NASA/CP-2000-209893

International VLBI Service for Geodesy and Astrometry

2000 General Meeting Proceedings

February 21-24, 2000
Kötzting, Germany

Nancy R. Vandenberg and Karen D. Baver, Editors

The NASA STI Program Office ... in Profile

Since its founding, NASA has been dedicated to the advancement of aeronautics and space science. The NASA Scientific and Technical Information (STI) Program Office plays a key part in helping NASA maintain this important role.

The NASA STI Program Office is operated by Langley Research Center, the lead center for NASA's scientific and technical information. The NASA STI Program Office provides access to the NASA STI Database, the largest collection of aeronautical and space science STI in the world. The Program Office is also NASA's institutional mechanism for disseminating the results of its research and development activities. These results are published by NASA in the NASA STI Report Series, which includes the following report types:

- TECHNICAL PUBLICATION. Reports of completed research or a major significant phase of research that present the results of NASA programs and include extensive data or theoretical analysis. Includes compilations of significant scientific and technical data and information deemed to be of continuing reference value. NASA's counterpart of peer-reviewed formal professional papers but has less stringent limitations on manuscript length and extent of graphic presentations.
- TECHNICAL MEMORANDUM. Scientific and technical findings that are preliminary or of specialized interest, e.g., quick release reports, working papers, and bibliographies that contain minimal annotation. Does not contain extensive analysis.
- CONTRACTOR REPORT. Scientific and technical findings by NASA-sponsored contractors and grantees.
- CONFERENCE PUBLICATION. Collected papers from scientific and technical conferences, symposia, seminars, or other meetings sponsored or cosponsored by NASA.
- SPECIAL PUBLICATION. Scientific, technical, or historical information from NASA programs, projects, and mission, often concerned with subjects having substantial public interest.
- TECHNICAL TRANSLATION. English-language translations of foreign scientific and technical material pertinent to NASA's mission.

Specialized services that complement the STI Program Office's diverse offerings include creating custom thesauri, building customized databases, organizing and publishing research results . . . even providing videos.

For more information about the NASA STI Program Office, see the following:

- Access the NASA STI Program Home Page at http://www.sti.nasa.gov/STI-homepage.html
- E-mail your question via the Internet to help@sti.nasa.gov
- Fax your question to the NASA Access Help Desk at (301) 621-0134
- Telephone the NASA Access Help Desk at (301) 621-0390
- Write to:
  NASA Access Help Desk
  NASA Center for AeroSpace Information
  7121 Standard Drive
  Hanover, MD 21076-1320

International VLBI Service for Geodesy and Astrometry

2000 General Meeting Proceedings

February 21-24, 2000
Kötzting, Germany

Nancy R. Vandenberg and Karen D. Baver, Editors

Available from:

NASA Center for AeroSpace Information
7121 Standard Drive
Hanover, MD 21076-1320
Price Code: A17

National Technical Information Service
5285 Port Royal Road
Springfield, VA 22161
Price Code: A10

Preface

This volume is the proceedings of the first General Meeting of the International VLBI Service for Geodesy and Astrometry (IVS), held in the town of Kötzting, Germany, February 21-24, 2000. The content of this volume also appears on the IVS web site at:

`http://ivscc.gsfc.nasa.gov/publications/gm2000`

The goal of the program committee for the General Meeting was to provide an interesting and informative program for a wide cross section of IVS members, including station operators, program managers, and analysts. The program included reports, tutorials, invited and contributed papers, and poster presentations. The tutorial papers should be particularly useful references because each one provides an overview and introduction to a topic relevant to VLBI.

This volume contains the following:

- **General information about the meeting.** This section includes the IVS Chair's welcome address, a summary with some photographs, and the meeting press release.
- **The papers presented at the meeting.** There are nine major sections of this volume, each corresponding to a meeting session. The tutorial papers were given at the beginning of each session, and appear as the first papers in each section. There were a total of 16 invited tutorials presented, 27 contributed oral papers and 35 poster papers. This volume includes 62 papers; abstracts only are printed for four papers for which a paper was not provided for publication. Poster papers about IVS component status are not included in this volume; they will be available in electronic version on the IVS web site later this year and will be published in the 2000 Annual Report.
- **Reports from splinter meetings.** Included are reports about the 2001 "chiefs" meeting, the RFI workshop held at Wettzell, and the first Analysis Workshop.
- **A list of registered participants.**
- **The meeting program.**

Acknowledgements

The editors would like to thank the following people who provided invaluable support throughout the preparation of this volume:

- Leonid Petrov for LaTeX programming and advice,
- Frank Gomez for systems support, and
- Carey Noll for graphics conversions and advice.

Thanks also to all the authors for preparing and submitting papers of such high quality, and thanks to the authors and their IVS components for the exceptional work that these papers represent. We look forward to the second General Meeting and future work with our colleagues.

Nancy Vandenberg and Karen Baver
IVS Coordinating Center
Editors, 2000 General Meeting Proceedings

Table of Contents

About the Meeting

IVS

Welcome Address, IVS 2000 General Meeting Proceedings, p.3–3
http://ivscc.gsfc.nasa.gov/publications/gm2000/welcome

Welcome Address

It is a great honor for the Bundesamt für Kartographie und Geodäsie (BKG) and especially for me to host the first General Meeting of the International VLBI Service for Geodesy and Astrometry in Kötzting. More than 120 participants registered for this conference. Considering that IVS has about 230 associated members, the participation in the General Meeting is highly encouraging and much more than expected. Nearly all the components have sent representatives.

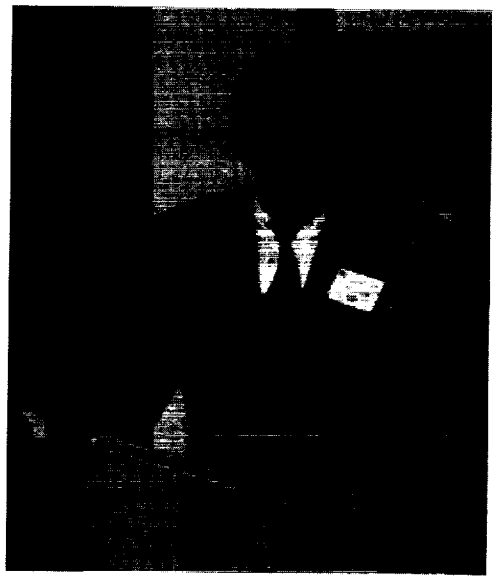

I am pleased to welcome Mr. Budrat as representative from the Ministry of Interior, which over the years supported the Fundamentalstation Wettzell as it grew up from a Satellite Observation Station to the Fundamentalstation. For our conference the Major of Kötzting, Wolfgang Ludwig, and the District Administrator, Landrat Theo Zellner, with their staff supported us actively by making available the convention facilities in "Haus des Gastes" and providing us additional conference rooms for splinter meetings. I express my gratitude and thank Mr. Zellner and Mr. Ludwig for their support.

As representative of the International Association of Geodesy Prof. Dr. Drewes, the president of the CSTG is welcomed. IVS is a service under the umbrella of the IAG and it is important for us to be recognized within IAG, which is for geodesy the most important international organization. He and Prof. Beutler of the University of Bern promoted the establishment of the IVS and supported actively the transition from the CSTG VLBI subcommission to the IVS.

The General Meeting of the IVS is the important meeting for all the representatives of the various components. During the conference experiences will be exchanged and new results will be reported. One of the goals of this meeting is to strengthen cooperation and to build bridges between the various components for a better understanding and for improvements. These goals were considered by the program committee. For this purpose each session starts with tutorials, in order to introduce the session topic to those who work in different areas. I express my thanks to the members of the program committee: Marshall Eubanks/USNO, Hayo Hase/BKG, Ed Himwich/NVI, Inc./GSFC, Yasuhiro Koyama/CRL, Chopo Ma/NASA-GSFC, Arthur Niell/MIT-Haystack, Axel Nothnagel/GIUB, Hans Peter Plag/SK, Rich Strand/GCGO, Nancy Vandenberg/NVI, Inc./GSFC and Alan Whitney/MIT-Haystack.

For the organisation of the conference we employed web-based technology, which I believe was a very efficient tool. In addition many things still had to be organized "manually". I thank the groups involved in the organisation very much for their excellent work. Specifically I thank Nancy Vandenberg from the Coordinating Center and Hayo Hase from the Local Organizing Committee.

The success of the first General Meeting will result from the contributions of the participants. Highly interesting and important contributions will be provided as oral presentations, as posters and during discussions. I thank all the speakers, the session chairpersons and the authors in advance for their excellent contribution. The value of the conference is maintained by providing your papers to be printed shortly after the conference in the proceedings. Thanks to all, let us keep up the excellent work.

My thanks to Dr. Tetsuro Kondo and to Dr. Shigeru Matsuzaka, members of the Directing Board for their agreement to arrange the next General Meeting in Japan. I hope to see you again there.

Wolfgang Schlüter, Chair

The First IVS General Meeting, IVS 2000 General Meeting Proceedings, p.4–5
http://ivscc.gsfc.nasa.gov/publications/gm2000/summary

The First IVS General Meeting

The first General Meeting of the International VLBI Service for Geodesy and Astrometry (IVS) was held in Kötzing, Germany on February 21-24, 2000. The purpose of the bi-annual General Meetings is to assemble representatives from all IVS components to share information, hear reports, and plan future activities. The meeting also provides a forum for interaction with other members of the VLBI and Earth science communities. All IVS Associate Members, representing all of the IVS components, are encouraged to attend the General Meetings. Any persons interested in VLBI are also cordially invited to attend these meetings.

The town of Kötzting is located in the Bavarian forest of Germany, close to the Fundamentalstation Wettzell. The host for the meeting was Bundesamt für Kartographie und Geodäsie (BKG), and the technical sessions were held at the convention center known as the "Haus des Gastes" in Kötzting. All of the arrangements for the meeting were handled by the Local Organizing Committee of Wolfgang Schlüter and Hayo Hase.

The mayor of Kötzting, Wolfgang Ludwig, received an IVS t-shirt in appreciation of the town's support for the General Meeting.

The president of BKG, Deitmar Grünreich, welcomed the participants at the reception. Traditional Bavarian music was provided by the brass band behind him.

At the reception on Sunday evening Wolfgang Schlüter, IVS Chair, gave an address (page 3) welcoming the participants and thanking the town of Kötzting and the district of Cham for all the support they provided for the meeting.

The meeting was extensively covered by the local radio, newspapers, and television stations because of the uniqueness associated with an international meeting in the small town of Kötzting. A press release, prepared (in German) by Wolfgang Schlüter, provided background information for the journalists (pages 6–7). Articles and photographs appeared in the newspapers Kötztinger Zeitung, Kötztinger Umschau, Mittelbayerische Zeitung, Passauer Neue Presse, and Viechtacher Bayerwaldbote. A short report was aired on "Bayern 1" and "Bayern 5" radio stations, and two television stations sent camera crews. A three-minute video was shown on Bavarian-wide television "BR 3" on Thursday evening, including pictures of the Wettzell antenna, shots of speakers at the meeting, and interviews with Wolfgang Schlüter and Nancy Vandenberg.

The registration desk was organized by members of the Wettzell staff. Hannelore Vogl holds a receipt, Richard Kilger is checking the list, and Rudolf Zernecke is delivering an IVS logo t-shirt.

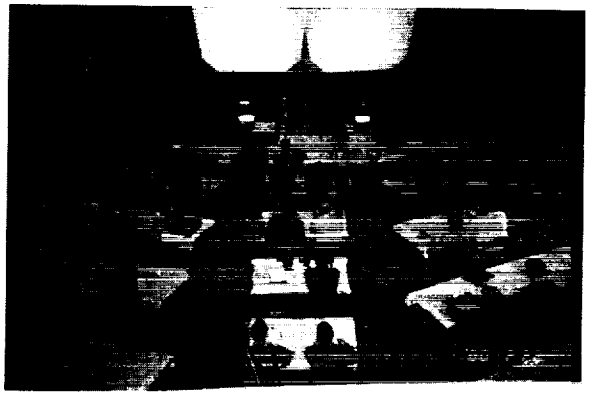

Participants attended all technical sessions in the meeting room of the "Haus des Gastes".

The meeting dinner was held at the Restaurant Gut Schmelmerhof, a former large farm house, in the village of Rettenbach. The chef prepared an excellent meal, and the highlight was the dessert plate that had elements from the IVS logo.

During the excursion to Wettzell on Thursday morning, participants toured the Wettzell antenna, the TIGO installation, and the laser system. An RFI workshop was held during the afternoon at Wettzell.

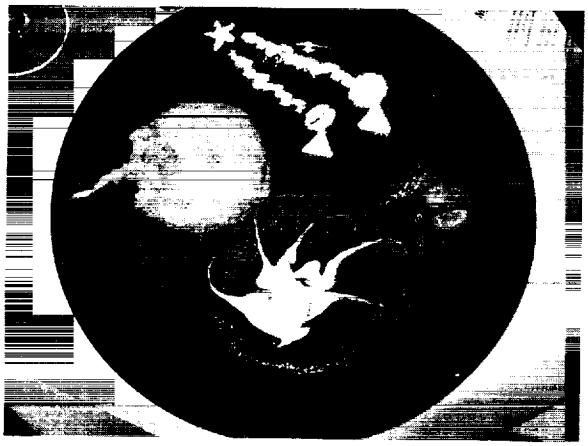

The dessert plate at the IVS dinner shows the basic elements of VLBI – two antennas, a quasar, and the radio waves. The intricate sauce design may be a quasar or it might be the Earth's core.

During the excursion to Wettzell, Hayo Hase described the TIGO installation. Hayo was a member of the Local Organizing Committee. Behind him is Armin Böer, another member of the TIGO team.

Press Release, IVS 2000 General Meeting Proceedings, p.6–7
http://ivscc.gsfc.nasa.gov/publications/gm2000/press

Press Release

This report is a translation of the press release provided to journalists from radio, television, and newspapers who reported on the first IVS General Meeting in Kötzting.

1. Information

In the period from February 21 to 24, 2000, the first General Meeting of the International VLBI Service for Geodesy and Astrometry (IVS) will take place in "Haus des Gastes" in Kötzting. The meeting will be hosted by the Bundesamt für Kartographie und Geodäsie (BKG), Fundamentalstation Wettzell. More than 100 guests from all over the world are expected, from the U.S.A., Canada, Japan, China, South Africa, Vietnam and from European countries.

2. What is VLBI?

VLBI is the abbreviation for Very Long Baseline Interferometry. Several radio telescopes, spread all over the world, simultaneously observe quasars (quasi-stellar objects). Quasars are billions of light years away from the Earth; therefore only very low-power microwave radiation is detected on the Earth. The telescopes are capable of receiving the weak signal and they record the signal together with time marks provided by highly precise atomic clocks. The data are recorded on magnetic tapes. After the observation of a complete experiment the magnetic tapes are shipped to a correlator. The correlator is a very sophisticated device, specially developed for this purpose to compare the signals from the different stations and to derive the times of arrival at the various stations. The different signal arrival times are used to calculate the distance between the radio telescopes—the so-called baselines. Also, Earth rotation is derived with respect to the quasars. VLBI is the most accurate technology to determine intercontinental baselines and Earth rotation parameters.

Quasars define a celestial reference frame which is fixed in space. The radio telescopes define a reference frame on the surface of the Earth that is fixed to the Earth. This enables us to fix points on the Earth's surface in relation to the celestial system.

Today we know that due to plate tectonics and geophysical phenomena there is no fixed point on the Earth. The task of realizing a reference frame thus becomes very complex. Nowadays not only the position of a radio telescope must be determined but also its motion.

VLBI plays a key role. On one hand VLBI allows us to determine the positions of quasars in the space-fixed reference system –which is the objective of astrometry. On the other hand the positions of the radio telescopes realize an Earth fixed reference system. Continuous observation series allow the monitoring of changes. The Earth orientation parameters describing the direction of the Earth's rotation axis and the rotation velocity provide the links between Earth fixed and space fixed reference frame—which is the task of geodesy.

Earth fixed reference frames are employed and are of great importance for satellite navigation systems such as GPS. GPS is used for navigation of vehicles, for land surveying, for the provision of basic information for geo-information, even in farming to measure the ground location of the harvest in order to spread fertilizer most efficiently. GPS today is used in a lot of daily applications. The global reference frame is the basis for development and application of such new technologies.

3. IVS

In the last few years the importance of VLBI and its results was recognized in research and in applications. In order to guarantee the delivery of VLBI products in a timely manner a service was required. In

1998 within the International Association of Geodesy and the International Astronomical Union a call for participation was released for the purpose of establishing wordwide the International VLBI Service. The first meeting of the Directing Board of the IVS was held in Wettzell on February 11, 1999. The IVS is supported by 15 nations and is formed through 30 radio telescopes, 7 correlators, 6 data centers, 19 analysis centers, 9 technology development centers and 1 coordinating center. Around 250 scientists and engineers are engaged in this effort.

4. Contribution of the German Research Group Satellite Geodesy

The Research Group Satellite Geodesy (Forschungsgruppe Satellitengeodäsie or FGS), formed by the Bundesamt für Kartographie und Geodäsie, Forschungseinrichtung Satellitengeodäsie of the Technische Universität München, Deutsche Geodätisches Forschungsinstitut (DGFI) and the Geodätisches Institut of the Universität Bonn, supports IVS enthusiastically. The FGS provides observations with the radio telescope at Wettzell, with TIGO (Transportables Integriertes Geodätisches Observatorium), and with the telescope located at O'Higgins/Antarctica. FGS also provides data and analysis centers and a correlator operated jointly by BKG, the University of Bonn and the Max Planck Institut für Radioastronomie. Important functions are carried out by Axel Nothnagel of the University of Bonn as the coordinator for analysis and by Wolfgang Schlüter, chair of the IVS Directing Board.

The first General Meeting is organized jointly by BKG and the IVS Coordinating Center, which is located at NASA Goddard Space Flight Center, Greenbelt/USA. Wolfgang Schlüter and Hayo Hase of BKG/Fundamentalstation Wettzell organized the local arrangements.

5. Objectives of the Meeting

The objectives of the General Meeting are to exchange experiences to support international cooperation, to present actual results and to discuss new projects. The program covers all areas starting from the observations up to the analysis. The first day summarizes some highlights and observation strategies. The second day covers VLBI technology. Data analysis is the topic of the third day. An excursion to the Wettzell observatory is planned for the fourth day. In the evening splinter meetings take place to discuss very special topics. All participants will take the opportunity for personal discussions. The next meeting will be in two years.

6. Thanks

We have to express our thanks to the city of Kötzting and especially to Mayor Wolfgang Ludwig; to Sepp Barth, the director of the tourist office; and to Theo Zellner, the Landrat of Cham, for their tremendous support in hosting our guests, providing the meeting facilities in the "Haus des Gastes" and for the warm welcome of the city of Kötzting.

Session 1

Highlights and Challenges of VLBI

Wolfgang Schlüter: Report of the IVS Chair, IVS 2000 General Meeting Proceedings, p.11–15
http://ivscc.gsfc.nasa.gov/publications/gm2000/schlueter2

Report of the IVS Chair

Wolfgang Schlüter

Bundesamt für Kartographie und Geodäsie
e-mail: schlueter@wettzell.ifag.de

Abstract

This report reviews the objectives and the current status of the IVS. It summarizes the activities and gives some prospects for the near future.

1. Objectives of the IVS

The International VLBI Service for Geodesy and Astrometry (IVS) is a Service of the International Association of Geodesy (IAG). The goal of IVS is to coordinate and organize the collaboration of organizations which operate or support Very Long Baseline Interferometry (VLBI) components. The inauguration date of IVS was March 1, 1999. At the IAG Executive Committee Meeting in Birmingham, July 1999, the IVS officially was recognized as a Service of IAG.

While in the past cooperation between organizations was more or less on a voluntary basis and each organization could withdraw its contribution, participation in the service is now an obligation because the respective organizations have applied to be members of IVS. Because the products of VLBI are in demand not only for scientific applications but also for operational activities, the pressure to guarantee the results for maintaining reference frames has increased. An international organization with an ongoing purpose is required in order to strengthen cooperation, to justify the participation of each participating agency and finally to guarantee in the long term the delivery of products for the whole community. The transition from the VLBI Subcommission of the CSTG (International Coordination of Space Techniques for Geodesy and Geodynamics) to the IVS was performed in the years 1997 to 1998.

The general objectives of IVS are, as documented in the Terms of Reference, to

- support geodetic, geophysical and astrometric research and operational activities,
- promote research and development for VLBI,
- interact with users of VLBI products.

IVS coordinates internationally the geodetic and astrometric VLBI activities and provides contributions to

- the International Terrestrial Reference Frame (ITRF), e.g. through the determination of the positions of the VLBI observatories and their motion,
- the International Celestial Reference Frame (ICRF), uniquely provided by the VLBI technique through the determination of the positions of the quasars,
- the determination of Earth Orientation Parameters (EOP), describing the orientation of the Earth's rotation axis with respect to the crust (polar motion) and Earth rotation (DUT1),

- the determination of the celestial pole, describing the motion of the rotation axis in space, with respect to the quasars (precession and nutation).

IVS activities closely interact with the International Earth Rotation Service (IERS) in order to ensure that VLBI products have suitable quality and timeliness.

2. IVS Components

IVS coordinates the VLBI observations, the data flow, the correlation and the data analysis and also technology developments. Various components of IVS are defined:

- Network Stations, which are high performance VLBI stations that acquire data,
- Operation Centers, which coordinate the activities of a network of Network Stations and generate observation schedules,
- Correlators, which process data, provide feedback to the stations on the data quality, and provide processed data to analysts,
- Analysis Centers, which analyze data and produce results and products,
- Data Centers, which distribute products to users, and provide storage and archive functions,
- Technology Development Centers, which develop new VLBI technology,
- Coordinating Center, which coordinates the daily and long term activities of IVS.

A call for participation in the IVS was released in fall 1998 and agencies which support VLBI proposed to provide different components. With their proposals the agencies documented their strong desire to guarantee their support within the service according to the ToR.

For the coordination of the components a steering body and coordinator functions were established:

- The Directing Board determines policies, standards and goals. It is composed of elected and ex officio members. The elected members represent the components while ex officio members are nominated by IAG, IAU, IERS and the Coordinating Center.
- The Network Coordinator is responsible for station data quality and performance standards,
- The Analysis Coordinator is responsible for VLBI product development and delivery,
- The Technology Coordinator is responsible for VLBI technique advancement and system compatibility.

Agencies supporting one or more IVS components are known as Member Organizations, and individuals who participate in the work of any of the IVS components are Associate Members. Agencies that provide no support of an IVS component but cooperate with IVS, e.g. in the development of technology, are known as Affiliated Organizations. Finally individuals who want to be informed of IVS activities are Corresponding Members. The current components of IVS are shown in figure 1.

Figure 1. Map of IVS Components.

3. Members of the Directing Board and Functions

The Members of the Directing Board are ex officio, selected or elected by the Directing Board or elected by the Associate Members representing IVS components. Ex officio members are nominated by the IAG, IAU, IERS and by the Coordinating Center. The coordinators are selected by the Directing Board upon review of proposals from the relevant IVS components. At large members are elected by the Directing Board for keeping a balanced representation from as many countries and institutions as possible. The members of the Directing Board are

- Ex Officio:
  - James Campbell, replacing Gerhard Beutler since July 1999 as IAG representative
  - Nicole Capitaine as IAU representative
  - Chopo Ma as IERS representative (IERS is currently reorganized)
  - Nancy Vandenberg as Director of the Coordinating Center
- Coordinators:
  - Axel Nothnagel as Analysis Coordinator (since October 1, 1999)
  - Ed Himwich as Network Coordinator
  - Alan Whitney as Technology Coordinator
- Representatives:
  - Chopo Ma for Analysis and Data Centers (October 1, 1999)
  - Marshall Eubanks for Operation Centers and Correlators
  - Shigeru Matsuzaka for Networks
  - Wolfgang Schlüter for Networks (chair)
  - Tetsuro Kondo for Technology Development Centers
- At Large Members:
  - Wayne Cannon
  - Paolo Tomasi

The Directing Board had its first meeting in Wettzell on February 11, 1999; second meeting in Birmingham on July 19, 1999, and third Meeting in Wettzell on February 20, 2000. The minutes of the board meetings are available on the IVS web site.

In addition a Coordinators meeting was held at GSFC on April 8, 1999, to discuss the activities of each coordinator with emphasis on areas where responsibilities of the Coordinators may overlap.

4. Summary of Activities

The following activities were performed:

- The IVS web site was set up at NASA Goddard Space Flight Center/USA, mirrored at Bundesamt für Kartographie und Geodäsie/Germany (BKG) and Communications Research Laboratory/Japan. It was officially announced March 1, 1999.

- A logo contest was held and more than 20 entries were received. The official logo is a composition of various accepted entries, designed by an artist. The final logo was officially accepted on September 23, 1999.
- A solicitation for IVS data and analysis was released to obtain proposals from the Operation Centers and Analysis Centers on the provision of products. In addition proposals for analysis functions (e.g. comparison) were requested and a call for proposals for the Analysis Coordinator was released.
- The IVS Annual Report was published in August 1999 (electronically). The printed version was distributed in September 1999. The Annual Report was intended to be a description and documentation of the current status of the various components of the IVS.
- The first IVS General Meeting held in Kötzting, Germany was organized.

5. Prospects

The next important steps of the IVS have to be aimed at strengthening the coordination of all resources and integrating all the components into a highly reliable service which will guarantee the highest achievable quality and timely products on a long term basis.

IVS standards have to be developed for the components, in order to enhance overall data quality, quantity and reliability. This will motivate the organizations to keep their components operating on a highly reliable level. Continuous monitoring of data quality and quantity will encourage the best products.

Improvements have to be considered in the network configuration. Today, the distribution of the network stations in the southern hemisphere is not sufficient. IVS has to investigate all resources, e.g. cooperation with related communities so that we can make use of their facilities. The standardization of data acquisition interfaces will help to combine the various data acquisition techniques (MK3/MK4, K4 and S2) and will support the implementation of more network stations. It should be pointed out that the Transportable Integrated Geodetic Observatory (TIGO) will be placed to Concepcion/Chile in 2001. With its 6-m VLBI offset antenna it will significantly improve the network. Additional network stations are urgently required in the Asian/Australian area.

New developments in data transmission will accelerate data exchange leading finally to near real time products. It will help to reduce the effort in maintaining tape drives and shipping tapes.

If we can employ more reliable components with an increased degree of automation, we can perform more observations without operators. Such developments will support an improved observation quantity on weekends.

Close cooperation with the other services will become important. As all the geodetic space techniques have their advantages, the combination of data will improve the results significantly. During the first IVS General Meeting the IVS established a Working Group jointly with the IGS and ILRS to study the feasibility of determining the location of the phase center of the GPS transmitters. The analysis of GPS data indicates that the assumption of the phase center as a point source is not precise and can cause systematic errors. VLBI may be able to map the GPS source with respect to the quasars, laser ranging can provide additional information on the scale and on the GPS orbits (for two satellites) with respect to the center of mass. A combination of all techniques might solve the problem.

Nancy R. Vandenberg: Coordinating Center Report, IVS 2000 General Meeting Proceedings, p.16–18
http://ivscc.gsfc.nasa.gov/publications/gm2000/vandenberg

Coordinating Center Report

Nancy R. Vandenberg

NVI, Inc./NASA Goddard Space Flight Center
e-mail: nrv@gemini.gsfc.nasa.gov

Abstract

This report summarizes the activities of the IVS Coordinating Center during the past six months, since the publication of the Annual Report (see Ref. [1]). This report summarizes recent activities and forecasts plans for the coming year.

1. Coordinating Center Operation

The IVS Coordinating Center is operated by NEOS (National Earth Orientation Service), a joint effort for VLBI by the U.S. Naval Observatory and NASA Goddard Space Flight Center.

The main mission of the Coordinating Center is to provide communications and information for the IVS community and the greater scientific community. Our primary activity is coordination of the day-to-day and long-term activities of IVS.

The web server for the Coordinating Center is provided by Goddard. The address of the IVS web site is

`http://ivscc.gsfc.nasa.gov`

The IVS web site holds all the charts and tables that describe the IVS as an organization. It has prominent links to data and products. The web site is mirrored at collaborating IVS institutions in Germany and Japan.

2. Activities

The main activities required of the Coordinating Center are defined in the Terms of Reference. During the past six months the Coordinating Center supported the following IVS activities:

- Supported the Directing Board at meetings in July 1999 and February 2000.
- Coordinated the Master Schedule for all geodetic observing.
- Maintained the web site, adding new pages with links to IVS data and products.
- Set up new mail lists as needed and maintained the mail archives for all lists.
- Published the first IVS Annual Report (Ref. [1]), which covered the period of the year prior to the establishment of IVS.
- Organized generation of the IVS logo (see figure 2) under direction from the Directing Board and made logo t-shirts.
- Organized the "global" part of the first IVS General Meeting, including announcements, the web pages, and registration.

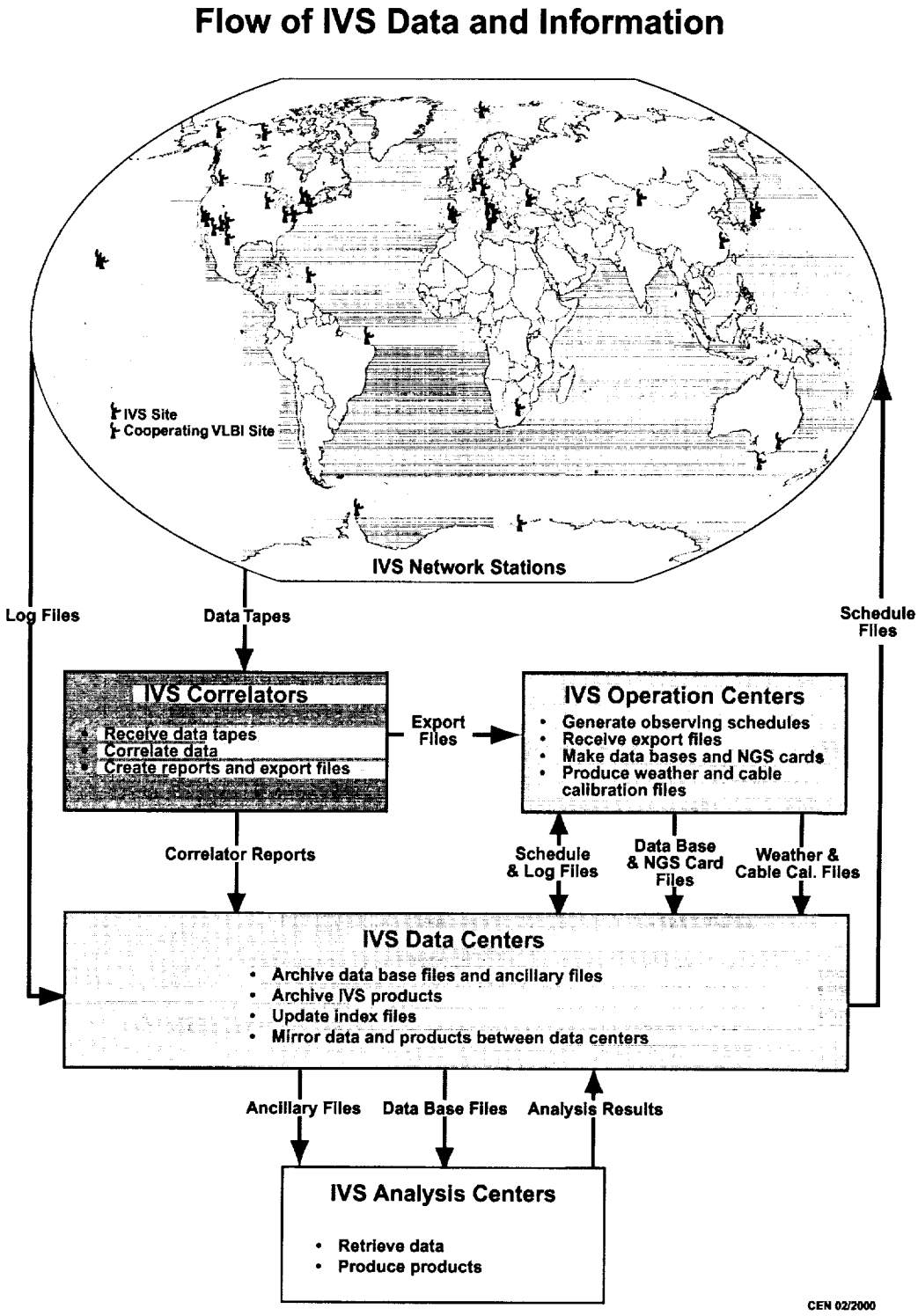

Figure 1. Flow of IVS data and information.

3. Plans

During the coming year, the Coordinating Center plans to do the following:

- Publish the proceedings of the first IVS General Meeting.
- Publish the 2000 Annual Report, which will cover the period through the year 2000.
- Improve access to data and products by working with the Analysis Coordinator and the Data Centers. Figure 1 is a diagram created by Carey Noll (GSFC) to show the data flow among all the IVS components.
- Establish a web-accessible data base of IVS information.
- Set up configuration files for all IVS components by working with the Network Coordinator.
- Coordinate the first IVS Chiefs Meeting in early 2001.

4. The Logo

The initial version of the IVS logo was designed by Ms. Jane Foltz of Raytheon, based on direction from the IVS Directing Board. The Directing Board decided to have a logo designed that contained the elements that it felt should be included: the Earth, two antennas, signals, and a quasar.

Figure 2. IVS Logo.

The Coordinating Center worked with the artist to refine the design after several reviews by the Board. The final design was released on September 23, 1999 and published on the IVS web site. This date still holds the record for the most accesses to the IVS web site.

The first official appearance of the logo was on IVS letterhead, used by the IVS Chair for official business.

The second official use of the logo was to produce screen-printed t-shirts for each registered participant at the first IVS General Meeting. Free t-shirts were provided to each person who submitted a logo to the logo contest.

References

[1] Vandenberg, N. R., "IVS Coordinating Center Report", in International VLBI Service for Geodesy and Astrometry 1999 Annual Report, edited by N. R. Vandenberg, NASA/TP-1999-209243, 1999.

J. Campbell: From Quasars to Benchmarks: VLBI Links Heaven and Earth, IVS 2000 General Meeting Proceedings, p.19–34
http://ivscc.gsfc.nasa.gov/publications/gm2000/campbell1

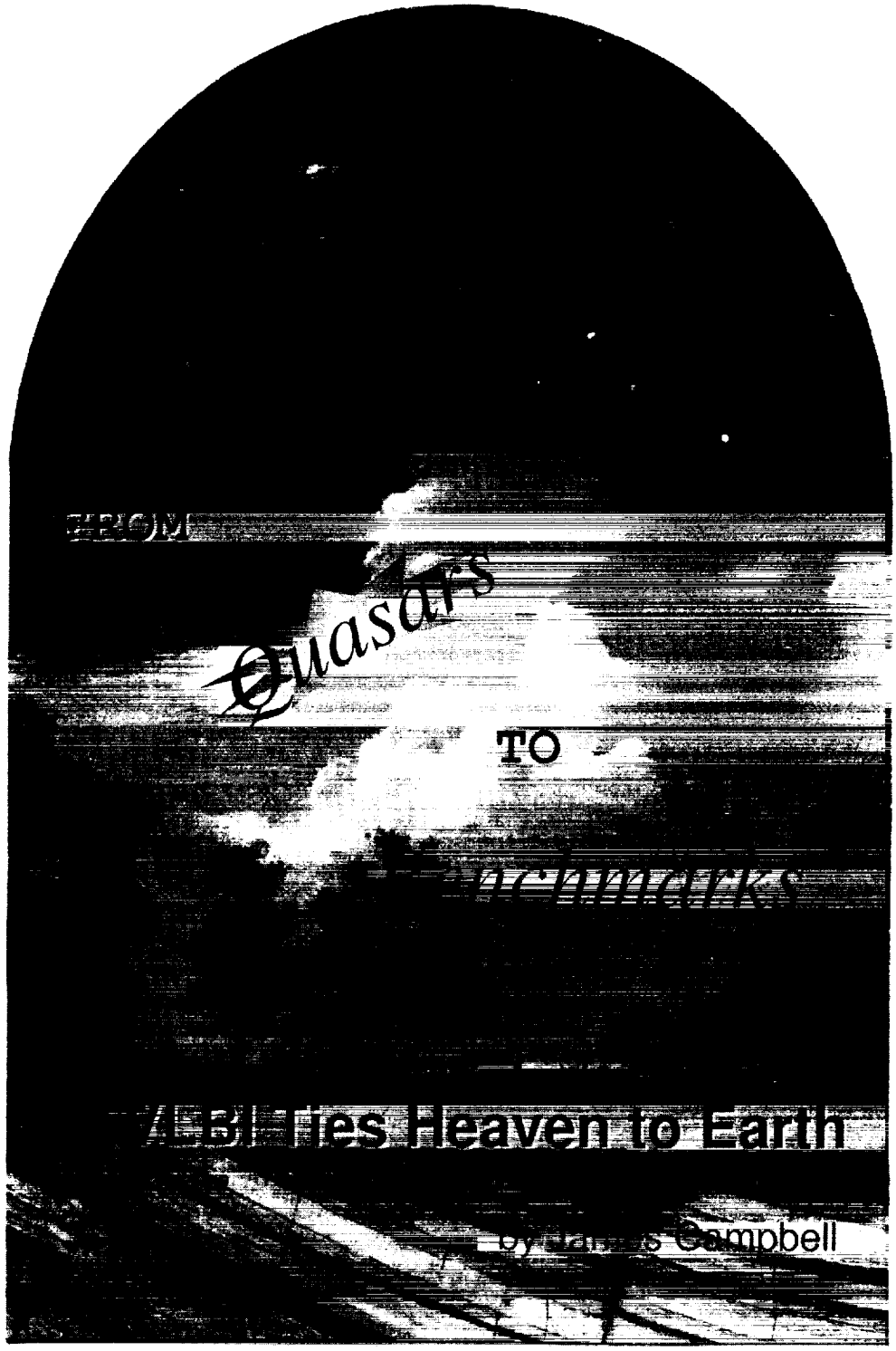

From Quasars to Benchmarks: VLBI Links Heaven and Earth

J. Campbell

Geodetic Institute of the University of Bonn
e-mail: campbell@sn-geod-1.geod.uni-bonn.de

Abstract

Very Long Baseline Interferometry is able to provide a direct geometrical tie to the extragalactic radio sources which represent the best possible realization of an inertial system. By this token, VLBI can measure Earth rotation and orientation as well as precise station positions and their velocities without involving the gravity field of the Earth. In the broader context of Earth observation and the monitoring of geodynamic processes, these and many more unique features have allowed the VLBI technique to achieve pioneering feats such as the determination of present-day plate tectonic motions, post glacial rebound, sub-daily Earth rotation variations and parameters of general relativity. In this contribution, some of the highlights of the history of VLBI will be passed in review and directions of future developments will be pointed out.

1. Introduction

At first glance it may seem rather bold to establish—as the title picture suggests—a direct link between two objects as disparate as the solid crust-fixed benchmark near our feet and the elusive quasi-stellar object at the ultimate confines of the universe. Yet, if we substitute the benchmark by a concrete foundation topped with a radio telescope and tune in to the wide bandwidth noise emanating from the tiny dots in the sky, radio astronomy is born and the way is opened for the concept of VLBI: adding in more telescopes and comparing the timed signals received at the different places on the Earth bestows us with an almost perfect tool for measuring angles and distances with extremely high precision on a global scale.

The geometric principle of VLBI is surprisingly simple and straightforward. It even precedes satellite geodesy, because the incoming radiation has plane wavefronts, thereby eliminating the parallactic angle and the distance to the emitter. The basic triangle for the determination of the baseline vector reduces to a rectangular one providing a direct relation between the baseline vector and the direction to the radio source, i.e. the scalar product representing the observed delay (Fig. 1 and Tab. 1). The interferometer being glued to the Earth's surface follows its diurnal rotation and in this way allows us to sample the radiation from all quasars coming into view.

If we leave abstract Euclidian geometry in empty space and return to the real world with curved space, flickering quasars, billowing atmospheres, wobbling axes and drifting continents, we have to delve into layers of complexity, fortunately not only as a chore but also as an opportunity to gain a wealth of new knowledge about our system Earth (Fig. 2).

Very Long Baseline Interferometry, initially named less ambitiously "Long Baseline Interferometry" is an outgrowth of radio interferometry with cable-connected elements designed to overcome the limited resolution power of single dish radio telescopes (Cohen et al. 1968).

In its simplest form, a radio interferometer consists of two antennas separated by a given distance and connected via the receivers, the down conversion systems and a phase stable electrical link to a phase (and amplitude) meter. To separate the actual radio signals from the unwanted

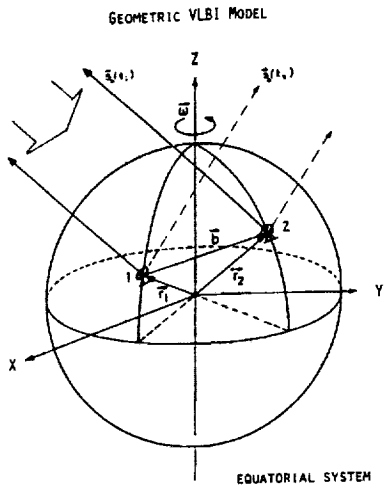

Fig. 1: Geometric VLBI model

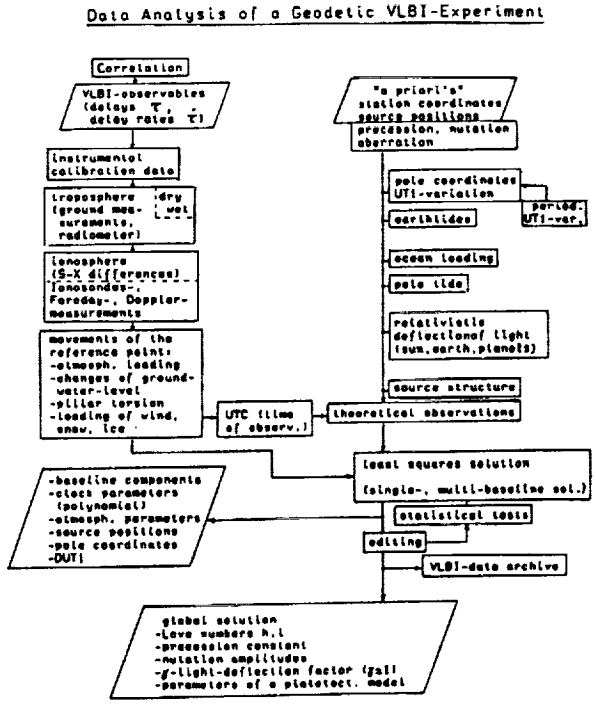

Fig. 3: Geodetic VLBI data analysis

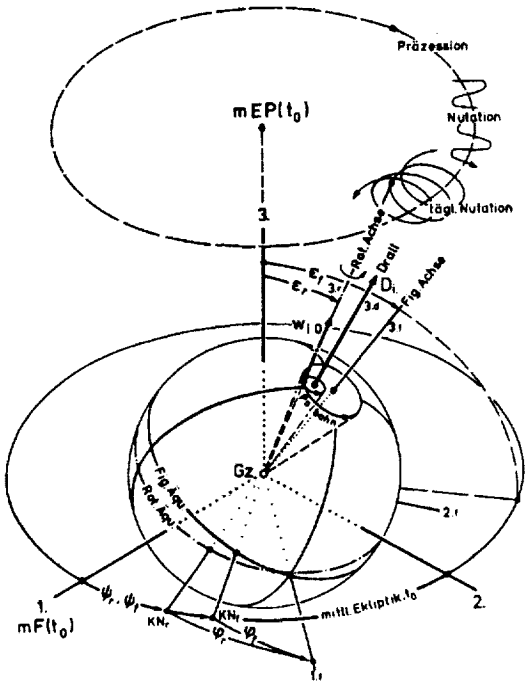

Fig. 2: Earth rotation in the space-fixed body-fixed systems (Heitz 1976)

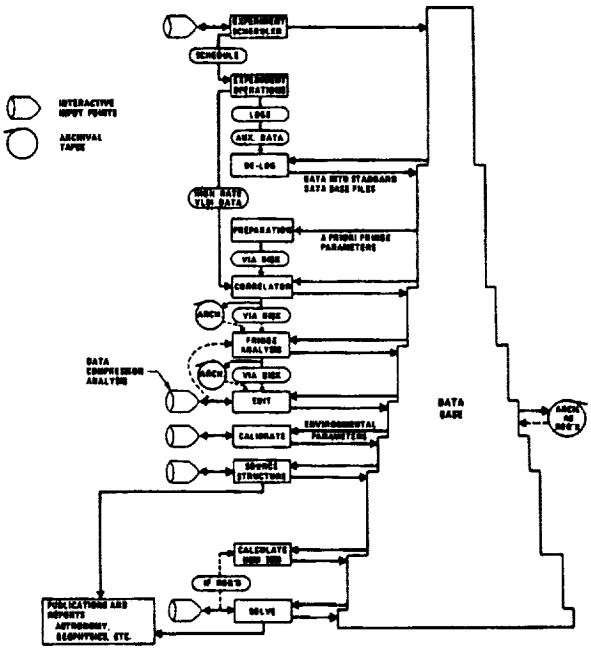

Fig. 4: The MkIII VLBI data analysis system

noise the correlation technique is normally used as the most efficient realisation of a phase meter. The response of such a system to the observed radio source carries information on its angular size and structure which are of prime interest to the astronomer.

To reveal the structure of extremely compact radio sources, the resolving power of Connected Element Radio Interferometers (CERI) was insufficient even at higher frequencies. A major breakthrough was made in the late sixties, when independent radio observatories in Canada and in the US were able to record their data on tapes using highly stable oscillators, and fringes were found during playback of the tapes at a correlator center, thus eliminating the need for a phase stable connection between the telescopes (Broten et al. 1967, Bare et al. 1967).

2. Phase or Group Delay in Geodetic VLBI?

The first experiments that were explicitly aimed at achieving geodetic accuracy on long baselines were conducted by the Haystack/MIT group on the 845-km baseline between the Haystack Observatory in the north of Massachusetts and the National Radio Astronomy Observatory of Green Bank, West Virginia (Hinteregger et al. 1972). The key to the high group delay resolution of ± 1 nanosecond attained in these experiments was the invention of the so-called bandwidth synthesis technique (Rogers 1970), which helped to overcome the limitations of tape recording equipment in terms of recordable bandwidth.

Considering the successful use of the phase observable in GPS, one could wonder why it is so important to strive for high bandwidth. After all, the fringe phase is among the VLBI observables that are derived from the correlator output. One 2-MHz channel would be enough to detect and measure the phase of a source (observing strong sources with large dishes and cooled receivers). Two channels in two different bands would take care of the ionospheric phase delay, so one would just have to follow the GPS recipe and solve the ambiguities by forming double differences.

Obviously this is not the way taken in geodetic VLBI. One important reason is that sources in different parts of the sky cannot be observed simultaneously. Radio telescopes have to be steered and pointed at the sources one after the other to collect enough signal strength to permit their detection during correlation. During telescope slewing, several instrumental and environmental effects have ample time to destroy the phase coherence between scans.

This situation evidences an intrinsic division between VLBI and GPS: no double differencing means no elimination of timing errors between receiving stations. Therefore VLBI has to rely on "error-free" time keepers at the stations to bind the sequential observations of the radio sources together. The tempting idea to use omnidirectional antennas at the VLBI stations and forget about H-maser oscillators has to remain a dream because quasars are at least six orders of magnitude weaker than the signals emitted by the GPS satellites (MacDoran et al. 1982).

Thus several factors are joining to hamper and obstruct the use of the phase observable in geodetic VLBI (Herring 1992, Petrov 1999). In any case, the natural ultra-wide band continuum radiation is offered free of charge by the majority of the compact radio sources and provides the means to use the essentially unambiguous wide band group delay as the prime geodetic VLBI observable.

The group delay resolution is proportional to the inverse of the SNR and the spanned bandwidth (Rogers 1970), so, if we increase the spanned bandwidth at a given SNR by a factor of ten, the group delay uncertainty will be reduced by the same factor, a relation with tremendous consequences. There are virtually no limitations to further improve the geodetic group delay performance, except

(evolving) technological constraints and costs. Phase delay, on the other hand, is still an issue of research and does provide very high accuracy on very short baselines (Herring 1992, Hase and Petrov 1999).

Before going into more details about the technical side of VLBI we have to take up the thread from the basic VLBI model to the fully grown analysis systems of the present day.

3. Models vs. Observations in Geodetic VLBI Data Analysis

The most commonly used way to extract significant and meaningful information from nature's ongoing processes is to try to model these processes by applying the laws of physics to the best of our knowledge. The less well known parts of our model will be equipped with a set of well seasoned unknown parameters. The least squares adjustment will then reveal the degree of correspondence we have achieved between theory and observation.

In VLBI, just like most other measuring techniques, the data analysis system has two main branches, one that takes in the raw observations and provides a number of instrumental and environmental corrections and the other that produces the "model observations" or "theoreticals" (Fig. 3).

The **fundamental geometric model** of the time delay forms the heart of the system. This model has evolved from its simple initial form in a geocentric system to the highly complex relativistic formulation in the solar system barycenter (Tab. 1). The complete formulation includes both the effects of **special relativity** (part of what is known as aberration in spherical astronomy) and of **general relativity**, which describes the curvature of space-time. The effect of gravity on the propagation of electromagnetic waves is considerable: even at an angle of 180° away from the sun the differential delay effect (for a 6000 km baseline) is still 0.4 ns. VLBI observations have been used to verify Einstein's theory (PPN formulation) to an accuracy of 0.1% (Counselman et al. 1974; Robertson and Carter 1984).

Table 1. Models for the geocentric (observed) time delay

Basic geocentric formulation		**Solar system barycentric formulation**
Cohen–Shaffer (1971)	**Thomas (1972)**	**Robertson (1975)**
$\tau_0 = -\frac{\mathbf{b}\cdot\mathbf{k}}{c}$	$\tau_g = \tau_0\left(1 - \frac{\dot{\mathbf{r}}_2\cdot\mathbf{k}}{c}\right)^{-1}$	$\tau_g = \tau_0\{1 - (\dot{\mathbf{R}}+\dot{\mathbf{r}}_2)\,\mathbf{k}/c$
+ **retarded baseline effect (or diurnal aberration at station 2)**	$\dot{\mathbf{r}}_2 = \boldsymbol{\Omega}\times\mathbf{r}_2$	$[(\dot{\mathbf{R}}\cdot\mathbf{k})^2 + 2\,(\dot{\mathbf{R}}\cdot\mathbf{k})\,(\dot{\mathbf{r}}_2\cdot\mathbf{k})]/c^2\}$ $+(\mathbf{b}\cdot\dot{\mathbf{R}})\,[(\dot{\mathbf{R}}\cdot\mathbf{k})/2 + (\dot{\mathbf{r}}_2\cdot\mathbf{k})]/c^3$ $-\tau_0(U + \dot{R}^2/2 + \dot{\mathbf{R}}\cdot\dot{\mathbf{r}}_2)/c^2$ $-(\mathbf{b}\cdot\dot{\mathbf{R}})/c^2$
+ **annual aberration**	+ **annual aberration**	
	+ **relativistic light deflection** $\Delta\phi_{\text{grav}} = 2r_g^{\odot}/d$	+ **General relativity** $\tau^{\odot}_{\text{grav}} = \frac{r_g^{\odot}\mathbf{b}(\mathbf{k}+\mathbf{R}_0)}{Rc(1+\mathbf{k}\cdot\mathbf{R}_0)}$

In principle, the description of the Earth's orientation with respect to the celestial system

(**precession, nutation**) and the motion of the Earth's axis with respect to the crust (**polar motion**) has to reach the same level of accuracy as all the other model components, which means roughly better than one milliarcsecond. The same holds for the rotational speed of the Earth about its axis: to compute the phase angle of the Earth's rotation at any epoch to better than 1 mas, the **UT1-variations** have to be known to better than 0.1 msec of time. Of course, our understanding of the origin of all these variations is still far behind these levels of accuracy and this is why at present we still have to regard all angles involved in the transformation between the terrestrial and the celestial systems as unknown parameters in our solution (Herring et al. 1986, Herring, this volume). It is due to the intrinsic strength of the geodetic VLBI observing strategy that we are still able to solve the system of observation equations, without ending up in singularity. Of course, if we stop the Earth, the instantaneous rotation axis vanishes and the system degenerates: we are left with three Eulerian angles between two non-aligned systems.

Already in the early seventies the periodic deformations of the Earth's crust could be seen in the VLBI observations: **solid Earth tides** cause diurnal and semidiurnal oscillations with vertical amplitudes of about 40 cm and horizontal displacements of up to 10% of the vertical effect. Although good models are available, the relevant parameters can be estimated from larger sets of data (Herring et al. 1983). More difficult to model are the **tidal loading** effects of the oceans, which amount to as much as a decimeter on some coastal or island sites (Scherneck 1991).

The fact that the VLBI stations are tied to the solid crust reveals itself alas as a rather deceptive assumption. Apart from the periodic convulsions of the Earth there are all sorts of aperiodic motions, the most prominent of which are the horizontal and vertical motions associated with **plate tectonics** (Minster and Jordan 1978). The obvious problem that arises for the definition of a terrestrial reference frame is akin to the problem of proper motions in the optical celestial reference frames: how do we fix the origin? Here we have to resort to the concept of a priori constraints, e.g. the "no net (to) rotation" (NNR), "no net translation" (NNT) constraints (Argus and Gordon 1996), but rigorously speaking there is no solution to this problem if we have different sets of defining stations in the global networks (Altamimi, this volume).

In global solutions with large data sets precise **source positions** can be determined simultaneously with the other parameters (Ma et al. 1993). The accuracy of the celestial reference frame may now be estimated to be around 0.3 milliarcsec on short as well as on longer time scales, although individual sources show greater variations (Feissel, this volume). The physical nature of quasars is still under debate, although models have been developed that are able to explain several of the observed features, such as the core-jet structure (Walker, this volume). For the geodesist the bitter fact remains that most of the observed compact sources are indeed showing **structure** at the level of several mas (Fey, this volume). This effect, in particular any changes in the structure, poses a limit on the accuracy of the radio reference system. However, permanent monitoring of the structure, which is accomplished in part by the same VLBI data, can be done in parallel to the geodetic analysis, thus providing a means to correct for the structure effects (Charlot and Fey 1999).

The systematic **instrumental effects** include clock instabilities, electronic delays in cables and circuitry and deformations of the telescope structure. Usually as a clock model a second order polynomial is introduced and occasionally a break has to be allowed for. Clock modelling is still very much an interactive procedure and belongs to the editing session. The instrumental delay changes are, or at least should be, monitored by the phase and delay calibration system, which is part of the MkIII system (Petrov, this issue). In the telescope the distance between the feed

horn and the axis intersection should be constant; in this case it becomes part of the clock offset parameter. Large telescopes such as the Effelsberg 100-m antenna exhibit direction dependent changes that have to be measured by local geodetic surveying techniques (Nothnagel 1999).

The effect of the **atmosphere** on VLBI observations is considered to be the most serious problem, because at widely separated stations the elevations of the telescopes during a scan differ greatly as well as the meteorological conditions themselves (Mathur et al. 1970). But while the **ionosphere** can be readily eliminated to first order by using two different observing frequencies, the neutral atmosphere, essentially the troposphere, presents the same problems in VLBI as in GPS observations. Its influence on radio signals adds up to an extra zenith path of 1.8 to 2.5 meters. The contribution of the dry part is rather stable, although care has to be taken to choose a proper mapping function for the lower elevations (Davis et al. 1985, Niell, this volume). The **wet component**, although the smaller part of the total tropospheric effect, changes rapidly and has to be monitored by some external means. Still today the only promising—albeit costly—method appears to be the radiometer technique, which consists of measuring the microwave thermal emission from water vapour near 22 GHz in the line-of-sight (Elgered et al. 1982, Resch, this volume).

In VLBI data processing there are two levels of least squares solutions, one in which only the "local" unknowns are estimated (such as clocks, atmospheric parameters, and Earth rotation parameters) thus creating a first data base version of a particular experiment, and another one which collects all available experiments for a comprehensive solution including the "global" unknowns (such as station and source positions, etc.). Among the various VLBI software systems the MkIII Data Analysis System (Fig. 4) should be mentioned, which is built around the CALC/SOLVE software system developed jointly by the US East Coast VLBI groups including additional improvements made at Bonn and has become a standard against which the other systems can be compared (Ma et al. 1989). Of course, modelling does not end here: a holistic approach of the system "Earth" still remains a task for the future.

4. Geodetic Observing Programs and Milestone Results

A detailed description of the great potential of VLBI for geophysical applications was presented as early as 1969 at a conference held in London, Canada on "Earthquake displacement fields and the rotation of the Earth" (Shapiro and Knight 1970). In subsequent years virtually all of the goals mentioned there were to be achieved. We cite the original list from page 295 of the proceedings:

(1) Global Geodesy.

(2) Tidal Oscillations.

(3) Crustal-Block Motions (including continental drift).

(4) Polar Motion.

(5) Earth Rotation.

(6) Precession and Nutation (including a test of general relativity).

(7) Obliquity of Ecliptic.

(8) Shape of Sea Surface.

(9) Geopotential.

(10) Global Time and Frequency Synchronisation.

Referring to item (1), the text reads "...improvements in geodetic ties, especially over long baselines, by several orders of magnitude. For example, the relative positions of the stations of the world-wide net of Baker-Nunn satellite-tracking cameras have uncertainties of the order of 10-20m. Interferometry offers the possibility of reducing such uncertainties to a few centimeters."

In the meantime, uncertainties at the cm level and even less have been demonstrated by thousands of VLBI experiments in networks connecting almost all major continents of the globe. In order to realise the initial goals and many more, the efforts in different countries around the world have been combined in setting up several programs that include international cooperation. Here, we can name only two of the most important ones:

The NASA Crustal Dynamics Project (CDP, 1979–1993)

This project is part of a US Federal program involving several government agencies for the application of space technology to crustal dynamics and earthquake research (Coates 1985). Under its predecessor, the "Pacific Plate Motion Experiment" (PPME, 1976-1979) the first geodetic intercontinental baseline measurements with the MkI VLBI system were carried out in September 1977 and February and May 1978 on the baseline Haystack-Onsala (Ryan et al. 1986).

A milestone was reached when the first significant estimates of the length change on the transatlantic baseline Haystack-Onsala were announced. A baseline rate of 17 ± 2 mm/y derived from 31 experiments observed with the newly installed MkIII system beween Sept. 1980 and Aug. 1984 was published by Herring et al. in 1986 (Fig. 5). This value agrees extremely well with today's best estimates for that same baseline.

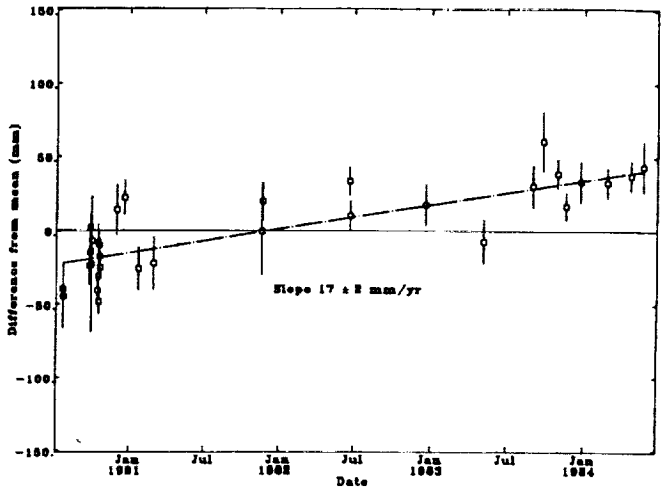

Figure 5. First estimate of intercontinental baseline rate Haystack - Onsala (Herring et al. 1986).

Cooperative arrangements had been made with several other countries extending the project to a truly international global research program. The VLBI part of the CDP comprised regular experiments (10–20 each year) of one to three days duration between all major geodetic VLBI facilities in the US, Europe, Asia, Australia, South Africa and South America. The annual reports of the CDP VLBI program constitute a detailed history of the successful application of the VLBI technique for the measurement of global tectonic motions (Ryan et al. 1993).

Project IRIS (International Radio Interferometric Surveying 1983-1990)

In contrast to the earlier VLBI programs which were based on the experiment-by-experiment philosophy (due to the limited correlator resources), the aim of the IRIS program was to increase the frequency of observing sessions to a level that permitted a quasi-continuous monitoring of the Earth rotation parameters. The monitoring concept was introduced at the IAG Symposium

No. 82 "Time and the Earth's Rotation" at San Fernando, Spain in 1978 under the acronym of POLARIS by the National Geodetic Survey, Rockville, MD (Carter et al. 1979). Observations began during the MERIT (Monitor Earth Rotation and Intercompare the Techniques) preliminary campaign (Wilkins and Mueller 1986) in the fall of 1980 with only one baseline (Westford-Ft.Davis) observing on a weekly basis. Later, the Swedish station of Onsala joined once per month to extend the POLARIS interferometer across the Atlantic. It soon became obvious that the long baselines across the Atlantic were essential to exploit the full accuracy of VLBI for Earth rotation monitoring, and at the end of 1983 the newly built geodetic radiotelescope at Wettzell in the southeast of Germany (Fig. 6) became an essential part of the IRIS network. Since 1984 this network has been routinely observing at a 5-day interval until 1990, when organisational and financial restructuring caused the Project to be taken over by the US Naval Observatory under the acronym of NEOS (National Earth Orientation Service). The IRIS Intensive campaigns, which were additional short daily measurements on the baseline Westford-Wettzell, were used to monitor the rapid UT1 variations between the 5-day epochs (Robertson et al. 1985).

Figure 6. Wettzell Geodetic Fundamental Station (1983, after completion of 20 m radio telescope).

In Wettzell, the construction of a dedicated geodetic radio telescope was part of the broader concept of a geodynamic "Fundamental Station" that would assemble the different space techniques such as Satellite Laser Ranging (SLR), Lunar Laser Ranging (LLR), Optical, Doppler and GPS systems, as well as supplementary geophysical monitoring intrumentation at one site to be able to compare and combine the data gathered as well as the results obtained from the different networks (Schneider et al. 1982). In recent years, the idea has been extended to build a transportable duplicate of the Fundamental Station, the TIGO (Transportable Integrated Geodetic Observatory) and operate the system at a site in the southern hemisphere, in order to improve the global coverage (Hase, Petrov 1999). Unfortunately, there are even today only very few stations in the world that have reached the status of a true Fundamental Station.

In the past decades, Wettzell has become a pivotal point for several global and regional networks and has provided some of the longest and most densely spaced time series of interstation distances and Earth orientation parameters. It is interesting to compare the Wettzell-Westford baseline length evolution from one of the most recent global solutions (L. Petrov, personal communication) (Fig. 7) with the earliest determinations of the transatlantic baseline rates (Fig. 5). The extraordinary smoothness and linearity of the length evolution postulates an absolutely uniform crustal motion, and by the same token a perfectly uniform spreading process at the oceanic ridges. In their extensive analysis of the global baseline changes and site motions observed by VLBI, Argus and Gordon (1996) find no really significant departures from **continuous** motion, except of course the coseismic displacements in very locally defined areas (Clark et al. 1990).

Another example of the potential of VLBI on longer time scales is the observed time series of the nutation angles appearing as corrections to the IAU 1980 reference model (Herring, this

volume). After some twenty years of intensive theoretical work by many groups in different parts of the world, the resulting new and thoroughly improved model will soon be published. It is quite certain that the continued time series of VLBI observations at well defined stations will contribute by their integrity to the solution of many more of the very intriguing and challenging questions in geodynamic research.

At the other extreme, VLBI observations have also lent themselves to investigate very short period, even down to sub-diurnal phenomena, such as the ocean tide induced variations in Earth rotation (Brosche et al. 1992, Clark et al. 1998). In this respect, the ultimate goal is of course a truly continuous observation program which will optimise the resolution power at the short periods down to a few hours. To achieve this goal, the CORE project has been devised at NASA/GSFC to combine the strengths of different station configurations on the globe and cover the seven days of a week without placing too much observational burden on any single one of the VLBI stations (Clark et al. 1998). This project has begun in an initial phase with on the average only two days per week and will be stepped up with the full deployment of the capabilities of the new MkIV VLBI system.

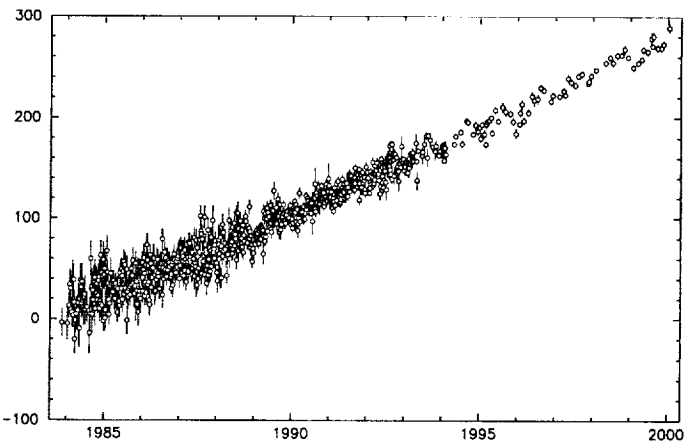

Figure 7. Wettzell-Westford baseline length evolution from recent solution (scale in mm)(Petrov, pers. comm.). The slope is 18.3 ± 0.1 mm/y with a WRMS of 8.5 mm.

There is just not enough space in this publication to present the many other projects in different parts of the world, such as China with two shared VLBI facilities for astronomy and geodesy (Tongshan et al. 1987); Japan with the Key Stone Project (Koyama et al. 1998) and several other domestic and international VLBI activities; Canada continuing its long tradition of VLBI both for astronomy and geodesy (Cannon et al. 1979, Klatt et al., this issue); Australia with an early involvement in geodetic VLBI (Harvey et al. 1983) and the long performance record of the stations of Tidbinbilla and Hobart; South Africa with the uniquely important station of Hartebeesthoek (Carter et al. 1980), and many more. Most of the presently active observing stations, analysis groups and technical development centers are listed and described in the first Annual Report (Vandenberg 1999) of the newly created:

IVS (International VLBI Service for Geodesy and Astrometry)

A strong incentive to introduce a more formal organisation that would provide the means for a better coordination of the activities in the global geodetic VLBI community towards a common goal and a more production-oriented approach, was given by the example of the GPS community in their International GPS Service for Geodynamics (IGS). The IVS was set up during 1998 and began its operations on the 1st of March 1999 (Campbell and Vandenberg 1999). The present first General Meeting at Kötzting gives proof of the successful start of a new, more internationally oriented phase of VLBI with even closer cooperation between its members (Schlüter, this volume).

5. From Bits to Gigabits/s: Progress in the Technical Realization of VLBI

The technical realization of VLBI is a perfect example of the concurrence of ingenious inventions and developments from many widely different sectors of electrical engineering, radar technology and communications technology, to name only a few. As mentioned earlier, the requirement for wide bandwidth and high sensitivity meant that there would be no way around the need to transfer extremely high data rates between the telescopes and the correlator center. Technically this is perhaps the most challenging part in the story of VLBI, i.e. to find cost-effective ways to perform this transfer. In consequence, the early phase of the technical development of VLBI is characterized by intensive experimentation with different ways to record the data on tapes.

The MkI system used standard computer tapes of 360 kHz bandwidth. The paper about the first VLBI experiment to prove general relativity (Sept–Oct. 1972 on the baseline Haystack-Green Bank) gives a vivid impression about the giant effort involved: for about 120 hours of observation ~5000 tapes had to be correlated (Counselman et al. 1974).

The MkII system was developed at the National Radio Astronomy Observatory (NRAO) on the basis of TV tape recorders with 2 MHz bandwidth (Clark 1973). The initial Ampex studio recorders were soon replaced by commercial cassette recorders opening the way for relatively cheap recordings. The wide spanned bandwidth was implemented in MkII just as in MkI by sequential switching of the IF to the different frequency channels in the band (Thomas 1972).

A turning point for geodetic VLBI was reached by the decision of NASA to support the development at Haystack of the multi-channel MkIII system that was designed to record 28 parallel tracks of 2 MHz bandwidth each, i.e. a maximum bit rate of 112 Mb/s. The geodetic setup included the dual S/X-band receiving with 14 channels recorded in one direction (forward pass), 6 channels for the S-band and 8 for the X-band. In this mode, a 1-inch wide instrumentation tape could carry about one to two hours of data in forward and reverse. If we add the successful upgrade of the hydrogen maser frequency standards to a level of 1 part in 10^{14} over many hours of operation, the preconditions for a quantum leap in geodetic accuracy were fulfilled (Clark et al. 1986). The first years of MkIII observations have given ample proof of the great success of the MkIII concept in geodetic VLBI.

However, also outside the US the momentum for technical developments in the field of VLBI was taken up, in particular of course in Canada, where the initial work (Broten et al. 1967) was pursued to debouch into the cassette-based S2 system (Cannon et al. 1997, Cannon, Petrachenko, this volume) and in Japan, where in the early 80s the MkIII-compatible K3 system was developed at the Radio Research Laboratories (Kunimori et al. 1993). As a follow-up system, a totally new concept based on cassettes was implemented with the K4 system which is being used now in the Key Stone project (Koyama et al. 1998). The 4-station network in the Tokyo area has been designed to run in a fully automated fashion, including a quasi-real-time transfer of the wide-band RF-signals. This development clearly paves the way for future e-VLBI systems that would make tape recordings obsolete.

Already in the early days of VLBI, hopes were high to be able to replace the cumbersome tape based systems by satellite-linked systems. A test experiment by Canadian and US groups on the communications satellite ANIK-B (Yen et al. 1977) proved the concept, while at the European Space Agency a project study on satellite linked VLBI went into great detail (ESA 1979), but was finally abandoned after being faced with the fact that the running costs at the required wide bandwidths would be prohibitive. At a recent meeting on the possibilities of e-VLBI (real time

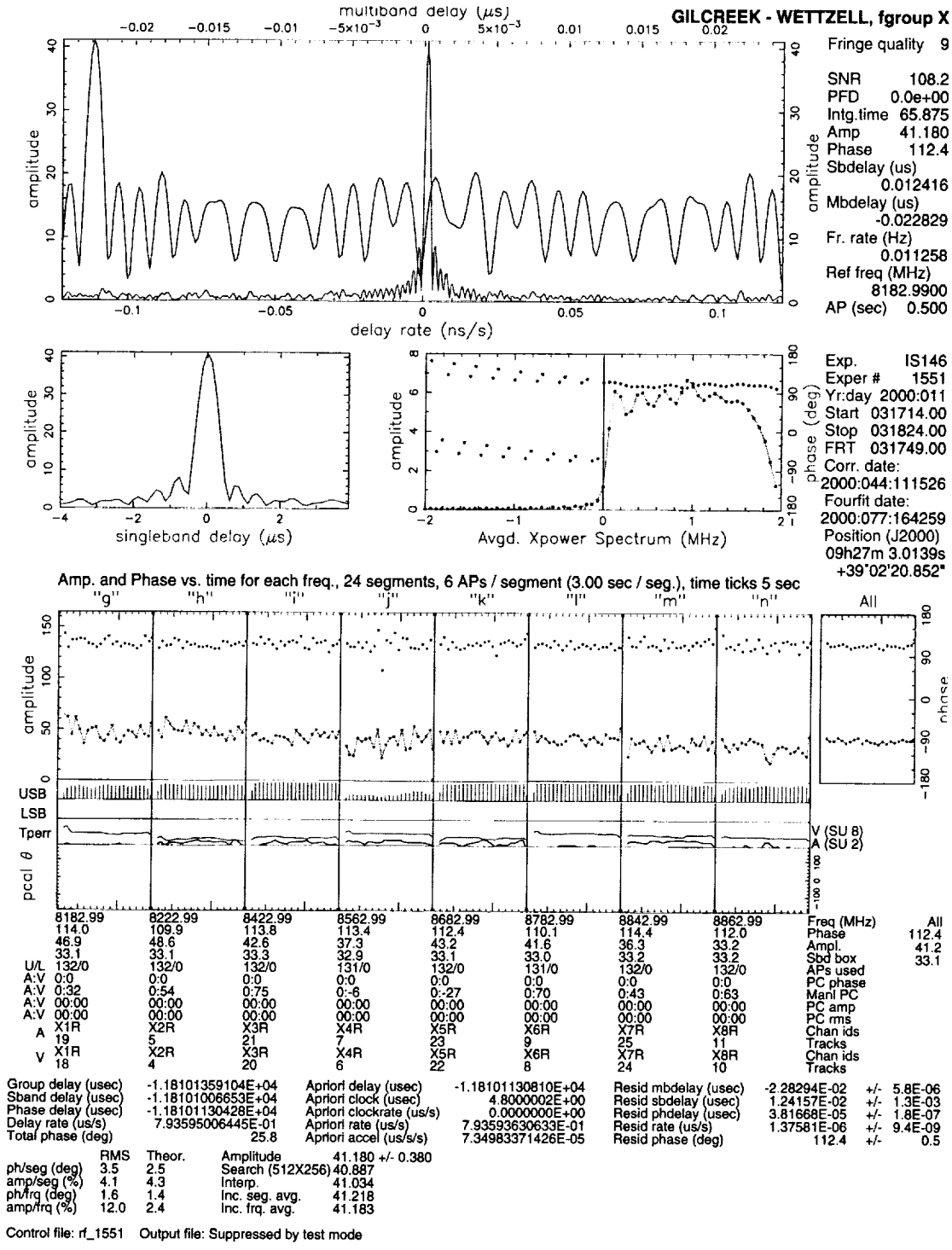

Figure 8. Mark IV fringe plot

VLBI forum at Haystack, Ray 1999) the feeling was that although it would be important to prepare the new systems for the day when e-VLBI would become feasible, the tape based systems would have to stay in place for a number of years to come.

In this situation, the development of the MkIV system as a natural follow-up of the MkIII and MkIIIA systems is a consistent and consequent step to maintain as well as improve the operational capabilities of VLBI (Whitney, this volume). It seems appropriate to conclude this overview with a closer look at one of the most recent fringe plots obtained at the new Bonn version of the MkIV correlator (Alef, this volume) to illustrate the state of development (Fig. 8). A beautiful coloured version now replaces the ~25-year old alphanumeric fringe plot (Whitney 1976), that has served generations to find fringes and sort out problems. The 8-channel 700 MHz multiband delay function shown in blue in the upper plot has a main peak halfwidth of 1.4 ns, which at an SNR of 108.2 (4C39.25 is a strong source) leads to a group delay resolution of 5.8 ps (first of the bottom lines) or 1.5 millimeter.

6. References

Argus, D.F., R.D. Gordon: Tests of the rigid-plate hypothesis and bounds on intraplate deformation using geodetic data from very long baseline interferometry, J. Geophys. Res. 101, 13,555-13,572, 1996

Bare, C.C., B.G. Clark, K.I. Kellerman, M.H. Cohen, D.L. Jauncey: Interferometry experiment with independent local oscillators, Science, 157, p. 189, 1967

Brosche, P., J. Wünsch, J. Campbell, H. Schuh: Ocean Tide Effects in Universal Time detected by VLBI. Astronomy & Astrophysics, Vol. 245, p. 676- 682, 1991

Broten, N.W., T.H. Legg, J.L. Locke, C.W. McLeish, R.S. Richards, R.M. Chisholm, R.M. Gush, J.L. Yen, J.A. Galt: Long Baseline Interferometry: A new technique, Science, 156, p. 1592, 1967

Campbell, J., N. Vandenberg: Very Long Baseline Interferometry (VLBI) - Subcommission Report - , IAG, CSTG-Bulletin No. 15, Progress Report 1998, Eds. G. Beutler, H. Drewes, H. Hornik, DGFI, p. 16-27, Munich 1999

Cannon, W.H., R.B. Langley, W.T. Petrachenko, J. Kouba: Geodesy and Astrometry by Transatlantic Long Base Line Interferometry, J. Geophys. Res., Vol. 84, p. 229-236, 1979

Cannon, W.H., Baer, D., Feil, G., Feir, B., Newby, P., Novikov, A., Dewdney, P., Carlson, B., Petrachenko, W.T., Popelar, J., Mathieu, P., Wietfeldt, R.D.: The S2 VLBI System, Vistas in Astronomy, Vol 41, No 2, p. 297-302, 1997.

Carter, W.E., D.S. Robertson, M.D. Abell: An Improved Polar Motion and Earth Rotation Monitoring Service Using Radio Interferometry, AGU-Symposium No. 82, Time and the Earth's Rotation, San Fernando, Spain, 8-12 May 1978, p. 191- 198, Reidel Publ. Co., Dordrecht 1979

Carter, W.E., Robertson, D.S., MacKay, J.R.: Geodetic Radiointerferometric Surveying: Applications and Results. J. Geophys. Res., Vol. 90, p. 4577-4587, 1985

Carter, W.E., D.S. Robertson, A. Nothnagel, G.D. Nicolson, H. Schuh, J. Campbell: IRIS-S: Extending Geodetic Very Long Baseline Interferometry Observations to the Southern Hemisphere. J. Geophys. Res., Vol. 93, p. 14947-14953, 1988.

Clark, B.G.: The NRAO Tape Recorder Interferometer System. Proc. IEEE, Vol. 61, p. 1242-1248, 1973

Clark, T.A., B.E. Corey, J.L. Davis, G. Elgered, T.A. Herring, H.F. Hinteregger, C.A. Knight, J.L. Levine, G. Lundqvist, C. Ma, E.F. Nesman, R.B. Phillips, A.E.E. Rogers, B.O. Rönnäng, J.W. Ryan, B.R. Schupler, D.B. Shaffer, I.I. Shapiro, N.R. Vandenberg, J.C. Webber, A.R. Whitney: Precision Geodesy using the Mk-III Very-Long-Baseline Interferometer System. IEEE Transactions on Geoscience and Remote Sensing, Vol. GE-23, No.4, p. 438-449, 1985

Clark, T.A., C. Ma, J.M. Sauber, J.W. Ryan, D. Gordon, D.B. Shaffer, D.S. Caprette, N.R. Vandenberg: Geodetic measurement of deformation in the Loma Prieta, California, Earthquake with Very Long Baseline Interferometry. Geophys. Res. Letters, Vol. 18, p. 1215-1218, 1990

Clark, T.A., C. Ma, J.W. Ryan, B.F. Chao, J.M. Gipson, D.S. MacMillan, N.R. Vandenberg, T.M. Eubanks, A.E.Niell: Earth Rotation Measurement Yields Valuable Information About the Dynamics of the Earth System. EOS, Vol. 79, No. 17, p. 205, 1998

Cohen, M.H., D.L. Jauncey, K.I. Kellerman, B.G. Clark: Radio Interferometry at One-Thousandth Second of Arc,

Science, Vol. 162, p. 88-94, 1968
Cohen, M.H., D.B. Shaffer: Positions of Radio Sources from Long Baseline Interferometry. Astronomical Journal, Vol. 76, p. 91-101, 1971
Coates, R.J., H. Frey, G.D. Mead, J. Bosworth: Space-Age Geodesy: The NASA Crustal Dynamics Project. IEEE Transactions on Geoscience and Remote Sensing, Vol. GE-23, No.4, p. 360-368, 1985
Counselman III, C.C., S.M. Kent, C.A. Knight, I.I. Shapiro, T.A. Clark, H.F. Hinteregger, A.E.E. Rogers, A.R. Whitney: Solar Gravitational Deflection of Radio Waves Measured by Very-Long-Baseline Interferometry. Physical Review Letters, Vol. 33, No. 27, p. 1621-1623, 1974
Davis, J.L. et al.: Geodesy by Radio Interferometry: Effects of Atmospheric Modeling Errors on Estimates of Baseline Length. Radio Science, Vol. 20, p. 1593-1607, 1985.
Elgered, G., Rönnäng, B., Askne, J.: Measurements of Atmospheric Water Vapour with Microwave Radiometry. Radio Science, Vol. 17, p. 1258-1264, 1982.
ESA: Satellite Linked VLBI, Phase-A Study. European Space Agency, Document SD/20545/AFB/MZ, Paris, December 1979
Harvey, B.R., A. Stolz, D.L. Jauncey, A. Niell, D. Morabito, R. Preston: Results of the Australian Geodetic VLBI Experiment. JPL, TDA Progress Report No. 42-75, p. 140-146, 1983
Hase, H., L. Petrov: The first Campaign of Observations with the VLBI-Module of TIGO. Proceedings of the 13th Working Meeting on European VLBI for Geodesy and Astrometry, Viechtach/Wettzell Feb. 12-13, 1999, Eds. W. Schlüter and H. Hase, p. 19-24, 1999
Heitz, S.: Mathematische Modelle der geodätischen Astronomie. Deutsche Geodätische Kommission, Reihe A, Nr. 85, Frankfurt am Main 1976
Herring, T.A., B.E. Corey, C.C. Counselman III, I.I. Shapiro, A.E.E. Rogers, A.R. Whitney, T.A. Clark, C.A. Knight, C. Ma, J.W. Ryan, B.R. Schupler, N.R. Vandenberg, G. Elgered, G. Lundquist, B.O. Rönnäng, J. Campbell, P. Richards: Determination of Tidal Parameters from VLBI Observations. Proc. Ninth Int. Sympos. on Earth Tides, New York, Aug. 17-22, 1981, ed. J. Kuo, p. 205-214, E. Schweizerbart'sche Verlagsbuchhandlung, Stuttgart 1983.
Herring, T.A., I.I. Shapiro, T.A. Clark, C. Ma, J.W. Ryan, B.R. Schupler, C.A. Knight, G. Lundquist, D.B. Shaffer, N.R. Vandenberg, B.E. Corey, H.F. Hinteregger, A.E.E. Rogers, J.C. Webber, A.R. Whitney, G. Elgered, B.O. Rönnäng, J.L. Davis: Geodesy by Radio Interferometry: Evidence for Contemporary Plate Motion. J. Geophys. Res. 91, 8341-8347, 1986
Herring, T.A., Gwinn, C.R., Shapiro, I.I.: Geodesy by Radio Interferometry: Studies of the Forced Nutations of the Earth, I. Data Analysis, J. Geophys. Res., Vol. 91, 4745-4754, 1986.
Herring, T.A.: Submillimeter Horizontal Position Determination Using Very Long Baseline Interferometry. J. Geophys. Res., Vol. 97, p. 1981-1990, 1992
Hinteregger, H.F., I.I. Shapiro, D.S. Robertson, C.A. Knight, R.A. Ergas, A.R. Whitney, A.E.E. Rogers, J.M. Moran, T.A. Clark, B.F. Burke: Precision Geodesy via Radio Interferometry. Science, 178, 396-398, 1972
Koyama, Y., N. Kurihara, T. Kondo, M. Sekido, Y. Takahashi, H. Kiuchi, K. Heki: Automated geodetic Very long Baseline Interferometry observation and data analysis system, Earth Planets and Space, 50, 709-722, 1998
Kunimori, H., F. Takahashi, M. Imae, Y. Sugimoto, T. Yoshino, T. Kondo, K. Heki, S. Hama, Y. Takahashi, H. Takaba, H. Kiuchi, J. Amagai, N. Kurihara, H. Kuroiwa, A. Kaneko, Y. Koyama, K. Yoshimura: Contributions and Activities of Communications Research Laboratory under the Cooperation with Crustal Dynamics Project. Contributions of Space Geodesy to Geodynamics: Technology, AGU Geodynamics Series, Vol. 25, p. 65-80, 1993
Ma, C., Ryan, J.W., Caprette, D.: Crustal Dynamics Project Data Analysis - 1988, VLBI Geodetic Results 1979-87. NASA Technical Memorandum 100723, Greenbelt, Md., February 1989.
Ma, C., J.W. Ryan, D. Gordon, D.S. Caprette, W.E. Himwich: Reference Frames from CDP VLBI Data. Contributions of Space Geodesy to Geodynamics: Earth Dynamics, AGU Geodynamics Series, Vol. 24, p. 121-145, 1993
MacDoran, P.F., D.J. Spitzmesser, L.A. Buennagel: SERIES: Satellite Emission Range Inferred Earth Surveying. Proc. 3rd Int. Sympos. on Satellite Doppler Positioning, Defense Mapping Agency and National Ocean Survey, Vol. 2, 1143- 1164, 1982
MacMillan, D.S., W.E. Himwich, N.R. Vandenberg, C.C. Thomas, J.M. Bosworth, B. Chao, T.A. Clark, C. Ma: CORE: Continuous, High-Accuracy Earth Orientation Measurements. Proc. 13th Working Meeting on European VLBI for Geodesy and Astrometry, Viechtach/Wettzell Feb. 12-13, 1999, Eds. W. Schlüter and H. Hase, p. 166-171, 1999
Mathur, N.C., M.D. Grossi, M.R. Pearlman: Atmospheric Effects in Very Long Baseline Interferometry. Radio Science, Vol. 5, No. 10, p. 1253-1261, 1970

Minster, J.B., Jordan, T.H.: Present-Day Plate Motions. J. Geophys. Res., Vol. 83, p. 5331-5354, 1978.

Nothnagel, A.: Local Survey at the Effelsberg Radio Telescope 1997 - Preliminary Results. Proc. 13th Working Meeting on European VLBI for Geodesy and Astrometry, Viechtach/Wettzell Feb. 12-13, 1999, Eds. W. Schlüter and H. Hase, p. 25-31, 1999

Ray, J., A. Whitney: Real-Time VLBI Forum, IAG, CSTG-Bulletin No. 15, Progress Report 1998, Eds. G. Beutler, H. Drewes, H. Hornik, DGFI, p. 28-31, Munich 1999

Robertson, D.S.: Geodetic and astrometric measurements with very long baseline interferometry. PhD Thesis, MIT, Cambridge, Mass., 1975

Robertson, D.S., Carter, W.E., Campbell, J., Schuh, H.: Daily Earth Rotation Determinations from IRIS Very Long Baseline Interferometry. Nature, Vol. 316, p. 424-427, 1985.

Robertson, D.S., W.E. Carter: Relativistic Deflection of radio signals in the solar gravitational field measured with very-long-baseline interferometry, Nature, 310, 572-574, 1984

Rogers, A.E.E.: Very Long Baseline Interferometry with Large Effective Bandwidth for Phase Delay Measurements. Radio Science, Vol. 5, p. 1239-1247, 1970.

Ryan, J.W., C. Ma, D. Caprette: NASA Space Geodesy Program - GSFC Data Analysis - 1992, Final Report of the Crustal Dynamics Project, VLBI Geodetic Results 1979-91. NASA Technical Memorandum 104572, Greenbelt, Md. 1993.

Petrov, L.: Steps towards phase delay VLBI. Proc. 13th Working Meeting on European VLBI for Geodesy and Astrometry, Viechtach/Wettzell Feb. 12-13, 1999, Eds. W. Schlüter and H. Hase, p. 144-151, 1999

Scherneck, H.-G.: A parameterized Solid Earth Tide Model and Ocean Tide Loading Effects for Global Geodetic Baseline Measurements, Geophys. J. Int., 106, 677-694, 1991

Schneider, M., R. Kilger, K. Nottarp, E. Reinhart, J. Campbell, H. Seeger: Concept and Realization of a 20m Radiotelescope for the Satellite Observation Station Wettzell. Proceedings of the IAG Symposium No. 5: Geodetic Applications of Radio Interferometry, Tokyo, Japan, May 7-8, 1982, NOAA Techn. Rep. NOS 95 NGS 24, p. 266-284, 1982

Shapiro, I.I., C.A. Knight: Geophysical applications of long baseline radio interferometry. In: Earthquake Displacement Fields and the Rotation of the Earth, ed. L. Mansinha, D.E. Smylie and A.E. Beck, pp. 284, Springer, New York 1970.

Sovers, O.J., J.L. Fanselow, C.S. Jacobs: Astrometry and geodesy with radio interferometry: experiments, models, results. Reviews of Modern Physics, Vol. 70, No. 4, p. 1393-1454, Oct. 1998

Tongshan, W., W. Huaiwei, W., Q. Zhihan, Z. Yunfei, F. Takahashi, N. Kawaguchi, H. Kuroiwa, J. Amagai: The first Sino-Japanese Experiment of Very- Long-Baseline Interferometry (VLBI). Scientia Sinica (Series A), Vol. 30, No. 3, p. 307-316, 1987

Thomas, J.B.: An Analysis of Long Baseline Radio Interferometry. Deep Space Network Progress Report, Technical Report 32-1526, Vols. VII, VIII, XVI, Jet Propulsion Laboratory, Pasadena 1972.

Vandenberg, N. (Ed.): IVS 1999 Annual Report, NASA Publication TP-1999- 209243, 1999

Whitney, A.R., A.E.E. Rogers, H.F. Hinteregger, C.A. Knight, J.I. Levine, S. Lippincott, T.A. Clark, I.I. Shapiro, D.S. Robertson: A Very-Long-Baseline Interferometer for Geodetic Applications. Radio Science, Vol. 11, p. 421-432, 1976.

Wilkins G.A., I.I. Mueller: On the Rotation of the Earth and the Terrestrial Reference System: Joint Summary Report of the IAU/IUGG Working Groups MERIT and COTES; Bull. Geod., Vol 60, p. 85-100, 1986

Yen, J.L., K.I. Kellerman, B. Rayhrer, N.W. Broten, D.N. Fort, S.H. Knowles, W.B. Waltman, G.W. Swenson: Real-Time, Very-Long-Baseline Interferometry Based on the Use of a Communications Satellite. Science, 198, p. 289-291, Oct. 1977

Hermann Drewes: The Role of VLBI Among the Geodetic Space Techniques Within CSTG, IVS 2000 General Meeting Proceedings, p.35–41
http://ivscc.gsfc.nasa.gov/publications/gm2000/drewes

The Role of VLBI Among the Geodetic Space Techniques Within CSTG

Hermann Drewes

Deutsches Geodätisches Forschungsinstitut (DGFI)
e-mail: drewes@dgfi.badw-muenchen.de

Abstract

The main objectives of the Commission on International Coordination of Space Techniques for Geodesy and Geodynamics (CSTG) for the near future are the optimum integration of all geodetic observation techniques in a unique global network, the International Space Geodetic Network (ISGN), and the combined processing of all heterogeneous space geodetic measurements in a common data analysis procedure. The combination of different techniques will provide more reliability and a higher accuracy of the results. Each of the techniques plays an important role in this procedure and provides some unique tools for the geodetic parameter estimation. VLBI is not only unique in connecting the celestial and the terrestrial reference frames, but it gives also other indispensable information about geodetic parameters, which the satellite techniques cannot solve for independently. Only the inclusion of VLBI observations will guarantee the continuity and stability of geodetic reference systems.

1. Introduction

The Commission on International Coordination of Space Techniques for Geodesy and Geodynamics (CSTG) is Commission VIII of the International Association of Geodesy (IAG) and Subcommission B2 of the Scientific Commission on Space Studies of the Earth-Moon System, Planets and Small Bodies of the Solar System of the ICSU Committee on Space Research (COSPAR). The general objectives of CSTG were defined during its establishment at the 17th IUGG General Assembly in Canberra, Australia, in 1979 with impetus from the 22nd Plenary Meeting of COSPAR in India. They may be summarized as follows:

- develop links between various groups engaged in the field of space geodesy and geodynamics by various techniques,
- coordinate the work of these groups,
- elaborate and propose projects implying international cooperation, follow their progress, and report on their advancement and results.

CSTG accomplished these tasks in the past by initiating several projects and installing subcommissions, which led to well-known international services. We may mention in particular:

- The MERIT (Monitoring Earth Rotation and Inter-comparison of Techniques) and the MEDOC (Motion of the Earth by Doppler Observing Campaign) projects in 1979, which led to the International Earth Rotation Service (IERS);
- The COTES (Conventional Terrestrial Reference System) in 1982, which led to the International Terrestrial Reference System (ITRS);

- The IRIS (International Radio Interferometric Surveying) Sub-commission, which was installed in 1983 and led to the International VLBI Service for Geodesy and Astrometry (IVS);
- The GPS and SLR Sub-commissions, which were established in 1987 and led to the International GPS Service (IGS) and the International Laser Ranging Service (ILRS), respectively.

Actually, there are two other sub-commissions in CSTG which are to prepare the fields for new international services, namely:

- The Space Geodetic Measurements Sites (SGMS) Sub-commission, established in 1991 and on the way to form the International Space Geodetic Network (ISGN);
- The Project on Doris, which was installed in 1999 in order to prepare an International Doris Service (IDS).

2. Main Objectives and Structure of CSTG in the Period 1999–2003

During the General Assembly of the International Union for Geodesy and Geophysics in Birmingham (UK) 1999, a new structure was given to CSTG identifying some major challenges for the next four years. Among those we shall mention in particular the following:

2.1. Coordination of Space Techniques

We have to make optimum use of the existing space geodetic networks by coordinating their work not only with respect to the individual observation activities, which are coordinated by the techniques' services, but also with respect to the relations between the techniques. This means in particular to solve the permanently existing problem of the eccentricity measures between the different techniques' observation instruments in order to get a direct link between the networks. As a result we should officially install an International Space Geodetic Network (ISGN) composed of the permanently operating stations of the different techniques, which shall routinely take care of these tasks. The ISGN should play a superior role in the International Terrestrial Reference Frame (ITRF). Therefore, a close cooperation with the IERS is necessary.

2.2. Combination of Data Analysis

Presently, the individual techniques' observation data are processed independently by the techniques' analysis centers. In these processings they estimate also some parameters which are common to all techniques and should get identical numbers from the individual adjustment procedures (e.g., atmospheric travel time delay). The results, however, are normally quite different for all techniques. When combining these results, the effect of an incorrect modeling cannot be reduced but enters into the final parameter estimation. We have therefore to strive for a rigorous combined adjustment, where all the phenomena affecting the different techniques' observations are parameterized and adjusted simultaneously.

2.3. Integrating New Techniques and Methods

The objective of CSTG has always been the coordination of geodetic research on modern technologies and evaluation methods. In the recent past, this task was focussed on techniques for precise point positioning. The upcoming decade will be dominated by the determination of

the Earth's gravity field. New satellite missions are in preparation (CHAMP, GRACE, GOCE). Another topic is the sounding of the atmosphere by satellite-to-satellite observations. A major requirement for both of these observations is the precise orbit determination of low Earth orbiters. CSTG will be active in this field. Furthermore, there was seen a need to better coordinate the dissemination and the use of satellite altimetry data. This will also be taken care of by CSTG.

As a consequence of the described main objectives, the structure of CSTG was designed by new sub-commissions and a project, the difference between both being given by their permanency: while a sub-commission is planned for a longer time period, a project is initiated to fulfill a more temporary task and may be abandoned after a short time interval when the objectives are satisfied. The structure for the period 1999–2003 is as follows:

- Sub-commission on the International Space Geodetic Network (ISGN),
- Sub-commission on the Coordination and Combination of the Analysis in Space Geodesy,
- Sub-commission on Precise Satellite Microwave Systems,
- Sub-commission on Multi-Mission Satellite Altimetry,
- Sub-commission on Precise Orbit Determination for Low Earth Orbiting Satellites,
- Project on DORIS.

The CSTG Executive Committee includes besides the president, past president and the chairmen of the sub-commissions and the project also one representative of each of the related IAG services, namely IERS, IGS, ILRS, and IVS as well as a representative of COSPAR.

3. The Role of VLBI Within the CSTG Objectives

VLBI plays an important role in the above mentioned objectives of CSTG, in particular in the coordination of space techniques and in the combination of the data analysis.

In the coordination of space techniques, especially in the establishment of the International Space Geodetic Network (ISGN), the VLBI observatories are most important stations, because they provide an extensive infrastructure and they guarantee the continuity of an observation site. The ISGN sites criteria, set up by a CSTG/IERS Working Group (ref. [2]) for the rating of candidate space geodetic stations, include seven main aspects:

- Geographical criteria ("optimum" location on the Earth's sphere),
- Geological criteria (location on a "stable crust"),
- Environmental criteria (no local disturbances),
- Site monumentation criteria (fixed monuments),
- Site surveying criteria (precise footprint survey),
- Operational criteria (good infrastructure and personnel),
- Instrumentation criteria (required instruments).

The last mentioned instrumentation criteria require, in order to qualify as an ISGN station, that there has to be at least one high-precision space geodetic system (SLR or VLBI) and a permanent,

high performance geodetic GPS receiver (accepted by IGS) or a Doris beacon. The criterion of a VLBI (or SLR) station has been included mainly because of the necessity to guarantee the continuity of the site. A GPS receiver may be removed easily; a fixed VLBI telescope, however, is rather immovable. In the compilation of candidate ISGN stations, we therefore find about 50 VLBI stations among a total number of some 80 sites.

In the combined data analysis of different techniques, VLBI provides unique capabilities for the parameter estimation in connecting the celestial (inertial) and the terrestrial reference frames (Earth orientation parameters). It is the only technique that can provide the nutation parameters and UT1 in a direct way. On the other hand, VLBI is independent of the stationary gravity field and its specific reference frames. This has sometimes been considered a loss of the VLBI technique, because it doesn't provide station coordinates with respect to the geo-center (center of mass) but primarily baselines or coordinates relative to an arbitrarily defined origin. One may, however, turn the apparent disadvantage around and argue that because of the missing gravity field dependency, VLBI is not affected by its specific errors:

- VLBI is not affected by satellite orbit errors caused by mismodeling of the gravity field;
- The fact that it is not related to the Earth's center of mass excludes influences of the variation of the geo-center on the estimated parameters, in particular on the heights;
- The independence of the gravity field includes that there is no dependency on GM, which causes scale problems in satellite methods because of its relatively great uncertainty.

4. Advantages and Disadvantages of VLBI in the Combination of Space Techniques

In addition to the above mentioned uniqueness of VLBI in connecting the celestial and the terrestrial reference frames and the independence of the gravity field, VLBI may contribute significantly to the estimation and reduction of common effects in all the space techniques when doing a combined data processing and analysis. Let us mention in particular:

- Ionospheric effects: VLBI uses a broad frequency spectrum (large difference of frequencies) which allows precise ionospheric parameter estimates and reductions;
- Tropospheric effects: VLBI is observing in one azimuth and one elevation angle only at one epoch. This facilitates a clear separation of tropospheric parameter estimation in space and time. In comparison, GPS is observing simultaneously all the horizon and elevations, but it is in general estimating an azimuth independent tropospheric travel time delay;
- Tidal and loading effects: VLBI is able to estimate pure geometric effects of the Earth's crust's deformation without indirect effects caused by gravity potential changes that affect the satellite methods in terms of orbit errors.

Besides these positive aspects of VLBI within the combination of space geodetic techniques, there are of course also some disadvantages in comparison with the satellite methods that shall not be suppressed. Special emphasis has to be given to these effects and problems:

- Telescope related effects: There are axis offset errors and telescope deformations that require a sophisticated treatment for reducing their effects from the parameter estimation;

- Instrumentation and operation: The VLBI instruments are expensive and not easily to be operated (e.g., in comparison with GPS). There are no continuous observations, the data handling is relatively complicated (transport of tapes) and not yet feasible in real time;
- Data processing and analysis: The data processing is relatively complicated (correlation and adjustment) and not yet possible in real time. The precision of the results depends strongly on the tropospheric path delay modeling (including a scale factor).

The principal geodetic parameters estimated in the VLBI data processing are the Earth orientation parameters (EOP) and the time dependent station coordinates (in general three- dimensional cartesian or ellipsoidal coordinates and the corresponding velocities). The original observables of VLBI are the baselines between two observatories (telescopes) and their time variations. By this means they are independent of the reference frame and its changes in time. This is a great advantage in comparison with satellite methods which provide coordinates with respect to a reference frame that may vary from one epoch to the other.

Table 1 presents the comparison of station velocities estimated from the different techniques VLBI (ref. [4]), SLR (ref. [3]), GPS (ref. [5]) and derived from an Actual Plate Kinematic and Deformation Model (ref. [1]). We see large differences between the solutions which often exceed the three times r.m.s. error of the estimates. Analyzing these differences, we find that a great part is due to a strong influence of the different datums of the individual solutions.

Table 1: Station Velocities from Different Space Geodetic Techniques and Combined Model

Station Country Plate	φ[°] λ[°] h[m]		APKIM9.0 (combined) [mm/a]	VLBI GLB1102 [mm/a]	SLR CSR96L01 [mm/a]	GPS CODE99 [mm/a]
Wettzell	49.1	$d\varphi/dt$	15.3 ± 0.1	13.6 ± 0.1	16.2 ± 2.9	14.1 ± 0.1
Germany	12.9	$d\lambda/dt$	19.5 ± 0.1	20.3 ± 0.1	25.9 ± 1.6	20.2 ± 0.1
EURA	670	dh/dt	–	-1.0 ± 0.1	4.4 ± 3.0	-2.2 ± 0.1
Haystack	42.6	$d\varphi/dt$	3.3 ± 0.1	5.9 ± 0.3	10.9 ± 2.8	3.9 ± 0.2
Mass., USA	-71.5	$d\lambda/dt$	-15.7 ± 0.1	-14.7 ± 0.1	-13.0 ± 1.9	-14.7 ± 0.1
NOAM	117	dh/dt	–	-0.2 ± 0.3	-27.7 ± 2.8	2.0 ± 0.2
Fort Davis	30.6	$d\varphi/dt$	-8.4 ± 0.1	-5.7 ± 0.2	-1.8 ± 0.9	-7.9 ± 0.1
Texas, USA	256.1	$d\lambda/dt$	-11.7 ± 0.1	-12.8 ± 0.1	-12.8 ± 0.8	-10.4 ± 0.1
NOAM	1607	dh/dt	–	-1.2 ± 0.2	-2.9 ± 0.9	1.2 ± 0.2
Hawaii	20	$d\varphi/dt$	31.2 ± 0.1	32.3 ± 0.4	35.2 ± 0.9	32.7 ± 0.6
USA	204	$d\lambda/dt$	-61.4 ± 0.1	-65.5 ± 0.4	-61.7 ± 0.8	-61.9 ± 0.7
PCFC	3400	dh/dt	–	5.3 ± 0.4	-5.2 ± 0.7	-2.6 ± 1.1

Table 2 shows the estimated kinematic datums of the different techniques with respect to the "no net rotation" (NNR) datum of APKIM9.0, which was determined there by constraining the integral of motions over the entire Earth's surface to become zero (ref. [1]). The units are arc seconds per million years; the corresponding maximum linear velocity due to the rotation around the three axis (i.e. in the equator or the meridian, respectively) is given in the lines below. It is obvious that the datum effect is in general much greater than the given r.m.s. errors of the estimated station velocities. We may therefore state that the kinematic datum of the individual space geodetic techniques, which is by definition fixed to the International Terrestrial Reference Frame (ITRF), is quite different for all the solutions. This is due to the different realization of the

datum by constraining individual station velocities which may not represent perfectly the whole frame. It seems that the realization is better in VLBI and GPS (the latter one because of the large number of constraint stations) than in SLR.

Table 2: Datum Parameters of Technique Dependent Kinematic Solutions w.r.t. NNR

Axis	GLB 1102	CSR96L01	CODE99
ω_X	-86.7 ± 6.9 "/Ma	-237.6 "/Ma	-13.7 "/Ma
	(< 2.7 mm/a)	(< 7.3 mm/a)	(< 0.4 mm/a)
ω_Y	45.8 ± 6.9 "/Ma	-25.9 "/Ma	39.6 "/Ma
	(< 1.4 mm/a)	(< 0.8 mm/a)	(< 1.2 mm/a)
ω_Z	45.1 ± 6.9 "/Ma	37.1 "/Ma	19.8 "/Ma
	(< 1.4 mm/a)	(< 1.1 mm/a)	(< 0.6 mm/a)
Total Datum Effect	107.9 "/Ma	241.9 "/Ma	46.3 "/Ma
	(< 3.3 mm/a)	(< 7.5 mm/a)	(< 1.4 mm/a)

As a conclusion from this example we see that the individual space geodetic techniques provide only relative results (in this case velocities) related to a specific realization of a datum or, in general, a given set of standards. The combination of all the techniques can improve significantly the parameter estimates and refer the results to a more objective system. VLBI plays an important role in this combination procedure because of its specific characteristics and realization of reference systems.

5. Conclusion

The cooperation between the new VLBI Service for Geodesy and Astrometry (IVS) and the Commission on International Coordination of Space Techniques for Geodesy and Geodynamics (CSTG) has started in a very harmonious and most promising way. For the future, CSTG would like to express some wishes and expectations from the VLBI community for the accomplishment of the common objectives. These are in particular:

- IVS should provide uniform (combined) VLBI solutions for Earth orientation, rotation parameters, station coordinates and velocities.
- IVS should cooperate with the other techniques' services and use identical models and standards (conventions).
- IVS should cooperate with CSTG and its sub-commissions in scientific research on new techniques and methodologies.

Last but not least, there is a need to express congratulations to the IVS team. They achieved an excellent start for the new service and they are on the best way to fulfill all the requirements of the international geodetic community on VLBI. There is no doubt that we need this service in geodesy and we can be sure that we'll have good and manifold results in the future.

References

[1] Drewes, H.: Realisierung des kinematischen terrestrischen Referenzsystems ohne globale Rotation (no net rotation). Deutsche Geodaetische Kommission, Reihe A, Nr. 116, 120-125, Muenchen 1999.

[2] Drewes, H., G. Beutler, J. Bosworth, C. Boucher, T. Herring, I.I. Mueller: The International Space Geodetic and Gravimetric Network (ISGN). IAG CSTG Bulletin, No. 15, 13-22, Muenchen 1999.

[3] Eanes, R.J., M.M. Watkins: Earth orientation and site coordinates from the Center of Space Research solution CST96L01. Internet ftp 128.183.10.141, 1996.

[4] NASA GSFC: GFSC VLBI solution GLB1102 August 1998. Internet ftp://gemini.gsfc.nasa.gov /pub/solutions/, 1998.

[5] Rothacher, M.: CODE station coordinates, velocities and Earth rotation parameters. Internet ftp://ubeclu.unibe.ch /code/iers/, 1999.

R. Craig Walker: Astronomical VLBI: Comparison and Contrast with Geodetic/Astrometric VLBI, IVS 2000 General Meeting Proceedings, p.42–51
http://ivscc.gsfc.nasa.gov/publications/gm2000/walker1

Astronomical VLBI: Comparison and Contrast with Geodetic/Astrometric VLBI

R. Craig Walker

National Radio Astronomy Observatory
e-mail: cwalker@nrao.edu

Abstract

The VLBI technique can be used for both high precision geometric measurements in geodetic and astrometric observations, and to study astronomical sources with high resolution. The equipment required for both types of observations is essentially the same and many telescopes and correlators are used for both. This synergy gives both the geodesy and astronomy communities access to more resources than either could support alone. The IVS membership is familiar with geodetic/astrometric VLBI, but perhaps less so with astronomical VLBI. Therefore this presentation will begin with an introduction to the existing astronomical VLBI instruments. That will be followed by a number of examples of astronomical VLBI results to give a flavor for the science. Then some direct comparisons between geodetic and astronomical VLBI will be made with emphasis on observing modes and on the importance of various aspects of the data. Finally, the interaction between the groups will be discussed, both in terms of how they are interdependent and how differences in style have created some complications.

1. Introduction

The output of a VLBI correlator consists of correlation coefficients as a function of time and frequency (or, equivalently through a Fourier transform, time and delay). These correlation coefficients are calculated for each baseline between pairs of antennas in an array. They can be determined for several baseband (video) channels at different frequencies. If both polarizations are detected at the antennas, they can be determined for both parallel and crossed hand polarizations (all stokes parameters). The magnitude of the correlation coefficients depends on the sensitivities of the antennas and on source strength and source structure. The phase of the correlations depends again on source structure but also on the separation of the antennas, the position of the source, and any propagation effects such as ionospheric and tropospheric delays.

In geodetic and astrometric VLBI (often lumped under the term geodetic VLBI in this text), the object is to use the measured data to determine the positions of the sources and antennas. Usually the measured phases, as a function of frequency across multiple basebands, are used to determine delays from which the geometry of the observation can be deduced. Astronomical VLBI is done with the data in a variety of forms, depending on the goals of the project. Astrometry is, of course, a form of astronomy and some astronomical observations are indistinguishable from astrometric observations. But usually the source structure, often as a function of frequency and/or polarization, is the information of interest and imaging techniques are used. In this case, the delays are simply a calibration offset to be removed.

2. Astronomical VLBI Instruments

Astronomical VLBI is dominated by the Very Long Baseline Array (VLBA), the European VLBI Network (EVN), and Global VLBI Network observations involving the VLBA, the EVN, and often other telescopes. In addition to these, there are the Asia Pacific Telescope (APT), involving antennas in the Eastern Hemisphere, the Coordinated MM VLBI Array (CMVA) for high frequency observations, and the Japanese VLBI spacecraft, *HALCA*. The Australia Telescope, besides being part of the APT, has an independent VLBI capability.

The VLBA is operated by the National Radio Astronomy Observatory[1] (NRAO) in the USA. It is a national facility open to all with time allocated on the basis of quality of scientific proposals. It has 10 antennas, each 25 meters in diameter, at locations in the United States chosen for optimum performance for imaging. Each antenna is equipped with nine receivers for frequencies between 0.33 and 43 GHz, with a tenth receiver at 86 GHz being added now. Each site has two tape recorders, which allows unattended operation for 21 hours at the nominal bit rate of 128 Mbps. There are two site technicians associated with each site. The array is operated from Socorro, New Mexico, with the sites unmanned much of the time. Also in Socorro are a 20 station correlator, central maintenance facilities, postprocessing facilities for staff and visitors, and a scientific staff. Operations are merged with an even larger NRAO instrument, the Very Large Array (VLA), that is located near Socorro.

The EVN is a network of independent radio astronomy observatories that have agreed to devote a fraction of their observing time to VLBI. The EVN allocates that observing time and helps coordinate technical issues across the Network. It is not a full time array and has much more diverse equipment than the VLBA. But it does have some larger antennas. The members of the EVN are Jodrell (2 antenans), Cambridge, Westerbork, Effelsberg, Medicina, Noto, Onsala (2 antennas), Sheshan, Nanshan, Torun, Simeiz, Metsaehovi, Yebes, Robledo, and Wettzell. A 16 station correlator is nearing completion at the Joint Institute for VLBI in Europe (JIVE) in The Netherlands.

For Global Network observations, usually the array includes the VLBA, six or more EVN antennas, Green Bank (currently in a gap between 140' and GBT availability), and the VLA (often as a phased array). Other common participants include various DSN antennas and Hartebeesthoek. Arecibo, with its huge collecting area (about 300 m diameter), will participate more often when its recorder system is available. For the last few years, most global observations have been correlated on the VLBA correlator in Socorro. It is expected that a major portion of such correlation will shift to the JIVE correlator when it becomes operational.

Observations at frequencies of 86 GHz and above are usually made using the CMVA, which includes various mm antennas around the world, along with those VLBA antennas that have been outfitted at 86 GHz. The CMVA is coordinated at Haystack and most observations are correlated there. MM VLBI is still at a level of technical and organizational difficulty somewhat like those experienced at cm wavelengths 20 years ago. The number of antennas available is small and lack of sensitivity and short coherence times make the observations difficult. Good work can be done, but it is still a struggle.

The development of VLBI was a natural result of the quest for resolution in radio interferometry and in astronomy in general. With normal VLBI, the resolution at a given frequency is limited

[1]The National Radio Astronomy Observatory is a facility of the National Science Foundation, operated under cooperative agreement by Associated Universities, Inc.

simply by the size of the Earth. For more resolution, it is necessary to have at least one antenna in space. The first space VLBI antenna is *HALCA*, launched by Japan in February 1997. It observes regularly with ground arrays consisting of many of the usual VLBI antennas around the world.

3. Some Astronomical Results

The sources used for geodetic VLBI are usually quasars, often at high redshifts. Such sources are sufficiently far away that any transverse motions of the underlying object, generally thought to be a massive black hole, must be extremely small in angular terms. Such sources can be very compact, but usually do show structure. That structure can change on time scales of months, with components often showing apparent motions of faster than the speed of light (superluminal motion) due to projection effects. The study of such sources, using single polarization, single frequency observations, occupied a significant fraction of the effort of astronomical VLBI for many years. An understanding of such data, besides providing information about relativistic jets, is important to understanding the effect of structure changes on geodetic results.

In recent years, as the capabilities available for astronomical VLBI have improved, the range of studies has increased significantly. The rest of this section will be devoted to a variety of examples of studies that utilize the new capabilities.

The study of astrophysical masers dates back to the earliest days of VLBI. But the capabilities provided by the VLBA have vastly increased the scale of possible observations. In one of the most ambitious projects yet attempted, Diamond and Kemball have imaged the SiO masers in the inner regions of the stellar wind from the Mira variable TXCAM every 2 weeks for well over a full 557 day period of the variability. The masers are at 43 GHz and are seen in roughly a ring around the star at a distance of a few stellar radii. The size of the maser shell is seen to grow during the cycle and to show various complex motions. Since spectral lines are being observed, the frequency information gives the radial velocity of the masing gas while the VLBI shows transverse motions. Also full polarization information is being obtained in order to study the magnetic fields in the wind. A movie based on the VLBI images can be found on the internet at www.aoc.nrao.edu/pr/txcam.a-ak.gif. An NRAO press release containing more information can be found at www.aoc.nrao.edu/pr/txcam99.html.

Another maser study has provided some of the best available evidence for the presence of a massive black hole in the center of a galaxy and has helped determine the extragalactic distance scale. Water masers in the center of the galaxy NGC 4258 are distributed in both position and velocity in such a way as to make it clear that they are in a gas disk at the galactic center [1]. The top portion of Figure 1 shows the positions of the masers superimposed on a model of the disk and on a VLBI continuum image of the core/jet structure at the galactic center. The bottom portion of the figure shows the spectrum of the water masers. The inset shows the distribution of radial velocities with position across the disk. The velocities follow a beautiful Keplerian rotation curve. The velocities and distances involved indicate that there are about 4×10^7 solar masses interior to the disk which is only about a light year in radius. The only reasonable way to have that much mass in such a small volume is for most of it to be in a black hole. Further studies of the transverse motions of the masers seen against the central source, and of the radial accelerations of those masers, have been used to determine a very accurate distance to the galaxy [1]. This distance determination is independent of the complicated chain of distance indicators usually needed to determine the distances to extragalactic objects. It is important in calibrating the indicators used

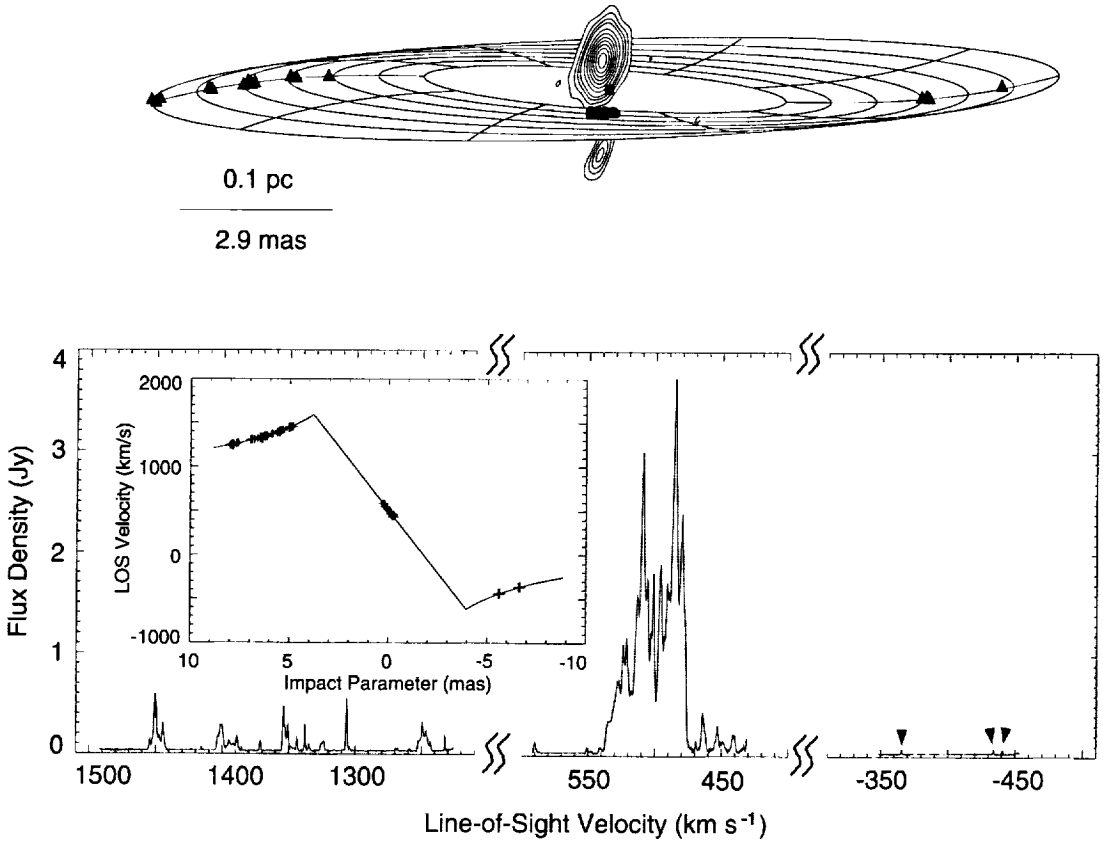

Figure 1. Water masers in NGC4258 from [1]. The top panel shows the distribution of the water masers, a continuum image of the central jet, and a warped disk model. The bottom panel shows the spectrum of the masers. The inset shows the maser velocities as a function of offset from the central source. The line indicates a Keplerian rotation curve model. Figure reproduced with permission from Nature.

to determine distances to more distant galaxies from which the scale and age of the universe are determined.

Another VLBI program that provides an extragalactic distance and provides information important in understanding an astrophysical phenomenon is the monitoring of supernova 1993J in the galaxy M81 [2]. Recently published images form a 13 frame movie that starts when the source was nearly unresolved at much smaller than a milliarcsecond in May 1993 and continues to Nov 1997 when it was a clear ring of about 5 mas in size. A distance measure can be determined by relating the expansion velocity seen in optical lines to the rate of increase of angular size. The observed angular expansion rate has slowed, which is important information in comparisons with models of the expansion of the blast wave into the surrounding medium. That medium is thought to be mainly from outflow from the precursor star. Asymmetries in the brightness of the ring and in its shape also provide information on the outflow.

One advantage that VLBI has over other forms of astronomical imaging is that the resolution is sufficiently high that even extragalactic sources can change structure on human timescales allowing

dynamical studies. The superluminal sources are a classic example. But there are surely longer time scale variations, perhaps related to variations in the amount of fuel being fed into the black hole accretion disks, that are still too long for human observation. There are much smaller black holes in our galaxy, remnants of stellar collapse, that have much shorter time scales. These holes and their associated accretion disks are essentially mini-quasars. A few such sources have been observed and indeed show a rich variety of behavior at all wavelenths. Included are episodes of superluminal expansion, much like those seen in quasars. But the scales are such that whole episodes are over in a few days. This can present challenging imaging problems because the structure changes by significant amounts during the course of an observation. A good example of such observations is the sequence of 7 VLBA images made over 1 month in 1994 of the source GRO J1655-40 [3].

While most VLBI studies concern the emission regions themselves, there are a variety of ways that the radiation can be used to study other material near galactic nuclei. This is possible if the radiation is absorbed by the other material, or if its polarization properties are affected. One example is the absorption by ionized gas of the radiation from the counterjet in 3C 84. The counterjet radiation has to pass through the accretion disk on the way to the Earth. There, ionized gas either in the disk or in a wind or corona above the disk absorbs the lower frequency radiation. The result, as seen in Figure 2, is that the counterjet is seen strongly at 22 GHz, but very weakly at 6 GHz, with intermediate amounts getting through at frequencies in between. The near side jet is not affected by any such absorption showing that that absorbing material is on the scale of the disk, not on a much larger scale. Multifrequency studies of the absorption have given measures of the amount of ionized material on parsec scales and have shown that it decreases rapidly with distance from the central parts of the source [4].

Another opportunity to study nuclear material arises when the neutral hydrogen in that material absorbs radiation from the jets. An example is 1946+708, a two sided jet source that shows variable hydrogen absorption along the jet. The widest lines are near the position of the "core" which spectral indices indicate is the origin of the jets and the likely location of the central mass. These wider lines indicate that there are rapid gas motions in this vicinity compared to other regions of the source [5].

When polarized radiation passes through a magnetized, ionized medium, its plane of polarization is rotated. The amount of rotation is frequency dependent in much the same way that the delay through the ionosphere is frequency dependent and can be determined using measurements at both S and X bands. The "rotation measure" can be determined using multifrequency, polarization sensitive observations. Many of the well known, complex core-jet sources have been the subject of studies of rotation measure as a function of position along the jet. The general result is that the rotation measure is much higher very near the compact core than further out. Since there are variations over the inner few parsecs of the jets, the ionized medium causing the rotation must be on that scale. The observations then provide information on the distribution of ionized gas near the central black holes of these systems (cf. [6]).

In almost all observations of jets, the jet is well formed and collimated by the time it is resolved transversely. Thus the jet must be formed on scales smaller than the resolution of the observations, which is typically a fraction of a light year. This is not too surprising considering that the massive black holes thought to be responsible for the jets are roughly the size of the solar sytem, some 5 orders of magnitude smaller than the typical resolution. One goal of high resolution observations is to see the collimation region. This may have been done recently using global VLBI observations

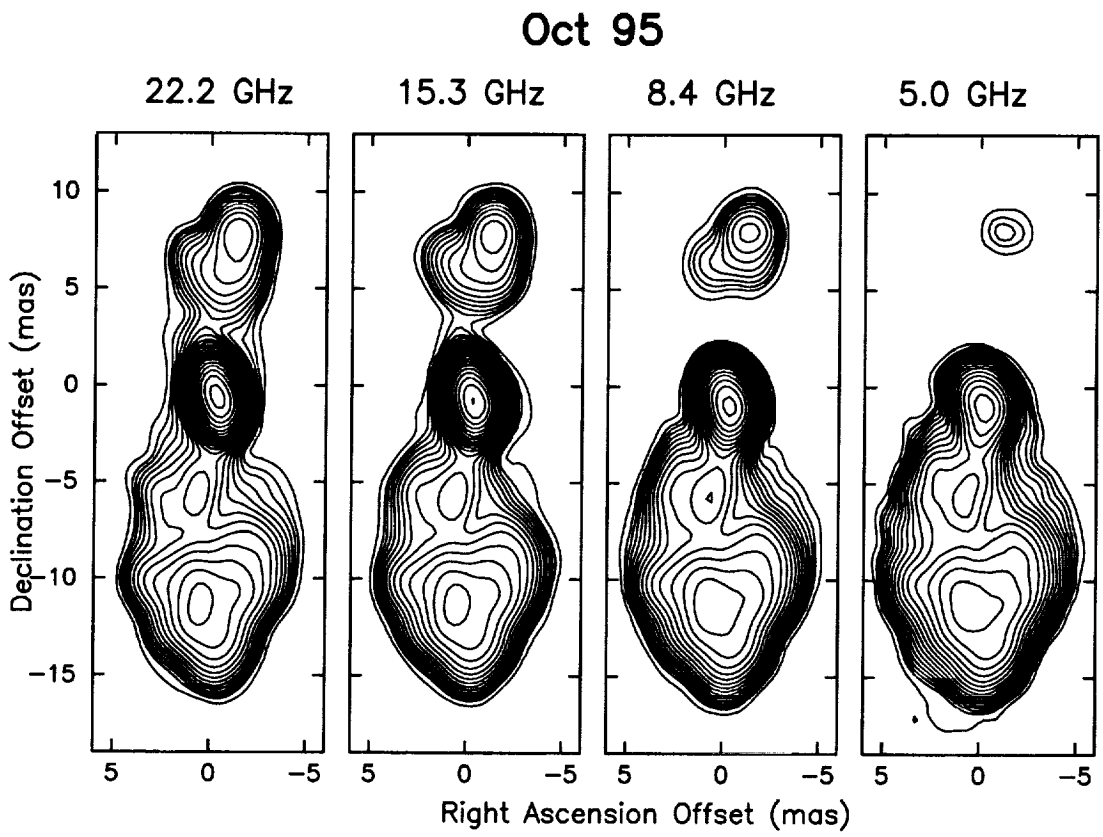

Figure 2. Free-free absorption in 3C 84. The images were made with the VLBA and, for 22 GHz, one VLA antenna. The contour levels start with 5, 10, 14, 20 mJy beam^{-1} and increase from there by factors of $\sqrt{2}$. The convolving beam for all images is 1.6 by 1.2 mas, elongated north-south. Note that the southern jet is stronger at low frequencies, which is typical for jets. But the northern feature almost disappears at low frequencies. This is the evidence for free-free absorption by structures associated with the accretion disk.

at 43 GHz of the jet in M87. M87 is an especially good source for this work because it contains a very massive black hole with a strong jet system, and it is very close compared to most sources. At least in the northern hemisphere, its black hole may have the largest angular size of any source. The 43 GHz observations have a resolution of 0.33 by 0.12 mas and show that the jet has a wide (60°) opening angle on the smallest resolved scales, compared to only a few degrees on all larger scales. This suggests that the jet is collimated on scales of around 30-100 times the size of the black hole. The observed structure of a flaring jet on the smallest scales provides important clues to the nature of the collimation region [7].

The last example is made possible by the interaction between the geodetic/astrometric community and the astronomical community. It relied on phase referencing, the observing style in which phases are calibrated on a strong source in order to allow long integrations on a weak source or in order to allow accurate relative positions to be obtained. This requires the use of a sufficiently good geometric model that phase errors are roughly the same on the calibrator and target sources. Such models come from the geodetic community and the one in CALC is used on the

VLBA correlator. Using that model with rapid switching between a calibrator and target that are no more than about 5 degrees apart, it is now possible to calibrate VLBI phases in much the same way that it is done on linked interferometers such as the VLA, Westerbork, and the AT. The importance of this method is simply seen in the fact that 30-50% of all observations on the VLBA use phase referencing. An example is the observation of the gamma ray burst source G970508 using the VLBA, VLA, and Effelsberg [8]. The source was observed 6 times at 8 GHz between 1 and 3 weeks after the burst. It was detected in all epochs, with flux densities ranging between 0.6 and 1.2 mJy and with positions consistent at about the 0.2 mas level. These flux densities are well below what could be detected by traditional fringe fitting.

4. Observing Modes

The primary observable for geodesy observations is the time interval between the arrivals at two stations of a wavefront from a source. A standard observing mode has been developed to measure this interval. Several well-separated baseband channels are measured and the slope of phase with frequency across these channels is determined. Since phase is frequency times delay and the frequencies are known, this determines the delay. This is done at both S and X bands and the difference is used to calibrate the ionosphere. To help determine the contributions from the troposphere and from clock variations, sources are observed as quickly as possible all over the sky, including at low elevations where the tropospheric effect is much enhanced. This style drives a desire for fast moving antennas. Often the antennas are subarrayed to increase the number of low elevation scans at each antenna. The final geometric results, such as source positions, station positions, and EOP, are determined, along with clocks and troposphere, in a least squares fit. This observing style, and the frequency bands used, are rarely altered for geodetic and astrometric observations.

In contrast to the uniformity of geodetic observing modes, astronomers use a very wide variety of frequencies, modes and capabilities. This is because the properties of sources vary with frequency and the goals of different projects can be quite different. Continuum source structure is usually frequency dependent and that dependency can tell much about source physics. Therefore observations are often desired over much of the possible RF range. This requires observing with several receivers, often band switching on time scales of minutes. Spectral line sources are frequency dependent over very narrow frequency ranges. This drives the need for narrow bandwidth capabilities in the data acquisition systems and for large numbers of spectral channels in the correlators. It is very common that the polarization properties of the sources are of interest so both RCP and LCP signals must be received and the correlator must deliver all the cross-hand correlations. The tradeoffs between source flux density (often highest at lower frequencies), resolution, phase stability and other factors depend on the nature of the sources and astronomical goals. Astronomical observations can be anything from very simple, with a long track on a single source at one frequency to highly complex with, for example, combined band switching, multiple sources, spectral line and full polarization. Astronomical observations also commonly push the capabilities of the instruments in such parameters as high or low frequency capability, weak source sensitivity and field of view (requires short integrations). The need to observe weak sources places a premium on large antennas, often at the expense the high slew speeds desired for geodesy.

5. Observables and Models

To some extent, geodetic and astronomical VLBI differ in what are considered to be observables and what are nuisance parameters. An obvious case is the delay. For both types of observations, the delays are determined with a fringe fit to phase slopes. For geodesy, most subsequent processing is based on the delays and the amplitudes and phases are not used beyond the fringe fit. For astronomy, the delays are only used to flatten the fitted phase slopes. Subsequent processing is based on the calibrated amplitudes and phases.

For geodesy and astrometry, the scientific targets of the observations are the geometric parameters. Source structure, to the extent that it affects the data, is a nuisance parameter. For astronomy, on the other hand, source structure is usually the scientific target and any errors in the a priori geometry are nuisance parameters. One thing that both groups agree on is that phase offsets introduced by the troposphere and ionosphere are nuisance parameters. An atmospheric physicist might disagree, but not much VLBI data has been used for such studies.

There are differences in the way models are treated for geodesy and astronomy. For geodesy, the correlator model only need be good enough to reduce the phase slopes in time (fringe rate) and frequency (delay) to allow a reasonable amount of averaging before the fringe fit. Fairly simple models can be used, and that was the tradition until the VLBA was built. After the fringe fit, the residuals are added to the model removed by the correlator to construct the "totals" that are used in all further processing. The most important aspect of the model is that it is accountable so that accurate totals can be constructed. Also, to simplify model independence, the baselines are often treated independently in both the correlator and the fringe fitting. The time tags on the data are usually the wavefront arrival time at one of the stations.

For astronomy, the model is rarely modified after correlation. For simple imaging experiments, the model quality is also not very important as errors are removed by the fringe fitting. But for phase referencing, a high quality model is required. Phase referencing is based on the assumption that the phase errors are the same on calibrator and target, and this is only true with a good model. It is is much simpler to analyze such observations if a good model is used on the correlator as on the VLBA.

For imaging, it is critical that closure offsets not be introduced. Closure offsets are violations of the concept that all instrumental offsets introduced by a station, or the atmosphere above a station, are the same on all baselines to that station. The word closure refers to the fact that such offsets cancel if phases are summed around a triangle. VLBI imaging is fundamentally based on the idea that, with N antennas, there are roughly N^2 baselines, each with independent information about the source structure, and only N calibration parameters that need to be determined. There is enough information to solve for both the source structure and the calibration. The easiest way to be sure that the closure parameters are preserved is to only ever introduce model or calibration factors that are station dependent and are the same on all baselines to a station. This is one reason that astronomy oriented correlators use Earth center models. The time tags are the wavefront arrival times at the Earth center and are the same on all baselines. Model calculations are done only once for each station and the results applied to all baselines to that station. Calibration parameters are stored and applied in the postprocessing software as pure station numbers. This guarantees that closure is preserved, but has complicated obtaining the desired independent baseline delays (treated as calibration parameters) for geodesy experiments processed in astronomy software.

6. Interaction

Despite the differences between geodetic and astronomical observations, the similarities are great. The same antennas, backend hardware, recording systems, and correlators can be used for both. By sharing resources, more of both types of science can be done than either community can afford by themselves. There has been a long history of cooperation in this regard and a large fraction of current systems are used for both geodesy and astronomy. As noted above, one group's fundamental observables are the other group's nuisance parameters in many cases. Having a whole community studying your nuisance parameters can be useful! The prime example of this is the tremendous impact that the high quality geodetic models have had on astronomy observations using phase referencing. This has effectively increased the sensitivity of the astronomical observations by well over an order of magnitude. In the other direction, the tools for imaging and the understanding of the behavior of compact sources provided by astronomy are of growing importance for geodesy as the accuracy reaches levels where source structure and evolution really matter.

Another area where interaction will hopefully be important is in dealing with those atmospheric effects that are nuisance parameters for all. Already, it looks like the global ionospheric models provided by the GPS side of the geodetic community will be of significant use for improving astronomical phase referencing projects. Dual band observations cannot be used in most such projects because the target sources are too weak. Both groups are interested in developing alternative methods of measuring tropospheric offsets. Water vapor radiometers are being tried in both contexts. It is possible that GPS data or other weather data may be helpful here. Also, it may prove advantageous for astronomers to mix periods of geodetic style observations all over the sky into phase referencing observations. Then geodetic type solutions for the atmosphere could be used to improve the astronomical results. This has not been done much so far, mainly because the postprocessing systems are so separate that it is extremely difficult to mix results. It would be useful to change this some day.

7. Culture

The style in which geodetic and astronomical observations are made is quite different. For geodesy, the community as a whole decides what observations should be made, then the resources are allocated to make those observations. The actual observing and data reduction are carried out by operational groups not necessarily consisting of the final users of the information produced. The operational groups produce data products such as reference frames and EOP parameters. They also prepare large data bases containing nearly all of the geodetic observations ever made. The geophysics is generally done by investigators who either use the data products, or who do their own fits to the overall data base.

In contrast, astronomy is more personal. A few collaborators, or even an individual, think up an observing project. They then write a proposal to one or more of the arrays or networks. The proposals are refereed along with all other submitted proposals. The referees are usually not people associated with the instruments. Each high ranking proposal is then given a block of time on the array. The detailed schedule is prepared by the astronomers and run by the instrument's operations staff. After correlation, the data are given to the astronomers who do all further processing and analysis and who eventually publish the results. The data do not, in general, become part of a large data base, although the correlator output is usually archived and can be accessed by others

after some proprietary period. In the past, the astronomer also participated in the observations and correlations, but that is now rare.

These differences have caused some problems when the operational geodesy groups have tried to observe with some of the astronomical instruments, particularly the VLBA. The astronomical referees needed to be convinced that the requested time was better devoted to geodesy than to astronomy. There were some problems as the VLBA was completed and the demand for astronomy time increased. Eventually, a number of geodesy projects were combined into the 6 RDV observations per year that use the 10 VLBA antennas plus up to 10 other antennas. This program has received good ratings and is now a regular part of VLBA activities. In fact the observing and correlation of those observations have been relatively trouble free compared to many Global Network projects. However the different styles of postprocessing software, combined with the need to fringe fit all VLBA correlator data in AIPS, are still causing some difficulties. The data path for geodesy is not very smooth, and there are still a few oddities in the output that are not yet understood (see Dave Gordon's contribution elsewhere in this volume). This has been compounded by the fact that the astronomical community is in transition between software packages so support for the old one (AIPS) is minimal and the new one (AIPS++) is not yet ready.

8. Summary

Astronomical and Geodetic/Astrometric VLBI involve many of the same techniques and equipment. Differences are minor compared to the similarities and both groups benefit from each other. Many of the interests of both groups in future developments are shared. Both would like improved tropospheric correction methods, wider bandwidths and more sensitivity, not to mention less costly systems to operate, perferably involving real time correlation. Hopefully the long history of cooperation between the groups will continue into the future.

References

[1] Herrnstein, J. R., Moran, J. M., Greenhill, L. J., Diamond, P. J., Inoue, M., Nakai, N., Miyoshi, M., Henkel, C.; Riess, A., "A geometric distance to the galaxy NGC 4258 from orbital motions in a nuclear gas disk.", 1999, Nature, 400, 539.

[2] Bartel, N., Bietenholz, M. F., Rupen, M. P., Beasley, A. J., Graham, D. A., Altunin, V. I., Venturi, T., Umana, G., Cannon, & W. H., Conway, J. E., "The Changing Morphology and Increasing Deceleration of Supernova 1993J in M81", 2000, Science, 287, 112.

[3] Hjellming, R. M. & Rupen, M. P., "Episodic ejection of relativistic jets by the X-ray transient GRO J1655-40", 1995, Nature, 375, 464.

[4] Walker, R. C., Dhawan, V, Romney, J. D., Kellermann, K. I., & Vermeulen, R. C., "VLBA Absorption Imaging of Ionized Gas Associated with the Accretion Disk in NGC1275", 2000, Ap. J. 530, 233.

[5] Peck, A. B., Taylor, G. B., & Conway, J. E., "Obscuration of the Parsec Scale Jets in the Compact Symmetric Object 1946+708", 1999, Ap. J., 521, 103.

[6] Taylor, G. B., "Magnetic Fields in Quasar Cores II", 2000, Ap. J. in press.

[7] Junor, W., Biretta, J. A., & Livio, M., "Formation of the radio jet in M87 at 100 Schwarzschild radii from the central black hole", 1999, Nature, 401, 891.

[8] Taylor, G. B., Frail, D. A., Beasley, A. J., and Kulkarni, S. R., "Position and parallax of the gamma-ray burst of 8 May 1997", 1997, Nature, 389, 263.

Chopo Ma: The International Celestial Reference Frame (ICRF) and the Relationship Between Frames, IVS 2000 General Meeting Proceedings, p.52–56
http://ivscc.gsfc.nasa.gov/publications/gm2000/ma1

The International Celestial Reference Frame (ICRF) and the Relationship Between Frames

Chopo Ma

NASA Goddard Space Flight Center
e-mail: cma@virgo.gsfc.nasa.gov

Abstract

The ICRF, a catalog of VLBI source positions, is now the basis for astrometry and geodesy. Its construction and extension/maintenance will be discussed as well as the relationship of the ICRF, ITRF, and EOP/nutation.

1. The Conceptual Basis of the VLBI Celestial Reference Frame

The conceptual basis of the VLBI celestial reference frame is simplicity itself, i.e., that the observed objects are stationary points. As these objects are all extragalactic radio sources, primarily quasars, their great distance makes this assumption plausible in a practical sense. Realistic transverse velocities would not change positions by more than 1 microarcsec/yr, entirely undetectable by current methods. The operational basis is that the relative positions of sources, i.e., the arclengths between sources, observed in a single one-day VLBI session are determined with high precision and accuracy. The precision is limited by the error in the basic astrometric observable, group delay, now on the order of 10 ps. The accuracy is a function of the geophysical, astronomical, and geometric/relativistic models needed to convert group delays into celestial and terrestrial geometry. While a one-day VLBI observing session covers the entire right ascension range of the sky (while the declination range may be limited by the north-south network geometry), the number of sources observed has increased from 10-15 in the early 1980s to 50-80 by the late 1990s, reflecting improvements in sensitivity and observing schedule design. If at all possible, each source is observed several times with varying geometry to break the geometric correlations. Since only a small fraction of the 600+ usable sources can be observed in one session, it is necessary to patch the whole sky together. This is accomplished by observing some of the same sources in different sessions along with other sources. The group of sources that are observed in both of two sessions links the other sources in these sessions and allows their relative position to be determined as well. Schematically, if the sources in session 1 are the set (A+B) and the sources in session 2 are the set (A+C), then the use of sources in set A in both sessions allows the relative positions of sources in set (B+C) to be estimated. The strength of the connection between sets B and C depends on the precision of the measurements and the geometric distribution of set A on the sky. The concatenation of many sessions provides both multiple links between sources and multiple direct measurements of arclengths. It should be mentioned that because most of the data come from geodetic observing programs, there is a small subset of sources with vastly more observations than the sources observed primarily in the limited number of purely astrometric sessions. The large number of relative positions is reduced to conventional right ascensions and declinations by adopting a right ascension origin and axis directions. The fundamental arclength information is retained in the full covariance matrix of the source coordinates.

2. The Process of Adopting the ICRF

While catalogs of VLBI source positions were generated independently by several groups with increasing sophistication starting in the 1970s, the process for adopting the ICRF as the defining celestial reference frame had several formal and scientific stages that were the joint effort of many people under the aegis of the IAU. The most important steps were taken at the 1988 IAU General Assembly in Baltimore, which called for the use of extragalactic objects when data and analysis were available, and the 1990 IAU Colloquium 127 along with the working groups leading up to the colloquium, which resolved the issues related to the adoption of a general relativistic framework, concluded that VLBI observations of extragalactic radio objects provided a suitable realization of a quasi-inertial celestial reference frame, and supported the continuity of optical and dynamical frames with the extragalactic frame. A working group was established at the 1991 IAU General Assembly to identify the objects to be used and another working group from the 1994 IAU General Assembly was charged with determining the positions of these objects. The actual VLBI source position catalog was generated by a subgroup of individuals from the main VLBI analysis centers at JPL, USNO, and GSFC along with representatives of the IERS to ensure continuity with the IERS celestial reference system, i.e., the orientation of the Cartesian axes in space. The 1997 IAU General Assembly in Kyoto adopted the ICRF positions, replacing the stellar FK5 on 1 January 1998, and the IERS celestial reference system as the International Celestial Reference System (ICRS). In the same resolution, the Hipparcos catalog, which had been aligned with the ICRF largely through specialized VLBI observations of radio stars, was adopted as the realization of the ICRS at optical wavelengths. The ICRF disengages the celestial reference frame from any real connection to the equinox, equator and ecliptic although the axes of the ICRF are very closely aligned to the equinox and mean equator of J2000.

3. The ICRF Analysis Configuration

The IAU subgroup for the ICRF catalog decided that the VLBI analysis should be optimized for the celestial reference frame, recognizing the limitations imposed by geophysical, astrophysical and astrometric reality. To the extent possible, state-of-the-art (ca. 1995) modeling and estimation methods were used and a final catalog was made from a single solution rather than a combination of catalogs. Four effects were most important. Since at some level a linear model of station motion must be insufficient, the station positions were estimated independently for each session. Tropospheric gradients were estimated to allow for time-varying asymmetry. The effect of gradients can be seen in Figure 1, which shows the declinations with gradients estimated minus the declinations without gradients estimated. (Points with formal errors >2 mas are omitted for clarity.) Although sources cannot move significantly in a material sense, their structure can change, leading to apparent changes in the positions estimated. This motion can be monitored by examining the time series of a source's position estimated independently from each session in which the source was observed successfully. Sources with excessive linear or random motions were treated as "arc" sources, i.e., their positions were estimated for each session instead of as a single value from all the data. Finally, to overcome the limitations of the standard precession and nutation models (amply demonstrated by VLBI data), offsets in nutation and longitude were estimated for each session. The offsets estimated from the data used for the ICRF are shown in Figure 2 along with a model fit. It might be noted that the model fit shows that nutation is not zero at J2000.0, an artifact of

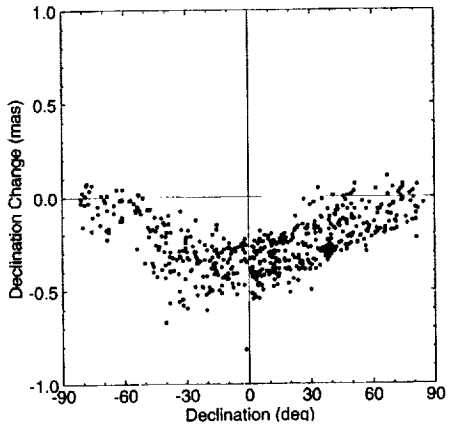

Figure 1. Effect of tropospheric gradients on source declinations

the original IERS definition of the ICRS made before the defects in the precession and nutation models became obvious. An essential aspect of the analysis was the development of a realistic error

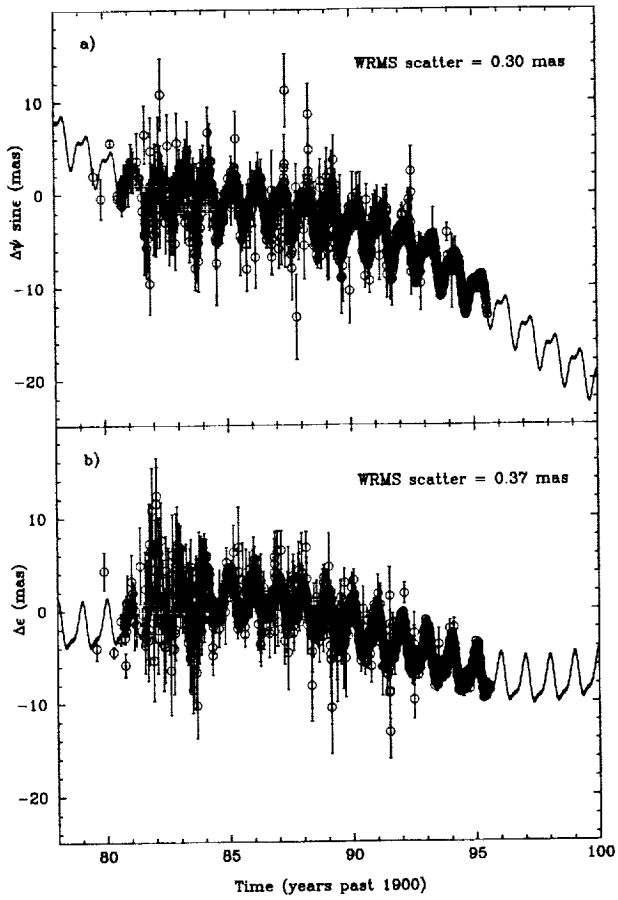

Figure 2. Nutation offsets estimated from the data used for the ICRF

model since formal errors as small as 0.01 mas were clearly too optimistic. The error model was derived from comparisons of software, comparisons of catalogs, and test solutions to study particular effects. The results indicated that a floor on source position uncertainty of 0.25 mas, while arbitrary, was credible. The sources of the ICRF were divided into three groups: 1) 212 defining sources with precise positions and absence of significant linear or random motion determined from sufficient observations and time interval, 2) 294 candidate sources with insufficient observations or time interval but no indication of significant linear or random motion, and 3) 102 "other" sources with significant apparent motion and treated as arc sources. In a formal sense the ICRF is defined by the numerical coordinates of the 212 defining sources. The positions of the candidate and other sources, however, are consistent with the ICRF as they were all estimated simultaneously in the same solution.

4. Maintenance and Extension of the ICRF

The maintenance and extension of the ICRF has two main elements, further observations and (limited) refinement of analysis. It is being carried out at present by task group T1 under the IAU Working Group for the ICRS with the close cooperation of the IVS and IERS. The original ICRF work used all relevant geodetic and astrometric data available through July 1995. The first extension, ICRF-Ext.1, added data through April 1999, 600 000 observations in 461 sessions. There are 59 new sources, shown in Figure 3. The observations currently contributing to the ICRF include geodetic observing programs such as CORE (Continuous Observations of the Rotation of the Earth), weekly NEOS (U.S. National Earth Observation Service), and RDV (Reserach and Development with VLBA). While these sessions use primarily the $\sim$ 100 best (most compact, strong) sources, they also observe the astrometric sources with the intention of repeating all sources over a few year interval. There are also a small number of purely astrometric sessions each year, which have concentrated on mid-south sources. The conceptual basis of analysis in the

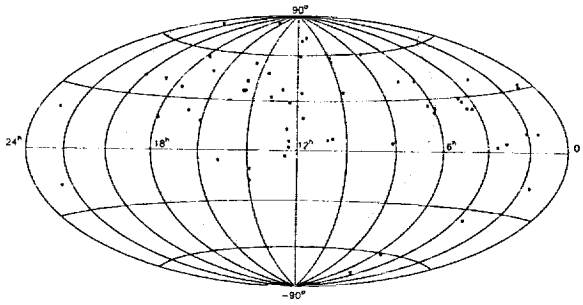

Figure 3. New sources added in ICRF-Ext.1

maintenance and extension phase is to make improvements but not to introduce systematic effects or to change positions generally beyond the ICRF error threshold. It is not practical or desirable to repeat exactly the analysis used for the original ICRF. On the other hand, the ICRF is now a conventional frame and requires stability to be most useful. Consequently the main features of the original ICRF analysis remain, and the positions and errors of the defining sources are not changed. However, the positions and uncertainties of the candidate sources may be improved by additional

data and better modeling. For example, the troposphere mapping function has been updated and the interval for troposphere parameters shortened. Some effects such as nonzero a priori mean gradients are not included because they cause small but systematic changes in the overall frame. The source position time series have also been brought up to date, and several additional sources have been shifted to the arc source category because of excessive position variation. It is expected that further extension/maintenance solutions will be made on a roughly annual basis. The realization of an entirely new ICRF requires a consensus that the improvement in accuracy and distribution of sources is needed to support scientific research.

5. The Relationship between Frames

The relationship between the celestial and terrestrial reference frames is shown in Figure 4. The central image is the undisturbed state. The effect of precession and nutation is to move the spin axis and geographic pole together in space. The effect called polar motion is the motion of the spin axis about the geographic pole while UT1 measures nonuniform rotation rate about the spin axis. In the figure, the North and South geographic poles (thick gray axes) are imaginary

Figure 4. Relationship between the terrestrial and the celestial reference frames.

fixed points on the Earth that define latitude. The spin axis (thin black axes) is the line about which the Earth rotates at a particular instant. At some time in the past (**middle globe**), the N and S poles were defined to coincide with the spin axis. Changes in the Earth's orientation are described in three ways, greatly exaggerated for clarity. In the **top globe** nutation and precession are the periodic and long-term motion of the spin axis in space. The tilt of the spin axis changes with respect to the distant quasars. In the **bottom left globe** polar motion describes the motion of the N and S poles about the spin axis. Over time the spin axis is spiraling away from the poles. In the **bottom right globe** UT1 describes the nonuniform daily rotation of the Earth. At any particular time, the rotation angle of the Earth differs from what would be predicted if the length of day were exactly 24 hours.

Zuheir Altamimi: ITRF Status and Plans for ITRF2000, IVS 2000 General Meeting Proceedings, p.57–61
http://ivscc.gsfc.nasa.gov/publications/gm2000/altamimi

ITRF Status and Plans for ITRF2000

Zuheir Altamimi

IGN, ENSG, LAREG

e-mail: altamimi@ensg.ign.fr

Abstract

The status of the International Terrestrial Reference Frame (ITRF) and the procedure of its implementation are presented. We will focus on VLBI contributions to ITRF and their relationships to the other IERS techniques in terms of TRF definition as well as quality assessment. Future plans for ITRF2000 will be outlined.

1. ITRF Combination Procedure

The current methodology of ITRF combination procedure is based on combining simultaneously station positions and velocities using full variance-covariance information provided, in SINEX format, by the IERS analysis centers. Moreover, a rigorous weighting scheme is used, based on the analysis and estimation of the variance components using the Helmert method. For a full description of the physical as well as statistical modelling, see Ref. [2].

The general physical model used in the combination software called CATREF is given by the following equation (1):

$$\begin{cases} X^i_s &= X^i_{itrf} + (t^i_s - t_0)\dot{X}^i_{itrf} + T_k + D_k X^i_{itrf} + R_k X^i_{itrf} \\ &+ (t^i_s - t_k)\left[\dot{T}_k + \dot{D}_k X^i_{itrf} + \dot{R}_k X^i_{itrf}\right] \\ \dot{X}^i_s &= \dot{X}^i_{itrf} + \dot{T}_k + \dot{D}_k X^i_{itrf} + \dot{R}_k X^i_{itrf} \end{cases} \quad (1)$$

where for each individual frame k, D_k is the scale factor, T_k is the translation vector and R_k is the rotation matrix. The dotted parameters designate their derivatives with respect to time.

2. VLBI Contribution to ITRF

Since the begining of the ITRF activities in 1988, VLBI Analysis Centers contributed significantly to ITRF by submitting station positions (and velocities). The high precision of VLBI observations is a key element for ITRF in terms of the unification of terrestrial references coming from VLBI, SLR, GPS and DORIS. The long history of VLBI observations is also a significant contribution for ITRF time evolution. The first ITRF velocity field estimated by space geodesy techniques is that of ITRF91, derived from a combination of VLBI and SLR TRF solutions [1].

Figure 1 shows the current distribution of VLBI stations contributing to ITRF.

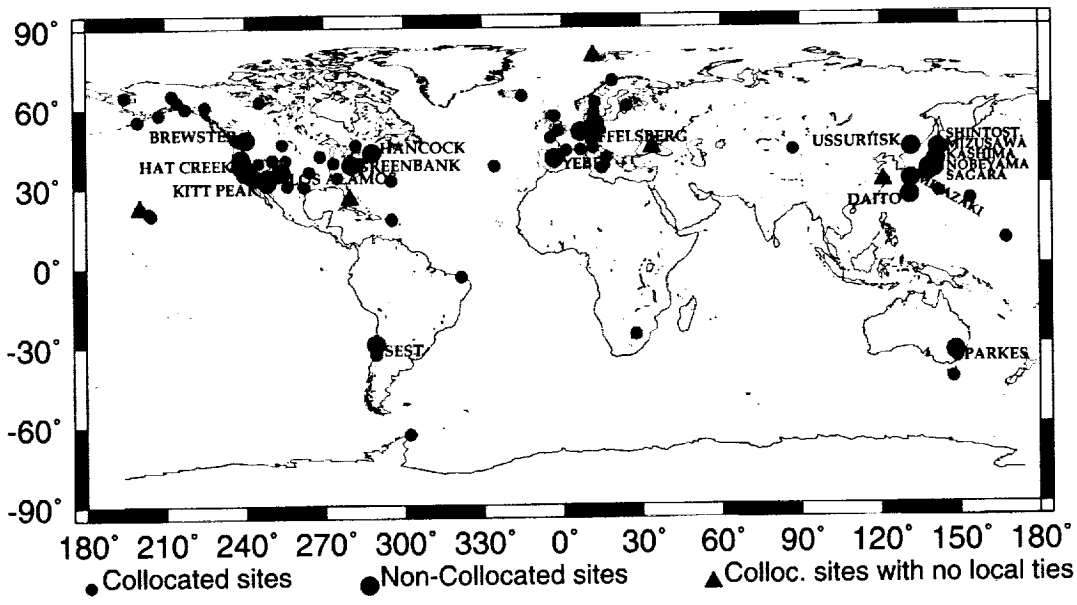

Figure 1. VLBI Network (Feb. 2000).

3. Analysis of VLBI TRF Solutions

In this paper we selected some VLBI TRF solutions in order to assess their relative quality to each other. Moreover we also included in this analysis solutions from SLR, GPS and DORIS techniques in order to evaluate their level of agreement and quality when combined together. The investigated solutions are as follows:

- Solutions used in ITRF97:
  - VLBI: GIUB, GSFC, USNO solutions
  - SLR: CSR free network solution
  - GPS: CODE solution (constraints are removable)
  - DORIS: IGN free network solution
- New VLBI loose solutions from GIUB and GSFC

The performed analyses are:

- Comparison of individual VLBI TRF's to ITRF97
- Global Combination of VLBI TRF's
- Global Combination of loose VLBI, SLR, GPS and DORIS solutions

We use in these comparisons and combinations full variance-covariance matrices provided in SINEX format.

4. Quality Assessment of VLBI TRF Solutions

When comparing or combining several TRF's, the quality assessment is evaluated upon the commonly computed Weighted RMS. The latter is based on post fit residuals as well as a priori variances. The WRMS is very sensitive in particular to the weighting as well as to the constraints imposed in the individual solutions one wants to combine.

In theory, for a given TRF solution, the variance-covariance matrix contains a natural noise coming from the observations and a TRF effect. Tightly constraining (or fixing) some parameters hides the observation noise and then in turn disturbs the quality assessment (WRMS).

A result from the VLBI TRF's analysis, figure 2 illustrates the WRMS in position and velocity as follows:

- the top plots are the results obtained from comparisons to ITRF97. We clearly see that the WRMS of the loosely constrained solutions are larger than those of the three constrained solutions used in the combination of the ITRF97.
- to see the impact of combining constrained and loosely constrained solutions, the bottom plots show the WRMS obtained from a global VLBI combination incorporating one constrained solution (USNO) and two loosely constrained solutions (GIUB and GSFC). The former appears better than the latter, meanwhile the three VLBI solutions are in principle of the same quality as indicated by the top plots.

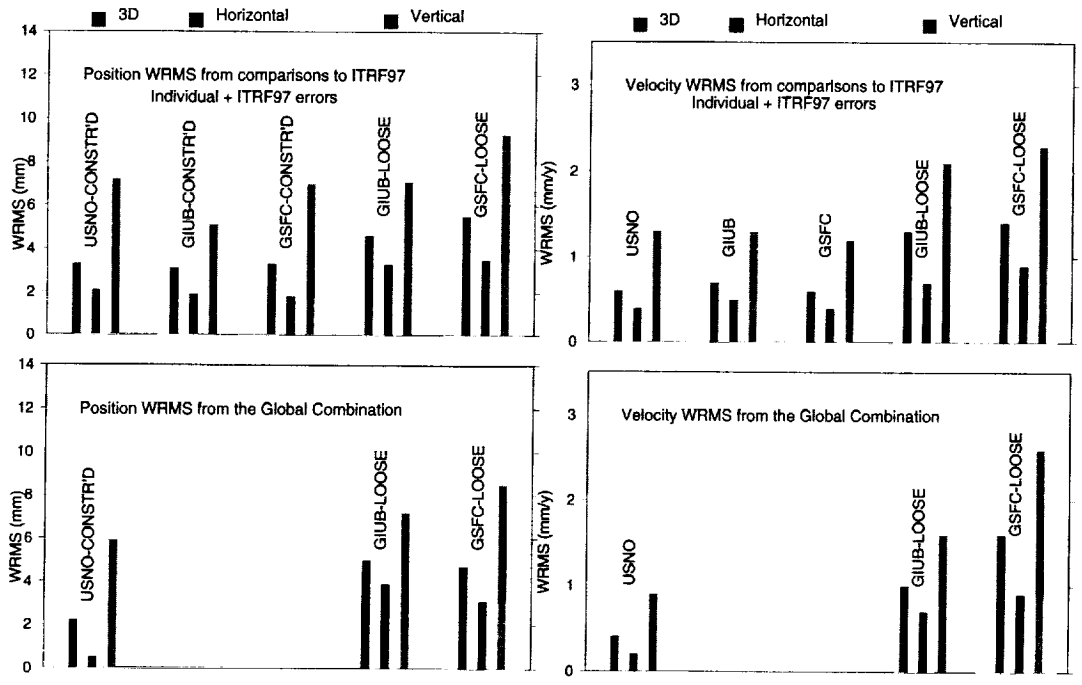

Figure 2. WRMS in position and velocity coming from VLBI TRF comparisons to ITRF97 (top) and the global VLBI combination (bottom).

5. Quality Assessment of VLBI, SLR, GPS and DORIS TRF Solutions

In order to evaluate the agreement level of TRF solutions provided by the four techniques (VLBI, SLR, GPS and DORIS), two global combinations were performed:

- the first combination includes two constrained solutions (VLBI from GSFC and GPS from CODE) and two free network solutions (SLR from CSR and DORIS from IGN)
- the second combination includes four loosely constrained solutions; the two SLR and DORIS as in the first combination and two VLBI loosely constrained solutions from GSFC and GIUB.

Figure 3 illustrates the WRMS valuse as obtained from these two global combinations.The figure indicates that while the WRMS of the two free network solutions (SLR and DORIS) remain unchanged, the WRMS of the two loosely constrained solutions (VLBI and GPS) are larger than those derived from the first combination.

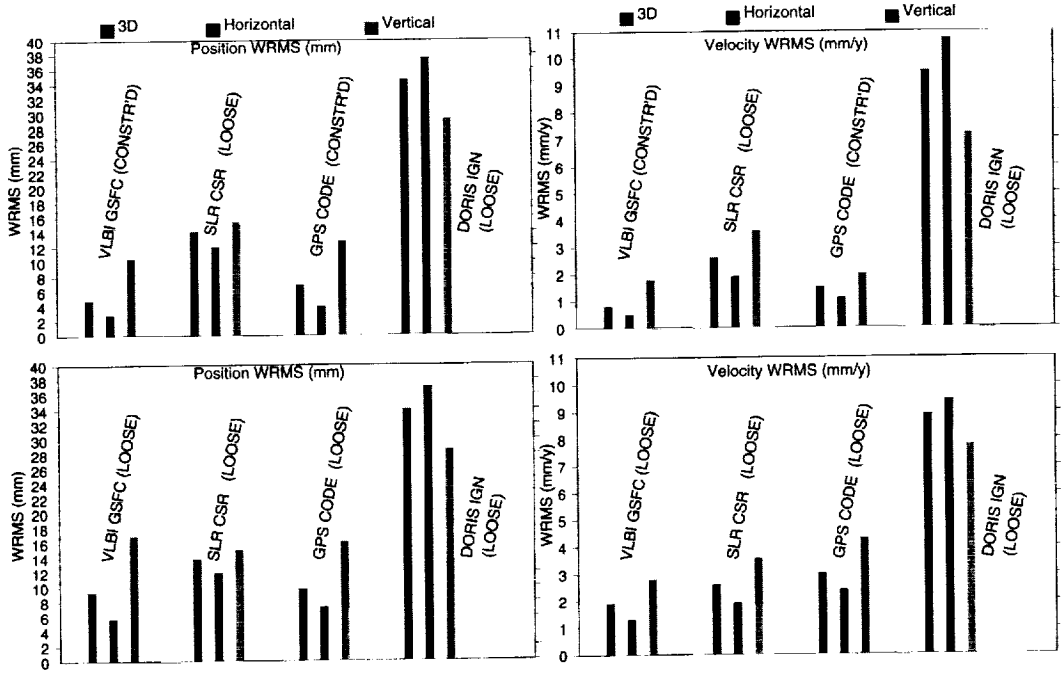

Figure 3. WRMS in position and velocity derived from two global combinations of VLBI, SLR, GPS and DORIS TRF solutions.

6. Plans for ITRF2000

The ITRF2000 is to be considered as a standard solution for a wide user community (geodesy, geophysics, astronomy, etc.). The ITRF2000 comprises on one hand primary core stations observed by VLBI, LLR, GPS, SLR and DORIS techniques and, on the other hand, significant extension provided by regional GPS networks for densifications as well as other useful geodetic markers tied to the space geodetic ones.

The IVS AC's should contribute to the ITRF2000 by submitting at least three independent loosely constrained or unconstrained solutions. These solutions should contain station positions and velocities using as much as possible of VLBI data and as many as possible of VLBI stations.

7. Conclusion

The main conclusion of the analysis presented in this paper is that the relative quality suggested by the preliminary global combination of loose VLBI, SLR, GPS and DORIS solutions could be summarized in the following table:

Technique	AC	Position 3D-WRMS mm	Velocity 3D-WRMS mm/y
VLBI	GSFC	10	2
SLR	CSR	14	3
GPS	CODE	10	3
DORIS	IGN	34	9

On the other hand, it is obvious that further analysis of more loose solutions is needed and the IVS AC's are encouraged to provide loosely constrained solutions.

Finally we see that combining constrained and loose solutions disturbs the quality assessment (WRMS).

References

[1] Altamimi, Z., C. Boucher and L. Duhem, 1993, The Worldwide Centimetric Terrestrial Reference Frame and its Associated Velocity Field, *Adv. Space Res.* **13**, (11)151-(11)160.

[2] Boucher, C., Z. Altamimi and P. Sillard, 1999, The 1997 International Terrestrial Reference Frame (ITRF97), IERS Technical Note 24, Observatoire de Paris.

Thomas A. Herring: Geophysical Applications of Earth Rotation Measurements, IVS 2000 General Meeting Proceedings, p.62–68
http://ivscc.gsfc.nasa.gov/publications/gm2000/herring

Geophysical Applications of Earth Rotation Measurements

Thomas A. Herring

Department of Earth, Atmospheric and Planetary Sciences, MIT
e-mail: tah@mit.edu

Abstract

Measurements of the variations in Earth rotation have improved dramatically over the last few decades. These measurements are usually viewed in three separate ways: (a) The motions of the Earth's rotation axis with respect to the crust (polar motion); (b) the variations in the rate of rotation (length-of-day, LOD); and (c) motions of the Earth's rotation axis in space (nutations). VLBI is the only technique available that can make reliable measurements of all of these components over long periods of time. The requirements for such stability are for (a) a stable terrestrial reference frame and for (b) and (c) a stable inertial reference frame with the latter being unique to VLBI. We discuss the relationship between and the accuracy of different space geodetic techniques for making measurements of Earth rotation variations and the geophysical applications of each of the measurement types.

1. Introduction

Changes in the rotation of the Earth are a balance between the changes in angular momentum and the applied torques. At any instant, three Euler angles can be determined that rotate between a coordinate system attached to the Earth and one attached to inertial space. The former is the Terrestrial Reference System (TRS) and is attached to the Earth in a predetermined fashion that accounts for the deformation of the Earth due to tides and other geophysical processes such as plate tectonic motions. The latter system is called the Celestial Reference System (CRS) and is defined now by extragalactic radio sources that are assumed to be stationary in this frame. The three Euler angles, to first order, represent the rotation about one axis and the position of that axis, either in the TRS or CRS, depending on which way the transformation is being made. The temporal variations of the Euler angles contain all frequencies but when the transformation is made from the TRS to the CRS, there are large components in the retrograde nearly diurnal band and at longer periods. These two bands are usually treated separately with the nearly diurnal band being referred to as nutations (and usually given in the CRS in which they have long period variations). Those components for the position of the rotation axis with long period variations are called polar motion. The rotation angle contains all frequencies and is usually expressed as the difference in time as measured by the rotation of the Earth, UT1, and atomic time, UTC. The time derivative of UT1-UTC represents the variations in the length-of-day (LOD).

The Liouville equation is the basic equation that is used to determine how a system rotating with angular velocity Ω and having angular momentum vector $\mathbf{H}$ changes in response to an applied torque Γ

$$\frac{d\mathbf{H}}{\mathbf{dt}} + \Omega \times \mathbf{H} = \mathbf{\Gamma} \tag{1}$$

The torque applied by external bodies on a biaxial ellipsoidal body is

$$\Gamma = -\Omega^2 e A \mathbf{i_3} \times \phi \tag{2}$$

where e is the dynamical ellipticity of the body given by $(A-C)/C$, A and C are the minimum and maximum moments of inertia, $\mathbf{i_3}$ is the Z principal axis and ϕ is the potential of the external body. For the torques from the Sun, Moon and planets, ϕ is well known. The corresponding equation to equation (1) in a non-rotating frame simply has Ω set to zero.

The three types of rotation variations can be deduced from equation (1). There are three important axes to consider: (a) the rotation axis denoted by Ω; (b) the angular momentum axis, $\mathbf{H}$; and (c) the $\mathbf{i_3}$ axis which for a rigid body is attached to the Earth. For a non-rigid Earth, the $\mathbf{i_3}$ axis is attached to the Earth in a pre-defined way usually given as being attached to the mantle after the effects of deformations such as Earth tides are removed. When Γ is zero i.e., no external torques, the angular momentum axis remains fixed in space (viewed from a non-rotating frame) and has a small motion relative to Ω, if Ω and $\mathbf{H}$ are not aligned (i.e., the $\times$ in equation (1) must balance the time derivative of $\mathbf{H}$. When Γ is non-zero, the angular momentum axis (along with all the other axes) move in space and with respect to each other. In this case, the motions relative to each other are much smaller than the motions in space. Because the Earth is very close in shape to a biaxial ellipsoid, the changes in the direction of the axes are largely decoupled from the magnitude of vectors that represent the axes. The external torques from the Sun and Moon do not change the rate of rotation of a biaxial ellipsoid, they only affect the direction of the rotation axis.

Equation (1) is often written in its linearized form and by use of a complex representation of direction of the rotation axis. In this form, we write $\tilde{m} = (x_p - iy_p)$ for the direction of the rotation axis in terms of the polar motion components x_p and y_p. The rate of rotation is given by $\Omega_3 = (1 + m_3)\Omega_0$ where Ω_0 is the average rotation rate. The value m_3 is often expressed as changes in length-of-day. In its linearized form, equation (1) can be written as a pair of equations:

$$\dot{\tilde{m}} = i\frac{(C-A)}{A}\Omega(\tilde{m} - \tilde{\chi}) \tag{3a}$$

$$m_3 = \chi_3 \tag{3b}$$

where $\tilde{\chi}$ is the complex excitation function. It can be decomposed into three parts: (a) contributions from external torques; (b) terms for changes in the moments of inertia, either due to mass motions or due to deformations; and (c) terms due to the momentum being carried by moving mass. In Earth rotation studies, it is the separation of these components along with forward models for their variations that are used to study the Earth. In general, for nutations the torques are well known and the response of the Earth can be directly determined. For polar motion and length-of-day variations, the excitations in terms of mass motions and the effects of mass are the quantities sought.

2. Nutations

Nutations provide unique insights into the physical characteristic of the Earth. In nutation studies, equation (1) is written for the major parts of the Earth: the mantle, the outer-fluid core, and the solid-inner core. The interaction between the components of the systems has a large impact on the rotational variations of the Earth. The major effect is from two resonances that develop due to differential rotation between the mantle, outer and inner cores. Both of these resonances are in the nearly retrograde band, when viewed from the rotating Earth, and are very sensitive to specific characteristics of the boundaries between these bodies. In current theories, the atmosphere and

oceans are not explicitly included. The oceans are accounted for through contributions that are computed directly from ocean-tide models. The atmosphere is included only through estimation. The currently adopted nutation series is the IAU-1980 nutation series which explicitly contains the effects of elasticity of the mantle and the pressure coupling of the fluid core to the mantle. The latter coupling is very dependent on the shape of the core-mantle boundary and in the IAU-1980 nutation series this shape is computed from the assumption that the Earth is in hydrostatic equilibrium. The International Earth Rotation Service (IERS) also developed a nutation series (IERS-1996) to better match VLBI data. In Figure 1 we show a comparison of these two series.

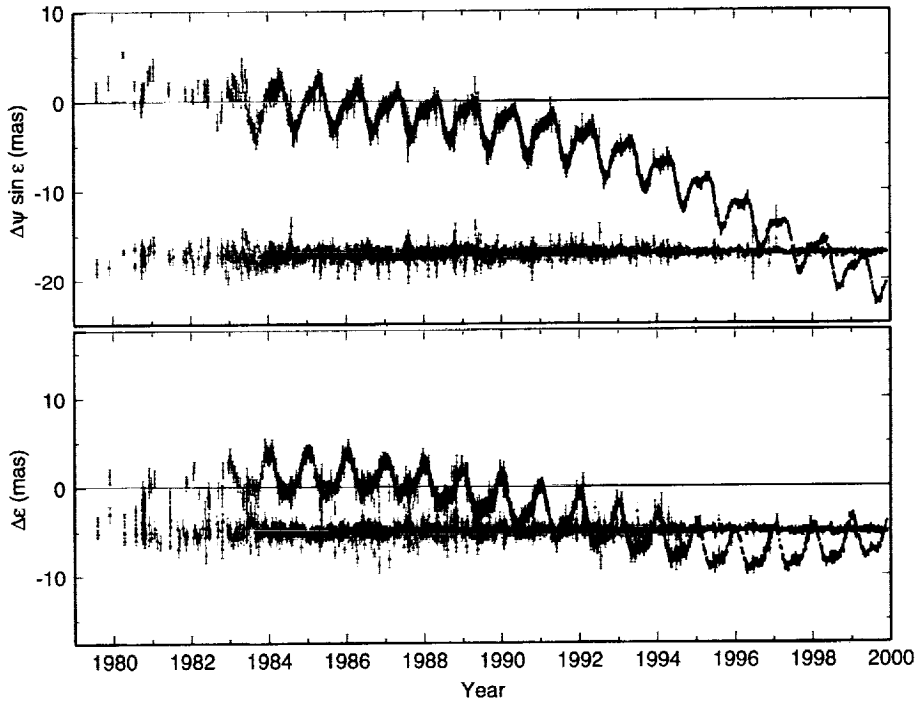

Figure 1. Differences between GFSC and USNO nutation angle determinations and the IAU-1980 nutation series (black) and the IERS-1996 series (red) for all measurements with standard deviations less than 1 mas. The weighted root-mean-square (WRMS) scatter of the differences to the IAU-1980 series are 5.6 mas for $\Delta\psi \sin\epsilon$ and 2.7 mas for $\Delta\epsilon$. The corresponding values for the differences to IERS-1996 series are 0.17 mas and 0.17 mas. The mean values of the differences to the IERS series are due to the method used to initially adopt the celestial coordinates of the quasars. The derivation of the IERS-1996 series used data through the end of 1995 and therefore the last 5 years of differences are based solely on predicted values.

Recently, a new nutation series has been developed that attempts to match the VLBI data to a geophysical model. The series MHB-2000 [1] is rigorously based on geophysical theory with certain parameters of the Earth estimated from the VLBI data. The WRMS difference between this theory and the VLBI measurements is 0.16 mas for both $\Delta\psi \sin\epsilon$ and $\Delta\epsilon$ where $\Delta\psi$ and $\Delta\epsilon$ are the nutation in longitude and obliquity, and ϵ is the mean obliquity of the ecliptic ≈ 23.4 deg. The main characteristics of this series are: (a) the dynamic ellipticity of the fluid core is 3.8% higher than the hydrostatic equilibrium value; (b) the base of the mantle needs a highly conductive layer of at least 200 m thickness; (c) the RMS of the radial magnetic field at the core-mantle boundary

is 7.2 Gauss; (d) the solid-inner core is coupled to the Earth through a 68 Gauss magnetic field at the solid-fluid boundary as well as pressure and gravitational coupling; and (e) corrections have been applied to account for mantle anelasticity, ocean tides and atmospheric effects at the S_1 tidal frequency (prograde annual nutation).

In addition to the predictable part of the nutations given by the MHB-2000 nutation series, there is a non-predictable part of the motion due to the random excitation of the Retrograde Free Core Nutation (RFCN) resonance mode (analogous to the Chandler wobble in polar motion). The precise reason that the amplitude of this mode has been decreasing is not clear at moment, but such variations show that continued measurements of the nutation angles are needed in order to monitor these variations.

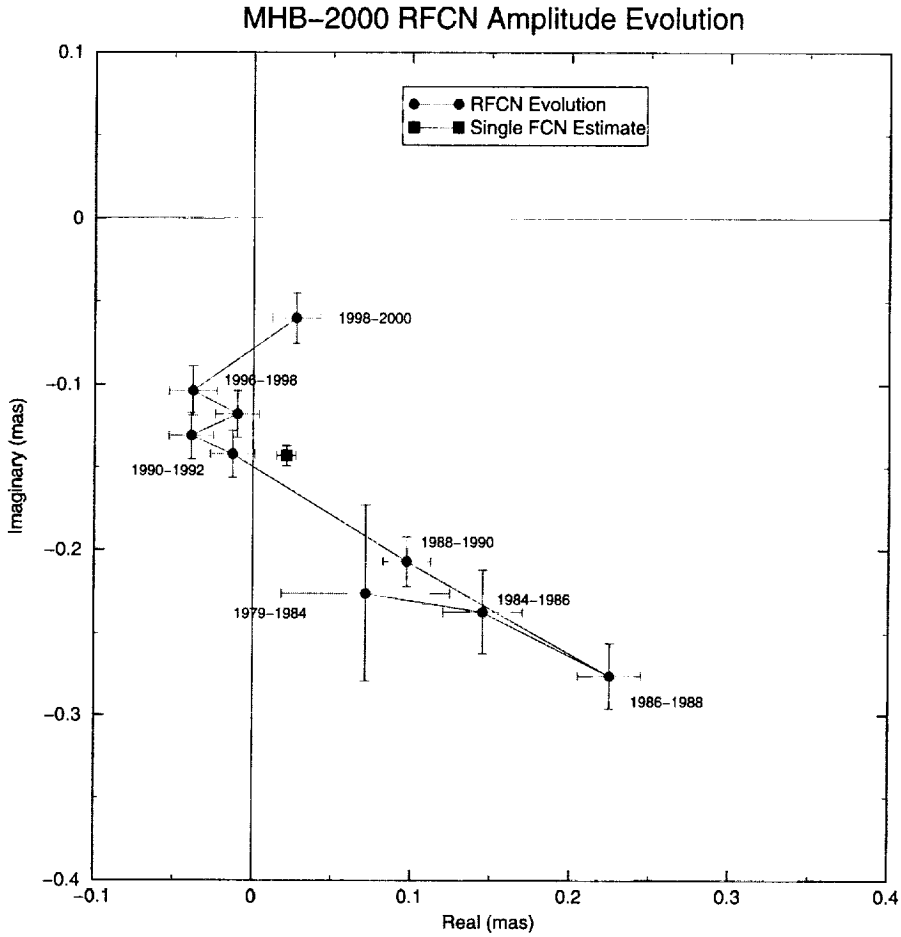

Figure 2. Evolution of the freely excited RFCN mode from 1979-2000. After 1984, estimates are made on a two-year basis. The single black estimate is the average value of the 20 year interval from 1980-2000.

3. Axial Rotation Rate Variations

The axial variations in rotation rate are usually expressed as length-of-day (LOD) variations. From equation (3*b*), the variations in length of day are a direct measure of the excitations about the Z-axis. On short time scales, such as the year of data shown in Figure 3, the variations of LOD are dominated by changes in the angular momentum of the atmosphere (AAM) caused by atmospheric winds. Once the wind contribution to AAM is removed, the dominant remaining signal is semi-annual and thought to arise from ground water seasonal variations in each hemisphere. For LOD the mass contribution to AAM from atmospheric pressure changes is small.

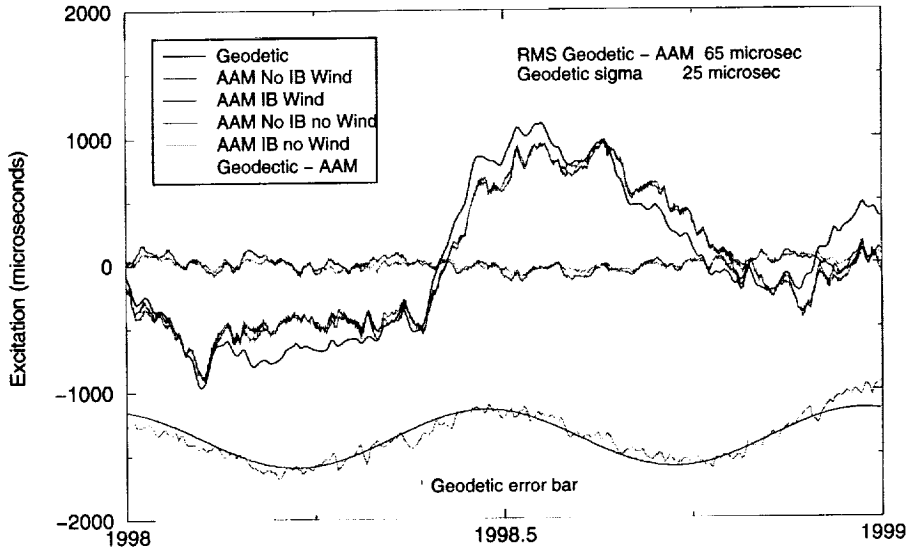

Figure 3. Comparison of LOD variations determined geodetically with the variations computed from changes in the angular momentum of the atmosphere (AAM) under various assumptions. The two curves which track the geodetic measurements closest include the angular momentum contribution from winds. The effects of atmospheric pressure changes are small independent of whether the oceans are assumed to behave rigidly (No IB) or according to the inverted barometer (IB) assumption. The bottom portion of the figure is the difference between the geodetic excitation and AAM contribution. The black line here is the fit of a semiannual signal to the difference. After removing this contribution, the RMS difference is 65 μs, compared to a geodetic uncertainty of 25 μs.

Decadal period variations in LOD are much larger than those shown in Figure 3 and are believed to arise from changes in the angular momentum of the fluid core. Recent results using core motions predicted from changes in the Earth's magnetic field have shown that such variations are possible with either topographic or electromagnetic coupling of the fluid core to the mantle. On all time scales, the oceans can be expected to influence LOD and results of recent ocean angular momentum (OAM) calculations, based on altimeter data and wind forcing, have been shown to be correlated with variations in LOD.

4. Polar Motion Variations

The excitation of polar motion is the least well explained of the EOP components. It is also the most difficult to compute accurately from geodetic data sets. The excitation is computed by re-arranging equation ($3a$) so that $\tilde{\chi}$ appears on the left-hand side of the equation. The excitation is then computed from the derivatives and values of polar motion. At high frequencies, noise in the estimates of the polar motion derivatives can greatly affect the accuracy of the excitation calculation. In recent years, the computation of geodetic excitations has improved greatly due to the availability of daily Global Positioning System (GPS) estimates of pole position and derivatives obtained directly from geodetic analyses of the data. Prior to this, the derivatives of polar motion were computed by interpolating non-uniformly spaced, in the case of VLBI, estimates of the pole positions. In Figure 4, we compare geodetic polar motion excitations with those computed from AAM. In this figure, the geodetic excitations are computed from daily IERS Bulletin A values of pole position. Comparison between the results shown in Figure 4 and excitation estimates computed directly from daily GPS estimates of pole position and its derivatives show RMS differences of 0.01" which is small compared to the differences between the geodetic and AAM excitations.

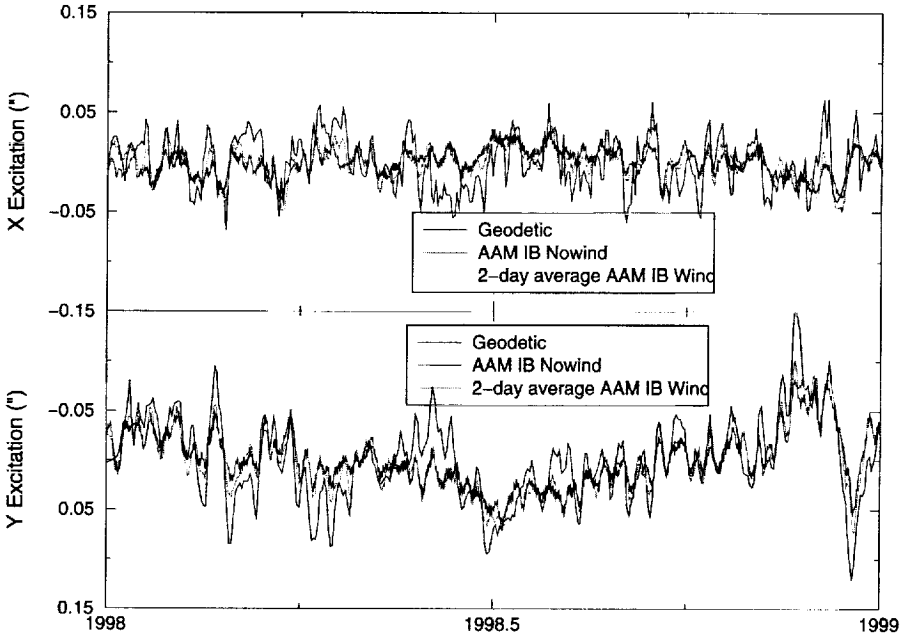

Figure 4. Comparison of polar motion excitations inferred geodetically and from changes in AAM. Unlike LOD, the wind term in the case of polar motion has large high frequency (nearly diurnal) variations. In this figure, the wind term has been smoothed with a 2-day moving average. Although the AAM computed excitation is correlated with the geodetic, especially for the Y-component of the excitation, there are large sources of excitation which are not accounted for by the atmosphere.

There is still much speculation about the origin of polar motion excitations. The noise in the geodetic excitations is now small compared to the differences. The short period correlations between the AAM and geodetic excitations, although often with different amplitudes, suggest that the excitation is related to atmospheric changes. Recent results from the analysis of OAM where

the ocean variations are driven by atmospheric winds are showing promise for explaining much of the difference between the series. On longer time scales, of order decades, there does appear to a role to be played by the fluid core but there have been few quantitative comparisons at this time.

5. Conclusions

In the table below we give the current capabilities for EOP determinations using the three main geodetic systems, VLBI, GPS and satellite laser ranging (SLR). The area in which VLBI is unique is long period nutation measurements. At short times, $\leq$10 days, GPS has yielded nutation results of accuracy similar to VLBI, but the errors grow rapidly with increasing time span. Much of the uncertainty in nutation models is for long period terms such as the 430-day period RFCN free mode and the 18.6 year nutation, and measurements at these period remain the sole domain of VLBI.

EOP Type	VLBI	GPS	SLR
Polar motion	0.2 mas	0.1 mas	0.4 mas
Polar motion rates	?	0.15 mas/day	?
UT1	0.01-0.03 ms	?	?
LOD	0.02 ms	0.02 ms	0.06 ms
Nutation	0.15 mas	0.2 mas, periods $\leq$10 days	

For the other components of EOP measurements, GPS is playing an increasingly important role primarily due to the large number of stations used and the continuous measurements. For daily measurements of pole position and its rate of change, the 100–200 GPS stations whose data is processed daily probably provides more accurate results than the current VLBI measurement programs. It is yet to be seen whether the fully operational CORE VLBI measurements, using a relatively small number of stations, will be as accurate as the GPS determinations at that time. Similarly for LOD variations, GPS gains from the large numbers of stations although it still depends on VLBI for long period integration of LOD to yield UT1 values. For geophysical studies, however, the LOD variations are of interest and these appear to be well determined by GPS.

The variations in Earth rotation are driven by changes in the fluid envelopes of the Earth and by external forces. The fluid changes also cause variation in quantities other than just EOP. There are mass loading terms, either external or internal, that cause deformations of the Earth, and there are gravity field changes also associated with these variations. In 2001 a satellite mission dedicated to measuring changes in the Earth gravity field will be launched. The combination of gravity field changes, surface deformations, and Earth rotation changes hold promise for allowing the detailed study of changes occurring in the Earth's fluid envelope.

References

[1] Mathews, P. M., T. A. Herring, and B. A. Buffett, "Modeling of nutation-precession: New nutation series for nonrigid Earth, and insights into the Earth's interior", submitted *J. Geophys. Res., March, 2000.*

Tom Clark: It's About Time!, IVS 2000 General Meeting Proceedings, p.69–69
http://ivscc.gsfc.nasa.gov/publications/gm2000/clark1

It's About Time!

Tom Clark

NASA Goddard Space Flight Center

e-mail: clark@tomcat.gsfc.nasa.gov

Abstract

Everything we do in VLBI is connected to time. In this contribution, we review 28 orders of magnitude of the spectrum of time ranging from a few hundred femtoseconds (i.e. one degree of phase at X-band $\sim \pi \cdot 10^{-13}$ seconds) upwards to tens of millions of years (i.e. ten million years $\sim \pi \cdot 10^{14}$ seconds). In this discussion, we will pay special attention to the relation between the underlying oscillator (the frequency standard that defines a clock's rate) and the time kept by the clock (which counts the oscillations of the frequency standard). We will consider two different types of time — time kept by counting an atomic frequency standard (Hydrogen Maser or Cesium), and time reckoned by the rotation of the Earth underneath the stars and sun.

Session 2

Field Stations and Data Acquisition

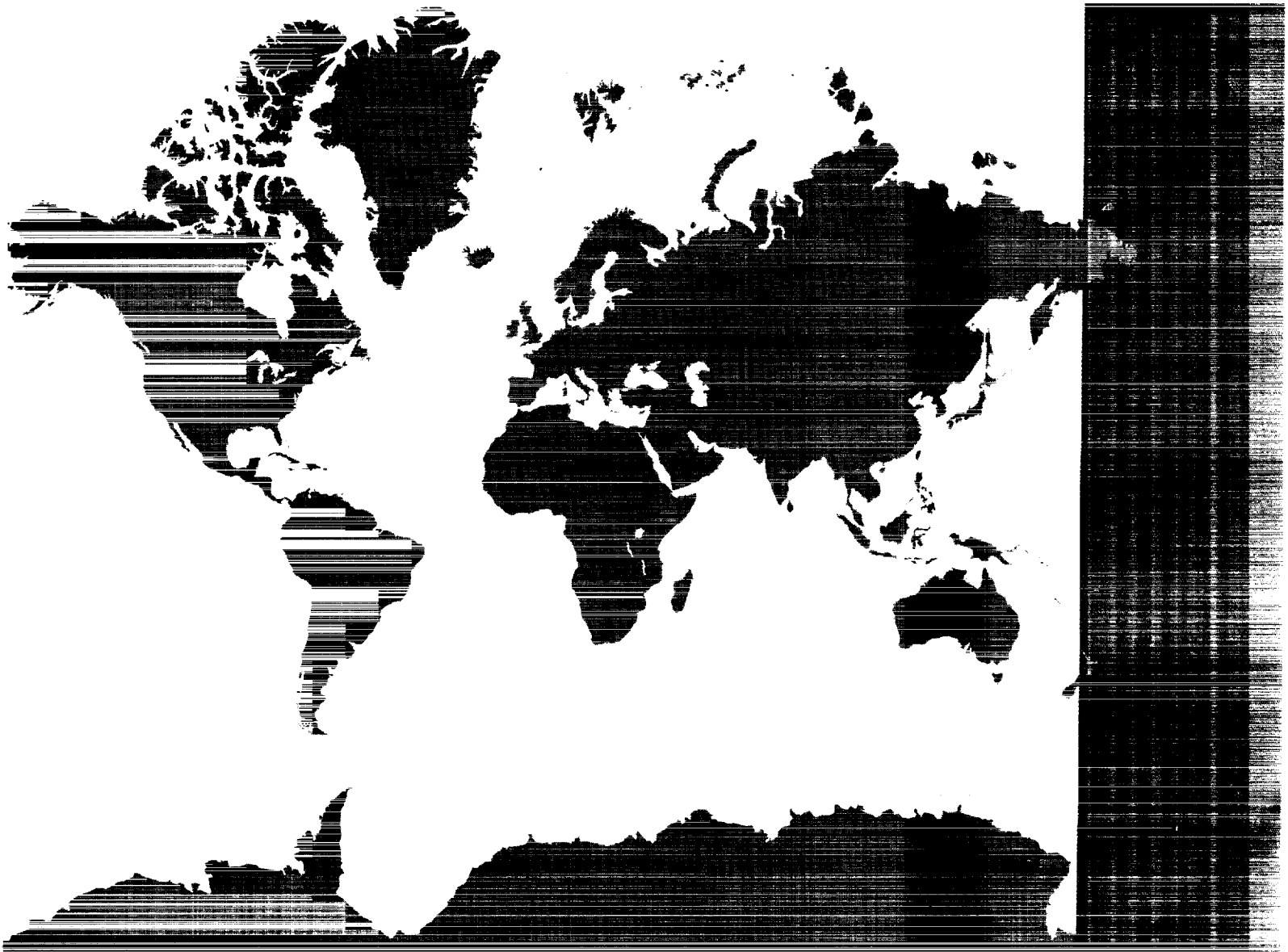

IVS

Ed Himwich: Network Coordinator Report, IVS 2000 General Meeting Proceedings, p.73–74
http://ivscc.gsfc.nasa.gov/publications/gm2000/himwich1

Network Coordinator Report

Ed Himwich

NVI, Inc./NASA Goddard Space Flight Center
e-mail: weh@vega.gsfc.nasa.gov

Abstract

This report summarizes the Network Coordination activities during the past six months, since the publication of the Annual Report (see Ref. [1]).

1. Network Coordination

The overall state of the network is good. The current IVS Network Stations are shown in Figure 1. There are no overwhelming problems at this time. However, there are some minor problems, some of which are chronic. Most stations survived the transition to Y2K without major incident. However, two station are still in the process of updating their software. Two areas of concern are that there is no centralized maintenance facility for the network and an aging antenna at Gilmore Creek that needs to be replaced. Both of these issues are being worked on.

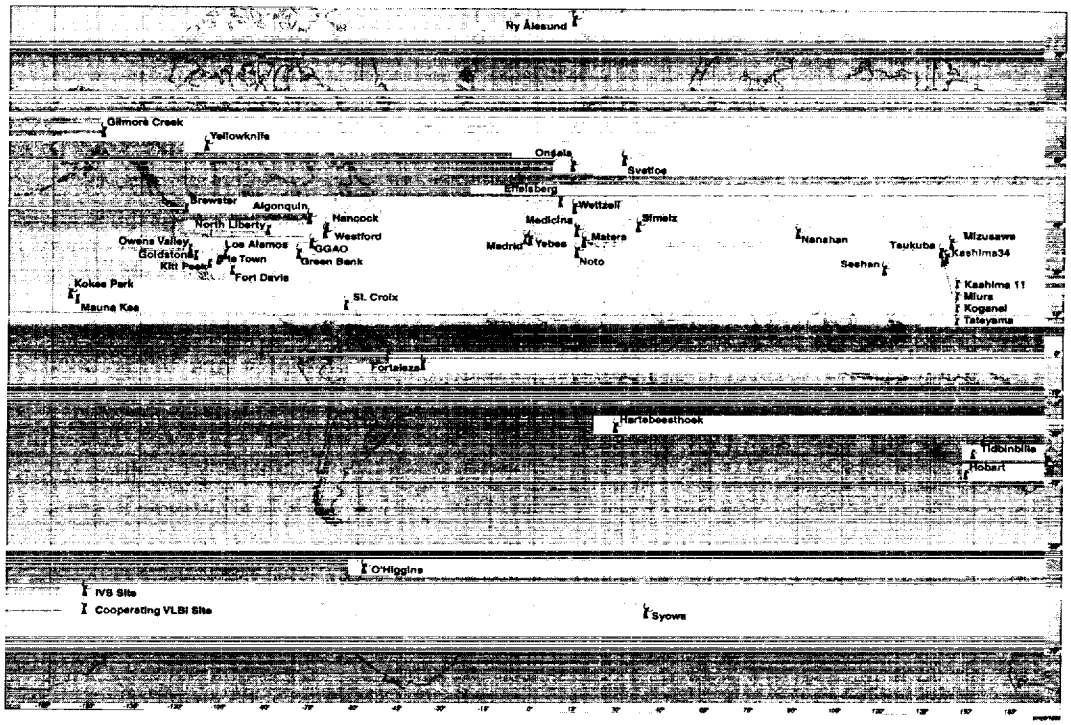

Figure 1. IVS Network Stations

2. Initiatives

There are several areas that are being developed. These include: performance standards, web-based performance plots, site visits, performance monitoring, collocation with other techniques, and site configuration databases.

The goal of performance standards is to give stations a tool for evaluating their own performance. This will developed first for IVS stations using the longitudinal recording systems Mark III, Mark IV, VLBA, and VLBA4. Once this is completed the standards will be expanded to include S2 and K4 systems. This approach is well matched to the distribution of equipment in the network. Relatively minor extensions are needed to expand the coverage to the additional systems. This also fits the resources available for this effort. The resulting standards should be useful for improving and maintaining data quality.

Web based performance data will provide an easy way to survey a summary of operational parameters for the stations. These are plotted for log data along with plots from the analysis results. This should assist trouble-shooting activities as well as make an archive of information on stations performance.

We are planning to organize site visits. These are important for maintaining high data quality at all the stations. Unfortunately, it is not possible to visit all stations as often as we would wish. This because of constraints both on funding and time. Stations will have to provides funds to help support visits. Ideally although we would like to visit every station every year, this is an impossible burden for the people involved. Even one visit every three years is too much. Instead visits will have to be planned on the basis of need and who can provide funds to support a visit. In order to help as many people and sites as possible benefit from the sites that are visited, we plan to make information about what was learned and what improvements were made available on the web.

Several people, including the Network Coordinator, have been monitoring "ops" messages, as well as correlator and analysis reports from observing sessions. Problems are referred to experts to assist their resolution. Web based performance data should assist with this activity.

We are trying to encourage collocation of other geodetic instrumentation at IVS sites. This is important for frame ties and other research including comparisons of time histories to find correlated signals.We are particularly trying to encourage all of the sites to become IGS sites as well if they are not already. IVS stations that currently do not have their own collocated IGS station can be divided into three categories: (1) stations that currently are being used or that have an existing history of measurements: NRAO20, CRIMEA, YEBES, and KASHIMA34, (2) stations that do not yet have any IVS measurements, these are all KSP stations: Kashima 11M, Koganei, Miura, and Tateyama, and (3) the transportable system: TIGOWTZL, which is currently at Wettzell and collocated there and will have its own IVS station with it wherever it goes. Clearly stations in category (1) are the highest priority candidates to become IGS stations.

We are developing a site configuration database that details the capabilities of the sites as well as other pertinent information such as other collocated geodetic systems.

References

[1] Vandenberg, N. R., "IVS Coordinating Center Report", in International VLBI Service for Geodesy and Astrometry 1999 Annual Report, edited by N. R. Vandenberg, NASA/TP-1999-209243, 1999.

Brian E. Corey: VLBI Electronics for Analysts: From the Feed to the Recorder, IVS 2000 General Meeting Proceedings, p.75–75
http://ivscc.gsfc.nasa.gov/publications/gm2000/corey1

VLBI Electronics for Analysts: From the Feed to the Recorder

Brian E. Corey

MIT Haystack Observatory

e-mail: bcorey@haystack.mit.edu

Abstract

This talk will describe how some of the critical electronic components in a VLBI system work, with an emphasis on analog electronics such as mixers, amplifiers, and phase calibrators. The ideal behavior of such devices will be described, as well as what the likely effects on VLBI observables are when a component fails or is used improperly (e.g., when an amplifier is overdriven). The basic principles of operation will be treated, without delving into the underlying semiconductor physics.

William T. Petrachenko: VLBI Data Acquisition and Recorder Systems: A Summary and Comparison, IVS 2000 General Meeting Proceedings, p.76–85
http://ivscc.gsfc.nasa.gov/publications/gm2000/petrachenko2

VLBI Data Acquisition and Recorder Systems: A Summary and Comparison

William T. Petrachenko

Natural Resources Canada, Geodetic Survey Division
e-mail: Bill.Petrachenko@hia.nrc.ca

Abstract

A brief description of each VLBI data acquisition and recorder system currently in use for geodetic applications (Mk3a/4, VLBA, K4, S2) will be provided. The similarities and differences between systems will be discussed and summarized in tables under the headings IF processing, baseband conversion characteristics, baseband processing capabilities, formatter capabilities, recorder characteristics, data quality analysis features and control characteristics.

1. Introduction

There are several VLBI Data Acquisition (DAS's) and recorder systems currently in use. In the Mk3 family there are the Mk3a, Mk4, VLBA, geodetic VLBA (VLBAg) and VLBA4. In the K4 family there are the K4-type1, K4-type2 and K4-VSOP. The S2 family, on the other hand, has only one official member. However, the S2 record terminals (RT's) have been interfaced to another DAS in reasonably widespread use, which was designed in Australia (S2Aus). Other than the fact that both of these DAS's interface to the S2 RT, they are unrelated. In addition, there are a few special purpose DAS's in existence. For example, in China, their transportable antenna uses an 8 BBC VLBA-style DAS which is interfaced to an S2 recorder; and, in the countries of the former USSR, there are a variety of DAS's which have been summarized in Table 1.

Antenna	Diameter(m)	Data Acquisition System	Recorder	S/X
Bear Lakes	64	1 BBC (2,4,8 MHz)	Mk2, S2	Soon
Evpatoria, Ukraine	70	Mk2	Mk2	Y
Kalyazin	64	K4-1, Australian DAS	K4-1, S2	Y
Puschino	22	4 BBC (2,4,8 MHz)	Mk2, S2	
Simeiz, Ukraine	22	Mk3	Mk2, Mk3, K4, S2	Y
St. Pustyn	14	1 BBC (2,4,8 MHz)	Mk2	
Svetloe	32	2x2 BBC (2,8,16 MHz)	S2	Y
Ussuriiysk	70			Y
Venspils, Latvia	32	Mk2	Mk2	
Zelenchukskaya	32	Antenna not complete		
Zimenki	15	Mk2	Mk2	

Table 1. DAS's in countries of the former USSR.

2. Brief Description of the Major VLBI Systems in Use Today

In this section, the major VLBI systems in use today will be described very briefly. Further details can be found in later sections where the similarities and differences between systems are discussed and summarized in tables.

2.1. The Mk3 Family

The Mk3 family of systems is characterized by its use of a large number of baseband converters (BBC's) and a multi-track longitudinal tape drive. [Note: the term BBC and video converter (VC) refer to the same thing.] In geodesy, a large number of BBC's are used to synthesize the wide effective IF bandwidths required to achieve high precision in the determination of the delay observable. Physically, the Mk3 systems are packaged in two 6' high racks. One rack holds the DAS and the other holds the recorder. All DAS modules are packaged in VLA-style bins and the rack is permanently wired using NIM connectors so that no cables need to be connected or disconnected when modules are exchanged. The recorder uses a modified Metrum 9600 transport equipped with a 36-head narrow track headstack which is capable of recording up to 16 passes on a tape with all heads enabled. Data are stored on 1" wide tape wound on 14" diameter open reels. There are 8 BBC's in the VLBA system and 14 in each of the Mk3a, Mk4, VLBAg and VLBA4 systems.

2.2. The K4 Family

Although there are also a large number of BBC's in the K4 system, it uses a single helican scan high data rate recorder. The modularity of the system is considerably different from the Mk3 family. In the Mk3 family, each BBC is packaged separately and is more or less self-contained. In the K4 family, BBC functions are grouped together in separately packaged modules. For example, one module contains a large number of LO's, another contains a large number of image reject mixers (IRM's), etc. [Note: an IRM refers to the same thing as a single sideband mixer (SSBM).] All DAS modules are packaged in 19" rack-mountable assemblies. Signal interconnections between assemblies is achieved using individual coaxial cables. The K4 uses a DIR-1000 series helical scan data recorder designed by Sony to VLBI specifications. The recorder is capable of a maximum data rate of 256 Mb/s at error rates better than 1×10^{-10} using error correction. Data are recorded on easy to handle 19 mm D-1 cassettes. In the K4-type1 system, BBC components are grouped in units of 16. In the K4-type2 and K4-VSOP systems, BBC components are grouped in units of 8.

2.3. The S2 Family

The S2 system is unique in its use of a small number of BBC's and a recorder made up of an array of 8 modified SVHS helican scan transports. Although there are only a small number of BBC's in the system, the LO in each BBC has been designed to switch frequencies rapidly so that a wide effective bandwidth can be synthesized by cycling each BBC LO through a sequence of frequency settings. Because the sequences are flexible, the system is very adaptable. The S2 DAS is packaged in a single 19" wide 9U high rack-mountable VME cage. The recorder uses proven, reliable SVHS industrial transports and is packaged in a transportable configuration which includes three 19" rack-mountable modules each weighing less than 37 kg. Data are recorded on

inexpensive easy to handle SVHS cassettes. A large amount of functionality is included in each BBC. In addition to LO's, SSBM's and baseband filters, it includes samplers and data quality analysis (DQA) functions. Each system can be outfitted with 1-4 BBC's, 2 being recommended for most applications.

Since the S2 record and playback terminals (RT and PT) are inexpensive and easy to interface and operate, they have also become an integral part of the Australian VLBI system. The Australian DAS is a very capable DAS for astronomy applications. Unfortunately, it lacks any means of synthesizing the wide effective bandwidths required by geodetic applications of VLBI. It is, however, reasonably widespread in the southern hemisphere, and will be included here. The Australian S2 DAS is almost completely digital.

3. Similarities and Differences between Systems

3.1. IF Processing

IF processing characteristics of the systems are summarized in Table 2. The column labeled Mk3 includes both the Mk3a and the Mk4 systems, the column labeled VLBA includes the VLBA, VLBAg and VLBA4 systems, and the column labeled K4-2 also includes the K4-VSOP system. IF processing in the Mk3 systems is somewhat more complicated than the others in that it includes 2 IF inputs with frequency range 100-500 MHz and 1 IF input with frequency range 600-900 MHz. The latter IF was added after the fact, when the X-band spanned bandwidth was increased from 360 MHz to 720 MHz. Even with the inclusion of the extra IF channel, 100 MHz of the wide X-band IF is still missing. As it turns out, this has no practical impact on bandwidth synthesis. In the S2 system, the wide X-band IF can be handled naturally since the frequency range of each IF input is 100-1000 MHz. In all other systems, wide IF's must be handled by band-splitting and frequency translation external to the system.

Parameter	Mk3		VLBA	K4-1	K4-2	S2	S2Aus
Number of Inputs	2	1	4	4	3	1-4	2
Freq. Range (MHz)	100-500	600-900	500-1000	100-500	500-1000	100-1000	<192
Sub-bands (MHz)	94-224	–	–	100-230	–	–	–
	216-504	–	–	200-520	–	–	–
Translation (MHz)	–	-500.1	–	–	–	–	–
Fan-out per Sub-band	7	4	8	4	8	4	–
Attenuation Range (dB)	0-63	0-63	0-20	0-15	Ext	0-30	na
Attenuation Step Size (dB)	1	1	20	1	Ext	2	na
Number of IF Total Power Detectors	2	1	4	4	Ext	1-4	none
IF Selection Method	Patch Panel		Electronic Switch	Cable Connect	Cable Interconnect	Electronic Switch	Direct

Table 2. IF Processing

Although the frequency range for the K4-type2 IF inputs is specified as 500-1000 MHz, an

option for 100-500 MHz inputs is also available.

Notice that sub-band filtering is included in a few systems. This is done to avoid contamination from third harmonic response of the SSBM's. Although it appears that this should be necessary in the S2 system as well, a two-step frequency conversion to baseband avoids third harmonic contamination at all frequencies.

In most of the systems, IF assignments to BBC's are handled by manual cable connections. However, in the VLBA systems and the S2 DAS the assignment is done by electronic switches. In the VLBA this was done because systems must be able to change operating modes remotely. In the S2 system, it was done because bandwidth synthesis is accomplished by frequency switching. Since, in general, switching sequences will include both X-band and S-band inputs, it must be possible to switch between these inputs automatically.

3.2. Baseband Conversion Characteristics

Baseband conversion characteristics for the systems are summarized in Table 3. Most entries in the table are self-explanatory. The exception is the column for the S2Aus system. In this case, baseband conversion is not accomplished in the normal way. Early in the signal path, an appropriately filtered IF signal is sampled with a high speed digitizer. If the IF signal is above the sampling frequency, it will be aliased to baseband. This is a form of baseband conversion in which the implied LO frequency is an integer multiple of the sampler frequency. Additionally, in the S2Aus DAS, an LO and mixer are implemented digitally such that, in effect, any frequency within the sampler bandwidth can be converted to baseband.

Parameter	Mk3	VLBA	K4-1	K4-2	S2	S2Aus
Number of BBC's per System	14	8:VLBA 14:VLBAg 14:VLBA4	16	16	1-4	2
Input Selector Switch	no	4:1	no	no	4:1	no
LO Range (MHz)	100-500	500-1000	100-500	500-1000	100-1000	0-64
LO Step Size	10 kHz	10 kHz	10 kHz	10 kHz	1 Hz	1 Hz
LO Settling Time	<4s	<1s	na	na	<1ms	Digital
No. of Mixer Stages	1	1	1	1	2	na
Conversion Method	SSBM	SSBM	SSBM	SSBM	SSBM	Aliased Sampler
Outputs per BBC	U/LSB	U/LSB	U/LSB	U/LSB	U/LSB	1 or 2
SSBM BW (MHz)	8:Mk3a 16:Mk4	16	8	32	16	na

Table 3. Baseband Conversion Characteristics

With the exception of the S2Aus DAS all systems produce two baseband channels per BBC, i.e. one USB and LSB. Since the S2Aus DAS does not use conventional baseband conversion, in certain modes it only has one baseband output per "pseudo" BBC.

Note that the S2 LO settling time is <1ms to enable frequency switched bandwidth synthesis.

3.3. Baseband Processing Capabilities

Baseband processing capabilities for the systems are summarized in Table 4 and output bandwidths are summarized in Table 5. Baseband processing systems can be divided into two distinct classes, one in which the baseband filters are implemented digitally and the other in which they are inplemented using analog circuits. In the digital systems, a fixed antialias filter and high resolution high speed fixed rate sampler are implemented early in the signal path. The digitized signal is then passed through finite impulse response (FIR) filters, requantized and decimated in time to produce an output sample rate which is double the filter bandwidth, i.e. the signal is Nyquist sampled. The amplitude and phase response of the digital baseband channels is very well controlled since filtering is done digitally. In analog systems, the antialias filters are of selectable bandwidths and, in fact, define the baseband bandwidth of the channel. In some analog systems the sample clock rate is programmable while in others it is fixed at the maximum sample rate. In the latter case, the output sample rate is generated through decimation, i.e. samples at regular intervals are simply discarded.

Parameter	Mk3	Mk4	VLBA	VLBAg	VLBA4	K4-1	K4-2	S2	S2Aus
Digital Filters							•		•
No. of Antialias Filters	28	28	16	28	28	32	16	2-8	2
Antialias Filter BW (MHz)	see Tbl 5	see Tbl 5	see Tbl 5	see Tbl 5	see Tbl 5	see Tbl 5	32	see Tbl 5	42
No. of BBC Total Power Detectors	28	28	16	28	28	4	4	2-8	0
Gain Control Range (dB)	10	≈25	54	54	54	15	15	54	12
Automatic Gain Control		•	•	•	•			•	•
No. of Samplers	28	28	16	28	28	16	16	2-8	2
Native Sample Rate (Ms/s)	0.25-8.0	0.5-32.0	32	32	32	4	64	32	128
Output Sample Rate (Ms/s)	0.25-8.0	0.5-32.0	0.5-32.0	0.5-32.0	0.5-32.0	4	Nyquist	4-32	Nyquist
No. of Native Digitizer Bits	1	2	2	1,2	2	1	8	2	8
No. of Output Digitizer Bits	1	1 or 2	1 or 2	1, 1 or 2	1 or 2	1	1, 2, 4 or 8	1 or 2	1 or 2

Table 4. Baseband Processing Capabilities

With the exception of the K4 system, all other systems have one digitizer per baseband channel. In the case of the K4 system, there are half as many digitizers as baseband channels. The selection of which baseband channels to digitize is accomplished by physical coaxial connections between the video converter module and the input interface unit where the digitizers are located.

In all systems, there is some ability to vary the baseband signal amplitude to keep it within the dynamic range of the digitizers. This is most critical for the 2-bit samplers since the $\approx 1\sigma$ level of the signal must be maintained near the $\pm$V digitizer threshold voltages to achieve optimum performance in the correlator.

With the exception of the S2Aus DAS, all systems have the ability to monitor the total power of each baseband channel. This is useful for radiometry and interference monitoring.

Since the VLBAg system can handle a total of 32 sampled bits in the formatter and there are a total of 28 baseband channels, it is not possible to 2-bit sample all channels. As a result the VLBAg sampler was designed to 2-bit sample two channels and 1-bit sample the rest. This allows the VLBAg systems to be compatible with VSOP modes in 2 baseband channels and Mk3a modes in up to 28 baseband channels.

Bandwidth (MHz)	Mk3a	Mk4	VLBA	K4-1	K4-2	S2	S2Aus
0.0625			•			•	•
0.125	•	•	•		•	•	•
0.250	•		•		•	•	•
0.500	•	•	•		•	•	•
1.0	•		•		•	•	•
2.0	•	•	•	•	•	•	•
4.0	•	•	•	•	•	•	•
8.0		•	•		•	•	•
16.0		•	•		•	•	•
32.0					•		•

Table 5. Output Bandwidths

3.4. Formatter Capabilities

Formatter capabilities for the systems are summarized in Table 6. Fan-in refers to the ability to record more than one sampled bit stream on a single track and fan-out refers to the ability to use more than one track to record a single sampled bit stream.

Barrel roll refers to the ability to cyclically change the assignment of sampled bit streams to tracks and then to undo the process at the time of playback. With barrel roll, a single track failure will degrade all sampled bit streams equally. Without it, a single track failure can lead to the complete loss of one sampled bit stream which can seriously degrade bandwidth synthesis performance. (Note: For the S2, the word transport should be substituted for the word track in the above text.)

Modulation refers to the process of combining a bit stream with a pseudo random sequence prior to recording and then undoing the process at the time of playback. This may improve data and clock recovery for some conceivable signal patterns such as all zeros.

Time codes are formatted differently from system to system. See Table 7. In this table, Y refers to digits of the year, D refers to digits of the day of the year, H refers to digits of the hour, M refers to digits of the minute, S refers to integer digits of the second, s refers to fractional digits of the second and J refers to the last 3 digits of the Julian date. In VLBA time codes, SSSSS refers to the second within the day.

Parameter	Mk3a	Mk4 VLBA4	VLBA VGLBg	K4-1	K4-2	K4-VSOP	S2
Max Fan-in	1:1	4:1	4:1	16:1	16:1	16:1	4:1
Max Fan-out	1:1	1:4	1:4	na	na	na	1:2
Barrel Roll		•	•				•
Across Track Parity			•				
Modulation		•	•				•
Data Replacement	•	•		•	•		

Table 6. Formatter Capabilities

Mk3a/Mk4/VLBA4	VLBA/VLBAg	K4-1/K4-2	S2
YDDDHHMMSSsss	JJJSSSSSssssss	YYDDDHHMMSS	YYYYDDDHHMMSS

Table 7. Time Format

3.5. Recorder Characteristics

Recorder characteristics for the systems are summarized in Table 8. Note the variation between allowable record and playback speeds among the systems. These are significant since they impose important limitations when considering compatible modes among the recorder systems.

Parameter	Mk3/VLBA	K4	S2
Recorder Type	Longitudinal	Helical	Helical
Transport	Modified Metrum 9600	ID-1	Modified SVHS
Max Record Rate (Mb/s)	224: Mk3a 1024: Mk4 256: VLBA	256	128
Bit Error Rate Spec	$< 3 \times 10^{-4}$	$< 1 \times 10^{-10}$	$< 1 \times 10^{-4}$
Error Correction	no	yes	no
Tape Package	14" Reel	D1-L Cassette	SVHS Cassette
Ship Weight - 24 hrs at 128 Mb/s (kg)	10	20	9
Tape Package Volume - 24 hrs at 128 Mb/s (cm^3)	5.8×10^3	29.9×10^3	16.9×10^3
Record Time at 128 Mb/s (hrs)	12	2	6
Tape Changer	no	yes	no
Record Speed	Mode dependent	Mode dependent	Fixed
Playback Speed	Fixed	Variable	Fixed (same as record speed)

Table 8. Recorder Characteristics

The development of high density helical scan recorders was supported by both commercial and industrial interests. The same was not true for high density longitudinal recorders where the primary motivation for development was from the VLBI community. As a result, VLBI developers and users have been forced to acquire considerable expertise in these systems and a greater degree of detail is of interest when describing and comparing these systems. See Table 9. Note that a data rate of 16 Mb/s, tape speed of 320 ips and a longitudinal bit density of 56,250 bpi can only be achieved when using thin tape.

Parameter	Mk3a	Mk4	VLBA/ VLBAg	VLBA4
No. of read headstacks	1	0	0	0
No. of write headstacks	1	1	0	1
No. of read/write headstacks	0	1	1	1
No. of heads/headstack	36	36	36	36
Head width (μm)	38	38	38	38
Head spacing (μm)	698.5	698.5	698.5	698.5
Positioner range (μm)	$\pm$1397	$\pm$1397	$\pm$1397	$\pm$1397
Positioner precision/ accuracy (μm)	$\pm$2	$\pm$2	$\pm$2	$\pm$2
Thin tape	–	•	–	•
Max data rate/track (Mb/s)	8	16	8	16
Max tape speed (ips)	270	320	270	320
Max longitudinal bit density (bpi)	33,333	56,250	33,333	56,250
No. of passes	12	16	14	16
Max no. of tracks per pass	28	64	36	64

Table 9. Longitudinal Recorder Characteristics

3.6. Data Quality Analysis (DQA) Features

In VLBI, it is difficult to know whether data is being recorded properly at the radio antennas. This is only known for certain after tapes have been shipped to a correlation site and processed. To reduce the risk of making errors when recording data, a number of data quality analysis features have been built into VLBI systems. These are summarized in Table 10.

All systems have plentiful front panel monitor points where signals can be connected to oscilloscopes, spectrum analyzers, counters, etc.

In the S2 system, the cable between the DAS and RT can be verified by injecting a pseudo random signal at the DAS and detecting it at the RT. The same cable can be verified indirectly in the Mk3 family of systems. There is one cable from the formatter to the recorder and another cable from the recorder to the decoder. If data returned to the decoder is decoded properly this indicates that both cables are functioning.

In Mk3 systems, buffers are included which can store data which is either generated directly in the formatter or has been recovered from the recorder. The stored data can either be used for

real time fringe tests using electronic transmission to a correlation site or for detailed analysis of the data at each site. The S2 system allows extraction of 4 bytes of data at a time.

The detection of PCAL tones at record sites is a powerful measure of system coherence. In the Mk3a system, an ad hoc method of detecting phase cal tones was developed which involved the use of an external 10 kHz filter and an oscilloscope. All other systems either have or plan to have PCAL detectors built into the systems. Each VLBA DAS can have up to 8 PCAL detectors in 2-bit mode and 16 PCAL detectors in 1-bit mode. It is also possible to reconfigure the PCAL detectors as stream statistics accumulators but the total number is limited to 8 (2-bit) or 16 (1-bit).

Stream statistics accumulators are useful with 2-bit sampling to determine the fraction of samples which have been taken in each of the four possible digitizer states. This verifies that the signal level has been set properly and that DC bias is at an acceptable level.

Parameter	Mk3a	Mk4/ VLBA4	VLBA/ VLBAg	K4	S2
Front Panel Monitor Points	•	•	•	•	•
Recorder Cable Verification	Indirect	Indirect	Indirect	–	•
Data Buffer Size (Bytes)	0.125M	60M	0.5M	0	4
Number of PCAL Detectors	External Filter	4 Future	8/16 (2)	2	2 per BBC
PCAL Frequency	10 kHz	Future	10 kHz increments	10 kHz	1 Hz increments
Number of Stream Statistics Counters	0	4	8/16	0	2 per BBC
Tape Error Rate Estimate	•	•	•	•	•
Formatter/Tape Read-back (Time, Aux Data)	•	•	•	–	•
Cable Cal	•	•	•VLBAg	•KSP	Future

Table 10. Data Quality Analysis Features

3.7. Control Characteristics

Control characteristics for the systems are summarized in Table 11.

Note that although the S2 system has no manual control, it has extensive high level and low level control options using a console attached either through an RS232 port or via Ethernet.

In general, automatic control of the Mk3a and Mk4 is accomplished using the MAT, automatic control of the VLBA and VLBAg is accomplished using the MCB, automatic control of the K4 systems is accomplished using the GPIB, and automatic control of the S2 system is accomplished using the Recorder Control Link. The VLBA4 system uses both the MCB and MAT since most

of the modules in the system are VLBA designs, but the formatter is Mk4.

Parameter	Mk3a/ Mk4	VLBA/ VLBAg	VLBA4	K4	S2
Scheduling support	•	•	•	•	•
PCFS Support	•	•	•	•	•
Manual Control	•			•	
Console Control (RS232/Ethernet)					•
Microprocessor Ascii Transceiver (MAT)	•		•		
Monitor Control Bus (MCB)		•	•		
GPIB IEEE488)				•	
Recorder Control Link					•

Table 11. Control Characteristics

4. Acknowledgements

The information for this paper was accumulated from numerous sources including manuals, data sheets, papers and web sites. Where the written information was incomplete, I was able get valuable assistance from individuals. In this regard I would like to thank Alan Whitney, Dan Smythe and Brian Corey from Haystack Observatory, Jon Romney and George Peck from NRAO, Tetsuro Kondo, Hitoshi Kiuchi and Mamoru Sekido from CRL, Georg Feil from CRESTech, Rick Wietfeldt from JPL, Igor Molotov from the Astro-Space Centre, Qian Zian from Shanghai Observatory, Dick Ferris from ATNF and Hayo Hase from BKG.

Ed Himwich: Introduction to the Field System for Non-Users, IVS 2000 General Meeting Proceedings, p.86–90
http://ivscc.gsfc.nasa.gov/publications/gm2000/himwich2

Introduction to the Field System for Non-Users

Ed Himwich

NVI, Inc./NASA Goddard Space Flight Center
e-mail: weh@vega.gsfc.nasa.gov

Abstract

This report provides a brief description of the Field System (FS) for non-users. The Field System (FS) is a suite of programs that provides the coordinating control of VLBI data acquisition at many stations. The basic features of the FS and experiment operations are described. Areas for future development are listed.

1. Basic Features

The Field System (FS) is a software package that provides an interactive and automated control of VLBI stations. The control language is Standard Notation for Astronomical Procedures (SNAP). The FS supports a wide variety of VLBI back-ends. The FS can be adapted to support unique hardware and the antenna found at virtually every station. All events are recorded in an ASCII log with time-stamps. An antenna independent package of programs is provided for pointing and sensitivity measurements. Schedules are provided that automate calibration of the supported longitudinal VLBI recorders. A significant feature of the FS which reduces its cost considerably is that it runs on the free (and freely available) Linux operating system.

2. Supported Equipment

The FS supports a plethora of VLBI back-ends. For practical purposes the FS divides the back-end into two parts: the Data Acquisition System (DAS) and the recorder. The supported DASs include: Mark III, Mark IV, VLBA (including VLBAG), VLBA4, and K4. The supported recorders include: Mark III, Mark IV, VLBA, VLBA4, S2 and K4. In addition the FS can support a second longitudinal recorder, any of: Mark III, Mark IV, VLBA, and VLBA4.

3. Station Adaptation

The FS provides several features that are useful for adapting or customizing it for a particular station. The most fundamental of these is that it is organized into station independent and station dependent parts. The station independent parts provide the basic support for the VLBI back-ends. The station dependent parts can be customized to support the different hardware and antenna interface that is found at a particular station. Distribution of the FS respects the station independent and dependent split. Typically updates only require recompiling and relinking any station dependent programs.

The most important part of the station dependent software is the ANTenna CoNtrol program (ANTCN). The design of the ANTCN program is such that once it is properly implemented at a station, the antenna has certain standard features from the FS's point of view. Once these features

exist, control of the antenna from a schedule and for pointing and sensitivity measurements can be carried out in a station independent fashion.

In addition to ANTCN, there can also be station specific SNAP commands, error messages, control files, equipment checking, and background programs that support the local station environment.

4. SNAP Command Language

The operator and schedule driven interface for the FS utilizes the Standard Notation for Astronomical Procedures (SNAP) command language. Experiment operations are conducted from "schedule files". Testing and equipment set-up is performed with a combination of interactive commands and schedules.

5. SNAP Procedures and Schedules

SNAP commands can be collected together in "procedures" which function as macros of commands to reduce typing of common operations. SNAP schedules contain typically longer sequences of commands such as those needed to carry out an entire observing session.

6. SNAP Syntax

Each command in SNAP starts with a keyword that is usually associated with a hardware module or sub-module. The keyword may also represent a more abstract concept such as a measurement process. Each keyword can typically be used in one of two forms. The first form is to command the set-up of the module and consists of the keyword followed by an equals sign (=), followed by one or more comma delimited parameters. For example:

```
keyword=parameter1,parameter2,...
```

The meanings of the parameters are determined by their order in the list. Usually required parameters are first in the list to minimize the amount of typing necessary. Many parameters may be omitted if sensible defaults exist. Such a command generally doesn't produce a visible response unless there is an error. The approach here is similar to that in UNIX, that "no news is good news".

The second form of a command is to monitor the state of a module. In this case, just the keyword is entered:

```
keyword
```

The response is in the form:

```
keyword/parameter1,parameter2,...
```

The parameters represent the state of the module. Adjustable parameters which can be set by the user are listed first in the same order that they are used in the set-up command form. Addi-

tional parameters that represent information that can only monitored, but not set (e.g., square-law detector power levels) follow.

7. Log File Output

All events that occur are recorded in an ASCII time-tagged log file. The recorded events include operator or schedule issued commands, command responses, and errors. The log file lines are divided into three parts: the time-tag, the type character, and the data. The example below shows a small fragment from a log:

```
2000.010.12:34:56.34;ifd=20,20
2000.010.12:35:10.34;ifd
2000.010.12.35:10.56/ifd/20,20,nor,nor,rem,2785,17345
```

This example shows three log entries. The first is a set-up command that sets the attenuation for the "ifd" module. The semi-colon ";" character between the time-tag and the "ifd=20,20" is the type character which in this case indicates that the command came from the operator rather than a schedule. The second entry is a command to monitor the state of the "ifd" module, again from the operator. The last entry is a monitor response for the "ifd" module. It shows that the attenuators are in fact set for 20 and 20 as previously request. Then some other settable parameters followed by some monitor only parameters are shown. In this case the type character is a slash "/" which indicates this is a module response. Other type characters which are typically seen include colon ":" which indicates a command that came from a schedule and question mark "?" which indicates an error message.

8. Operational Use - Session Preparation

The normal flow of operations begins with the schedule writer (more commonly called the P.I. by astronomers) who provides a VEX or optionally, a Mark III format schedule file (*.skd or *.drg). The schedule file is deposited on a data center server. The stations pick up the schedules from the server.

At each station the DRUDG program is run to create a SNAP schedule (*.snp) and a corresponding session procedure file (*.prc).

Just before the experiment begins the operator makes any necessary manual preparation, connecting cables, setting switches that are not computer controlled, etc.

Figure 1 shows a typical operator at the FS console.

9. Operational Use - Session

Once everything is ready the operator starts the schedule with the "schedule=..." command. The SNAP schedule is run by the FS and the back-end equipment is all set up automatically. Operators usually perform certain "pre-checks" to verify correct operation of the system and check the sign of the cable before the first scan is recorded.

The session runs with the FS controlling the antenna and the back-end. Monitor data and some ancillary data such as cable calibration are placed in the log file (*.log). During the session

operator intervention is normally only required to change tapes or to restart the system if a serious fault such as a power failure should occur.

Figure 1. Seated at the FS console is a typical operator, taking a rest from being the Local Organizing Committee of the first IVS General Meeting.

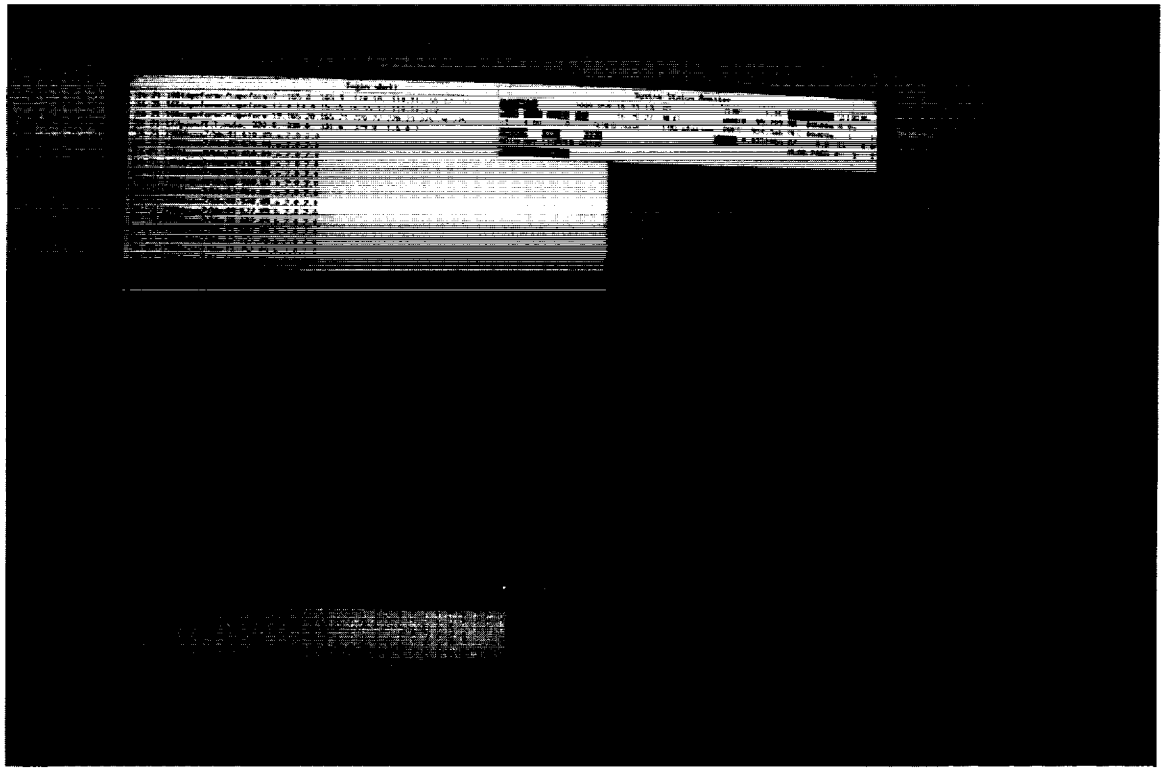

Figure 2. Typical FS console display.

The typical display the user sees when the FS is running is shown in Figure 2. The display includes a small operator in/out window in the lower left corner, a log display and output window, a larger window in the upper left, and a status and monitor display in the upper right. FS displays vary in size; on most systems these windows take up most of the display.

10. Operational Use - End of Session

After the session the operator may perform some final checks to verify that the system is still healthy. Data from the log file (*.log) is plotted to verify that none of the ancillary data types has developed a problem. The log file is placed on the data center server for use by the correlator and analysts. The tapes are sent to the correlator.

11. Future Improvements

Several improvements in the FS are planned in the fairly near term. These include: (1) automated Tsys measurements, (2) remote operation, (3) more automation, (4) a new utility to standardize "ops" messages, (5) improved log display and searching, (6) S2 DAS support, (7) more test software, and (8) control structures and variables in SNAP.

Session 3

Technology Development

Alan R. Whitney: Technology Coordinator Report, IVS 2000 General Meeting Proceedings, p.93–97
http://ivscc.gsfc.nasa.gov/publications/gm2000/whitney3

Technology Coordinator Report

Alan R. Whitney

MIT Haystack Observatory
e-mail: awhitney@haystack.mit.edu

Abstract

Much progress has been made over the last year in defining a "VLBI Standard Interface" specification. This specification, a joint effort between the geodetic and astronomy VLBI communities, is being developed in an effort to specify standard interfaces to/from a VLBI "data transmission system" so that data collected on inhomogeneous systems can be processed together at a correlator. The first step of defining a hardware interface is almost complete, and efforts at software standardization are planned. This presentation will explain the philosophy of the VSI as well as some of the details of the interface specification. Though it will take some years before all VLBI systems adhere to VSI, this step should lead to an eventual major improvement in worldwide VLBI compatibility.

1. Introduction

Over the past year the IVS Technology Coordination effort has been dominated by a concerted effort to define a VLBI Standard Interface (VSI). This effort has been international in scope and has involved the contributions of several groups. The first part of this effort, to define the hardware interfaces (so-called VSI-H), is nearing completion and is expected to be approved within the next few months. A standardized software interface (dubbed VSI-S) will follow.

2. Goals of VSI

The VSI specification is being designed to achieve the following goals:

- To define a standard interface to and from a VLBI Data Transmission System (DTS) that allows heterogeneous DTS's to be interfaced to both data-acquisition and correlator systems with a minimum of effort.
- To be compatible with all potential forms of data transmission, including traditional recording/playback systems, network data transmission and even direct-connect systems.
- To largely or completely hide the detailed characteristics of the DTS and allow the data to be transferred from acquisition to correlator in a transparent manner.
- To be expandable to arbitrarily high data rates that may be supported by future systems.

VSI is *not* intended to be completely "plug and play" at the first level of implementation, but instead should help to relieve many of the existing incompatibilities that now exist between various VLBI data systems. The VSI specification is primarily aimed at normal data-taking and data-correlation tasks commonplace to VLBI. However, other activities such as media translation (tape copying, for example) and parallel operation of multiple DTS's is also addressed. The VSI specification is being developed as a joint effort between the geodesy and astronomy communities, spearheaded by IVS and GVWG (Global VLBI Working Group).

3. The VSI Process and Schedule

The following summarizes the VSI process and schedule:

- Draft proposal created Feb 1999 as a result of informal meetings held at Jan 99 GEMSTONE meeting.
- VSI committee selected with wide international representation from both geodetic and astronomy communities.
- Decision to separate hardware (VSI-H) and software (VSI-S) specifications; do VSI-H first.
- Primary communications via e-mail.
- Several iterations of draft VSI-H have been circulated.
- VSI-H meeting held at Haystack end of January 2000 with representatives from Japan, Canada, Europe, Australia and U.S.
- Review of final draft specification in progress.
- Submission to IVS and GVWG for final approval expected in first half 2000.
- Work to begin on VSI-S specification in near future

4. VSI-H Committee

The VSI-H committee consists of representatives from both the geodesy and astronomy communities and from all groups actively involved in the design of VLBI data systems. In order to maintain a reasonable size and broad representation, appointment to the committee was limited to a single individual per organization:

Wayne Cannon	York University	Canada
Brent Carlson	DRAO	Canada
Dick Ferris	ATNF	Australia
Dave Graham	MPI	Germany
Tetsuro Kondo	CRL	Japan
Nori Kawaguchi	NAO	Japan
Misha Popov	ASC	Russia
Sergei Pogrebenko	JIVE	Netherlands
Jon Romney	NRAO	U.S.
Ralph Spencer	Jodrell	England
Rick Wietfeldt	JPL	U.S.
Alan Whitney	Haystack	U.S.

Of course, the VSI-H work carried out at these institutions has also involved a large number of other people who have also contributed to the VSI definition.

5. VSI-H Assumptions

The starting point of the VSI specifications is a set of four simple declarations about the generic characteristics of a VLBI data-transmission system:

- The VSI Data Transmission System (DTS) is fundamentally a receiver and transmitter of parallel bit streams between a Data-Acquisition System (DAS) and a Data Processing System (DPS).
- The meaning of individual bit streams is not specified; normally, a bit-stream will be a stream of sign or magnitude bits associated with particular samples, but the actual meaning is to be mutually agreed upon between the DAS and DPS.
- The received and transmitted bit-stream clock rates may be different (e.g. the playback rate into the DPS may be speeded-up or slowed-down), however all bit-stream clock rates on acquisition must be the same, and all bit-stream clock rates on transmit must be the same.
- A single time-tag applies to all parallel bit streams. The DAS time-tag of every bit in every bit-stream must be fully recoverable at the output of the DTS.

With these assumptions as a starting point, the VSI-H specification was developed.

6. VSI-H Basics

The basic model of a VSI-H data-transmission system is shown in Figure 1. For purposes of the specification, the DTS is divided into two logical modules:

- The "Data Input Module" (DIM) is responsible for accepting multiple parallel bit streams, accompanied by a common clock and common 1-second tick, applying a common time-tag ("observe time"), and sending them to a *transmission medium* (tape, disc, fiber-optic, etc.).
- The "Data Output Module" (DOM) accepts data from the transmission medium, decodes the accompanying "observe-time" information, and recreates the data-streams in accordance with an external clock and "1-second" tick.

The DIM and DOM may reside either in a single physical module or in separate physical modules. The details of the interfaces shown in Figure 1 are contained in the VSI-H specification itself, which we won't go deeply into here. However, it is useful to point out some of the features and characteristics which result from the specification:

- A "quantum channel" is defined whose data-rate capacity is 1.024 Mbits/sec. A DTS may include one or more "quantum channels" to reach arbitrarily high data rates.
- One standardized 80-pin connector is used for each "quantum channel"
- The signal and timing interfaces to/from the DTS are all defined using the LVDS (low-voltage differential signal) standard that is now popular in the computer industry.
- The method of time-tagging the data is entirely internal to the DTS and is not specified by VSI-H.
- The method of data transmission between the DIM and DOM is entirely internal to the DTS and is not specified by VSI-H. This allows for any conceivable media or transmission method, including tape, disc, fiber-optic, Internet, or any other method.

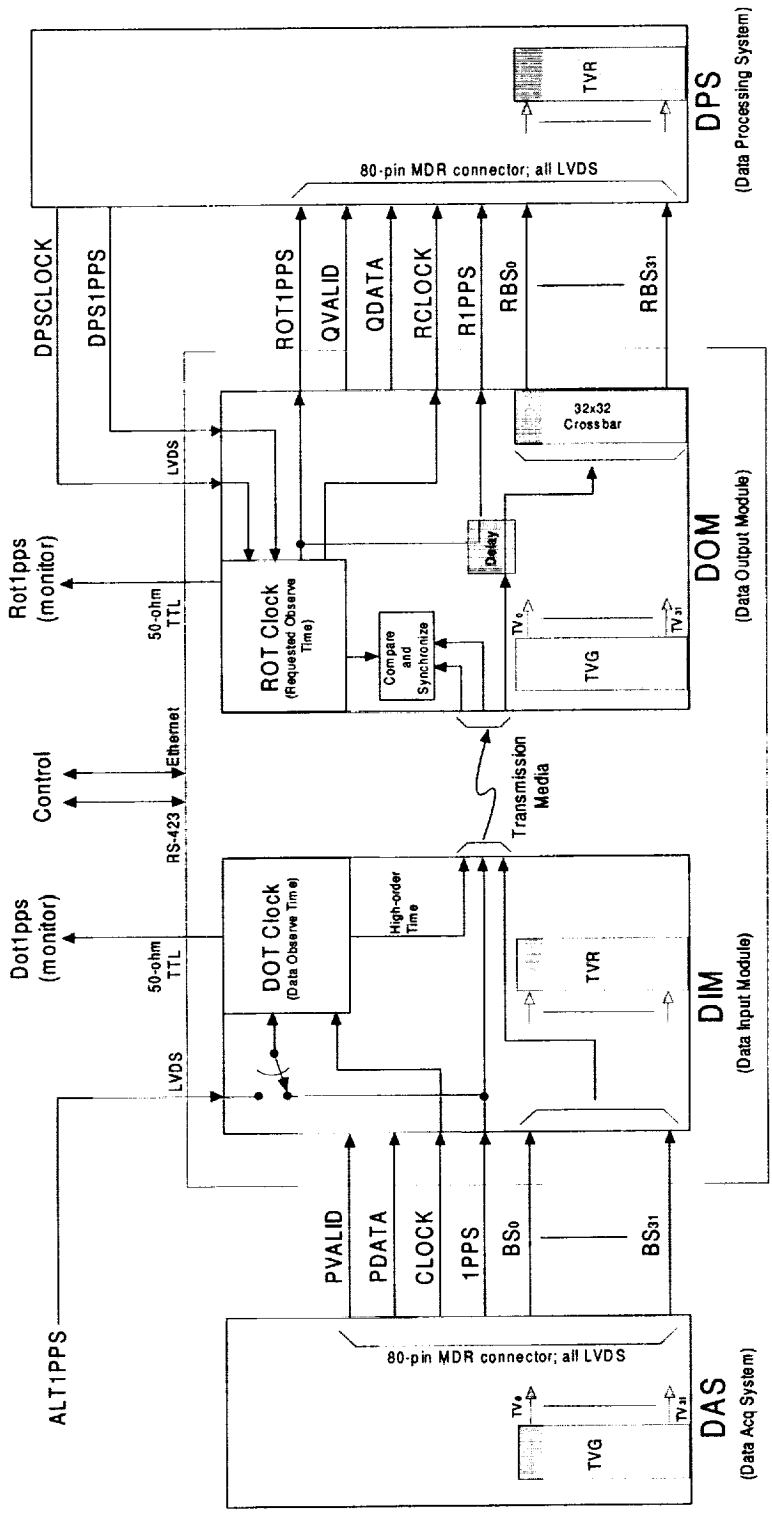

Notes:
1. Shaded items are for illustrative purposes only.
2. PVALID is optionally transmitted from DIM to DOM.
3. PDATA is optionally transmitted from DM to DOM.
4. Data delay in DOM is optional.
5. If DIM/DOM in single box, ALT1PPS/DPSCLOCK/DPS1PPS share single MDR-14 connector.
6. This diagram does not show all functions and options -- see VSI-H specification for details.

Figure 1: VSI-H Functional Block Diagram

VSI6.DRW
ARW 7 Feb 2000

- A built-in vector test facility is mandated for easy verification of system function.
- DTS control may be either through RS-423 (compatible with RS-232) or 10/100Base-T Ethernet.
- The system is designed to accommodate easy media translation (tape copying, for example).
- Two levels of VSI-H compliance are defined to ease the transition to new systems.

The VSI-H specification itself goes into great detail regarding electrical and timing specifications to guarantee as much possible that heterogeneous VSI-H-compliant systems will be interoperable.

7. Coming Next: VSI-S

With the VSI-H specification nearly complete, attention will soon be turned to the software part of the VSI specification. The goal is to define a set of DTS-specific commands that focus on that part of the DTS that is independent of the details of the technology actually used. It is recognized from the outset that VSI-S cannot be complete to the extent that heterogeneous systems will be completely "plug'n'play" since there will always be technology-specific control that will be required. Nevertheless, we feel that it is useful to pursue this effort as far as possible to minimize the pain in developing software to support various VSI-H-compliant systems. If all goes well, VSI-S should be well along towards completion in about a year. Stay tuned!

Yasuhiro Koyama et al.: Geodetic VLBI Observations using the Giga-bit VLBI System, IVS 2000 General Meeting Proceedings, p.98–102
http://ivscc.gsfc.nasa.gov/publications/gm2000/koyama

Geodetic VLBI Observations using the Giga-bit VLBI System

Yasuhiro Koyama [1], *Tetsuro Kondo* [1], *Junichi Nakajima* [1], *Mamoru Sekido* [1], *Ryuichi Ichikawa* [1], *Eiji Kawai* [1], *Hiroshi Okubo* [1], *Hiro Osaki* [1], *Hiroshi Takaba* [2], *Minoru Yoshida* [2], *Ken-ichi Wakamatsu* [2]

[1] *Kashima Space Research Center, Communications Research Laboratory*

[2] *Gifu University*

Contact author: Yasuhiro Koyama, e-mail: koyama@crl.go.jp

Abstract

A series of geodetic VLBI experiments have been performed with the giga-bit VLBI system using a baseline between Kashima and Koganei stations in the Key Stone Project VLBI Network, and a baseline between the 34-m antenna station at Kashima and a mobile VLBI station at Gifu University. The baseline vector was successfully estimated from the first test experiment on October 19, 1999. The results are still preliminary, but the challenge became the first success of the geodetic VLBI experiment at the recording speed of 1024 Mbps. Details of the giga-bit VLBI system and the geodetic VLBI experiments using the system are reported in this paper.

1. Introduction

Communications Research Laboratory has been developing the giga-bit VLBI system which has a capability to perform VLBI observations with a continuous bandwidth of 512 MHz from the baseband. The primary purpose of developing the system is to observe weak radio sources by the means of VLBI since the wide bandwidth of the giga-bit VLBI system can improve the observation sensitivity. Since the bandwidth of the giga-bit VLBI system is four times wider than the currently used other operational systems, an improvement of the signal-to-noise ratio is a factor of two. This unique characteristic is considered to be most effectively utilized in the radio astronomical applications. Several observation sessions were already performed and are planned with the baseline between 34-m antenna station at Kashima and either 45-m antenna station at Nobeyama or 64-m antenna station at Usuda. Geodetic VLBI experiments are usually performed with multiple channels and these channels are allocated to X-band and S-band frequency bands. It is because the precise time delay is obtained by using the bandwidth synthesis technique and the ionospheric propagation delay has to be corrected by performing observations in two frequency bands. The single-channel architecture of the giga-bit VLBI system prevents to apply both the bandwidth synthesis technique and the ionospheric delay correction. However, on the other hand, the giga-bit VLBI system has a potential to improve the observation sensitivity so that small aperture antennas can be used for geodetic VLBI observations. In addition, the system does not require base-band converter units and phase-calibration tone signals, and has a possibility to simplify the geodetic VLBI observation system. By considering these advantages, we determined to try to apply the giga-bit VLBI system for the geodetic VLBI observation.

2. The Giga-bit VLBI System

The giga-bit VLBI system consists of six components, i.e. sampler units, data recorder units, a correlator unit and three kinds of interface units. The entire view of the giga-bit VLBI system is shown in Figure 1. The sampler unit has been developed based on a commercially available digital oscilloscope products (Tektronix TDS784/TDS580). The oscilloscope unit has a high speed analog-digital sampler chip which operates at the speed of 1024 Mbps (bit-per-second) with a quantization level of 4 bits for each sample. One of the 4 quantization bits is extracted from the digital oscilloscope and is connected to the sampler interface unit. The sampler interface unit demultiplexes the 1024 Mbps of serial data stream to 32 parallel lines. The parallel data are then formatted by a time control unit (DRA1000) and the data are recorded by the data recorder unit (Toshiba GBR1000). The time control unit uses the track set ID counts in the data recorder unit to control the precise timing so that recorded data can be precisely reproduced with the recorded time. The data recorder unit records digital data in the D6 standard format. The recording speed of the data recorder unit was increased so that it can record the input data stream at 1024 Mbps. The correlator interface unit (DRA2000) is used in the data correlation processing and it absorbs the large time delay which can not be absorbed in the correlator unit (Giga-bit Correlator: GICO). The correlator interface unit also multiplexes and demultiplexes 32 parallel data into 64 parallel data since the correlator unit requires the 64 parallel data lines for the input data. In the correlation processing, two DRA1000 units are connected to a common 1 PPS signal and each unit synchronizes the reproduced data by controlling the GBR1000 data recorder. The correlator system was first developed at Nobeyama Radio Observatory for the Nobeyama Millimeter Array. It has a capability to correlate data stream of 1 GHz of 2-bit data and only half of the processing speed is used for the giga-bit VLBI system.

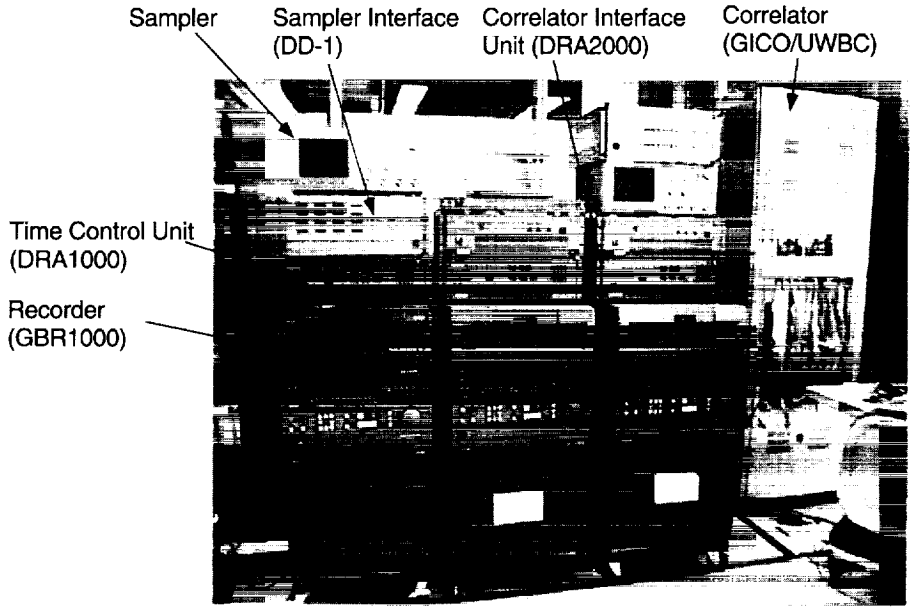

Figure 1. Entire view of the giga-bit VLBI system.

In the observations, the GBR1000 data recorder is controlled by a notebook PC using a PCM-

CIA GP-IB interface card. The observation program has been originally developed to control K-4 VLBI system and a 3-m mobile antenna system using a basic command interpreter. In the data correlation processing, the GICO and GBR1000 units are controlled by a Unix workstation over the GP-IB interface. The correlated data are saved in a file on the workstation and the time delay and its rate of change are calculated. For the geodetic VLBI data analysis, a set of programs have been developed to create Mark III database files from the output file generated by the correlator control program.

3. Experiments

The first geodetic VLBI experiment using the giga-bit VLBI system was performed for about 6 hours on October 19, 1999 with the KSP VLBI stations at Kashima and Koganei. Several softwares have been developed to process the correlator outputs using the actual data obtained in the test experiment. Following the test experiment, two full-day geodetic VLBI experiments were performed with a baseline between a mobile VLBI station at Gifu University and the 34-m antenna station at Kashima on January 18 and on February 29, 2000. The mobile VLBI system with a 3-m VLBI antenna was transported to the campus of the Gifu University in November, 1999 for the experiments. Figure 2 shows the 3-m transportable antenna and the observation shelter of the mobile VLBI system installed at Gifu University. Figure 3 shows the geographic locations of the observation stations.

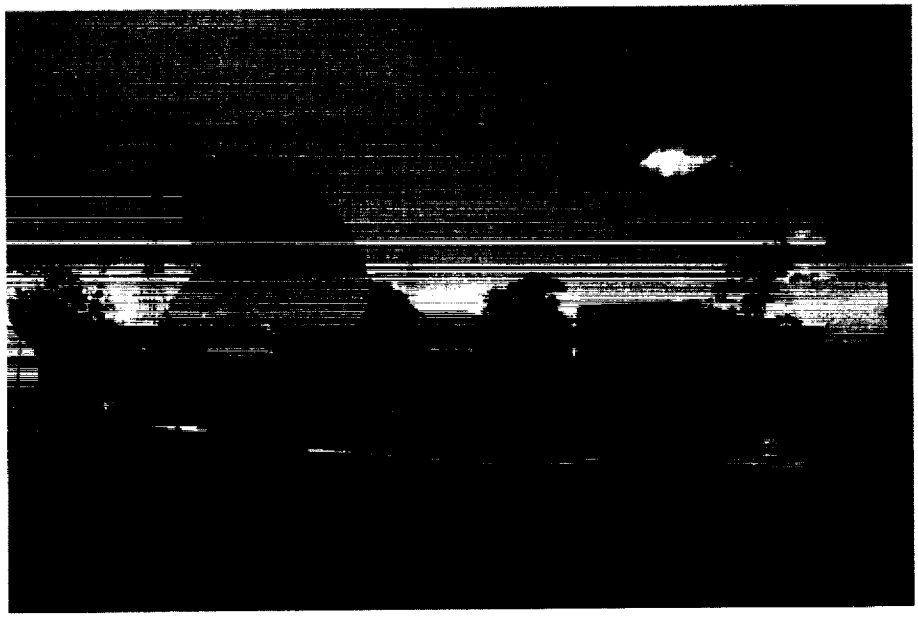

Figure 2. 3-m mobile antenna and VLBI observation shelter system at the campus of Gifu University.

The mobile VLBI system was developed in 1987, and has been used in geodetic VLBI experiments at Kashima, Koganei, Wakkanai, Okinawa, and Minamidaito island. Minamidaito island is located on the Philippine Sea Plate and the motion of the plate with respect to the North American Plate was detected by the means of geodetic VLBI technique for the first time by using the mobile VLBI system [Amagai *et al.*, 1990; Kondo *et al.*, 1992]. The 3-m antenna system does not have a

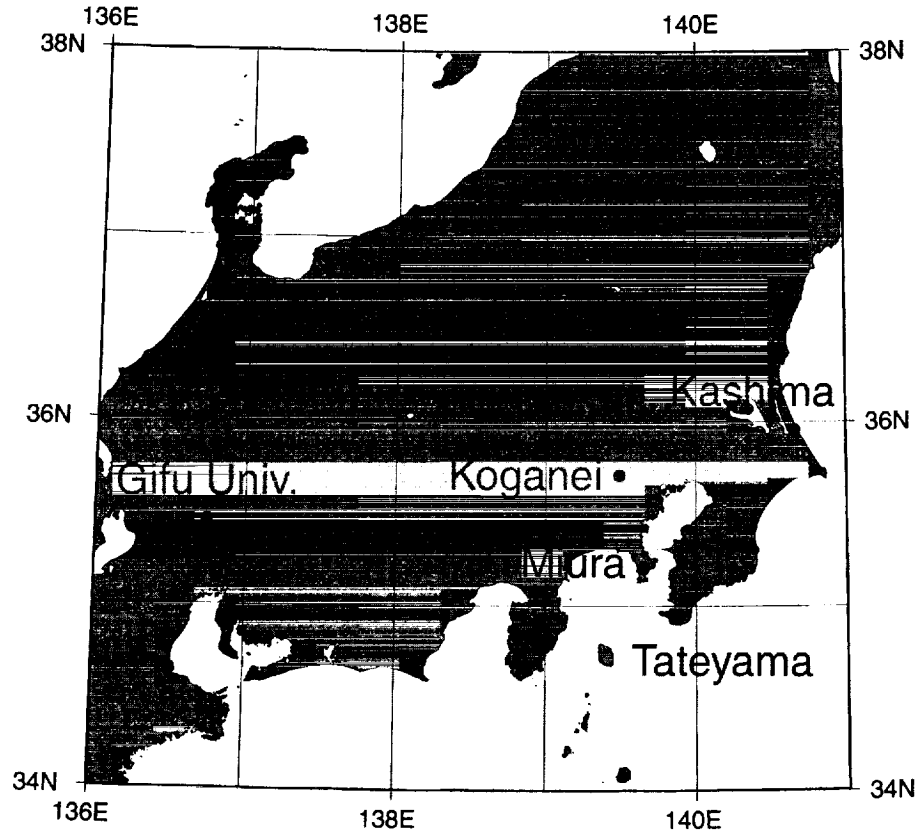

Figure 3. Geographical locations of the observation sites in the Key Stone Project VLBI Network and the new site in the campus of Gifu University.

receiver for S-band, but instead, it has two X-band receivers to expand the frequency bandwidth within the frequency band. Although the small aperture of the antenna degrades the sensitivity of the observations, the wide frequency bandwidth of the receiver helps to improve the precision of time delay measurements. The maximum slewing speed of the antenna is 3 degrees per second for both elevation and azimuth angles, and the fast slewing capability increases the number of observations within a certain length of time, which also contribute to improve the results.

The giga-bit VLBI system improves the observation sensitivity by a factor of two compared with the conventional VLBI recording system with the recording speed of 256 Mbps. The high sensitivity of the giga-bit VLBI system is considered to be most effectively demonstrated in the VLBI experiments with a small aperture antenna like the 3-m antenna system. In this scope, it was decided to conduct two geodetic VLBI experiments by using the 3-m antenna and the giga-bit VLBI system. Since the giga-bit VLBI system allows to sample baseband signal up to the frequency of 512 MHz, phase calibration signals and baseband converter units are not required and the VLBI observation system can be greatly simplified.

During the first test experiment and two full day experiments, the K-4 VLBI system was also used for the observations in addition to the giga-bit VLBI system for the comparison between the results from two independent systems. The observation tapes recorded during the two full day experiments have not been processed yet, but the observation tapes from the first test experiments

have been processed and the preliminary results are compared in Table 1.

Table 1. Comparison with analysis results from the KSP system.

	K-4 system	giga-bit VLBI system
Baseline Length	109099666.04±3.69 mm	109099667.87±13.14 mm
RMS Delay Residual	48 psec.	183 psec.

Although the estimated baseline lengths are in good agreement, both the estimated error of the baseline lengths and the root-mean-square of the residual time delays obtained from the observations with the giga-bit VLBI system were worse than the results obtained with the K-4 VLBI system. This fact suggests that there remains some problem either in the data processing software or the hardware system. In either case, we are planning to continue our efforts to eliminate these problems.

4. Conclusions and Future Plans

The giga-bit VLBI system was used for three geodetic VLBI experiments and we succeeded in estimating the baseline vector for the first time with the unprecedented speed of data recording at 1024 Mbps. Although the results are still preliminary, the high sensitivity of the system will give us many potential possibilities for innovation in the technical developments in the field of geodetic and astronomical VLBI observations.

The observation tapes recorded in the two full-day experiments will be correlated as soon as the GBR1000 and related systems return to the Kashima Space Research Center from Nobeyama Radio Observatory after an astronomical VLBI experiment which was just finished on March 12, 2000. The improvements of the data processing software and the hardware systems will be continued by using the actual data taken in these experiments.

We are also planning to develop a new data transmission system for real-time VLBI observations based on the Internet Protocol. The 3-m antenna mobile VLBI station at Gifu University and the 34-m antenna station at Kashima will be used for the technical developments and test observations using the high speed network connection which will become available in the near future between Gifu University and the Communications Research Laboratory. We are looking forward to expand the real-time VLBI network to international baselines by using the Internet Protocol and are hoping to make another innovation in the technical developments for the geodetic and astronomical VLBI observations.

References

[1] Amagai, J., H. Kiuchi, A. Kaneko, and Y. Sugimoto, "Geodetic experiments using the highly transportable VLBI station", J. Commun. Res. Lab., Vol. 37, p. 63, 1990

[2] Kondo, T., J. Amagai, and Y. Koyama, "Data Analysis of Geodetic VLBI Organized by the Communications Research Laboratory", published by Commun. Res. Lab., October 1992

Alan R. Whitney: Concept for an Affordable High-Data-Rate VLBI Recording and Playback System, IVS 2000 General Meeting Proceedings, p.103-110
http://ivscc.gsfc.nasa.gov/publications/gm2000/whitney1

Concept for an Affordable High-Data-Rate VLBI Recording and Playback System

Alan R. Whitney

MIT Haystack Observatory
e-mail: awhitney@haystack.mit.edu

Abstract

Recent and continuing developments of magnetic-tape data-storage systems for the computer industry provide a basis on which to create a high-performance, affordable high-data-rate (HDR) recording and playback system. Such a system would be suitable for VLBI and other applications which demand sustained data rates of a gigabit/sec (Gbps) or higher. These systems should be based on mostly-off-the-shelf hardware which will be readily available from the computer industry, with a minimum of custom design, and which can easily grow to higher data rates as the recording industry advances. Furthermore, they must be capable of unattended operation for at least 24 hours. Based on currently-announced tape products and projected industry roadmaps, the cost per Gbps for such systems will drop from a Year 2000 cost of ~$100K/Gbps to ~$14K/Gbps by ~2007. This suggests that HDR systems in the range of ~8 Gbps may be available for ~$110K before the end of the next decade.

1. Goals for a Next-Generation VLBI HDR System

The goals for a next-generation VLBI HDR system can be stated fairly succinctly:

- Minimum of 1 Gbps data rate (native, uncompressed)
- Economically upgradeable/expandable to ~8 Gbps over the coming decade
- Design based primarily on unmodified off-the-shelf subsystems and components
- Modular, easily upgradeable as better/cheaper technology becomes available
- Robust operation, low maintenance cost
- Easy transportability
- Conformance to emerging VLBI Standard Interface (VSI) specification
- Flexibility to support electronic transfer ("e-VLBI") and computer processing of recorded data
- Easy adaptability to HDR applications other than VLBI
- Minimum of 24-hour unattended operation

Though this list of goals may appear idealistic, we believe they can be achieved in a system which can be designed today, and which will evolve in the following years to ~8 Gbps with minimal additional engineering effort.

2. The Computer Industry to the Rescue

The demands of the computer industry have been driving several technologies that are key to meeting the stated goals of the next-generation VLBI HDR system. We shall examine each of these key technologies.

2.1. Tape Recording Technology

Figure 1 shows the historical progression of the native storage capacity of a single tape for several commercial systems, both of the helical scan and linear variety, and all of which use a tape cartridge format. Also shown is the industry projection for storage capacity over the next 7-8 years. We note that today's single-tape capacity of roughly 100 GB is expected to rise to ~1 TB by ~2007; capacities of 0.5 TB/tape have already been demonstrated in commercial laboratories. Though projecting future technology is clearly a risky business, some credibility to these projections may be gained by noting that the disc drive industry has handily outstripped nearly all predictions made for that industry over the past 5 years; tape technology is quickly picking up steam and is now beginning to move very aggressively in the same direction.

Figure 2 shows the history of single-drive data rates for the same set of systems, as well as industry projections for single-drive data rates over the next 7–8 years. The currently available data rates of 10–12 MB/sec will rise to 16–18 MB/sec in announced products available within the next 4–8 months, and are expected to rise to the order of 128 MB/sec/drive by ~2007, roughly mirroring the growth rate of data storage capacity.

Current costs of a single tape drive, regardless of type, is on the order of $5–7K each in small quantities. Based on past experience and on industry projection, the cost per drive will remain relatively constant as the technology progresses over the next 7–8 years.

Whatever the details of the tape technology to be used, whether linear or helical-scan or something else, the implications are clear. Within the next year, 8 *standard commercial tape drives* at 16 MB/sec each can, in principle, be paralleled to achieve 1 Gbps data rate for an investment of < $60K in tape drives. In 7–8 years, as shown in Figure 2, *a single* tape drive is expected to be capable of 1 Gbps (128 MB/sec), so that a bank of 8 such machines will be able to achieve 8 Gbps for the same < $60K investment in tape drives!

2.2. Industry Standard Buses and Interfaces

Of course, tapes and tape drives aren't the only component of a recording or playback system, and projections based on that aspect alone are obviously not the whole story. In this section we will investigate the state of standardized buses and interfaces that will be needed to support the tape drives.

3. Concept for an HDR VLBI Recording System

Figure 3 shows a simple block diagram of such a system based on the standardized components and interfaces discussed above. A 64-bit-wide PCI-X bus operating at 133 MHz forms the backbone of the system, supporting a data transfer rate of up to 1 GB/sec (8 Gbps). A standard CPU, probably of the high-speed Intel or Motorola variety, along with its attendant semi-conductor memory, will attach to the bus for control and monitor. Two standard SCSI interfaces are shown

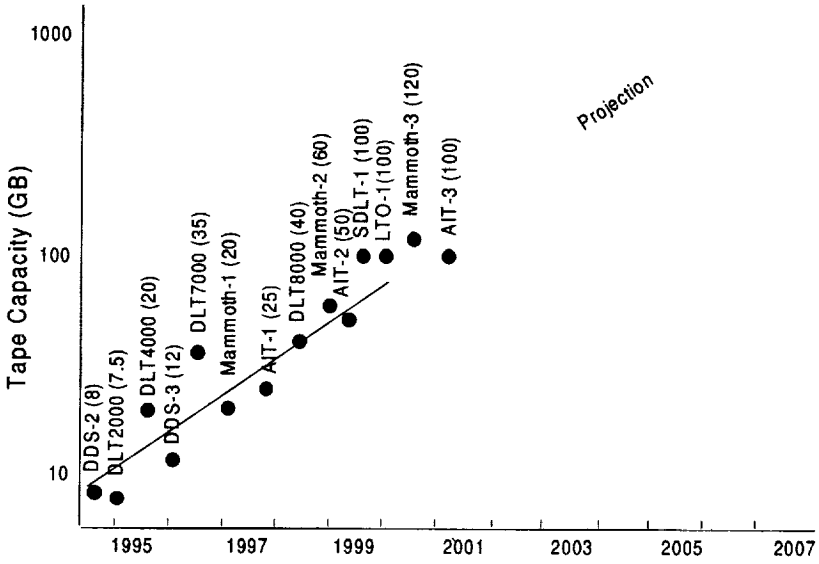

Figure 1: Tape Capacity vs. Time

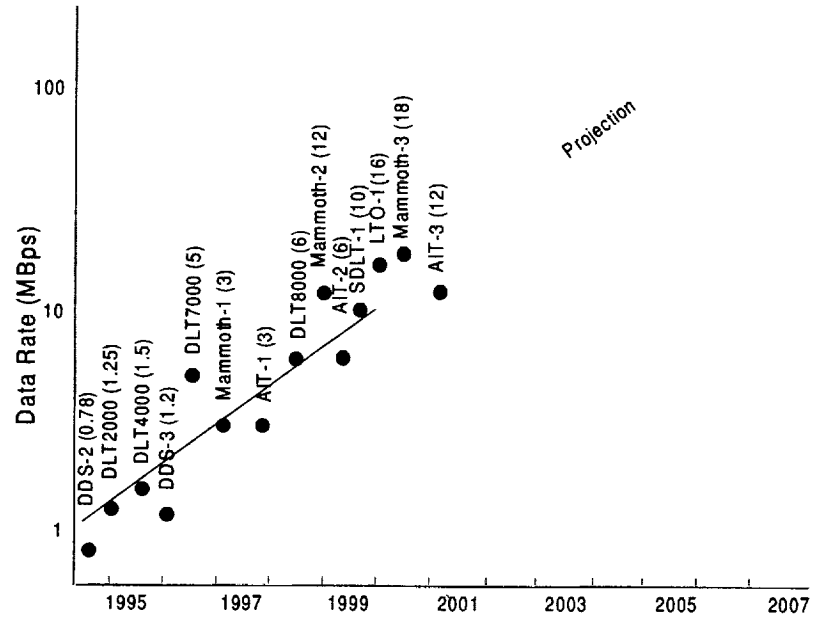

Figure 2: Tape Data-Rate vs. Time

Note:
AIT: Sony, helical scan
DDS: Sony: helical scan
DLT: Quantum, linear
LTO: HP, IBM, Seagate, linear
Mammoth: Exabyte, helical scan

TAPE1.DRW
ARW 990927

attached to the PCI-X bus, each of which supports two standard commercial recording devices; for most VLBI applications these devices would be magnetic tape recording devices of the types described above, but they could also be other types of recording devices such as optical and/or magnetic discs and tapes. The important point is that these are all standard off-the-shelf devices with standard interfaces.

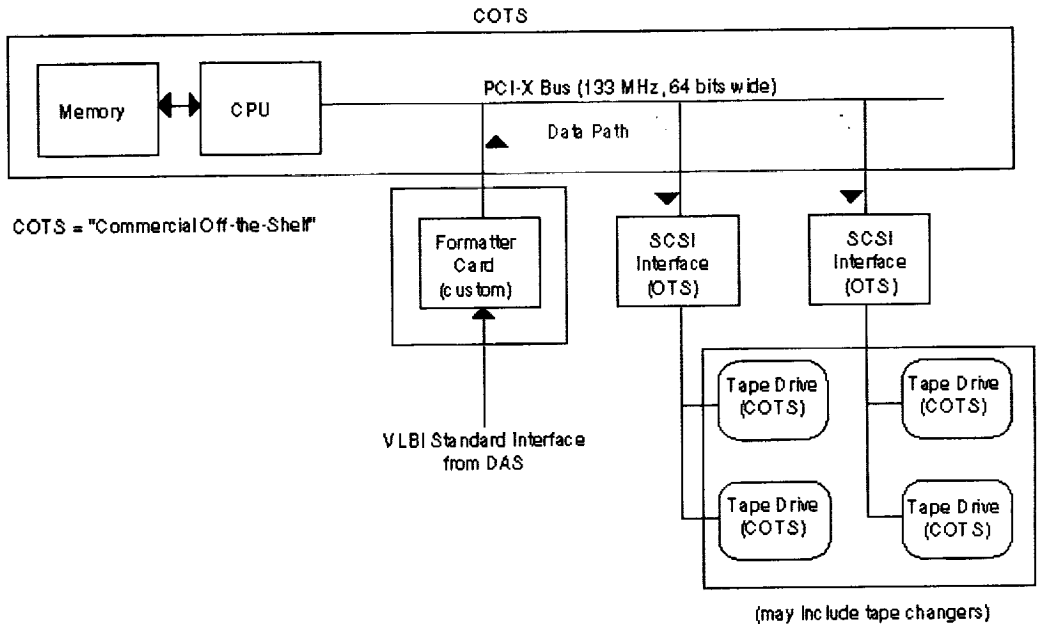

Figure 3. Example Block Diagram of HDR VLBI Data-Recording System.

The *only* custom hardware in the HDR recording system is a plug-in VSI formatter card which implements the VLBI Standard Interface specification and acts as a PCI-bus master device to transfer data *directly* to the SCSI recording interfaces with no interaction with the CPU or its memory. Initial investigation suggests that a single VSI formatter card should easily handle at least 1 Gbps and possibly substantially more.

The software operating system for the HDR system will also be a standard off-the-shelf product, chosen from among several potential candidates after careful investigation. Possible contenders in this arena are such systems as Linux, LynxOS, OS-9, QNX, VxWorks and pSOS. The final choice will depend on many considerations, from robustness of implementation to ease of application development. Networking capabilities will be of significant importance, both for future support of e-VLBI and for remote operation and monitoring.

4. Concept for an HDR VLBI Playback System

Figure 4 shows a block diagram of a complementary HDR playback system. The hardware is identical to the recording system except a custom VSI *de-formatter* card replaces the VSI formatter

card for collection of the data from the SCSI devices for transmission to the VLBI Standard Interface and the user. Alternate data paths exist for collection of the playback data into the computer memory for local processing or transmission through a standard network interface (e-VLBI).

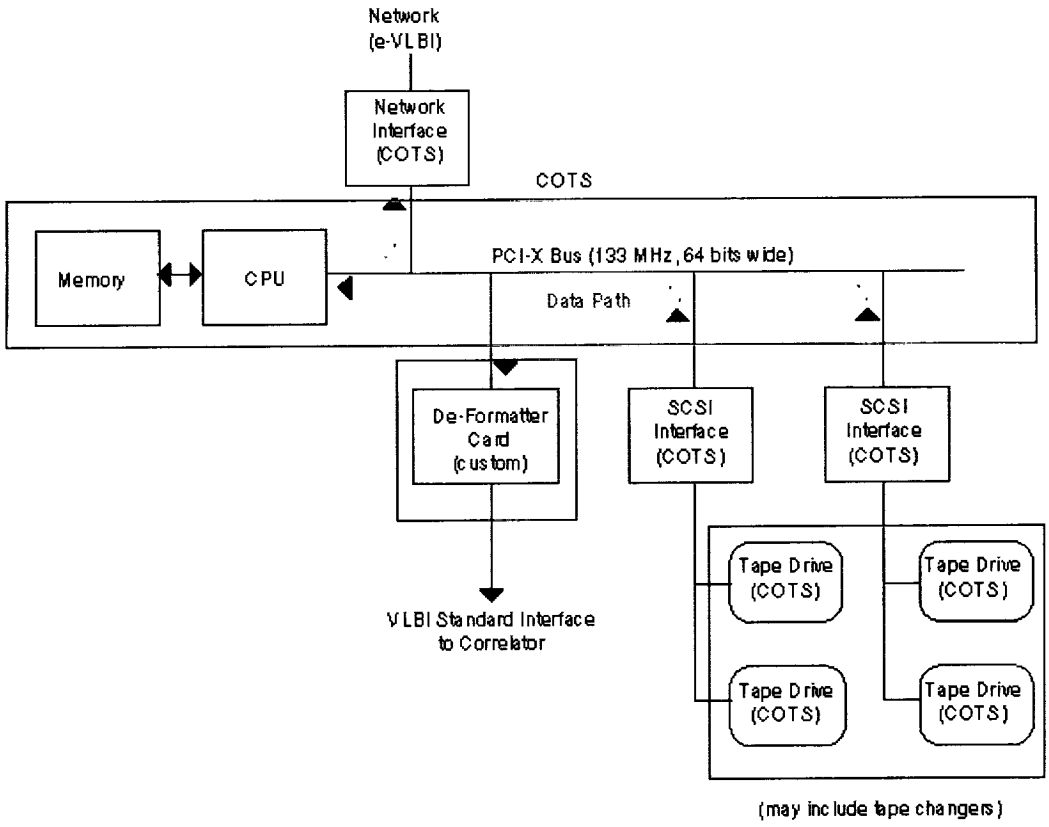

Figure 4. Example Block Diagram of HDR VLBI Playback System.

5. What Can Be Done Today for What Cost?

A survey of the computer marketplace today allows us to estimate the performance and cost of an example system that can be built with hardware available today or in the very near future. For a recording device, we can choose one of the soon-to-be-available systems that supports a data rate of at least 16 MB/sec (see Figure 2). These devices, whether using linear or helical scan recording, can sustain a continuous recording data rate of 128 Mbps for at least 104 minutes on a single tape cartridge, at a cost of $\sim$ \$7000/device. If we implement the system shown in Figure 3 using these devices, we can make a conservative estimate of the total hardware system cost:

Computer, memory, backplane	$5,000
SCSI interface cards (2)	$2,000
VSI Formatter card (1)	$2,000
Tape drives (4)	$28,000
Cabinets	$1,000
Contingency	$2,000
Total	$40,000

System capability: 512 Mbps for ~104 minutes
Tape cost: 4 tape cartridges at ~ $70 each = ~ $280

These cost estimates are based on current small quantity prices and should become even more economical at quantity prices.

The costs for the playback system are approximately the same, only with a VSI de-formatter card replacing the VSI formatter card.

6. The 24-Hour Challenge

We stated at the outset that 24-hour unattended operation is a major goal of a new HDR system. Here again the computer industry has risen to the challenge, with solutions from many vendors. As an example, a 14-tape changer from ATL Products is readily available for ~ $2000 each to support DLT-style tapes; other similar changers are available for other styles of tape cartridges. The changer and its attendant drive will fit into a 7" standard-rack space. We need four changers, so the system (dubbed "HDR-1") cost becomes:

System "HDR-1"-	
Basic system (from above)	$40,000
14-tape changers (4)	$8,000
Total	$48,000

System capability: 512 Mbps for 24 hours
Tape cost: 56 tape cartridges at ~ $70 each = $3920
Possible physical configuration: 3 small (~ 18" high) racks with changers and electronics

Two such systems operating in parallel will achieve 1 Gbps for 24 hours unattended operation for < $100,000 (not including tape). And this is just the beginning, since the computer industry is investing hundreds of millions of dollars to help us.

7. What Does the Future Hold?

Fortunately, we can be fairly certain that, by building on widely accepted computer standards and subsystems, the future is very bright. As shown in Figures 1 and 2, by ~ 2007 single-tape capacity is expected to reach 1 TB at a data rate of 1 Gbps, *and the per drive cost is expected to remain essentially the same.* This would be hard to believe if we did not have the demonstrated example of the disc drive industry already meeting or exceeding projected price/performance growth

rates. The projected system of ~ 2007 (dubbed "HDR-4") looks and costs about the same as the system described above:

System "HDR-4"-	
Computer, memory, backplane	$5,000
SCSI interface cards (2)	$2,000
VSI Formatter card (4)	$8,000
Tape drives (4)	$28,000
Cabinets	$1,000
14-tape changers (4)	$8,000
Contingency	$2,000
Total	$54,000

System capability: 4 Gbps for ~ 30 hours
Tape cost: 56 tape cartridges at ~ $70 each = $3920
Possible physical configuration: 3 small (~ 18" high) racks with changers and electronics

Depending on the capabilities of the interface cards and backplane, it may be possible to add additional interface cards and tape drives directly to this system to reach 8 Gbps; alternatively, two HDR-4 systems operating in parallel will reach 8 Gbps and cost only marginally more since the foundation computer and bus are inexpensive. In either case, the cost would be <~ $110K for a system capable of recording 8 Gbps for 24 hours unattended.

Table 1 illustrates several of the relevant system parameters for current and other proposed VLBI data systems, as well as projections for four generations of HDR systems (HDR-1 through HDR-4) through ~ 2007. What we see is an astonishing projection of costs declining from ~ $100K/Gbps in the near term to ~ $14K/Gbps around 2007 for systems which can record for at least 24 hours unattended. Even if these projections prove to be too optimistic by a factor of 2, it is clear that the cost of VLBI HDR systems will decline rapidly, *provided they are largely based on standard off-the-shelf technology.*

8. References

A more complete paper outlining this proposed system is available from Haystack Observatory. Please contact the author.

Table 1: Characteristics of various current and proposed VLBI recording systems (best estimates)

	Mark IV	Mark IV Thin-Film	S2	S3	K4 (Sony)	D6 (Toshiba)	HDR-1 (buildable Y2000)	HDR-2 (projected)	HDR-3 (projected)	HDR-4 (projected)
When available?	now	?	now	2002?	now	now	(2000)	(2003)	(2005)	(2007)
Technology	linear	linear	helical	helical	helical	helical	linear or helical	?	?	?
Max data rate (Gbps)	1-2	2-4	1/8	1	1/4	1	1/2	1	2	4
#tape transports	1	1	8	8	1	1	4	4	4	4
Single Tape capacity (TB)	0.5	1.0-2.0	0.04	0.14	0.1	0.46	0.1	0.25	0.5	1.0
Est. system cost (**$GBPS**):										
w/o changer	$250-140K	$130-70K	$235K	$100K	$300K	$500K	-	-	-	-
w/changer	-	-	-	?	?	?	$100K	$50K	$30K	$14K
Unattended operation (hrs at max rate):										
w/o changer	1.1-0.5	~1.1	5.7	2.5	1.0	1.0	1.7	2.2	2.2	2.2
w/changer(s)	-	-	-	24	24?	>24	24	30	30	30
Tapes/24 hrs (at max rate)	~22-44	~22	~32	~80	24	24	56	44	44	44
TB/24 hrs (at max rate)	11-22	22-44	1.4	11	2.8	11	5.5	11	22	44
Media cost (**$/TB**)	$1950	$975-490	$360	$312	$2000	$1090	$710	$280	$140	$70
Shipping weight (**kg/TB**)	21	10.5-5.2	9.3	2.7	14.4	3.6?	3.8	1.5	0.7	0.35
Heads:										
Est. lifetime (hrs)	3-5K	>10K?	3-5K?	3-5K?	?	1K	>10K	>10K	>10K	>10K
Replacement cost	$20-40K	$2.5K		~ $8K	?	$30K	?	?	?	?
$/hr head cost	$5-8	<$0.25		~$2	?	$30	<$1	<$1	<$1	<$1
Speedup on playback for data-rates < max	Y	Y	N	N	Y	Y	Y	Y	Y	Y

Session 4.

Local Surveys

James L. Long et al.: The Importance of Local Surveys for Tying Techniques Together, IVS 2000 General Meeting Proceedings, p.113–117
http://ivscc.gsfc.nasa.gov/publications/gm2000/long

The Importance of Local Surveys for Tying Techniques Together

James L. Long [1], *John M. Bosworth* [2]

[1)] *Honeywell Technology Solutions Inc.*
[2)] *NASA Goddard Space Flight Center*
Contact author: James L. Long, e-mail: jim.long@honeywell-tsi.com

Abstract

The synergistic benefits of combining observations from multiple space geodesy techniques located at a site are a main reason behind the proposal for the establishment of the International Space Geodetic and Gravimetric Network (ISGN). However, the full benefits of inter-comparison are only realized when the spatial relationships between the different space geodetic systems are accurately determined. These spatial relationships are best determined and documented by developing a local reference network of stable ground monuments and conducting periodic surveys to tie together the reference points (for example: the intersection of rotation axes of a VLBI antenna) of the space geodetic systems and the ground monument network. The data obtained from local surveys is vital to helping understand any systematic errors within an individual technique and to helping identify any local movement or deformation of the space geodetic systems over time.

1. Introduction

Over the past two decades, the space geodesy techniques, VLBI, SLR, GPS, and DORIS, have developed into very powerful measurement tools for geodetic science, with accuracies of a few millimeters. During this same time period the number of permanent collocation sites with multiple techniques has grown significantly. However, the ability to compare the data from the different techniques is often limited by missing or inaccurate local survey ties. In analyzing geodetic data from the space techniques, it is necessary to separate the tectonic motion from any motion due to locally induced instabilities, such as the settlement of an antenna foundation. This paper will provide a perspective on local surveys within international programs and provide recommended criteria and examples of local surveys from NASA GSFC experience.

Local surveys are very important to the success of the goals of the following two international efforts relating to the intercomparison of space geodesy techniques.

2. The International Space Geodetic Network (ISGN)

The ISGN is being established under the charter of the IAG Commission on International Coordination of Space Techniques for Geodesy and Geodynamics (CSTG) with the goal of improving cooperation between the individual technique services (IVS, ILRS, and IGS) and defining the recommended network station criteria. The accomplishments of the former CSTG Geodetic and Geophysical Sites Subcommission (GGSS), pertaining to site surveys and monumentation are being incorporated as a basis for the ISGN site criteria.

3. The IERS International Terrestrial Reference Frame (ITRF)

The IERS publishes revised ITRF positions on an annual basis for a global network of geodetic stations. The collocated stations offer an extremely valuable opportunity to compare the solutions for the various techniques. However, missing or inaccurate local survey data at some stations significantly impedes this analysis. IERS issues a periodic report to identify problems with local survey ties. The adopted threshold for identifying an uncertainty in a local survey as "imprecise" is 5 millimeters in any component, regardless of length.

In some cases, the accurate survey has been completed, but the data is not transmitted in a usable format, which allows independent evaluation of the data quality. To help alleviate this problem, IERS has adopted SINEX as the format for the submission of local survey data.

4. Description of Model Collocation Site

The following is a description of a model collocation site developed by the NASA/GSFC Space Geodesy Program. The purpose of the extensive set of ground monuments is to facilitate the surveys of the reference point of the different space technique systems and help identify any local instability. The ground monument network should be designed with consideration for geometric strength of figure and inter-visibility between the monuments.

The site should have a central ground monument, to which all other monuments and space systems can be referenced. This central monument may be used in surveys to tie the site to the regional or national, high-accuracy geodetic control networks. The central ground monument is surrounded by three reference monuments at a distance of 25 to 100 meters, in an equilateral triangle configuration. The ground reference monument network is extended as required to enclose the area around all the space geodetic systems. SLR systems often require ground calibration targets, which can be included in the ground reference monument network.

As it is most important that the ground monuments remain stable over a long period of time, they should be designed with consideration of the site specific geological information. Traditionally, the ground monuments have been constructed by excavating a hole, approximately 0.3 meters in diameter and 1 meter deep, filling the hole with concrete, and placing a brass survey disk at the top. A better design is a tall, reinforced concrete pier with a self-centering device, compatible with survey instruments, at the top. The dimensions of the pier are approximately 0.3–0.5 meters in diameter and 1.3–2.0 meters above the ground surface. The depth of the pier into the ground should be a minimum of 2.0 meters, but can vary depending on the geological characteristics of the site. The utilization of the concrete pier eliminates the errors associated with plumbing over a traditional style mark with a tripod.

There should be a network of three or four distant ground monuments, called "footprint" monuments, at a distance of 10 to 25 kilometers from the collocation site. The locations for the footprint monuments must be carefully chosen to select areas geologically stable with the collocation site, but far enough away to avoid local disturbances affecting both the collocation site and the footprint monument. The footprint network will aid in recognizing the difference between local, regional, and tectonic plate motions.

Type of Instrument	Manufacturer's Accuracy	Standard Error Used
Leica THEOMAT 3000 (theodolite)	0.5 seconds	1 mm + 1 second
Leica DI 2002 (distancer)	1 mm + 1 ppm	1 mm + 1 ppm
Leica NA3003 (digital level)	0.4 mm in 1 km (with invar rod)	1 mm
Trimble 4000SSI (GPS)	Horiz.: 5 mm + 1 ppm Vert.: 10 mm + 1 ppm	5 mm + 5 ppm(<1 km) 5 mm + 1 ppm (>1 km)

Table 1. Instrument Accuracy Table

5. Examples of Local Surveys

NASA GSFC has been performing local surveys in support of space geodesy at many sites over a number of years. As the accuracy of the space systems has improved, the survey methods and equipment have been upgraded and improved correspondingly. This experience has resulted in the following recommendations for a high-precision, local survey.

- Utilize the best quality, highest precision equipment available. The type of equipment typically used by the NASA GSFC surveyors is shown in table 1 above. Use conventional survey equipment over short lines (less than 1 kilometer), where there is visibility between the stations.
- Calibrate distance measurement equipment on a regular schedule over an established calibration baseline.
- Measure distances both ways over each line and use two different instruments, if possible.
- Repeat observations (both direct and reverse) for horizontal directions and zenith angles to reduce the effect of pointing errors.
- Measure instrument and target heights accurately to within 1 millimeter.
- Utilize differential leveling methods to measure differences in heights.
- When using a tripod or instrument stand over a monument, utilize a high quality optical plummet and re-plumb tribrachs daily, at a minimum.

The documentation of the survey is also very important. A project file and a brief report should be compiled at the completion of the survey. The report should include the following:

- A narrative description of the project objectives, methods, and conclusions.
- A discussion of the observation plan and equipment utilized.
- A network diagram and sketches of the reference points of the space geodesy systems.
- A summary of the least-squares adjustment and the quality of the survey.

The results of the survey at a collocated site should be submitted to the IERS in the SINEX format.

6. Antenna Survey Procedures

The following is a general description of the procedures used by the NASA GSFC surveyors to perform local surveys at the VLBA antenna sites. The 10 identical VLBA antennas have a 25-meter diameter dish with an elevation over an azimuth wheel and track drive configuration. The elevation axis is offset from the vertical axis by 2.135 meters. None of the antennas are enclosed in a radome.

1. Construct three or four ground monuments in a network around the antenna. These monuments will be used as control points for the antenna survey. At least one of these monuments is a reinforced concrete pier constructed to enable the eventual installation of a GPS antenna on a permanent basis.

2. Perform a precise conventional, electro-optical survey to tie the new ground monuments to previously established survey control monuments. Measurements with GPS are used over long lines and to supplement the conventional measurements.

3. Temporarily mount a specially fabricated, pointed rod survey target at the apex of the antenna quadripod feed support structure. The location of the target should be chosen to optimize simultaneous visibility from the most ground stations and to ensure stability.

4. Mount a survey target, on an X-Y (horizontal motion) translation stage and trivet plate, on a structural platform at the approximate location of the vertical axis of rotation. Using the translation stage, adjust the target to lie on the vertical axis of rotation while viewing the target through a theodolite as the VLBA antenna is rotated in azimuth.

5. Observe directions and distances, from each of the survey reference marks, into the survey target on the vertical axis of rotation.

6. Perform an extensive set of survey observations to position the survey target rod, mounted at the antenna apex, over a wide variety of antenna positions. Observations are made from each reference survey mark that will see the target rod, at each antenna position. Systematically rotate the antenna through 48 point positions (i.e. azimuths: 000, 090, 180, and 270 degrees; elevations at each azimuth: 10, 20, 30, 40, 50, 60, 70, 80, 90, 100, 110, 120 degrees).

7. Utilize differential level methods and equipment to measure the difference in height between each of the ground monuments and the target located on the vertical axis of rotation.

8. A least squares adjustment program is used to determine the coordinates of each position point for the tip of the target rod. A circle-fit software is used to calculate the center of each of the four circles, as described by the 12 points on the arc at each of the four azimuths. The mean of these four circle centers determines the elevation axis offset.

The NASA GSFC surveyors have used this method (with some minor modifications) at 8 of the 10 VLBA sites, since 1990. The results of the surveys have been consistent and appear to be accurate to within 3 mm. There has been no attempt made to account for antenna structural deflection in this solution, however, this topic may be addressed in the future.

7. International Cooperation

Under the guidance of the ISGN Subcommisson, we hope to promote the idea of an international cooperative team to facilitate local surveys at the ISGN sites. The Subcommission would provide a forum for discussion on survey methods and procedures and encourage their improvement to achieve greater accuracy.

As an example, recently a cooperative survey effort was accomplished in support of the installation of the new Matera Laser Ranging Observatory (MLRO) system at the Italian Space Agency Space Geodesy Center (ASI-CGS) near Matera, Italy. A NASA GSFC surveyor traveled to the site and worked with the ASI-CGS personnel to perform a survey to determine the preliminary coordinates of the MLRO telescope and the ranges to the new calibration targets. In addition, the survey effort was expanded to include the local ties directly to the SAO-1 SLR system and the IGS permanent GPS station. The ground reference marks surrounding the VLBI antenna were included in the survey so that data from a previous survey of the VLBI antenna will be used to determine the tie between the VLBI antenna and the MLRO.

The raw survey measurements were reduced and adjusted by each group, independently. The preliminary results indicate an agreement of around 1 millimeter, in each coordinate, between the two solutions.

Ludwig Combrinck: Local Surveys of VLBI Telescopes, IVS 2000 General Meeting Proceedings, p.118–127
http://ivscc.gsfc.nasa.gov/publications/gm2000/combrinck

Local Surveys of VLBI Telescopes

Ludwig Combrinck

Hartebeesthoek Radio Astronomy Observatory
e-mail: ludwig@hartrao.ac.za

Abstract

With geodetic VLBI techniques we are able to determine station coordinates and displacement rates at millimetre accuracy levels. These results are very sensitive to local telescope displacements caused by natural phenomena or by man-made modifications. In order to separate the local effects from those which are of interest like crustal movements, land uplift and subsidence, we need to measure the position of the telescopes in the local vicinity. Local networks in walking distance of the telescope should be complemented by extended networks which provide links to geologically stable areas. In this paper we introduce the holistic approach to footprints and geodetic monuments. In order to achieve millimetre precision, local effects such as slope movement, weathering and thermal effects can no longer be ignored. The geodesist must recognise and be aware of potential instabilities caused by such factors.

1. Introduction

In order to achieve the current objectives of geodesy, several space geodetic techniques are utilised at facilities all over the world. Very Long Baseline Interferometry (VLBI), Global Positioning System (GPS) and Satellite Laser Ranging (SLR) are the three main space geodetic techniques supported. Determining the stability of each geodetic fiducial site on a local scale, tying reference points, and determining the eccentricities between these points require small geodetic networks which surround the geodetic sites. These *footprint* networks cover a radius of some tens of metres to tens of kilometres. Conventional surveying techniques and instrumentation could be used, utilising optical instruments such as theodolites and electronic distance measuring instruments, or GPS equipment. All these techniques are capable of providing good results and it will depend to a large extent on a station's available equipment and expertise as to which instrumentation is used for the local surveys and ties. It is time however to adopt a new approach to footprints, using an holistic approach which could add more meaning to the term *footprint*. This paper does not allow a full discussion of the subject at hand so a more detailed version is to be published as an IVS monograph. The IVS monograph will contain detailed examples of both conventional (optical) and GPS procedures.

2. Footprints: an Introduction

This short introduction is partially based on an unpublished report by Bell et al. (1994) and personal communication received from C. Noll (Crustal Dynamics Data Information System (CDDIS)) and R. Allenby. Conventional geodetic surveys are usually performed to ascertain reference points of SLR and VLBI instrumentation and the relative positions of reference monuments or other collocated geodetic instruments within the immediate site area. The measurements are done in order to differentiate between local instability effects (local groundwater fluctuations, soil movement or monument instability) and geodetically measured motion from larger scale effects. The

larger scale effects include coseismic displacement during an earthquake, subsidence or uplift due to glacial or fluvial loading or unloading, steady state slip resulting from plate motion, or displacement due to volcanic eruptions. A footprint measurement can provide crucial information when a site suddenly exhibits anomalous displacement.

As mentioned by Bell et al. (1994) the objectives of the NASA/GSFC Site Stability Program are:

- Assuring the integrity of geodetic measurements taken at principal space geodetic observing sites (VLBI, SLR, and GPS)
- Implementing and measuring local GPS networks around the main observing monument that are representative of the local tectonic environment they encompass (5-30 km scale)
- Repeating conventional surveys of the reference markers relative to the main observing monument (less than 1 km) to assure monument stability
- Providing first and second epoch GPS footprint measurements at many of the essential fiducial geodetic sites used in the worldwide global networks, beginning with the U.S.
- Providing raw survey data and final geodetic results to NASA's CDDIS.

2.1. Conventional Site Surveys

Physical stability of the main observing monuments is assessed by conventional geodetic surveys of the reference markers. If a permanent tracking instrument (VLBI, SLR, GPS) is installed at the site, these conventional surveys determine the reference point of the fixed observing instrument, and the relative positions of reference monuments, an azimuth mark, as well as other collocated geodetic instruments within the site area. When a site contains a marker that is frequently used by mobile geodetic systems, a mark to mark survey is simply conducted. The relative station position estimates from these classical surveys generally agree at the several mm level.

2.2. GPS Footprint Surveys

From 1990 onwards, NASA's Site Stability Program has implemented and measured local GPS networks (1-30 km scale) centred around main observing monuments with the aim to determine local stability of the area occupied by the main reference point. Similar work has been done at other sites, including HartRAO. In comparison to the footprint survey, local GPS networks have been and are being measured by scientific teams in areas of tectonic interest to identify geological structures that are accommodating strain seen between and around geodetic fiducial sites. There is a basic difference between these two efforts. The footprint encompasses a single tectonic feature which is occupied by the main site, whereas the regional strain network encompasses an entire deformation field including all of its regional characteristics.

3. The Footprint System in General

Basically the stability of the footprint area is inferred from the measured stability of the footprint reference points, referred to (in HartRAO's case) the SLR pad, radio telescope and the IGS station HRAO. Several of the reference points at HartRAO are located on rocky outcrops, which are essentially free of soil and can be regarded as continuous or nearly continuous bodies of exposed rock. These outcrops owe their form to the intact strength of the rock, the continuity,

dip, strike and spacing of their partings. Any movement of the rock on which the monument is located might not be due to crustal instability in the footprint area, but might be the result of other natural factors which influence and even control the nature and extent of the dominant processes in rock slope evolution. The current form of such an outcrop is a result of long term evolution of the ridge on which the outcrop is located. Each outcrop will have its own inherent stability, dependent on the current state of balance with the dominant processes in its evolution.

Form is an important parameter in any footprint as the processes which created the form are the same processes which will cause movement of the monument. Therefore the footprint does not concentrate on the evolution of the form, but on the effect the processes have on the stability of the monument. In order to understand and correctly interpret small movements of the reference points one has to approach the footprint in a holistic way. Therefore, consideration needs to be given to the individual reference point as a system, and a combination of all these systems into the footprint system. These systems can be simply defined as structured sets of objects and/or attributes with specific relationships between them. In order to solve this particular geodetic problem, use should be made of all relevant disciplines, in a multi-disciplinary approach.

3.1. The Open Dynamic System

The type of system in which it is convenient to describe the footprint and its components is the **open dynamic system**, as its main matter component is the surface of the Earth, which is open to the flow of matter and energy. Using GPS as an example, the system's main measurement component is GPS, which is open to influence from other systems, such as the ionosphere, troposphere and time. We have thus an external input, some processes internal to the system, such as rock movement or soil heave and an output consisting of radiated energy or matter which leaves the system. Each component in the footprint system can be described as a subsystem and this approach allows a methodical, structured approach which aids in describing the footprint system holistically.

The footprint as an open system, in the case of HartRAO can be described as having:

- **Boundaries**: an inner boundary set by the five inner monuments, an intermediate boundary, set by the four outer monuments and an outer boundary set by the three reference points of the outer network.
- A **focal point**, chosen as the main reference point, which is the area surrounding the radio telescope and which contains the radio telescope, the SLR pad and IGS reference point HRAO and monuments close (< 200 m) to the radio telescope.
- A **set of coordinates** which defines the boundaries and focal point. The focal point has fixed coordinates whereas the boundary reference points have dynamic coordinates. For instance, the IGS station HRAO was used as the "fixed point" in the final adjusted values of the footprint.
- **Inputs and outputs** of varying nature such as energy, matter and information (e.g. satellite ephemerides), which cross the boundaries of the system.
- **Processes** within the system which affect measurement accuracy and monument stability.
- A **steady state**, in which the footprint shows no signs of instability; it is in dynamic equilibrium. An **unsteady state**, where one or more reference points shows instability; the system will either move towards a new state of equilibrium or return to its previous state. During the crossover from one steady state to the next, the footprint system is in a **transient state**.

The footprint is mostly a cyclic, dynamic system in which the energy and other factors which constitute the inputs increase and decrease in a cyclic manner. As an example the measurement system is affected by diurnal changes in total electron content and periodic repetition in the geometry of the GPS satellites. The Earth's surface, i.e. the crustal component, is affected by diurnal variation in incident solar radiation, which causes possible thermal expansion and contraction. This component is also affected by the drying and wetting cycle of summer rain and winter dry periods.

4. Footprint Geology and Geomorphology

Causes and factors involved in site stability are mentioned here as these should be taken into account during site selection and during the lifetime of the geodetic monuments. For instance, weathering can cause apparent site instability through affecting the stability of a monument by transport of surface material; or weathering of subsurface rock could lead to progressive settlement of a monument.

4.1. Natural Slopes

The geodesist should be aware of the danger that slope movement presents to his footprint monument stability. This is especially true if the monument is located on a slope and not tied to bedrock. Many footprint areas over the world will be located on terrain which is not perfectly flat and not all sites will have zero slope movement. Slope movement and development is a common, natural occurrence and is an important factor in footprint stability. Giani (1992) mentions some of the principal phenomena which can contribute to an increase in shear stress and/or to a reduction of shear strength, both being causes which determine sliding movement in a slope. Contributions to an increase in shear stress are mainly from the slope surface or toe weakening, or slope surcharging. Natural surcharging results from water percolation in rock discontinuities, rain water or snow weight. Man also plays a role when constructing embankments, heavy buildings and other structures, and large water reservoirs.

Slope surface or toe weakening could be the result of erosion by streams, rivers, glaciers, waves, tidal currents, sub-aerial weathering, wetting and drying and frost action. Subsidence, previous rock fall, toppling, sliding and superficial scaling play a role as well as phenomena connected to human activity such as excavations and mining. The main causes contributing to a decrease in shear strength include soil texture rock fabric and structural defects, physical and chemical reactions as well as changes in intergranular forces. Slope studies should form part of the footprint systems approach; local movement will in most cases be due to some form of slope movement unless the footprint is situated in an active earthquake zone. Even in earthquake zones, slope movement would still be very important as slope activity could be increased by seismic activity.

5. Monumentation and the Geodesist

Monumentation is one of the most important aspects of a geodetic installation, where long and short term stability is the main requirement. Using a tripod to locate a theodolite or GPS antenna is an inferior approach and should **not** be used for high precision work. Self-centring devices which are permanently fixed to the monument should be used because reoccupation errors

are tens of microns instead of a tripod's millimetres. In order to determine crustal stability or measure relative plate motions, conduct a footprint or measure Earth rotation, one needs to fix the geodetic monuments to be used to the Earth's crust.

The more interfaces we have between the geodetic reference point and the solid crust, the more leeway is allowed for indeterminate errors. If data are collected over a long time, local and short term effects which induce positional errors tend to be averaged out, which give some observers confidence in a weak interface. However, as is well known, statistically it is far better practice to have better data than more but poor data. It is obvious that the closer the monument is located to the crust, the better, but even the shortest interface can be weak if made from the wrong material or incorrectly constructed. All of this sounds like common sense but when one inspects some geodetic reference points, it is obvious that more regard has been given to other factors such as ease of installation, cost considerations, accessibility, safety and security of equipment and personnel. Before one can design and construct a suitable interface between the reference point and the crust, one must first decide how the crust, in our terms of reference (considering crustal dynamics and footprint networks) can be defined.

A monument located on soil or on a building would be more unsuitable than one that has been built on the bedrock as the interface between the monument and the crust would be strengthened by limiting the material separating the monument and the crust. The upper layer of the crust may not necessarily be that fixed either, as sediments and crystalline basements exhibit the presence of cracks, joints, fractures and fissures for at least the first 10 km of depth, but the topmost 10 m or so is normally the zone where bedrock acts as parent material for soil. This is a zone which should preferably be bypassed when installing a geodetic monument. Using this simple introduction one can create a definition of the crust from a surveying point of view.

This crust varies in composition and physical characteristics. One could therefore write:

- *Monumentation crust = the layer of the Earth, overlaid by man made structures, water, vegetation and organic matter, soil and regolith. Its depth varies from the surface where it can be exposed, to depths exceeding 100 m. It is the thin layer that separates the soil forming part of the uppermost layer of the Earth from the more stable and subjected to significantly less weathering processes, solid crust and is normally the parent material for the soil.*

The rock close to the monumentation crust could be weathered to such an extent that a residual soil is formed, which could take the form of several layers of rock-like soil or soil-like rock transitions in between. This residual soil, or saprolite, should be bypassed by drilling until true bedrock is reached and not be confused with the monumentation crust. From a stability and accessibility point of view, the ideal location for a geodetic monument would be on exposed, unweathered bedrock. Regardless of the inaccessibility to the monumentation crust, maximum effort should always be exerted to have the reference point located as close to and connected as strongly as possible to this crust.

In the geotechnical field, rock and soil stability analyses are used to allow evaluation and prediction of instability, especially those caused by excavation and construction on natural slopes. The analyses are designed to support the safe and functional design of slopes to be cut, and incorporate features such as consolidation works (drainage systems, retaining walls) which can aid in stabilising a slope. Evaluation is made of the role played by design parameters such as excavation height and slope angle, in order to determine their role in the work excavation stability. Unless the researcher is placing his monument on an absolutely flat location, which is not a very likely scenario, it is being placed on a slope. Geotechnical engineering and geomorphology provide

us with information which is useful when selecting a site for a geodetic monument. The purpose of this section is to describe, in a general way, what one should keep in mind when selecting a site from a stability point of view.

5.1. Field Investigation

Once a decision has been made on the geographical region for the monument installation and one has studied available geological and geotechnical data, a field reconnaissance should be undertaken to gather information on the proposed site. Note the presence of exposed bedrock, note the strike and dip of the rock, joint spacing and condition. One should draw a map of the site and its immediate surroundings, keeping in mind the requirements of a stable monument. Factors which might influence the stability of the monument on rock are:

- Presence of faults, joints, fractures, shear zones.
- Varying ground water levels.
- Rock slope instability, rock which could cause problems due to swelling, dissolving and shrinking.
- Presence of cavities due to karstic formations, such as found in dolomitic regions.
- Human engineering activity, gas,water and sewer pipes, drainage ditches.
- The type and condition of the rock.

The effect of these factors are quite obvious. For instance joints, fractures and shear zones may be filled with compressible soils such as expansive clay. During drying and wetting cycles, expansive minerals, for instance montmorillonite and anhydrite, shrink and expand, leading to a seasonal signal in the time series. Cavities develop in soluble rocks, especially dolomite, limestone, rock salt and gypsum. This might not have an immediate effect on the monument, but an existing cavity may lead to the monument disappearing into a sinkhole when the cavity roof collapses. Flow of water dissolves gypsum and can cause tilting of the monument. Certain types of rock are less suitable for a stable site, as the density of the rock is normally a factor in the swelling characteristics of the rock. Shales for instance are affected by moisture content, density, weathering and mineral structure.

5.2. Monumentation Located on Rock

Rock mass strength is an important determinant of slope form, especially in the absence of structural controls. Rock properties such as intact strength, spacing of joints and other geological discontinuities determine to some extent the form of the equilibrium slope. Any changes in the slope form over time will affect the stability of the monumentation. Generally the emphasis in the literature has been on processes as controls of rock slope development (Wood 1942), (King 1953), but more recently rock mass properties have been recognised as controls in rock slope evolution (Terzaghi 1962, Moon 1985). The study of the properties of materials, although a relative newcomer to the field of geomorphology, emerged in recognisable form with the work of Yatsu (1966) and found its way into the mainstream of geomorphology by Whalley (1976). Compressive strength, the degree of rock weathering and elasticity have been found to affect control on morphometric variables such as valley slope gradients and drainage density (Cooks 1979, 1981, 1983). A technique to determine rock mass strength was developed by Selby (1980) which allows for the expression of rock mass strength on a scale from 25 to 100. Rock mass strength

can be regarded as the resistance of a rock mass to surface processes and it being the foundation of the reference monument, it follows that rock mass strength is directly related to the long term stability of the monument. Application of rock mechanics was taken further by Selby (1982) and Moon (1985) and led to a better understanding of rock resistance and joint roughness as controls of the stability of different rock slopes. It is important to bear in mind the main finding that joint spacing and intact rock strength are some of the prime determinants of slope form. The detailed analyses of individual properties of rock masses will enhance the understanding of the development of rock slopes and consequently of long term monument stability. Study of the materials, or at least taking them into account in some way, will aid in evaluating potential stability or instability and has important implications for monument design and site selection. Rock mass classification systems exist which have been used extensively in correlation with parameters applicable to the design of rock foundations (ASCE 1996). The geodesist should be aware of these approaches, as they provide valuable insight as to the possible instabilities, especially in the long term, which could affect a monument's stability.

5.3. Monuments Located on Soil

Classical soil mechanics can be put to use to give one a good indication of the expected stability and movement of a monument located on soil. There are two basic groups of calculations, *settlement calculations* and *stability calculations* which are commonly used in geotechnical engineering. Settlement calculations are of direct importance to us as it is concerned with the stiffness of the soil beneath the monument. Stability calculations are used to model complete failure of soil masses, where large deformations occur on rupture planes followed by collapse of the geotechnical structure. Useful calculations can be done for a given monument and examples as well as the mathematical theory supporting various approaches can be found in the literature (see for instance Lambe 1964, Bowles 1977).

5.3.1. Volumetric Variables

A large proportion of the volume occupied by soil consists of voids, normally filled by air or water (pore fluids). When deformed, large and often irreversible changes in volume can occur due to the change of relative positions of the soil particles. In contrast, rock is more homogeneous at the particulate level so it is easier to describe it in terms of stresses and strains. However, the geotechnical structure on which the monument is located is normally much larger than the individual soil particles and as long as we take into account the possibility of large volumetric changes, stresses and strains can be averaged over the soil. The soil particles form a highly redundant skeletal, cellular framework, so any changes in the volume of this particle structure leads to the flow of pore fluid through the soil. The mechanical behaviour of the geomaterial on which a monument is located depends on its state, which in turn is defined by its structure and texture.

State parameters are:

- porosity (density)
- water content (consistency)
- stress (stress level, degree of isotropy, stress path)
- strain

- time
- temperature

These parameters are not isolated; instead they act in combination. It is outside the scope of this paper to give a detailed description of each parameter, but the geodesist should be aware of the following points:

- The stress fields of porous continuous materials are not homogeneous (Feda 1992) and sources of progressive failures at higher stress levels, different stress gradients, their distribution and intensity, depend on the pore-size curve, as well as the overall porosity and its homogeneity.
- An increase in water content can lead to structural breakdown or decrease in strength and peak shear resistance. Monuments should not be built in a depression where water can accumulate.
- The mechanical response of soils is related to the magnitude of their strain (Ishihara 1981, quoted by Feda 1992). The response is elastic for $\epsilon < 10^{-5}$; elastoplastic for $10^{-2} > \epsilon > 10^{-5}(\epsilon = 10^{-1}$ representing the approximate failure strain); loading rate and frequency becomes relevant when $\epsilon > 10^{-3}$. The value $\epsilon > 10^{-3}$ is the threshold for major structural changes before dilatancy and contractancy appear.

5.4. Monuments Located on Buildings

Many geodetic monuments are actually buildings. If one attaches a GPS antenna to a pole which is attached to a building, the pole is not the monument, nor is the antenna mount the monument, the monument is the building. Buildings are not necessarily bad monuments, they often meet requirements in respect of accessibility, safety, power and convenience. Hardly ever are they evaluated in terms of their long-term stability. Building foundations suffer from primary consolidation, which results in the pore-water pressure being diffused. The theory and calculations can be found in the engineering literature (see for instance Holtz and Kovacs 1981, ASCE 1996) and indicates that even for geodetic monuments, depending on soil type and state, some primary consolidation is to be expected. Secondary consolidation should also be taken into acount. All buildings will show some settlement; the best will be those which have had pilings done to bedrock. It is probably good practice to avoid using buildings as monuments. When a building is constructed, its foundations may or may not be fixed to bedrock. The load imposed by the structure at the foundation level will always be accompanied by strain which results in settlement of structures. This is true for the monument as well to a certain extent. The total settlement of the monument or building foundation in general is given by

$$S = S_e + S_c + S_s \tag{1}$$

where S_e = immediate settlement, S_c = primary consolidation settlement and S_s = secondary consolidation settlement. In granular soils the predominant part of the settling is during the immediate settlement phase. In areas where saturated inorganic silts and clays occur the primary consolidation settlement predominates. If the monument is located on highly organic soils or peats the secondary consolidation settlement forms the major part of the settlement.

The expected settlement is not easy to calculate due to the many variables involved such as modulus of elasticity, shear modulus and Poisson's ratio obtained from triaxial tests, but reasonable estimates are possible; one can find many different approaches in the literature. If one is installing a monument on a newly constructed building, mortar shrinkage will produce some instabilities, these last about six months. Typical primary consolidation over a period of 10 years is on the

several cm level. The settlement depends a lot on how close the foundation is to bedrock—the closer, the more stable the monument will be. So within reason, if one has to choose a building for a monument location, it becomes part of the monument and in general older buildings should be more stable.

6. Footprint Networks

In a way, footprints are like fingerprints, not one is alike and each footprint will show the influence of its owner. The smaller inner network should possibly be called the fingerprint, as it is usually given much more attention. At HartRAO, during the footprint planning stages, fair consideration was given to network geometry and accessibility to reference points. Using self-centering plates and existing standard trig beacons did lead to a suitable geometrical configuration and practical network which was cost effective. During the construction of the 26 m radio telescope and the years following, several beacons were constructed surrounding the telescope and some of these were very suitable for the inner network. The outer and intermediate networks were designed by using as a starting point a topographical map on which the trig beacons have been marked. Some apparently suitable beacons were selected from the map. This was followed by a field investigation to ascertain their overall suitability, leading to a final selection of the existing footprint network. This consists basically of an outer network of three points, an intermediate network of four points and an inner network of five points with radii centred around the VLBI telescope of approximately 60 km, 20 km and 1 km.

7. Conclusions

The footprint for a specific geodetic site is defined by the operations required to make it scientifically useful and is not determined by any one particular definition set up with special circumstances in mind. Footprints determine geodetic site integrity, identify local instabilities, determine eccentricities between different geodetic techniques, and can vary in scale from very local (tens to hundreds of metres) to several tens of kilometres scale or more, depending on specific local requirements. Footprints are not technique dependent, nor are they bound by particular disciplines and can be regarded as an open dynamic system. Footprints should include some investigation of the geology and geomorphology of the area encompassed by the footprint networks as well as a substantial area beyond these networks. Evidence of historical and present/future instability can be had from several sources such as faults, seismics and geomorphology. The main point to be stressed here is that one should approach the footprint study from an holistic viewpoint and one should take into consideration the history, structure and slow evolution of the Earth on which the footprint is located. Final results of a footprint or any other geodetic network depend to a large extent on the stability and suitability of the monumentation used.

References

ASCE 1996. *Rock Foundations.* Technical engineering and design guides as adapted from the U.S. Army Corps of Engineers, by the American Society of Civil Engineers. Series TA775. R63. ASCE. USA.

Bell, L., Bryant, M., Nelson, V. and Allenby, R. 1994. *NASA's Space Geodesy Project: A*

Summary of GPS Footprint Results. Unpublished report provided by C. Noll of the NASA Crustal Dynamics Data Information System (CDDIS).

Bowles, J.E. 1977. *Foundation Analysis and Design.* McGraw-Hill. New York.

Cooks, J. 1979. Die verband tussen litologie en landvorme. *South African Geographer*, **7**, 127-135.

Cooks, J. 1981. Rock quality measured by seismic wave velocity as a factor in landform development. *South African Journal of Science*, **77**, 517-521.

Cooks, J. 1983. Geomorphic response to rock strength and elasticity, *Zeitschrift für Geomorphologie* ,**27**, 483-493.

Giani, G.P. 1992. *Rock Slope Stability Analysis.* A. A. Balkema. Rotterdam.

Holtz, G.T and Kovacs, W.D. 1981. *An Introduction to Geotechnical Engineering.* Prentice-Hall. New Jersey.

Ishihara, K. 1981. Strength of cohesive coils under transient and cyclic loading conditions. State-of-the-art in earthquake engineering. In: Ergunay O. and Erdik M. (eds), *Turkish National Committee on Earthquake Engineering.*

King, L.C. 1953. Canons of landscape evolution. *Bulletin of the Geological Society of America*, **64**, 721-751.

Lambe, T.W. 1964. Methods of estimating settlement. *J. Soil Mech. Found. Div. Am. Soc. Civ. Eng.*, **90**, no. SM5.

Moon, B.P. 1985. Controls on the form and development of rock slopes in fold terrane, in *Hillslope Processes*, ed. A.D Abrahams. Allen & Unwin. Boston. USA.

Selby, M.J. 1980. A rock mass strength classification for geomorphological purposes: with tests from Antarctica and New Zealand, *Zeitschrift fur Geomorphologie*, **24**, 31-51.

Selby, M.J. 1982. Controls on the stability and inclinations of hillslopes formed on hard rock. *Earth Surface Processes and Landforms*, **7**,449-467.

Terzaghi, K. 1962. Stability of steep slopes in hard unweathered rock. *Geotechnique*, **12**, 251-270.

Whalley, B.W. 1976. *Properties of materials and geomorphological explanation.* Oxford University Press. Oxford.

Wood, A. 1942. The development of hillslide slopes. *Proceedings of the Geological Association*, **53**, 128-140.

Yatsu, E. 1966. *Rock control in geomorphology.* Sozosha. Tokyo.

Sten Bergstrand et al.: A New GPS–VLBI Tie at the Onsala Space Observatory, IVS 2000 General Meeting Proceedings, p.128–132
http://ivscc.gsfc.nasa.gov/publications/gm2000/bergstrand

A New GPS–VLBI Tie at the Onsala Space Observatory

Sten Bergstrand, Rüdiger Haas, Jan Johansson

OSO, Onsala Space Observatory
Contact author: Sten Bergstrand, e-mail: sten@oso.chalmers.se

Abstract

Onsala is a collocated reference site for IVS as well as IGS. In order to establish a new type of tie between the two reference frames, we have installed two Dorne Margolin GPS choke ring antennas on the 20 m VLBI telescope that is situated inside a radome. One of the antennas is permanently mounted on the subreflector support structure, the other one is intermittently attached close to the vertex of the parabola with a rigid support. Since mid 1999, repeated measurements have been performed pointing the VLBI telescope to the zenith position. In addition we made experiments with a moving 20 m dish, but without success. To obtain accurate positions of the two antennas, we found that measurements inside the radome are feasible without further multipath suppression than that already provided by the choke rings and that a data set consisting of 24 hour uninterrupted measurements was necessary.

1. Introduction

The Onsala Space Observatory (OSO) is a joint IVS (International VLBI Service for Geodesy and Astrometry) and IGS (International GPS Service) component. With increasingly improved accuracy within and interaction between the VLBI and the GPS techniques, the demand for accurate ties at common reference points has increased. Since the 20 m VLBI antenna at Onsala is operating inside a radome and the reference point is immaterially suspended in free air inside a stainless steel cabin, optical measurement of the reference point is quite complicated to achieve.

Our main objective has been to improve the local connection between VLBI and GPS, inspired by Combrinck and Merry [1], and Matsuzaka *et al.* [2]. We try to develop a method for frequent measurements of the tie to check monument stability. A second order objective is the ability to perform GPS measurements inside the radome, an environment anticipated to have serious multipath problems caused by the aluminium frame for radome support and the 20 m dish. Currently, we use an invar rod to measure height deformation of the concrete foundation. We hope to be able to detect that signal with the GPS and possibly also the thermal deformation of the subreflector support structure. The general idea has been to mount GPS antennas on the 20 m antenna and do measurements while pointing to the zenith. As an extracurricular activity, we have tried to measure during VLBI experiments in order to monitor the reference point simultaneously with the different techniques.

At OSO, previous ties between the the two techniques have been made in two ways, the first being a combination of classic surveying techniques and construction drawings; the second a combination of mobile VLBI and classic surveying. The disagreement between the ties is on the centimetre level and partly poorly documented. A new accurate tie would certainly contribute to connect the IVS and IGS reference frames. The present work involves a combination based on GPS data, classic measurements and technical drawings; something we hope to be able to reduce to a combination of GPS data and classic measurements in the future.

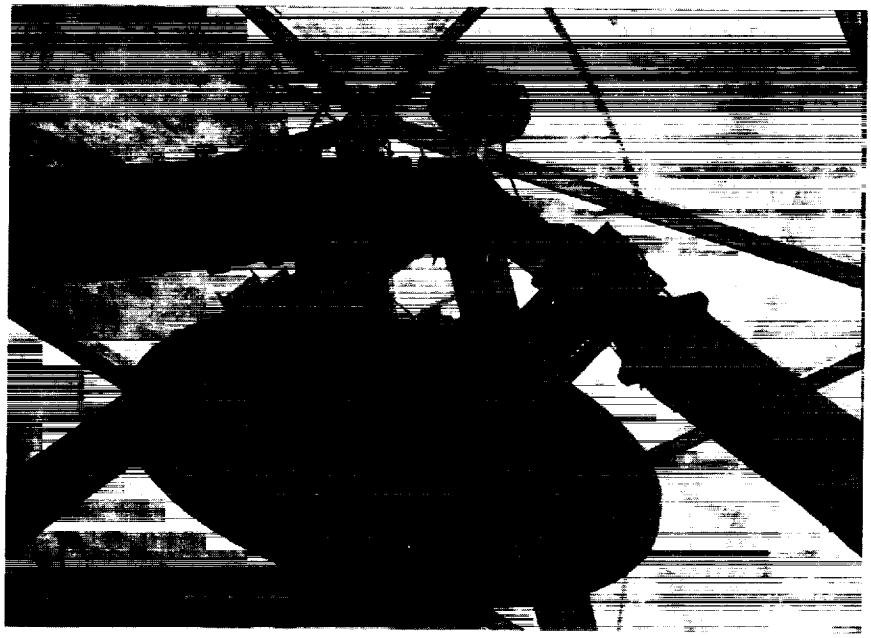

Figure 1. APEX antenna on top of the subreflector support structure.

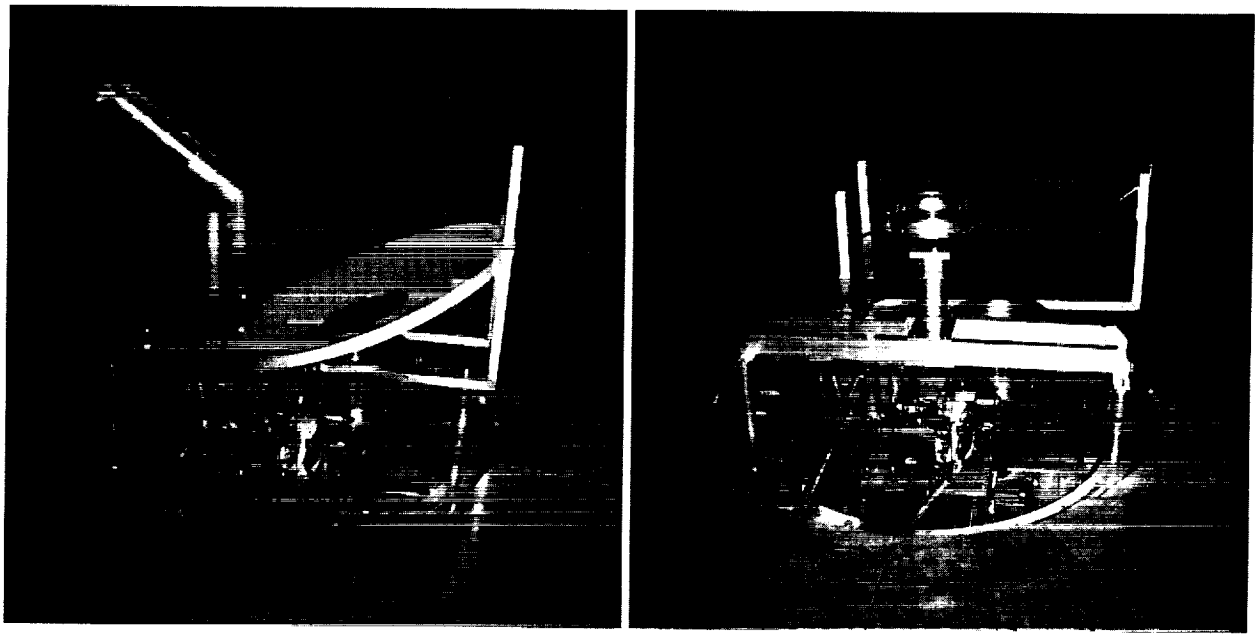

Figure 2. a) Normal S/X set-up with dichroic surface and S-band waveguide. b) VTEX antenna mounted, S-band waveguide removed.

2. Set-up

In order to pursue both objectives, GPS measurement of the IVS reference point as well as thermal deformation of the antenna, we have mounted two Dorne Margolin choke ring antennas on

the structure. One is permanently mounted on top of the subreflector support structure, henceforth referred to as APEX (Fig. 1), and one is intermittently mounted close to the vertex of the parabola, hence VTEX (Fig. 2). APEX is permanently connected and should in principle be able to measure at all times. When OSO is measuring S/X-band, a dichroic reflector surface is mounted in front of the X-band horn. The dichroic surface reflects S-band signals into a waveguide that redirects the signals into the S-band horn. When VTEX is used, the normal VLBI configuration's dichroic surface and S-band waveguide have to be removed in order to get rid of objects that affect the electromagnetic environment. On the 20 m antenna at OSO, this procedure seemed to be the best compromise between proximity to the actual vertex and rapid mounting with submillimetre repeatability. Measurements may now commence within an hour from antenna hand-over. The actual antenna in VTEX is electrically insulated from the remaining structure in order to maintain the antenna's a priori characteristics and refrain from disturbing interaction of the 20 m dish. For acquisition and recording, we use Turbo-Rogue receivers and sample once every 30 seconds. Experiments have been made with as well as without absorbing material on the subreflector in order to evaluate the possible impact on multipath effects (Fig. 3).

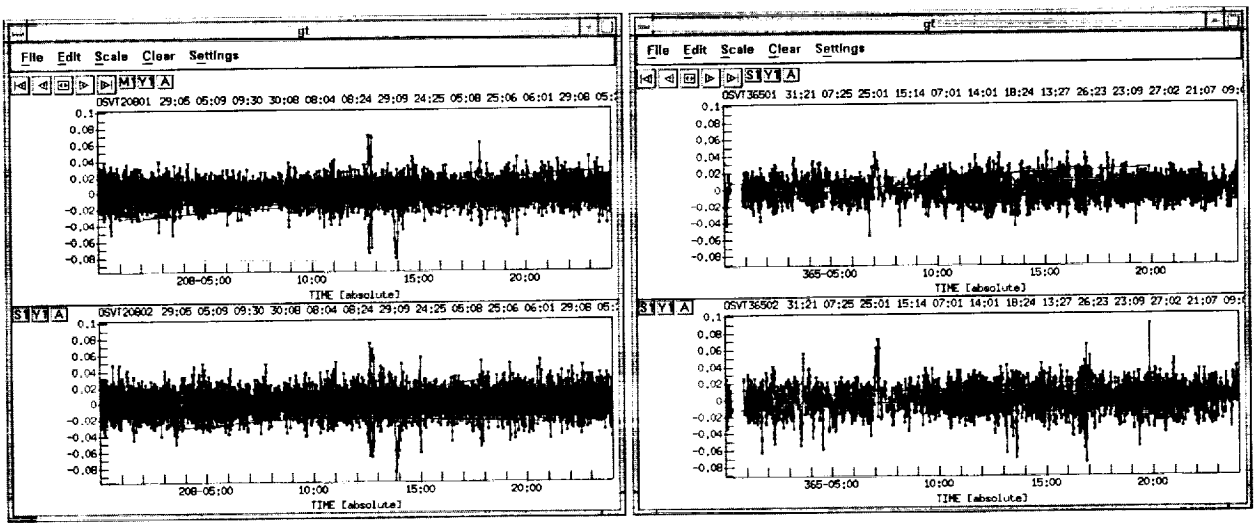

Figure 3. a) Residuals with absorbing material. b) Residuals without absorbing material. Absorbing material on subreflector has no significant impact on multipath suppression.

3. Data Acquisition

Data have mainly been acquired during maintenance periods and with benevolent permission from fair-weather astronomers (the 1999 Onsala autumn has favoured our measurements). That meant that most experiments were recorded from Friday afternoon to Monday morning. Excluding preliminary tests, we have performed five successful experiments commencing with a full week in July, the rest being "weekend experiments". We have also tried to measure at APEX during VLBI experiments, but in the most favourable cases the receiver lost track of satellites, started "open sky search"-mode and obtained preposterous results (worst cases meant losing track of satellites completely).

4. Data Analysis

We processed the recorded data of APEX and VTEX together with data from the IGS permanent station at Onsala as a three station network. For preparation, we used the Bernese 4.1 software [3] in "manual-automatic" mode. We used the graphic option to manually reduce the influence of obvious outliers in the residuals when satellites were getting close to the horizon. From the VTEX antenna, the rim of the 20 m dish is at 12 degrees elevation, and the used software elevation cut-off is 15 degrees. Solutions were obtained from 24 hour periods, midnight to midnight whenever possible. During processing, we assumed the IGS reference antenna to be the most stable in the set-up and determined the position of the other two antennas relative to that. When we analysed the data, we realized that days with less than 24 hours of observations, i.e. the Fridays and Mondays of our weekend experiments, showed outlying results and larger formal errors as compared to days with 24 hours of observations, although they appeared to be reasonable at first inspection. In other words, we do have a multipath problem, but the longer the observation period, the better the results. Apparently, the averaging reduces the impact from multipath. Therefore, we use the 24 hour period as a criterion for position fidelity (Fig. 4).

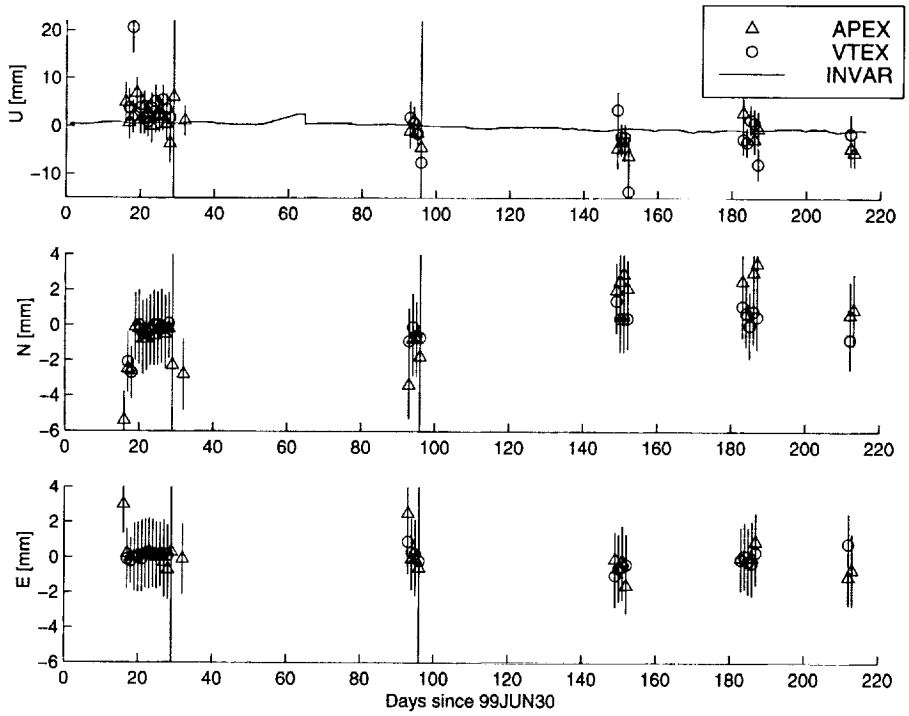

Figure 4. Up, North and East residuals from mean positions. Days 29 and 96 have less than 12 hours of data and larger formal errors. Invar measurement for comparison of vertical components.

5. Results

Although the radome is causing serious multipath, RMS errors of the APEX and VTEX positions are of the same order as measurements made outside. As a fiducial solution we have run an

automatic check with the GIPSY/OASIS software [4] for the "favourable" measurement days. The automatic GIPSY solutions that model data differently than the Bernese software accommodate the Bernese values within their error limits.

Since our GPS results are still somewhat preliminary and too many distances on the telescope remain to be measured with high accuracy, we prefer not to communicate the results yet, but consider this to be a status report and show only the residuals. Formal errors for North and East components are of equal order, whereas the Up-component, as expected, has larger formal errors. The errorbars shown in Fig. 4 are Bernese repeatability output. For the Up component (first row) we also show the relative height measurement of the telescope obtained by the invar rod device installed inside the concrete foundation. For more details on the invar measurement system see for example Haas *et al.* [5]. Experience from GPS experiments with stable monuments for determination of crustal movement in Scandinavia (Bergstrand et al., in preparation), suggest an up-scaling of formal errors from GPS analysis software packages by a factor of three.

6. Conclusion and Outlook

We have tried to establish a new tie between the IGS and IVS reference frames at the collocated site Onsala by mounting GPS antennas on the 20 m VLBI antenna. We found that the quality of GPS measurements inside the radome is comparable to the quality of measurements in a less multipath prone environment (even without absorbing material on subreflector), given that measurements are made over at least a 24 hour period. The GPS antennas need therefore to be positioned with an accuracy of 1 millimetre in order to get a good tie. Since the results are more accurate than anticipated, we are currently exploring the possibility to monitor the GPS antenna positions and align them with the azimuth axis of the 20 m antenna more accurately. We anticipate that a receiver with a quicker update (e.g. Ashtech ZXII) will be able to track satellites even when the 20 m antenna is moving. If we can utilise such receivers, we will try to determine the reference point of the VLBI telescope as the centre of a hemisphere created by the positions of the roving GPS antennas.

Acknowledgment. Rüdiger Haas is supported by the European Union within the TMR programme under contract FMRX-CT960071.

References

[1] Combrinck, W. L., Merry, C. L.: "Very long baseline interferometry antenna axis offset and intersection determination using GPS", *JGR*, Vol. 102, No. B11, pp. 24,741–24,743, Nov 1997.

[2] Matsuzaka, S., Ishihara, M., Nemoto, K., Kobayashi, K.: "Local tie between VLBI and GPS at Geographical Survey Institute", In: *Proceedings of the international Workshop on GEodetic Measurements by the collocation of Space Techniques ON Earth (GEMSTONE)*, pp. 68–72, 1999.

[3] Beutler, G., Brockmann, E., Fankhauser, S., Gurtner, W., Johnson, J., Mervart, L., Rotacher, M., Schaer, S., Springer, T., Weber, R.:"Bernese GPS Software Version 4.0", 1996.

[4] Webb, F. H., Zumberge, J. F.: "An Introduction to GIPSY/OASIS-II Precision Software for the Analysis of Data from the Global Positioning System", *JPL Publ. No. D-11088*, JPL, 1993.

[5] Haas, R., Elgered, G., Scherneck, H.-G.: "Onsala Space Observatory – IVS Network Station", *IVS 1999 Annual Report*, edited by N. R. Vandenberg *NASA/TP-1999-209243*, pp. 90–93, 1999.

Rüdiger Haas et al.: VLBI Determinations of Local Telescope Displacements, IVS 2000 General Meeting Proceedings, p.133–137
http://ivscc.gsfc.nasa.gov/publications/gm2000/haas1

VLBI Determinations of Local Telescope Displacements

Rüdiger Haas [1], *Axel Nothnagel* [2], *Dirk Behrend* [3]

[1]) *Onsala Space Observatory (OSO), Chalmers University of Technology (CUT)*
[2]) *Geodetic Institute of the University of Bonn (GIUB)*
[3]) *Institut d'Estudis Espacials de Catalunya (IEEC)*

Contact author: Rüdiger Haas, e-mail: haas@oso.chalmers.se

Abstract

At three telescopes involved in the European geodetic VLBI network track and wheel repair work had to be performed during 1996 and 1997, possibly changing the positions of the geodetic reference points. In order to monitor these changes conventional geodetic surveys have been done with respect to the local geodetic footprints of the telescopes. Knowledge of the position and possible change of position of the geodetic reference point of a telescope is of great importance for the geophysical interpretation of the results obtained from geodetic VLBI. In our paper we derive the changes of the geodetic reference points directly from the VLBI data observed in the European geodetic VLBI network and compare our results to the ones obtained by conventional geodetic surveys.

1. Introduction

One of the goals of geodetic VLBI is to monitor interplate and intraplate crustal motion with high precision and accuracy. The geophysical interpretation of crustal motion results derived from geodetic VLBI requires that the movement of the telescopes are representative for the part of the Earth's crust they are attached to. This basic requirement relies on the precise knowledge and a precise monitoring of the position of the geodetic reference point of the VLBI telescopes with respect to the Earth's crust. Normally this is ensured by repeated conventional geodetic surveys of the reference point and the geodetic footprints of the telescope.

The geodetic reference point of an alt-azimuth VLBI telescope is the intersection of its elevation and azimuth axes. Unfortunately it is usually not directly accessible and so its position is difficult to observe with conventional geodetic survey methods. The reference point is normally invariant to the surrounding of the telescope. However, its position changes for example when repair work of the mechanical parts of a telescope are carried out.

Three telescopes involved in the European geodetic VLBI network were repaired in the last four years. Track and wheel repair had to be done at Medicina (Italy), Effelsberg (Germany) and Madrid (Spain) in 1996 and 1997. These telescopes are large steel constructions of azimuth-elevation mount type, see Figure 1. Turning the telescopes in azimuth the constructions run with wheels on circular tracks placed on concrete foundations.

The Medicina 32 m telescope was repaired during early summer 1996 and the work was completed July 1st, 1996. Cracks in the concrete foundation of the track had developed over the years and so the telescope had to be lifted and the concrete foundation had to be repaired. Similar problems were detected at the Effelsberg 100-m telescope which was lifted during autumn 1996 and the foundation and the track were repaired. The work was completed October 1st, 1996. The Madrid 34-m telescope finally was repaired during spring 1997. Here a deformation of the foundation and cracks had been detected. The track was repaired and the work was completed April 30, 1997.

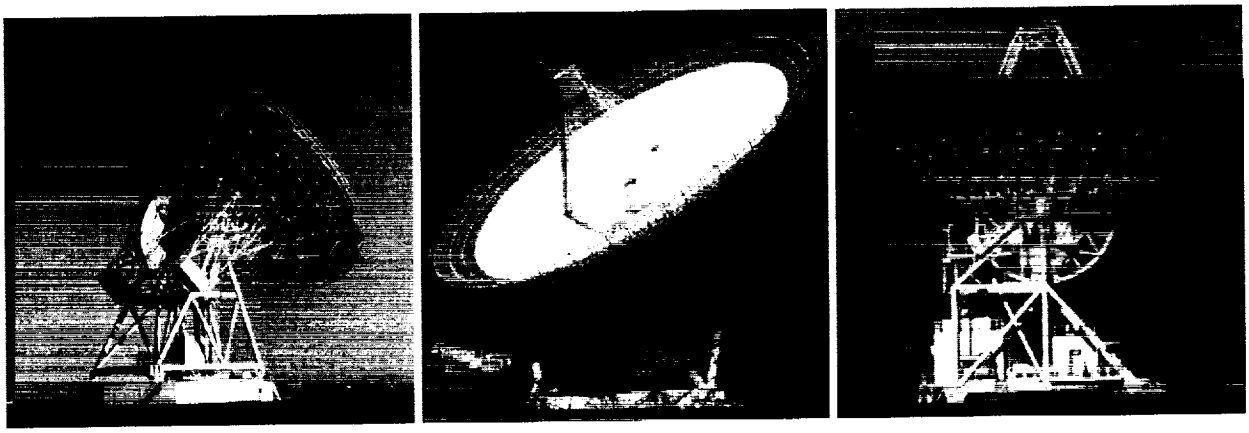

Figure 1. Three telescopes involved in the European geodetic VLBI network with track and wheel repair in 1996 and 1997. Left to right: Medicina (32 m), Effelsberg (100 m) and Madrid (34 m).

Conventional geodetic surveys of the geodetic reference points before and after the repair work have been performed at all three telescopes [1], [2], [3].

A second method of determining the displacements of the reference point is to analyse the VLBI data directly, provided that sufficient geodetic VLBI observations are available before and after the repair work. These results can then be compared to the ones derived from the conventional geodetic surveys.

2. The VLBI Data Analysis

For 10 years now the European geodetic fixed station VLBI network has been carrying out regular observing sessions for the determination of station coordinates and tectonically induced displacements [4]. Since the European network is very sensitive to displacements of the telescopes as such a special analysis of the data was carried out in order to determine the displacements of local origin, e.g. caused by repair work.

The analysis was performed using the CALC/SOLVE analysis software [5], [6] as a so-called "baseline solution", i.e. keeping one reference station fixed in the network and determining the coordinates of all other stations. We used Wettzell as reference station and adopted Earth orientation parameters and radio source positions from a recent global VLBI solution [7]. A refined frequency and latitude dependent solid Earth tide model and a recent ocean loading model [8] were applied.

The analysis provides time series of geocentric Cartesian coordinates for all stations except the reference station. Subtracting the global drift of the European plate according to the Nuvel-1A-NNR plate tectonic model [9] yields station coordinates in a Europe-fixed system. These were transformed into local topocentric coordinates using the parameters of the WGS84 ellipsoid. Subtracting mean positions, time series of topocentric east, north and height components were derived which were then used to compute topocentric drift rates with respect to the reference station.

We estimated additional offsets for each of the topocentric components on the days when the repair work was completed. The drift rates were forced to be the same before and after the offset.

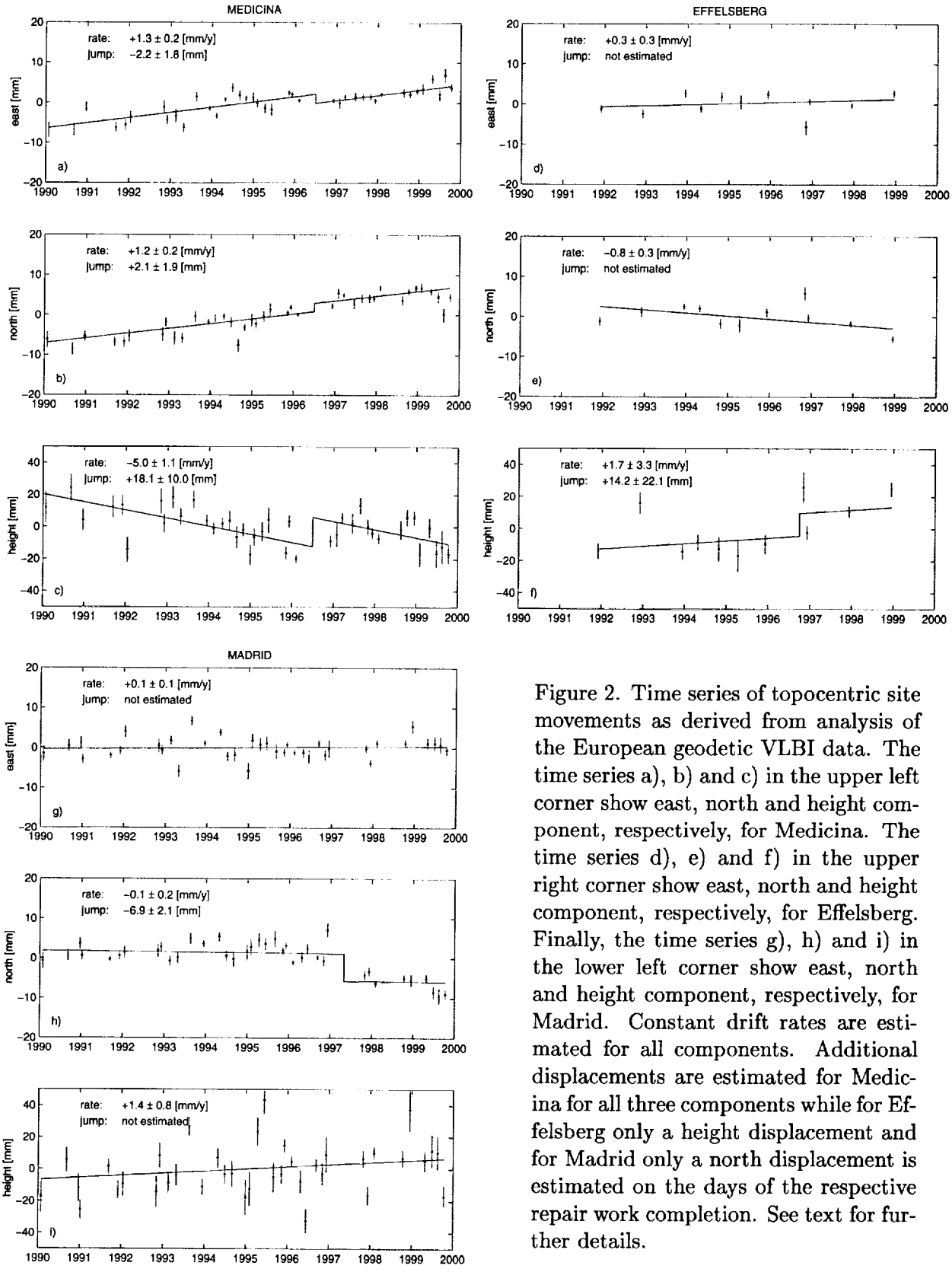

Figure 2. Time series of topocentric site movements as derived from analysis of the European geodetic VLBI data. The time series a), b) and c) in the upper left corner show east, north and height component, respectively, for Medicina. The time series d), e) and f) in the upper right corner show east, north and height component, respectively, for Effelsberg. Finally, the time series g), h) and i) in the lower left corner show east, north and height component, respectively, for Madrid. Constant drift rates are estimated for all components. Additional displacements are estimated for Medicina for all three components while for Effelsberg only a height displacement and for Madrid only a north displacement is estimated on the days of the respective repair work completion. See text for further details.

Statistical tests were then applied in order to decide which of the abrupt displacements may be considered significant. For the station Medicina all three-dimensional topocentric displacements are significant at the 95% confidence level. The test statistics are $T_e = 29.5$, $T_n = 8.3$ and $T_h = 19.0$, for east, north and height displacement, respectively. The null hypotheses testing whether one of the displacements does not differ significantly from zero have an alpha-quantile of $F_{0.95;1,37} = 4.1$ and so are rejected. From a statistical point of view it is therefore quite safe to introduce the abrupt displacements in the analysis.

For Effelsberg none of the three-dimensional displacements is significant in a statistical sense. The test statistics are $T_e = 2.2$, $T_n = 0.7$ and $T_h = 0.1$ for east, north and height displacement, respectively, while the alpha-quantile is $F_{0.95;1,8} = 5.3$. Nevertheless, the inclusion of an additional height displacement causes the height drift to reduce from +4.5 [mm/y] to +1.7 [mm/y] as compared to a linear regression without the additional height displacement. Thus, for the final analysis, we decided to estimate a height displacement and to keep the horizontal position unchanged.

For the station Madrid only the north displacement is significant at the 95% confidence level. The test statistics are $T_e = 0.1$, $T_n = 7.7$ and $T_h = 1.7$, for east, north and height displacement, respectively, while the alpha-quantile is $F_{0.95;1,35} = 4.1$. Hence, we decided to only estimate the north displacement and to keep the other two components unchanged for a final analysis.

In the final step we estimated the topocentric drift rates of the three telescopes including only significant displacements found in the previous step (cf. Table 1). The corresponding results are depicted in Figure 2.

3. Comparison to Conventional Surveys

In Table 1 we compare our results derived from the analysis of VLBI data to the results obtained by conventional surveys. The latter are available and published for Effelsberg and Madrid in [2] and [10] while the results for Medicina will be available soon.

Table 1. VLBI determinations and conventional survey results of local station displacements.

station name	completion of repair work	type of determination	east [mm]	north [mm]	height [mm]
Medicina	96-07-01	VLBI determination	-2.2 ± 1.8	$+2.1 \pm 1.9$	$+18.1 \pm 10.0$
		Conventional survey	not yet available		
Effelsberg	96-10-01	VLBI determination	0	0	$+14.2 \pm 22.1$
		Conventional survey	-0.4 ± 0.9	$+2.7 \pm 0.9$	$+21.8 \pm 1.0$
Madrid	97-04-30	VLBI determination	0	-6.9 ± 2.1	0
		Conventional survey	$+1.5 \pm 3.9$	-7.0 ± 3.8	$+6.0 \pm 2.8$

In general it can be stated that the agreement between the two different approaches is on the level of several millimetres. The VLBI results for Effelsberg suffer from the limited number of data points after the track and wheel repair. We are looking forward to determine the offsets more accurately when more observations after the repair work become available.

There is a good agreement in the north displacement of Madrid between conventional and VLBI determination, while we do not see a significant height displacement from VLBI analysis

yet. Simliar to the case of Effelsberg more observations are required after the repair work in order to determine the displacements more accurately.

Medicina has sufficient observation data before and after the repair work in order to determine the displacements from VLBI data. Here we are waiting eagerly for the results obtained from conventional geodetic surveys.

4. Conclusions and Outlook

We demonstrated that it is possible to determine the displacements of the VLBI reference points caused by repair work directly from the VLBI data. However, as a prerequisite this requires a sufficient number of VLBI observations before and after the repair work. A better agreement is expected as soon as more VLBI observations after the repair work become available and can be included in the analysis. For a continuing surveillance of the local site stability we recommend the performance of conventional surveys on a regular, e.g. annual, basis. We plan to build up a database collecting all determinations of changes of the positions of the reference points at all telescopes in use for IVS. This information should be used in analysis and interpretation of crustal motion results from geodetic VLBI.

Acknowledgment. Rüdiger Haas and Dirk Behrend are supported by the European Union within the TMR programme under contract FMRX-CT960071.

References

[1] Nothnagel, A., "Conventional survey at the Medicina radio telescope", personal communication, 1998.

[2] Nothnagel, A., "Conventional Survey at the Effelsberg radio telescope – Internal Report 1999", *Geodetic Institute Internal Report*, available at http://giub.geod.uni-bonn.de/~nothnage/publications.html, Geodetic Institute of the University of Bonn, 1999.

[3] Behrend, D., "Invariant Point I, Geodetic Determination of the Invariant Point of the DSS65 VLBI Antenna", *Technical Report 98-01, Evaluation of Four IGN Measurement Campaigns*, Institut d'Estudis Espacials de Catalunya, Consejo Superior de Investigationes Científicas, Barcelona, Spain, 1998.

[4] Campbell J., A. Nothnagel, "The European VLBI Project", In: Proceedings of the First IVS General Meeting, this issue, 2000.

[5] Caprette D.S., C. Ma, J.W. Ryan, "Crustal Dynamics Project Data Analysis - 1990", *NASA Technical Memorandum 100765, A-1*, NASA Goddard Space Flight Center, Greenbelt MD, 1990.

[6] Ma, C., J. M. Sauber, L. J. Bell, T. A. Clark, D. Gordon and W. E. Himwich, "Measurement of horizontal motions in Alaska using very long baseline interferometry", *JGR*, **95**, 21991–22011, 1990.

[7] Ma, C. and J. W. Ryan, "NASA Space Geodesy Program – GSFC Data Analysis – 1998, VLBI Geodetic Results 1997-1998", http://lupus.gsfc.nasa.gov, August 1998.

[8] Scherneck, H.-G., R. Haas and A. Laudati, "Ocean Loading Tides for, in and from VLBI", In: Proceedings of the First IVS General Meeting, this issue, 2000.

[9] De Mets, C., R. G. Gordon, D. F. Argus and S. Stein, "Effect of recent revision to the geomagnetic reversal time scale on estimates of current plate motions", *GRL, Vol. 21*, **20**, 2191–2194, 1994.

[10] Behrend, D., and A. Rius, "Geodetic Control of the Madrid DSS65 VLBI Antenna", In: *Proceedings of the 13th Working Meeting on European VLBI for Geodesy and Astrometry*, held at Viechtach, February 12–13, 1999, edited by Wolfgang Schlüter and Hayo Hase, BKG, Wettzell, 1999.

Session 5

Observing Programs

Cynthia C. Thomas et al.: CORE: Continuous Observations of the Rotation of the Earth, IVS 2000 General Meeting Proceedings, p.141–145
http://ivscc.gsfc.nasa.gov/publications/gm2000/thomas

CORE: Continuous Observations of the Rotation of the Earth

Cynthia C. Thomas [1], *Chopo Ma* [2], *Nancy R. Vandenberg* [1]

[1)] *NVI, Inc./NASA Goddard Space Flight Center*
[2)] *NASA Goddard Space Flight Center*
Contact author: Cynthia C. Thomas, e-mail: cct@gemini.gsfc.nasa.gov

Abstract

Various aspects of the Continuous Observations of the Rotation of the Earth (CORE) program are presented, including the science goals, validation strategy, and evolutionary plan.

1. CORE Program Science Goals

The goal of the program for Continuous Observations of the Rotation of the Earth (CORE) is to use VLBI to continuously monitor the integrated response of the Earth. This will provide a data set for Earth system science. With the data researchers can study continuous momentum exchange among oceans, atmosphere, and solid Earth.

Two critical elements of the CORE program are the Mark IV correlator that is capable of processing much more data than the Mark III correlator and the Mark IV data acquisition hardware that can record data rates up to 1 Gb/s, more than an order of magnitude greater than the current geodetic usage of 56 Mb/s. With the Mark IV system, we expect to produce data with a daily precision of 12 μsec for UT1 and 25-50 μarcsec for polar motion. This is approximately three times better than the current precision of the NEOS network. Figure 1 shows the expected UT1 precision as CORE evolves. Estimation of the lower curve assumed a perfect TRF in which station positions are known perfectly and estimation of the upper curve accounted for a realistic level of station motion.

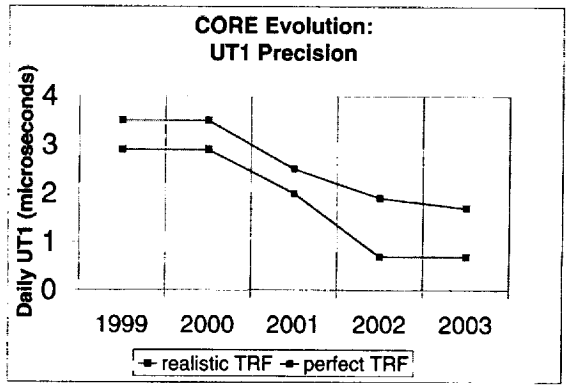

Figure 1. CORE Evolution UT1 Precision Chart. The chart shows that UT1 will improve as the years progress. This is attributed to the increased observing and better correlator efficiency.

Variations in Earth orientation are caused by external torques from gravitational forces or by angular momentum exchange between the solid Earth, atmosphere, oceans, and inner core. Measurements of nutation due to external forces can be used to correct parameters of Earth models, for instance to determine ellipticity of the inner core or to improve nutation models. Polar motion and UT1 measurements are used to study periodic signals such as tides, non-periodic signals such

as atmospheric and oceanic angular momentum, and episodic signals such as earthquakes. When complete, the CORE program will provide a continuous Earth orientation series for Earth system science. This data series will constrain the integrated effect of all of the geophysical components.

A major challenge for analysis of CORE data is separating the many geophysical signals. For signals that are periodic, long-term averaging will enable us to detect even weaker signals for such phenomena as sub-daily and long term ocean tides.

2. Observing Scenario

The observations for CORE will be made by an international network of 15 to 20 high performance Mark IV stations. There will be seven different sub-networks of five to six stations each for each day of the week. For instance, CORE-1 will be designated for Monday, CORE-2 for Tuesday and so forth.

Each of the participating stations must have Mark IV capability, a calibrated timing system, and adherence to high performance standards. The data from the stations will be processed on the Mark IV correlators. Most of the stations have been upgraded to Mark IV data acquisition equipment, but a few remain. The following table lists for each year the planned number of observing days per week. This shows how the full CORE program will evolve.

Year	Number of Sessions per week
1997-9	pre-CORE sessions, Mark III, 2.7 days/week
2000	transition to Mark IV, 2.4 days/week
2001	Mark IV, 3.5 days/week
2002	Mark IV, 4 days/week
2003	Mark IV, 6 days/week

Figure 2 shows the evolution of the CORE program in more detail. The chart visually shows how the weeks are being filled in as the years progress. The goal is to have six sessions per week by the year 2003. This goal will require additional funding at the stations so that station personnel can observe on the weekends, or improved software and two tape recorders at each site for unattended recording. The latter will make it easier to observe six or seven days a week.

3. 1997–1999 Activities

The period of 1997 through 1999 was named "Pre-CORE" while the Mark IV system was being implemented. The technical goals during the "Pre-CORE" period were to:

- evaluate the sub-network concept,
- determine the accuracy of the EOP measurements,
- develop timing calibration and procedures, and
- establish a set of standards for station performance.

The simultaneous CORE-A/NEOS sessions were designed to determine VLBI EOP accuracy by using different networks to make a measurement of what should be the same EOP. A complete explanation of the differences between the measurements on each network is still lacking, but progress is being made toward understanding them (see [1]).

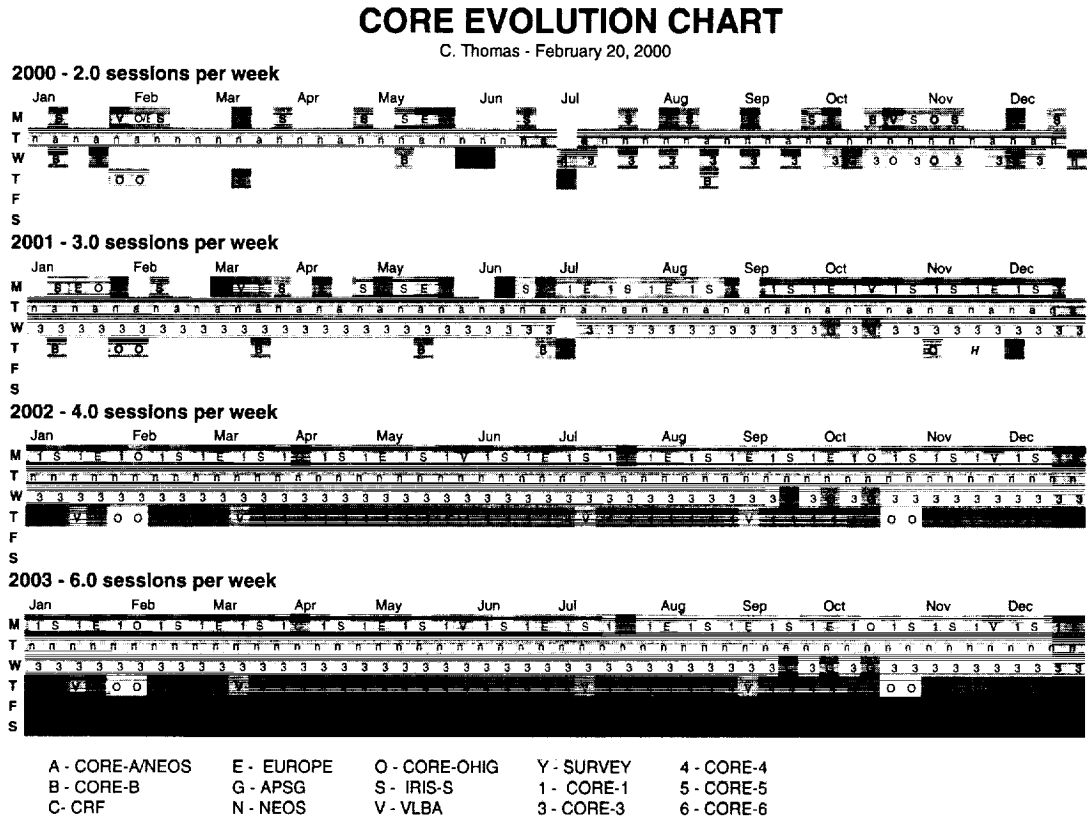

Figure 2. CORE Evolution Chart. Each shaded box indicates a 24 hour observing session. The number of days per week increases in later years.

4. Plans for 2000

The 2000 observing plan was sized to accomodate the shakedown period of the Mark IV correlator. The current 2000 observing plans are the following:

- NEOS network weekly
- CORE-A monthly, simultaneous with NEOS
- CORE-B quarterly, on days adjacent to NEOS
- CORE-3 begins in July, biweekly

The accuracy goals for all CORE networks during 2000 are to achieve formal errors better than 100 μarcsec in the pole position and formal errors better than 3.5 μsec for UT1.

5. Resources for CORE

Until the year 2001 correlator throughput (due to the shakedown period) will be slightly lower than the amount of data to be acquired. This will produce backlogs at the three Mark IV correla-

tors, Haystack, Washington, and Bonn. After the shakedown period, it is expected that correlator efficiency will improve and the backlog will be worked off. This increased efficiency is based on

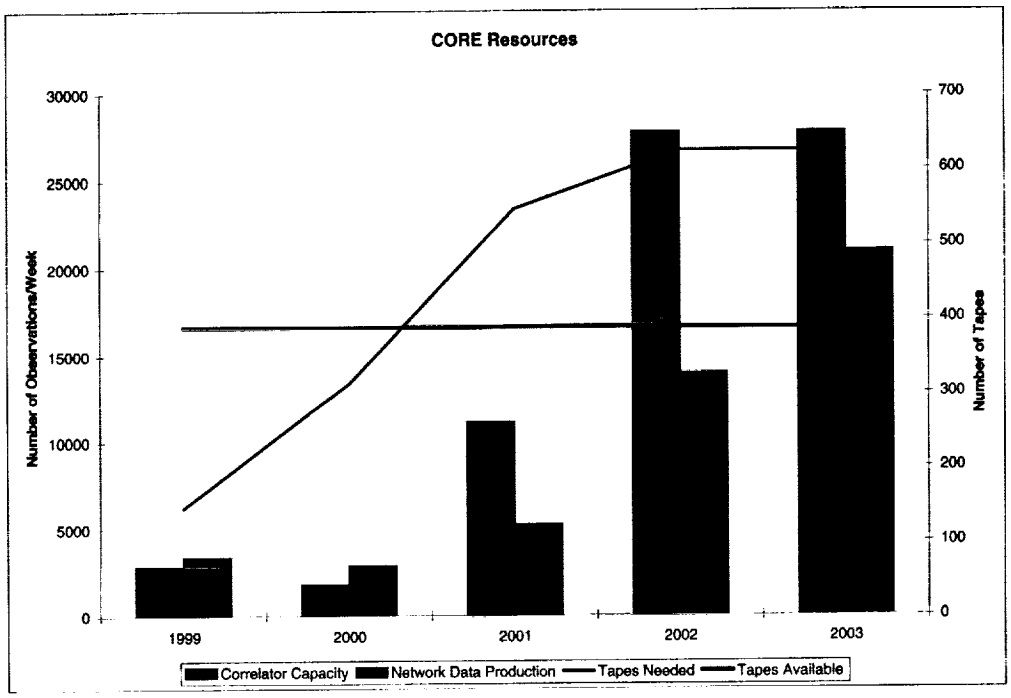

Figure 3. CORE Resources Chart. The chart shows the projected plan for major resources needed for the CORE program: correlator capacity, data production, and tapes. As the correlator reaches its full capacity, more observing is planned which will require more tapes. The current number of tapes is shown as a horizontal line.

planned correlator features and software development. The driving force in the CORE plan is the Mark IV correlator capacity, and the CORE program observing cannot begin until after the Mark IV correlator completes its shakedown period.

The stations will have to observe more and additional thin tapes will be needed to accomplish the CORE observing plan. Therefore, additional thin tapes will have to be purchased to utilize the increased station days and improved correlator efficiency. Figure 3 shows the estimated resources for CORE: correlator capacity, data production, and tapes. The figure shows the dramatic increase in correlator capacity from 2000 to 2002 as the Mark IV correlator reaches its potential. The figure also shows the planned increase in data production and tape usage. Both station time and tapes will soon become the most needed resource.

Figure 4 displays the planned increased usage of stations from 2000 to 2003. The chart is not a precise projection since the stations participating in CORE require the Mark IV upgrade and it is not known at this time when stations like Algonquin, Fortaleza, and Hobart will become Mark

IV stations. Another factor that affects usage is station availability.

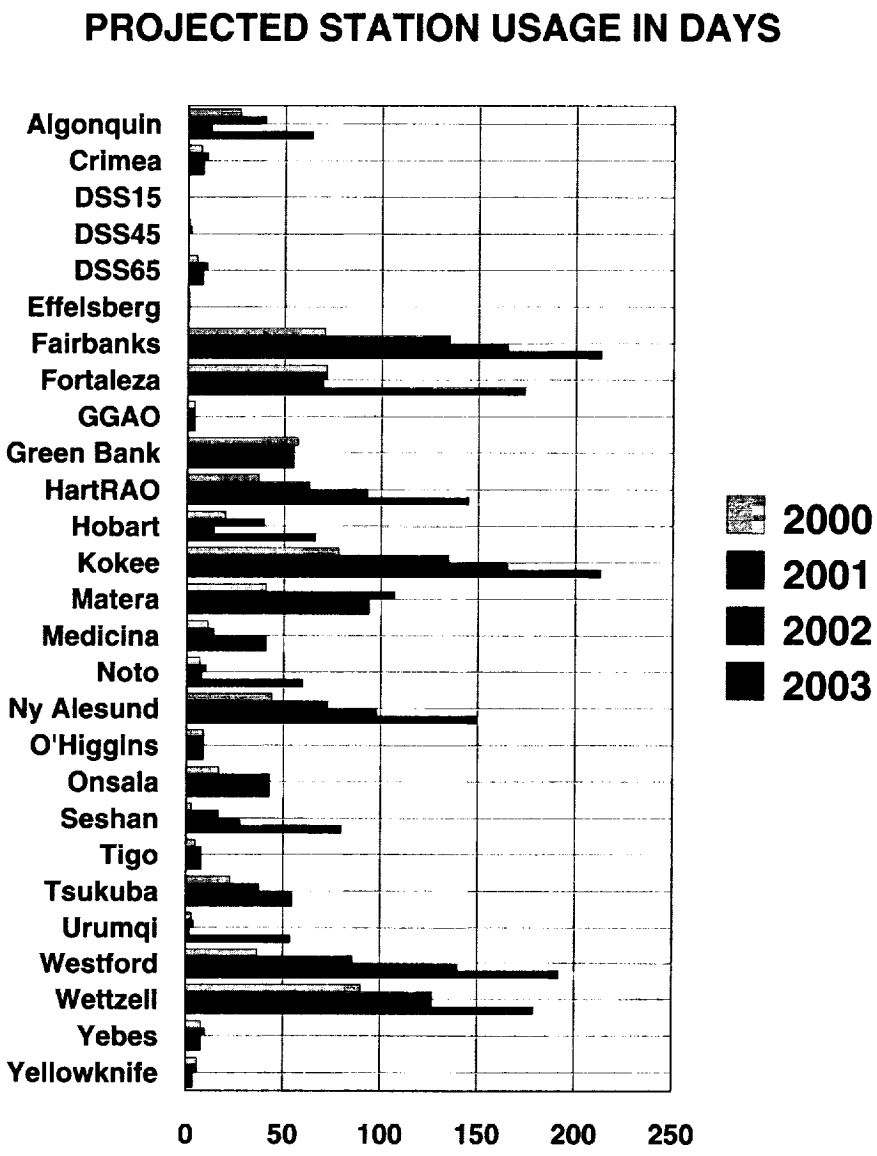

Figure 4. Projected Station Usage in Days. The chart shows the number of observing days needed from each station to support the CORE plan.

References

[1] MacMillan, D. S. and C. Ma: "Improvement of VLBI EOP Accuracy and Precision", in this volume.

J. Campbell et al.: The European VLBI Project, IVS 2000 General Meeting Proceedings, p.146–150
http://ivscc.gsfc.nasa.gov/publications/gm2000/campbell2

The European VLBI Project

J. Campbell [1], *R. Haas* [2], *A. Nothnagel* [1]

[1] *Geodetic Institute of the University of Bonn*

[2] *Onsala Space Observatory, Chalmers University of Technology*

Contact author: J. Campbell, e-mail: campbell@sn-geod-1.geod.uni-bonn.de

Abstract

The European geodetic VLBI project in its current phase aims at determining present-day vertical crustal motions by measuring relative vertical positions at regular intervals between the fixed VLBI stations in Europe. The VLBI observations have been carried out between 1990 and 1999 at a rate of six experiments per year with slightly different station configurations. The vertical site motions derived in the analysis of a 9-year time series are showing significant trends relative to Wettzell: at the station of Medicina we found a subsidence rate of 4.8 mm/y, probably related to groundwater and gas withdrawal in the Po plains. At Onsala and Ny Ålesund small uplifts of about 1 to 2 mm/y were detected. These may be associated with the postglacial uplift in Scandinavia. The uplift of 2.3 mm/y at Madrid may be due to local effects which are also seen in the GPS data from the nearby IGS station. More extensive comparisons and combinations with the results from the GPS permanent stations in Europe are planned.

1. Introduction

The high concentration of relatively large and sensitive radio telescopes in Europe has provided a strong incentive to use these facilities to exploit the full geodetic potential of the VLBI technique (Campbell 1988). The moderate size of the network with baselines ranging between a few hundred to one or two thousand kilometers lends favourable conditions to achieve the highest possible accuracy, one important aspect being the good simultaneous visibility for all stations which leads to a strong geometry for both horizontal and vertical control.

After an initial phase of observing sessions in the frame of the NASA Crustal Dynamics Project (CDP), funding for regular operations was secured from the European Commission within the 2nd Framework Programme "Science". In this first phase under the title "European VLBI for Crustal Dynamics" the work has been concentrated on the measurement of horizontal crustal motions which were expected to show up in the baseline and coordinate time series fairly soon, i.e. within three or four years. The continuation and expansion of the project has been accepted by the European Commission under the 4th Framework Programme "Training and Mobility of Researchers (TMR)", enabling a second phase of funding of geodetic VLBI observations in Europe. This second phase emphasizes the determination of vertical site motions, which are much more difficult to detect. Accordingly, the project contains an expanded work programme with an increased frequency of observations, new VLBI stations, and also includes comparisons and combinations with GPS results. Together with the already existing series of observations, the entire project will include an EC-funded observation time span of nearly 9 years (1993-2001).

For the determination of significant vertical motions at the millimeter per year level this longer data set, together with a refined modeling of the atmospheric path delay, should provide the necessary strength and integrity. The results are of high importance for the monitoring of land

uplift and subsidence, sea level changes, glaciology and other vertical motion applications and are hoped to contribute to the evaluation of global climatic changes and other environmental effects.

The training scheme, which is an intrinsic part of the EU-TMR programme, is implemented through the employment of young researchers from the EU-member states and includes tuition courses on various topics related to the project. In the organisational frame, the VLBI group at the Geodetic Institute of the University of Bonn has assumed the role of coordinator.

2. Status of the European Geodetic VLBI Network

At present, the European Network consists of 10 stations (Fig. 1), six of which have a geodetic observing record longer than 10 years. In October 1994 a 20 m antenna established by the Norwegian Mapping Agency at Ny Ålesund on the arctic archipelago of Spitsbergen (78° latitude!) has taken on routine participation in the European VLBI experiments. The 14 m antenna of the Instituto Geografico Nacional at Yebes, about 80 km east of Madrid, has been equipped for geodetic VLBI and made its first experiments in 1996. With the help of NASA the station of Simeiz on Crimea (Ukraine) has been able to take part in several of the European geodetic sessions. Moreover, several astronomical radio observatories have shown their interest in the geodetic campaigns: Effelsberg (Germany) is taking part once per year, and Westerbork (The Netherlands) is preparing to take part in the near future.

3. The Observations

All observing sessions are set up according to the same principles, to attain a full sky coverage over a period of one complete revolution of the Earth. With a specially designed algorithm within the scheduling program SKED the observations of the participating telescopes are automatically selected for an optimized sky coverage at each station (Steufmehl 1991). At the same time all conditions regarding telescope slewing speeds and limits, tape recorder operations, and integration time are taken into account by the software.

The recorded data from the observatories are sent for processing to the VLBI Correlator Center at the Max-Planck-Institute for Radioastronomy in Bonn, where the geodetic observables, the time delays of the radio signals between the different telescopes, are derived from the raw data. An observing session with 10 stations produces on the average nine thousand delay observations.

Between January 1990 and December 1999 a total of 52 observing sessions with up to 10 stations in slightly varying configurations have taken place. From 1994 onwards the rate of six sessions per year has been achieved with the existing time available at the Bonn correlator. Plans are to increase the rate to eight per year from 2000 onwards.

4. Data Analysis

In the frame of the European VLBI Project, the data are being analysed by several of the participating groups and the results are compared and discussed at regular intervals (Börger 1999). Most of the groups are using the CALC/SOLVE analysis software developed at the NASA GSFC (Caprette et al. 1990) or the OCCAM package (Zarraoa et al. 1990), but the strategies and the amount of data actually used are left to the discretion of each team. Thus, the influence of different analysis approaches on the estimated quantities can be evaluated and used to assess the stability

and significance of the results.

In one of the most recent analyses (Haas et al. 1999) all European sessions from 1990 to April 1998 were treated in a combined least squares adjustment including atmospheric wet zenith path delays for every 60 minutes using the NMF 2.0 mapping functions (Niell 1996). Horizontal gradients were estimated every 8 hours.

One of the preferred analysis strategies for the European Network, which has the benefit of showing the baseline and site coordinate evolution with time, is to run a combined adjustment of all sessions, but estimate station coordinates for all epochs in relation to one station fixed (for more details see e.g. Nothnagel and Campbell 1993). In this case, of course, the Earth Orientation Parameters (EOP) have to be taken from an external source, e.g. from a global VLBI solution such as the NASA Goddard Space Flight Center solution 1102g (Ma and Ryan 1998) used here. In this case, we are using the inherent stability of the global solution to orient our regional network in space (the translations are inhibited by fixing one station, e.g. Wettzell). With a conservative estimate for the orientational stability of 0.3 mas (1 cm at one Earth radius) over short as well as longer time scales we may put an upper bound on the influence of the reference system on a baseline vector of 1000 km length at 1.5 mm (Herring 1986, Ma et al. 1993).

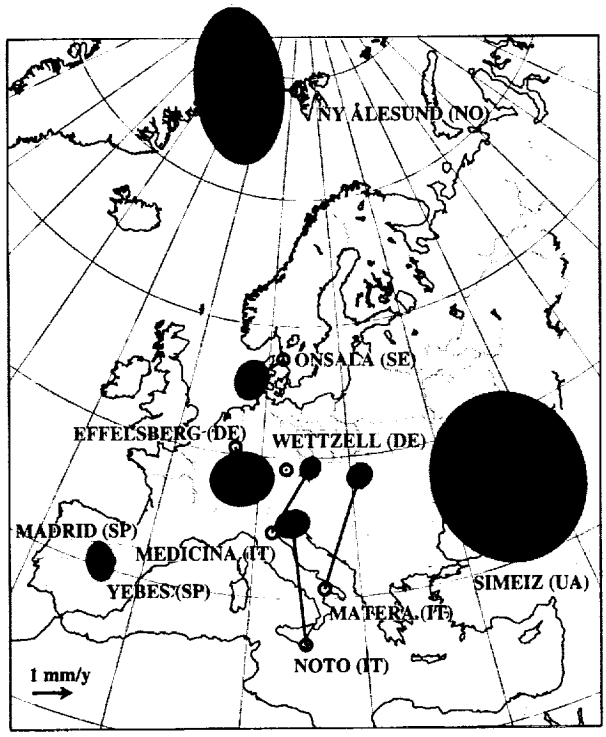

Figure 1. Observed horizontal station motion with respect to Wettzell

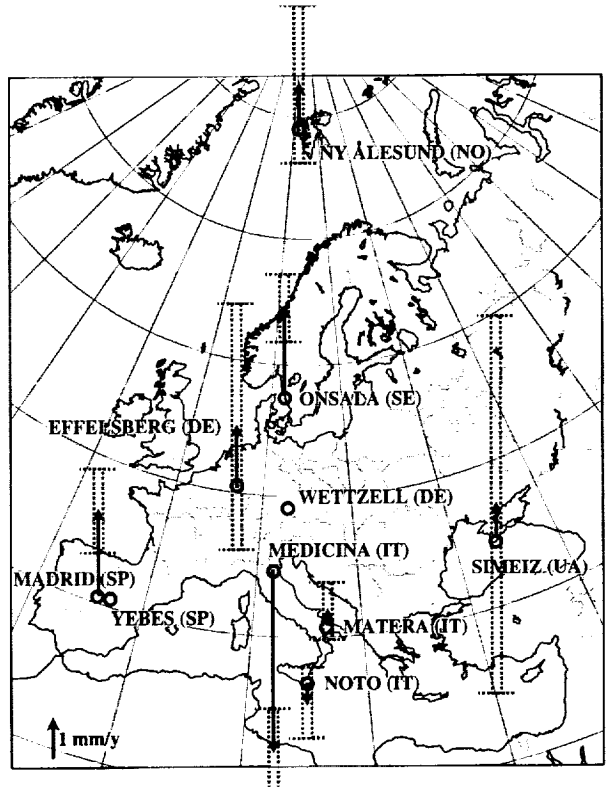

Figure. 2: Observed vertical station motion with respect to Wettzell

The baseline length repeatability obtained from the time series has proved to be the best indicator of the inherent accuracy of VLBI because it is essentially free from orientational errors of the reference system. For the European baselines we obtain a weighted RMS (WRMS) of

2.0 mm + 0.8 mm*b, where b is the baseline length in units of 1000 km (Haas et al. 1999). The horizontal coordinate WRMS repeatabilities range from 1.5 to 5.7 mm (Ny Ålesund north) whereas the values for the vertical are about three times larger, i.e. 8.0 to 14.4 mm.

Fixing the motion of Wettzell to its value in the NUVEL-1A-NNR frame, we were also able to estimate velocity vectors from the time evolution of the coordinates of each station with repect to Wettzell (Haas et al. 1999) (Fig. 1). The most prominent horizontal motions are concentrated on the Italian peninsula with the effect of the northward moving African plate on the Adriatic plate being obvious at Matera and partly also at Medicina, while Noto is probably even directly affected by the African motion. Compared to earlier determinations, the velocities are somewhat smaller and by the fact that they are now much more reliable this will help to better interpret the interactions between the converging African plate and the smaller blocks in the Mediterranian area (Ward 1994, Gueguen and Tomasi 1999).

In spite of their larger uncertainty the vertical site motions of some of the stations derived in the analysis of the 9-year time series are showing significant trends relative to Wettzell: at the station of Medicina we found a subsidence rate of 4.8 mm/y, probably related to groundwater and gas withdrawal in the Po plains. At Onsala and Ny Ålesund small uplifts of about 1 to 2 mm/y were detected. These may be associated with the postglacial uplift in Scandinavia. The uplift of 2.3 mm/y at Madrid may be due to local effects which is also seen in the GPS data from the nearby IGS station.

The vertical motions have to be interpreted with even greater care than the horizontal ones because of the large number of local effects that interfere with the more global picture. In this situation, it is important to establish close links to the European GPS Permanent Network within the EUREF organisational frame. The Bundesamt für Kartographie und Geodäsie (former IfAG), a partner in the European VLBI project, is strongly involved in the establishment of a European vertical reference frame and is carrying out a substantial part of the data analysis of the permanent GPS stations in Europe (Gubler, Hornik 1999).

The scientific aspects of vertical crustal motions and sea level variations in the European region are also an important topic in the WEGENER Working Group, which covers the contribution of geodynamic observing networks from different techniques (Plag 1998). The particular value of the VLBI contribution to the European geodynamic monitoring networks resides in the fact that VLBI can provide the geometrically stable platform for tying in all other systems that are prone to systematic short and long-term errors in their reference.

5. References

Börger, K.: Comparison of European network solutions. Proc. 13th Working Meeting on European VLBI for Geodesy and Astrometry, Viechtach/Wettzell Feb. 12-13, 1999, Eds. W. Schlüter and H. Hase, 121–137, 1999

Campbell, J.: European VLBI for Geodynamics. Proc. of the Third International Conference on the WEGENER/MEDLAS Project, Bologna, May 25-27, 1987, Eds. P. Baldi, S. Zerbini, The University of Bologna, 361–374, 1988

Caprette D.S., C. Ma, J.W. Ryan: Crustal Dynamics Project Data Analysis - 1990, NASA Technical Memorandum 100765, A-1, NASA Goddard Space Flight Center, Greenbelt MD, 1990

Gubler, E., Hornik, H. (Eds): IAG/EUREF Publication No.7/I and No.7/II, Reports on the EUREF-Symposium Bad Neuenahr, June 10-13, 1998 and on the results of the European vertical Reference Network GPS Campaign 97 (EUVN'97), Mitt. Bundesamt f. Kartographie und Geodäsie, Frankfurt am Main, 1999

Gueguen, E., P. Tomasi: Geodynamic interpretation of the Central Mediterranean combining geological and VLBI data. Proc. 13th Working Meeting on European VLBI for Geodesy and Astrometry, Viechtach/Wettzell Feb. 12-13, 1999, Eds. W. Schlüter and H. Hase, 198–205, 1999

Haas, R., E. Gueguen, H.-G. Scherneck, A. Nothnagel, J. Campbell: Crustal Motion Results derived from observations in the European Geodetic VLBI network. Submitted to Earth, Planets, Space, Japan, 1999

Herring, T.A.: Precision of Vertical Position Estimates From Very Long Baseline Interferometry. J. Geophys. Res., 91, 9177–9182, 1986

Ma, C., J.W. Ryan, D. Gordon, D.S. Caprette, W.E. Himwich: Reference Frames from CDP VLBI Data. Contributions of Space Geodesy to Geodynamics: Earth Dynamics, AGU Geodynamics Series, Vol. 24, 121–145, 1993

Ma C., J.W. Ryan: NASA Space Geodesy Program - GSFC Data Analysis - 1998 VLBI Geodetic Results 1997-1998, http://lupus.gsfc.nasa.gov

Niell A.E.: Global mapping functions for the atmosphere delay at radio wavelengths. J. of Geophys. Res., Vol. 101, No. B2, 3227–3246, 1996

Nothnagel, A., J. Campbell; European Baseline Rate Determinations with VLBI; Proceedings of the Ninth Working Meeting on European VLBI for Geodesy and Astrometry; Bad Neuenahr, FRG; Sept. 30 - Oct. 1, 1993; in Mitteilungen aus den Geodätischen Instituten der Rheinischen Friedrich-Wilhelms-Universität Bonn, Nr. 81, Bonn, 1993

Plag H.-P. (ed.) The Ninth General Assembly of WEGENER, Book of Extended Abstracts - Second, Revised Edition, Statens Kartverk, Hønefoss, 1998

Steufmehl, H.: AUTOSKED - Automatic creation of optimized VLBI observing schedules. Proc. of the 8th Working Meeting on European VLBI for Geodesy and Astrometry, June 13-14, 1991, Dwingeloo, The Netherlands, Report MDTNO-R- 9243, Survey Dept. of Rijkswaterstaat, Delft, IV-23–IV-29, 1991

Ward, S.N.: Constraints on the seismotectonics of the central Mediterranean from Very Long Baseline Interferometry. Geophys. Journ. International, Vol. 117, 441–452, 1994

Zarraoa N., A. Rius, E. Sardon, H. Schuh, J. Vierbuchen: OCCAM: A Compact and Transportable Tool for the Analysis of VLBI Experiments, Proc. of the 7th Working Meeting on European VLBI for Geodesy and Astrometry, A. Rius (ed.), 92–102, Madrid, 1990

Acknowledgements:

The project has been supported by the EU (grants SCI CT92-0829 and FMRX CT96- 0071) from Feb. 1993 through to the present. The work described in this report could not have been accomplished without the technical and logistic assistance of the NASA/GSFC VLBI group. We are also indebted to the many individuals in the participating observatories and institutes who ensured the enormous routine work of data collection and correlation. Specifically we should like to mention the support of the Max-Planck-Institut für Radioastronomie (VLBI Correlator Center), Bonn, Germany, the Land Nordrhein-Westfalen with its programme "Förderung der Spitzenforschung" (VLBI staff at the Geodetic Institute Bonn) and the Deutsche Forschungsgemeinschaft (special research grants).

Huib Jan van Langevelde: Current Activities in the EVN, IVS 2000 General Meeting Proceedings, p.151–154
http://ivscc.gsfc.nasa.gov/publications/gm2000/vanlangevelde

Current Activities in the EVN

Huib Jan van Langevelde

Joint Institute for VLBI in Europe
e-mail: langevelde@jive.nl

Abstract

This report describes the current (February 2000) technical developments in the (astronomical) European VLBI Network (EVN). The EVN has switched over to observing in MkIV and VLBA modes mostly and is currently in the process of upgrading VLBA type terminals to the MkIV standard. The new observing formats, replacing the MkIII modes, have proven to work reliably. Other new developments have been the advent of UHF and 5 cm receivers and progress on frequency agility of the telescopes. It is noteworthy that more and more observing programs use phase referencing techniques. The situation with correlators for the EVN is tight. Using the MkIV/VLBA modes initially has been made possible through the VLBA correlator. The EVN MkIV correlator at JIVE is now also operational, albeit for a limited number of observing modes and with limited throughput.

1. Introduction to the EVN

The EVN is a consortium of radio-astronomy institutes operating 16 telescopes (14 sites) in 10 countries, not limited to Europe but also extending to China. The main characteristic of the network is that, although quite inhomogeneous, it is very sensitive, as it contains a number of very large antennas. The sensitivity makes it attractive for a large range of scientific projects. However, the diversity of antenna characteristics poses a challenge when it comes to operations and observing strategies. For instance the receiver capabilities and (polarization) characteristics vary considerably across the network.

The EVN has three deadlines for observing proposals per year and about 40 experiments are scheduled in three or four observing sessions. This number excludes observations within the VSOP (space VLBI) context. A large fraction of the target sources are of the type familiar to geodetic VLBI: continuum observations of active galactic nuclei (AGN). But also a considerable number of stellar objects can be observed in the same continuum mode. Quite a lot of these experiments employ either parallel or full polarization to obtain additional information on the physical conditions.

2. New Capabilities of the EVN

In order to extend these observations to sources that are so weak they cannot be detected in the coherence time, a considerable fraction is done nowadays using phase referencing. This leads to specific requirements for the experiment schedules. For instance, short scans are necessary and therefore fast slewing is beneficial. This is however difficult to establish in the EVN where the dishes are quite large and mostly not built for VLBI applications in the first place. Continuous tape motion, in which tapes are not stopped during source changes, has been implemented to overcome sync up times at the correlator. The technique of phase referencing has become much more accessible now that it can be performed with the residual phases. This has been made possible

because the correlators now use very accurate geodetic models. In the EVN there are a number of telescopes for which the positions are still not accurately known, because a few never participate in geodetic campaigns. Further enhancements in the data acquisition terminals to accurately flag the data during slewing would improve the system. Likewise, improvements in the gain calibration are pursued.

Another area of increasing interest are spectral line studies. One category concerns masers, for example interstellar OH and H_2O masers. These observations require narrow bandwidth, 500 or 125 kHz, which in practice is accomplished by oversampling in the MkIV system. Another type of spectral line observations target HI (or OH) absorption in extragalactic sources. These usually require slightly wider (2 – 4 MHz) bandwidths than the Galactic masers. These systems are often cosmologically red-shifted. For galaxies that have their HI shifted outside the traditional L-band, some EVN antennas are equipped with UHF receivers. Another unique frequency band for the EVN is the 5 cm system, which enables observations of methanol masers. In these non-standard bands, as well as in the protected astronomy bands, RFI is becoming a severe problem. In some astronomical experiments there is a need for switching receivers during the observation. Several EVN antennas have introduced frequency agility for a selection of receivers. This also makes the switch-over between observing sessions faster and more reliable.

As mentioned earlier, these observations are now predominantly done using MkIV (VLBA) compatible modes, including 2-bit sampling and fan-out recordings. The operational situation for correlating the observations is complicated by the fact that in 1999 and 2000 three correlators are being used for processing EVN projects. Traditionally the Bonn correlator at the MPI Bonn has been used for MkIII experiments. The JIVE correlator (see below) has started operations, focusing on simple MkIV observations. The VLBA correlator in Socorro is also processing a considerable fraction of the EVN data. Besides the "global" experiments, also the more complicated observing modes, such as oversampled spectral line experiments, have been sent to Socorro.

The new MkIV observing modes seem to function reliably; very few problems associated with operating the new formatters have been encountered. The observations are scheduled with Sched, which also schedules NRAO's VLBA telescopes directly. Currently the recording bit-rates are still limited to 256 Mb/s. The main reason why higher data rate modes have not been tested yet is that only half of the EVN stations have been upgraded to MkIV. Stations which originally had VLBA type equipment are expected to be upgraded to MkIV sometime in 2000. For these systems the VLBA formatter will be replaced with a MkIV formatter and the recorders will be equipped for 320 ips tape speeds and two-head recording.

Because some telescopes participate in different programs and provide recordings to a number of correlators, stations are forced to switch between thick and thin tapes. This does not seem to be a healthy situation, even for recorders equipped with triple-cap heads. It is certainly a source of recording problems, which affect the reliability of the EVN. Another origin of reliability problems could be the fact that many telescopes in the EVN do not have a permanent setup for VLBI; outside the session they are involved in other, single dish, astronomical programs. The many receiver changes could be another occasion of problems. Clearly, the sites with multiple recorders or dishes are the most complicated in this respect. An EVN project is underway which will allow the stations to make improvements to their equipment leading to higher reliability.

A bright prospect for the EVN is the construction of two more sensitive antennas: a 64-m dish at San Basilio, Sardinia, Italy and a 40-m at Yebes, Spain.

3. The EVN MkIV Data Processor at JIVE

A central item in the MkIV upgrade of the EVN is the construction of the EVN MkIV data processor at the Joint Institute for VLBI in Europe. JIVE is hosted by NFRA in Dwingeloo, the Netherlands, and funded by science councils in a number of European countries. Special projects have been funded by the EU. Nowadays, a majority of the $\approx$ 20 staff members are involved in further development and operations of the correlator. Other efforts at JIVE include support of the EVN, by carrying out Network Monitor Experiments, as well as maintaining the central information depot (http://www.jive.nl/jive/evn/evn.html). An important aspect of the efforts is user support: assistance to astronomers during all steps in carrying out a VLBI experiment. The facilities include top end computing facilities for visitors.

The construction of the MkIV data processor was completed in October 1998. It was built within the context of an international consortium, in which also the other (geodetic) MkIV correlators were built. The correlator at JIVE differs in several aspects. For one thing, it is a 16 station processor and therefore the total correlator capacity has been quadrupled with respect to the others to yield a total of 262144 lags. A large interconnection switch distributes the data to the four correlator crates which contain 1024 special purpose chips. This Data Distributor Unit became operational on February 21, 2000. The drives are of a different make (P+G) than those at the other MkIV processors and use tension arms rather than vacuum to control the tape guidance. Finally, the complete control software and the data product have been derived independently and are currently tailored for astronomical use. It uses aips++ data storage for inspection and export of the data, currently in FITS format to classic AIPS.

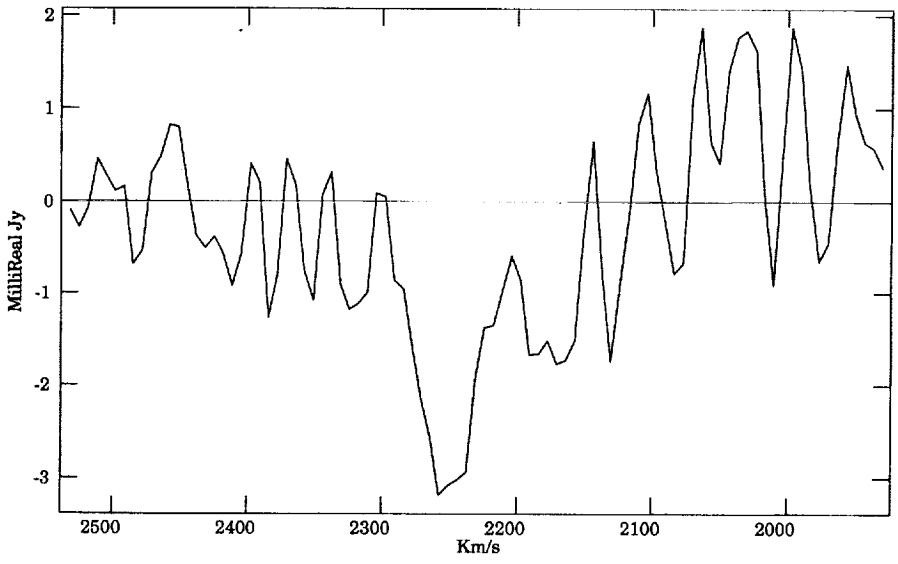

Figure 1. Weak HI absorption towards the nucleus of NGC4261, a good example of what the EVN can achieve.

The first image obtained with the data processor emerged in April 1999. From September 1999 the focus at JIVE was to get user data for a number of astronomical projects completed. These "pilot projects" have exercised the operational procedures at JIVE as well as a number of

MkIV modes. About 10 projects have been completed and delivered to the investigators. The overall data quality has proven to be quite satisfactory, although several subtle problems have been discovered in the process. In addition there are a number of special features which still require considerable development. By February 2000 these included oversampling capabilities, MkIII experiment processing, large output data rates, and modes with more than 256 Mb/s. Some special astronomical capabilities are planned, such as ultra-high spectral resolution, pulsar gating, multiple telescopes per tape, multiple field centers and space VLBI.

The results from a "first science" project have recently appeared in press (Van Langevelde et al., 2000, Astronomy & Astrophysics Letters 354, L45). The paper describes the detection of HI absorption against the counterjet, very close to the AGN in NGC4261 (Fig. 1). The object is a famous radio source associated with an elliptical galaxy. In the inner part of this galaxy the Hubble telescope has found evidence for a massive black hole and an accretion disk of molecular material. The new data shows that close to the nucleus the disk gets heated so much it turns from molecular into atomic form. The very weak detection of 3.5 mJy over a 450 kHz band, highlights what is possible with the "MkIV EVN": very sensitive baselines, even more sensitive with 2-bit sampling, enough bandwidth to span line and continuum, and new correlator capabilities which yield much better spectral resolution.

R. Craig Walker: Overview of Observations on the VLBA, IVS 2000 General Meeting Proceedings, p.155–159
http://ivscc.gsfc.nasa.gov/publications/gm2000/walker2

Overview of Observations on the VLBA

R. Craig Walker

National Radio Astronomy Observatory
e-mail: cwalker@nrao.edu

Abstract

The VLBA is a dedicated instrument for VLBI that includes 10 antennas, a 20 station correlator, and an operations center. The capabilities of the instrument are reviewed along with the operating style. The current usage, in terms of amount of time spent observing, the distribution of observing by frequency band, and correlator usage, are summarized. Some of the current and desired upgrade projects are described.

1. Introduction to the VLBA

Since the Very Long Baseline Array [1] (VLBA) is primarily an astronomical instrument, it is possible that not all of the IVS membership is familiar with its characteristics. Therefore this presentation will begin with a description of the array. For more information, consult the VLBA home page, reached from the NRAO home page at www.nrao.edu.

The VLBA is a dedicated VLBI array that consists of 10 antennas, a correlator, and an operations and maintenance center. It is operated by the National Radio Astronomy Observatory[1] (NRAO) as a national facility. It is open to all scientific users, with time allocated on the basis of the scientific merit of proposals as determined by external referees. It is operated from the Array Operations Center (AOC) in Socorro, New Mexico. Operations are tightly integrated with those of an even larger NRAO instrument located near Socorro, the Very Large Array (VLA).

The antennas of the VLBA are located at sites across the United States chosen for good imaging performance. The shortest baselines are near the VLA to take best advantage of the sensitivity of that instrument when used as a VLBI station. This will also greatly enhance a planned future expansion that includes additional antennas to fill the intermediate length baselines. The longest baseline of the VLBA, from Hawaii to St. Croix, is 8600 km in length, which is within roughly 20% of the longest usable Earth based baselines. Each antenna is 25 meters in diameter and is outfitted with nine receivers, seven of them cryogenic. All receivers are always available. The desired receiver can be selected by rotating the asymmetric subreflector which takes less than 20 seconds. The receivers cover frequencies ranging from 327 MHz to 43 GHz. A tenth system for use at 86 GHz is being installed. All receivers accept both left and right circular polarization. Separate receivers are provided for S and X band. For dual frequency geodetic style observations, a dichroic reflector/ellipsoidal reflector combination is used to direct X band radiation aimed at the S band feed over to the X band feed. The ellipsoid can be moved out of the way for higher sensitivity, X band only observations popular in astronomy.

Each site is operated with only two employees, which drives the operational style. The site technicians work normal week days plus visit the site once per day on weekends and holidays.

[1]The National Radio Astronomy Observatory is a facility of the National Science Foundation, operated under cooperative agreement by Associated Universities, Inc.

Most of the time, the antenna is run unattended. An operator is always on duty in Socorro during any observing and is able to monitor all 10 sites via network connections. The antennas have a variety of safety features and are able to continue observing for extended periods even if the network connections are broken. Because of the long periods of unattended operation, frequent tape changes are not possible, except by special arrangements. Therefore each station is outfitted with two VLBA tape recorders. Together, they can cover 21 hours between tape changes at the nominal sustained bit rate of 128 Mbps.

Maintenance of station equipment is done mainly by personnel in Socorro or at the VLA site. The local site technicians take care of the site and make some repairs. But most failures are handled by a module swap. The modules are repaired at the AOC, which is also where most spares are kept. When major maintenance of items that cannot be moved is needed, personnel from New Mexico travel to the sites. As an example of the advantage of this scheme over the usual VLBI Network maintenance style, consider that the VLBA recorder group maintains about 50 drives — 22 at the stations including the VLA, 24 on the correlator, and various spares and test units. They gain a lot more experience than someone maintaining one drive at a typical VLBI site. Because of the remote maintenance style, there are very few knobs and dials on VLBA hardware. It is explicitly designed to be as easy to exercise remotely from Socorro by computer as locally. Also this precludes the possibility that some switch will be left in the wrong position.

At the AOC, there is a 20 station correlator. It uses the FX architecture in which the Fourier transforms to convert to spectra are done before cross multiplication. It is highly station oriented, with all station adjustments, such as delays, fringe rotation, and the Fourier transform, happening before the signals are fanned out to the baseline modules for cross multiplication. The correlator uses CALC, from the geodetic community, for the geometric model. The effect of this has been tremendous. Often the raw residual phases only show a few turns across a many hour observation at the intermediate frequencies. This has made phase referencing for weak source observing, or for relative position determinations, reasonably routine, which is a dramatic change from pre-VLBA practice. Around 30-50% of VLBA observations now use phase referencing. The correlator typically plays back observations at twice the record rate which allows it to keep up with observing. Usually, pure VLBA observations are correlated within two weeks of observing. Correlations involving other stations take more effort to set up so usually take a week or two longer.

2. Multiple Projects Per Tape and Dynamic Scheduling

The need to limit tape changes at the stations has caused some operational styles to be used that are not used elsewhere. Most VLBA observations use automatic tape allocation. Under this scheme, the on-line system decides where to put the data on a tape, based on what is already recorded. The schedule only says whether to run the tape or stop it. If the end of tape is reached in the middle of a scan, the tape is turned around and keeps going in the other direction with the loss of a few seconds of data. The big advantage of this scheme, besides allowing observers to not be concerned about tape management, is that it allows more than one project to be put on a tape. That avoids the extra tape changes that are forced at project boundaries in the traditional operating environoment.

Another non-traditional scheduling style that has begun to be used on the VLBA is dynamic scheduling. Under this scheme, the project schedules are submitted with times specified as some sort of sidereal time, typically that for the Pie Town station. The actual project to be observed in

an available slot is chosen very close to the time of observing so that account can be taken of the current weather and equipment conditions. This mode has always been planned, but was started somewhat earlier than it might have been when problems with the *HALCA* spacecraft caused many observations to be canceled on rather short notice. With dynamic scheduling, it became a relatively simple matter to find a substitute project when that happened. Currently, about 50% of projects are dynamically scheduled.

3. Operations Breakdown

The ideal goal for VLBA operations would be to be doing scientific observations all the time. But reality intrudes. Time is needed for maintenance and for test observations. Also the inability to change tapes at arbitrary times means that there occasionally have to be dead times while waiting for personnel to reach the sites. This is most easily understood when projects are using more bandwidth than the sustainable 128 Mbps. The higher 256 Mbps mode is used reasonably often and uses up tape twice as fast. Soon there will be a 512 Mbps capability using both drives in parallel. That will further complicate the tape change situation. Finally, there are scheduling inefficiencies due to the fact that it is not always possible to fit projects together so that one is ready to start just as the previous one finishes. On the VLA, with 27 antennas, short gaps caused by this effect can be used effectively for test or scientific observations because of the "snapshot" capability. But 10 antennas is not enough for this so those gaps are generally not filled.

In practice, the VLBA currently spends about 60% of full time on scientific projects. About 10% each go to maintenance and tests. The tape change and scheduling inefficiencies account for the remaining 20%. It is expected that the scientific observing could increase to 65% with better schedules and perhaps 75% if the tape change constraints were removed. The correlator does not now, and is not expected in the future, to constrain the available observing time. Note that the VLA, with no tapes and with the ability to productively use time slots as short as an hour, is used about 80% of the time for scientific observing. Also note that the VLA has a 28th antenna so one can always be out of the array for major maintenance without affecting observing.

4. Correlator Usage

As noted above, the VLBA correlator keeps up with observing without a problem. VLBA projects are correlated not long after the tapes become available. The GPS clocks are trusted and production correlation is done without fringe searches. Projects involving other stations require more effort and take longer to prepare for correlation. The preparation includes gathering and reading logs (automatic for VLBA sites) and performing clock searches and trial runs to be sure everything is working. Nevertheless, it is uncommon for an observation to be correlated more than a month after observing.

Table 1 shows the breakdown of projects correlated in 1999. Times are the sum of the elapsed times for each project. This breakdown roughly reflects the use of the array, although a few projects are correlated that do not involve any VLBA antennas. The "VLBA" projects include a number that use one or both of the VLA (single dish or phased array) and Effelsberg (which has a special agreement for observing with the VLBA outside of Network sessions). Note that Global Network use will increase as *HALCA* reaches the end of its lifetime because many *HALCA* observations occur during what would otherwise be Global Network sessions. The Global Network

and EVN times on the VLBA correlator will decrease in the future as the JIVE correlator becomes fully operational. But the use of higher bit rate modes, for which the correlator achieves less of a speed up factor, will probably increase. Note that the RDV projects account for most of the geodesy done on the VLBA.

TABLE 1
VLBA Correlator Projects in 1999

Type	Number	Observing Hours	Percent
VLBA	269	2962	59.5
Global Network	24	281	5.6
HALCA	123	1242	25.0
EVN	16	275	5.5
RDV	6	150	3.0
Test	14	67	1.3
TOTAL	452	4977	

5. Frequency Usage

An indication of the popularity of the frequencies available on the VLBA is given in Table 2. These are actually the times for projects correlated on the VLBA correlator, so a few frequencies not available on the VLBA are included thanks to some EVN projects correlated in Socorro. Note that the 3 mm system is just beginning to be used and was only available on a couple of VLBA antennas during this time. Those antennas were used in CMVA sessions, a few projects of which were processed in Socorro. "Hours" are time on-source at the band, which is less than the elapsed times of Table 1. Dual band (mostly S/X and 50/90cm) observations count half for each band.

TABLE 2
VLBA Correlator Frequency Usage in 1999

Band	Freq (GHz)	Hours	Percent	
90cm	0.327	62	1.6	
50cm	0.610	19	0.5	
—	0.7-1.1	51	1.3	EVN
20cm	1.1-1.8	724	18.1	
13cm	2.3	155	3.9	
6cm	5	899	22.5	
—	6	60	1.5	EVN
4cm	8.4	501	12.5	
2cm	12-15	453	11.3	
1cm	22	478	12.0	
7mm	43	543	13.6	
3mm	86	55	1.4	CMVA
TOTAL		4000		

It is clear that the 6 and 20 cm bands are the most popular at about 20% each. All of the fully functional higher frequency bands are about even at a bit over 10% each. The 6 cm band is probably most popular because that is where many of the complications of VLBI are least severe and phase referencing is most effective. The frequency is low enough that the tropospheric effects

are not severe and high enough not to be badly affected by the ionosphere. The 20 cm band is probably so popular because it not only is the lowest sensitive band for continuum observations, but also has both the hydrogen and OH spectral lines and is good for pulsars. The 50 cm and 90 cm bands are strongly affected by the ionosphere and the VLBA receivers are not very good, so they aren't very popular. The 13 cm band is often used in conjunction with 4 cm band (S/X). For those observations, only half the time is counted for 13 cm. Also it is close to the 20 cm band and it is not available on the VLA so many observers are not accustomed to using it.

6. Development Projects

The most significant effort currently in progress to improve the VLBA is the addition of the 3 mm (86 GHz) system. Four receivers have been built with NRAO funds. There is funding from the MPIfR to build the rest of the receivers needed to outfit most of the antennas plus Effelsberg. Unfortunately efforts to obtain other special funding in the US for this effort have not succeeded. This project involves more than just adding receivers. Most of the antennas have efficiencies of only 10 to 20% which should be improved. So the project will include efforts to measure and improve the surfaces. This is complicated by the fact that there are two surfaces, the main dish and the subreflector, and they are used in different orientations with respect to each other at different frequencies. Errors in one cannot be fixed by adjusting the other and only one, the main dish, is easy to adjust. Also the pointing of between 6 and 10 arcseconds rms is marginal. Efforts will be made to improve it.

Another area of ongoing development effort is in phase referencing. We have recently tested the use of GPS based global ionosphere models, obtained from CDDIS, for correction of VLBI phases. Improvements of on the order of a factor of 2 to 5 were obtained. This should improve as the models improve. On the WVR front, the new 22 GHz receivers being installed on the VLA have a capability to measure broadband powers around the water line. There is an effort to use that information to correct VLA phases. If that is successful, we will eventually try to use it on the VLBA, but that would require a receiver upgrade. Finally, the 512 Gbps recording mode is being installed. This uses both tape recorders at each site, each recording at its maximum rate of 256 Mbps. A 1 Gbps mode is also being investigated. There is NASA funding to pursue that development.

The big upgrade hopes center around the proposed VLA Expansion Project. Phase I of that project is being proposed to the NSF now. That involves fiber optic data transmission, new receivers for continuous frequency coverage, and a new correlator with 80 times the bandwidth of the current one. Phase II, to be proposed later, is mainly what is being called the "New Mexico Array". This will involve adding new antennas, perhaps eight, within about 350 km of the VLA. A very compact VLA configuration may also be proposed. Once this is done, there will effectively be one instrument consisting of the VLA, the New Mexico Array, and the VLBA, that covers all baselines between 25 m and 8600 km. A project can use whatever portions of that instrument are appropriate for the scientific goals of the observation.

References

[1] Napier, P. J., Bagri, D. S., Clark, B. G., Rogers, A. E. E., Romney, J. D., Thompson, A. R., & Walker, R. C., "The Very Long Baseline Array", 1994, Proc. IEEE, 82, 658

Nobuyuki Kawano et al.: Differential VLBI Observations among a Lunar Orbiter, the Moon and a QSO, IVS 2000 General Meeting Proceedings, p.160–163
http://ivscc.gsfc.nasa.gov/publications/gm2000/kawano

Differential VLBI Observations among a Lunar Orbiter, the Moon and a QSO

Nobuyuki Kawano [1], *Hideo Hanada* [1], *Takahiro Iwata* [2], *Yasuhiro Koyama* [2]

[1] *National Astronomical Observatory, Division of Earth Rotation*
[2] *Communications Research Laboratory, Kashima Space Research Center*
Contact author: Nobuyuki Kawano, e-mail: kawano@miz.nao.ac.jp

Abstract

The Japanese lunar explorer, SELENE will be launched in 2004. It will send two radio transmitters to the Moon for differential VLBI. One is a mission instrument on board the orbiter, and the other is placed on the Moon or on board another free flyer. They transmit carrier signals at three frequencies of S-band and one of X-band. It is expected that many VLBI stations take part in the observations of these transmitters for selenodesy. In addition to the VLBI observations, it is also expected that a lunar orbit and lunar libration will be observed at LLR stations.

1. The Japanese Lunar Explorer, SELENE

Differential VLBI observations among the transmitters both on a lunar orbiter and on the Moon as well as a QSO are planned in order to estimate the precise lunar gravity field and to know the lunar core density. This plan is a part of Japanese lunar exploration project (SELENE Project), SELENE is the abbreviation of SELenological and ENgineering Explorer. It is going to be launched in 2004. It has 14 mission instruments, and three of them are for precise determination of lunar gravity field and the lunar topography. These are two VLBI transmitters, a relay satellite and a laser altimeter. The explorer consists of a main orbiter, a relay satellite and a propulsion module. The relay satellite, in which one of the transmitters for differential VLBI (VRAD-1) is installed, is a free flyer and is separated from the explorer just after the explorer is injected into an elliptic lunar orbit. Its orbit has an apoapsis of 2400 km altitude and periapsis of 100 km altitude. The main orbiter gradually decreases its altitude and finally it has a circular orbit with 100 km altitude. After about one year of observations, a part of the propulsion module attached to the main orbiter is separated and lands softly on the lunar surface together with another VLBI transmitter (VRAD-2). Instead of soft-landing of the module, it is also discussed that VRAD-2 is installed in another free flyer.

2. The Concept of Observations for Selenodesy

The relay satellite relays radio waves from the Earth to the main orbiter, and the return waves from the orbiter are also relayed to the Earth by this satellite. The relay satellite makes Doppler shift measurements called 4-way possible in the far side of the Moon. These measurements must give us the precise information on lunar gravity field of the far side [1] since they are achieved with resolution of 0.1 mm/s. The laser altimeter emits laser pulses. The pulses are reflected on the lunar surface and return back to the orbiter. The altimeter measures round trip time with an accuracy of 17 ns (5 m in altitude), and knows the altitude of the orbiter [2]. Since the

orbiter is tracked by 2-way Doppler frequency measurements, the position of the orbiter is precisely determined. Therefore, we can draw the figure of the Moon from the observed altitudes and the estimated position of the orbiter. In order to determine the orbit of the relay satellite, two radio transmitters (VRAD-1 and VRAD-2) both on the satellite and on the Moon play the important role. Differential VLBI between two radio sources as well as Doppler measurements determine its precise position, and VLBI between VRAD-2 and a QSO gives us the information on lunar librations in addition to LLR data. Fig. 1 shows the concept of the observations.

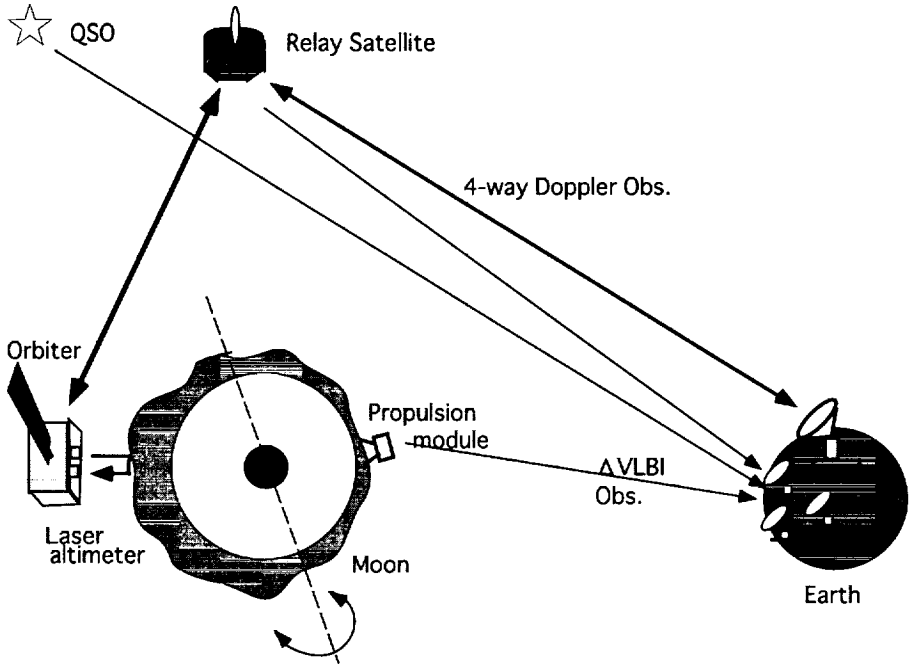

Figure 1. The concept of the observations

3. Scientific Targets

One of our scientific targets in the SELENE project is the estimation of lunar core density [3]. Lunar principal moment of inertia is derived from a set of dynamic flattenings, and C20, C22. Unfortunately, the observation error of C22 or C20 is larger than that of dynamic flattening so far. If the error is improved by one order of magnitude or so, the lunar core density can be estimated more precisely from the moment of inertia assuming three layer model, for example. The lunar core density is closely related to the origin of the Moon because several hypotheses of the origin anticipate different core density or chemical compositions, especially total amount of ferrite. Radio signals from both VRAD-1 and VRAD-2 are received at the VLBI stations on the Earth, and derive delay and delay rate in addition to Doppler frequency measurements to determine the precise position of the relay satellite. Although these data are not sensitive to higher degree gravity coefficients because of larger semi-major axis, they improve the lower degree gravity coefficients such as C20 and C22. On the other hand, 4-way Doppler tracking of the main orbiter has a potential to derive higher degree gravity coefficients in both the near side and the far

side. The laser altimeter measures the distance between the orbiter and the lunar surface with an accuracy of 5 m, although the resolution of the elevation depends on the accuracy of the estimated orbit. If differential VLBI observations are conducted between the main orbiter and VRAD-1 or VRAD-2, a digital elevation map over the whole Moon with the resolution of several meters will be made. These wide-range spherical harmonic coefficients and the topography provide precise gravity anomaly and give us information on the lunar crust.

4. Radio Transmitters VRAD-1 and VRAD-2

One of the radio transmitters is installed in the relay satellite, and another one is attached to the landing unit of the propulsion module if the part of propulsion module softly lands. Both of the transmitters emit signals at three frequencies of S-band and one of X-band as shown in Table 1. VRAD-2 is attached with thin belts to the landing unit and is packed with a thermally insulated compartment to survive severe cold and heat for two months.

Table 1. Specifications for VRAD

Frequency	S-band: 2212, 2218, 2287 MHz
	X-band: 8456(synchronized in phase with S-band)
Frequency stability	$< 1 \times 10\text{-}6$
S-band antenna	Cross-dipole antenna with the gain
	greater than -3dBi, RHCP
X-band antenna	Cross-dipole antenna with the gain
	greater than -3dBi, RHCP
Transmission power	S-band: 130 mW, X-band: 100 mW
Electric heater	Control by Thermostat
Coaxial cable	CuNi and stainless steel
Lifetime	2 months

Table 2. Desired specifications for a VLBI station

Antenna diameter	10 m
Aperture efficiency	>38 % at S-band
	>60 % at X-band
Tsys	<310 K at S-band
	<350 K at X-band
Rsn	>5.7 both at S and X-band
VLBI video converter	Mark-IIIa or K-3, 4 (2MHz×16ch)
RISE terminal	BW=100kHz, 200 ksps of 4 channels
	Data for 8 hours are recorded on 8-mm
	cassete tape

5. VLBI Station

Desired specifications for a VLBI station are shown in Table 2. The VERA network is going to be operated for these differential VLBI observations, as a main VLBI network. Three stations of the network got started in Dec. 1999 and will be completed next year. Although the network will be operated all the time when the Moon is in view, the observation period of about 8 hours in one network is not enough to precise estimation of lunar gravity field. We hope that VLBI stations, as many as possible, take part in our observations.

References

[1] Namiki N., H.Hanada, T.Tsubokawa, N.Kawano, M.Ooe, K.Heki, T.Iwata, M.Ogawa, T.Takano and RSAT/VRAD/LALT mission groups:@Selenological experiments of SELENE: Relay satellite, differential VLBI and laser altimeter, Adv. Space Res. vol.23, No.11, pp. 1817-1820, 1999.

[2] Araki H., M.Ooe, T.Tsubokawa, N.Kawano, H.Hanada and K.Heki: Lunar Laser Altimetry in the SELENE Project, Adv. Space Res. vol.23, No.11, pp. 1813-1816,1999.

[3] Hanada H., Ooe M., Kawaguchi N., Kawano N., Sasao T., Tsuruta S., Fujishita M., and Morimoto M., Study of the lunar core by VLBI observations of artificial radio sources on the moon, Journal of Geomag. Geoelectr., 45, 1405-1414, 1993.

Alan L. Fey et al.: A Southern Hemisphere Observing Program to Strengthen the ICRF, IVS 2000 General Meeting Proceedings, p.164–167
http://ivscc.gsfc.nasa.gov/publications/gm2000/Fey1

A Southern Hemisphere Observing Program to Strengthen the ICRF

Alan L. Fey [1], *Kenneth J. Johnston* [1], *David L. Jauncey* [2], *John E. Reynolds* [2], *Anastasios Tzioumis* [2], *James E. J. Lovell* [2], *Peter M. McCulloch* [3], *Marco E. Costa* [3], *Simon J. Ellingsen* [3], *George D. Nicolson* [4]

[1] *United States Naval Observatory*
[2] *Australia Telescope National Facility*
[3] *University of Tasmania*
[4] *Hartebeesthoek Radio Astronomy Observatory*

Contact author: Alan L. Fey, e-mail: afey@usno.navy.mil

Abstract

We outline a program of planned Southern Hemisphere astrometry and imaging observations aimed specifically toward improvement of the International Celestial Reference Frame.

1. The Observations

We plan to strengthen the ICRF in the Southern Hemisphere by a) increasing the reference source density with additional S/X band (2.3/8.4 GHz) bandwidth-synthesis astrometric VLBI observations, and b) VLBI imaging at 8.4 GHz of ICRF sources south of $\delta = -20°$. These observations will allow us to determine the contribution of the intrinsic source structure to the measured positions, to investigate possible systematic errors in source positions, and to provide a strong tie between the Northern and Southern Hemisphere through the overlap with common sources measured from the north.

1.1. Astrometry

Our earlier S/X band Southern Hemisphere VLBI astrometry program (Russell *et al.* 1994; Reynolds *et al.* 1994; Johnston *et al.* 1995) proved most successful in providing the fundamental Southern Hemisphere reference frame for the ICRF, as well as the basis for the southern component of the Australia Telescope Compact Array reference frame currently in use. We plan to continue this successful astrometry program by repeated observations of $\sim$ 150 Southern Hemisphere ICRF sources, both to better define the reference frame and to provide high quality sources for phase referencing observations. We note that much of the present VLBA observations are now undertaken in phase referencing mode. Details of the planned observations are as follows:

- ATNF Long Baseline Array Proposal submitted and approved
- Mark III/IV format
- Standard dual-frequency S/X band
- Correlated at Washington (USNO)

- About 150 sources
- 2–3 24^{hr} experiments per year for 5 years
- Array of telescopes
  - Parkes and/or Tidbinbilla (Australia)
  - Hobart (Tasmania)
  - Hartebeesthoek (South Africa)
  - Kashima (Japan)
  - Kokee Park (USA)
  - Syowa (Antarctica)
  - TIGO (South America)

1.2. Imaging

A program of multi–epoch imaging of all the Northern Hemisphere sources of the ICRF is currently underway using the VLBA, with promising early results. We plan to extend this important work to the Southern Hemisphere by imaging at 8.4 GHz, with milliarcsecond resolution, $\sim$ 200 ICRF sources. Over the proposed five year lifetime of the program we plan for two observations of each source separated by one to two years in order to determine component proper motions. Details of the planned observations are as follows:

- ATNF Long Baseline Array Proposal submitted and approved
- S2 format
- Standard X band frequency
- Correlated at Epping (ATNF)
- About 200 sources
- 2–3 24^{hr} experiments per year for 5 years
- Array of telescopes
  - Narrabri (Australia)
  - Mopra (Australia)
  - Parkes and/or Tidbinbilla (Australia)
  - Ceduna (Australia)
  - Hobart (Tasmania)
  - Hartebeesthoek (South Africa)
  - Kashima (Japan)
  - Kokee Park (USA; S2 on loan from ATNF)

2. Motivation for Observations

Despite its significance and stated accuracy, the International Celestial Reference Frame (ICRF) (Ma *et al.* 1998) suffers from a deficit of defining sources in the Southern Hemisphere. Defining sources are those that set the initial direction of the ICRF axes and were chosen based on their observing history and the stability and accuracy of their position estimates. Of the 212 ICRF defining sources, less than 30% are in the Southern Hemisphere. This is illustrated in Figure 1 which shows the ICRF defining sources on an Aitoff equal area projection of the celestial sphere. In order to control local deformations of the ICRF, it is crucial to increase the density of sources in the Southern Hemisphere. Although systematic effects should be greatly reduced in frames derived from extragalactic radio sources, there is no *a priori* reason to assume that the radio frame will be completely free of systematic errors.

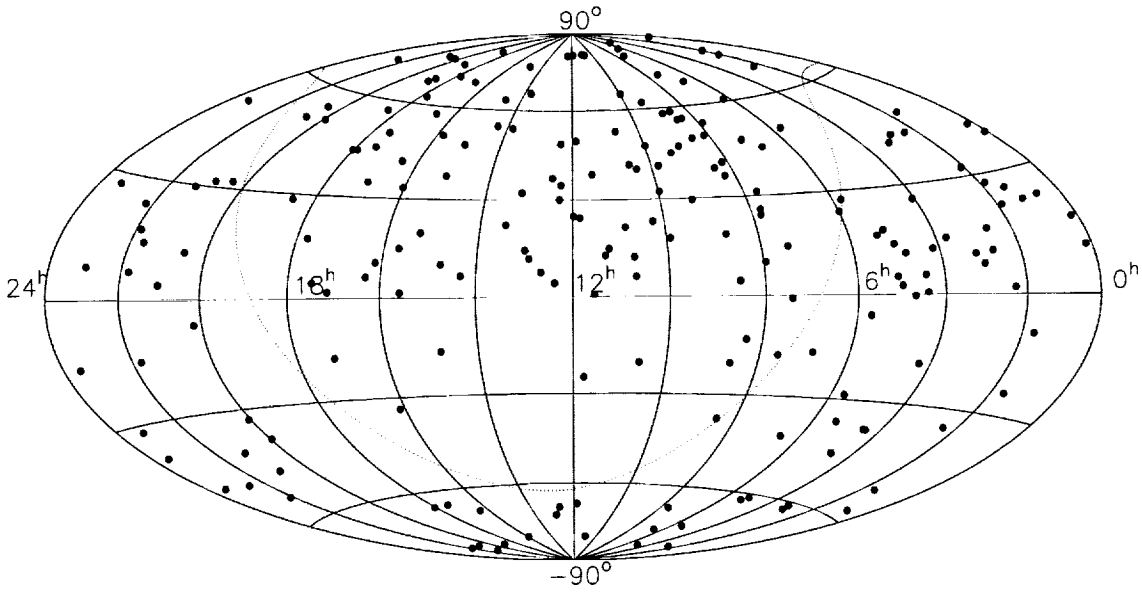

Figure 1. The distribution of ICRF defining sources on an Aitoff equal area projection of the celestial sphere. The dotted line represents the Galactic equator. Note the deficit of defining sources in the Southern Hemisphere.

Fey *et al.* (2000) have used up–to–date radio astrometric and ancillary data to evaluate the extragalactic sources which make up the ICRF in terms of their suitability for use by the Space Interferometry Mission as radio/optical frame tie sources. As a general result, they present an estimate of the radio astrometric quality of the sources based on an evaluation of the available radio data. This estimate of astrometric quality is shown in Figure 2 plotted versus declination. As can be seen in this figure, the astrometric quality of the sources rapidly decreases for sources south of the celestial equator. Additional high quality astrometric observations are needed to improve the quality of these sources and to improve the ICRF.

It is well known that the extragalactic radio sources which comprise the ICRF have variable emission structure on angular scales larger than the precision of their position estimates. The Very Long Baseline Array (VLBA) telescope of the National Radio Astronomy Observatory has been used successfully to image ICRF sources in the Northern Hemisphere (Fey & Charlot 2000

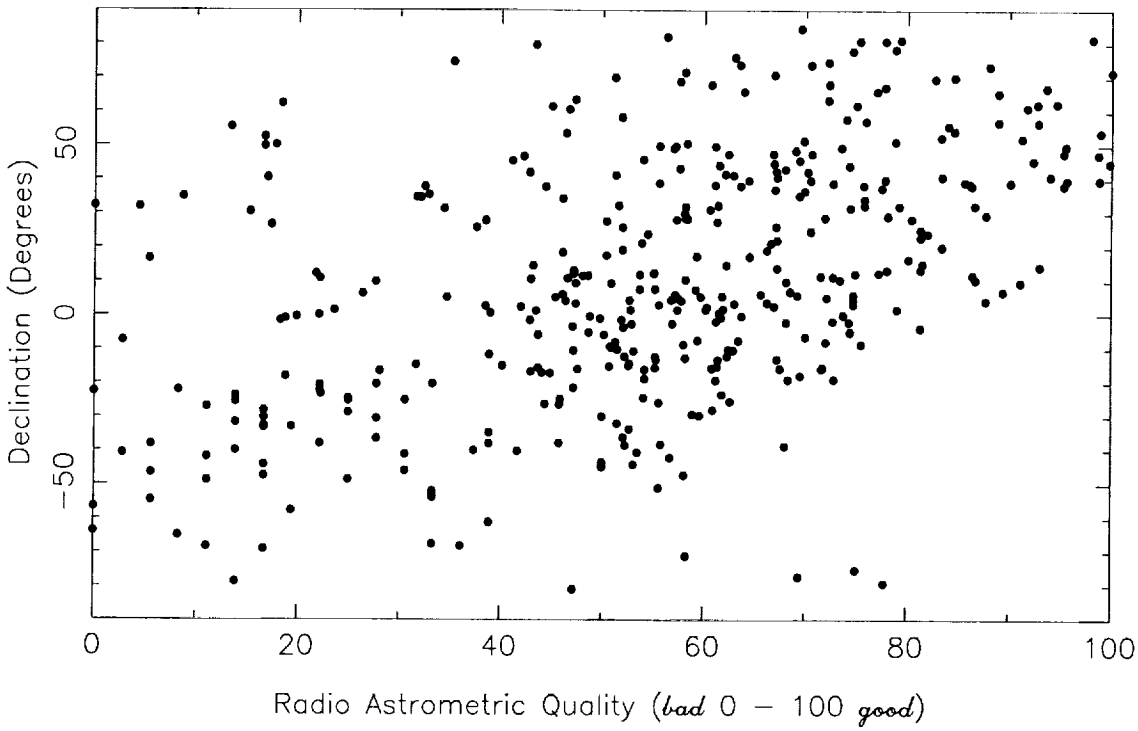

Figure 2. The distribution of radio astrometric quality as defined in Fey *et al.* (2000) with respect to source declination for the extragalactic radio sources in the ICRF. Note the decrease in astrometric quality for sources in the Southern Hemisphere.

and references therein), at least for sources with $\delta > 30°$. The resultant VLBA images have been used to calculate a source "Structure Index" (SI) based on the analysis of Charlot (1990). The SI can be used in conjunction with other data to obtain an estimate of the astrometric quality of the sources. SI values for 388 ICRF sources are reported by Fey & Charlot (2000). Continued viability of the ICRF at a high level of accuracy requires measuring and monitoring of the sources for changes in intrinsic structure.

3. References

Charlot, P. 1990, AJ, 99, 1309
Fey, A.L., & Charlot, P. 2000, ApJS, in press
Fey, A.L., *et al.* 2000, in preparation
Johnston, K.J., *et al.* 1995, AJ, 110, 880
Ma, C., *et al.* 1998, AJ, 116, 516
Reynolds, J.E., *et al.* 1994, AJ, 108, 725
Russell, J.L., *et al.* 1994, AJ, 107, 379

Patrick Charlot et al.: A Proposed Astrometric Observing Program for Densifying the ICRF in the Northern Hemisphere, IVS 2000 General Meeting Proceedings, p.168–172
http://ivscc.gsfc.nasa.gov/publications/gm2000/charlot

A Proposed Astrometric Observing Program for Densifying the ICRF in the Northern Hemisphere

Patrick Charlot [1], *Bruno Viateau* [2], *Alain Baudry* [1], *Chopo Ma* [3], *Alan Fey* [4], *Marshall Eubanks* [4], *Christopher Jacobs* [2], *Ojars Sovers* [5]

[1] *Observatoire de Bordeaux*
[2] *Jet Propulsion Laboratory, California Institute of Technology*
[3] *NASA Goddard Space Flight Center*
[4] *US Naval Observatory*
[5] *Remote Sensing Analysis Systems*

Contact author: Patrick Charlot, e-mail: charlot@observ.u-bordeaux.fr

Abstract

The International Celestial Reference Frame (ICRF) could be of significant importance to the astronomy community for observing weak objects angularly close to ICRF sources with the phase-referencing technique. However, the current distribution of the ICRF sources is found to be largely non-uniform, which precludes the wide use of the ICRF as a catalog of calibrators for phase-referencing observations. We show that adding 150 new sources at appropriate sky locations would reduce the distance to the nearest ICRF source for any randomly-chosen location in the northern sky from up to 13° to up to 6°, close to the requirement of the phase-referencing technique. Accordingly, a set of 150 such sources, selected from the Jodrell Bank–VLA Astrometric Survey and filtered out using the Very Long Baseline Array Calibrator Survey, has been proposed for observation to the European VLBI Network (EVN) extended with additional geodetic stations. The use of the EVN is essential to this project since most of the new sources will be weaker and thus difficult to observe with standard geodetic networks.

1. Scientific Objectives

The International Celestial Reference Frame (ICRF) (Ma *et al.* 1998), the most recent realization of the VLBI celestial frame, is currently defined by the radio positions of 212 extragalactic sources distributed over the entire sky. These "defining" sources set the initial direction of the ICRF axes and were chosen based on their observing histories with the geodetic networks and the stability and accuracy of their position estimates. The highest quality positions in the ICRF are accurate at the 0.25 milliarcsecond (mas) level. In addition, positions for 294 less observed candidate sources and 102 other sources unsuitable for defining the frame at this level of accuracy were given, primarily to densify the frame and make it more accessible. The first maintenance and extension of the ICRF, ICRF-Ext.1, provides positions for 59 newly observed sources and refines the positions of candidate sources from additional observations (IERS 1999).

Despite its stated accuracy, the ICRF suffers from a deficit of sources with an average of only one object per 8° × 8° on the sky, which is a limitation for attaching other reference frames (e.g. at optical wavelengths) to the ICRF. Moreover, the distribution of the 667 ICRF-Ext.1 sources is found to be largely non-uniform (see e.g. the northern-sky distribution in Fig. 1). For example, the distance to the nearest ICRF source for any randomly-chosen sky location is up to 13° in the northern sky and 15° in the southern sky. This precludes the use of the ICRF as a

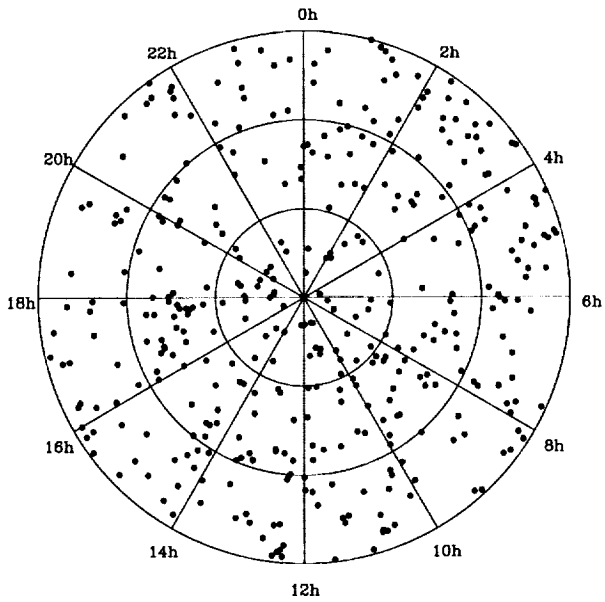

Figure 1. Northern-sky distribution of the ICRF-Ext.1 sources in polar coordinates. The outer circle corresponds to a declination of 0° while the inner central point is for $\delta = 90°$. The intermediate circles correspond to declinations of 30° and 60°.

catalog of calibrators serving as fiducial points to determine the relative positions of nearby weaker objects (radio stars, pulsars, weak quasars) with the phase-referencing technique (e.g. Lestrade *et al.* 1990), because the separation between the calibrator and the target source should be a few degrees at most in such observations. The non-uniform source distribution also makes it difficult to assess and control any local deformations in the ICRF. Such deformations might be caused by tropospheric propagation effects and the apparent motions of the sources due to variable intrinsic structure (see Ma *et al.* 1998).

The primary objective of our proposed observing program is to densify the ICRF using an approach that will also improve the overall sky distribution of the sources. A secondary objective is to identify new sources of high astrometric value which could potentially be used as defining sources in a further future realization of the ICRF. For this reason, the newly selected sources will be required to have no or limited extended structure to ensure the highest possible astrometric accuracy. The proposed observing program, as described below, will focus on the northern sky to take advantage of the existing standard VLBI networks like the European VLBI Network (EVN) and the Very Long Baseline Array (VLBA).

2. Strategy for Selection of New Sources

The approach used for selecting new sources to densify the ICRF was to fill first the "empty" regions of the sky. The largest such region for the northern sky is located near $\alpha = 22$ h 05 min, $\delta = 57°$, where no ICRF source is to be found within 13°. A new source should thus be preferably added in that part of the sky. By using this approach again and repeating it many times, it is then possible to progressively fill the "empty" regions of the sky and improve the overall ICRF

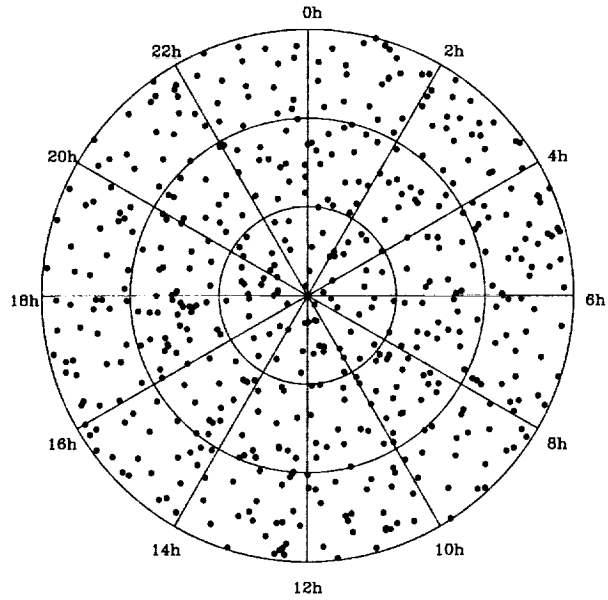

Figure 2. Northern-sky distribution of the ICRF-Ext.1 sources together with the additional 150 proposed new sources in polar coordinates. The outer circle corresponds to a declination of 0° while the inner central point is for $\delta = 90°$. The intermediate circles correspond to declinations of 30° and 60°.

source distribution. The input catalog for selecting the new sources to observe was the Jodrell Bank–VLA Astrometric Survey (JVAS) which comprises 2118 compact radio sources distributed over all the northern sky (Patnaik *et al.* 1992, Browne *et al.* 1998, Wilkinson *et al.* 1998). Each JVAS source has a peak flux density at 8.4 GHz larger than 50 mJy at a resolution of 200 mas, contains 80% or more of the total source flux density, and has a position known to an rms accuracy of 12–55 mas. For every "empty" region in ICRF-Ext.1, all JVAS sources within a radius of 6° (about 10 sources on average) were initially considered. These sources were then filtered out using the VLBA calibrator survey (Peck & Beasley 1998) to eventually select the source with the most compact structure in each region. The VLBA calibrator survey is an ongoing program to image all JVAS sources with milliarcsecond resolution at 2.3 GHz and 8.4 GHz.

The results of this iterative source selection scheme show that 30 new sources are required to reduce the distance to the nearest ICRF source from up to 13° to up to 8°. Another 40 new sources would further reduce this distance to a maximum of 7° while for a maximum distance of 6°, approximately 150 new sources should be added to ICRF-Ext.1. Carrying this procedure further, it is found that the number of required new sources doubles for any further decrease of this distance of 1° (approximately 300 new sources for a maximum distance of 5° and 600 new sources for a maximum distance of 4°) with the limitation that the JVAS catalog is not uniform enough to fill all the regions below a distance of 6°. Based on these results, the choice of 150 new sources to add to the ICRF appears to be a good compromise between the amount of VLBI observing time required and the improvement of the source distribution. With at least one source within 6° of any target in the northern sky, the proposed densified ICRF catalog is much improved (see Fig. 2) and would be especially useful as a catalog of reference sources for phase-referenced VLBI observations of weak objects.

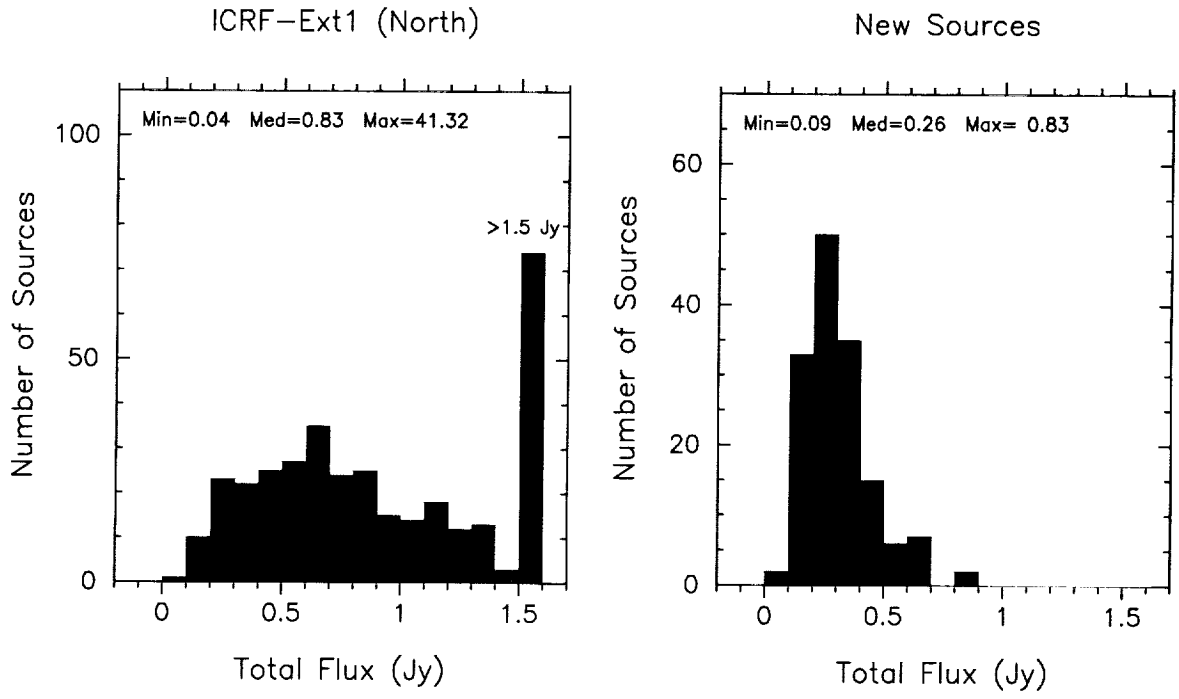

Figure 3. Comparison of the total flux of the ICRF-Ext.1 sources (left) with that of the 150 new sources proposed for densification of the ICRF (right). The total flux values are from the JVAS catalog and were measured at 8.4 GHz. All ICRF-Ext.1 sources present in the JVAS catalog (341 sources out of a total of 392 northern sources) are included. The minimum, median and maximum of the total flux values are indicated in each panel.

3. Proposed VLBI Observing Program

The goal of our observing program is to determine the VLBI astrometric positions of the first 150 sources selected above for possible inclusion of these sources in a further future extension of the ICRF. A comparison of the total flux of these new sources with that of the current ICRF sources (Fig. 3) indicates that the new sources are much weaker (median total flux of 0.26 Jy against 0.83 Jy for the ICRF-Ext.1 sources). For this reason, we have considered using the EVN, which includes large radio telescopes like the 100 m Effelsberg antenna, for carrying out these observations. Additional non-EVN geodetic stations will also be added to increase the baseline length. In particular, the external stations of Algonquin Park (Canada), Hartebeesthoek (South-Africa) and Ny Ålesund (Spitsbergen) have been contacted and agreed to participate in such observations.

The proposed observing strategy will consist in observing about 50 new sources in each experiment of 24-hr duration, and repeating the observation of each source three times over a time scale of two years to ensure the position accuracy required for inclusion in the ICRF (see Ma *et al.* 1998). Our observing program will therefore require a total of nine 24-hr experiments for completion. The new sources will be scheduled jointly with a set of 10 highly-accurate ICRF sources so that their positions can be linked directly to the ICRF. Accordingly, a proposal has been submitted to the

EVN for carrying out these observations, with the initial request consisting of a single experiment to first demonstrate the feasibility of this project. This initial request has been approved and the proposed experiment is planned for May-June 2000. For the future, we are also considering using the global VLBA+EVN network to observe all the 150 new sources at once, which would reduce the amount of observing time required for this project. This observing strategy, however, needs to be further studied, especially in terms of scheduling feasibility.

References

Browne, I. W. A., Patnaik, A. R., Wilkinson, P. N., Wrobel, J. M.: 1998, Interferometer Phase Calibration Sources – II. The Region $0° \leq \delta_{B1950} \leq +20°$, *MNRAS*, 293, 257.

IERS: 1999, First extension of the ICRF, ICRF-Ext.1, *1998 IERS Annual Report*, Ed. D. Gambis, Observatoire de Paris, p. 87.

Lestrade, J.-F., Rogers, A. E. E., Whitney, A. R., Niell, A. E., Phillips, R. B., Preston, R. A.: 1990, Phase-Referenced Observations of Weak Radio Sources – Milliarcsecond Position of Algol, *AJ*, 99, 1663.

Ma, C., Arias, E. F., Eubanks, T. M., Fey, A. L., Gontier, A.-M., Jacobs, C. S., Sovers, O. J., Archinal, B. A., Charlot, P.: 1998, The International Celestial Reference Frame as Realized by Very Long Baseline Interferometry, *AJ*, 116, 516.

Patnaik, A. R., Browne, I. W. A., Wilkinson, P. N., Wrobel, J. M.: 1992, Interferometer Phase Calibration Sources – I. The Region $35° \leq \delta \leq 75°$, *MNRAS*, 254, 655.

Peck, A. B., Beasley, A. J.: 1998, A VLBA Calibrator Survey, *IAU Colloquium 164: Radio Emission from Galactic and Extragalactic Compact Sources*, Eds. J. A. Zensus, G. B. Taylor, & J. M. Wrobel, *ASP Conference Series*, Vol. 144, p. 155.

Wilkinson, P. N., Browne, I. W. A., Patnaik, A. R., Wrobel, J. M., Sorathia, B.: 1998, Interferometer Phase Calibration Sources – III. The Regions $+20° \leq \delta_{B1950} \leq +35°$ and $+75° \leq \delta_{B1950} \leq +90°$, *MNRAS*, 300, 790.

Calvin Klatt et al.: The S2 Geodetic VLBI Program in Canada: System Validation Experiments and Results, IVS 2000 General Meeting Proceedings, p.173–179
http://ivscc.gsfc.nasa.gov/publications/gm2000/klatt

The S2 Geodetic VLBI Program in Canada: System Validation Experiments and Results

Calvin Klatt [1], *Mario Bérubé* [1], *Marc Bujold* [1], *Wayne H. Cannon* [3], *Georg H. Feil* [2], *Alexander Novikov* [2], *William T. Petrachenko* [1], *Josef Popelar* [1], *Anthony Searle* [2]

[1)] *Geodetic Survey Division, Natural Resources Canada*
[2)] *Space Geodynamics Laboratory, CRESTech*
[3)] *York University*

Contact author: Calvin Klatt, e-mail: klatt@geod.nrcan.gc.ca

Abstract

In this report we discuss a number of S2 geodetic system validation experiments and their results. These experiments are those in which we use one or more VLBI baselines, observe a number of geodetic radio sources (full sky coverage) and use frequency-switching to achieve bandwidth synthesis.

The experiments performed to date used the three geodetic antennas in Canada: ALGOPARK, YELO7296 and the Canadian Transportable VLBI Antenna (CTVA). ALGOPARK and YELO7296 are IVS Network stations, while the CTVA is a 3.6 m antenna being operated as part of the development center activities [2]. Each of the three antennas is equipped with an S2 RT, an S2 DAS, a PC Field System computer and a hydrogen maser frequency standard.

The S2 Recording Terminal (RT) is a well established VLBI recording system utilizing an array of eight commercial video cassette recorder (VCR) transports to record at rates of up to 128 Mbits/sec.

The focus of much recent activity is the frequency-switching S2 Data Acquisition System (DAS). Currently the DAS systems in use utilize two baseband converters and switch frequencies in order to synthesize a larger bandwidth [1].

Correlation is done at the Canadian S2 Correlator, which is currently configured with six playback terminals.

1. Operational Considerations

We report here on a variety of operational issues in which our S2-based program differs from other geodetic VLBI programs. These differences all relate to the use of cassette tapes and the frequency-switching technique used to achieve bandwidth synthesis.

1.1. The S2 RT and Cassette Handling

The S2 RT is a proven VLBI recording system that is fully supported by the PCFS. Status monitoring and control are via a console or Ethernet (window open on PCFS). PCFS support means that errors are reported to the operator via the Field System. The RT has a power-on self-test.

The S2 RT uses high-quality reusable cassette tapes in sets of eight. Cassette changes during experiments are easy to perform and are currently given four minutes in the schedule. Cassettes are automatically ejected and rewinding is done at the correlator. Tapes are numbered from 0-7 to correspond with the cassette transports. If the order is not followed the correlator will resolve the problem without operator intervention.

The cost of cassettes is approximately $12.50 Canadian or $8.50 U.S., and 32 to 48 cassettes are used at each station for each 24-hour experiment (4-6 sets of 8 cassettes) depending on tape control mode and speed.

Experiments have been conducted using adaptive tape control (cassettes are stopped if the time between valid data exceeds some preset value) at SLP speed. This combination gives approximately 7 hours between tape changes. One experiment was performed using continuous tape control at LP speed, giving approximately 4 hours between tape changes. The latter combination improved time synchronization at the correlator. We found that additional tape changes were not an operational problem because each one is so simple to perform. We intend to experiment with continuous tape control at SLP mode, which we expect to give approximately 6 hours between tape changes.

The S2 cassettes are very easy to work with when a schedule is aborted for any reason. If in adaptive mode, the cassette motion should be stopped. The schedule will restart recording. In continuous motion the operator need not do anything with the cassettes, except a cassette change if one was scheduled during the time of the failure.

1.2. The S2 DAS and Frequency-Switching

The instantaneous bandwidth of the system now in use is 32 MHz, 16 MHz in each BBC. We use a 2-bits/sample mode, at a Nyquist sampling rate. The recorded data rate is 128 Mbits/sec.

The spanned bandwidth of any frequency-switching sequence is determined by the receiver bandwidth. The maximum switching rate is 50 Hz. There is no maximum or minimum number of states. Optimizing the frequency sequence is a similar exercise to that in parallel channel systems such as the MkIV. See [1] for a discussion of frequency-switching sequence design.

The PC Field System (PCFS) does not yet fully support the S2 DAS. DAS mode setup and loading of the frequency sequence from the PCFS is partially implemented. A locally modified version of the PCFS is used with the transportable antenna to read system temperatures from the S2 DAS for SEFD determination, etc.

DAS status monitoring and control is performed via a console. Alternatively a window can be raised on the Linux PCFS to monitor behavior. When fully operational, error messages will be communicated to the field system and the console will be necessary only in exceptional circumstances. A power-on self-test for the DAS has recently been completed. Phase-cal extraction features, useful for status monitoring, are currently in development.

1.3. General Scheduling Notes

The standard geodetic scheduling software is SKED, maintained by the Goddard VLBI group. This software has not yet been adapted for the S2 DAS or RT but preliminary work is underway to add S2 support. Both the astronomical scheduling software SCHED and the DRUDG program, used to produce SNAP and procedure files, support the S2 RT.

Local changes to the SKED software were performed to allow an interim scheduling process to be developed. SKED was modified to not rewind tapes and to correctly specify S2 tape change times. This local version of SKED was then used to produce optimized geodetic schedules. The list of scans (sources, scan start times, dwell times, tape change times) is extracted from the SKED output and ported into a SCHED command file. SCHED then is run to produce a S2 schedule, which can be run through DRUDG. The entire process after generating the SKED output is done through a UNIX script, which is run as a single command.

Schedule optimization is performed using a feature in SKED which exports a fake database that can be loaded into SOLVE. The simulation results are not as accurate as they are for MkIII systems because frequency-switching schemes aren't supported. This affects the simulated delay resolution function, and has a minor effect on the simulated results and a very minor effect on schedule optimization.

1.4. Validation Network Considerations

The antennas used in the system validation experiments are described in Table 1. Note that there is one very sensitive antenna, one of moderate sensitivity and one low-sensitivity antenna. More stations and baselines are required to determine Earth Orientation Parameters or to determine accurate Celestial Pole offsets (Nutation). The S2 data rate, 128 Mbits/sec, is higher than that typically used in MkIII CORE-A experiments at ALGOPARK, increasing the sensitivity somewhat. At 128 Mbits/sec ALGO-CTVA is approximately as sensitive as two 16 m-diameter antennas at 56 Mbits/sec.

Meteorological data at the current CTVA location, the Dominion Radio Astrophysical Observatory (DRAO) in Penticton, British Columbia has now been integrated with the PCFS but was not available for any experiments in 1999. Meteorological data will be available at all proposed CTVA sites.

A cable calibration system for the CTVA is not yet available.

Antenna Name	Diameter (m)	X SEFD	S SEFD	Equipment
ALGOPARK	46	200	250	Mk-III, S2
YELO7296	9	7600	6500	Mk-III, S2
CTVA	3.6	70000	100000	S2

Table 1. Antenna Characteristics

1.5. Canadian S2 Correlator

The Canadian S2 Correlator is located at DRAO and has been operating in production mode now for three years. The correlator was designed for both Space VLBI (VSOP/HALCA and RadioAstron) and Geodetic VLBI. The correlator currently has six playback terminals but has the electronic components for ten playback terminals. The correlator can be expanded to 128 stations.

Cassette playback is 1:1 speed, but jobs from small networks can be broken up and placed in any available transport. For example correlation of a 24-hour two-station experiment can be broken up into three jobs and completed in 8 hours. Correlation of a 24-hour three-station experiment can be correlated in 12 hours.

Implementation of support for frequency switching schemes is complete. Data quality analysis software tools (to create so-called "fringe plots") are in development.

1.6. Analysis Issues

The correlator output data format is UVFITS. A program called CGFF (Canadian Geodetic Fringe Fitting) is used to process the UVFITS file and output geodetic data in a CGLBI format.

This CGLBI format is an ASCII text format based on the NGS format with a significant increase in information content. The most recent CGLBI format description is available at the CGLBI website (www.sgl.crestech.ca/cglbi). An additional program (CGGLBIDB) is used to convert the CGLBI format file into a CALC/SOLVE database. The initial steps in the analysis process for S2 data is described on the CGLBI website.

Because of minor hardware dependencies incorporated in the CALC/SOLVE database design, S2 databases are slightly different from those of the MkIII system. The bulk of the differences relate to the 14 channels of the MkIII system. There were a small number of changes required in the CALC/SOLVE software that we expect to be incorporated in future releases. These changes typically involve *not* making calculations if the data is determined to be S2. The S2-specific ionospheric calculations are performed when the CGLBIDB program is called and are thus not part of CALC/SOLVE. Documentation on the software changes made to CALC/SOLVE is available on the CGLBI website.

Group delay ambiguities are 200 ns at both X-band and S-band, but none have been observed. Some 200 ns jumps in the data have been observed when the phase-cal was interrupted at one station. After the data has been edited and the ionospheric correction performed, the group delay residuals (25-50 ps) match those expected by the scan SNRs.

In our current analysis we are holding ALGOPARK fixed to its ITRF97 position and the coordinates of the other antennas are adjusted. A priori EOPs and nutation are used (IERS Bulletin B values are used). The clock and troposphere parameterization adjusts new clock offsets every 180 minutes and new troposphere delays every 60 minutes, with standard constraints on the changes in these values. ALGOPARK is used as the reference clock.

For comparison purposes the databases from all 1999 CORE-B experiments which used both ALGOPARK and YELO7296 were analyzed in a similar manner to the above. A spacing of 120 minutes between clock parameters was used because the CORE-B network clock behavior was not as well known.

2. Experiments Performed

Table 2 lists the system validation experiments performed to date. Several other experiments (CG005, CG007 and CG009) were single-source experiments designed to study other aspects of the system. Frequency switching was first done with the S2 DAS in July 1998. The experiments listed were all 24-hour multiple-source frequency-switching experiments. The main objectives of these experiments have been:

- Testing of new features in the S2 DAS (frequency-switching, automatic gain control, etc.)
- CTVA functionality and sensitivity
- Overall interferometer sensitivity
- Scheduling and analysis software and procedure development
- Correlation software and procedure development
- PCFS functionality and control of the S2 DAS, S2 RT and the CTVA

CG006 is the first geodetic-type experiment that can be analyzed in CALC/SOLVE. CG008, a 48-hour experiment that has been broken into two 24-hour segments for analysis purposes, followed

Experiment Name	Date	Baselines	Number of Delays Obtained
CG006	June 1999	ALGOPARK-CTVADRAO	106
CG008-Day 1	August 1999	ALGOPARK-CTVADRAO	105
CG008-Day 2	August 1999	ALGOPARK-CTVADRAO	143
CG010-Day 1	October 1999	ALGOPARK-CTVADRAO ALGOPARK-YELO7296 YELO7296-CTVADRAO	302
CG010-Day 2	October 1999	ALGOPARK-CTVADRAO ALGOPARK-YELO7296	242

Table 2. System Validation Experiments

two months later. The first half of CG008 has fewer scans than the second half due to antenna problems. CG010 is an experiment that is in two parts, each 24 hours long with a 24-hour gap between. This experiment used YELO7296 for the first time. The first 24 hours of CG010 had special long scans on bright sources placed hourly to obtain scans between YELO and CTVA. The second day of CG010 had some S2 equipment problems that reduced both the quality of the data and the number of observables. The cause of this problem has now been resolved.

There is a general trend of increasing numbers of scans as our scheduling ability improved and the idle time at the stations was gradually reduced. We are now achieving 1% idle time at ALGOPARK (the slowest antenna). The three station schedules were produced by first creating an optimal schedule using ALGOPARK and the CTVA and then tagging along the YELO station.

The baselines ALGOPARK-CTVADRAO and ALGOPARK-YELO7296 are both approximately 3000 km in length.

3. Experiment Results

Analysis of each 24-hour data set was done independently. The additional delay measurements between the CTVA and YELO obtained during CG010 Day 1 were used in the analysis. When they are removed from the solution there is very little difference; their contribution to the solution is very weak.

Figure 1 shows the baseline length determination for ALGOPARK-CTVA. The X, Y and Z positions of the CTVA are available from the author. No survey of the CTVA position at DRAO is currently available: the line shown illustrates the ITRF97 baseline velocity.

Figure 2 shows the baseline length determination for ALGOPARK-YELO7296. The X, Y and Z positions of YELO7296 are available from the author. The ITRF97 baseline length and velocity is also shown. There are only two CGLBI experiments involving YELO7296, CG010 days 1 and 2. The values obtained from similar analysis (see above) of CORE-B databases are shown here for comparison purposes.

The CTVA results show repeatability of the baseline lengths below 1 cm, better than could be expected from the individual measurement uncertainties.

The YELO results show that the S2 data is generally consistent with the CORE-B experiments and with the position given by ITRF97. A number of problems occurred during day 2 of CG010 and this is seen in the results.

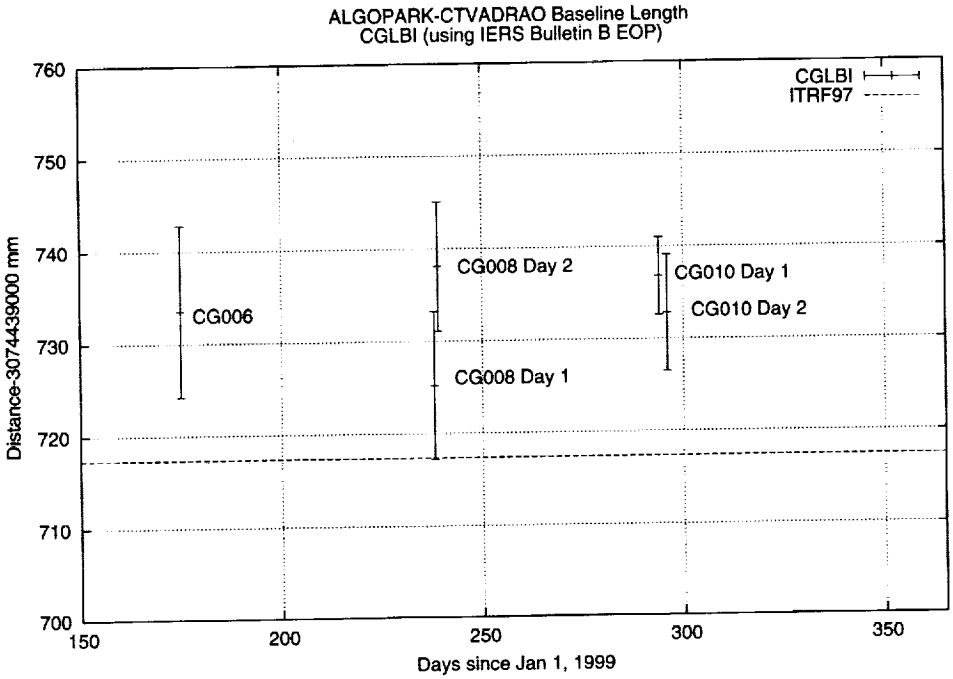

Figure 1. ALGOPARK-CTVADRAO Baseline Length

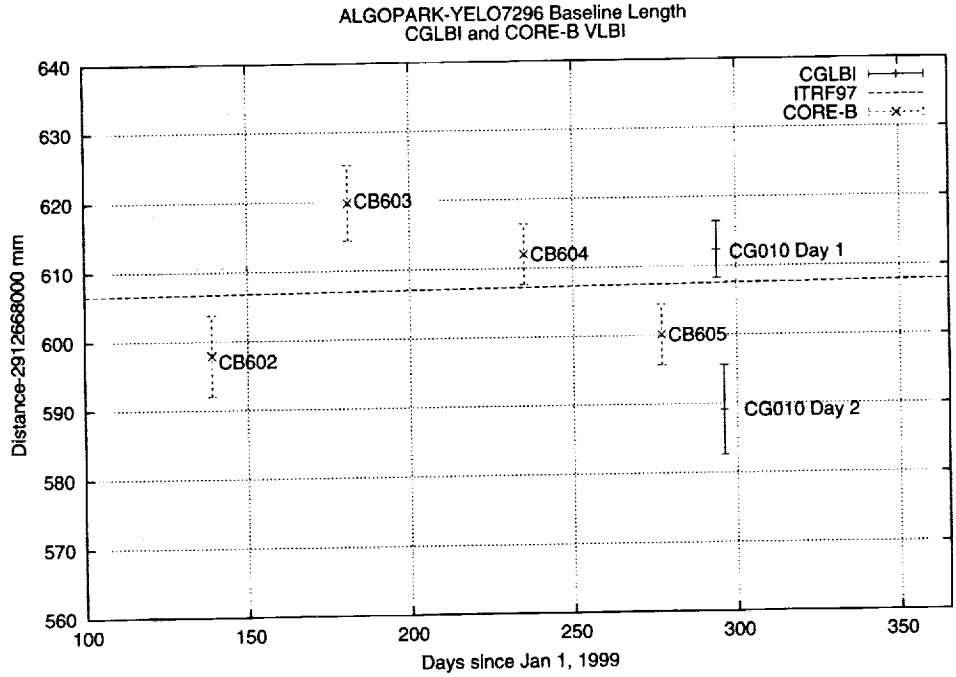

Figure 2. ALGOPARK-YELO7296 Baseline Length

The results are very promising, but it should be remembered that these experiments were system tests. There have not been enough experiments for us to make any definitive statements about data scatter, repeatability, etc. In the next stage of this research program we will obtain a significant amount of new data, allowing us to gain a more complete understanding of the performance of the S2 geodetic VLBI system.

4. Future Plans

We plan to begin trial operations using the Canadian antennas in April 2000. These trials should involve at least 10 experiments over the spring and summer of 2000. During this period a number of outstanding development issues should be resolved and the operations themselves will give us significantly more experience using the equipment. This number of experiments will be useful for us to investigate optimal strategies in a number of areas including frequency sequences, tape modes, SNR targets and analysis parameterization. The first production release of the DAS operating system software should be made this summer, with phase-cal extraction features.

During this time we should be able to make progress in partnership with other groups toward obtaining official support for the S2 system in scheduling software and the field system.

References

[1] Petrachenko, W.T., *et al.* "The S2 VLBI System: DAS, RT/PT and Correlator", This Volume.

[2] Bérubé, M. "The Canadian Transportable VLBI Antenna", This Volume.

Tom Clark: New Uses for the VLBI Network, IVS 2000 General Meeting Proceedings, p.180–184
http://ivscc.gsfc.nasa.gov/publications/gm2000/clark2

New Uses for the VLBI Network

Tom Clark

NASA Goddard Space Flight Center
e-mail: clark@tomcat.gsfc.nasa.gov

Abstract

This paper suggests some potential new uses for the existing VLBI network.

It seems that every VLBI group in the world faces some common problems:

We do not have enough money to operate!
We do not have enough money to make improvements!!

In this contribution I discuss several possibilities for new business that might help to support the network stations without causing serious impacts on the primary VLBI programs.

1. Deep Space Tracking

We have experimented with using a few stations from the geodetic VLBI network to track the MARS Global Surveyor (MGS) spacecraft with respect to extragalactic radio sources. At the distance of Mars, an angular accuracy of $\sim$ 100 μarcseconds translates into a positional accuracy $\sim$100 meters. Initial results are promising, but they show how much work we need to do!

The main technical problems we encountered were related to differences between the normal VLBI extragalactic inertial frame and the dynamical coordinate system used to describe the position of objects in our solar system to "feed" the correlator and to analyze the data. These were made more difficult by having very little financial support for the program.

Nevertheless, Marshall Eubanks and I think we could have prevented the Mars Climate Observatory ("Metric vs. English units") disaster by using VLBI for supplementary tracking.

In the first decade of the new millennium there are plans to launch a virtual armada of satellites to study the inner solar system – Mars, Mercury, asteroids and Lagrangian points. As I look at the mission planning activities, I doubt that all the world's resources devoted to Deep Space Tracking can handle all the missions.

The typical S/X geodetic VLBI station is already equipped with most of the hardware to support telemetry downlinks from such spacecraft:

- $\sim$ 20 Meter Aperture
- Cryogenic Receiver
- Time/Frequency Standard
- Automatic Telescope Control
- Internet access

To add downlink telemetry to a VLBI station, I envision a Pentium-class PC streaming raw baseband data onto a 10-20 GByte hard disk, while also doing software decoding for on-line monitoring. After a data acquisition pass was over the data could be shipped by Internet (or the Hard Drive could be removed and shipped) to the sponsoring "customer".

To evaluate this possibility, I took a look at a private initiative by SpaceDev (http://www.spacedev.com) called the Near Earth Asteroid Prospector (NEAP) which will rendezvous with an asteroid. Table 1 shows link budget calculations comparing a typical ~20m geodetic VLBI station with a 34m DSN station. The ~8 dB sensitivity difference (i.e. SEFD ratio = 6.5:1) translates into a 6.5:1 ratio in the deliverable data rate.

- If the cost of operating a VLBI station to track spacecraft can prove to be significantly (i.e. a factor of ten) cheaper than operating the DSN, and
- if we can work out observing schedules that allow for tracking without compromising the VLBI programs,

then the customer would find our resources to be a useful alternative.

2. Global Frequency/Time Network

At present, global time/frequency is defined by BIPM based on a global array of atomic clocks (Cesium Beam, Hydrogen Maser and recently Cesium Fountain standards). Because this clock is distributed, it is can be called a "paper clock". The quality is dependent on the accuracy of synchronization that can be achieved over intercontinental distances. Several techniques are used for clock synchronization including:

- Travelling Clocks,
- Two-way satellite time transfer,
- Common-View GPS and GLONASS satellite observations, and
- GPS carrier-phase (i.e. geodetic) observations with a large (IGS) network.

In the past, carrying travelling clocks as "passengers" on commercial airliners and in vans used to be quite common, but other techniques are now much easier and more cost-effective. The two-way satellite and common-view GPS techniques provide nsec-level accuracy, while carrier-phase measurements deliver precision at levels of ~50 picoseconds.

VLBI is a user of this global "paper" clock – our correlators require a priori time synchronization at the sub-μsec level for efficient operation and at the μsec level to produce UT1. The use of GPS code-phase data with simple timing receivers (like my "TAC") provides blind synchronization anywhere in the world at accuracy levels ~20 nanoseconds. As the VLBI data is analyzed, the "paper clock" parameterization of the clocks at each station over a day is precise at levels ~10-50 picoseconds. As early as 1977 [1] VLBI showed that it could provide time synchronization as a "product" at accuracy levels of 10-20 nanoseconds.

For the future, I would like to suggest that the Hydrogen Masers, as calibrated with geodetic VLBI and GPS measurements, *could* be a significant addition to the global clock network. We need to develop calibration techniques for both VLBI and GPS that allow the incredibly **precise** (~10-50 picosecond) measurements to be used for timing **accurate** at the sub-nsec level.

Table 1: NEAP -- Near Earth Asteroid Prospector

Downlink (Space-to-Earth) Link Budget

DSN 34M vs Typical 20M VLBI Ground Station
1 Meter Spacecraft Antenna with 20W transmitter
X-Band at Time of End of Encounter

Spacecraft:	**Value:**
Transmitter RF Power Output:	20 Watts
Carrier Frequency:	8471 MHz
Wavelength:	3.5 cm
Antenna Diameter:	1 m
Antenna Aperture Efficiency:	55 %
Antenna Gain:	36.4 dBiC
Antenna -3dB Beamwidth:	2.5 deg.
Line/Cable Losses:	-1.0 dB
Switch Losses:	0.0 dB
Misc. Tranmission Losses:	-0.7 dB
Spacecraft Pointing Error:	0.7 deg.
Spacecraft Pointing Losses:	-0.8 dB
Spacecraft EIRP:	46.8 dBW

Path Losses, etc:	
Range to Spacecraft	1.21 AU
Range to Spacecraft (meters)	1.82E+11 m
Derived Path Loss:	-276.2 dB
Polarization Loss Allowance:	-1.5 dB
Atmospheric Loss Allowance:	-0.1 dB
Ionospheric Loss Allowance:	-0.1 dB
Rain/Water Vapor Attenuation:	-1.0 dB
Signal Level at Earth	-232.1 dBW

Ground Station (GS):	**34M DSN STATION**	**TYPICAL VLBI STATION**
GS Antenna Diameter:	34	20 m
GS Antenna Aperture Efficiency:	65	45 %
GS Antenna Gain:	67.7	61.5 dBiC
GS Antenna -3dB Beamwidth:	0.073	0.124 deg.
GS System Noise Temperature:	42	65 K
GS Pointing Loss:	0.1	0.1 dB
System G/T Figure of Merit:	51.4	43.3 dB/K
G/T in VLBI SEFD units:	101	630 Jy
GS C/No:	47.9	39.8 dB*Hz
Data Rate:	13000	2000 bps
Interleave Coding Rate:	0.5	0.5 rate
Symbol Rate:	26000	4000 sps
Available Matched Filter Eb/No:	6.8	6.8 dB
Real-World Demod. Implementation Loss:	0.5	0.5 dB
Req'd Eb/No for 10e-7 BER with CCSDS Convolutional Encoding/Reed Solomor	2.6	2.6 dB
Signal Margin	3.7	3.7 dB

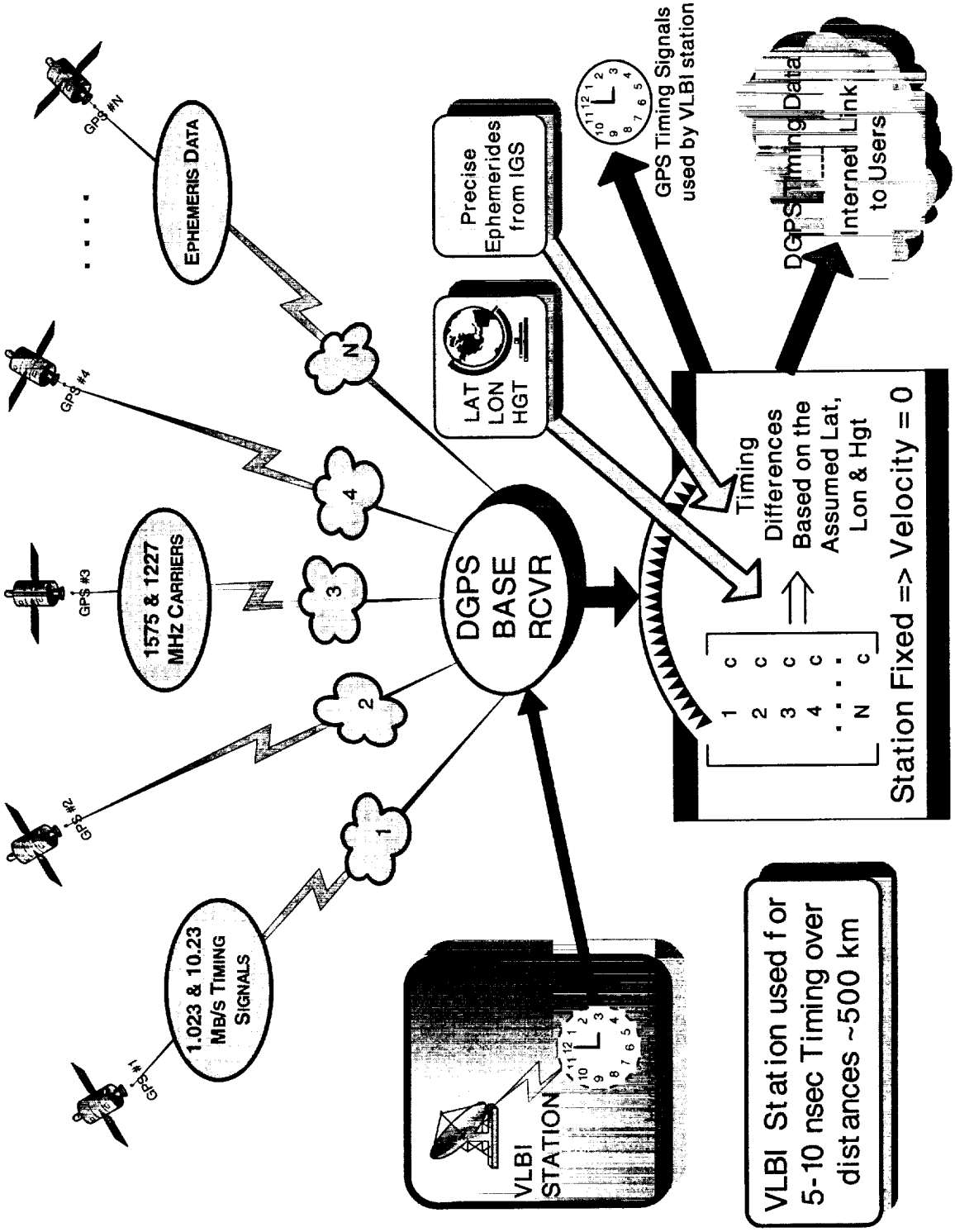
GPS #N
GPS #4
GPS #3
GPS #2
GPS #1
EPHEMERIS DATA
1575 & 1227 MHz CARRIERS
1.023 & 10.23 MB/S TIMING SIGNALS
DGPS BASE RCVR
VLBI STATION
Precise Ephemerides from IGS
LAT LON HGT
GPS Timing Signals used by VLBI station
DGPS Timing Data
Internet Link to Users
Timing Differences Based on the Assumed Lat, Lon & Hgt
Station Fixed => Velocity = 0
VLBI Station used for 5-10 nsec Timing over distances ~500 km

Some commercial ventures are considering a scheme that uses GPS to provide nsec-level timing accuracy over continental scale distances. This involves DGPS-like clock corrections being distributed in real-time via the Internet from primary clock sites equipped with atomic standards. The global VLBI stations might host these operations by providing access to their Masers, VLBI and GPS data and Internet connectivity. The accompanying cartoon illustrates the concept.

References

[1] Clark et al., "Synchronization of Clocks by Very-Long-Baseline Interferometry", IEEE Trans Inst. And Meast. IM-28, 1979, 184.

Session 6.

Correlators

Alan R. Whitney: How Do VLBI Correlators Work?, IVS 2000 General Meeting Proceedings, p.187–205
http://ivscc.gsfc.nasa.gov/publications/gm2000/whitney2

How Do VLBI Correlators Work?

Alan R. Whitney

MIT Haystack Observatory
e-mail: awhitney@haystack.mit.edu

Abstract

The VLBI correlator is the "glue" that brings the data from separate antennas together and processes it to form the basic observables used in astronomy and geodesy. In this introductory tutorial, we will examine the operations that the correlator executes by following through a set of simple examples from raw data to multi-band delay estimates. What we will find is that the operations performed inside a correlator are really quite simple and understandable. What is not so simple are the practical realities of dealing with tapes, the precise control of huge torrents of data from tape, and the complicated bookkeeping to keep track of everything. Four our purposes, however, we will completely ignore these difficulties and examine the correlator as a simple machine.

1. Introduction

VLBI correlators have always tended to be large and complicated machines, but the functions they perform are fundamentally fairly simple. Their apparent complexities have more to do with dealing with the difficult nature of tapes and their attendant problems rather than with the actual computations that occur. In this short tutorial, we will attempt to explain the basic workings of a VLBI correlator with little attention paid to the complexities of tapes or other implementation details. In addition, the mathematics attending correlation will be kept to an absolute minimum so that a more intuitive understanding can be gained.

2. Why Correlate (Figure 1)

The VLBI data-processing procedure can be viewed from both the astronomy and geodesy perspectives, in which case the goals are a bit different.

For *astronomy*, the goal is generally to make high-resolution maps of radio sources. This is done by combining the data from two or more antennas in such a way that the data appear to have been collected by a single antenna that happens to have geographically-separated elements. A single antenna effectively gathers its signal by summing the signals from all the various parts of its surface in an operation that is nearly identical to correlation. The correlation processing of a VLBI correlator effectively adds the signals from multiple antennas together in such a way that the result appears to have come from a single antenna whose surface is made of the actual individual antennas. If the actual single antennas are distantly separated, the synthesized antenna has a beam pattern with very narrow lobes which allows the mapping of small radio objects with very high resolution, sometimes approaching the micro-arcsecond level, which is, incidentally, the highest angular resolution achievable by any known existing technique! Correlating the signals between all pairs of individual antennas allows the signals to be properly "added" to form the synthesized mapping beam.

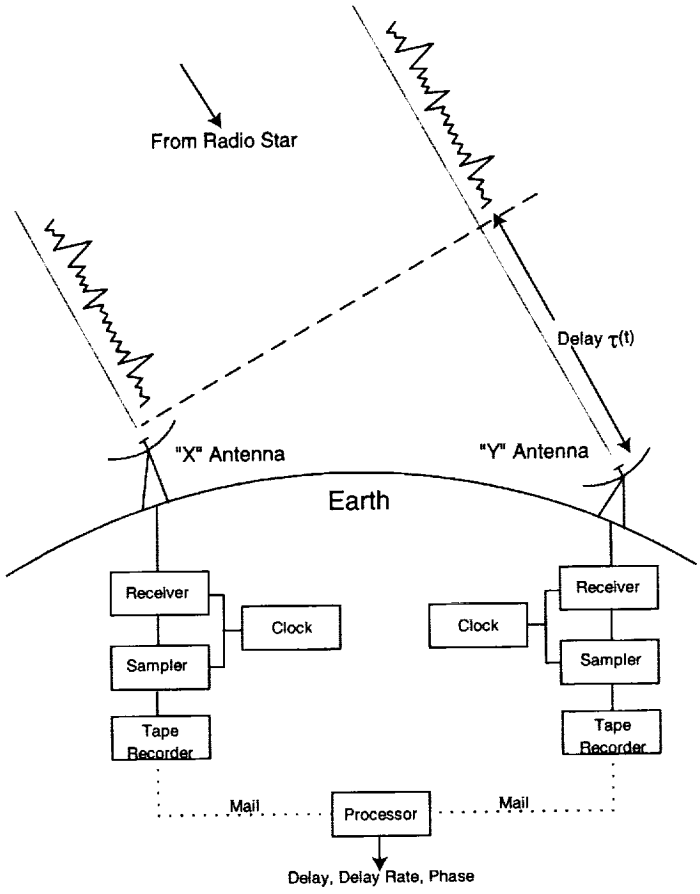

Figure 1. Basic VLBI Block Diagram

For *geodesy*, the goal is usually to measure the time-of-arrival difference of signals from a radio star, as illustrated for a single antenna pair in Figure 1. Assuming that the radio star is a point object and that the clocks at the individual stations are exactly synchronized, the time-of-arrival difference, $\tau(t)$, can be measured by comparing the signals with different trial delays until they match. In practice, this is done by multiplying them together with different trial delays until a maximum is discovered at the actual delay. This multiplication process with many different trial lags is called *correlation*, which can be shown to be the optimal processing procedure for the so-called *maximum-likelihood estimate* of the delay [1] As we shall see later in this tutorial, the correlation process may actually be implemented in a couple of different ways that involve Fourier transforms. But the underlying process is always equivalent to a multiplication process with many different trial lags.

[1] In actual practice, of course, a large number of antennas are used that have imperfectly synchronized clocks. By collecting a sufficiently large amount of data, the relative synchronization of the clocks can be determined, as well as the actual delay measurements. In this tutorial, however, we will assume that the clocks are all perfectly synchronized.

3. A Simple Real Correlator (Figure 2)

In the real world of VLBI, signals at each antenna are normally converted to digital samples before writing to tape. These samples are usually taken at a regular interval corresponding to $1/(2\times BW)$ where BW is the bandwidth of a channel.[2] Each sample consists of either 1 or 2 bits[3].

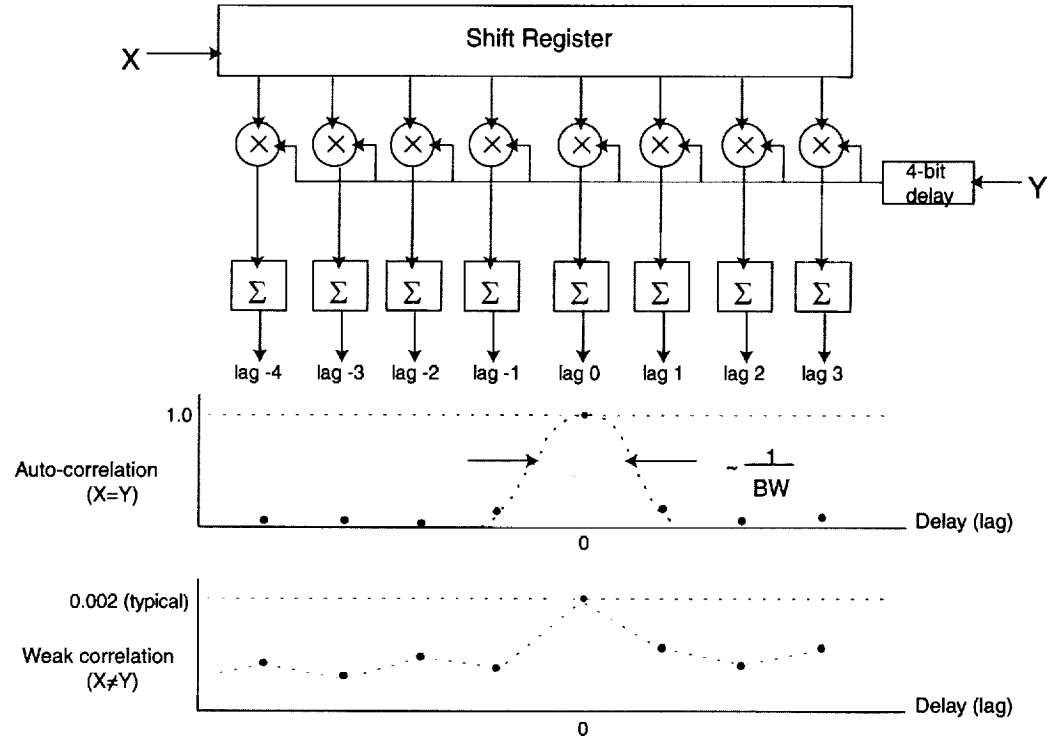

Figure 2. Simple Real Correlator

In the 1-bit/sample case, for example, the sample value is chosen to be 0 if the voltage at the sampling instant is < 0 v, or 1 if the voltage is ≥ 0 v. For 2 bits/sample, a threshold voltage is chosen and each sample is assigned one of four possible values according to whether the sampled voltage is positive or negative, and whether it is inside or outside of the absolute threshold voltage[4].

Figure 2 shows a "simple real correlator". The X signal is impressed directly on a shift register and shifts one position to the right at every sample period. The Y signal is first delayed by three sample-periods and is then impressed on the eight multipliers in parallel, and the output of the multiplier at each lag is summed. If the X and Y signals are identical, a little thought will convince you that the signals are exactly correlated at lag 0 where, by definition, the *correlation coefficient* is 1. If X=Y, the function of correlation amplitude versus delay (lag) is called the *auto-correlation function.* For the case of white Gaussian signals, most of the energy of the correlation

[2]This is called the "Nyquist rate" and is optimal for geodetic VLBI observations observing wideband continuum radio sources. Typically, many independent parallel channels, widely separated in observing frequency, are recorded.

[3]It turns out that recording more than 2 bits per sample is inefficient by the metric of signal-to-noise ratio per bit recorded, so is almost never used.

[4]The actual coding scheme used is system dependent; the correlator must, of course, be aware of the particular coding scheme used.

is concentrated at lag 0, though a few percent is in adjacent lags -1 and $+1$. If we were to draw a curve through correlation coefficients at lags -1,0,$+1$, the width of the function is $\sim 1/BW$, as shown in Figure 2. If X and Y have zero delay between them and are weakly correlated[5], as is usually the situation with VLBI, the correlation function might look like the plot in the lower plot of Figure 2. In the case illustrated, only a small fraction of a percent of the signals in X and Y is correlated at lag 0; the other lags are mostly just noise.

4. Real Correlator with Delay (Figures 3-4)

If signal Y has a fixed delay with respect to X, but is otherwise identical, the correlator shown in Figure 3 may be used to process the data. A delay is provided for at the X input to compensate before correlation is done. Since this delay is limited to be an integral number of sample periods,

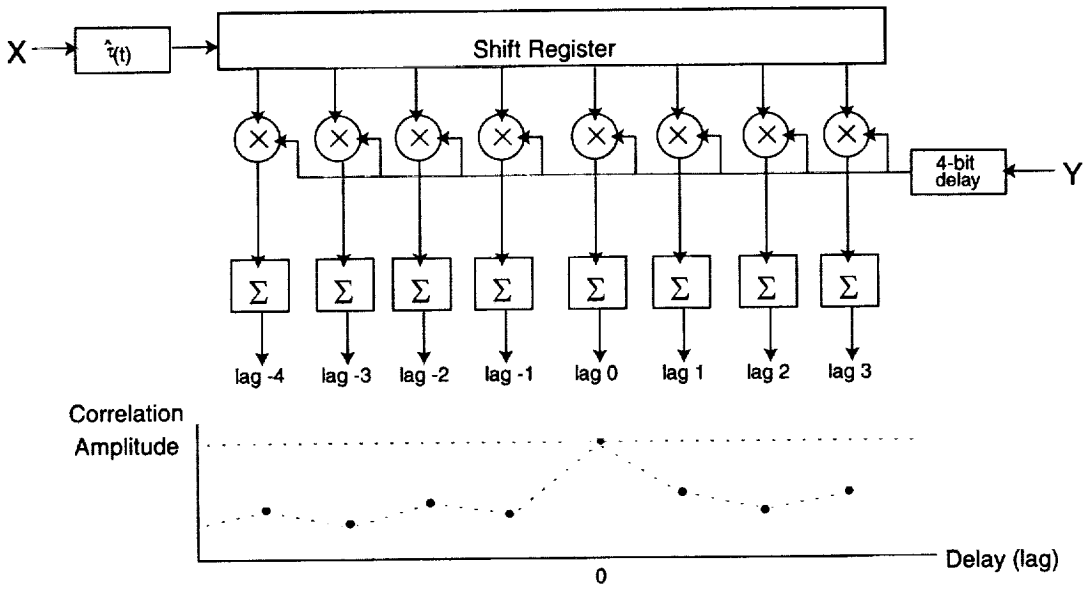

Figure 3. Real Correlator with Delay

it usually cannot be set precisely to the desired delay, but can *always* be set to be within $\pm$ 0.5 sample periods of the desired delay. If the "error" in the delay setting is non-zero, a small loss in signal-to-noise ratio (SNR) will result, and the correlation function will not be centered on a particular lag.

If the delay of Y with respect to X is changing, but the signals are otherwise identical[6], the delay applied to the X signal must change as a function of time in a quantized fashion, as shown in Figure 4. The dashed line represents the "model" (or desired) delay, but the actual X-delay

[5] "Weakly correlated" means that a small component of X and Y is identical, but that the primary components of X and Y are uncorrelated noise.

[6] In this scenario, the local oscillators at the stations must be adjusted to remove any differential Doppler frequency that would otherwise result.

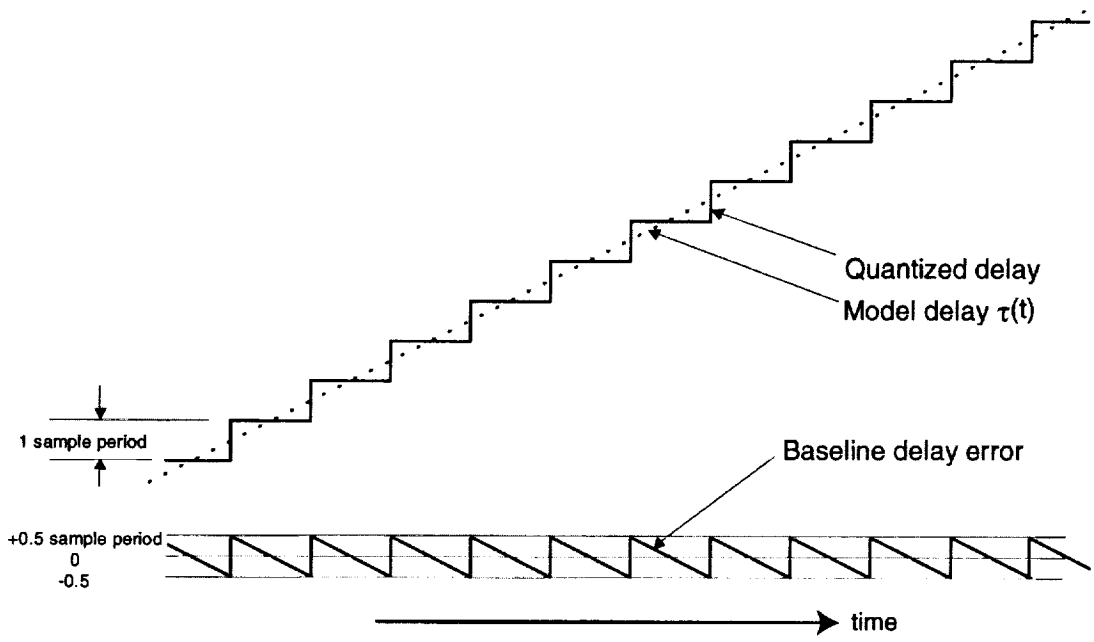

Figure 4. Quantized Delay-tracking Example

must step in integral sample periods as shown. This results in a sawtooth "baseline delay error" shown at the bottom of Figure 4, which varies between +0.5 and −0.5 sample periods. Because the correlator delay cannot exactly track the desired delay, a small SNR loss occurs (~4% in most cases).

5. Baseline-Based XF Complex Correlator (Figures 5-7)

In most modern VLBI systems, the RF receiving frequencies are set to be identical at all stations. This means that not only is there a signal delay between stations but, due to the rotation of the earth and the resulting difference in velocity (or delay rate) along the line-of-sight to the source, a frequency shift as well. This frequency shift is known as the "differential Doppler" frequency or "fringe rate" frequency, and is directly related to delay rate [7] Before a cross-correlation of X and Y can be done, compensation must be made for both the delay and fringe rate. One way to do this is shown in Figure 5; we will see an alternative way in Figure 10.

In Figure 5, we have moved the delay to the Y signal and reversed its sign[8]. The X signal is multiplied by sine and cosine waveforms corresponding to the "fringe rate" and the resulting two signals are individually correlated with the delayed Y signal. This type of sine/cosine multiplication is known as "quadrature mixing" and is effectively a single-sideband mixing operation that shifts

[7]Strictly speaking, the differential Doppler or fringe rate must be referred to a particular reference RF frequency, but often the terms are used loosely and interchangeably with "delay rate".

[8]In theory, the delay can be compensated either at the X or the Y inputs; only the sign of the delay changes. With tapes, data can be adjusted to have an arbitrary positive or negative delay.

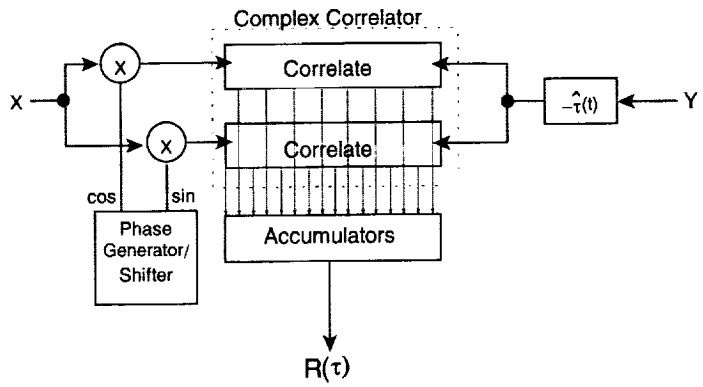

Figure 5. Baseline-Based XF Complex Correlator

the frequency spectrum of the X signal to match that of the Y signal. The correlator has a "cosine" and "sine" sum at each lag; such a correlator is known as a "complex correlator" since the cosine/sine sum pair form a complex number. The cross-correlation function, $R(\tau)$, is a discrete function consisting of one complex number for each value of lag τ. This type of correlator is known as an "XF" correlator due to the order of mathematical operations it executes. The "X" stands for cross-correlation and "F" for Fourier transform. As we will see later, the data from an XF correlator are Fourier transformed in a post-correlation processing step. Due to mathematical reciprocity, it is possible to perform an equivalent set of mathematical operations by first performing a Fourier transform ("F") on the data, followed by a multiplication ("X"). A correlator which performs the operations in this order is known as an "FX" correlator, which we will examine later. The sine and cosine waves generated by the Phase Generator in Figure 5 are not perfect sine/cosine waves, but are digital approximations.

Figure 6 shows a block diagram of a simple hardware realization of a phase generator of the type that is often used. It consists of three registers: 1) a phase register, typically 32 bits wide, where the full range of possible register values maps a single rotation from 0 to 360 degrees, 2) a phase-rate register, which holds the value by which the phase register is incremented at every sample period (clock cycle), as shown, 3) a phase-acceleration register which holds the value by which the phase-rate register is incremented at every sample period. The actual values of the cosine/sine waveforms are determined only by the 4 MSBs of the phase register, which map into 16 discrete cosine/sine phase segments as shown in Figure 6. As you can see, each waveform has only the value of $-1,0,+1$ in a rough approximation to an actual cosine/sine waveform. In the 1 bit/sample case, the quadrature multipliers in Figure 5 have a simple job: if the cos/sin value is 1, the sample is passed through unchanged; if the cos/sin value is -1, the sample is inverted to the other possible value; if the cos/sin value is zero, the output value is zero and the correlator does no accumulation regardless of the Y sample value. Though this procedure is simple and seemingly crude, it works well but does result in an $\sim$15% loss in SNR, which is normally quite tolerable considering the complexities of alternative schemes. The lost energy is scattered into data mixed with the higher harmonics of the cos/sin waveforms and is seen as slight additional noise.

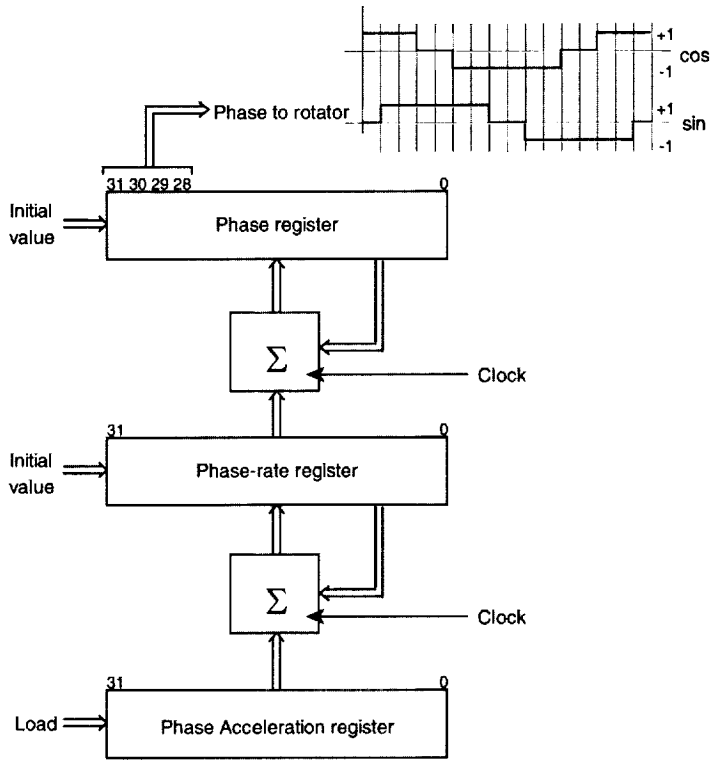

Figure 6. Sample 3-level Phase Generator

The frequency of the phase generator is usually chosen to be the fringe rate (or differential Doppler) at the center of observed BBC channel. This choice minimizes the average SNR loss over a correlation interval. However, for practical reasons it is desirable to reference the correlation processing to a frequency at one edge of the observing channel.[9] This requires one to adopt a delay-shift/phase-shift algorithm illustrated in Figure 7, which shows the rotator phase as a function of time. During each period of time for which the delay is held constant (i.e. during the interval over which the quantized delay error tracks from -0.5 to $+0.5$ sample periods) the phase rotator operates at a phase rate corresponding to the fringe rate at the middle of the channel (band). However, because we want the overall processing to be referenced to the DC edge of the video band, the phase of the phase rotator must be stepped exactly 90 degrees[10]at each instant that the delay is shifted by one sample period. This results in the sawtooth-like rotator phase pattern shown in Figure 7. Note that the gross progression of the rotation phase follows the BBC DC edge phase, but the instantaneous rotator phase rate is always appropriate for mid-band. This type of algorithm was first used on the Mark III correlator and is also incorporated into the Mark IIIA, Mark IV, and other correlators.

[9]In particular, by processing the data from the USB/LSB channel pair of a single BBC to the same reference RF frequency, they can be easily combined in post-correlation processing since they share a common LO chain. This operation would be much more complex if USB and LSB were processed with different reference frequencies.

[10]The sign of the phase shift depends on the sideband and the sign of the delay rate. A 90-degree phase shift is appropriate for Nyquist-sampled data. If a channel is oversampled, the phase shift is corresponding reduced by the oversampling factor.

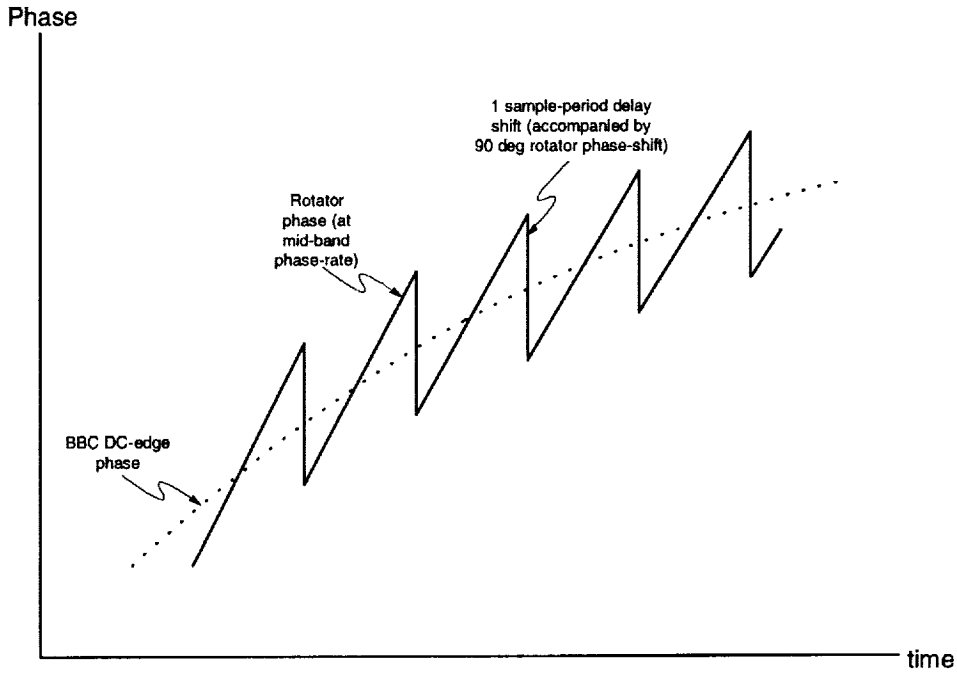

Figure 7. Delay Shift/Phase Shift Algorithm

The number of lags used in VLBI correlation is a function of the type of signal and the uncertainty in the model. For geodetic VLBI, the signals are always wideband white Gaussian noise; if the computer model is known to be highly accurate so that the signal is always nearly centered in the lag range, 3 lags will suffice. In practice, a minimum of 8 lags is usually processed in order to account for uncertainties in the correlation model, most particularly clock synchronization uncertainties. For spectral-line observations in radio astronomy, the target signals may be much narrower than the recorded bandwidth, in which case the signal energy is spread out over many more lags, with the number of processed lags often being as large as 512 or 1024.

6. Station-Based XF Complex Correlator (Figures 8-9)

A drawback of the baseline-based XF correlator of Figure 5 is that the delay element must be implemented individually for every baseline since every baseline, in general, has a different delay. This is tolerable for a relatively small correlator system, but because the number of baselines goes as the square of the number of stations, this scheme quickly becomes unwieldy and expensive. An alternative is the Station-Based XF Complex Correlator as illustrated in Figure 8.

In the system shown in Figure 8, the X data and Y data are delayed individually with respect to some common reference point, usually the center of the earth. But there is a problem. Because the delay-error of each station tracks between -0.5 and $+0.5$ sample periods as the delay changes, the baseline delay error will track between -1.0 and $+1.0$ sample periods. This is illustrated in Figure 9 where the Y delay, Y delay error, X delay and X delay error for a sample observation

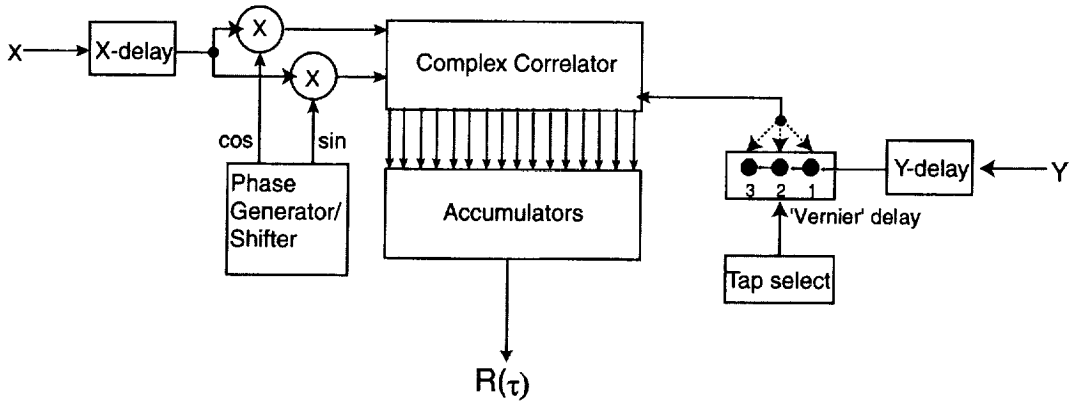

Figure 8. Station-Based XF Complex Correlator

are shown independently in the upper four traces. If the Y and X delay errors are differenced, representing the *uncorrected baseline delay error* the result is the dashed line in the bottom trace.[11] As you can see, the uncorrected baseline delay can behave quite peculiarly. Before correlation can be done, the baseline delay error must be brought within the normal bounds of -0.5 to $+0.5$ sample periods at all times. This requires the insertion of a "vernier delay" as shown in Figure 8, which is nothing more than a 3-tap shift register that allows the Y delay to be changed by ± 1 sample period. By suitably selecting the appropriate vernier-delay tape at any instant, a single sample-period delay can be added or subtracted in the Y data path and the baseline error can be tamed to the "corrected baseline error" shown in Figure 9 (solid line).

The details of the control of the vernier delay tap setting is beyond the scope of this tutorial, but suffice it to say that, based only on the knowledge of the X and Y delay errors and rates alone over an integration period of a second or so (no more than ~64 bits of information), a set of simple algorithms allows one to wiggle the tap in precisely the correct manner to achieve the *corrected baseline delay error* trace in Figure 9. The X and Y data then flow into the correlator with a baseline delay error that looks just like the baseline-based correlator of Figure 5.

There are other complications as well. For example, every time the X-delay shifts by a sample period, the discontinuity requires a corresponding discontinuity in the phase generator in order that the rotator phase be continuous with respect to the station X clock. If the X- delay changes such that an X sample is dropped, the phase generator in Figure 8 must respond by doubling the phase increment for that sample period; conversely, if the X-delay changes such that an X sample is added (usually duplicated), the phase generator must respond by zeroing the phase increment for the added sample. Furthermore, the phase generator must still execute a 90-degree phase shift every time the baseline delay increments or decrements by one sample period. Again, fairly simple algorithms can be used to control all of these parameters. All of the details of the precise control of the vernier-delay tap and the phase-generator can be transmitted to the correlator as simple *station-based* parameters (no more than ~256 bits from each station each second or so) on which simple calculations are made and algorithms are executed.

[11] Where the dashed line of the uncorrected baseline delay error overlaps the corrected delay error, a solid line is shown.

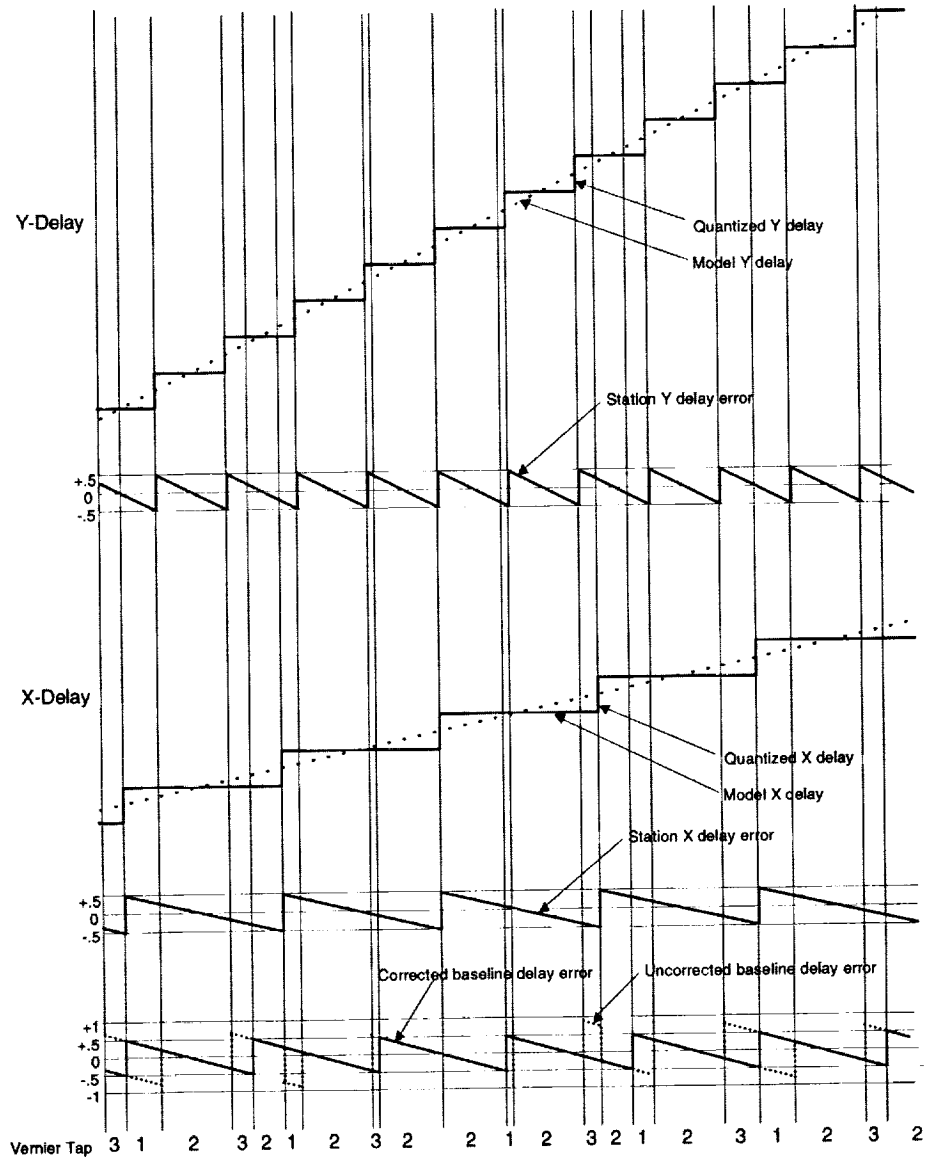

Figure 9. Baseline "Vernier Delay" Correction

A logical question to ask is why, in the station-based XF correlator, is not phase rotation done on a station basis as well as delay? In principle, this is possible, but in practice creates two difficulties. The first is that the SNR loss of the rotator would be suffered not just once, but twice, once each on X and Y data streams. The second reason is a bit more insidious. Because the rotation waveforms are rough approximations of true cos/sin curves, a rotator generates a set of undesired harmonics in addition to the fundamental rotation frequency. In a baseline-based correlator, only one set of rotator harmonics enter the correlator (from X), and it is unlikely that there are signals in the Y data that will correlate with these harmonics. However, if both X and Y are rotated before entering the correlator, there is a reasonable probability that some of the *harmonics of the two rotators* will correlate and produce undesirable spurious correlations. This is

generally not so much a problem for geodetic or continuum VLBI, but can be potentially disastrous for spectral-line VLBI.

One difference between the baseline-based and station-based correlators is that the spatial reference points to which their observations are referred are naturally different. In the case of the baseline-based correlator, observables (i.e. delay, delay-rate, fringe phase) are naturally referenced to the position of one of the stations of the baseline, whereas the station-based-correlator observables are more naturally referenced to a common point such as the center as the Earth. The differences are somewhat subtle and must be taken into proper account during post-correlation data analysis.

The Mark IV correlator uses a station-based XF architecture of the type outlined above. The Mark III and Mark IIIA correlators, which can process only a relatively small number of stations, are built on a baseline-based architecture. The Canadian S2 correlator is of a station-based XF architecture, but uses different algorithms for developing phase rotation and delay correction.

7. Station-Based FX Complex Correlator (Figure 10)

As we discussed earlier, a VLBI correlator can be built to process data in the "XF" fashion (correlation followed by Fourier transform) or "FX" (Fourier transform followed by multiply). Mathematically they are equivalent, but the implementations are obviously different. Figure 10

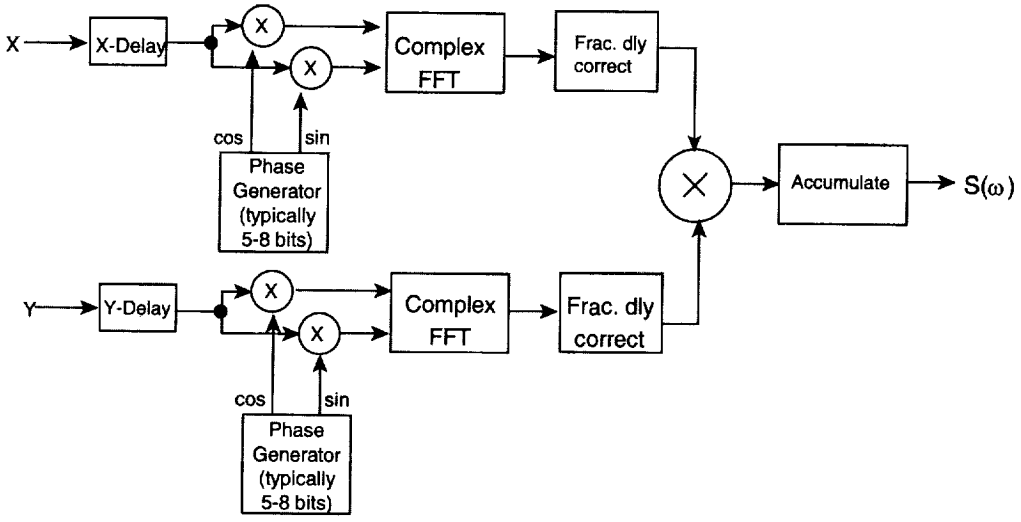

Figure 10. Station-Based FX Complex Correlator

illustrates the basic elements of a station-based FX correlator. One of the attractive features of the FX design is that it is more naturally "station based". A station-based delay is applied to both X and Y in a similar manner to the XF correlator and quadrature rotation is applied to remove the gross station-based fringe rate. Unlike the XF case, however, many bits (typically 5-8) are used in the phase generator to lower SNR losses and reduce harmonic generation. The data from each station are then blocked into fixed-length segments of (typically) 1024 to 8096 samples and each segment is Fourier transformed to obtain the complex station spectra. In order to maintain precision, the output of the Fourier transform is typically 8-12 bits per point. A simple fractional-

delay correction is applied to each station by multiplying the spectra by a linear phase ramp to correct for the quantized delay prior to the Fourier transform. The X and Y complex spectra are then multiplied and accumulated to obtain the complex cross-correlation spectra, $S(\omega)$. $S(\omega)$ itself is the Fourier transform of the lag-based cross-correlation function, $R(\tau)$, so that the mathematical equivalence to the XF correlator is complete.

Several correlators of the FX type have been built (VLBA correlator, for example; VSOP correlator is also FX design). Typically FX correlators have a fixed number of spectral points set by the size of the FFT; the number of spectral points in an XF correlator is set by the number of lags. Typically, XF correlators are designed to be able to trade off number of baselines with number of lags/baseline. The benefits of one type over the other in this regard are not black and white, however. An occasional difficulty of the FX design is that the data rate from the FFT typically exceeds the raw input data rate by a factor of 4 to 8 since so many significant bits must be kept at each transform point; with raw data rates approaching or exceeding 1 Gbps, this expansion in data rate may impose significant engineering or cost challenges.

8. Signal and Noise Vectors (Figure 11)

Figure 11 illustrates the nature of VLBI signals and noise as vectors. This is a useful representation for understanding the nature of VLBI correlation results. The VLBI signal is fundamentally a vector quantity with an amplitude and phase, illustrated as "Signal Vector" in Figure 11. In principle, this signal vector has a phase corresponding to the phase-delay difference between the signals arriving at the two antennas of a baseline at a particular reference time, but in practice for most systems the signal vector for each channel is ambiguous by many 2π rotations. Assuming that data are collected with stable instrumental systems and with a stable atmosphere and ionosphere, this signal vector is essentially constant at the correlator output, but is corrupted by an additive "Noise Vector" as shown in Figure 11. This noise vector has a random phase and an amplitude which is proportional to $\sqrt{1/(BW \cdot T)}$ where BW is the channel bandwidth and T is the observing time. Therefore, the signal-to-noise ratio, SNR, is proportional to $\sqrt{BW \cdot T}$. In the graphical representation of Figure 11, the SNR is roughly the ratio of the lengths of the signal vector to the noise vector. It is also obvious from Figure 11 that the approximate average phase error of the Signal+Noise vector (in radians) is just the ratio of the noise vector to signal vector, which is just 1/SNR.

The actual phase of the signal vector at the correlator output is affected by many things, including the LO phase and the instrumental and ionospheric stability and other unmodelled effects.

9. Single-Band Fringe-Search and Fitting (Figure 12)

Figure 12 illustrates the fringe-search procedure for a single frequency band (single BBC channel). Typically, the correlation data from the correlator is segmented into *accumulation periods* (APs), each of length ΔT ranging from $\sim$ 0.1–5.0 seconds, covering the duration of a scan, T, typically several minutes. In an XF correlator, the lag correlation function for each AP is Fourier transformed to obtain the cross-spectral function, $S(\omega)$, and a "fractional-bit correction" is applied as necessary to compensate for a non-integral number of delay shifts during the AP. Depending on the sideband of the channel, either the positive or negative frequencies of $S(\omega)$ will simply be

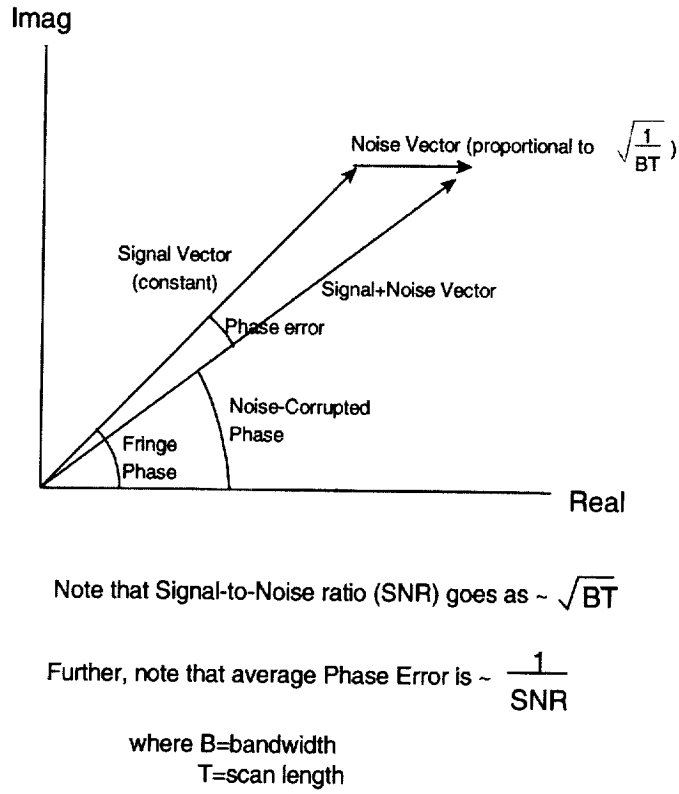

Figure 11. Signal and Noise Vectors

noise and are discarded (set to zero). The resulting cross-spectral function is the same as that which comes directly from an FX correlator, so that XF and FX correlator outputs are equivalent at this point.

For a strong continuum signal, $S(\omega)$will typically appear as shown in Figure 12. Although noisy, the amplitude vs. frequency reflects the passband of the BBC filters (ideally flat), while the phase vs. frequency has a slope which is proportional to the difference between the actual group delay and the model group delay (this difference is called the *residual group delay*) used by the correlator. Note that a wider bandwidth allows a better determination of the phase slope and hence a more precise determination of residual group delay. If both sidebands of a BBC have been correlated and the RF reference frequency for both sidebands is identical (typically the RF sky frequency which is translated to DC in the BBC video output), then the cross-spectral functions of the two sidebands can be combined into a single cross-spectral function spanning both positive and negative frequencies. Since both sidebands share the same LO chain, this combining can be done without respect to any phase calibration. The modified cross-spectral function for each AP is Fourier transformed back to the lag domain to form a complex single-band delay function, $D(\tau)$, as shown in Figure 12. Choosing the value of τ corresponding to the peak of $D(\tau)$ is mathematically equivalent to performing a least-squares fit of a straight line to the phase-slope of $S(\omega)$. The signal

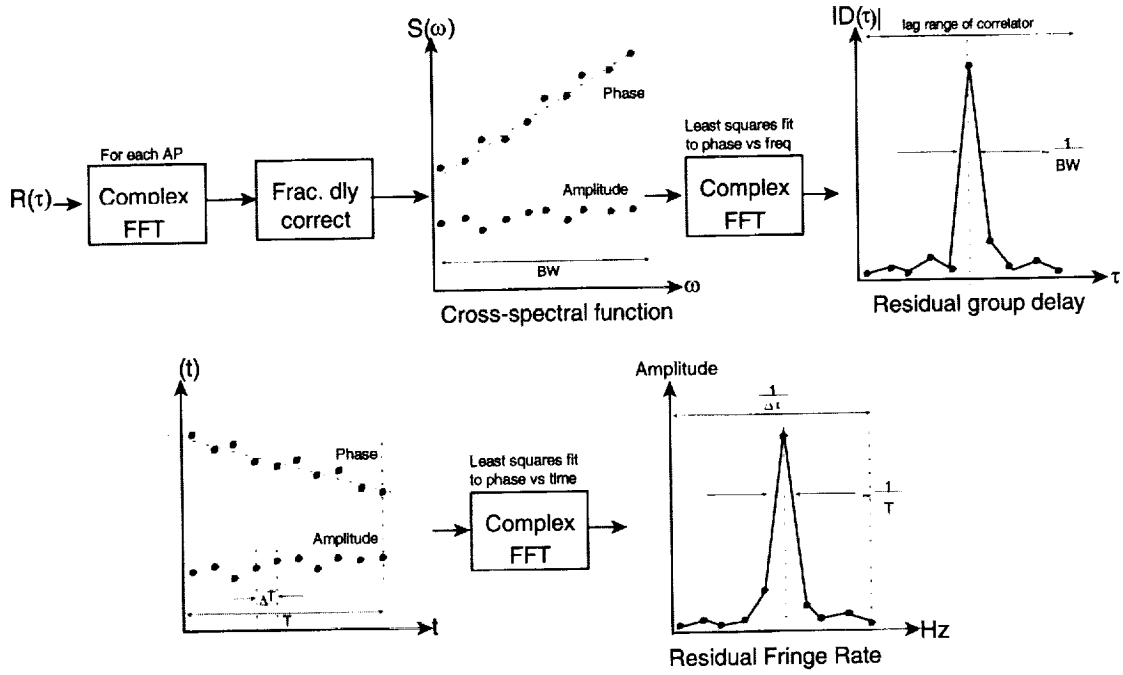

Figure 12. Single-Band Fringe Search and Fitting Procedure

peak of D(τ) has an approximate width of 1/BW, where BW is the bandwidth of the channel represented by S(ω), so that the peak is narrower and better determined for wider bandwidths. Often the cross-spectral function is padded with extra zeroes prior to the Fourier transform in order to increase the resolution of D(τ); this somewhat increases the probably of identifying a weak signal whose actual delay falls in between the coarser lag spacing.

Next, the complex value of D(τ) from each AP for a single trial value of τ is collected into an array, Q(t), which is illustrated for a strong signal case at the lower left of Figure 12. The amplitude vs. time is approximately constant with time while the phase has a slope. The phase slope of this function indicates the difference between the actual signal phase rate and the model phase rate (this difference is called the *residual phase rate* or *residual fringe rate*). Now, a Fourier transform is performed on Q(t) to create a "fringe-rate spectral function". Choosing the value of residual fringe rate corresponding to the peak of the fringe rate spectra is mathematically equivalent to performing a least-squares fit of a straight line to the phase-slope of Q(t). This Fourier transform procedure is done over all APs (i.e. over time) for each lag value in D(τ). The point of highest amplitude point among all these Fourier transforms determines the best estimates of the residual group delay and residual fringe rate.[12] These residuals, when added to the original model, form the best estimates of the total group delay and delay rate (since fringe rate is directly related to delay rate). It is instructive to note a couple of characteristics of the fringe rate spectra as illustrated in Figure 12. The width of the peak of the fringe-rate spectra is $\sim$1/T (Hz), where T is the length of the scan; this implies that a long scan has a better determination of fringe rate, which is true

[12]In practice, some additional work is usually done to iterate to the actual peak, which in the general case does not sit exactly on any of the discrete Fourier transform points.

to the extent that other causes, such as instrumental, atmospheric or ionospheric instabilities, do not significantly corrupt the fringe phase. The total width of the fringe-rate spectra is $1/\Delta T$ (Hz), where ΔT is the AP length; this implies that the fringe rate model used by the correlator must place the residual fringe rate within this window. Furthermore, there are significant SNR losses as the signal moves towards the end of this fringe-search window due to losses within the individual APs.

The single-band fringe-search procedure we have outlined here is not the only procedure that can be used. A more direct procedure is to consider the AP-by-AP cross-spectra as a two dimensional function, S(ω,t), and perform a direct 2-dimensional Fourier transform to find the peak in delay and rate. This is computationally more expensive, but may be acceptable with some modern computers.

10. Multi-Band Delay Determination (Figure 13)

You will recall from the above discussion that a wider channel bandwidth leads to a more precise determination of group delay because it allows a better measure of the slope of the fringe phase vs.

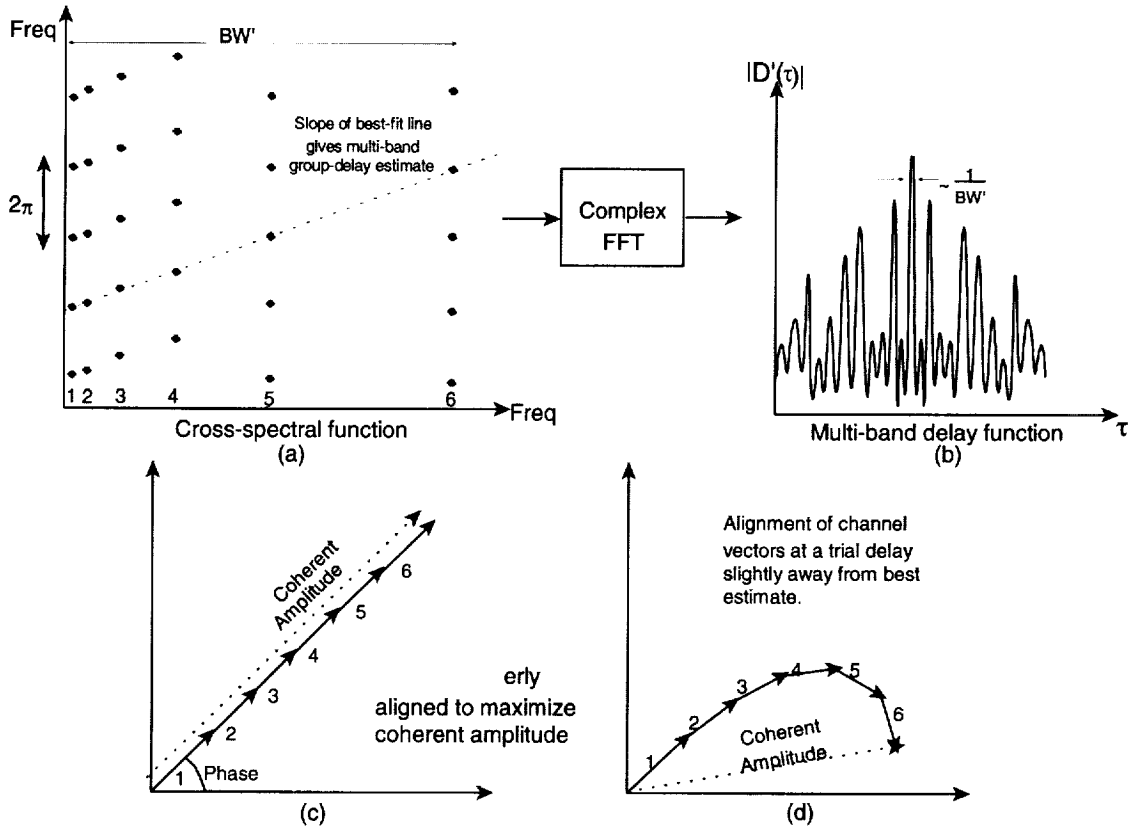

Figure 13. Multi-Band Delay Determination

frequency (which, by definition, is the *group delay).* If VLBI systems could record single-channel bandwidths of a GHz or more, there would be no need for multi-channel delay determination (or

bandwidth synthesis).[13] That not being the case, however, VLBI system designers have devised a method of recording many thin slices of bandwidth *spanning* the total bandwidth of a GHz or so that the precision of the group delay measurement is nearly comparable. Figure 13a illustrates an example of a phase vs. frequency plot for a sample multi-band observation for which all single-band fringes have already been found[14]. In this example, six frequency channels have been observed (labeled 1-6), the individual channel bandwidths being small with respect to the frequency spacing between the channels; the fringe phase for each channel[15] is ambiguous by 2π, as we discussed earlier, so there are a number of possible actual phases for each channel, separated by multiples of 2π as shown in Figure 13a. The group delay estimate is determined simply by finding the slope of the "best fit" straight line through this set of phase points[16]. Again, the Fourier transform is the tool of choice; transforming the multi-band spectral function results in a multi-band delay function, $D(f\tau)$, as illustrated in Figure 13b. Due to the sparse nature of the frequency coverage, the multi-band delay function has many subsidiary peaks in addition to the main peak. The main peak is at the position of the best estimate of the multi-band group delay, while the subsidiary peaks are at delay ambiguities. If a system is not well calibrated by phase-cal tones or if there are other systematic defects in the system, the amplitude of a subsidiary peak may exceed the amplitude of the "proper" peak, resulting in an error in the delay estimate. The placement of the frequency channels within the large band is chosen to have as many different combinations of frequency spacings as possible in order to minimize the problems of *delay ambiguities*. But there is always a tradeoff between the precision of the delay determination and the probability of choosing the wrong peak of the delay function. You will recall that the peak of the single-band delay function is $\sim 1/\mathrm{BW}$, where BW is the channel bandwidth. Correspondingly, the width of the peak of a multi-band delay function, as indicated in Figure 13b, is $\sim 1/\mathrm{BW}f$ where BWf is the total bandwidth spanned by all the channels. For BWf=1 GHz, which is approximately the bandwidth spanned at X-band by many geodetic observations, the width of the peak is $\sim$1 nsec, which corresponds to one full rotation at 1 GHz. For an observation with an SNR$\sim$ 50, the phase error is $\sim 1/50$ radian or $\sim$1 degree, which corresponds to $\sim$3 psec at 1 GHz. 3 psec of light travel time corresponds to a distance of $\sim$1 mm, which illustrates the power of the multi-band delay technique.

Figures 13c and 13d illustrate another way of looking at the multi-band delay estimation procedure. Each channel of the multi-band observation can be considered as a vector, as shown, with the coherent amplitude of the multi-band observation being the vector sum of these channel vectors. The best estimate of multi-band group delay occurs when all the channel vectors are aligned to maximize the vector sum, as shown in Figure 13c. As the trial multi-band group delay changes, each vector rotates at a rate according to its position in the frequency sequence. Consider channel vector 1 to be at the RF reference frequency so that it is essentially fixed. Suppose channel 2 is spaced at 5 MHz, where a full rotation of its vector occurs over 200 nsec, then channel 3 at, say, 20 MHz for a rotation period of 50 nsec, up to channel 6 which is spaced at, say, 1 GHz for a rotation period of 1 nsec. When the trial delay is slightly off the best estimate, the channel vectors

[13] All is not quite so simple, because the effects of the ionosphere and instrumental instabilities, for example, would still complicate matters well beyond what we discussed in single-band delay finding.

[14] Due to space limitations, we will not discuss the procedure for full-sensitivity fringe search procedure in multi-band data using all channels simultaneously.

[15] At this point, the individual channel phases must have been calibrated using the phase-cal tones present in each channel.

[16] This ignores possible effects of frequency-dependent dispersive effects on delay, such as the ionosphere.

might appear as in Figure 13d, with a reduced coherent amplitude as shown. As the trial delay moves away from actual delay, you can see that the vector sum (coherent amplitude) will vary quite rapidly, but will only be maximized at the actual delay.[17]

Of course, life is never quite so simple as we have made it out to be. The ionosphere complicates delay measurements because it is dispersive, meaning that different frequencies travel through it at different velocities. However, the dispersion coefficients can be quite accurately determined by also measuring the group delay at a very different RF frequency, such as S-band. The simultaneous measurements at S-band and X-band allow a sufficient calibration of the ionospheric effects such that they may be removed from the data. For standard geodetic VLBI, the primary group delay measurements come from a very wide X-band observation, while the S-band is present only to calibrate the ionosphere.

For completeness, we should mention a more direct, but much more computationally intensive, method of determining the multi-band group delay estimate. If individual channel cross-spectra for each AP are placed suitably along a RF frequency axis so that the whole of the data lie in a large 2-dimensional array by time and RF frequency, this array may be directly Fourier transformed to obtain the multi-band group delay estimate. In principle, this is straightforward, but in practice, the size of the array is so large that it is computationally impractical. Therefore, other algorithms have been developed, some as illustrated above, to take advantage of the sparse nature of the frequency coverage and significantly improve computation efficiency.

11. Phase-Cal Processing (Figure 14)

In nearly all geodetic VLBI observations, short pulses are injected into the front-end receivers to produce a set of calibration tones that are used to calibrate the LO chain for each of the individual

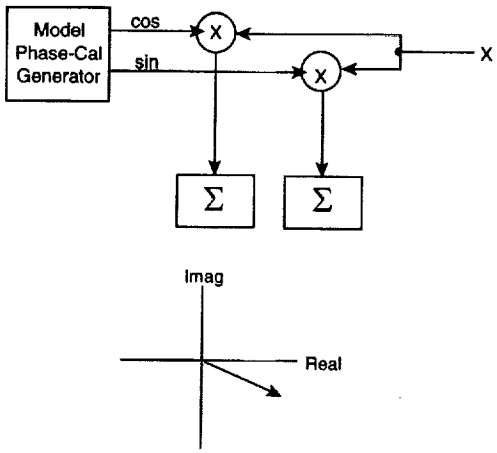

Figure 14. Phase-cal Processing (basically a 1-lag complex correlator)

[17]In the example, if the frequency spacings are all multiples of 5 MHz, the vectors will come into the same alignment every 200 nsec. This is known as the *primary ambiguity* of the delay function, and is chosen to be large enough that *a priori* information is sufficient to choose the proper ambiguity peak.

channels. Typically, the pulses are at a repetition rate of 1 microsecond, which produces a set of tones spaced 1 MHz apart across the entire receiving band. These tones are typically very weak and increase the total power in each channel by no more than a few percent. The BBC LOs are typically set so that these tones appear in the BBC output at a frequency of 10 kHz in upper-sideband channels. There are also tones present at 10 kHz+1 MHz, 10 kHz+2 MHz, etc. In the lower-sideband channels, the tones are then at 990 kHz, 990 kHz+1 MHz, etc.

Traditionally, only the tones in the USB channel at 10 kHz are detected and used to correct the channel phase. Since USB and LSB channels share a common LO chain, it is not necessary to separately calibrate the LSB channels. Some newer correlators are capable of detecting more tones, which has the advantage of better calibration of the phase across the BBC bandpasses.[18] The phase-cal tones can be detected either at the station or at the correlator, and there are several ways that the detection can be done. One simple method to detect a single tone is shown in Figure 14. This is basically a 1-lag complex correlator, where the data signal (X) is correlated against a quadrature model of the expected phase-cal tone, typically a 10 kHz sine/cosine wave. The resulting output is a vector with a phase corresponding to the phase of the tone. If the LO system is not fully stable, this vector may slowly rotate with time, which must also be accounted for in the analysis.

12. Correlator Models and Testing

It is important to understand that a correlator processes data using a computer model that includes the location of the antennas, radio-source positions, clock synchronization, atmospheric thickness, and many other parameters. From this model are generated the model delays, delay rates and phases that the correlator actually uses to process the data. Of course, this model is never quite accurate (if it were, we wouldn't have to make the observations in the first place!), but instead is accurate enough that the differences between the model and reality are small and are within the *search range* of the correlator processing. These differences are called the *residual differences*, or just *residuals*. In our discussions of single-band and multi-band delay determinations, we are dealing with residuals to the computer model and trying to determine the best estimate delay, delay rate and phase of these residuals. Once determined, the residuals are added to the original model parameters to arrive at the *total observables* (delay, rate, phase, etc) that are used in post-correlation analysis. One crucial test of a properly operating correlator system is that the *total observables are invariant to the computer model.* If this is not the case, the answers from a correlator cannot be trusted. Another crucial test is to "reverse" the sense of baselines, so that the stations corresponding to X and Y are reversed. Depending on the reference system used by the correlator software, the total observables may or may not be identical, but in any case they should differ in a predictable way. A third crucial test is that the baseline fringe phases, when all consistently referenced in both space and time, must add to zero around any triangle of baselines for observations of a truly point-like radio-source. If a radio source has significant structure, this phase summation may legitimately be non-zero and, in fact, provides information about the structure of the source. Most sources used for geodetic VLBI are chosen carefully to not exhibit structure on a scale that would cause the delay or phase summation to be non-zero.

[18] Potentially, extraction of multiple phase-calibrations tones within each channel will allow the multi-band group delay to be automatically resolved by a more precise knowledge of the single-band group delay.

13. Conclusion

This short tutorial has attempted to explain how VLBI correlators work in a straightforward and mostly non-mathematical way. As you can see, the concepts are really quite simple. The actual implementation of VLBI correlators, on the other hand, is generally quite complex because of the difficulties of reading and synchronizing tapes, and precisely controlling the data streams as required for accurate processing. This is complicated by the fact that the aggregate data rates from each station are now pushing towards 1 Gbps and beyond, providing further challenges to correlator designers. Of course, the delay, delay-rate and fringe phase results from a VLBI correlator are only the first step in a long series of processing steps required to turn raw VLBI data into baseline vectors, source positions, earth orientation, etc. But hopefully you will now have a better understanding of the first and crucial process of VLBI correlation.

Kerry A. Kingham et al.: Early Experiences with the Mark 4 Correlator, IVS 2000 General Meeting Proceedings, p.206–209
http://ivscc.gsfc.nasa.gov/publications/gm2000/kingham

Early Experiences with the Mark 4 Correlator

Kerry A. Kingham, James O. Martin

U.S. Naval Observatory
Contact author: Kerry A. Kingham, e-mail: kak@CygX3.usno.navy.mil

Abstract

We detail the early operating experiences with the new Mark 4 Correlator at the Washington VLBI Correlator Facility. The emphasis is on the progress of operational efficiency since that area is of concern to the IVS members because of the resulting changes to the observational schedule. During the startup phase, NEOS Intensives were processed with an efficiency matching the previous experience with the Mark IIIA correlator; but the 6-station, 24 hour NEOS experiments took almost three times as long. Later improvements cut the time required for NEOS processing with the Mark 4, but still have not equalled the mature Mark IIIA. A short analysis of the reasons for this, and some suggested improvements are offered.

1. The Washington Correlator Facility

The Washington Correlator Facility began operations in early 1986 with the first Mark IIIA correlator to enter production processing. The primary purpose of the Washington Correlator is to process geodetic/astrometric VLBI observations as efficiently and as quickly as possible, with an emphasis on routine Earth Orientation observations. At the time the facility opened, the typical turn-around time for an EOP observation was on the order of 4 to 6 weeks. The facility reduced that to a few days. In the late 1980s, it was typical for 24-hour, 4-station IRIS-A and NAVNET observations to be completely processed within 3 days of the end of the experiment.

In recent years, the following was typical of the facility's responsibilities:

Earth Orientation Observations:	1 24-hour, 5- or 6-station experiment/week
	5 1-hour, 2-station "Intensives"/week
CORE:	26 CORE-A 24-hour, 6-station experiments/year
	Some CORE-B 24-hour, 9-station experiments
Reference Frame:	Several 5–12 station reference frame experiments/year

The Washington Correlator Facility presently runs 120 hours per week with a staff of 6 operators, 1 tape librarian, 1 manager and 2 technical staff. All experiment preparation, quality control, diagnostics and repairs are done by this staff.

2. Mark 4 History

The Washington Correlator's involvement with the Mark 4 project goes back to 1990 when USNO started funding a "Prototype Next Generation Correlator". With the addition of the VLBI group at Goddard Space Flight Center, this became the "Mark 4 Correlator" by 1993; and with the addition of the Joint Institute for VLBI in Europe (JIVE), the Smithsonian Center for Astrophysics, and the Netherlands Foundation for Research in Astronomy (NFRA) in 1994, it

became the "International Advanced Correlator" project. The primarily geodetic VLBI correlators at Haystack and Washington, and the MPIfR/Bonn correlator continue to be called "Mark 4".

Due to requirements placed on the Washington Correlator Facility to verify Y2K compliance, the first hardware, a combination of prototype and production units, was delivered in June, 1999. Once the "Y2K test" was completed, the prototype units were removed and the Mark 4 was idle until December, 1999 when the full production correlator was assembled. In mid-December, two-correlator tests were begun, comparing the results of experiments processed on both the Mark IIIA and the Mark 4 correlators. Since these tests are reported on elsewhere in this volume, we will concentrate on describing the experience with operational processing.

In the second week of January, 2000, full production processing was initiated, starting with the NEOS Intensives. The first Intensive completed by the Mark 4 correlator was submitted to the IERS on January 13, 2000. By the end of the month, the Intensive processing was up to date. The 24-hour NEOS experiments were a different story. The Mark 4 correlator was running in "6 X 8" mode, which means 6-stations with 8 frequency channels. This required two passes for a 14 channel experiment (there was also a "2 X 16" mode, which allowed the Intensives to be processed in one pass). Unlike the one pass Intensive processing, which was operating at close to Mark IIIA efficiency, the NEOS experiments were being done with a processing factor (PF) of 6.5; that is, it was taking 6.5 times as long to correlate as it did to observe. This was three times as long as the Mark IIIA, which had an average PF of 2.3. Even worse, it was taking 157 hours to process a 24-hour NEOS and the Washington Correlator was operating only 120 hours per week. Since the NEOS experiments are weekly, the correlator was falling behind observations.

It was this situation that led to a cut-back in the observing schedule while the Mark 4 correlators were undergoing their initial startup period. Fortunately, on February 10, a software upgrade allowed "6 X 16" processing (6-station with 16 frequency channels). This reduced the processing factor for NEOS experiments to 3.5, and, at least, allowed the Mark 4 correlators to keep up with the weekly observations.

3. Operational Capabilities

At the time of the IVS General Meeting, the Mark 4 correlator at the Washington Correlator Facility was processing 6-station NEOS 24-hour experiments and 2-station 1-hour NEOS Intensives. Some CORE A processing was also being done. A review of the operations indicated a few areas of poor efficiency, even allowing for start-up problems. As a result of the review, we expect a PF of 3 for the NEOS and CORE processing and a PF of 1.1 for the Intensives.

	Weekly Loading	
NEOS	PF = 3	72 hrs.
Intensives	PF = 1.1	5.5 hrs.
Total		77.5 hrs.
CORE-A	120−77.5 =	42.5 hrs

4. Suggested Improvements

Several areas of correlator operations require improvements if, in the near term, Mark IIIA-type efficiencies are to be realized. Most of these are software and possibly firmware changes. Some are procedural.

Operator Training The operator interaction with the Mark 4 is quite different than that of the Mark IIIA. Also, with a less mature system, more operator interaction is required. Both of these areas have caused difficulties for all or some of our operators. There is now enough experience with the Mark 4 to identify places where operator training is indicated.

Pass Finding One big difference between the Mark IIIA and the Mark 4 is the present state of finding the proper pass on a narrow-track tape. The Mark IIIA has an automatic pass-finding algorithm developed and refined over 12 years. It is a parallel process (all drives at once) and very effective. The Mark 4 has no automatic system, requiring operators to align the passes manually. Operators do this one drive at a time, a serial process. This requires much more time, and, in our experience, is slightly less reliable than the automated Mark IIIA.

SU Delays The Mark 4 Station Units are also slow at present. They cannot handle commands spaced too closely together, and they delay before sending commands to the tape drives. This can lead to long "wait states" where nothing is going on. These periods add up over hundreds of scans to cause several hours of delays in a 24-hour experiment. Cutting the delays would speed things up considerably.

Near Realtime Diagnostics Unlike the mature Mark IIIA, the Mark 4 does not provide near–realtime processing diagnostics. With such a system, operators can catch problems shortly after they occur and implement fixes. Reprocessing can be scheduled "on-the-fly" saving time. With the present Mark 4, reprocessing requirements often don't appear until after the first pass through an experiment. With the Mark 4 problems listed above, this can be very inefficient.

5. Long Term Outlook

Several expected improvements over the next 12 months should lead to improvements in both processing quality and efficiency. Some highlights:

Phase Cal At present the Mark 4 is not extracting the phase cal tones. This is expected to change by April, 2000.

Increased Playback Speed Speeding up playback rates by 2 or (eventually) 4, will allow a "speed up" factor in processing. While this won't give as great an increase in efficiency as the "speed up" might indicate, it will reduce the PF for all experiments.

Mark 4 Modes The implementation of Mark 4 recording modes will allow wider bandwidth observations and a potential for reducing lost data. This should allow more creative observations and less reprocessing.

Additional Playbacks The Washington Correlator expects to increase the number of playbacks from six to eight by the end of the calendar year. Since the Mark 4 Correlator has 8 station capability (with 16 stations being possible with some additional hardware as is done at JIVE),

this will allow more stations to observe in an experiment without increasing the processing time. With the Mark 4 "multiple streams" it will also allow smaller experiments to be processed in parallel, which will pack more processing into the available time.

6. Final Thoughts

The Mark IIIA correlator took almost two years to reach its full potential. In 1987, with the advent of narrow-track recording, processing was even worse than with the present Mark 4. Additionally, we know how we fixed the problems in 1987, some of which we're reprising now (such as pass-finding). The improvements in Mark 4 operations, from the initial attempts in January, 2000 to the situation at the time of the IVS General Meeting in February, are cause for cautious optimism. It is entirely within reason to expect Mark IIIA efficiencies in the next few months. Additional capabilities after that will improve the situation even more.

W. Alef et al.: The Bonn MK IV Correlator Project, IVS 2000 General Meeting Proceedings, p.210–214
http://ivscc.gsfc.nasa.gov/publications/gm2000/alef

The Bonn MK IV Correlator Project

W. Alef [1], *D. A. Graham* [1], *J. A. Zensus* [1], *A. Müskens* [2], *W. Schlüter* [3]

[1)] *Max-Planck-Institut für Radioastronomie*
[2)] *Geodätisches Institut, Universität Bonn*
[3)] *Bundesamt für Kartographie und Geodäsie*
Contact author: W. Alef, e-mail: walef@mpifr-bonn.mpg.de

Abstract

We describe the present status of the VLBI correlator in Bonn. The old MK III correlator has been made Y2K compliant, but it is expected to be taken out of operation this year. We report our first experience with the new MK IV correlator, jointly operated by the MPIfR and the BKG, as well as our short-term and long-term plans, both with respect to astronomical and geodetic requirements.

1. Introduction

Participation in astronomically motivated VLBI activities at the Max-Planck-Institute for Radioastronomy (MPIfR) dates back to the early seventies. The first VLBI processor — a copy of NRAO's 3-baseline MK II correlator — was installed at the institute in 1978. Already in 1979, the first geodetic observation was correlated under the direction of the Geodetic Institute of the University of Bonn. In 1980 routine correlation for the European VLBI Network (EVN) began. The MK II correlator was taken out of operation in 1992.

In 1982 a MK III correlator was acquired from Haystack Observatory; geodetic correlation switched to the MK III system in Bonn in 1983. The first correlation of the IRIS series was performed in Bonn in 1984. The MK III correlator remained operational until summer 1999.

In 1989 a copy of Haystack's MK IIIA correlator became operational with a capacity of up to 12 baselines. It had been implemented at MPI with the "multi-wire" technique. It will probably be taken out of operation in mid-2000. The first of the geodetic EUROPE observation series was correlated in 1990, the first O'Higgins observation in 1995. At about the same time the load of EVN correlation increased substantially due to the introduction of the narrow track recording capability in the EVN.

In 1991 the Institut für angewandte Geodäsie (IfAG; now BKG) agreed with MPI to jointly acquire and operate a MK IV correlator. It was installed by Haystack at MPIfR in December 1999. (Figures 1 and 2 show the present setup at Bonn)

2. Present Status

2.1. MK IIIA Correlator

The MK IIIA correlator was made Y2K compliant in January 2000. The required changes in the software were fairly limited. They would allow us to run the MK IIIA correlator for another two to three years. The first geodetic observation from 2000 — IRIS 146 — was successfully

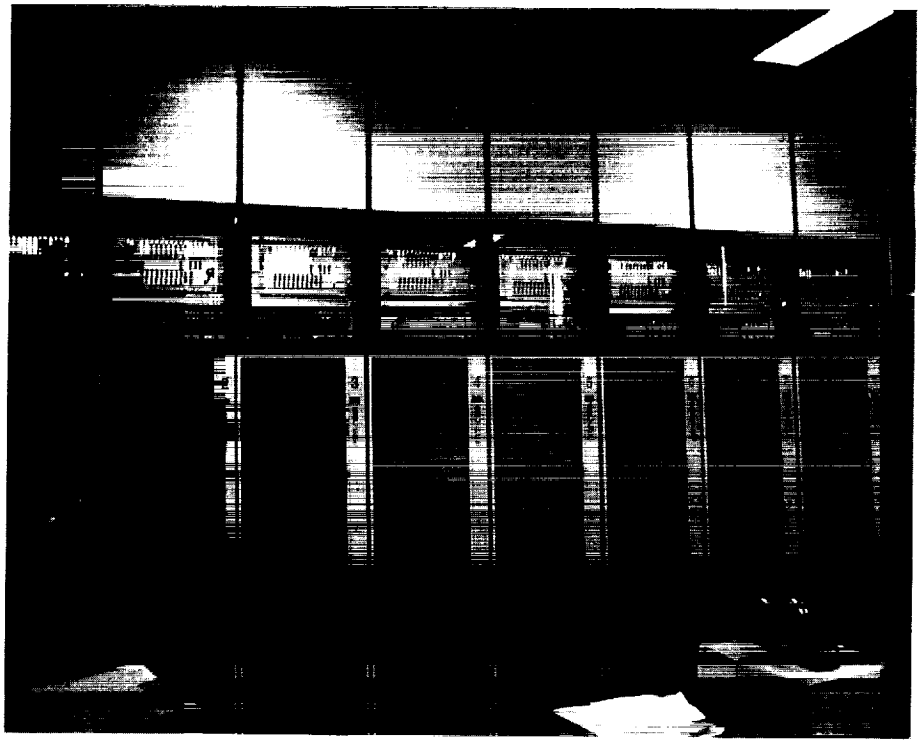

Figure 1. Eight of the nine correlator tape drives with new station units on top.

processed and read into CALC/SOLVE. This correlator is operated with up to seven simultaneous tape drives and up to 12 or 6 baselines, depending on the recording bandwidth.

We expect to operate the MK IIIA correlator at least up to the middle of 2000.

2.2. MK IV Correlator

In December 1999 a MK IV correlator was received from Haystack. It is the same correlator configuration with two crates and 16 correlator boards as had been installed at USNO shortly before. The Bonn version is connected to nine tape drives and station units. The tape drives can be switched between both correlators easily and in a short amount of time.

The initial operation was restricted by the available software to four simultaneous tape units and six baselines. Only mode C single-polarization had been available initially as a tested mode of operation.

As might be expected, the software is currently in an early pre-production stage of development, with a number of unimplemented features which reduce the productivity well below that available with the MK III correlator. In addition, hardware problems — mostly in the station units — further reduce the throughput.

The operator interface is much more user friendly and easier to master than that of the MK III correlator. The productivity is increasing. The ease with which, e.g., the correlation of mode B was achieved is encouraging (see below).

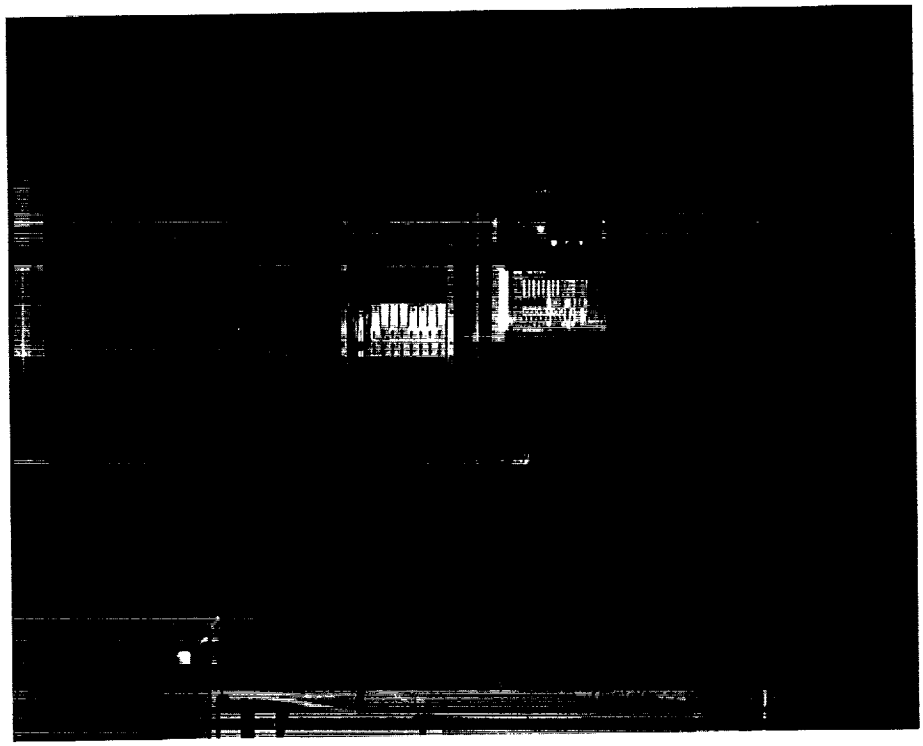

Figure 2. Opposite side of the correlator room shows from left to right two racks with the old MK IIIA correlator, one rack with the MK IV correlator, one station unit and the 9th tape unit.

2.2.1. Astronomical Test Correlation

For a first test we repeated the correlation of a so-called EVN network monitoring observation, which had been recorded at 10 EVN stations in September 1999 at 1.6 GHz in MK III mode A with dual polarization. Owing to the restriction of the MK IV correlator to 16 output channels, we correlated only one polarization which is then equivalent to a mode B recording with 14 channels. The correlation was done in several passes for 9 of the 10 stations.

After one of us had fixed a small bug in MK4FIT the data was fringe-fitted successfully, and thus we could verify that the MK IV correlator can also process MK III mode B (a double-sideband mode) (see figure 3).

For a more complete astronomical comparison of the results of both correlators, we exported the data with "alist" to A-file format, calibrated the amplitudes with the system temperatures and efficiencies of the antennas, changed the A-file format to the older MK III format, and translated this to FITS with Haystack's "atofits" program. The data was them mapped with Caltech's "difmap" program.

Unfortunately, several stations performed very badly in this experiment which resulted in very large noise in the data. This had not been taken into account when the observation was selected for this test, so that the quality of the resulting map is very bad, but it agrees with the map derived from the original MK III correlation.

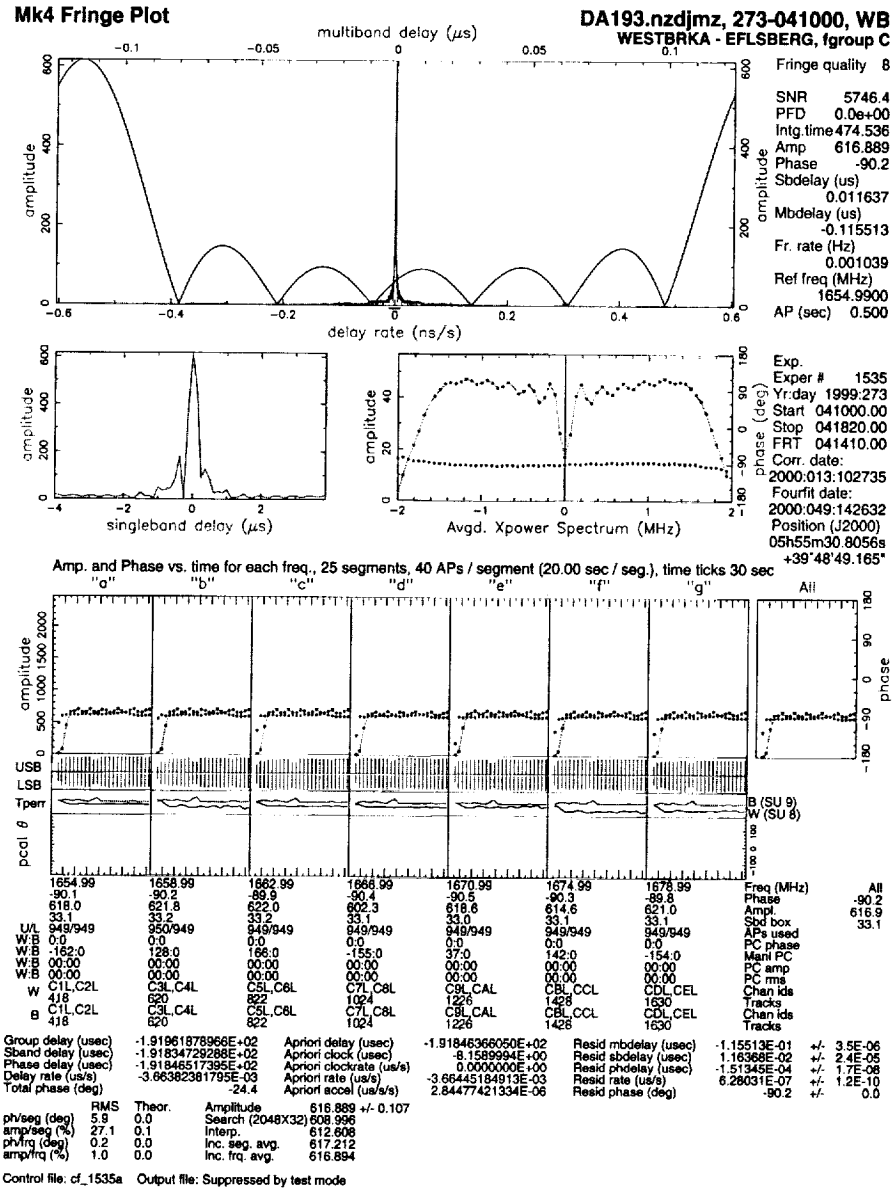

Figure 3. MK4FIT plot of a MK III mode B correlation. The usage of upper and lower sideband is visible in the plot of the averaged cross-spectrum ("Xpower").

2.2.2. First Geodetic Correlation

A new version of the correlator software allowing six simultaneous tape drives with 14 baselines was installed on February 11. Subsequently IRIS 146 observed on the 10th of January was partly correlated. Due to lack of time, a full comparison of this data with the data processed on the MK IIIA correlator could not be finished in time for the IVS meeting. One baseline though, correlated on the same tape drives with both correlators, was compared in detail and a high level

of agreement was found. It is planned to perform a full comparison when phase-cal extraction becomes available on the MK IV correlator.

3. Future Outlook

Of immediate importance to the astronomical community is an interface for data from the MK IV correlator to NRAO's AIPS software. It is planned to write such a program this year in collaboration with Haystack.

Astronomical phase-referencing observations could be improved by adding actual ionosphere and atmosphere corrections as measured with GPS receivers to the correlator model. We are actively pursuing such a program.

Stock taking of the available documentation and research of available test hard- and software both at Haystack and JIVE are the main objectives for our support personnel. Progress in these areas is absolutely essential for reliable correlator operations.

In the course of the next few months we expect that more correlation modes will be implemented and tested in collaboration with Haystack Observatory. The most important additional features which a MK IV system has to have are: fan in/out modes, fringe search capability, phase-cal extraction, spectral line modes, polarization correlation (seems to work already except for fringe fitting), VLBA modes, barrel roll, correlation with up to nine tape drives, double speed correlation, and later the ability to correlate dual head recordings with playback units which have only one read head.

We plan to use the MK IV correlator for processing geodetic experiments and for cutting-edge astronomical observations. The bulk of routine EVN correlation is expected to shift to JIVE in the course of 2000.

Session 7.

Analysis Part 1

A. Nothnagel: Report of the IVS Analysis Coordinator, IVS 2000 General Meeting Proceedings, p.217–218
http://ivscc.gsfc.nasa.gov/publications/gm2000/nothnagel3

Report of the IVS Analysis Coordinator

A. Nothnagel

Geodetic Institute of the University of Bonn
e-mail: nothnagel@uni-bonn.de

Abstract

On October 1, 1999, the author took over the tasks of the IVS Analysis Coordinator. On the basis of the preparations made by the Acting Analysis Coordinators a number of topics were addressed in the first five months. Regular submissions of the Analysis Centers are being received and have to be monitored. First comparisons are available and can be checked by the users on a special Analysis Coordinator web site. The first IVS Analysis Workshop took place at Kötzting, Germany, on February 24, 2000.

1. Introduction

In the absence of a formal proposal for an Analysis Coordinator at the inauguration of the IVS on March 1, 1999 the function of the Coordinator was provisonally carried out by a team of Acting Analysis Coordinators. T. Marshall Eubanks (US Naval Observatory), Chopo Ma (NASA Goddard Space Flight Center) and Nancy R. Vandenberg (NVI/GSFC) established the first procedures for the service functions of the IVS (EUBANKS et al. 1999).

At the second IVS Directing Board Meeting in conjunction with the Birmingham IUGG General Assembly in July 1999 a proposal of the Geodetic Institute of the University of Bonn to commit personnel and resources to the function of the IVS Analysis Coordinator was accepted. From October 1, 1999 the author has taken over the responsibilities of the IVS Analysis Coordinator.

The Acting Coordinators had already prepared the basic structure of IVS data analysis and data storage with great success. In addition, a number of activities were brought on the way which facilitated the start of the current Analysis Coordinator very much. We greatly appreciate all their efforts and achievements.

2. IVS Data Analysis and Data Storage Components

As set forth in the IVS Terms of Reference "*the IVS Analysis Coordinator is responsible for coordinating the analysis activities of the IVS and for stimulating VLBI product development and delivery*". In the framework of the IVS, the Data Centers play a central role since all data and products are kept up to date at the Data Centers. In terms of data flow all interaction between Operation Centers, Analysis Centers and the group of users is maintained by the Data Centers. Three data centers have taken up the responsibilities of primary data centers:

- Bundesamt für Kartographie und Geodäsie, Leipzig, Germany
- Observatoire de Paris, Paris, France
- NASA Goddard Space Flight Center, Greenbelt MD, USA

The Operation Centers submit their data to the nearest Data Center which in turn mirrors their contents at six hour intervals. The Analysis Centers then retrieve the data from their Data Center of choice and submit their products after the analysis. Three more IVS Data Centers concentrate on the data storage of regional VLBI campaigns.

To date 19 analysis centers have proposed to IVS to take over analysis functions within the IVS framework. In a response to a comprehensive analysis solicitation carried out by the Acting Analysis Coordinators eight centers envisaged to regularly produce and submit to IVS one or more VLBI products.

So far four of the IVS Analysis Centers regularly submit EOP results to the IVS data centers. These products are compared routinely and the comparison results are accessible via Internet in numerical and graphical form (Analysis Coordinator's page on IVS home page). Although the methods of comparison are still fairly rudimentary their results provide some valuable insight already. One aspect which has to be taken care of in particular is the handling of sessions which were observed simultaneously. Since these sessions produce EOP results which are biased (MACMILLAN AND MA, this volume) special care has to be taken that only results of the same sessions are compared.

The transition to the Mark IV Correlator has inevitably led to some loss in productivity. However, as more components of the correlator software become available, the overall capacity will increase considerably. Nevertheless, the data and product flow has to be monitored in order to guarantee smooth operation and a timely delivery of the results.

3. Plans

During the first IVS Analysis Workshop at Kötzting on February 24, 2000, a number of organisational and scientific topics were discussed (NOTHNAGEL, this volume). Five IVS Analysis Working Groups were established which will work on specific topics and will report on their initial activities by June 30, 2000.

The Analysis Centers are encouraged to streamline their operations so that the data flow and product delivery for all sessions can be optimized. Special emphasis will be given to an optimized distribution of tasks especially within the Associate Analysis Centers.

The refinement of the comparisons will consequently lead to a solid basis for combinations. For the time being these activities will be pursued primarily at the Analysis Coordinator's office. However, other IVS Analysis Centers are very welcome to join these combination activities. Additional combination centers would help to provide another level of quality control and redundancy.

4. References

Eubanks T.M., C. Ma, N. Vandenberg (1999): *Analysis Coordinator Report*, IVS 1999 Annual Report, NASA Publication TP-1999-209243, 27–28.

MacMillan D.S., C. Ma (2000): *Improvement of VLBI EOP Accuracy and Precision.* Proc. of the First IVS General Meeting, this volume.

Nothnagel A. (2000): *Excerpts from the first IVS Analysis Workshop* Proc. of the First IVS General Meeting, this volume.

Harald Schuh: Geodetic Analysis Overview, IVS 2000 General Meeting Proceedings, p.219–229
http://ivscc.gsfc.nasa.gov/publications/gm2000/schuh1

Geodetic Analysis Overview

Harald Schuh

Institut für Geodäsie und Geophysik, Techn. Univ. Wien
e-mail: hschuh@luna.tuwien.ac.at

Abstract

For the VLBI data analysis the best presently available knowledge is used to mathematically recreate, as closely as possible, the situation at the time of observation. The goal is to determine precise values of the parameters geodesists, geophysicists and astronomers are interested in, e.g. baseline components, radio source positions or Earth orientation parameters. A general overview about data analysis of geodetic/astrometric VLBI experiments is given. The procedure of data analysis is explained and the geophysical, environmental and instrumental effects which have to be taken into account are presented. A sample of the most interesting results is presented.

1. Introduction

The geodetic and geophysical interest in VLBI is based on the use of an inertial reference frame formed by a given set of extremely compact extragalactic radio sources. VLBI measures very accurately the angles between the Earth-fixed baseline vectors and the space-fixed radio sources. Thus, even the most subtle changes in the baseline lengths and in the angles between the reference systems can be detected. The main geodynamical phenomena such as polar motion, UT1 variations, nutation and precession, Earth tides, ocean tidal response, and tectonic plate motions can be monitored with unprecedented accuracy.

The research fields that profit most from the geometric potential of VLBI are those dealing with the motions of the celestial bodies, in particular the Earth-Moon system, and the orientation and the size of the Earth itself: astrometry and geodesy. These fields are usually meant to imply a much broader area, namely fundamental astronomy and geosciences, such as geophysics, meteorology and oceanography. The topic of gravitational light deflection is also intimately related to all of these fields, because it forms part of the fundamental space-time model describing the physical reality of VLBI. A comprehensive overview about the fundamentals of geodetic/astronomic VLBI is given by Schuh and Campbell (1994).

2. Analysis of High Precision Interferometry Observations

The term high precision interferometry is used here to include all those applications of VLBI that rely on the exploitation of the group delay observable τ. It is this quantity which allows to determine the "macroscopic" geometry of the interferometer, i.e. the baseline-source geometry that relates the location of the radio telescopes on the revolving Earth to the infinitely distant compact radio sources. These pointlike emitters without proper motion are ideally suited to serve as fixed beacons in the heavens, allowing to monitor even the smallest departures from the computed motions of the receiving stations.

The VLBI data analysis model is developed using the best presently available knowledge to mathematically recreate, as closely as possible, the situation at the time of observation. Then either

a least-squares parameter estimation algorithm, a Kalman filter or other estimation methods are used to determine the best values of the quantities to be solved for. Before this process starts, the raw observations have to be cleaned from several systematic effects, which in fact limit the final accuracy of the results. The flow diagram of a geodetic VLBI data analysis is shown in Figure 1.

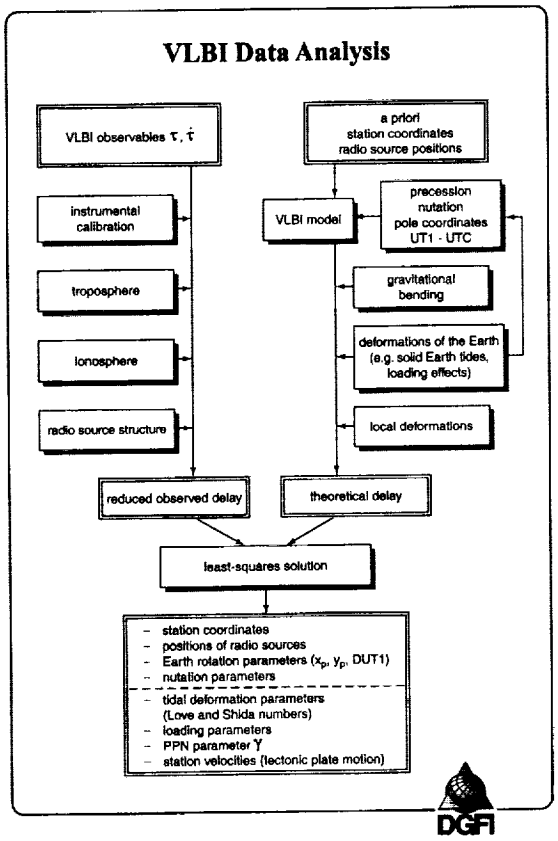

Figure 1. Flow diagram of a geodetic VLBI data analysis.

The system can be seen to have two main streams, one containing the actual observations which undergo instrumental and environmental corrections, and the other to produce the "theoreticals", beginning with the "a-prioris", a set of starting values for the parameters of the VLBI model. Both streams converge at the entrance to the parameter estimation algorithm, e.g. the least-squares fit, where the "observed minus computed" are formed. The instrumental effects include systematic clock instabilities, electronic delays in cables and circuitry and the group delay ambiguities. The latter are due to observation by a multichannel frequency setup covering the total spanned bandwidth around the X-band frequency of 8.4 GHz and the S-band frequency of 2.3 GHz. The group delay ambiguities can be made visible (see Figure 2) and removed by the analyst when for a first solution only the group delay rates $\dot{\tau}$ are used but the group delay residuals are plotted, too. As the group delay ambiguity spacing is well-known, e.g. 50 nsec, 100 nsec or 200 nsec, the analyst can select one level on which all residuals – and thus the corresponding group delay observables – are shifted. Care has to be taken that the group delay closure within each triangle of the multistation VLBI network is zero.

The instrumental delay changes are monitored by the phase and delay calibration system which is part of the MkIII system and the MkIV system. Figure 3 shows the cable calibration data recorded and entered into the station log file at the station Fortaleza, Brasil. At the beginning and the end of the VLBI session the cable sign check readings are done that allow the determination of the sign which is needed when applying the cable calibration correction to the observables. It happens frequently that the station log files contain wrong entries (outliers, offsets, gaps, ...) which have to be edited manually by the analyst.

At the telescope the distance between the feed horn and the axis intersection, which constitutes the baseline reference point, is assumed to be constant at the mm level. In this case it becomes part of the clock offset parameter which will be described later in this section. An axis offset model is applied to each antenna where the pointing axes do not intersect. Large telescopes such as the Effelsberg 100-m antenna exhibit elevation dependent changes in the focal distance which can however be modeled to a level of a few millimeters (Rius et al., 1987).

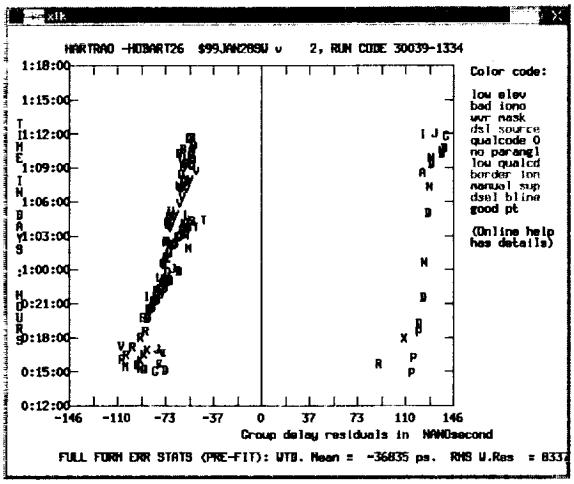

Figure 2. Group delay residuals of a first "delay rate only" solution spaced by the group delay ambiguities of 200 nsec (S-band, standard MkIII frequency setup).

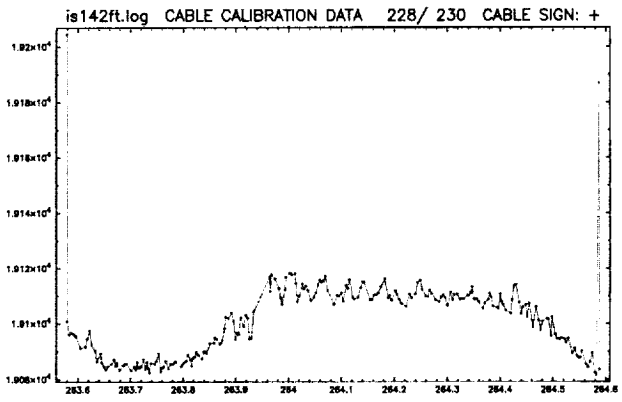

Figure 3. Cable calibration data recorded at Fortaleza, Brasil, with cable sign check readings at the beginning and the end of the session.

The effect of the atmosphere on VLBI observations is still considered to be the most serious problem, because at widely separated stations the elevation angles of the telescopes pointing to the same source differ greatly as well as the meteorological conditions themselves. The neutral atmosphere, essentially the troposphere, presents similar problems in VLBI as in GPS observations. Its influence on radio signals adds up to an extra zenith path of 1.8 to 2.5 meters. The contribution of the dry part is rather stable, although special care has to be taken to choose a proper mapping function (Davis, 1985; Niell, 1996) for the elevation angles lower than 20°. The wet component, although the smaller part of the total tropospheric effect, changes rapidly and can also be monitored by some means. The most promising – albeit costly – method appears to be the water vapor radiometer (WVR) technique, which consists of measuring the microwave thermal emission from water vapor near 22 GHz in the line-of-sight (Elgered et al., 1982; Emardson et al., 1999).

The ionosphere, which is a highly dispersive medium in the radio frequency band, can be dealt with to first order by using two different observing frequencies. In geodetic VLBI the frequency pair of $f_S = 2.3$ GHz (S-band) and $f_X = 8.4$ GHz (X-band) is used throughout. The ionospheric group delay corrections for the X-band observations are computed from the differences of group delay measurements at X-band and S-band:

$$\Delta\tau_x^{ion} = (\tau_x - \tau_s) f_s^2 / (f_x^2 - f_s^2) \tag{1}$$

In contrast to GPS, where a very close frequency pair has been chosen, in VLBI the factor to convert the difference into a correction for the higher band is very small: 0.081, so that there is no appreciable error contribution from the S-band observations.

A major problem is constituted by the fact that most of the observed "compact" radio sources tend to show structure at the level of a few mas. These effects, in particular the changes in the structure, pose a limit on the accuracy of the radio reference frame. Permanent monitoring of

the structure, which is also accomplished by analysing VLBI data, can be done in parallel to the geodetic analysis, thus providing a means to correct for the structure effects (Schalinski et al., 1988; Campbell et al., 1988; Charlot, 1993; Zeppenfeld, 1993; Charlot and Fey, 1999).

Now let us turn to the model side of the geodetic VLBI analysis. The geometric time delay of signals arriving at the two radio telescopes is to first order a function of the baseline vector $\boldsymbol{b}$ between the two telescopes and of the unit vector $\boldsymbol{k}$ in the direction of the radio source:

$$\tau(t) = -\,\boldsymbol{b}' \cdot \boldsymbol{k}(t)/c \tag{2}$$

where

$$\boldsymbol{b}' \cdot \boldsymbol{k}(t) = b_x \cos\delta \cos h(t) + b_y \cos\delta \sin h(t) + b_z sin\delta \quad , \tag{3}$$

with the geocentric baseline components b_x, b_y, b_z, the radio source positions α, δ and the Greenwich hour angle $h(t)$ of the source $h(t) = GST - \alpha$ (GST - Greenwich sidereal time). The negative sign reflects the conventions used in defining τ and $\boldsymbol{b}$. c is the velocity of light.

The fundamental geometric model of the time delay τ_g forms the heart of the system. This model has evolved from its basic form in a geocentric system [equation (2)] to the fairly complex relativistic formulation referred to the solar system barycenter (SSB). Initially the basic model of equation (2) was extended by the so-called retarded baseline effect, which accounts for the finite travel time of the signals between reception at the two telescopes on the revolving Earth. In spherical astronomy this effect is known as diurnal aberration and in fact it turns out that to first order the application of the retarded baseline effect is equivalent to correcting the source vector $\boldsymbol{k}$ at station 2 for diurnal aberration.

The relativistic formulation includes both the effects of special relativity (SRT) and of general relativity (GRT), but for reasons of practicality these are treated separately and added together on the level of the time delay (Preuss and Campbell, 1992; Schuh and Campbell, 1994):

$$\tau_g = \tau(SRT) + \tau(GRT) \tag{4}$$

The effects of special relativity to compute $\tau(SRT)$ arise from the fact that quantities defined in coordinate frames moving relative to each other have to be related by transformations of the Lorentz type with v/c^2 as the characteristic quantity in the time delay correction terms. The choice of two particular coordinate systems (the celestial system referred to the SSB and the terrestrial system referred to the geocenter) used to describe the VLBI model arises from practical considerations: the motions of bodies in the solar system and the positions of the radio sources are most readily defined in a celestial system, while the actual baselines between the telescopes are usually required in a terrestrial system. The velocity of the geocenter with respect to the SSB ($\sim$ 30 km/sec) and the velocity of station 2 with respect to the geocenter ($<$ 0.46 km/sec) are entered. In the geometric VLBI model these velocities have to be computed with an accuracy of better than 10^{-6}. The equation for $\tau(SRT)$ accounts also for the difference in SSB coordinate time and the geocentric proper time as well as for the fact that the station clocks are located at fixed points on the Earth's crust. In Oct. 1990 a workshop was held at U.S. Naval Observatory to bring the VLBI model builders (mostly theoretical relativists) and the model users (mostly geodesists with little experience in relativity) together. As an output of this workshop a so-called *consensus model* to guarantee picosecond delay accuracy was obtained for the geodetic VLBI observables (Eubanks (ed.), 1991).

The effect of gravity on the propagation of electromagnetic waves (GRT) is no less important. According to GRT, space-time is deformed by the presence of masses. $\tau(GRT)$ is computed as a sum of the influences of all gravitating bodies which are close to the signal path in particular the Sun and the Earth itself. Thus, the Schwarzschild radii of the Sun and the Earth are needed and the vectors from these bodies to the VLBI antennas. The most massive object in our vicinity is of course the Sun, which accounts for more than 99% of the total effect. Even at an angle of 90° away from the Sun the differential delay effect (GRT) for a 6000 km baseline is still 0.56 nsec (Table 1). For the other bodies of the solar system the corresponding Schwarzschild radii have to be used, if necessary, i.e. if the radiation from the observed radio source passes close to that body. At the present level of accuracy of VLBI the major planets also contribute a bending effect which cannot be entirely neglected. If Jupiter arrives within less than 1° of an observed source, its influence on ray bending has to be taken into account as can be seen from Table 1. Another small but significant contribution (< 20 psec) comes from the gravity field of the Earth itself. If neglected, this effect shows up as a scaling error in the geodetic results.

Θ (Sun) [°]	τ^s_{grav} [ns]	Θ (Jupiter)[°]	τ^J_{grav} [ns]
0.267	169.52	Rim	1.582
1	45.30	0.017 (≙ 1')	0.605
5	9.06	0.167 (≙ 10')	0.062
10	4.54	0.5	0.021
30	1.53	1	0.010
60	0.79	5	0.002
90	0.56	10	0.001
120	0.46		
150	0.41		
180	0.40		

Table 1: Gravitational path delay as a function of spherical distance from the Sun and Jupiter. Given are maximum values for a 6000 km baseline (Schuh, 1987).

As already mentioned above the baseline vector $\boldsymbol{b}$ is normally expressed in a terrestrial three-dimensional cartesian coordinate frame defined by a number of VLBI radio telescopes, while the radio source positions are given in a quasi-inertial celestial reference frame in space. In order to express $\boldsymbol{b}$ and $\boldsymbol{k}$ in the same coordinate system, several transformations are necessary. These can be applied to either vector. Equation (2) can be written as:

$$\tau = -\frac{1}{c}\, \boldsymbol{b}'\mathbf{WSNP}\, \boldsymbol{k} \tag{5}$$

where $\boldsymbol{W}$ is the rotation matrix for polar motion (wobble), $\boldsymbol{S}$ is the diurnal spin matrix, $\boldsymbol{N}$ is the nutation matrix and $\boldsymbol{P}$ is the precession matrix.

The description of the Earth's orientation with respect to the celestial system (precession, nutation), the motion of the Earth's axis with respect to the crust (polar motion) and the phase angle of the Earth's rotation (expressed by UT1-UTC) have to reach the same level of accuracy as all the other model components, which means roughly 0.0001 arcsec (0.1 milliarcsecond). Models are used to calculate a priori the periodic variations of the Earth rotation parameters (ERPs) due

to the Earth tides (e.g. Yoder et al., 1972; Tamura, 1993) and due to the ocean tides (e.g. Brosche et al., 1989; Wünsch and Seiler, 1992; Ray et al., 1994).

The parameters in equation (5) or combinations of parameters can be determined from VLBI experiments depending on the configuration of the network and the objectives of the session. The precision of the Earth rotation parameters observed by VLBI is to first order proportional to the baseline lengths of the network. Thus, only measurements carried out in large networks, i.e. with baselines longer than 6000 km, are used for the determination of the Earth's orientation. Present VLBI networks observe up to 25 radio sources several times in a predetermined sequence during a period of 24 hours providing 1000 to 2000 individual delay observables τ. Today, the formal error of the pole position determined in a standard 24-hour observing session lies in the range of about 0.1 to 0.2 milliseconds of arc (mas).

Another important factor is the geometry of the VLBI network. Long east-west baselines are mainly sensitive to UT1 whereas networks with long north-south components allow to measure precisely both components of the pole position. The sensitivity can be derived from the influence on the delay observable:

$$\Delta\tau_{xp} = \frac{\partial\tau}{\partial x_p}\Delta x_p, \tag{6}$$

$$\Delta\tau_{yp} = \frac{\partial\tau}{\partial y_p}\Delta y_p. \tag{7}$$

where Δx_p, Δy_p are the changes in the pole components and Δx_p, Δy_p are the respective changes in the delay observable. The partial derivatives $\partial\tau/\partial x_p$, $\partial\tau/\partial y_p$ are dependent on the baseline components b_x, b_y, b_z, the declination δ_s and the Greenwich hour angle h_s of the radio source:

$$\frac{\partial\tau}{\partial x_p} = -\frac{1}{c}\left[(b_x \sin\delta_s - b_z \cos\delta_s \cos h_s)\right], \tag{8}$$

$$\frac{\partial\tau}{\partial y_p} = -\frac{1}{c}\left[(b_y \sin\delta_s - b_z \cos\delta_s \sin h_s)\right], \tag{9}$$

For instance, the baseline between the Wettzell Geodetic Fundamentalstation (Germany) and the Hartebeesthoek Radio Astronomy Observatory (South Africa) whose z component of 7580 km is about eight times its x component and five times its y component, yields large values for the partial derivatives with strong variations due to the multiplication by $(\sin h_s)$ or $(\cos h_s)$. Thus, this baseline provides high sensitivity for changes in both components of polar motion.

Periodic and aperiodic deformations of the Earth's crust have to be taken into account as well. Solid Earth tides show diurnal and semidiurnal oscillations which cause vertical deformations in a range of $\pm$ 20 cm and horizontal displacements of about 30% of the vertical effect (e.g. Mathews et al., 1997). More difficult to model is the loading by the water masses of ocean tides and currents (ocean loading), which amounts to as much as a decimeter on some coastal or island sites (Scherneck, 1991). The loading effects due to air pressure variations (atmospheric loading) also reach the level of significance in VLBI modeling (Rabbel and Schuh, 1986; Haas el al., 1997).

Finally, deformations of the telescope structure which occur during the 24 hours of an observing session or between the observing sessions have to be taken into account. They can be caused by thermal expansion of the telescopes or snow and ice loading of the antenna (Haas et al., 1999).

The so-computed *theoretical delays* are then compared with the *reduced observed delays* by a parameter estimation process, e.g. a least-squares fit. The parameters which are estimated belong to different groups:

1. Auxiliary parameters which have to be computed but are usually not interesting for the geodesists, e.g. clock parameters and atmospheric parameters.

2. Geodetic/astrometric parameters which are of interest for the user community, e.g. baseline components or station coordinates with respect to a reference station, Earth orientation parameters (UT1-UTC, pole coordinates, nutation coefficients) or radio source positions.

Let's start with the auxiliary parameters. As a clock model usually second order polynomials are entered and occasional clock breaks have to be introduced. Clock modeling is still very much an interactive procedure and belongs to the editing session. In present standard VLBI solutions the clock estimation algorithm is designed to model short-term, random clock variations while enforcing realistic physical constraints on continuity and rates of change. When all clocks are "well behaved" a typical algorithm which is applied is as follows: the clock at one site is designated the reference clock and the differences between this clock and the other site clocks are modeled. These differences are modeled as the sum of two functions: a second order polynomial and a continuous, piecewise-linear function with an initial value of zero. The three coefficients of the polynomial correspond to clock epoch offset, clock frequency offset, and clock frequency drift. They are unconstrained in the solution because these parameters can be of any size for real hydrogen masers. In the piecewise-linear function, the offset at the end of each linear segment is estimated. In the solutions done by the NASA/GSFC VLBI group, the linear segments are only one hour long each (Ryan et al., 1993) whereas European VLBI experts usually choose longer segments, e.g. four or six hours (Nothnagel and Campbell, 1993). Residuals for the group delay observables on the baseline Ny Ålesund-Wettzell of a first solution with a simple clock model are plotted in figure 4. Figure 5 shows the clock of Wettzell station modeled by a piecewise-linear function as described above clearly corresponding to the behavior of the residuals.

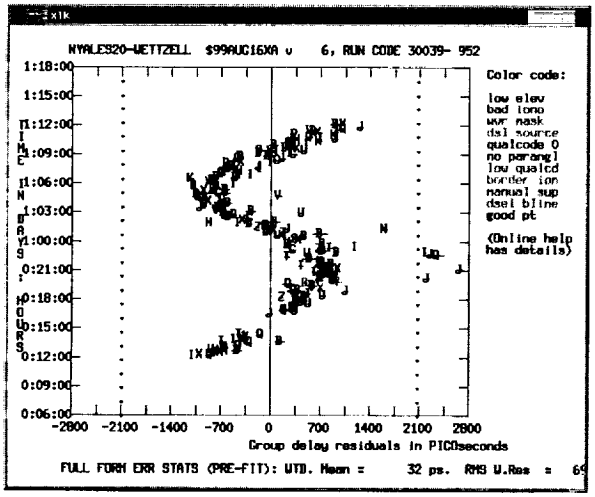

Figure 4. Group delay residuals of a first solution with a simple clock model for Wettzell station. Time axis is from bottom to top.

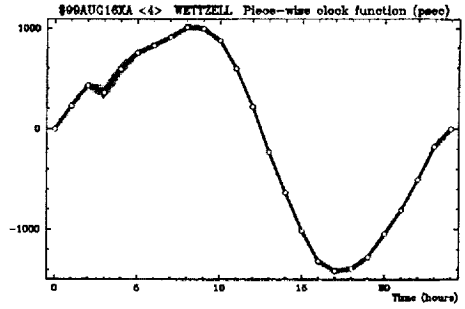

Figure 5. Clock of Wettzell station modeled by a piecewise-linear function as described above. Time axis is from left to right.

There are also different strategies for modeling the influences of the troposphere on the radio signals. Some of the VLBI analysis groups solve for tropospheric wet delay corrections only, some others for total zenith delay corrections, again approximated by a piecewise-linear function. Also so-called gradients are determined to take into account azimuthal dependencies (Davis et al., 1993).

Now, we continue with those parameters which are the subject of geodetic and astrometric VLBI observations. In geodetic VLBI data processing there are two levels of least-squares solutions, one in which only the "local" unknowns are estimated from a single session (such as clock and atmospheric parameters for the participating stations as described above, Earth orientation parameters UT1-UTC, components of polar motion x_p, y_p, and nutation parameters in longitude and in obliquity) thus creating a first data base version of each particular experiment, and another which collects a considerable number of available experiments covering a long time base for a combined solution including the "global" unknowns such as station and source positions and further geodynamical and astronomical parameters.

The latter can be parameters of a model for the solid Earth tides where the relevant parameters, i.e. the Love and Shida numbers, can be estimated (Mitrovica et al., 1994; Schuh and Haas, 1998). Deformation due to ocean loading is a small second order effect but large enough to be revealed by detailed analyses of VLBI measurements (Schuh and Möhlmann, 1989). Ocean loading parameters could be successfully determined from VLBI, e.g. by Sovers (1994) and by Haas and Schuh (1998). The loading effects due to air pressure variations (atmospheric loading) were also investigated based on VLBI measurements and relevant parameters were determined from VLBI (Haas et al. 1997).

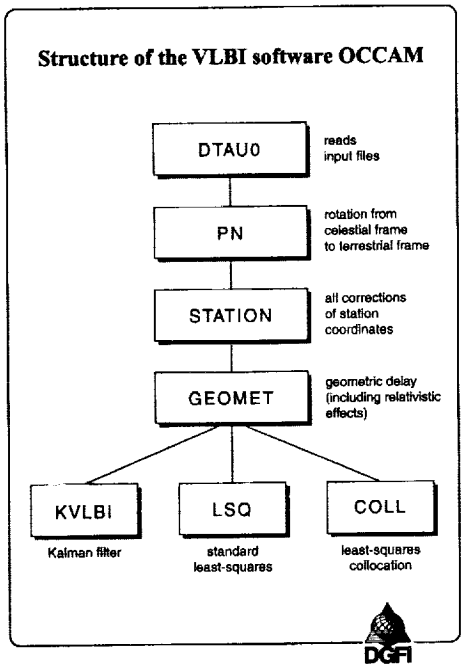

Figure 6. Flow chart of OCCAM.

Since the early 80's VLBI observations have been used extensively to verify Einstein's theory in its Parameterized Post Newtonian formulation (PPN). Two approaches have been used, one designing special experiments to observe sources such as 3C279 and 3C273 during their close approach to the Sun and the other using all available data from routine geodetic experiments to achieve the accuracy by the sheer number of the observations. The γ-factor, which in the Einstein theory should be equal to unity, has been found to show no significant departure from this value to the level of 0.1% (Carter et al., 1985). More recently, this accuracy level has been further improved to 0.02% (Robertson et al., 1991). Attempts have also been made to verify the gravitational bending near Jupiter (Schuh et al., 1988), but the effect is only marginally significant (< 100 psec) at very close encouters, i.e. less than a few arcmin (Campbell, 1989; Treuhaft and Lowe, 1991).

The theory of plate tectonics, which stipulates that the Earth's crust is formed by a mosaic of separate major plates that are in motion relative to each other, has now been universally accepted. Predictions derived from geophysical evidence yield motions of a few centimeters per year. With the large global VLBI data sets including now almost two decades of regular observations, parameterised plate models have been successfully determined based on VLBI solutions (e.g. Ryan et al., 1993).

In view of the extremely high precision inherent to VLBI, the modeling accuracy has to be

brought down to better than a few millimeters on the global scale. Great efforts have been made to develop comprehensive geodetic VLBI data analysis software systems, which include all aspects of the multi-faceted reality of VLBI. Among the various VLBI software systems the MkIII Data Analysis System is probably the most prominent one. It is built around the CALC/SOLVE software system developed jointly by the US East Coast VLBI groups. At present CALC version 9.1 is used. This software has become a sort of standard against which the other systems can be compared. Other software systems at the same level of accuracy are the OCCAM package (see fig. 6) developed by European VLBI groups in Bonn, Madrid and Saint Petersburg (Schuh, 1987, Zarraoa et al., 1993; Titov and Zarraoa, 1997) and the MASTERFIT/MODEST software developed at Jet Propulsion Laboratory, Pasadena (Sovers, 1991; Sovers et al., 1998).

References

[1] Brosche, P., Seiler, U., Sündermann, J., Wünsch, J.: Periodic Changes in Earth's Rotation due to Oceanic Tides. Astron. Astrophys., 220, p. 318-329, 1989.

[2] Campbell, J., Schuh, H., Zeppenfeld, G.: On the Computation of Group Delay Corrections Caused by Radio Source Structure. IAU-Symposium No. 129 "The Impact of VLBI on Astrophysics and Geophysics", eds. M.J. Reid and J.M. Moran, p. 427, Kluwer Academic Publ., Dordrecht 1988.

[3] Campbell, J.: Mésure de l'effect relativiste de Jupiter par VLBI. Systèmes de référence spatio-temporels, N. Capitaine ed., Observatoire de Paris, p. 55-63, 1989.

[4] Carter, W.E., Robertson, D.S., MacKay, J.R.: Geodetic Radiointerferometric Surveying: Applications and Results. J. Geophysical Research, Vol. 90, p. 4577-4587, 1985.

[5] Charlot, P.: Evidence for Source Structure Effects Caused by the Quasar 3C273 in Geodetic VLBI Data. Proc. of the 9th Working Meeting on European VLBI for Geodesy and Astrometry, Bad Neuenahr, 1993, Mitteil. aus den Geodätischen Instituten der Rhein. Friedr.-Wilh.-Univ. Bonn, Nr. 81, p. 171-178, 1993.

[6] Charlot, P., Fey, A.L.: A Classification of ICRF Sources Based on Observed Structure for Ultra-precise VLBI Astrometry and Geodesy. Proc. of the 13th Working Meeting on European VLBI, Viechtach, W. Schlüter and H. Hase (eds.), BKG, 217-223, 1999.

[7] Davis, J.L. et al.: Geodesy by Radio Interferometry: Effects of Atmospheric Modeling Errors on Estimates of Baseline Length. Radio Science, Vol. 20, p. 1593-1607, 1985.

[8] Davis, J.L. et al.: Ground-based measurement of gradients in the "wet" radio refractivity of air, Radio Science, Vol. 28, p. 1003-1018, 1993.

[9] Elgered, G., Rönnäng, B., Askne, J.: Measurements of Atmospheric Water Vapour with Microwave Radiometry. Radio Science, Vol. 17, p. 1258-1264, 1982.

[10] Emardson, T.R., Elgered G., Johansson J.M.: External atmospheric corrections in geodetic very-long-baseline interferometry, Journal of Geodesy, 73, 375-383, 1999.

[11] Eubanks, T.M. (ed.): Proceedings of the U.S. Naval Observatory Workshop on Relativistic Models for Use in Space Geodesy. U.S. Naval Observatory, Washington DC, June 1991.

[12] Haas, R., Schuh, H.: Ocean Loading Observed by Geodetic VLBI, Proc. of the 13th Intern. Symposium on Earth Tides, Brussels, July 1997, ed. by B. Ducarme, p. 111-120, 1998.

[13] Haas, R. et al.: Atmospheric Loading Corrections in Geodetic VLBI and Determination of Atmospheric Loading Coefficients, Proc. of the 12th Working Meeting on European VLBI, B.R. Pettersen (ed.), Statens Kartverk Geodesidivisjonen, Honefoss, p. 122-132, 1997.

[14] Haas, R. et al.: Explanatory Supplement to the Section "Antenna Deformation" of the IERS Conventions (1996), DGFI Report No. 71, H. Schuh (ed.), p. 26-29, 1999.

[15] Mathews, P.M., Dehant, V., Gipson, J.M.: Tidal station displacement, Journ. Geophys. Res., Vol. 102, B9, p. 20469-20477, 1997.

[16] Mitrovica, J.X., Davis, J.L, Mathews, P.M., Shapiro, I.I.: Determination of tidal h Love number parameters in the diurnal band using an extensive VLBI data set. Geophys. Res. Letters, Vol. 21, No. 8, p. 705-708, Apr. 1994.

[17] Niell, A.E.: Global mapping functions for the atmosphere delay at radio wavelengths, Journal of Geophysical Research, Vol. 101, No. B2, 3227-3246, 1996.

[18] Nothnagel, A., Campbell, J.: European Baseline Rate Determinations with VLBI. Proc. of the 9th Working Meeting on European VLBI for Geodesy and Astrometry, Bad Neuenahr, 1993, Mitteil. aus den Geodätischen Instituten der Rhein. Friedr.-Wilh.-Univ. Bonn, Nr. 81, p. 42-48, 1993.

[19] Preuss, E., Campbell, J.: Very-Long-Baseline Interferometry in Astro-, Geo-, and Gravitational Physics. Lecture Notes in Physics (eds. J. Ehlers and G. Schäfer), Springer-Verlag, p. 100-130, 1992.

[20] Rabbel, W., Schuh, H.: The Influence of Atmospheric Loading on VLBI-Experiments, Journal of Geophysics, Vol. 59, Number 3, p. 164-170, 1986.

[21] Ray, R.D., Steinberg, D.J., Chao, B.F., Cartwright, D.E.: Diurnal and Semidiurnal Variations in the Earth's Rotation Rate Induced by Oceanic Tides, Science, Vol. 264, p. 830-832, 1994.

[22] Rius, A., Rodriguez, J., Campbell, J.: Geodetic VLBI with Large Antennas. Mitt. Geod. Inst. Univ. Bonn, No. 72, eds. J. Campbell and H. Schuh, p. 59-67, Bonn 1987.

[23] Robertson, D.S., Carter, W.E., Dillinger, W.H.: New measurement of solar gravitational deflection of radio signals using VLBI. Nature, Vol. 349, p. 768-770, 1991.

[24] Ryan, J.W., Ma, C., Caprette, D.S.: NASA Space Geodesy Program - GSFC Data Analysis - 1992, Final Rep. of the CDP VLBI Geodetic Results 1979-91, NASA Techn. Memorandum 104572, 1993.

[25] Schalinski, C.J., Alef, W., Campbell, J., Witzel, A., Schuh, H.: First Results of the VLBI-Investigation of Sources from Geodetic IRIS-Experiments. IAU-Symposium No. 129 "The Impact of VLBI on Astrophysics and Geophysics", eds. M.J. Reid and J.M. Moran, p. 359, Kluwer Academic Publ., Dordrecht 1988.

[26] Scherneck, H.-G.: A parameterized solid earth tide model and ocaen tide loading effects for global geodetic baseline measurements, Geophys, J. Int., Vol. 106, p. 677-694, 1991.

[27] Schuh, H.: Die Radiointerferometrie auf langen Basen zur Bestimmung von Punktverschiebungen und Erdrotationsparametern. DGK Reihe C, Heft Nr. 328, 1987.

[28] Schuh, H. et al.: On the Deflection of Radio Signals in the Gravitational Field of Jupiter. Physics Letter A, Vol. 129, number 5,6, p. 299-300, May 1988.

[29] Schuh, H., Möhlmann L.: Ocean Loading Station Displacements Observed by VLBI. Geophysical Research Letters, Vol. 16, No. 10, p. 1105-1108, Oct. 1989.

[30] Schuh, H., Campbell, J.: VLBI in geodynamical investigations, Acta Geod. Geophys. Hung., Vol. 29 (3-4), p. 397-420, 1994.

[31] Schuh, H., Haas,R.: Earth Tides in VLBI Observations, Proc. of the 13th Intern. Symposium on Earth Tides, Brussels, July 1997, ed. by B. Ducarme, p. 101-110, 1998.

[32] Schwegmann, W., Schuh, H.: Status of IADA: An Intelligent Assistant for Data Analysis in VLBI, Proc. of the 1st IVS General Meeting, Kötzting, this Volume, 2000

[33] Sovers, O.J.: Observation Model and Parameter Partials for the JPL VLBI Parameter Estimation Software "MODEST" - 1991. JPL Publication 83-39, Rev. 4, Aug. 1991.

[34] Sovers, O.J.: Vertical ocean loading amplitudes from VLBI measurements. Geophysical Research Letters, Vol. 21, No. 5, p. 357-360, March, 1994.

[35] Sovers, O.J., Fanselow, J.L., Jacobs, C.S.: Astrometry and geodesy with radio interferometry: experiments, models, results. Reviews of Modern Physics, Vol. 70, No. 4, p. 1393-1454, 1998.

[36] Tamura, Y.: Periodic Series of DUT1. Geodesy and Physics of the Earth (ed. by Montag and Reigber), p. 435-438, Springer-Verlag, 1993.

[37] Titov, O., Zarraoa, N.: OCCAM 3.4 User's Guide, Communications of the Institute for Applied Astronomy (IAA), St. Petersburg, No. 69, 1997.

[38] Treuhaft, R.N., Lowe, S.T.: A Measurement of Planetary Relativistic Deflection. Astronomical Journal, Vol. 102, N. 5, Nov. 1991.

[39] Wünsch, J., Seiler, U.: Theoretical Amplitudes and phases of the periodic polar motion terms caused by ocean tides, Astron. Astrophys., 266, p. 581, 1992.

[40] Yoder, C.F., Williams, J.G., Parke, M.E.: Tidal Variations of Earth Rotation. Journ. of Geophys. Res., No. 86, p. 881-891, 1981.

[41] Zarraoa, N., Rius, A., Sardon, E., Schuh, H.: Introduction to the OCCAM V2.0 Models. Proc. of the 8th Working Meeting on European VLBI for Geodesy and Astrometry, Dwingeloo 1991, p. IV-59 - IV-69, Rep. MDTNO-R- 9243, Surv. Dep. of Rijkswaterstaat, Delft 1993.

[42] Zeppenfeld, .G.: Source structure enhanced MKIII Data Analysis Software. Proc. of the 8th Working Meeting on European VLBI for Geodesy and Astrometry, Dwingeloo 1991, p. IV-16 - IV-21, Rep. MDTNO-R-9243, Surv. Dep. of Rijkswaterstaat, Delft 1993.

L. Petrov: Instrumental Errors of Geodetic VLBI, IVS 2000 General Meeting Proceedings, p.230–235
http://ivscc.gsfc.nasa.gov/publications/gm2000/petrov1

Instrumental Errors of Geodetic VLBI

L. Petrov

Geodetic Institute of the University of Bonn
e-mail: petrov@picasso.geod.uni-bonn.de

Abstract

A model of VLBI observables includes effects of geometry, environment of signal propagation and delays in the data acquisition system itself. Imperfection of the model of instrumental effects can be a considerable source of errors in the estimates of the targeted parameters. Two effects are considered in detail: spurious signals in phase calibration and instrumental polarization. Methods of their detection, evaluation and calibration are outlined. Influence of these effects on the final results is shown.

1. Introduction

A model of VLBI observations includes contributions to time delay due to 1) geometry, 2) source structure, 3) effects of medium of signal propagation from the source to the point of injection of phase calibration impulses, 4) signal propagation from the point of injection of phase-cal impulses to a formatter. The latter term we will call instrumental delay.

Mismodeling instrumental delay spawns instrumental errors. Two effects are investigated:

- errors in phase-cal phases,
- instrumental polarization.

The signal enters the data acquisition system after passing a point of injection of phase-cal impulses. Then it goes through a variety of different radioelectronic devices such as amplifiers, mixers; it propagates through waveguides and cables. Ideally, the phase calibration system should calibrate all delays which the signal acquires after passing through the point of injection of phase-cal impulses. The fringed phases become referred to that point when phase-cal phases are subtracted from raw fringed phases. In practice the phase-cal system itself is affected by spurious signals which distort phase calibration phases. Mismodeling this effect may give a noticeable contribution to an error budget [1]. It will be shown that in many cases it is possible to considerably reduce the influence of spurious signals on group delay by performing a special analysis.

Another source of instrumental delay is related to the transformation of a circularly polarized wave falling on the antenna's aperture into the signal propagating through cables to the formatter. Instrumental polarization of radiotelecopes causes an additional delay.

2. Investigation of Phase-cal Phases and Phase-cal Amplitudes

A phase-cal antenna unit generates a rail of short impulses which are injected in a feed horn every microsecond. The phase calibration signal travels the same path as the signal from a source, and it is affected by the same transformations. Phases of the phase-cal signal at each channel are extracted during correlation and subtracted from fringe phases. The amplitude of the phase-cal

signal is not used in routine data analysis but it provides valuable information for calibration of the phase-cal system itself.

Since the amplitude of the phase-cal signal which is injected by the antenna unit is known and is constant, we can expect that the amplitude of the recorded signal should also be constant. Variations in recorded phase-cal amplitudes indicate that recorded phase-cal phases would have similar variations. However, variations in path length themselves do not change the amplitude of a signal. One of the reasons for variations in the recorded amplitude is the presence of narrow-band signals which are coherent with the true phase-cal signal. B. Corey proposed [2] to call them "spurious signals" or spurs for brevity.

If we could determine the amplitude and phase of spurious signals we could subtract their contribution from the recorded phase of the phase-cal signal and improve measurements of instrumental delay [3].

The correlator computes sine and cosine components of the phase-cal signal as a fraction of the amount of correlating bits to the total amount of recorded bits. The measured phase-cal amplitude is expressed as a fraction of the total system noise. Therefore, the amplitude of the extracted and injected phase-cal signal are tied as $A_e \sim \frac{A_i}{\sqrt{T_{sys}}}$.

The measured phase (ϕ_m) and amplitude (A_m) of phase-cal are related to the true phase and amplitude of phase-cal (ϕ_o, A_o) and spurious signal (A_s, ϕ_s):

$$\begin{aligned} \sqrt{\frac{T_{sys}}{T_o}} A_m - A_o &= A_s \cos(\phi_o - \phi_s) + O\left(\frac{A_s}{A_o}\right)^2 \\ \phi_m - \phi_o &= -\frac{A_s}{A_o} \sin(\phi_o - \phi_s) + O\left(\frac{A_s}{A_o}\right)^2 \end{aligned} \qquad (1)$$

where T_o is an averaged system temperature.

We see that the measured amplitude of the phase-cal can be affected by the variations caused by changes in system temperature and spurious signals. Normally, system temperature is measured before each scan and it is recorded in log files. The amplitude of a spurious signal can be determined by LSQ fitting provided we know how to model the phase of the spurious signal ϕ_s.

The phase of the spurious signal depends on its origin. B. Corey proposed a list of possible sources of spurious signals [2]. Some types of spurs can be parameterized as $\phi_s = f\,\phi_o + \phi_i$ where ϕ_i is a constant and f is a parameter.

Then spurs can be classified according to the following scheme:

- A-spur. $f_s = 0$ — Additive spur. It is generated by the electronics of the data acquisition system and is not related to the signal.
- B-spur. $f_s = -f_0$ — Image spur. It occurs due to an admixture of the signal at the image of the intermediary frequency.
- C-spur. $f_s = \frac{\omega_{\rm LO}}{\omega_{\rm LO}^{opp}}$ — Cross-band spur. It occurs due to an admixture of the signal from the opposite band.
- D-spur. $f_s = -\frac{\omega_{\rm LO}}{\omega_{\rm LO}^{opp}}$ — Image cross-band spur. It occurs due to an admixture of the signal at the image band of the intermediary frequency of the opposite band.

- L-spur. $A_m = A_o + L\,\phi_o, \quad \phi_m = \phi_o + L\,\phi_o$ — Linear spur. The origin is unclear.

Here $\omega_{\rm LO}$ and $\omega_{\rm LO}^{opp}$ are the frequencies of local oscillator (LO) at the current and opposite bands.

The presence of a spurious signal results in a harmonic dependence of the measured amplitudes and phases on the total phase of the phase-cal signal. The frequency of this dependence is $1 - f$ for all spurs, except L-spur, and it can be represented in this table (units are 1/cycle):

Spur	X-band	S-band
A-spur	1.0	1.0
B-spur	2.0	2.0
C-spur	0.75	1.25
D-spur	3.00	5.00

The following algorithm for determination of amplitudes and phases of spurs from the amplitudes of the phase-cal is proposed and implemented in the program Phase_Doctor:

- Modeling system temperatures as $T_m = T_o \cdot a(e) \cdot b(t)$, editing, outliers rejection. Here $a(e)$ is a function of elevation angle and $b(t)$ is a function of time. Then normalization of phase-cal amplitudes.
- Resolving ambiguities in phase-cal. (Assumptions: a dominating contribution is LO variations which are common at X- and S- bands; phase variations in the individual channels are smaller than one phase turn);
- LSQ fitting the model of harmonic variations in $A_m(\phi_m)$. Iterative refining for taking into account non-linear terms $O\left(\frac{A_a}{A_o}\right)^2$;
- Computation of contribution of spurs to group and phase delays.

Figure 1. Amplitude of phase-cal versus its phase at station MATERA, experiment 99APR26XA

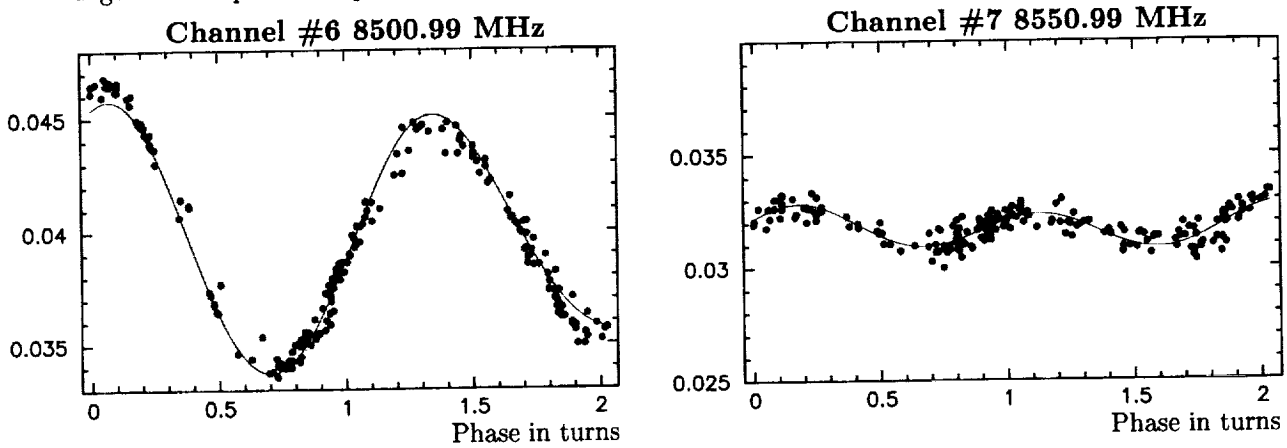

An alternative way is to use the phase of the phase-cal signal in the individual channel itself for spurious signal detection. The phase of phase-cal ϕ_i in the i-th channel can be modeled as

$$\phi_i(t) = \omega_o \tau_p(t) + \omega_i \tau_g(t) + \phi_o(t) + \phi_r(t) \qquad (2)$$

where ω_o is a reference frequency, $\tau_p(t)$ is the phase delay of phase-cal, ω_i is the frequency of the individual channel, $\tau_g(t)$ is the group delay of phase-cal, $\phi_o(t)$ is the phase offset at the channel and it may have a small number of breaks, $\phi_r(t)$ is the residual phase of the phase-cal signal.

Having combined equations (2) for all scans and for each band we can adjust a series of $\tau_p(t)$, $\tau_g(t)$ and find estimates of ϕ_o at the initial epoch and at the epochs of phase breaks by using LSQ method. Residual phases would have harmonic variations if spurious signals affected one or several channels. However, this approach does not allow us to detect spurs which have the same phase and amplitude at all channels of the band. An advantage of this approach is that the measurements of phase-cal phases are not affected by variations of system temperature and therefore the errors of measurements of system temperature do not affect residual phases.

The following algorithm for determination of amplitudes and phases of spurs from the residual phases of the phase-cal signal is proposed and implemented in the program Phase_Doctor:

- Resolving ambiguities in phase-cal phases;
- Building a model of phase-cal phases:
  - determination of phase break epochs in the individual channels;
  - determination of which spurs affect the phases.
- Adjustments of parameters of the phase-cal phase model usng LSQ:
  - Values of a phase offset and phase breaks for each channel;
  - Amplitudes and phases of spurs;
  - An array of phase delays in phase-cal over a band for each scan, each band;
  - An array of group delays in phase-cal over a band for each scan, each band.
- Iterations for taking into account non-linearity of the problem.
- Computation of contribution of spurs to group and phase delays.

Figure 2. Residual phase in phase-cal (in rad) versus full phase at station MEDICINA, experiment 99AUG16XA

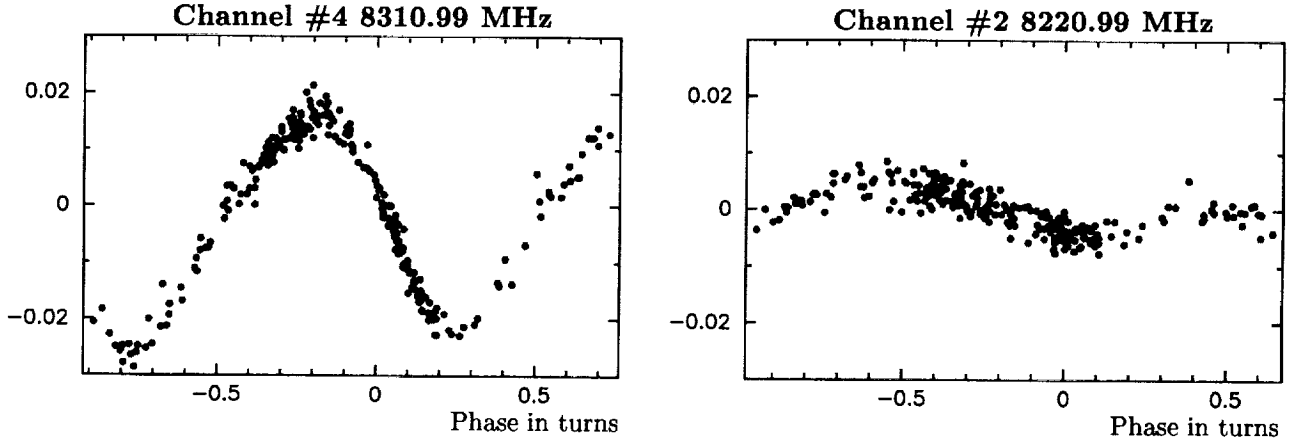

Figure 3. Contribution of spurious signals to group delay (in psec)

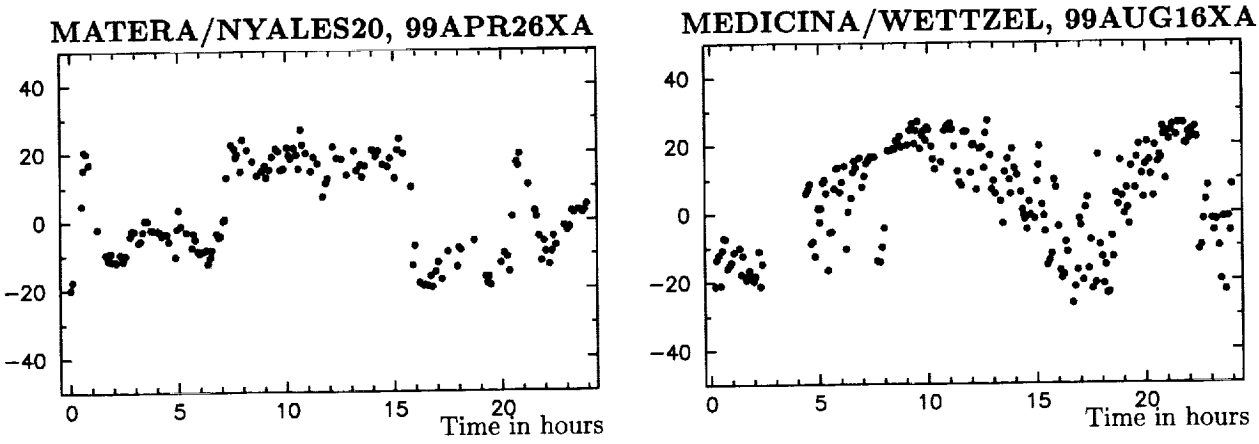

3. Investigation of Effects of Instrumental Polarization

Antennas receive not only wanted right circular polarization (RCP), but some amount of unwanted left circular polarization (LCP). Fringe phases of RR and LL scans are not the same:

$$\phi_{RR} - \phi_{LL} = k \sin\Big(2\,(\psi_1 - \psi_2) + \phi_o\Big)$$

$$k \approx \frac{\mathrm{Amp}_{LL}}{\mathrm{Amp}_{RR}}$$

where ϕ is the fringe phase, and ψ is the parallactic angle and Amp is the fringe amplitude. The coefficient k is a parameter of the radiotelescope and may depend on frequency and elevation.

Special polarization experiments were conducted in order to investigate the effects of instrumental polarization. Some antennas swapped polarization and observed LCP in one scan and RCP in the next scan while other antennas observed RCP only. The ratios of fringe amplitudes of RL cross scans to the amplitudes of normal RR scans for the same source were investigated. In the case of observations of unpolarized sources $\frac{\mathrm{Amp}_{LL}}{\mathrm{Amp}_{RR}} \approx \left(\frac{\mathrm{Amp}_{RL}}{\mathrm{Amp}_{RR}}\right)^2$ and therefore this method is rather more sensitive to instrumental polarization. Fringe amplitude of RL scans should be zero if a system is perfect.

- Extension of **euro46** experiment 1998.12.14: two RL and two RR scans were obtained. MEDICINA and CRIMEA swapped polarization, other stations observed RCP-polarization. Result: $\frac{\mathrm{Amp}_{RL}}{\mathrm{Amp}_{RR}} \approx 0.05 - 0.2$ for European VLBI stations.
- **brd01** experiment 1999.07.01: RL and RR scans were obtained. MEDICINA swapped polarization 96 times during 24-hours experiment. Some results are presented in the figure 4.

4. Conclusions

- Phase-cal phases can be cleaned up to the 0.01 rad level. Typically root mean square of contribution of a phase-cal noise to group delay is about 5–10 psec. It can be reduced to a level below 2 psec by LSQ adjustment of a parametric model.

Figure 4. Ratios of RL to RR fringe amplitudes for three sources observed in brd01 experiment

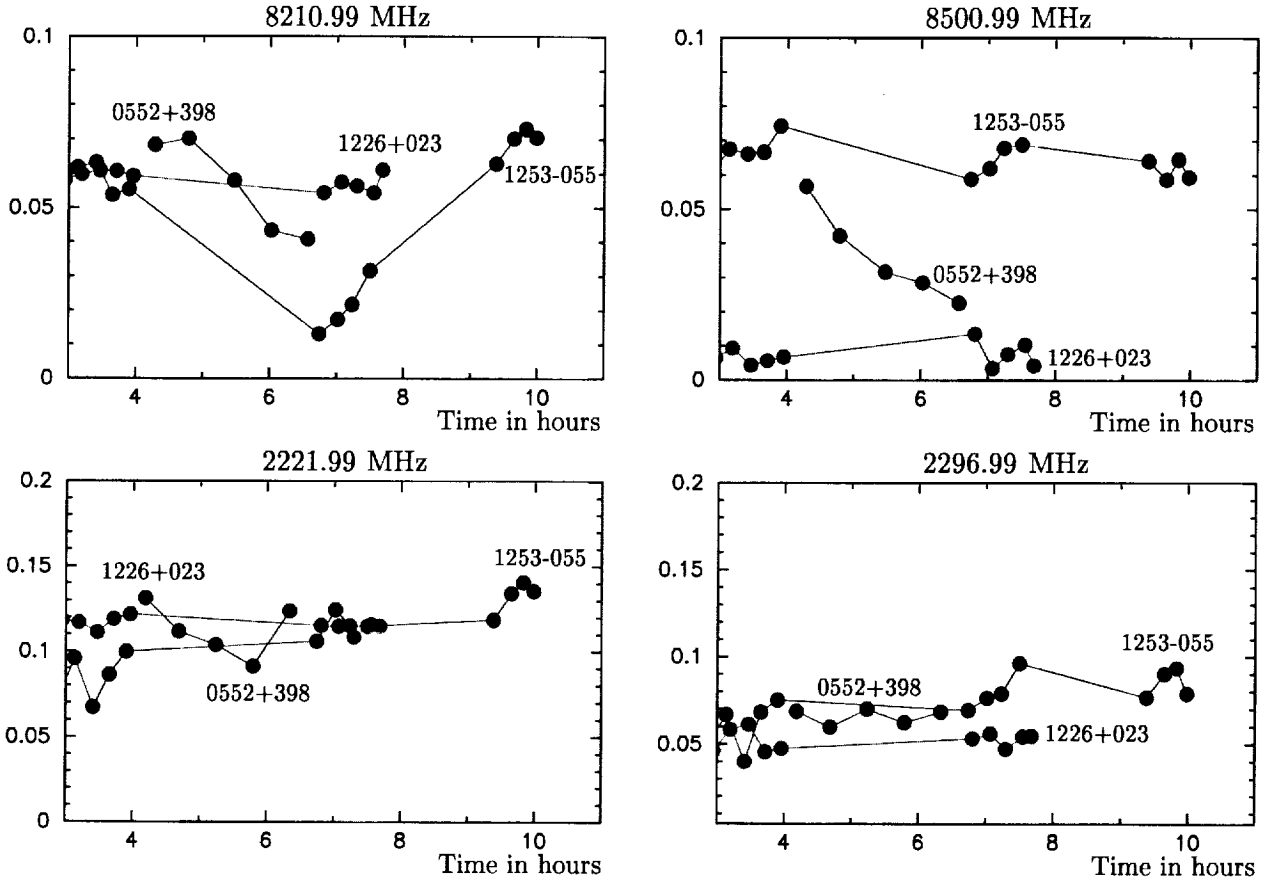

- Spurious signals in phase-cal were detected at all stations.
- Removal of spurious signals reduces the scatter of the residual fringe phases significantly, while it improves solutions only marginally. Spurious signals affect a solution at about the same level as the cable calibration.
- Instrumental polarization of European VLBI antennas is 5–20%. It has a strong dependence on frequency and antenna orientation.

References

[1] J. R. Ray, B. E. Corey, "Current precision of VLBI Multi-Band Delay Observations", In Proceedings of the AGU Chapman Conference on Geodetic VLBI: Monitoring global Change", NOAA Technical report NOS 137, NGS 49, Washington D.C. 1991, p. 123-134.

[2] B. Corey, "Spurious phase calibration signals: how to find them and how to cure them", Proceedings of VLBI Chiefs Meeting, 1998

(Web: `http://giub.geod.uni-bonn.de/vlbi/development/spur/spurs_bec.ps.gz`)

[3] T. Herring, "Precision and accuracy of intercontinental distance determinations using radio interferometry", Ph. D. Thesis, Cambridge MA, 1983, 442 p.

Brent A. Archinal: Mark IV Data Analysis – Software Changes and Early Experiences, IVS 2000 General Meeting Proceedings, p.236–236
http://ivscc.gsfc.nasa.gov/publications/gm2000/archinal

Mark IV Data Analysis – Software Changes and Early Experiences

Brent A. Archinal

United States Naval Observatory
e-mail: baa@CasA.usno.navy.mil

Abstract

Data from the Mark IV correlator hardware/software system should first become available in late November, 1999. For various reasons, this data is formatted differently than that of the earlier Mark III and IIIA systems, for example because additional types of data and diagnostic information are available. Changes have been made and will continue to be made to the "Calc/Solve" analysis system in order to process the data in this new format. These changes and early experience in processing such data will be discussed, and some questions will be raised about whether further changes, i.e. in algorithms, weighting, and databases may be appropriate or even necessary.

Harald Schuh et al.: Considering A Priori Correlations in VLBI Data Analysis, IVS 2000 General Meeting Proceedings, p.237–242
http://ivscc.gsfc.nasa.gov/publications/gm2000/schuh'tesmer

Considering A Priori Correlations in VLBI Data Analysis

Harald Schuh [1], *Volker Tesmer* [2]

[1)] *Institut für Geodäsie und Geophysik, Techn. Univ. Wien*
[2)] *Deutsches Geodätisches Forschungsinstitut (DGFI)*
Contact author: Harald Schuh, e-mail: hschuh@luna.tuwien.ac.at

Abstract

The complete model of least-squares adjustment contains the full variance-covariance matrix of the observables. However, in present standard VLBI solutions, only the variances of the observed time delays are introduced, whereas the covariances are set to zero, i.e. no a priori correlations between the observables of a VLBI-session are taken into account. In this study, correlation coefficients for 36 IRIS-S sessions since 1994 were determined empirically, the a priori correlation matrices were designed and entered into the VLBI data analysis. The OCCAM 3.4 VLBI software had been modified for that purpose by introducing the full variance-covariance matrix. The results were compared with those of an uncorrelated approach. The formal errors of the results usually increased and hence became more realistic. The repeatability of the baseline lengths and of the vertical and horizontal components improved significantly.

1. Introduction

In geodetic VLBI usually the least-squares method is applied for the estimation of the unknown parameters such as station coordinates, Earth rotation parameters or clock parameters. The complete model of a least-squares adjustment contains the full variance-covariance matrix. Its diagonal elements (variances) can be computed from the a priori errors σ_i; the off-diagonal elements (covariances) can be derived from the σ_i and from the correlation coefficients $\rho_{i,j}$ for each pair of observables. However, in all present standard VLBI solutions, only the variances of the observations are used whereas the covariances are set to zero. This can lead to a distortion of the results and to too optimistic formal errors. Reasons for neglecting a priori correlations in the past are that a correlated approach needs considerably more space on the computer and more CPU time. It is also not trivial to determine reasonable a priori correlations.

2. Reasons for Correlations between VLBI Observables

In this paragraph causes for a priori correlations between VLBI observables will be described (see also Schuh and Wilkin, 1989).

Correlations due to temporal closeness

Observables which are close in time will be more strongly correlated than observables which are far apart in time. Similar external influences, e.g. slowly varying atmospheric conditions, and also errors in the models for global, regional or local deformations of the Earth (e.g. Earth tides, oceanic and atmospheric loading or deformations of the antennas) can cause such correlations.

They will be especially high, if the observations were taken on the same baseline.

Correlations between observables of the same radio source

Temporally close observables can be even more strongly correlated if the same radio source was observed. This is due to systematic influences of the structure of the source or because of errors of the source position. Additionally, the tropospheric contribution to the total correlation coefficients will be in particular high, because the signal path through the troposphere will not differ very much for subsequent observations of the same radio source.

Geometric correlation

During a VLBI experiment, a radio source is usually observed simultaneously from all or from most of the participating stations. Thus, observables from geographically close stations, in particular made on baselines which have one common station, will be more strongly correlated than observables from baselines which are far apart.

Technical or other reasons

There are many reasons of technical nature which can cause correlations between observables. For example all observables which were obtained by the same correlation process may be correlated in a stochastic sense. All other instrumental components of the VLBI system (station clocks, instrumental calibration system, ...) can cause the "technical correlations".

3. Variance-Covariance Matrix of the Observations

The stochastic model of the least-squares method contains a main diagonal weight matrix P_{diag} ($p_i = const./\sigma_i^2$, with σ_i the a priori sigmas of the observables). In standard VLBI data analysis the off-diagonal elements of the a priori variance matrix Q of the observables are set to zero. Thus, Q is a main diagonal matrix and is computed according to eq. (1).

$$Q = P_{diag}^{-1/2} \cdot P_{diag}^{-1/2} \qquad (1)$$
$$\text{with} \quad q_{i,i} = \sigma_i^2 \quad and \quad q_{i,j} = 0$$

In a complete stochastic model, off-diagonal elements have also to be considered in the a priori variance-covariance matrix Q of the observables. Q is computed by the a priori sigmas σ_i of the observables, and the correlation matrix R, with correlation coefficients $\rho_{i,j}$ for each pair of observables (eq. (2)).

$$Q = P_{diag}^{-1/2} \cdot R \cdot P_{diag}^{-1/2} \qquad (2)$$
$$\text{with} \quad q_{i,i} = \sigma_i^2 \quad and \quad q_{i,j} = \sigma_i \cdot \sigma_j \cdot \rho_{i,j} \neq 0$$

4. Determination of A Priori Correlations

In this study, the determination of a priori correlation coefficients was carried out in three steps:

1: Empirical correlation coefficients were derived from "corresponding" residuals $\hat{e}_i$ and $\hat{e}_j$ of an uncorrelated approach according to eq. (3) (Qian, 1985). By fitting a polynomial of low degree through the empirical correlation coefficients obtained from a high number of VLBI sessions, the empirical correlation functions were obtained (fig. 1).

$$\rho_{i,j} = \frac{[\hat{e}_i \cdot \hat{e}_j]}{\sqrt{[\hat{e}_i^2] \cdot [\hat{e}_j^2]}} \qquad (3)$$

with $\hat{e}_i, \hat{e}_j$ - residuals of an "uncorrelated" approach

$\rho_{i,j}$ - empirical correlation coefficient

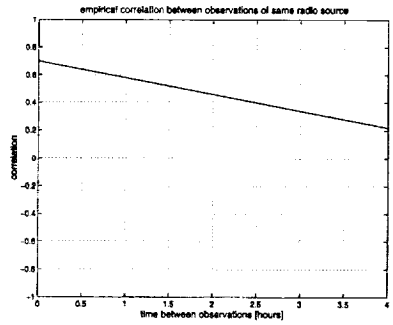

Figure 1. Empirical correlation function for observables of the same radio source

2: As a kind of test, the empirical correlation functions were compared with the a posteriori correlations between the observables within individual sessions, which were derived from the a posteriori variance-covariance matrix $\hat{Q}$ of the observations according to eq. (4). An example is plotted in figure 2.

$$\hat{Q} = A \cdot (A^T \cdot P_{diag} \cdot A)^{-1} \cdot A^T \qquad (4)$$

with A - Jacobian matrix

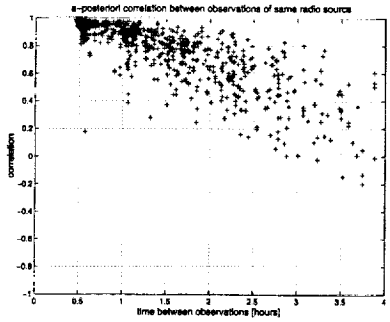

Figure 2. A posteriori correlations for observables of the same radio source

3: When designing the full a priori variance-covariance matrix Q of the observables, correlation coefficients due to k different reasons $(\rho_{1_{i,j}} \ldots \rho_{k_{i,j}})$, as derived in step 1, had to be considered. They were combined to final correlation coefficients $\rho_{i,j}$ for each pair of observables using eq. (5). The $\rho_{i,j}$ (fig. 3) and the a priori sigmas of the observations σ_i were used to determine the covariances of the variance-covariance matrix (eq. (2)). The variances were adopted according to a reweighting procedure recommended by Koch (1999).

$$\rho_{i,j} = \sqrt{{\rho_{1_{i,j}}}^2 + {\rho_{2_{i,j}}}^2 + \ldots + {\rho_{k_{i,j}}}^2} \qquad (5)$$

with $\rho_{i,j} < 1$

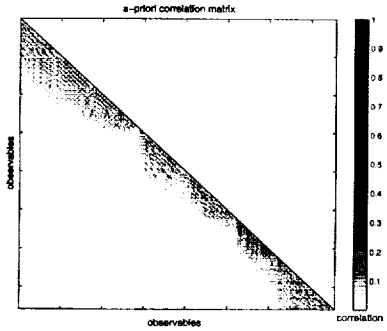

Figure 3. Full a priori correlation matrix R (main diagonal elements are 1)

5. Results

36 IRIS-S experiments from December 1994 till December 1998 were analysed using the OCCAM 3.4 VLBI software (Titov and Zarraoa, 1997). A simple parameterization was chosen in the least-squares fit: three coordinates and three clock parameters per station, wet tropospheric zenith delay parameters every four hours and corrections to the IAU nutation model (IERS Conventions (1996)). The a priori correlation matrices were designed according to steps 1.-3. as described in section 4. In this investigation, only a priori correlations were considered between temporally close observables and between observables of the same radio source. The results are presented in terms of baseline lengths (fig. 4, 5, 6, 7) and horizontal components (fig. 8, 9).

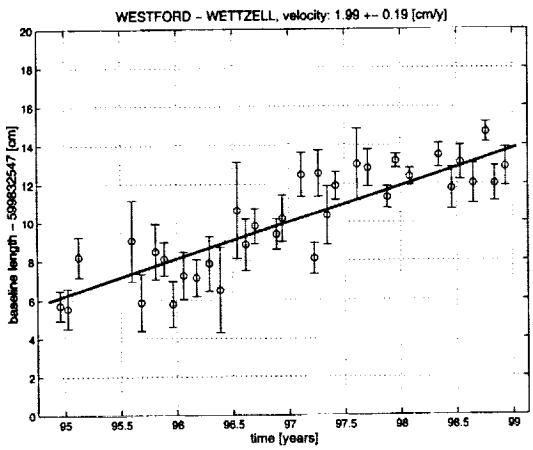

Figure 4. Length of baseline Westford-Wettzell obtained by the **"uncorrelated"** approach

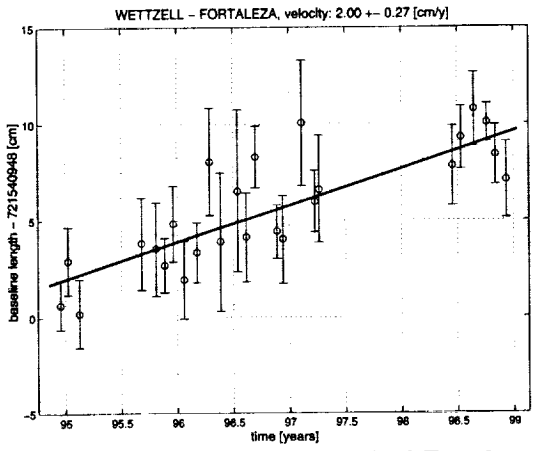

Figure 5. Length of baseline Westford-Fortaleza obtained by the **"uncorrelated"** approach

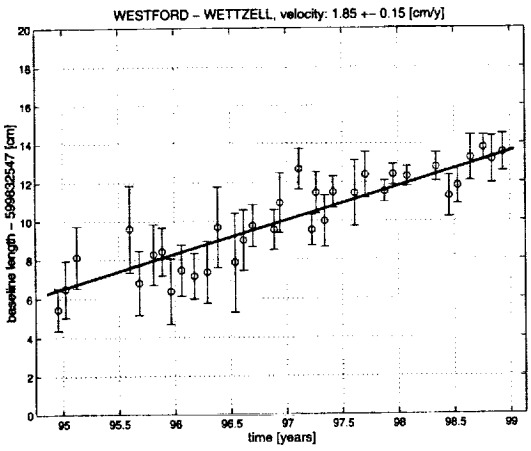

Figure 6. Length of baseline Westford-Wettzell obtained by the **"correlated"** approach

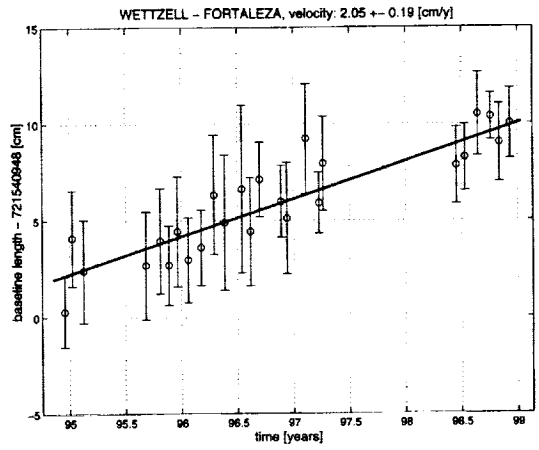

Figure 7. Length of baseline Westford-Fortaleza obtained by the **"correlated"** approach

The formal errors of the annual rates representing the scatter around the best-fit straight line, are significantly smaller for the "correlated" solutions, which shows that in spite of the usually higher formal errors of the individual baseline lengths, the repeatability of the baseline lengths has improved.

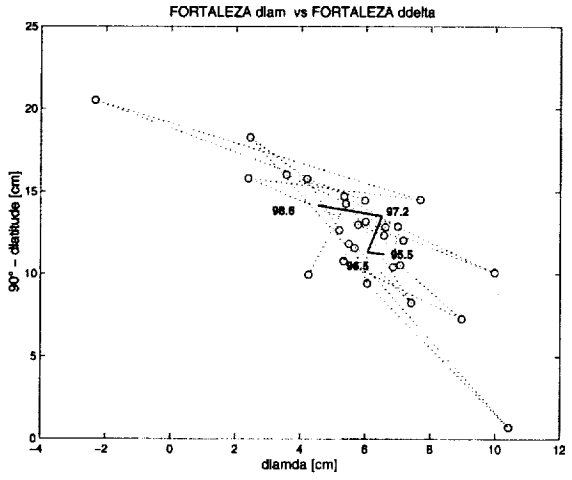

Figure 8. Horizontal components of Fortaleza, obtained by the **"uncorrelated"** approach

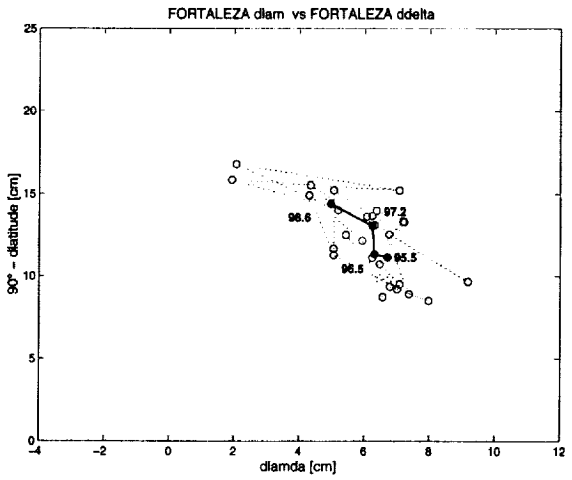

Figure 9. Horizontal components of Fortaleza, obtained by the **"correlated"** approach

The cluster of the horizontal coordinates has become much smaller; the repeatability of the station heights (not shown here) has improved, too. There are still unrealistic trends in the vertical components of most of the stations (see also table 2), which is a hint to a possible rotation of the VLBI network within the OCCAM solutions and has to be studied in more detail.

In table 1, the estimated annual rates of the baseline lengths are presented. All of them became more significant when applying the correlated approach. Most of the annual rates are similar to the results of the NASA/GSFC global solution (GSFC VLBI Group Homepage) and to the NUVEL-1a model. Differences can be explained by the short time base and the relatively small number of VLBI sessions used in this study (36 IRIS-S sessions during four years, only), compared to the global solution of the GSFC. Some of the baselines were determined by a few experiments, e.g. the Gilmore Creek radio telescope took part in experiments from 1997 to 1998, only. Table 2 shows the horizontal and vertical velocities of all stations in the IRIS-S network. All of them became more significant when using the correlated approach.

6. Conclusions

The comparisons show that by taking into account the a priori correlations between the observables, the formal errors of the results usually increase and hence become more realistic. The repeatability of the baseline lengths and of the spherical coordinates improves significantly, which is an indication that using the full variance-covarianace matrix is preferable to the "uncorrelated" approach. If the number of parameters to be estimated in the least-squares fit will be increased, the effect of neglecting a priori correlations will be less severe.

In this study, the a priori correlation coefficients were determined empirically from a sufficient number of VLBI sessions; thus they are a combination of mathematical and physical correlations. Another option could be to derive the physical correlations by external means, e.g. a procedure which was proposed by Treuhaft and Lanyi (1987) based on WVR measurements. Finally, it should be mentioned that the problem of neglected a priori correlations in GPS data analysis was discussed recently by Howind et al. (1999).

Table 1. Rates of baseline lengths obtained in this study, from the NASA/GSFC VLBI global solution, and the Nuvel-1a model.

Baseline	Rates of baseline lengths (this study, VLBI)[1]		GSFC (VLBI)[2]	Nuvel-1a
	uncorrelated [cm/y]	correlated [cm/y]	[cm/y]	[cm/y]
Westford-Wettzell	1.99 +-0.19	1.85 +-0.15	1.70 +-0.01	1.89
Westford-Fortaleza	0.16 +-0.51	0.13 +-0.33	0.09 +-0.12	0.17
Westford-Gilcreek	0.29 +-0.71	0.12 +-0.35	-0.03 +-0.01	0.00
Westford-Hartrao	0.91 +-0.63	0.11 +-0.50	0.96 +-0.07	1.20
Wettzell-Fortaleza	2.00 +-0.27	2.05 +-0.19	1.42 +-0.05	1.52
Wettzell-Gilcreek	-0.05 +-0.41	-0.06 +-0.28	1.04 +-0.02	1.06
Wettzell-Hartrao	-0.33 +-0.40	-0.90 +-0.34	-0.49 +-0.05	-0.66
Fortaleza-Gilcreek	-0.41 +-1.59	1.65 +-1.27	0.50 +-0.09	0.17
Fortaleza-Hartrao	2.17 +-0.44	1.88 +-0.41	1.84 +-0.14	2.46
Gilcreek-Hartrao	1.93 +-1.46	1.13 +-1.26	0.06 +-0.23	0.05

1) VLBI-Software: OCCAM 3.4, data from 1994–1998 (36 IRIS-S sessions)
2) VLBI-Software: CALC/SOLVE, data from 1979–1998 (several hundred sessions, global solution)

Table 2. Velocities of the spherical station coordinates obtained in this study.

Coordinates		uncorrelated [cm/y]	correlated [cm/y]
Wettzell	Δr	1.56 +-0.70	1.47 +-0.53
	$\Delta\lambda$	1.44 +-0.69	1.41 +-0.48
	$\Delta\delta$	-1.11 +-0.29	-1.04 +-0.19
Fortaleza	Δr	2.21 +-0.49	2.52 +-0.29
	$\Delta\lambda$	-0.53 +-0.38	-0.49 +-0.23
	$\Delta\delta$	0.96 +-0.56	1.12 +-0.32
Gilcreek	Δr	-1.89 +-0.84	-1.89 +-0.66
	$\Delta\lambda$	-2.18 +-2.88	-2.10 +-1.49
	$\Delta\delta$	-0.55 +-0.45	-0.21 +-0.43
Hartrao	Δr	2.23 +-0.51	1.29 +-0.46
	$\Delta\lambda$	-1.03 +-0.64	-0.85 +-0.53
	$\Delta\delta$	2.10 +-0.53	2.11 +-0.35

References

[1] Howind, J., Kutterer, H., Heck, B.: Impact of temporal correlations on GPS-derived relative point positions, Journal of Geodesy 73, p. 246-258, 1999.

[2] Koch, K.-R.: Parameter Estimation and Hypothesis Testing in Linear Models, Springer Verlag, 1999.

[3] Qian, Zhi-han: The Correlations on VLBI Observables and its Effects for the Determination of ERP, Columbus 1985, Proc. Vol.1, p. 369-165, 1985.

[4] Schuh, H., Wilkin, A.: Determination of Correlation Coefficients between VLBI-Observables, Proceedings of the 7th Working Meeting on European VLBI, Madrid, Spain, CSIC, A. Rius (ed.), p. 79-91, 1989.

[5] Titov, O., Zarraoa, N.: OCCAM 3.4 Users Guide, Communications of the Institute for Applied Astronomy (IAA), St. Petersburg, No. 69, 1997.

[6] Treuhaft, R. N., Lanyi, G. E.: The effect of the dynamic wet troposphere on radio interferometric measurements, Radio Science, Vol. 22, p. 251-265, 1987.

[7] ... Homepage of GSFC VLBI group: http://lupus.gsfc.nasa.gov

[8] ... IERS Conventions (1996), D. D. McCarthy (ed.), IERS Technical Note 21, Observatoire de Paris, 1996.

L. Petrov: Optimal Estimation of the Earth Orientation Parameters Using VLBI, IVS 2000 General Meeting Proceedings, p.243–246
http://ivscc.gsfc.nasa.gov/publications/gm2000/petrov2

Optimal Estimation of the Earth Orientation Parameters Using VLBI

L. Petrov

Geodetic Institute of the University of Bonn
e-mail: petrov@picasso.geod.uni-bonn.de

Abstract

The problem of the best strategy for estimation of the Earth orientation parameters using VLBI is considered. The present strategy for evaluation of six parameters for each session, UT1, UT1 rate, pole coordinates, nutation offsets, contains internal contradictions and it has known deficiencies. An alternative parameterization is presented. The ways of its implementation and some results are discussed.

1. Introduction

Aims of the determination of the Earth orientation parameters (EOP) are a) to provide a numerical model to our consumers — to answer what was the Earth's orientation in the past and what will be the Earth's orientation in the future; b) to improve our knowledge of the Earth interior — roughly speaking to measure deviations from the rotation of the absolutely solid body.

Two approaches for a description of a phenomenon of Earth rotation are used: kinematic and dynamic. The kinematic approach deals with the question *how* the Earth is rotating. The dynamic approach answers the question what are *the reasons* for the variations in Earth rotation. The kinematic approach considers constituents of the rotation as predictable/unpredictable. The dynamic approach considers them as deterministic/stochastic. As a result EOP are represented by three Euler angles as a function of time in the framework of the first approach and as a zoo of different components: precession, nutation, polhode, high-frequencies variations and so on, in the framework of the second approach.

The choice of the approach inspires the particular strategy of parameter estimation. Two extremes are possible: 1) the theory describing the phenomenon is perfect and it is formulated up to a finite set of parameters; 2) no theory is established and the character of functional dependence is also a subject of evaluation. The more degrees of freedom — the less certain results. The more strict theory — the less chances to disclose new effects.

The dynamic approach is nearer to the first strategy of EOP estimation, while the kinematic approach assumes more freedom in parameterization.

Earth rotation is a complicated process and there is no parameterization which would be optimal for all problems and for all data sets. The choice of the best parameterization depends on the selected estimation strategy and on the properties of available data.

2. Strategy of EOP Estimation

Constituents of Earth rotation which are considered in the framework of the kinematic approach are summarized in table 1.

Table 1. Constituents of Earth rotation as reckoned from the rotating Earth

	Component	Time scales	Frequencies	
1	Slowly variating terms	$> 2^d$	$< 4 \cdot 10^{-5}$	rad/sec
2	Harmonic components	$8^h - 18.^a6$	$1 \cdot 10^{-8} - 2 \cdot 10^{-4}$	rad/sec
3	High frequency aharmonic components	$8^h - 2^d$	$4 \cdot 10^{-5} - 2 \cdot 10^{-4}$	rad/sec

A traditional strategy of EOP estimation implies a two-step procedure: a) splitting the dataset into 24-hour segments (sessions) and adjustment of 6 parameters: X_p, Y_p, $UT1$, $\frac{\partial}{\partial t}UT1$, $\Delta\psi$, $\delta\epsilon$ for each session; b) analysis of the obtained EOP time series: filtering, LSQ fitting and etc.

Each coordinate of polar motion is modeled by two parameters: a pole coordinate and a daily nutation offset. However, these parameters are separated perfectly only if duration of the session is exactly one Earth rotation cycle and changes of nutation angles during the session are negligible. In practice both these assumptions are violated, and the resulting series of pole coordinates and nutation angles are corrupted. This approach does not allow one to estimate a constituent in the pole coordinates which has a frequency far away from zero or diurnal frequency, for example semidiurnal polar motion. More important, the traditional method has an internal contradiction. If we assume that nutation is a purely harmonic process, with known frequencies, which corresponds to a quasi-diurnal polar motion then we need to estimate only amplitudes and phases of the harmonic components, but not to represent nutation angles as a time series. If we assume that there are aharmonic components in nutation, e.g. free core nutation, with a broad spectrum, then we cannot strictly separate them from the pole coordinates.

I proposed an alternative way: a one-step approach. All parameters are determined in one global solution. The following parameters are estimated:

- Station positions and velocities, source coordinates.
- X_p, Y_p, $UT1$ and their rates of change for each session. They model slowly varying components.
- Set of sine and cosine terms for X_p, Y_p and $UT1$ at frequencies within the diurnal and semidiurnal bands (with respect to the rotating Earth). They include precession, Celestial Ephemeris Pole offset, nutations, tidal diurnal and semi-diurnal EOP variations, ad hoc harmonic variations. Frequencies are taken from theory [1].
- Linear spline for X_p, Y_p and $UT1$ with segment length 1.5 hours. These parameters model stochastic components in Earth rotation.
- Nuisance parameters.

However, this choice of parameterization has some difficulties:

- The theoretical spectrum of EOP variations has multiplets: a set of components with closely-spaced frequencies which cannot be resolved using the given data set.
- There are synonymous constituents, e.g. nutation and diurnal high frequency variations in polar motion.
- Three constituents are overlapping and are not independent:
  - A session-average parameter and an average value of linear spline over the session are indistinguishable.
  - A session-rate parameter and a linear rate of change of linear spline over the session are indistinguishable.

  - There is a quasi-linear dependence between a harmonic parameter and linear spline. The more nodes of the spline that are used, the better a linear spline approximates a harmonic signal.
- There are "blind" frequencies due to sampling.

But we can overcome these difficulties.

- Set the lowest frequency. The harmonic components with frequencies which are nearer than the lowest frequency are grouped into multiplets. A common narrow-band amplitude and phase are estimated for all aliases. The assumption that ratios of amplitudes within a narrow band are known from theory is used.
- Exclude synonymous frequencies.
- Impose stiff de-correlation constraints on linear spline for each session:
  - Average is zero (de-shifting);
  - Average rate is zero (de-trending);
  - Sine and cosine components at the specified frequencies are zero (de-harmonization).

3. Results

The approach outlined above has been implemented in the CALC/SOLVE program package. All available VLBI observations for 1979.7–2000.0 ($2.8 \cdot 10^6$ observations, 2961 sessions) were used in a single combined solution.

There were 736 harmonic parameters estimated. They include parameters for precession, celestial pole offset, harmonic parameters at 148 nutation frequencies, 34 additional tidal frequencies and 3 ad hoc frequencies. The lowest frequency $1 \cdot 10^{-8}$ rad/sec (period 18.6 years) was used. The 2559 daily pole coordinates and UT1 as well as their rates and the 44150 parameters of linear spline for pole coordinates and UT1 were obtained.

Formal uncertainties of harmonic variations are 20-300 prad. The largest correlation of 0.91 is between the 18.6 years terms nutation and precession: Only 89 correlations out of 270 480 are greater than 0.7. The estimates of stochastic components of EOP are shown in the figures 1–2.

Figure 1. Residual variations in Earth rotation for a routine VLBI experiment

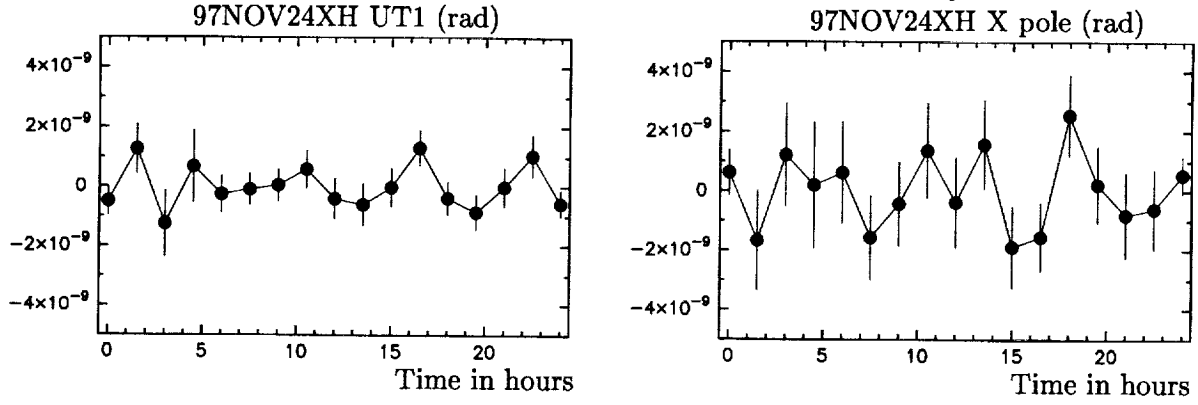

Figure 2. Residual variations in Earth rotation for one of the best VLBI experiments

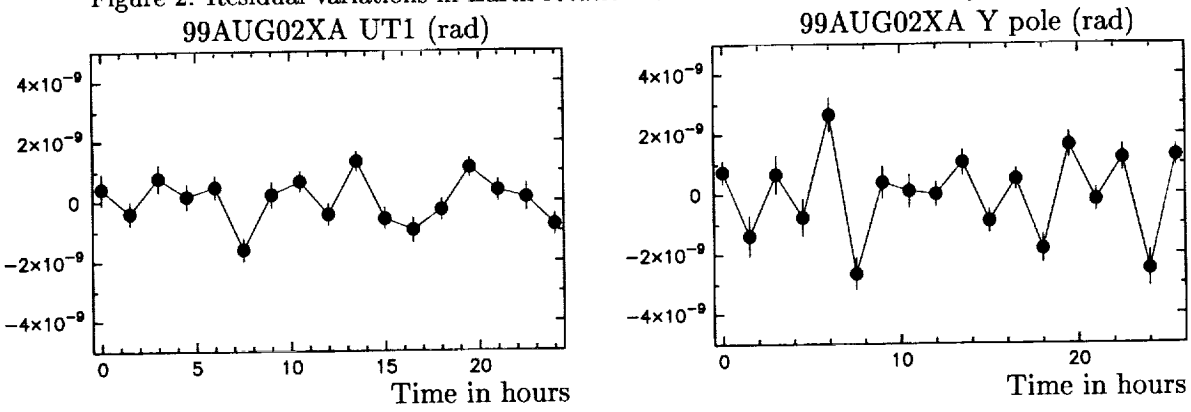

Results of comparison of the estimates of precession in longitude and obliquity rate are shown in table 2. Comparison with the empirical nutation coefficients obtained by Souchay et al. [2] showed that the differences are within 1-2 nrad.

Table 2. Estimates of precession

Precession in longitude:	-2.96 ± 0.02 mas/yr	(IERS96: -2.96 mas/yr)
Obliquity rate:	-0.27 ± 0.009 mas/yr	(IERS96: -0.23 mas/yr)

4. Conclusion

- It is shown that an empirical expansion of harmonic variations in Earth rotation can be obtained in one step.
- Advantages of the proposed approach:
  - A uniform treatment of harmonic variations in Earth rotation at diurnal and semi-diurnal frequencies;
  - No $\Delta\psi$, $\Delta\epsilon$ time series.
  - An ability to estimate correctly short-period nutation amplitudes.
- Disadvantage:
  - High computation cost.

References

[1] J. Souchay, B. Loysel, H. Kinoshita, M. Folguera, "Correctiona and new developments in rigid earth nutation theory", Astron. Astrophys. Suppl. Ser., vol. 135, pp. 111-131, 1999

[2] J. Souchay, M. Feissel, C. Bizouard, N. Capitane, M. Bougeard, "Precession and nutation for a non-rigid Earth: comparison between theory and VLBI observations", Astron. Astrophys., vol. 299, p. 277-287, 1995

Daniel MacMillan et al.: Improvement of VLBI EOP Accuracy and Precision, IVS 2000 General Meeting Proceedings, p.247–251
http://ivscc.gsfc.nasa.gov/publications/gm2000/macmillan

Improvement of VLBI EOP Accuracy and Precision

Daniel MacMillan [1], *Chopo Ma* [2]

[1)] *NVI, Inc./NASA Goddard Space Flight Center*
[2)] *NASA Goddard Space Flight Center*
Contact author: Daniel MacMillan, e-mail: dsm@leo.gsfc.nasa.gov

Abstract

In the CORE program, EOP measurements will be made with several different networks, each operating on a different day. It is essential that systematic differences between EOP derived by the different networks be minimized. Observed biases between the simultaneous CORE-A and NEOS-A sessions are about 60-130 μas for PM, UT1 and nutation parameters. After removing biases, the observed rms differences are consistent with an increase in the formal precision of the measurements by factors ranging from 1.05 to 1.4. We discuss the possible sources of unmodeled error that account for these factors and the biases and the sensitivities of the network differences to modeling errors. We also discuss differences between VLBI and GPS PM measurements.

1. Introduction

The international VLBI community is involved in a program called CORE (Continuous Observations of the Rotation of the Earth) to make continuous EOP (Earth Orientation Parameter) measurements beginning in about 2003 ramping up from 2.5 24-hour sessions per week during 1999. Two necessary elements of CORE are the MarkIV correlator that can process much more data and the MarkIV VLBI hardware that will provide much more precise measurements due to an increase in recorded bandwidth by a factor of eight. The MarkIV correlator will be capable of supporting continuous data acquisition. To make continuous measurements of EOP, several networks will be used. Therefore, for the CORE program to be successful, EOP derived from the different VLBI networks need to agree. To investigate this, we have been running a series of VLBI experiments starting in 1997, that are either simultaneous (CORE-A) with the weekly NEOS network or on adjacent days (CORE-B). Here we present results of comparisons of EOP measurements made by the CORE-A and NEOS networks as well comparisons with simultaneous GPS measurements. We also report on the differences between PM rates estimated by the two VLBI networks and GPS.

2. CORE-NEOS Comparisons

The precision of VLBI measurements has continued to improve by about an order of magnitude each decade. The best VLBI measurements of UT1 and PM have a precision of 30–40 μas. One of the principal problems with high precision VLBI EOP is determining the measurement accuracy. In the CORE program, EOP measurements will be made with several different networks, where each network will operate on a different day. We need to determine how much systematic and random error there is in the differences between EOP derived from different networks. Our basic test of this consists of examining the differences between EOP derived from independent VLBI measurements made by different networks. From the history of VLBI sessions from 1980 to the

present, there are about 300 simultaneous sessions. Comparisons of these simultaneous sessions imply that the formal EOP errors should be increased by a factor of 1.5–2.0. It is difficult to determine from this comparison whether the differences are caused by random or systematic errors since the formal errors range over two orders of magnitude.

To determine the current level EOP precision and accuracy, we have compared measurements made by the CORE-A and NEOS networks. The least squares estimation program (SOLVE) used in the analysis and the theoretical models applied in the analysis are generally described by Ma et al. [1990]. The weekly NEOS network uses Kokee, Green Bank, Fortaleza, Ny Ålesund, and Wettzell. The CORE-A network sessions are simultaneous with NEOS sessions and nominally use antennas at Fairbanks, Westford, Algonquin Park, Hobart, Hartebeesthoek, and Matera.

Based on the rms differences from all CORE/NEOS experiments during 1997-1999 (without removing any biases), and the χ^2/dof of these differences (262 μas and 2.9 for PM-X, 152 μas and 1.5 for PM-Y, 152 μas and 2.8 for UT1), there are clearly unmodeled sources of random or systematic error. Over this time period the actually observing networks have varied from the nominal set of stations because of unavailability of sites for certain observing sessions. A large component of the EOP differences is due to changes in networks. Of the 59 CORE-A/NEOS experiment pairs, 15 pairs used exactly the nominal set of stations. The statistics of the differences for this reduced set of experiments is given in Table 1. After removing the biases, the residual rms scatter for each difference pair is 100–150 μas, where the largest residual scatter is for PM-X. The observed rms scatter is somewhat greater than the formal uncertainty in each case. The χ^2/dof indicate that the formal uncertainties are too small, especially for UT1 for which the formal error should be scaled up by a factor of about 1.4.

Table 1. NEOS - CORE-A Offset Differences

Component	Bias (μas)	χ^2/dof	Wrms (μas)	$< \sigma_{CORE} >$ (μas)	$< \sigma_{NEOS} >$ (μas)
PM-X	-133±37	1.1	152	94	113
PM-Y	- 57±31	1.1	126	84	92
UT1	127±23	1.9	122	54	72
$\psi \sin\epsilon$	-97±24	1.4	106	69	81
ϵ	90±23	1.6	109	64	82

3. Station Position Errors

The observed biases between CORE and NEOS measurements implies that there are errors in the underlying TRF. The observed residual scatter of the differences imply that there is significant unmodeled nonlinear station motion. To quantify this, we can estimate the size of the effect of unmodeled or mismodeled station motion error by simulating the effect of a 1 mm station displacement at each of the sites in the CORE-A and NEOS networks. The first result of this simulation is that horizontal displacements couple much more strongly to EOP estimates than vertical displacements (by a factor of 5–10). This is fortunate in the sense that most geophysical effects result predominantly in vertical change. A second result is that EOP is much more sensitive

to motion at certain sites than others. For all components, this horizontal sensitivity ranges from 3–25 μas/mm depending on the site. If one assumes that unmodeled errors are random, these simulations show that the combined effect of a 1 mm rms unmodeled variation in the horizontal coordinates of all stations in the CORE-A network yields EOP rms errors of 30–40 μas.

There are several possible sources of unmodeled error that could contribute to observed residual station position motion. The current tropospheric gradient delay model [MacMillan and Ma, 1997] used in our VLBI analysis is reasonably good at describing large spatial scale (> 50 km) gradients. Applying this model in our analysis reduced residual EOP scatter by about 50% (about 100 μas). The current model has larger errors in modelling smaller scale wet troposphere turbulence. Errors in tropospheric gradient modeling are probably not more than 20% of the effect of the current gradient model or about 15–30 μas.

There are errors in the tidal ocean loading model but these should primarily affect subdaily EOP estimation (see Scherneck and Haas, [1999]). We have estimated the tidal loading amplitude adjustments from the a priori Schwiderski model values for the CORE and NEOS sites directly from VLBI data. In the vertical, the adjustments are as large as 5 mm (M2, K2, and O2 are the largest). In the horizontal, the adjustments are much smaller. They are as large as 1.5 mm for subdaily tidal components and as large as 1 mm for tidal periods longer than 1 day.

In our standard VLBI processing, the vertical effect of pressure loading is modeled using only local pressure and a pressure admittance that is site dependent [MacMillan and Gipson, 1994]. The horizontal effect is about a third of the vertical and is not currently modeled. In order to model the horizontal, it is necessary to compute pressure loading by convolving the spatial pressure distribution with a loading Green's function. Haas and Scherneck [1997] have done this and show that the effect of pressure loading is 0.5–1.0 mm rms in the horizontal coordinates. Based on the above simulations, the horizontal effect of atmospheric loading is then expected to contribute 20–40 μas of rms variation to each EOP parameter. Unmodeled tropospheric and loading effects would then contribute 30–60 μas of rms EOP variation.

The comparison in Table 1 indicates that there are significant biases of 60–130 μas between EOP estimates from the CORE-A and NEOS networks. When EOP parameters are estimated, it is assumed that site positions are evolving linearly at a rate that is close to that given by the NUVEL-1A plate motion model. The resulting set of estimated site positions and velocities is the terrestrial reference frame (TRF). The large observed EOP biases are an indication that there are errors in the underlying TRF. We are currently investigating this error and methods for correcting it. One test we have done is to compute the TRF from different time periods of VLBI data. Using a TRF based on data from 1997–99 reduced the bias for PM-X significantly to -54 μas, but the residual scatter increased to 181 μas. However, with a TRF generated from 1990–99 data, there was little effect on the network biases.

4. VLBI and GPS PM Comparison

We have also compared VLBI PM estimates with GPS estimates. The IGS "Final" series that we used is produced from a combination of GPS analysis center solutions. The VLBI estimates are given for the midpoint of each 24-hour session, which occurs at approximately 6 hours UTC. We have simply interpolated the IGS series given at half integer Julian days to the VLBI times. Table 2 shows the difference between PM estimates from the IGS and the VLBI networks when only the 15 identical networks are considered.

Table 2. VLBI-IGS Offset and Rate Differences

Component	Offsets			Rates		
	Bias	χ^2/dof	Wrms	Bias	χ^2/dof	Wrms
CORE-IGS						
PM-X	-260±25	1.3	111	160±60	0.7	199
PM-Y	134±24	1.5	113	-50±75	1.4	340
NEOS-IGS						
PM-X	-389±30	0.8	101	80±97	1.0	385
PM-Y	83±26	1.5	122	-94±82	1.4	382
IGS PM-X $<\sigma>$	40 μas	84 μas/d				
IGS PM-Y $<\sigma>$	50 μas	68 μas/d				

There are significant biases of 300–400 μas between the IGS PM-X estimates and both VLBI estimates. As discussed above, these biases are likely caused by errors in the underlying TRFs used in the respective VLBI and GPS solutions. For PM-Y, the biases are less than 100 μas. After removing a bias, the wrms differences between the IGS and VLBI estimates is reduced to 100–150 μas. (If all 59 VLBI network pairs are included, these wrms differences are 150–200 μas.) The χ^2/dof imply that the formal errors should be multiplied by a factor of at most 1.2. The formal precision of the GPS PM measurements given under Table 2 is better than the VLBI formal precision (see Table 1). This is because the number of globally distributed sites used in the GPS analysis (30–40) is much larger than the number of sites in the VLBI networks. The wrms differences between the IGS estimates and the two VLBI estimates are generally smaller than the difference between the VLBI estimates. If errors are random, this implies that the observed precision of the IGS estimates is better than the VLBI estimates. Assuming random errors, the three differences between GPS and two VLBI networks yields observed PM-X precision of 112 μas for CORE-A, 103 μas for NEOS, and $<$ 100 μas for IGS. For PM-Y, we get 83 μas for CORE-A, 94 μas for NEOS, and 77 μas for IGS.

5. EOP Rates

We have done some comparison of EOP rates from the two VLBI networks. The rates were estimated at noon rather than at the session midpoints in order to compare with GPS rates given at integer Julian days. The comparison results are shown in Tables 2 and 3. The χ^2/dof of 2.1 for PM-Y implies that the observed error is underestimated by the formal error by about a factor of 1.4. Doing the comparisons with all 59 VLBI experiments does not significantly change these results. Comparison with IGS PM rates indicates that the precision of the observed GPS rates are significantly better than the VLBI PM rates, particularly for Y-pole. If one assumes that the observed residual differences are random, then the observed PM-X rate precision is 153 μas/d for GPS, 127 μas/d for CORE-A, and 354 μas/d for NEOS. For PM-Y, the observed precision is $<$ 100 μas/d for GPS, 412 μas/d for CORE-A, and 441 μas/d for NEOS. Based on the NEOS/CORE differences, the observed VLBI LOD precision is about 230 μas/d assuming that the two networks are equally precise.

Table 3. NEOS - CORE-A Rate Differences

Component	Bias (μas/d)	χ^2/dof	Wrms (μas/d)	$< \sigma_{CORE} >$ (μas/d)	$< \sigma_{NEOS} >$ (μas/d)
PM-X	-93±113	0.7	376	235	375
PM-Y	-36±110	2.1	610	304	316
UT1	-71±68	1.5	323	149	222

6. Conclusions

Analysis of the 15 identical NEOS/CORE network pairs where only the nominal NEOS and CORE stations observed shows that the formal errors of the measurements are too small by a factor of 1.05–1.4, where the largest factor is for UT1. We have found evidence of biases between the EOP measurements made by the two networks as well as between PM measurements from these VLBI networks and from GPS. More investigation is needed to correct these errors, which are probably caused by errors in the underlying VLBI or GPS TRFs. The rms difference between PM rates from the VLBI networks are mostly comparable to those between each VLBI network and GPS. The exception, which will be investigated, is that the difference between CORE and NEOS is twice as large for PM-Y as for PM-X.

References

[1] Ma, C., J. M. Sauber, L. J. Bell, T.A. Clark, D. Gordon, W. E. Himwich, and J. W. Ryan, Measurement of horizontal motions in Alaska using very long baseline interferometry, J. Geophys. Res., 95(B13), 21991-22011, 1990.

[2] MacMillan, D. and C. Ma, Atmospheric gradients and the VLBI terrestrial and celestial reference frames, Geophys. Res. Lett., 24, 453-456, 1997.

[3] MacMillan, D.S. and J. Gipson, Atmospheric pressure loading parameters from very long baseline interferometry observations, J. Geophys. Res, 99,18081-18087, 1994.

[4] Haas, R., Scherneck, H.-G., H. Schuh, Atmospheric loading corrections in geodetic VLBI and determination of atmospheric loading coefficients, Proceedings of the 12th Working Meeting on European VLBI for Geodesy and Astrometry, Honefoss (Norway), 1997, September 12-13, ed. Bjorn R. Pettersen, 122-132, ISBN 92-90408-41-2, 1997.

[5] Scherneck, H.-G., and R. Haas, Effect of horizontal displacements due to ocean tide loading on the determination of polar motion and UT1, Geophys. Res. Lett., 26, 501-504, 1999.

A. Nothnagel et al.: First Results of the 1999 Tsukuba - Wettzell UT1 Test Series, IVS 2000 General Meeting Proceedings, p.252–256
http://ivscc.gsfc.nasa.gov/publications/gm2000/nothnagel1

First Results of the 1999 Tsukuba - Wettzell UT1 Test Series

A. Nothnagel [1], *G. Engelhardt* [2], *H. Hase* [2], *R. Kilger* [3], *S. Ogi* [4], *K. Takashima* [4], *V. Thorandt* [2], *D. Ullrich* [2]

[1] *Geodetic Institute of the University of Bonn*
[2] *Bundesamt für Kartographie und Geodäsie*
[3] *Forschungseinrichtung Satellitengeodäsie*
[4] *Geographical Survey Institute of Japan*

Contact author: A. Nothnagel, e-mail: nothnagel@uni-bonn.de

Abstract

In May and June 1999 the radio telescopes of the Wettzell Geodetic Fundamental Station in Germany and of the Geographical Survey Institute of Japan at Tsukuba observed a series of quasi-daily VLBI sessions of short duration for precise determination of UT1-UTC. Similar to routine UT1 observations on the Wettzell - Green Bank baseline this long east-west baseline is ideal for the accurate determination of UT1. For the first time a K4 data acquisition terminal was used for this type of observation. First analyses produce one-sigma formal errors of $\pm 12 \mu s$ with a bias of -55 μs relative to the IERS C04 Earth orientation parameter series.

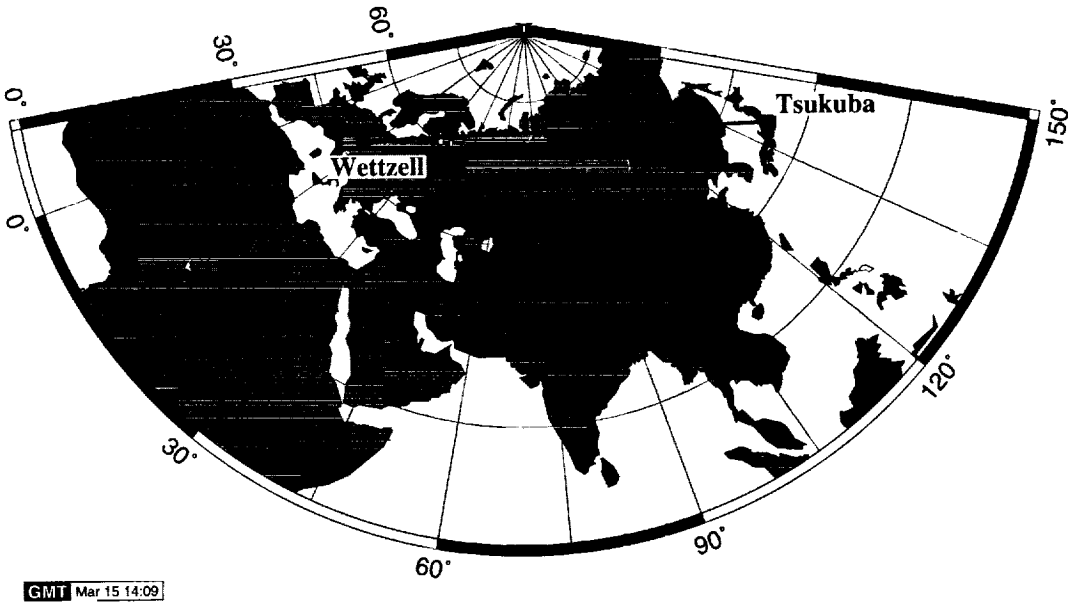

Figure 1. Tsukuba - Wettzell baseline.

1. Introduction

For almost two decades Earth rotation is monitored in a concerted effort by many agencies using geodetic Very Long Baseline Interferometry (VLBI) (e.g. CAMPBELL, this issue). Special

emphasis is placed on regular determinations of UT1 which can be measured accurately over a longer time span only by VLBI. In a long-standing series on a single east-west baseline with telescopes at Green Bank, West Virginia, USA, and at Wettzell Geodetic Fundamental Station in Bavaria (Germany) regular observations have been carried out for the determination of UT1 in short duration VLBI sessions (EUBANKS et al. 1994).

Due to the lack of a second series of this type these measurements remain uncontrolled through other series. Only adjacent sessions observed with multi-station intercontinental networks over observing periods of 24 hours each provide some kind of independent bound to the series. So far only two short series observed on another east-west baseline almost in parallel to the Wettzell - Green Bank sessions established an independent control (NOTHNAGEL et al., 1994).

The new 32 m radio telescopes of the Geographical Survey Institute of Japan at Tsukuba together with the 20 m radio telescope of the Wettzell Geodetic Fundamental Station offer the possibility to set up similar observing sessions of short duration. Both stations form an east-west baseline of approximately 8450 km length which theoretically provides an excellent sensitivity for the determination of UT1 (Fig. 1). In order to investigate the sensitivity of this baseline a test observing campaign was set up with these two stations. This campaign was also planned as a pilot project which aimed at studying the feasibility of such observations as a regular service.

2. Observations

Between May 25 and June 18, 1999 a series of 13 sessions was observed on the Wettzell - Tsukuba baseline with four different radio sources and 20 scans per session. In an observing session for the determination of UT1, radio sources near the celestial equator strongly contribute to the accuracy of the results. On the other hand the long east-west baseline between Tsukuba and Wettzell which is located fairly far in the north provides only a very limited area of mutual visibility of the sky near the equator. Therefore, the sidereal time for the observations had to be selected carefully in order to find a radio source near the equator which is observable long enough for several observations (Fig. 2).

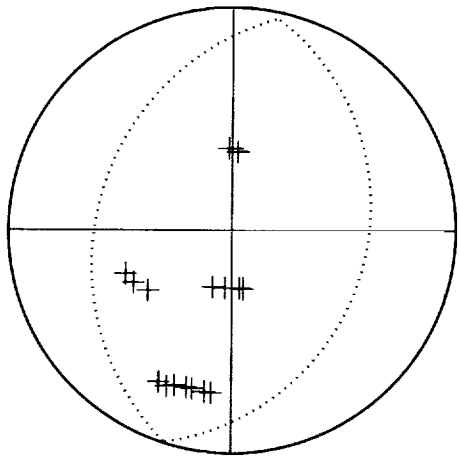

Figure 2. Stereographic projection of mutually visible sky for the Tsukuba – Wettzell baseline together with observations carried out in the schedule.

In preparing the observing schedule we tried to keep the observations above an elevation cut-off of 20°. However, the long baseline and the need for a number of observations near the celestial equator required that a small number of the observations had to be scheduled below 20°but still above 10°elevation. Each observing session lasted about 70 minutes with identical observing schedules for each day just being shifted by 4 minutes per day to match the sidereal time.

In order to calibrate the ionospheric refraction dual frequency observations were carried out with the same frequency setup as used in the majority of Mark III VLBI observations, i.e. 8 channels between 8212.99 and 8932.99 MHz (X band) and 6 channels between 2220.99 and 2345.99 MHz (S band). The VLBI data was recorded with a K4 data aquisition terminal which was on loan at Wettzell for the period of the campaign.

3. Data Analysis

The analysis of short duration measurements for the estimation of selected components of Earth rotation parameters has to rely on externally determined terrestrial and celestial reference frames as well as on the remaining components of Earth rotation and on precession and nutation models. The coordinates of the two stations were computed within a global solution of a large number of geodetic VLBI Mark III sessions available at the Bonn Geodetic Institute. Since the Tsukuba 32 m telescope is fairly young and has not yet participated in so many sessions its coordinates and velocity are not yet accurate to the full extent possible. The radio source positions of the International Celestial Reference Frame (ICRF) 1995 and its first extension (MA et al. 1996) were used. The station coordinates and the radio source positions provide a framework which had to be kept fixed in the analysis. Precession and nutation are modeled according to the IERS Conventions 1996 (MCCARTHY, 1996).

All sessions of the campaign were individually reduced using the CALC 9.1/SOLVE software system (CAPRETTE et al. 1990, GORDON 1999). The hydrostatic component of tropospheric refraction was calibrated using the Saastamoinen dry zenith delay computed from surface pressure together with improved constants according to DAVIS et al. (1985) and the NMF 2.0 mapping function (NIELL 1995) based on global meteorological data.

In the least squares adjustments of the east-west baseline measurements only UT1-UTC, the offset and rate between the two station clocks as well as one troposphere offset at each station were estimated. The troposphere offsets should account for the refraction caused by water vapor applying partial derivatives according to the NMF2.0 wet mapping function. The weights of the observations were adjusted to produce a unity χ^2 per degree of freedom by quadratically adding an average noise floor of 38 psec individually for each session. The effects of high frequency variations in UT1 were corrected for by applying corrections to the results computed from the model developed by GIPSON (1996).

4. Results

The formal errors (1σ) of the UT1-UTC determinations range from ± 6 to ± 17 microseconds of time (μs) with an average of ± 12 μs. However, the geometry may provide non-optimal sensitivity for systematic errors like those of the refraction model as compared to a schedule with more radio sources and a wider sky distribution as used in the Wettzell - Green Bank intensive series.

In order to investigate the influence of atmospheric refraction on the UT1-UTC results a closer

look has been given to the zenith wet delays estimated from the observations. At Tsukuba zenith wet delays of 646 picoseconds (ps) with a scatter of ±275 ps were estimated while at Wettzell the wet delay was estimated with an average of 397±81 ps. These values when converted into excess path lengths result in about 19 and 12 cm, respectively. The air temperatures at Tsukuba are all, except at one day, at or above 21° C with moderate relative humidities at the ground while at Wettzell the temperatures ranged from 10 to 20° C. Considering these meteorological circumstances the estimated zenith wet delays at both stations are quite plausible indicating that the observing schedule is robust.

For a reliable estimate of the absolute accuracy of our results we performed a direct comparison of the UT1 results with those of the IERS C04 series (IERS, 1999). Figure 3 displays the results of the 1999 series as differences to the IERS C04 daily normal points. Since our series has different reference epochs for each data point a quadratic interpolation was chosen for the computation of the respective data points in the C04 series. Comparisons with other methods like cubic spline interpolations yielded very similar results for the individual differences.

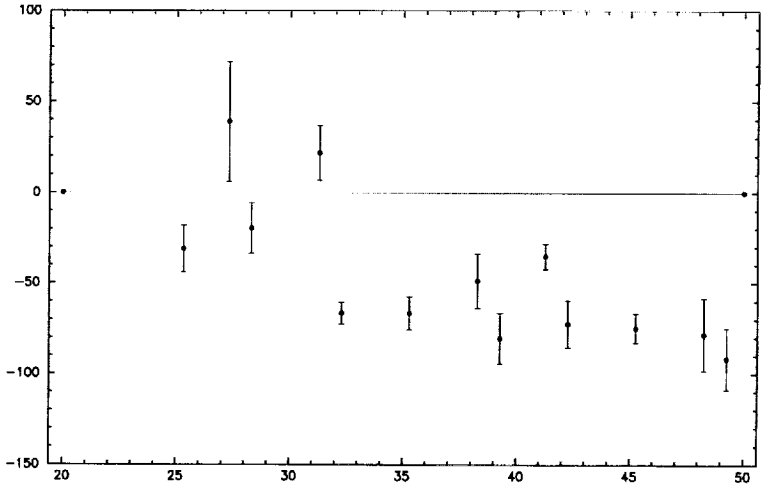

Figure 3. Differences relative to IERS C04 in μs at days since May 1, 1999.

A visual inspection of the residuals shows a picture which can be separated in two parts. The first four sessions seem to have a different behaviour than the rest of the sessions. However, there could easily be a linear trend in the data as well. This deficit of a clear interpretation of the residuals show already that the number of sessions is much too small to draw solid conclusions.

From a purely numerical point of view an offset of -55.1 ± 7.4 μs exists but, due to the fairly large deviations at the beginning of the series, is accompanied by an RMS of 25.6 μs. An offset of the series relative to the IERS UT1-UTC results may be attributed to a possible inconsistency in the terrestrial reference frame caused by a comparably low number of network sessions in which Tsukuba has taken part so far.

5. Conclusions and Outlook

This VLBI test series aimed at checking the feasibility of quasi-daily determinations of UT1-UTC with short duration sessions on the Tsukuba - Wettzell baseline. This baseline is much

longer than the Wettzell - Green Bank baseline which is used regularly for the determination of UT1-UTC with daily sessions of short duration. The longer baseline provides a higher sensitivity for changes in UT1 but, on the other hand, heavily restricts the mutual visibility of sources near the celestial equator which are of crucial importance for the determination of UT1. Therefore, special consideration has to be given to the selection of the radio sources and the time of day of the observations. Taking into account that only a very small number of sessions was observed the series can be considered a success. The accuracies achieved seem to be comparable to those of the daily Wettzell - Green Bank sessions although a much longer series has to be observed for conclusive evidence of the accuracy on this baseline. Using a K4 recording terminal is by all means equivalent to using a Mark III data acquisition terminal since it permits the use of the same frequency setup and bandwidth.

The analysis of the data is planned to be refined by using GPS induced zenith wet delays for both stations which can be computed from adjacent IGS GPS stations. More sessions of the Tsukuba 32 m telescope in the worldwide VLBI network will help to improve its coordinates and velocity reducing the effects of reference frame uncertainties. This will reduce and eventually eliminate the reference frame induced offset relative to the IERS series. Finally, it can be stated that this test series is a good basis for further single baseline observations on this baseline. Routine observations would be a very good complement to existing VLBI series for Earth rotation determinations. They would help to place upper bounds on the absolute accuracy, they may serve as an independent backup and to control each other.

6. References

Caprette D.S., C. Ma, J.W. Ryan (1990) *Crustal Dynamics Project Data Analysis - 1990* NASA Technical Memorandum 100765, A-1, NASA Goddard Space Flight Center, Greenbelt MD

Davis J., T.A. Herring, I.I. Shapiro, A.E.E. Rogers, G. Elgered (1985): *Geodesy by Radio Interferometry: Effects of atmospheric modelling errors on estimates of baseline length.* Radio Science, Vol. 20, 1593-1607

Eubanks M., B.A. Archinal, M.S. Carter, F.J. Josties, D.N. Matsakis, D.D. McCarthy (1994) *Earth Orientation Results from U.S. Naval Observatory VLBI Program.* IERS Technical Note 17, Observatoire de Paris, R65-R79

Gipson J. (1996) *VLBI Determination of Neglected Tidal Terms in High Frequency Earth Orientation Variation.* JGR, **101**, No. B12, 28051-28064

Gordon D.G. (1999) *Calc 9 Release Notes* Internal Report, NASA Goddard Space Flight Center, Greenbelt MD

IERS (1999), data publically available under http://hpiers.obspm.fr/webiers/results/eop/README.html

Ma C., M. Feissel (eds.) (1996) *Definition and Realization of the International Celestial Reference System by VLBI Astrometry of Extragalactic Objects.* IERS Technical Note 23, Observatoire de Paris, Paris

McCarthy D.D. (ed.) et al., (1996) *IERS Standards 1996* IERS Technical Note 21, Observatoire de Paris, Paris

Niell A.E. (1996): *Global mapping functions for the atmosphere delay at radio wavelengths.* J. of Geophys. Res., Vol. 101, No. B2, 3227-3246

Nothnagel A., Q. Zhihan, G.D. Nicolson, P. Tomasi (1994) *Earth Orientation Determinations by Short Duration VLBI observations.* Bulletin Géodésique, **86** 1-6

Hans-Georg Scherneck et al.: Ocean Loading Tides For, In, and From VLBI, IVS 2000 General Meeting Proceedings, p.257–262
http://ivscc.gsfc.nasa.gov/publications/gm2000/scherneck

Ocean Loading Tides For, In, and From VLBI

Hans-Georg Scherneck, Rüdiger Haas, Alessandro Laudati

Chalmers University of Technology, Onsala Space Observatory
Contact author: Hans-Georg Scherneck, e-mail: hgs@oso.chalmers.se

Abstract

The general problem of predicting surface displacements due to ocean tide loading is reviewed. This includes the procedures in the IERS Conventions and suggestions for their next issue. In order to increase modeling accuracy we focus on the tides in the Gulf of Maine. This area is difficult to represent in global tide models. The VLBI station of Westford is located close enough to open up a model inversion opportunity. We have revived an ocean tide model to compute fully time-dependent solutions; in one run we included forcing by air pressure using ECMWF pressure fields and the corresponding geostrophic wind. We show observed ocean loading parameters and discuss the remaining discrepancies with respect to the model results.

1. Introduction

Ocean loading tides have become a significant process in VLBI observations. We can show that amplitudes regularly exceed the resolution capability of larger databases tenfold. It is therefore indicated to address the problem with renewed scrutiny.

The article is organized into three parts, each a little article in its own right. We first review the current situation with supply of loading parameters **for** space geodesy and VLBI in particular. Then we discuss how the tidal processes are implemented **in** VLBI analysis software and come up with suggestions for improvement. Finally we show the high resolution of sub-millimeter harmonic processes possible to obtain **from** utilizing most of the available VLBI data bases.

1.1. For

At present a range of ocean loading files with coefficients are available from the ftp server at Onsala Space Observatory. The following ocean tide models have been used to generate ocean loading coefficients: Schwiderski (1980) [1], Le Provost et al., (1994) [2], CSR3 and CSR4 by Eanes and Bettadpur (1996, 1999) [3], and GOT99.2 by Ray [4]. Of these, only the Le Provost et al. (1994) model is completely numerical, the others using empirical tide information: The Schwiderski (1980) model is numerically driven by tide gauge observations, and the remaining models on the list utilize TOPEX/POSEIDON (T/P) satellite altimetry.

The demand in application for ocean loading is a good global coverage, good spatial resolution, representation of many partial tides, and good coverage of the shelves and smaller basins. The T/P based models fill in the Le Provost et al. (1994) tide in the high latitude regions not sensed by the satellite. As regards spatial resolution the Schwiderski (1980) model is inferior with its 1×1 deg to the others (0.5×0.5 deg); however, it is still the only one that provides the long-period partial waves M_f (fortnightly), M_m (monthly), and S_{sa} (semi-annually). Since the S_{sa} tide in Schwiderski (1980) appears unreasonably different from an equilibrium tide, which would be expected to approximate the semi-annual hydrodynamic response of the ocean even better than

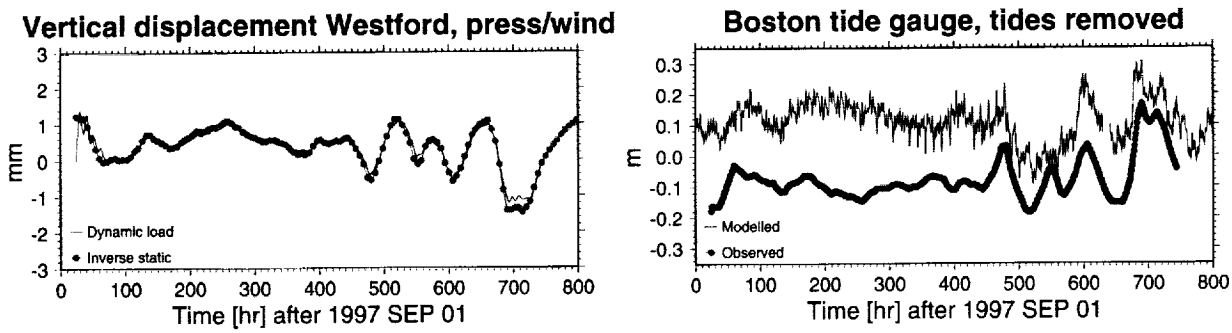

Figure 1. The left hand diagram shows the Gulf of Maine loading effect, vertical displacement at Westford, due to dynamic response to air pressure and wind (slight curve) and using an inverse barometer assumption (curve with circle symbols). The right hand diagram shows the modelled water level at Boston (curve with circle symbols) and a recording of the Boston tide gauge (slight curve), from which the luni-solar tides have been removed using a least-squares fit.

what seems to be evident in the case of the monthly tide, we regularly use an equilibrium tide to compute the loading effects at semi-annual period.

1.1.1. Computation of Surface Displacements

The method to compute the coefficients is by means of a point load Green's function, with which the tidal mass is convolved in a discrete approximation of a surface integral. The problem here is to resolve the coast fine enough when the field point, the location of a VLBI antenna, is at close distance. Experience shows that the five arc minute resolution of the TerrainBase or ETOPO5 topographic files are sufficient for loading induced displacements. The coastal refinement is carried out when a station is within 150 km from the coast and involves manual, interactive work to correctly edit the binary mask that distinguishes land and sea.

For the limited number of VLBI stations in the world, this work load is acceptable. Larger efforts are required for the ever increasing number of stations where satellite receivers are installed.

1.1.2. Tide Modelling on the Continental Shelves

We have also investigated the impact of a nearby body of water that possesses a profound resonance in the tidal band on load induced displacement of the Earth surface. We chose the Gulf of Maine as it is near the Westford site. A hydrodynamic model was created to model the shallow water tides of the area, including the Bay of Fundy and the Gulf of Saint Lawrence. The model was excited with either a large frequency set of tides (39 simultaneous waves) or with air pressure and wind fields from the European Centre for Medium Range Weather Forecast (ECMWF).

In short our results indicate that the dynamics of the area can be simulated by the model accurate enough to be used for loading effects. Most interesting, however, is an account of the dynamic response of the basin to excitation by weather conditions and the comparison of ensuing loading effects with the much simpler assumption of an inverted barometer response even on the continental shelf. Figure 1 shows the comparison of dynamic loading effects to the inverted barometer response. The effective net loading effect, equal to the difference between both, is

regularly less than 0.1 of the total, and much less than one millimeter.

The result is encouraging in so far as atmospheric loading for most stations will be accurately represented using an inverse barometer assumption for the ocean response. A small and over the oceans spatially uniform load will arise only due to the water mass budget constraint.

1.1.3. Atmospheric Loading Time-series

Time-series for predicted atmospheric loading displacements can be retrieved from our http server `http://www.oso.chalmers.se/~hgs/apload.html`. The time series comprise of three-dimensional displacements, vertical, east and north, in meter units, one sample per six hours for most VLBI stations used in geodetic experiments.

1.2. In

Ocean loading displacement of a site at time t can be specified using harmonics

$$\vec{\mathbf{u}} = \sum_j \hat{\mathbf{x}}_j \mathcal{R}eal \sum_k \mathcal{Z}_j^*(\omega_k)\gamma(\omega)H_k e^{i\omega_k(t-t_0)+i\phi_k} \tag{1}$$

where ϕ_k is the astronomical argument of partial tide k, and its angular speed at time t_0 is $\omega_k = d\phi/dt$. The sum involves those partial tides that belong to the same spherical harmonic degree of the astronomical potential H_k, and it is only harmonic degree two that is considered in the present context to have important oceanic tides. Thus, equation (1) is a first order Taylor expansion in time of a time convolution process of astronomical tides and solid earth tides driving the ocean that generates elastic deformation. The frequency domain function $\mathcal{Z}_j^*(\omega_k)$ is the ocean loading admittance. In each frequency band (long-period, diurnal, semi-diurnal) it is assumed to be a smooth function of frequency, especially if the core resonance, $\gamma(\omega)$, in the tide generating potential is factored out (but this requires that the ocean tide model has been generated with the core factor instituted; this is only rarely encountered). A method recently revived in TOPEX/POSEIDON tidal altimetry is termed Orthotides [5], [3]. It should be noted that the spectrum domain-based formulation of the ocean loading tide of equation (1) would work well together with a spectral domain formulation of the solid Earth tide as suggested in [6].

Originally, Schwiderski (1980) specified 11 tide waves. This might have inspired early programmers to limit the ocean loading formula in analysis software to these 11 terms. This went well along hand in hand with the storage efficiency of the solid Earth tide formula being based on the direct gravity action, knowing the ephemerides of the tide raising bodies. The major effect of the solid Earth core was accounted for using one correction for the K_1 tide, the argument of which is the sidereal hour angle. Thus, the most important effects were conveniently programmed.

With the 1996 issue of IERS Conventions [7] some additional terms were introduced (modulation of primary tides due to lunar node revolution in the loading tides). With steadily increasing sensitivity, more and more correction terms to the tide formulas are required, and they typically turn out as terms of a frequency domain formula like equation (1). The time may soon come when a revision of the presently used tide formulas is inevitable. For further discussion see [6].

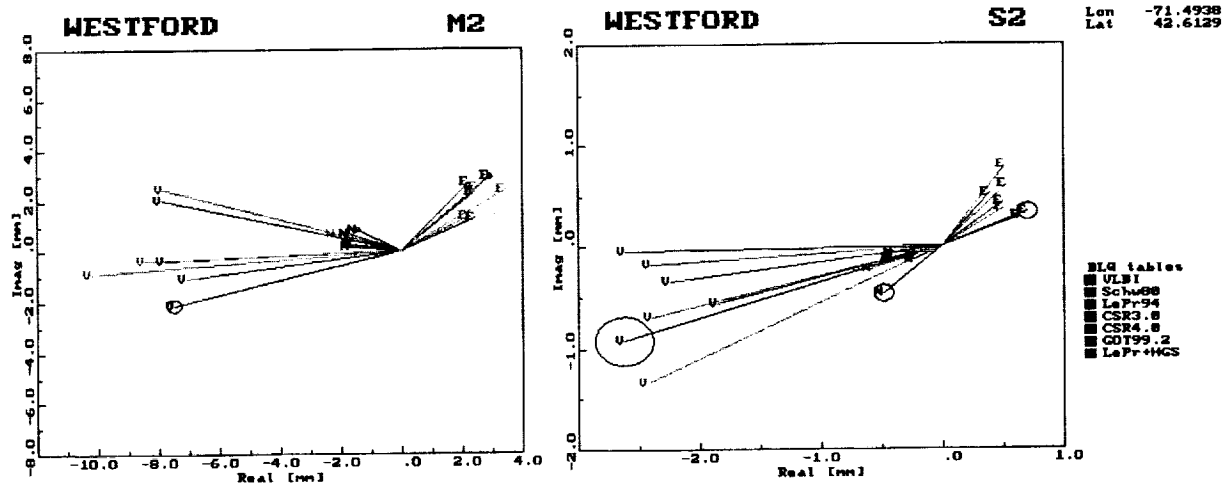

Figure 2. Plots of tidal phasors, observed (black and with circle showing a one-sigma limit) and predicted using a range of tide models. The model labeled LePr+HGS is composed of a regional model of the Gulf of Maine and the global Le Provost et al. (1994) model. Left hand diagram shows M_2, right S_2 vertical displacement at Westford.

1.3. From

Using data bases from 1979 on, we have estimated ocean loading parameters from VLBI observations. The method works as follows (also refer to [8]): The ocean loading tides are predicted using the standard model. At a set of target stations, pairs of signals in phase and at quadrature phase with respect to the eight most important solid earth partial tides are added in each spatial component, and the amplitude coefficients are adjusted in the least-squares stage.

In the most favorable cases we obtain one-sigma formal errors of 0.2 mm (vertical) and 0.1 mm (horizontal). Comparison with models show that a greater part of the observations are explained. Only the K1 tide seems to be offset by some perturbation, affecting both the vertical and the horizontal components at almost all stations, see Figure 3. As of now we have not found the systematics behind the perturbation.

Excepting the K_1 tide from an analysis of goodness of fit, Figure 4, we can show that the ocean loading models do explain 50 to 90 percent of the observed effects. The residual normalized chi^2 is found between 5 and 20. In the case of Wettzell, where ocean loading effects are small and the standard error is extremely small because of the great number of experiments, the goodness of fit looks a bit pessimistic. Translated into displacements, the discrepancy for the largest loading tide at Wettzell, M_2, is 2 mm of a loading effect of 5 mm.

There are no substantial differences between different ocean loading models. The general trend is that more recent models perform slightly better. Their greatest advantage is that the coverage of the models, GOT99.2 [4] in particular, extends over practically all important and interesting tidal waters, and that even difficult areas, like the Gulf of Maine, are represented with high accuracy.

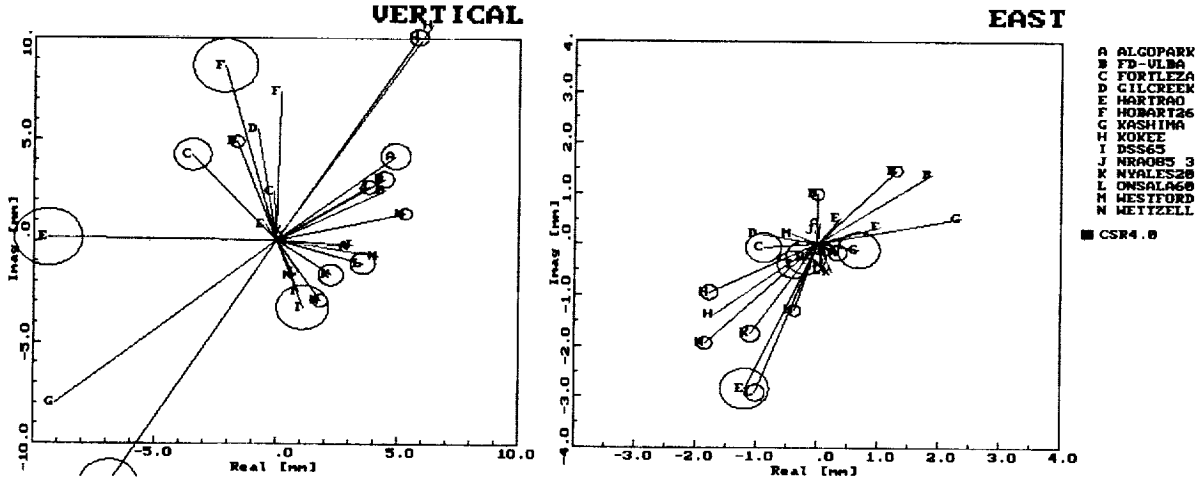

Figure 3. Plots of tidal phasors for the K_1 tide, observed (black and with circle showing a one-sigma limit) and predicted (grey) using the CSR4.0 model [3]. The discrepancies between observations and model are much larger than what could be explained by uncertainty in the ocean tide. All components are affected at practically all stations.

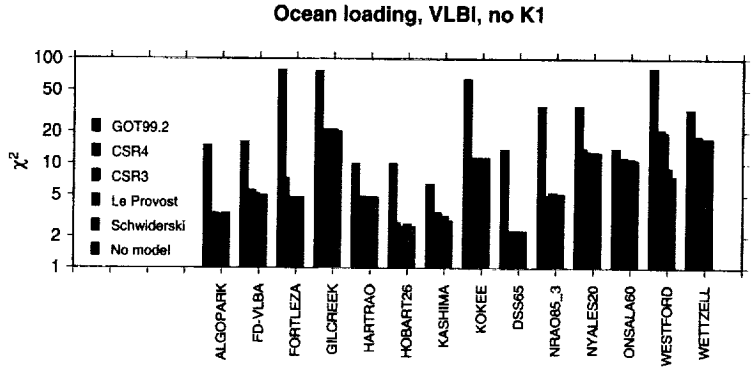

Figure 4. Goodness of fit

2. Conclusions

We showed that ocean loading tides are a significant phenomenon in VLBI observations of station motion. Currently available models predict the effects with approximately 90 percent agreement. Future work is indicated regarding the formulation of the process in the VLBI software.

Acknowledgment. This work is supported by EU-TMR under contract FMRX-CT960071.

References

[1] Schwiderski, E. W., On charting global ocean tides, *Rev. Geophys. Space Phys.*, 18, pp. 243–268., 1980

[2] Le Provost, C., Genco, M. L., Lyard, F., Vincent, P., and Canceil, P., Spectroscopy of the world ocean

tides from a finite element hydrological model, *J. Geophys. Res.*, **99**, 24,777–24,798, 1994.

[3] Eanes, R. and S. Bettadpur, *The CSR 3.0 global ocean tide model,* Center for Space Research, Technical Memorandum, CSR-TM-96-05, 25pp., 1996.

[4] Ray, R., *A Global Ocean Tide Model From TOPEX/POSEIDON Altimetry: GOT99.2*, NASA Technical Memorandum, NASA/TM-1999-209478, National Aeronautics and Space Administration, Goddard Space Flight Center, Greenbelt, MD, 1999.

[5] Groves, G.W. and Reynolds, R.W., An orthogonalized convolution method of tide prediction. *J. Geophys. Res.*, **80**, 4131–4138, 1975.

[6] Scherneck, H.-G., A parametrized solid earth tide model and ocean tide loading effects for global geodetic baseline measurements, *Geophys. J. Int.*, 106, 677-694, 1991.

[7] McCarthy, D. D. (ed): *IERS Conventions* IERS Technical Notes, Observatoire de Paris, 94 pp., 1996.

[8] Scherneck, H.-G., and Haas, R., Effect of horizontal ocean tide loading on the determination of polar motion and UT1. *Geophys. Res. Letters,* **26**, 501–504, 1999.

Arthur Niell: Improved Mapping Functions for GPS and VLBI , IVS 2000 General Meeting Proceedings, p.263-266
http://ivscc.gsfc.nasa.gov/publications/gm2000/niell

Improved Mapping Functions for GPS and VLBI

Arthur Niell

MIT Haystack Observatory
e-mail: aniell@haystack.mit.edu

Abstract

New atmospheric mapping functions have been developed which make use of in situ data available from numerical weather prediction or analysis. At mid-latitudes the hydrostatic component appears to be about a factor of two better at five degrees elevation than previous versions, while the wet component may be as little as twenty-five percent better. The improvement comes at the expense of simplicity.

1. Introduction

In this note I will give a brief description of what a mapping function is, describe the new mapping functions, compare them with those mapping functions that are currently most used, indicate the state of development, and describe some of the implementation questions.

2. Intuition

A mapping function is defined as the ratio of the electrical path length along the observation direction to the electrical path length in the zenith direction. For the same zenith electrical path length the mapping function is approximately proportional to the ratio of the thickness of the atmosphere to the radius of the earth. A measure of the thickness of the hydrostatic component of the atmosphere is the geopotential height (almost the the same as geometric height) of a constant pressure level. Such a height of constant pressure is called an isobaric surface. This led me to investigate if there is a strong correlation between the isobaric heights and the "true" mapping functions at a low elevation. For evaluation I used an elevation of 5 degrees. The mapping functions used for comparison are calculated by doing a raytrace along the elevation of interest using a vertical profile of temperature and humidity obtained usually from radiosonde data.

3. How is a Mapping Function Used?

A simplified model of the observed delay, τ, for either a VLBI baseline or for a single GPS receiver is:

$$\begin{aligned}\tau(\epsilon) &= \tau_g(\epsilon) + \tau_{clock} \\ &\quad +m_h(\epsilon) * \tau_h(90^\circ) \\ &\quad +m_w(\epsilon) * \tau_w(90^\circ)\end{aligned}$$

where m_h and m_w are the hydrostatic and wet mapping functions and ϵ is the elevation angle.

The observed delay is measured, and the mapping functions and a priori value for the hydrostatic zenith delay ($\tau_h(90^\circ)$) are assumed to be known. The unknown parameters are site position

(which is used to calculate τ_g), the station clock, and the wet zenith delay, $\tau_w(90°)$. The observations from typically twenty-four hours of data are used in a least-squares program (such as SOLVE or GIPSY) to estimate the values for the unknown parameters.

4. What are the Inputs to Mapping Functions?

Historically, it was known that mapping functions depend on the conditions of the atmosphere at all levels (e.g. CfA2.2 [1], and MTT [2]). However, since measurements of the atmosphere can be easily made only on the surface of the Earth, most mapping functions included surface meteorology as input data. However, the surface data can be mis-leading because of lower troposphere anomalies such as the very strong inversion layers that exist at high latitudes in the winter. A new set of mapping functions that depend only on site location and time of year was developed (NMF [3]). Although it is more accurate (less systematic error) it misses real variations on a time scale of days to weeks. It was clear that some information about the vertical distribution of atmosphere conditions was needed to improve the mapping functions.

To develop the new mapping functions data for the year 1992 were obtained from the GSFC Data Assimilation Office. Among the data available are the geopotential heights of specific pressure levels and the temperature and relative humidity for many more levels. The geopotential heights are used for the hydrostatic mapping function and the temperature and relative humidity for the wet mapping function. The correlation between geopotential height and the hydrostatic mapping function calculated from the radiosonde profiles at the same location are shown in Figure 1.

Both the hydrostatic mapping function based on the 200 hPa isobars, and the wet mapping function based on temperature and relative humidity profile information, were evaluated for twenty-six radiosonde sites spanning latitudes from 65° south to 80° north. Using an empirical rule-of-thumb, I estimated an approximate vertical scatter from the RMS scatter of the calculated mapping functions about the corresponding ones calculated by raytracing the radiosonde data. The results are shown in Figure 2 for both NMF and the new mapping functions, which I have called IMFh and IMFw. The dashed lines are of the form constant1 + constant2 × cos(2 × latitude), and the constants are approximate fits to the total effect (the quadratic sum of hydrostatic and wet) of each mapping function. However, the improvement of the new mapping functions is evident.

An important question raised by this figure is whether the improvement in the wet mapping function is significant enough to require the considerably larger data set needed. The hydrostatic mapping function needs only the geopotential heights at one pressure level. The wet mapping function needs the temperature and humidities at many levels. A possible implementation would use the new hydrostatic mapping function and use the wet mapping function from NMF.

5. How to Get in situ Information on a Global Basis

The best local information on the state of the atmosphere is obtained from radiosondes, but the locations for which these data are available are rather sparse on the global scale. An alternative source of information is from a global numerical weather analysis. These data are given on a uniform grid over the earth at specific levels in the atmosphere typically every six hours. The values at the locations of interest can then be obtained by interpolation.

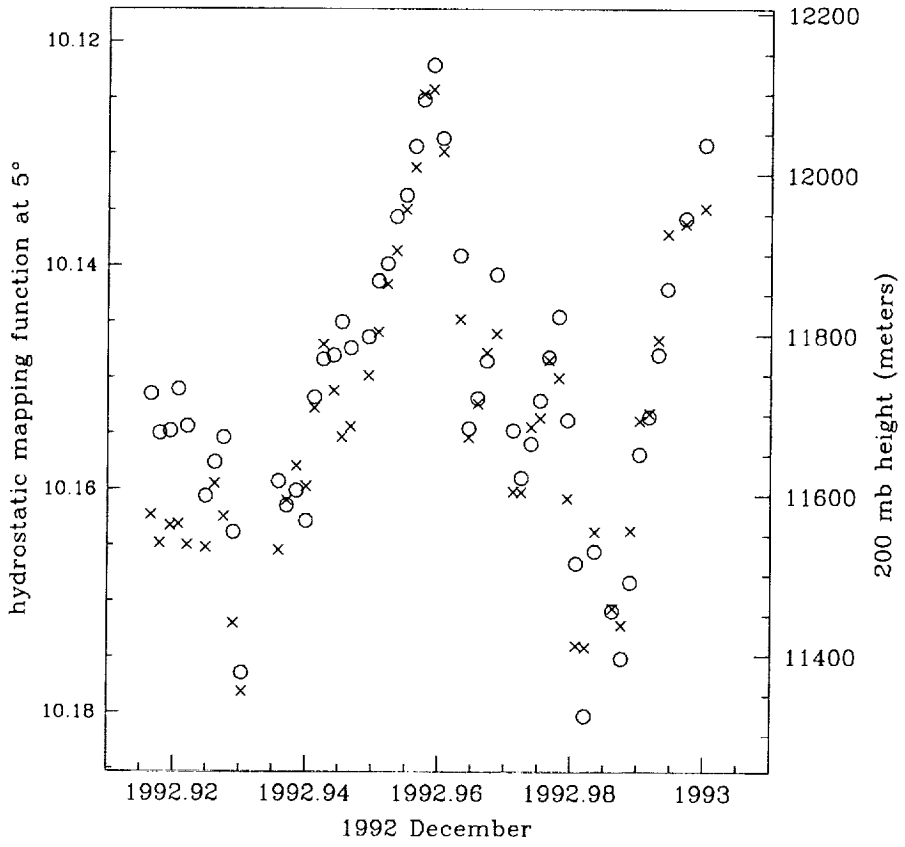

Figure 1. Hydrostatic mapping function at 5° elevation from radiosonde data (open circle) and 200 hPa geopotential height (cross) for site ALB for 1992 December.

6. Status of Development

The algorithms and constants of the new mapping functions are defined, and both fortran and matlab routines have been coded. For testing purposes I have obtained the temperatures, specific humidities, and geopotential heights for 1994 January from the GSFC Data Assimilation Office. In order to be able to utilize this information I must establish a practical mechanism for extracting the data from these very large files and inputting them to the VLBI estimation procedure. I then can test the inclusion of these mapping functions to see if they improve the repeatability of baseline lengths as expected.

7. Implementation Questions

The question of sequence must be evaluated. Should the atmosphere data be interpolated to the position of the site and the mapping functions be calculated once, or should the mapping functions be calculated at the grid points and interpolated to the site position?

When these questions are answered, the results using the new mapping functions must be

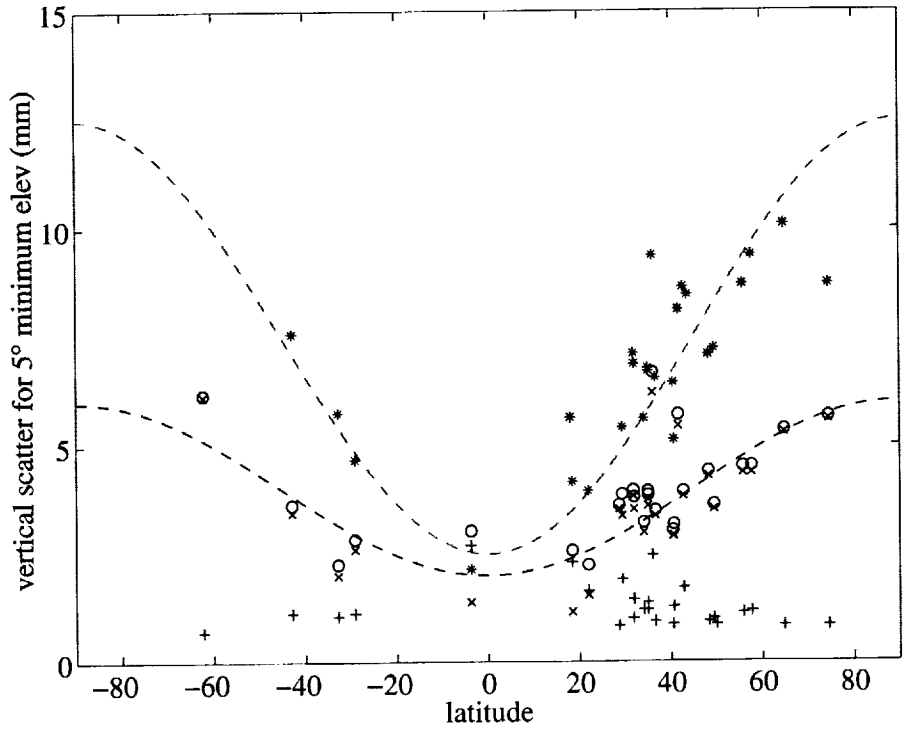

Figure 2. Standard deviation of apparent height for the combined errors of the hydrostatic and wet mapping functions. Except at very low latitudes the error due to the wet mapping function is insignificant. (IMFw - plus sign; IMFh - cross; IMFw + IMFh - open circle; NMFw+NMFh - asterisk).

compared to those using previous mapping functions to determine if sufficient improvement is obtained to warrant the more complicated system.

For an operational system the data must be obtained on a regular basis from one of the weather product services and then made available to all analysis centers.

References

[1] Davis, J. L., T. A. Herring, I. I. Shapiro, A. E. E. Rogers, and G. Elgered, Geodesy by radio interferometry: Effects of atmospheric modeling errors on estimates of baseline length, Radio Science, 20, 1593-1607, 1985.

[2] Herring, T. A., Modelling atmospheric delays in the analysis of space geodetic data, in Symposium on Refraction of Transatmospheric Signals in Geodesy, J. C. DeMunk and T. A. Spoelstra, eds., Netherlands Geodetic Commission Series No. 36, 157-164, 1992.

[3] Niell, A. E., Global mapping functions for the atmosphere delay at radio wavelengths, J. Geophys. Res., 100, 3227-3246, 1996.

Session 8

Analysis Part 2

Rüdiger Haas et al.: Atmospheric Parameters Derived from Simultaneous Observations with Space Geodetic and Remote Sensing Techniques at the Onsala Space Observatory, IVS 2000 General Meeting Proceedings, p.269–273
http://ivscc.gsfc.nasa.gov/publications/gm2000/haas2

Atmospheric Parameters Derived from Simultaneous Observations with Space Geodetic and Remote Sensing Techniques at the Onsala Space Observatory

Rüdiger Haas, Lubomir P. Gradinarsky, Gunnar Elgered, Jan M. Johansson

Onsala Space Observatory, Chalmers University of Technology
Contact author: Rüdiger Haas, e-mail: haas@oso.chalmers.se

Abstract

We compare estimates of zenith wet delay and horizontal delay gradients from 54 days of simultaneous observations with independent collocated space geodetic and remote sensing techniques at the Onsala Space Observatory. The impact of the choice of the constraints for the atmospheric parameters used in the analysis of the space geodetic data on the comparison with water vapour radiometer results is studied. We find estimated weighted RMS differences below the 10 millimetre level and correlation coefficients between 0.73 and 0.87 for the zenith wet delays derived from the different techniques while the agreement for the estimated horizontal delay gradients is less clear.

1. Introduction

Space geodetic techniques using microwave signals as e.g. Very Long Baseline Interferometry (VLBI) or the Global Positioning System (GPS), and microwave radiometry are influenced by water vapour in the Earth's atmosphere. Usually for the space geodetic techniques the atmospheric influence on the radio wave propagation is treated as an error source. Accordingly the atmospheric parameters derived from the analysis of VLBI and GPS data are normally treated as nuisance parameters. This is in contrast to the water vapour radiometer (WVR) which is often used for atmospheric studies.

In recent years the aspect of a possible use of atmospheric parameters derived from space geodetic techniques for atmospheric research and especially weather monitoring and prediction becomes more and more interesting [1]. This is especially due to the ongoing establishment of dense permanent GPS networks in many regions of the world which may be used as multiple-purpose interdisciplinary networks.

One question is whether the atmospheric parameters which are derived from space geodetic techniques can be used for meteorological and climate studies. Comparing these results with independent remote sensing data will also give us information on the impact of the atmospheric parameters in analysis of space geodetic data in terms of the measurement uncertainties. A plausible way to address these questions is to study and to compare the atmospheric parameters derived from simultaneous observations with collocated space geodetic and remote sensing techniques. The Onsala Space Observatory is equipped with collocated space geodetic and remote sensing techniques since many years and an extensive data base to perform such comparison studies is available. We analysed simultaneous observations from VLBI, GPS and WVR and compared the derived atmospheric parameters, i.e. the zenith wet delays and the horizontal gradients. A special focus was on the impact of the choice of constraints for the atmospheric parameters used in the analysis of VLBI and GPS on the agreement of the results with respect to those from the WVR.

2. The Data Set, the Analysis Strategy, and Results

The Onsala Space Observatory (OSO) is active in geodetic VLBI since 1969 [2] and contributes as a network station to the International VLBI Service for Geodesy and Astrometry (IVS). OSO also participates as a network station in the International GPS Service for Geodynamics (IGS) operating a permanent GPS site since 1987. Since 1993 OSO runs a water vapour radiometer (WVR) continuously in sky mapping mode. For more information on these techniques see e.g. [3].

Both, the GPS receiver and the WVR, are acquiring data continuously while 24-hour long VLBI experiments are carried out once or twice a month. In 1999 a total of 18 experiments were performed. Moreover there were also maintenance periods for the WVR and problems at individual days occurred, e.g. not enough useful WVR observations due to unfavourable weather conditions. Finally for the period 1993 to 1998 a data set of 54 days resulted that contains simultaneous observations with all three techniques.

We determined atmospheric parameters from the three techniques averaged over intervals of 90 minutes. The WVR data were analysed applying an in-house software package. In a preprocessing step the wet delay values were derived from the observed sky brightness temperatures. Then the gradient model [4] was fit to the wet delay values in a least squares analysis and the zenith wet delay values and the horizontal north and east gradient components were determined. The VLBI data were analysed using the CALC/SOLVE software package [5], applying the Niell mapping functions [6] and estimating the zenith wet delay and horizontal delay gradients by a least squares analysis. The GPS data were analysed using the Kalman filter software package GIPSY [7]. We used the Precise Point Positioning strategy [8], again applying the Niell mapping functions.

We identified eight out of the 54 days that showed the most variable atmosphere as sensed by the WVR. The VLBI and the GPS data of these eight days were then analysed using all possible combinations of the constraints for zenith wet delay and horizontal delay gradients given in Table 1 which meant that 400 different solutions were processed for each of these days.

Table 1. Constraints of a random walk model for zenith wet delay and horizontal gradients used in the VLBI and GPS data analysis. Characters are used as combination identifiers.

zenith wet delay constraint $[mm/\sqrt{h}]$										horizontal delay gradient constraint $[mm/\sqrt{h}]$									
A	2	E	6	I	12	M	23	Q	40	a	0.2	e	0.6	i	1.2	m	2.3	q	4.0
B	3	F	7	J	14	N	27	R	45	b	0.3	f	0.7	j	1.4	n	2.7	r	4.5
C	4	G	8	K	17	O	31	S	50	c	0.4	g	0.8	k	1.7	o	3.1	s	5.0
D	5	H	10	L	20	P	35	T	56	d	0.5	h	1.0	l	2.0	p	3.5	t	5.6

Figure 1 shows the time series for the atmospheric parameters for one out of the eight days studied in detail. For VLBI and GPS we only show the four "corner-solutions" Aa, At, Ta and Tt with the tightest and weakest constraints since all other results lie in-between. We calculated and compared the weighted RMS differences (WRMSD) of the atmospheric parameters derived from VLBI and GPS to those obtained from the WVR, depending on the constraints used. As an example Figure 2 shows the average of the WRMSD for the zenith wet delay results for all eight days. We found relative minima of the WRMSD for zenith wet delay constraints of 5–15 mm/$\sqrt{h}$ and horizontal delay gradient constraints of 0.5–2.0 mm/$\sqrt{h}$. Using a combination of constraints in this range we processed the data of all 54 days again. The results are shown in Figure 3.

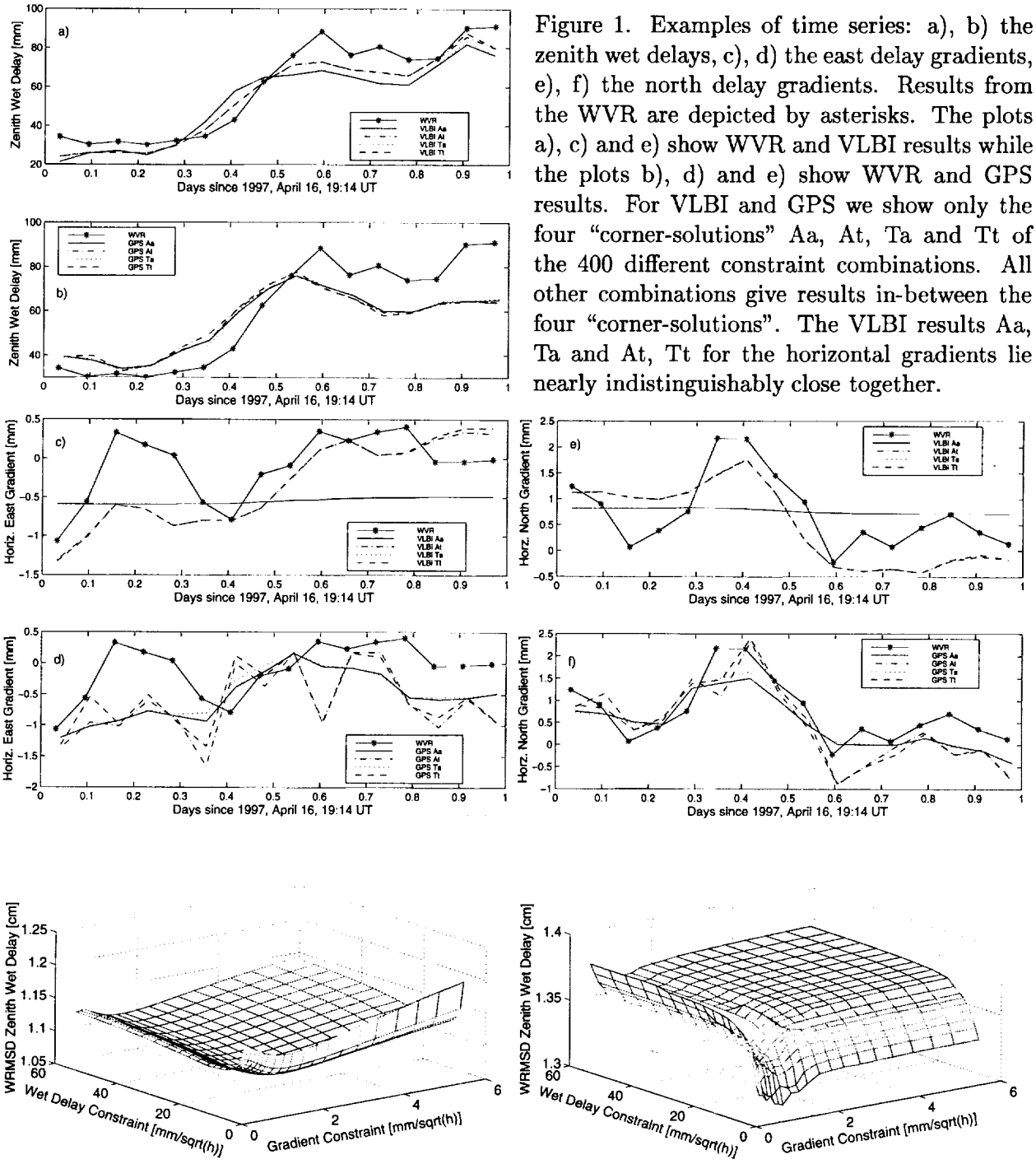

Figure 1. Examples of time series: a), b) the zenith wet delays, c), d) the east delay gradients, e), f) the north delay gradients. Results from the WVR are depicted by asterisks. The plots a), c) and e) show WVR and VLBI results while the plots b), d) and e) show WVR and GPS results. For VLBI and GPS we show only the four "corner-solutions" Aa, At, Ta and Tt of the 400 different constraint combinations. All other combinations give results in-between the four "corner-solutions". The VLBI results Aa, Ta and At, Tt for the horizontal gradients lie nearly indistinguishably close together.

Figure 2. Average weighted RMS differences for zenith wet delay vs. the constraints used for the zenith wet delay and the horizontal gradients: left plot WVR-VLBI, right plot WVR-GPS.

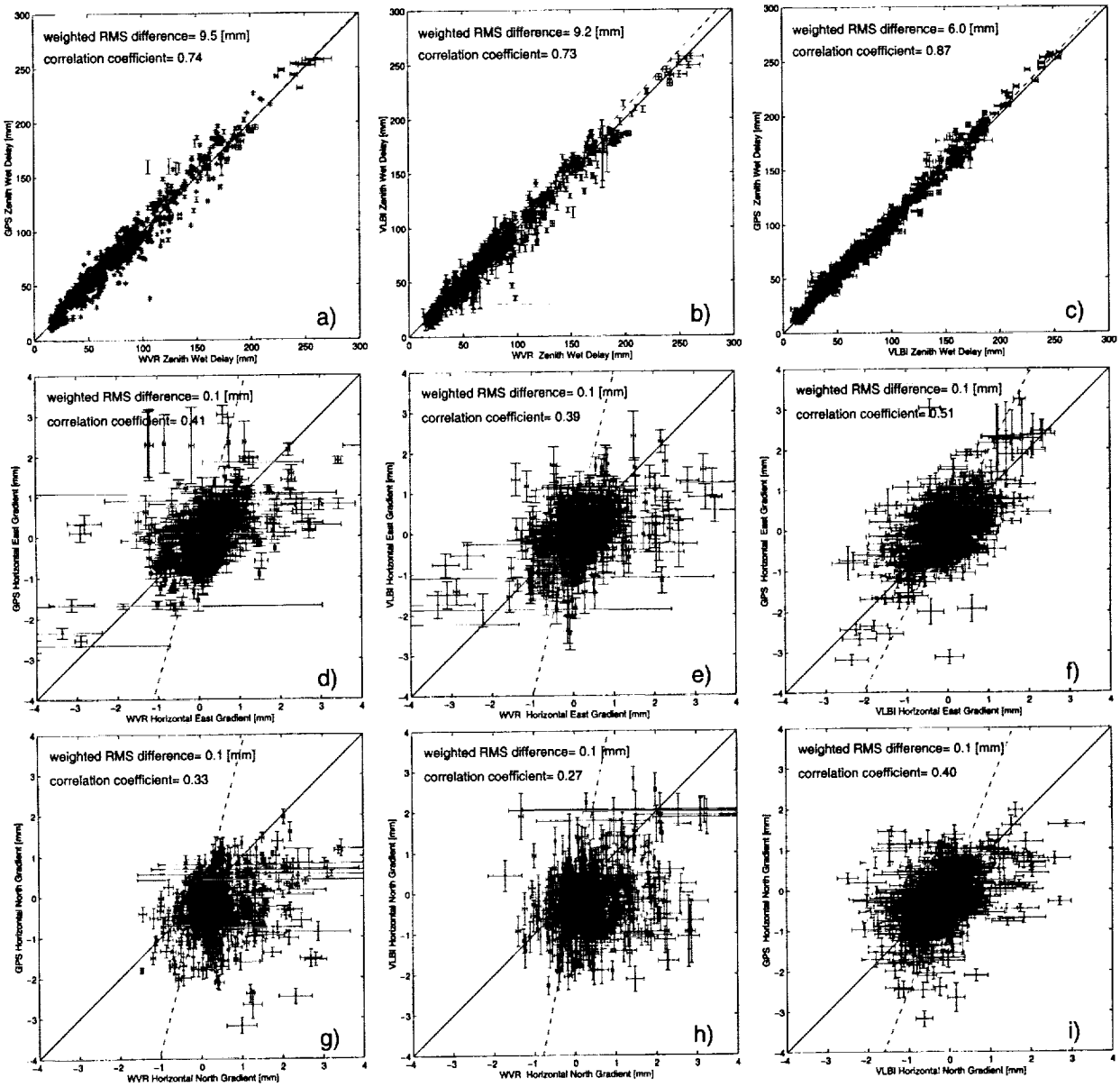

Figure 3. Scatter plots for the atmospheric parameters: The upper, middle and bottom row shows the zenith wet delay, east gradient and north gradients, respectively. The left, middle and right column shows GPS vs. WVR, VLBI vs. WVR, and GPS vs. VLBI, respectively.

3. Conclusions and Outlook

We find that the choice of the constraints for the atmospheric parameters used in the analysis of the space geodetic data does not drastically influence the agreement of the results with respect to the ones from WVR. The minimum average weighted RMS differences have relative minima for

constraints in the range of 5–15 mm/$\sqrt{h}$ and 0.5–2.0 mm/$\sqrt{h}$ for random walk models for the zenith wet delay and the horizontal delay gradients, respectively. This conclusion is based on the detailed analysis of eight out of the 54 days only and for the future we plan to analyse more data and search for a possible seasonal dependence.

Using constraints for the atmospheric parameters in these ranges for the space geodetic data analysis we obtain good agreement for the zenith wet delay results from the three techniques. The correlation coefficients are in the range of 0.73 to 0.87, where the higher correlation is obtained for the two space geodetic techniques. This can be partly explained by the fact that both techniques share some common error sources, e.g. the same mapping functions are used, and they do not suffer from rain effects as does the WVR.

The agreement of the results for the horizontal delay gradients is less pronounced. Here the correlation coefficients are between 0.27 and 0.51, where again the best agreement is found between the two space geodetic techniques. We do see a systematic behaviour for the north gradients where the WVR results would appear to indicate a positive contribution while the space geodetic techniques sense a negative contribution. This cannot be explained alone by the inclusion of the pressure term in the refractivity gradients which is of course not sensed by the WVR. An average positive north delay gradient has also been found from the analysis of a larger WVR data set [9].

Given that the Onsala site is on the coast further investigations especially with respect to pressure and local temperature gradients are necessary. The acquisition of more data and further comparisons are planned.

Acknowledgment. Rüdiger Haas is supported by the European Union within the TMR programme under contract FMRX-CT960071.

References

[1] Naito, I., *et al.*: Global Positioning System Project to Improve Japanese Weather, Earthquake Predictions, *EOS, Transactions, American Geophysical Union*, **79**, p. 301, p. 308, p. 311, June, 1998.

[2] Scherneck, H.-G., *et al.*: Space Geodetic Activities at the Onsala Space Observatory: 25 years in the Service of Plate Tectonics, *Phys. Chem. Earth*, **Vol. 23, No. 7–8**, 811–823, 1998.

[3] Gradinarsky, L. P., *et al.*: Wet path delay and delay gradients inferred from microwave radiometer, GPS and VLBI observations, submitted to *Earth Planets Space*, 1999.

[4] Davis, J. L., *et al.*: Ground-based measurements of gradients in the "wet" radio refractivity of air, *Radio Science*, **28(6)**, 1003-1018, 1993.

[5] Ma, C., *et al*: Measurement of horizontal motions in Alaska using very long baseline interferometry, *J. Geophys. Res.*, **95**, 21991–22011, 1990.

[6] Niell, A.: Global mapping functions for the atmosphere delay at radio wavelength, *J. Geophys. Res.*, **101(B2)**, 3227-3246, 1996.

[7] Webb, F. H., and J. F. Zumberge: An introduction to GIPSY/ OASIS-II, *JPL Publication D-11088*, Jet Propulsion Laboratory, Pasadena, California, 1993.

[8] Zumberge J. F., *et al.*: Precise point positioning for the efficient and robust analysis of GPS data from large networks, *J. Geophys. Res.*, **102**, 5005–5017, 1997.

[9] Gradinarsky, L. P. and G. Elgered: Horizontal gradients in the wet path delay derived from four years of microwave radiometer data, submitted to *Geophys. Res. Lett.*, 2000.

George Resch et al.: Calibration of Atmospherically Induced Delay Fluctuations due to Water Vapor, IVS 2000 General Meeting Proceedings, p.274–279
http://ivscc.gsfc.nasa.gov/publications/gm2000/Resch

Calibration of Atmospherically Induced Delay Fluctuations due to Water Vapor

George Resch, Christopher Jacobs, Steve Keihm, Gabor Lanyi, Charles Naudet, Abraham Riley, Hans Rosenberger, Alan Tanner

Jet Propulsion Laboratory

Contact author: George Resch, e-mail: George.M.Resch@jpl.nasa.gov

Abstract

We have completed a new generation of water vapor radiometers (WVR), the A- series, in order to support radio science experiments with the Cassini spacecraft. These new instruments sense three frequencies in the vicinity of the 22 GHz emission line of atmospheric water vapor within a 1 degree beamwidth from a clear aperture antenna that is co-pointed with the radio telescope down to 10 degree elevation. The radiometer electronics features almost an order of magnitude improvement in temperature stability compared with earlier WVR designs. For many radio science experiments, the error budget is likely to be dominated by path delay fluctuations due to variable atmospheric water vapor along the line-of-sight to the spacecraft. In order to demonstrate the performance of these new WVRs we are attempting to calibrate the delay fluctuations as seen by a radio interferometer operating over a 21 km baseline with a WVR near each antenna. The characteristics of these new WVRs will be described and the results of our preliminary analysis will be presented indicating an accuracy of 0.2 to 0.5 mm in tracking path delay fluctuations over time scales of 10 to 10,000 seconds.

1. Introduction

Two water vapor radiometers (WVRs) have been constructed in order to calibrate fluctuations in the line-of-sight path delay at radio wavelengths due to atmospheric water vapor. These WVRs will be used to calibrate fluctuations in the Doppler signals during the Gravitational Wave Experiment (GWE) with the Cassini spacecraft that is scheduled to start in December 2001 and repeat in 2002 and 2003 during the spacecraft cruise to Saturn. The GWE has been described by Armstrong et. al. [1], and Tinto and Armstrong [2]. Studies of atmosphere delay fluctuations [3, 4] indicate that this phenomenon is likely to dominate the error budget for the GWE on time scales of 100 to 10,000 sec.

The new WVR is shown in Figure 1 and has been described by Tanner [5]. This unit is located near Deep Space Station 13 (DSS 13) at NASA's Goldstone complex in the Mojave desert. In the background, slightly to the right of center in the photograph one can also see the microwave temperature profiler (MTP) and a WVR of earlier design (J-series).

The WVR measures equivalent blackbody brightness temperature at 22, 24, and 32 GHz. There is a spectral line originating from a rotational transition of the water vapor molecule centered at a frequency of the 22 GHz whose strength is proportional to the columnar content of water vapor along the line-of-sight which is related to the path delay.

The radiometer feed illuminates a main reflector of 1 m diameter in an offset configuration such that there is no blockage of the reflector that could cause scattering into the feed. The reflector can point in azimuth and elevation along the same line-of-sight as a nearby large communications antenna and has approximately a 1 degree beamwidth with very low sidelobe levels. Finally,

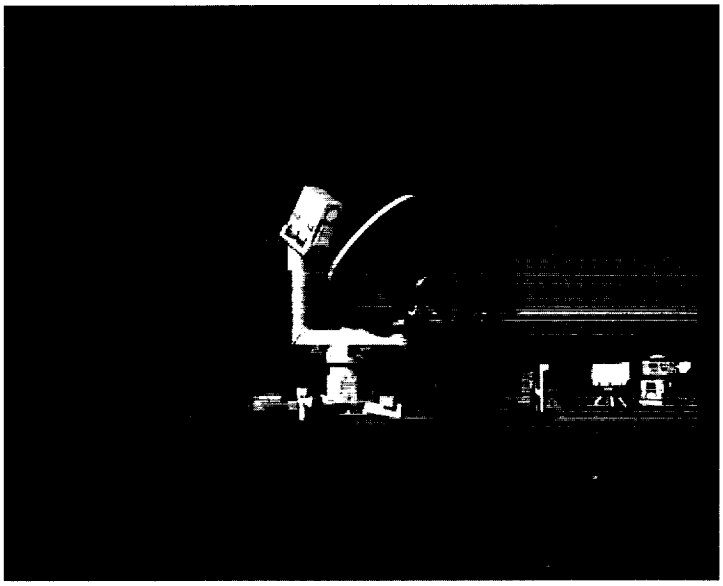

Figure 1. Photo of the new WVR taken at Goldstone near DSS 13. The MTP and a J-series WVR are shown in the background to the right.

the gain stability of the radiometer had to correspond to roughly 10 mK variation of brightness temperature for time scales as long as 10,000 sec.

2. Performance Demonstration

In order to demonstrate the performance of this new media calibration subsystem we examined its capability to calibrate another measurement technique that we knew to be sensitive to line-of-sight path delay fluctuations. The experiments were approximately modeled after the ones described in references [6, 7] using WVRs of an earlier design. The basic concept of the experiment is illustrated schematically in Figure 2.

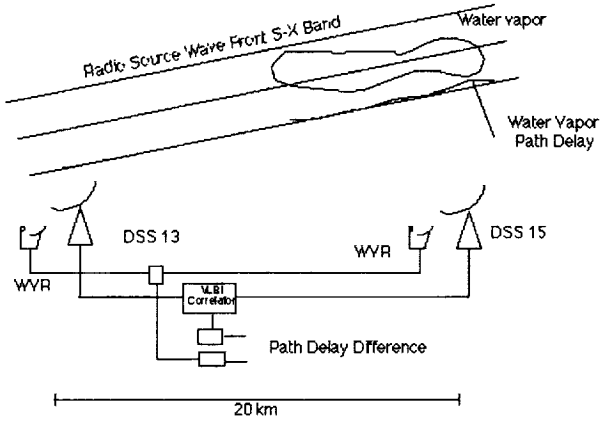

Figure 2. Schematic representation of the WVR/CEI comparison experiments

Each new WVR was located within 50 m of the base of a 34 m antenna, located at the Goldstone Deep Space Communications Complex in the Mojave desert. In our experiments, the stations DSS 13 and DSS 15 were used and are separated by approximately 21 km. The WVRs were monitored in real-time but all data reduction was done in post-data acquisition. Each WVR measured the brightness temperature along its line-of-sight at sub-second intervals and produced a time tagged series of data that included the azimuth and elevation. The brightness temperature data were integrated for 6 sec. These time series were then used with two retrieval algorithms [8, 9] to estimate the line-of-sight delay. The data from each WVR were then differenced to provide an estimate of the differential phase delay between the two stations that could then be compared with the Connected Element Interferometer (CEI) residual phase delay. Finally, we calculate the Allan Standard Deviation [10] of the interferometer phase residuals before and after correction by the WVR data in order to estimate the ability of the WVRs to calibrate atmospheric fluctuations as a function of time. This quantity is directly related to the requirements set by the Cassini GWE.

Typically the experiments were scheduled during night time hours using a two antenna CEI configuration. Only very strong sources ($S > 1$ Jy) whose positions were very well known (accuracy of better than 0.2 mas) were used. The objective in these experiments was to directly probe the quality of phase delay calibration on time scales of 10 to 10,000 sec under conditions similar to what is expected during the Cassini GWE. Each scan was scheduled for 1560 sec (i.e. the duration of a single pass on the Mark IV tape recorder). Several passes produced less data due to a variety of instrumental problems or operator errors.

The correlation process on the CEI data uses a priori estimates of several parameters in order to produce residual path delay and delay rate. Our fringe fitting software [11] removes a term in the phase delay estimate which is linear in time. This results in an estimate of phase delay that is zero mean over the entire scan. A similar linear rate was removed from the differenced time series of path delay for the WVRs.

Figures 3 and 4 illustrate the best tracking accuracy we observed. In Figure 3 we plot the residual delay of the interferometer from scan 11 (day 240, 1999) after accounting for all geometric effects together with the differenced WVR delays and removing a linear trend in the differenced WVR data. The rms of the CEI data in this plot is 0.65 mm and the correlation between the two data types is obvious. In Figure 4, we use the differenced WVR data to calibrate the CEI data. The rms of the residual in this case is reduced to 0.21 mm of path delay. Figure 5 shows the distribution of residuals for each step of the data analysis in scan 11. In panel (a) the CEI residuals are plotted, in panel (b) the differenced WVR data, and in panel (c) the calibrated CEI data. The reduction in variance is clearly evident.

Figure 6 plots the Allan Standard deviation as a function of integration time for scan 11. The dotted line is the requirement for media calibration during the Cassini GWE.

3. Discussion

We have described the results from a preliminary analysis of a single scan from a series of experiments that are designed to determine the performance of a new generation of WVR. During each scan in these experiments we observed a different radio source and tracked over a range of azimuth and elevation angles. When the WVR data is used as a calibration, the CEI residuals are reduced by a factor of 2 to 3.

The distribution of the calibrated data, as illustrated in the bottom panel of Figure 5 represent

the quadratic sum of CEI errors plus WVR errors. In order to assess the performance of the new WVR we must independently assess the error budget for each technique. For the WVRs, the components of the error budget are: a) precision, b) stability, c) beam size, d) separation from main antenna, and e) retrieval accuracy [12, 13].

For the CEI data the components of the error budget that are most important in these tests are: a) electronics stability, b) instrumental delay mis-modeling (including antenna deformation and subreflector motion), and c) baseline accuracy. All of these components must be reduced or estimated in order to infer the intrinsic accuracy of the WVRs. Our preliminary results strongly suggest that this error budget must be critically re-evaluated and this process is underway. Data analysis and additional experiments aiming to explore longer time scales are underway.

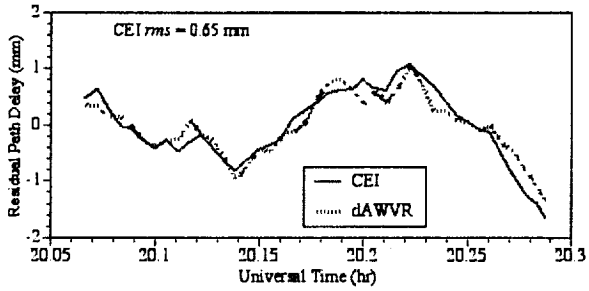

Figure 3. Residual delay of the connected element interferometer together with the residual delay of the differenced Water Vapor Radiometers for scan 11. Both data types mapped to zenith. The actual azimuth was 97 deg. and the elevation 29 deg.

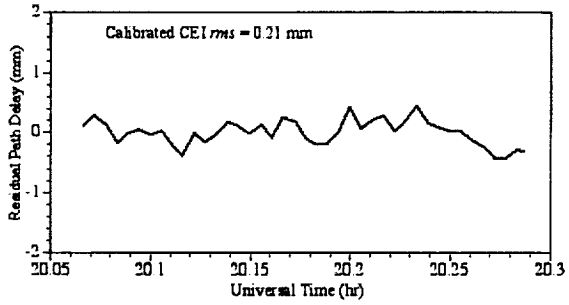

Figure 4. Residual delay of the connected element interferometer during scan 11 after correction by the differenced WVR data.

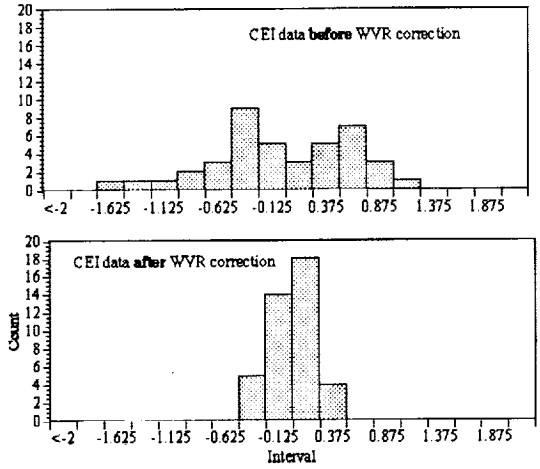

Figure 5. Histogram of the residuals from scan 11. Top panel shows the residual CEI path delay and the bottom panel shows the calibrated CEI data.

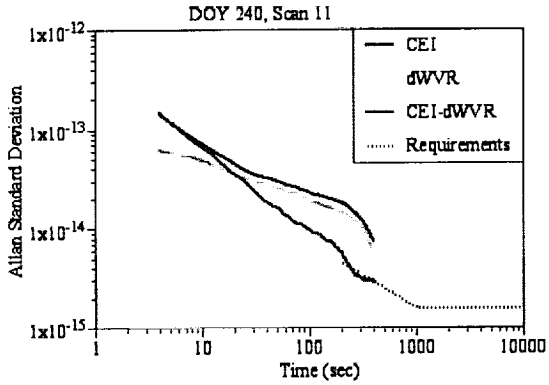

Figure 6. Allan standard deviation versus interval for scan 11 from DOY 240. This plot shows the CEI residuals, the differenced WVR data, the calibrated CEI data (CEI-dWVR), and the requirements for the Cassini GWE.

4. Acknowledgements

We are very grateful to Lyle Skjerve, Leroy Tanida, J. Eric Clark, Charles Snedeker, the staff at DSS 13, and the Operations crews at the Goldstone Signal Processing Center for the invaluable assistance provided during these experiments.

References

[1] Armstrong, J.W, B. Bertotti, F.B. Estabrook, L. Iess, and H.D. Wahlquist, "The Galileo/Mars Observer/Ulysses Coincidence Experiment", *Proc. of the Second Edoardo Amaldi Conf. on Gravitational Waves,* Ed., E. Coccia, G. Pizzella, and G. Veneziano; Edoardo Amaldi Foundation Series, Vol. 4,

World Scientific, 1998.

[2] Tinto, M., and J.W. Armstrong "Spacecraft Doppler tracking as a narrow-band detector of Gravitational Radiation", *Phys. Rev. D,* **58**, 042002, 1998

[3] Armstrong, J.W., and R.A. Sramek, "Observations of tropospheric phase scintillations at 5 GHz on vertical paths," *Radio Science,* **17**, pp. 1579 - 1586, Nov. 1982

[4] Keihm, S.J. "Water Vapor Radiometer Measurements of the Tropospheric Delay Fluctuations at Goldstone Over a Full Year," *TDA Prog. Report* 42-122, pp. 1-11, 1995

[5] Tanner, A.B., "Development of a high-stability water vapor radiometer," *Radio Sci.,* **33**, pp. 449-462, Mar. 1998

[6] Resch, G.M., D.E. Hogg, and P.J. Napier, "Radiometric correction of atmospheric path length fluctuations in interferometric experiments," *Radio Sci.,* **19**, pp. 411-422, Jan. 1984

[7] Teitelbaum, L.P, R.P. Linfield, G.M. Resch, S.J. Keihm, and M.J. Mahoney, "A Demonstration of Precise Calibration of Tropospheric Delay Fluctuations With Water Vapor Radiometers," *TDA Prog. Report 42-126,* pp. 1-8, 1996

[8] Resch, G.M., "Inversion Algorithms for Water Vapor Radiometers Operating at 20.7 and 31.4 GHz," TDA Prog. Report 42-76, pp. 12-26, Oct. 1983

[9] Keihm, S.J. and S. Marsh, "Advanced algorithm and system development for Cassini radio science tropospheric calibration," *TDA Prog. Report 42-127,* pp. 1-19, 1996

[10] Allan, D.W., "Statistics of Atomic Frequency Standards," *Proc. IEEE,* **54**, No. 2, pp. 221-230, Feb. 1966

[11] Lowe, S., "Theory of Post-Block II VLBI Observable Extraction," *JPL Publ. 92-7,* 15 July 1992

[12] Linfield, R.P., and J. Wilcox, "Radio metric errors due to mismatch and offset between a DSN antenna beam and the beam of a tropospheric calibration instrument," *TDA Prog. Report 42-114,* pp. 1-13, 1993

[13] Linfield, R.P., "Error Budget for WVR-based Tropospheric Calibration System," *JPL IOM 35.1-96-012,* 5 Jun 1996

Martine Feissel et al.: Stability of ICRF, a Time Series Approach, IVS 2000 General Meeting Proceedings, p.280–284
http://ivscc.gsfc.nasa.gov/publications/gm2000/feissel

Stability of ICRF, a Time Series Approach

Martine Feissel, Anne-Marie Gontier

Observatoire de Paris/CNRS UMR8630
Contact author: Martine Feissel, e-mail: feissel@ensg.ign.fr

Abstract

The qualification and the maintenance of the International Celestial Reference Frame (ICRF) source directions are currently based on global statistics on the complete data set of observations. As the founding hypothesis in the selection of extragalactic objects for accessing a quasi-inertial reference system is that their directions are fixed in space, the time variability of some of the sources is only used as a rejection criterion. We show that a significant proportion of the sources have apparent motions with non-random noise spectrum. We suggest that time series statistics be introduced in the computation of ICRF in order to take into account the error spectrum of the source motions. Test computations using different statistical approaches are performed. Their results are compared with those of the classical method.

1. Introduction

The IAU recommended in 1997 to use as conventional celestial reference system the International Celestial Reference System (ICRS) (see Feissel and Mignard 1998), materialized by coordinates of extragalactic compact radiosources observed with VLBI, the International Celestial Reference Frame (ICRF). The initial realization of the ICRS was published in 1997 (Ma et al. 1998, see also Ma and Feissel 1997). It includes 608 objects. The most recent update and extension, ICRF-Ext.1, is now available with 667 objects. (IERS 1999; `http://hpiers.obspm.fr/webiers/results/icrf/README.html`). The computation for ICRF-Ext.1 is based on the same analysis options as that for ICRF.

The radiosource coordinates in ICRF and ICRF-Ext.1 are derived from the complete set of observations over 1979–1999. They are qualified in two ways, 1) by ascribing realistic uncertainties that take into account both the random and systematic errors, and 2) by categorizing them, in decreasing order of confidence, as "defining", "candidates", and "other". This complex assessment scheme is made necessary by the existence of variabilities in the apparent directions of the sources. Thanks to the computation of the session-per-session coordinates of over 500 sources of ICRF-Ext.1, it is possible to investigate this instability in a time series approach.

According to Ma et al. (1998) there are two major causes for the current limitation in accuracy of source positions.

- Tropospheric delay modelling. The uncertainty in the modelling of the propagation delay due to the wet component of the troposphere, combined with deficiencies in the network geometry (majority of stations in the northern mid-latitudes, short N-S components of the baselines yielding to the observation of low declination objects at low elevation, where the mis-modelling of the delay has the largest effect), may give rise to systematic errors in declination at the level of 0.5 mas (milliarcsecond) in the zone around the equator. The consequences of this defect can be investigated on the basis of time series.

- Source structure. No radiosource is really point-like when observed in centimetric wavelength with baseline lengths around 6000 km. If the source structure is extended or not circular, its apparent direction may change as a function of the length and orientation of the baselines. This effect should be minimized with the practice of running 24-hour sessions, during which the Earth's sidereal rotation leads to the diversification of the projections of the baselines on the source structure. Moreover, despite the selection of quiet objects for astro-geodetic work, any of them may exhibit changes in their emission structure that will make their apparent direction change with time. In principle it is possible to accurately correct this effect, provided that repeated maps of the sources are available (Charlot & Sovers, 1997). In the framework of the ICRF maintenance, a systematic program for source mapping (Fey 1999; `http://maia.usno.navy.mil/rorf/rrfid.html`) and astrometric correction computation (`http://www.observ.u-bordeaux.fr/public/radio/PCharlot/structure.html`) is under way. However, the overall correction procedure is not yet implemented in the existing global analysis softwares. This mismodelling may propagate errors into the source positions at the level of 0.2 mas. We investigate this effect hereafter, based on the computed coordinates of the radiosources in a homogeneous reference frame, with one determination for each of the sessions in which the source was observed (Eubanks 1999).

2. Time Series Statistics on Radio Source Coordinates

For historical reasons, the numbers of observations per source are extremely uneven. Some sources that were used to provide reference directions in the early years of VLBI appeared too variable or too extended after some years and were discarded to the benefit of other, fainter sources that became usable thanks to the progress in technology. Some sources considered as best fitting the astro-geodetic needs are repeatedly observed, while others, considered as less useful for this purpose, are re- observed less frequently, mainly for astronomical studies.

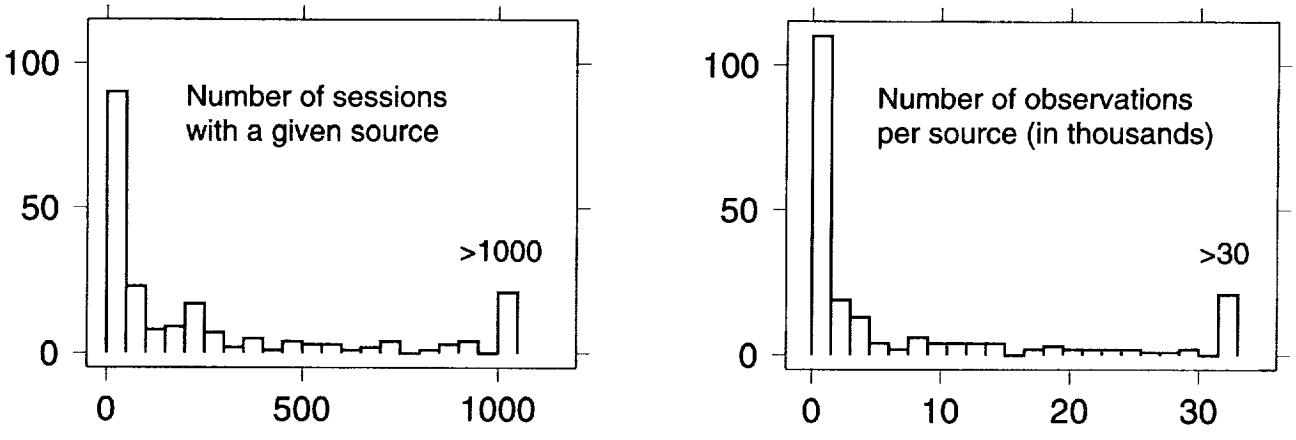

Figure 1. Histograms of rates of observations over 1988-99 for the 208 best observed ICRF sources

Our study is based on the computed coordinates of the radiosources in a homogeneous reference frame, with one determination for each of the sessions in which the source was observed (Eubanks 1999). Figure 1 shows the histograms of rates of observation for the 208 most regularly observed

sources over 1988-1999. These sources provide the backbone of the ICRF. About half of them have less than 1500 observations in less than 60 sessions. Twenty-one sources have more than 30 thousand observations in more than 1000 sessions.

The spectral characteristics of the time series of source coordinates can be investigated using the Allan variance method (Allan 1966, see a review of these methods in Rutman 1978). The Allan variance analysis allows one to characterize the variability power spectrum from time series of measurements. This method identifies white noise (spectral density S independent of frequency f), flicker noise (S proportional to f^{-1}), and random walk (S proportional to f^{-2}), and it allows one to specify the time frame in which a given type of noise is valid. Note that one can simulate flicker noise in a time series by introducing steps of random amplitudes at random dates. In the case of a white noise spectrum (an implicit hypothesis in the current ICRF computation strategy), accumulating observations with time eventually leads to the stabilisation of the mean position. In the case of flicker noise, extending the time span of observation does not improve the quality of the mean coordinates.

An example of spectral characterisation is given by Gontier et al. (1999) for the 65 best observed sources over 1988-1999. About 3/4 of the series of coordinates have white noise and 1/4 have flicker noise. This classification is uncorrelated with the "definition/candidate/other" classification currently used in the ICRF maintenance process.

3. Time Series of Celestial Reference Frames

For two sets of sources with reasonably continuous observations selected with two different levels of accepted interruptions, we consider yearly differential celestial reference frames based on the average differences with the mean coordinates for each source. The two sets of selected sources include 208 objects for the looser continuity condition (135 categorized as "definition" or "candidates" in the ICRF, and 73 "other") and 68 sources for the tighter condition (resp. 36 and 32). We then compute the systematic differences under the classical parametrisation of rotation angles dA1, dA2, dA3 around the axes of the equatorial system of coordinates. Figure 2 shows the time evolution of the dA1, dA2, dA3 angles in the two cases (blue/dark for the 208 sources selection, brown/light for the 68 sources one), estimated both by weighted minimum L2-Norm (least squares) and minimum L1-Norm analyses, with weighting based on the standard error of each yearly average. The L2-Norm results are shown as isolated points (circles for the 208 sources selection, diamonds for the 68 sources) with their standard errors, and the L1-Norm results are connected by a line. The double horizontal line shows the band of $\pm$ 0.2 μas that the authors of the ICRF claim to be the accuracy of the definition of the ICRF axes. The effective numbers of sources present in each yearly solution are given with the dA2 graph (bottom line for the 208 source selection, upper line for the 68 sources).

A striking feature is that the least square solutions are not regularized by doubling the number of sources. This effect, added to the least sensitivity of the L1-Norm solutions to the number of sources, suggests that even at the level of yearly averages source coordinates have large irregularities, as the L1-Norm estimation is known to be more robust with respect to outliers than the L2-Norm estimation.

The preliminary results presented here show that the analysis approach based on time series analysis deserves further development in the context of the maintenance of the ICRF.

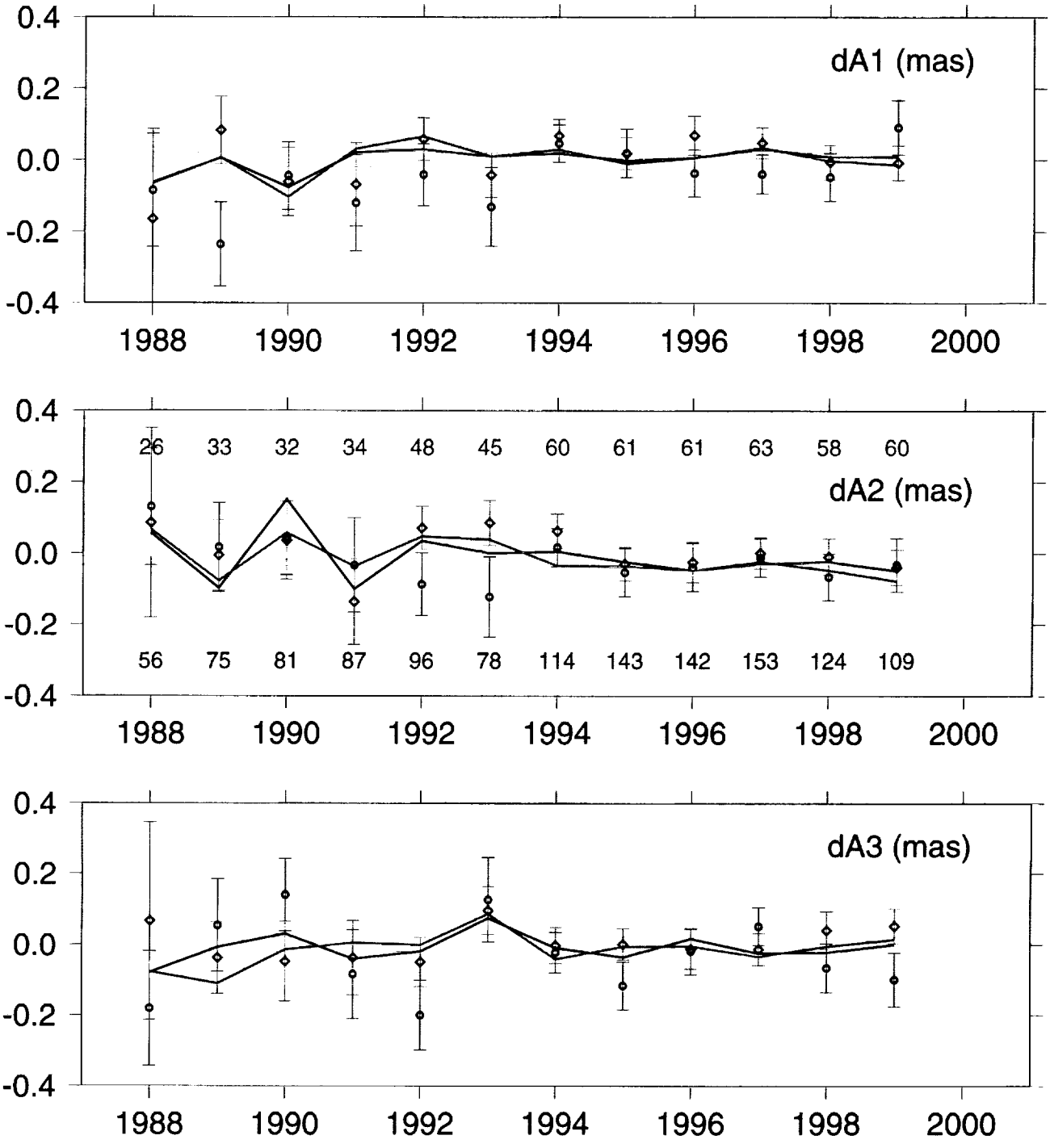

Figure 2. Relative rotation angles of yearly CRFs
(see explanations in the text)

References

[1] Allan, D.W.,1966, Proc. IEEE vol. 54, 221

[2] Charlot, P. & Sovers, O. J. 1997, The New International Celestial Reference Frame, 23rd meeting of the IAU, Joint Discussion 7, 22 August 1997, Kyoto, Japan., 7, E6

[3] Eubanks, T.M., 1999, private communication

[4] Feissel, M. & Mignard, F. 1998, AA, 331, L33

[5] Fey, A. L. & Charlot, P. 1998, ASP Conf. Ser. 144: IAU Colloq. 164: Radio Emission from Galactic and Extragalactic Compact Sources, 387

[6] Fey, A. L. 1999, Highlights in Astronomy , 11, 317

[7] Gontier, A.-M., Feissel, M., Essaifi, N., Jean-Alexis, D., 1999, 1999 IVS Annual Report, NASA/TP-1999-209243, p. 227.

[8] International Earth Rotation Service (IERS), 1999, 1998 Annual Report, 83. Observatoire de Paris.

[9] Ma, C., Feissel, M., (eds.)1997, IERS TN 23, Observatoire de Paris.

[10] Ma, C., Arias, E.F., Eubanks, T.M., Fey, A.L., Gontier, A.-M., Jacobs, C.S., Sovers, O.J., Archinal, B.A., Charlot, P., 1998, AJ 116, 516

[11] Rutman, J., 1978, Proc. IEEE vol. 66, 1048

Alan L. Fey et al.: Improving the ICRF Using the Radio Reference Frame Image Database, IVS 2000 General Meeting Proceedings, p.285–287
http://ivscc.gsfc.nasa.gov/publications/gm2000/Fey2

Improving the ICRF Using the Radio Reference Frame Image Database

Alan L. Fey, David A. Boboltz, Ralph A. Gaume, Kenneth J. Johnston

United States Naval Observatory
Contact author: Alan L. Fey, e-mail: afey@usno.navy.mil

Abstract

We describe applications of the Radio Reference Frame Image Database aimed specifically toward improvement of the International Celestial Reference Frame.

1. What is the Radio Reference Frame Image Database?

The Radio Reference Frame Image Database (RRFID) is a collection of multiple epoch and multi-frequency imaging observations of International Celestial Reference Frame (ICRF) (Ma *et al.* 1998) sources. The RRFID data are the result of an ongoing program to image the ICRF sources on a regular basis. The goal is to establish a database of images of all of the ICRF sources at the same wavelengths as those used for precise astrometry (2.3 and 8.4 GHz). The RRFID currently consists of over 2200 images of about 425 sources at frequencies of 2.3 and 8.4 GHz with images of selected sources available at 15 GHz. Imaging observations are carried out using the Very Long Baseline Array (VLBA) telescope of the National Radio Astronomy Observatory. Images using the VLBA together with several geodetic antennas are also available for some sources. These "VLBA+" observations provide enhanced uv–plane coverage and up to twice the resolution of the VLBA alone. Images made using observations taken only with geodetic antennas are available as well. A large fraction of the sources have been observed at multiple epochs, some as often as about every two months. The RRFID data are available for scientific use by anyone at:

http://www.usno.navy.mil/RRFID/

2. Uses of the RRFID

It is well known that the extragalactic radio sources which comprise the ICRF have variable emission structure on angular scales larger than the precision of their position estimates. The RRFID data allow us to assess the astrometric quality of the ICRF sources (based on intrinsic radio structure) and to monitor the sources for variability or structural changes so they can be evaluated for continued suitability as ICRF objects.

2.1. Structure Index

VLBA images from the RRFID have been used by Fey & Charlot (1997; 2000) to calculate a source "Structure Index" (SI) based on the analysis of Charlot (1990). The SI is an estimate of the intrinsic source structure contribution to the measured group delay and is based on radio images at one epoch. The SI can be used in conjunction with other data to obtain an estimate of

the astrometric quality of the sources. Values for 388 ICRF sources are reported by Fey & Charlot (2000).

2.2. Astrometric Quality

We have used the RRFID together with up–to–date radio astrometric and ancillary data to evaluate the extragalactic sources which make up the ICRF in terms of their suitability for use by the Space Interferometry Mission as radio/optical frame tie sources. As a general result, we have calculated an estimate of the radio astrometric quality of the ICRF sources based on an evaluation of the available radio data. Our estimate of astrometric quality is based on four criteria: 1) position uncertainty; 2) position stability; 3) source compactness; and 4) "Structure Index."

We use position uncertainties from an astrometric solution similar to that made for the ICRF (cf. Ma *et al.* 1998) but using all data in the U.S. Naval Observatory astrometric/geodetic database observed up until March 1999. An indication of the stability of the source positions is obtained from an astrometric analysis similar to that used to obtain position uncertainties but in which a separate source position is estimated for each VLBI session in which the source was observed. The weighted root-mean-square of these position time series are then our estimate of position stability. Fey & Charlot (1997; 2000) found correlations between the observed radio structure and the astrometric position accuracy and stability of the ICRF sources that they studied. These correlations indicate that the more extended sources have larger position uncertainties and are less positionally stable than the more compact sources. It is therefore logical to use observed radio frequency structure as an indicator of the astrometric quality of extragalactic sources. We use source models derived from RRFID data to characterize the compactness of the sources.

To obtain an estimate of radio astrometric quality, each source is evaluated and graded individually for each of the four selection criteria, usually on a scale of from one to ten. The individual scores based on each selection criteria are then totaled for each source. Because sources with no structure information are not evaluated for these criteria (they receive no score so the maximum possible score is different than for those sources with structure information), they are consequently on an absolute scale different from those sources for which this information is available. Thus, we normalize the total score for each source to a scale ranging from zero (for the worst astrometric sources) to one hundred (for the best astrometric sources). The resulting score is our estimate of radio astrometric quality. The distribution of radio astrometric quality for selected ICRF sources is shown in Figure 1. A complete discussion of this work, together with the estimated astrometric quality for individual sources, can be found in Fey *et al.* (2000).

The astrometric quality parameter described here would be an ideal selector for choosing the defining sources in the next realization of the ICRF.

3. Future Work

Continued viability of the ICRF at a high level of accuracy requires measuring and monitoring of the sources for changes in intrinsic structure.

3.1. Structure Variability Index

Since extragalactic radio sources are assumed to be very distant they should exhibit little or no detectable motions. Time variation of the astrometric coordinates of extragalactic radio sources is

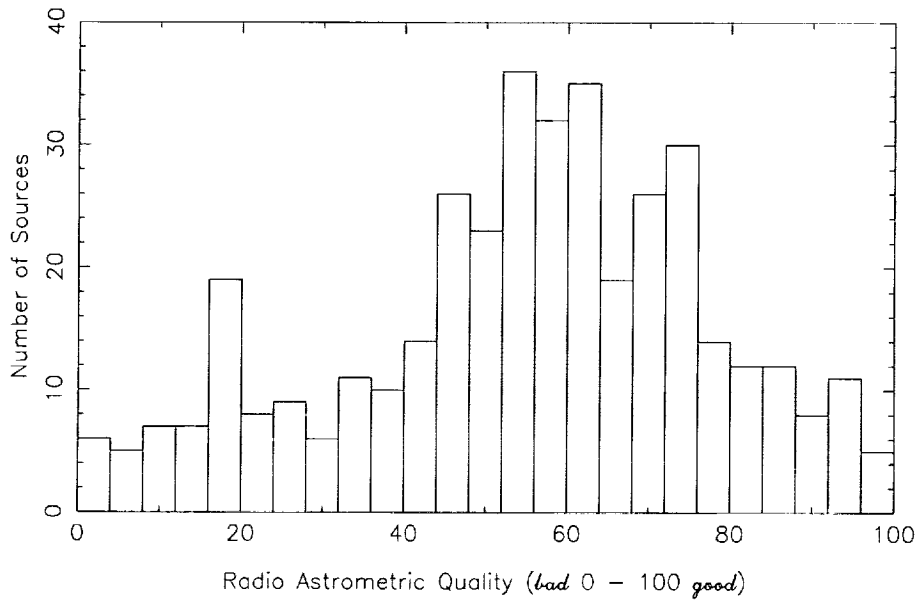

Figure 1. Distribution of radio astrometric quality for selected ICRF sources. The astrometric quality is described in Fey *et al.* (2000) and ranges from zero for the worst astrometric sources to 100 for the best astrometric sources. The estimated astrometric quality for individual sources can be found in Fey *et al.* (2000).

usually attributed to variability of their intrinsic structure (cf. Fey, Eubanks, & Kingham 1997). Since a large fraction of the ICRF sources have been observed at multiple epochs, some as often as about every two months, the RRFID is an ideal resource for estimating the structural variability of the ICRF sources. One method would be to determine a "Structure Variability Index," similar to the SI discussed above but defined as an estimate of the amount of variability expected in group delay measurements taken at multiple epochs, based on the magnitude of the spatial variability of the intrinsic structure of the ICRF sources. This variability index could then be used as an additional criteria used in the calculation of astrometric quality described above with the end result being a refined estimate of the astrometric quality for each ICRF source.

4. References

Charlot, P. 1990, AJ, 99, 1309
Fey, A.L., & Charlot, P. 1997, ApJS, 111, 95
Fey, A.L., Eubanks, T.M., & Kingham, K.A. 1997, AJ, 114, 2284
Fey, A.L., & Charlot, P. 2000, ApJS, in press
Fey, A.L., *et al.* 2000, in preparation
Johnston, K.J., *et al.* 1995, AJ, 110, 880
Ma *et al.* 1998, AJ, 116, 516

Per Helge Andersen: Combination of VLBI, GPS and SLR Data at the Observation Level - A Status Report, IVS 2000 General Meeting Proceedings, p.288–288
http://ivscc.gsfc.nasa.gov/publications/gm2000/andersen

Combination of VLBI, GPS and SLR Data at the Observation Level - A Status Report

Per Helge Andersen

FFI Forsvarets forskningsinstitutt

e-mail: per-helge.andersen@ffi.no

Abstract

A significant number of VLBI and SLR stations are equipped with GPS receivers. A few true fundamental stations with all three techniques even exist. Each technique has its strength and weakness with respect to the determination of geodetic parameters and together they complement each other in a way that should be fully taken advantage of in the data analysis. The simultaneous analysis of different data types at the observation level, due consideration of the physical interrelations, and presentation of results in a common reference system, are the main ideas behind the development of the GEOSAT software. A new and improved version of the software has been implemented with automatic generation of 1) observation residuals and observation partial derivatives for VLBI, GPS and SLR, consistent at the 0.1 ppb level, and 2) a simultaneous arc-by-arc UD-filtering at the observation level. A very advanced multi-level (presently four parameter levels including stochastic parameter representations at each level) SRIF arc combination software for long-term solutions has been developed and validated. The main elements of the processing scheme will be presented. The first results with a simultaneous analysis of different space geodetic data types (VLBI, GPS, and SLR) at the observation level were presented at the IERS-98 symposium in Potsdam and at GPS99 in Tsukuba. The analysis has recently been extended with significantly more observations. Results (Earth orientation parameters, geocenter, radio source coordinates, station coordinates, ...) from the new analysis will be presented. It is demonstrated that UT1 and nutation parameters can be determined also for days where VLBI data is unavailable.

Jim R. Ray: New Timing Products from the IGS: IGS/BIPM Time Transfer Pilot Project and UT1-like Estimates from GPS, IVS 2000 General Meeting Proceedings, p.289–295
http://ivscc.gsfc.nasa.gov/publications/gm2000/ray

New Timing Products from the IGS: IGS/BIPM Time Transfer Pilot Project and UT1-like Estimates from GPS

Jim R. Ray

Earth Orientation Dept., U.S. Naval Observatory
e-mail: jimr@maia.usno.navy.mil

Abstract

The International GPS Service (IGS) and its Analysis Centers are engaged in developing new products related to timekeeping, some of which are relevant to the IVS community. Global comparisons and techniques for dissemination of atomic time are being developed in a Pilot Project with the Bureau International des Poids et Mesures (BIPM). Full project information is available at http://maia.usno.navy.mil/gpst.html. In addition, high-quality estimates of Universal Time are now being made based on the observed motions of the GPS orbit planes. While these cannot replace the need for VLBI determinations of UT1, they are nonetheless very valuable for densifying the VLBI-based time series and for providing extremely rapid turnaround results necessary for real-time applications.

1. IGS/BIPM Time Transfer Pilot Project

The "IGS/BIPM Pilot Project to Study Accurate Time and Frequency Comparisons using GPS Phase and Code Measurements" was authorized in December 1997 jointly by the IGS and the BIPM. A Call for Participation was issued shortly afterwards with responses received from about 35 groups. The respondents have formed a working group, which was formally initiated on 18 March 1998 and is co-chaired by F. Arias, BIPM, and J. Ray, U.S. Naval Observatory (USNO).

A number of groups have been working for several years to develop the capability of using geodetic GPS techniques for accurate time and frequency transfer. A variety of convincing demonstrations has already been performed showing the potential for determining clock differences at the level of a few hundred picoseconds or better. The current state of maturity of both the global GPS tracking network and data analysis techniques now allows practical applications to be considered. The central goal of this Pilot Project is to investigate and develop operational strategies to exploit GPS measurements for improved availability of accurate time and frequency comparisons worldwide. This will become especially significant for maintaining the international UTC time scale as a new generation of frequency standards emerges with accuracies of 10^{-15} or better.

The respective roles of the IGS and BIPM organizations are complementary and mutually beneficial. The IGS and its collaborating participants bring a global GPS tracking network, standards for continuously operating geodetic-quality, dual-frequency GPS receivers, an efficient data delivery system, and state-of-the-art data analysis groups, methods, and products. The BIPM and its timing laboratory partners contribute expertise in high-accuracy metrological standards and measurements, timing calibration methods, algorithms for maintaining stable time scales, and formation and dissemination of UTC. The progress of the Project and other related information is maintained at the Web site http://maia.usno.navy.mil/gpst.mil.

2. Project Activities – Deployment of GPS Receivers

In addition to the GPS receivers already installed as part of the IGS global tracking network, other receivers at laboratories having accurate time standards are sought. These should be high-quality geodetic receivers capable of recording and rapidly transmitting dual-frequency pseudorange and carrier phase observations. The station configuration and data distribution should conform to IGS standards and appropriate documentation must be filed with the IGS Central Bureau. A log file should be completed and sent to the IGS Central Bureau for each IGS station. For this Project, due consideration should be given to electronic stability, environmental control, and other factors which might affect the timing results. Upgrading of existing tracking stations for better timing performance is also encouraged. Deployment of dual-frequency GLONASS receivers, especially collocated at IGS sites, would provide an additional data source of interest.

The IGS network currently consists of about 200 permanent, continuously operating geodetic stations globally distributed. Of these, external frequency standards are used at about 30 with H-masers, 20 with cesium clocks, and 20 with rubidium clocks. Most of the remaining sites rely on internal crystal oscillators. Currently 13 IGS stations are located at timing laboratories; additional installations are under development.

3. Project Activities – GPS Data Analysis

Strategies for analyzing GPS phase and pseudorange observations are required, consistent with other IGS products, to allow the routine, accurate characterization of time standards at a large number of independent GPS receiver sites and onboard the GPS satellites. This work is being done in close cooperation with the IGS Analysis Center Coordinator.

Of the IGS Analysis Centers, all but two already provide satellite clock estimates, which are combined and distributed with the IGS orbit products. The IGS is in the process of expanding its operational products to include combined clocks for the tracking receivers as well. A detailed plan for doing this was developed and considerable progress has been achieved.

4. Project Activities – Analysis of Instrumental Delays

In order to relate receiver clock estimates derived from GPS data analysis to external timing standards it is necessary to understand the instrumental electronic delays introduced by the associated hardware. There are, as yet, no geodetic receiver systems for which the timing calibration bias is known. This situation is a fundamental challenge to exploiting GPS geodetic techniques for time transfer. Two types of instrumental calibration approaches are being pursued by various groups. One method characterizes the delay through individual components of the receiver system. A second method attempts the end-to-end calibration of a complete (or near-complete) system by injecting simulated GPS signals. Both methods involve significant technological feats. Generally, the first method is more accessible, at least for certain components, and has the advantage of permitting the most sensitive system elements to be identified. An overall accurate system calibration determination, which is ultimately required for time transfer applications, can be difficult to obtain, however. The end-to-end methods are clearly desirable for practical uses but they require unique, expensive test equipment and may not be suitable for routine operational settings.

The level of understanding and control of environmental factors that affect frequency compar-

isons is much more advanced than time calibration. Standards of metrological control are well known in the timing community and have been implemented to varying extent at several IGS stations. Frequency comparisons at the level of 10^{-15} over one day, or better, appear entirely feasible already provided that care is taken to minimize environmentally induced variations (e.g., Bruyninx et al., 1999; Petit et al., 1999).

5. Project Activities – Time Transfer Comparisons

Simultaneous, independent time and frequency comparison data are needed to compare with the GPS-derived estimates. Collaborations are sought with groups performing time transfer experiments using a variety of techniques, particularly two-way satellite time transfer. Close cooperation is maintained with the Consultative Committee for Time and Frequency (CCTF) of the Comite International des Poids et Mesures (CIPM).

6. Project Objectives – Accurate and Consistent Satellite Clocks

Satellite clock estimates are among the core products of the IGS (Kouba et al., 1998). The IGS combined solutions for satellite clocks are distributed together with the IGS combined orbits in the sp3 product files. It is essential that the clock information be as accurate as possible and also that it be fully consistent with the other IGS products. Kouba et al. (1998) describe the importance of global consistency to ensure that the point positioning technique (Zumberge et al.,1997) can be applied without degradation.

A type of point positioning likely to become increasingly important is for tracking low Earth-orbiting satellites equipped with onboard GPS receivers. For this application the 15-minute tabulation interval of the sp3 orbit files is not adequate because the SA corruption of the broadcast clocks does not allow accurate interpolation over intervals longer than about 30 s (Zumberge et al., 1998a). For this and other applications, the IGS has been asked to consider providing satellite clock products with 30-s sampling rates. Methods for efficiently computing high-rate satellite clocks have been presented by Zumberge et al. (1998b) and Soehne (1998). A new exchange format has been developed that can permit easy distribution of the new high-rate clock results.

7. Project Objectives – Accurate and Consistent Station Clocks

Presently, the IGS does not produce clock information for the GPS ground stations although doing so is mentioned in the IGS Terms of Reference. There is a clear interest in the user community for this information. Apart from time transfer uses, it could be used to characterize and monitor the performance of station frequency standards. Clock solutions from stations equipped with very stable frequency standards (especially H-masers) are needed to apply the method of Zumberge et al. (1998a) to estimate high-rate satellite clocks. For this purpose, station clock determinations at intervals of about 5 minutes can be accurately interpolated to the 30-s intervals needed to solve for the satellite clocks provided that the ground stations are referenced to stable clocks.

For time transfer applications, such as envisioned for this Pilot Project, accurate analysis results for the station clocks are mandatory. As with high-rate satellite clocks, a suitable exchange format is required and has been developed. Preliminary summary reports to describe the analysis results characterizing satellite and station clocks are available, which will soon become an official IGS

product.

From geodetic analyses of the GPS data, the effective clock of each station is determined for the ionosphere-corrected L3 phase center of the antenna displaced by the electronic delay to the point in the receiver where the time tags are assigned to the pseudorange measurements. These clock determinations are relative measurements in the sense that usually a single station is chosen as a time reference and not adjusted. From the viewpoint of geodetic applications, the precise reference point of the analysis clocks is irrelevant. As a result, manufacturers of geodetic receivers have generally not taken care to provide easy or accurate access to the time reference points. However, for timing applications, such as time transfer comparisons with other techniques, the precise location of the clock reference and accurate access to it are essential. Consequently, the investigation of instrumental path delays and access points is critical to the success of the Pilot Project. The effects of environmental influences are generally important and must be minimized. Doing so will require new approaches for isolating GPS receiver equipment, such as efforts by Overney et al. (1997).

8. Project Objectives – Accurate and Stable Reference Time Scale

Ultimately, it is necessary that all clock information, for satellites and stations, be referenced to a common, consistent time scale. Individual sets of results from different Analysis Centers generally refer to different reference clocks. Thus, in the IGS combination process, the individual submissions must be realigned. This is currently done by choosing one submission as a reference solution, realigning its satellite clock estimates to GPS time based on the broadcast clocks for all the satellites (using only daily offset and rate terms), and then realigning all the other submissions to the reference solution (Springer et al., 1998). Corrections are applied to each solution set to account for radial orbit differences compared to the IGS combined orbits. The IGS combined satellite clock estimates are then formed from the weighted average of the realigned, corrected submissions.

It has been suggested that the clock realignment and combination process would be improved if a common set of fiducial station clocks were used in all analyses and included in the IGS submissions (Springer et al., 1998). Naturally, only stations equipped with very stable frequency standards (preferably geometrically well distributed) should be considered as candidate fiducials. Recommendations for this station set have been adopted.

Likewise, it is questionable whether GPS time is an appropriate choice for the underlying IGS time scale. The ideal choice should be accurate, accessible, and stable over all relevant time intervals (namely, 30 s and longer). GPS time is readily accessible but not with an accuracy comparable to other IGS products due to SA effects. Nor is GPS time particularly stable. The clocks of the GPS constellation are monitored from USNO and this information is provided to GPS operations with the goal of maintaining GPS time within 28 ns (RMS) of UTC(USNO), allowing for accumulated leap second differences. In practice, the two time scales have been kept within about 6.5 ns (modulo 1 s) over the last two years (for 24-hour averages). However, the GPS time steering algorithm has a bang-bang character resulting in a saw-tooth variation with a typical cycle of about 25 days. This is equivalent to a frequency error greater than 10^{-14} over days to weeks, which changes periodically in an abrupt, nearly step-like fashion.

Almost certainly, an internal ensemble of the frequency standards used in the IGS network can be formed which would possess better stability than GPS time (Young et al., 1996). There are

currently about 30 IGS stations using H-masers, and about 40 with cesium or rubidium standards. Addition of new IGS sites located at primary timing laboratories would only improve this situation. A purely internal IGS time scale would not be stable against long-term drifts so some linkage to external laboratory time scales is required. Indeed, traceability to UTC is most desirable. In principle, this could be accomplished using the instrumental calibration data mentioned above, especially for the fiducial clock sites. It will be technically difficult, however, to achieve comparable accuracies for the calibration measurements to the few hundred picosecond level possible for the data analysis clocks. This will be one of the greatest challenges for this Pilot Project.

An alternative approach to provide external linkage that can be readily implemented uses monitor data for the GPS constellation that are collected and compared at the timing labs. USNO collects such data using pseudorange timing observations and makes the results publicly available. Using the observed offsets of GPS time relative to UTC(USNO), the corresponding IGS clock estimates can be related to UTC(USNO). Because of the effects of SA such comparisons would only be useful to remove long-term differences. This is probably sufficient, at least for an initial realization. Other timing laboratories would be encouraged to provide similar monitor data for a more robust tie to UTC. A potential problem with this approach is possible biases between the effective clocks transmitted by the satellites as measured from the pseudorange and carrier phase observables.

Apart from the issues discussed above concerning calibration and external referencing for an IGS time scale, there are other practical questions that must be resolved. In particular, it may be difficult to form and maintain a time scale within the IGS product delivery schedule. This is likely to be especially true for the Rapid products even though that is probably also where the greatest user interest lies. Fundamentally, this does not seem overwhelming although it will require entirely new and highly automated IGS processes. Other practical concerns are minimizing discontinuities at day boundaries, dealing with clock discontinuities and drop-outs in the ensembling process, and finding an appropriate robust ensembling algorithm. These subjects, together with those mentioned above, should be studied during this Pilot Project.

9. UT1-like Estimates from GPS

UT1 cannot normally be estimated in the analysis of satellite tracking data used also to determine the satellite orbit. The UT1 rotation angle is perfectly correlated with the ascending node of the orbit. However, if a priori constraints are applied to the node parameter, such as by imposing continuity with the preceding data arc, then UT1-like variations can be estimated. Such constraints can risk degrading the orbit determination so they are not commonly used. The EMR Analysis Center (at Natural Resources Canada, Ottawa) is the only IGS group which uses this method.

Length of day (LOD) can normally be estimated and this is routinely done in high-accuracy GPS analyses. There is a perfect correlation between LOD and the rate of change of the ascending orbit node, but the latter is not ordinarily an adjusted parameter. On the other hand, any error in the modeling of the node rate will cause an error in the LOD estimates. In particular, GPS-based LOD estimates tend to be sensitive to biases, which is equivalent to a net nodal drift of the constellation.

All IGS Analysis Centers provide LOD estimates, which are combined after bias-correction and weighting based on comparison to the IERS Bulletin A series for a recent 21-day sliding period

(Mireault et al., 1999). The combination and the best individual submissions have random short-term errors (after bias correction) of roughly 20 μs and larger. The GPS-based LOD time series can be integrated to form a UT1-like series, where the errors will behave as a random walk (Ray, 1996).

In the IERS Bulletin A combination (for rapid service and prediction applications), the most recent IGS combined LOD values are integrated and included for epochs after the latest VLBI data. The 21 most recent days of directly estimated UT1-like values from EMR are also included, after calibration in offset and rate by comparison with overlapping VLBI results.

10. New UT1-like Series from USNO

Kammeyer (2000) has developed an alternative technique for extracting UT1-like variations by comparing observed, Earth-fixed GPS satellite ephemerides to numerically propagated models of their orbital planes. The modeled orbit planes are propagated using empirical models for the orbit-normal component of the radiation pressure acceleration. These models are expressed in terms of the angle from the orbital angular momentum to the Sun direction and the angle from the projection of the Sun direction onto the orbit plane to the position vector of the satellite. For each satellite and each time, there is a unique axial rotation angle which brings the observed Earth-fixed positions into alignment with the propagated orbit plane. The difference between the ascending node of the modeled orbit plane and that of the actual orbit plane for each satellite causes this rotation angle to differ by an offset from Greenwich apparent sidereal time. Adding to the rotation angle an estimate of this offset gives a single-satellite estimate of sidereal time and equivalently of UT. Taking the median of these estimates for the 12 satellites modeled (soon to increase to 16) gives the UT estimate reported to IERS Bulletin A.

By comparison with VLBI results, we have established that Kammeyer's GPS-based series has errors which can be characterized by two components which should be added in quadrature. The short-term noise floor is approximately white and has a variance of about $(25\ \mu s)^2$. As with any satellite-based determination, there is also a random walk component, the variance of which is about $40\ \mu s^2 \times t$ where t is the duration in days since calibration with VLBI. This performance is much better than for any other satellite-based estimates, particularly for the long-term behavior.

IERS Bulletin A has grown increasingly reliant on the IGS estimates of LOD and UT1-like variations, especially since the development of Kammeyer's series. In June 1999, the method used to assimilate the latter series was changed to incorporate it entirely beginning 8 July 1998, rather than only for the most recent period. A calibration trend is computed and applied based on a smoothing of low-frequency differences compared with VLBI. Calibration of the most recent GPS results, after the end of the latest VLBI data, is based on an ARIMA model extrapolation of the earlier low-frequency trend. This new assimilation method provides better UT1 values in the historic Bulletin A series by improving the "interpolation" where gaps in VLBI data occur. It also provides better rapid service performance by enhancing the stability of "extrapolation" after the latest VLBI data. Note that the GPS results from the IGS Rapid product delivery are available daily at 17:00 UTC for the previous day. This very rapid turnaround relieves the pressure for fast turnaround of VLBI Intensive data. However, it does not remove the critical need for frequent VLBI observations which remain necessary for calibration of the GPS-based results and for the development of the underlying empirical orbit models.

References

[1] Bruyninx, C., P. Defraigne, and J-M. Sleewaegen, "Time and frequency transfer using GPS codes and carrier phase: Onsite experiments", GPS Solutions, 3(2), 1-10, 1999.

[2] Kammeyer, P., "Determining a UT1-like quantity by comparing observed GPS orbits to numerically-propagated models of orbit planes", submitted to Celestial Mechanics and Dynamical Astronomy, 2000.

[3] Kouba, J., J. Ray, and M.M. Watkins, "IGS reference frame realization", in 1998 IGS Analysis Center Workshop Proceedings, European Space Operations Centre, Darmstadt, Germany, 139-171, 1998.

[4] Mireault, Y., J. Kouba, and J. Ray, "IGS Earth rotation parameters", GPS Solutions, 3(1), 59-72,1999.

[5] Overney, F., Th. Schildknecht, and G. Beutler, "GPS time transfer using geodetic receivers: Middle-term stability and temperature dependence of the signal delays", Proc. 11th European Frequency and Time Forum, 504-508, 1997.

[6] Petit, G., C. Thomas, Z. Jiang, P. Uhrich, and F. Taris, "Use of GPS Ashtech Z12T receivers for accurate time and frequency comparisons", IEEE Trans. on Ultrasonics, Ferroelectrics, and Frequency Control, 46(4), 941-949, 1999.

[7] Ray, J., "Measurements of length of day using the Global Positioning System", J. Geophys. Res.,101, 20141-20149, 1996.

[8] Soehne, W., "Precise high-rate satellite clocks at GFZ", in 1998 IGS Analysis Center Workshop Proceedings, European Space Operations Centre, Darmstadt, Germany, 57-64, 1998.

[9] Springer, T.A., J.F. Zumberge, and J. Kouba, "The IGS analysis products and the consistency of the combined solutions", in 1998 IGS Analysis Center Workshop Proceedings, European Space Operations Centre, Darmstadt, Germany, 37-54, 1998.

[10] Young, L.E., D.C. Jefferson, S.M. Lichten, R.L. Tjoelker, and L. Maleki, "Formation of a GPS-linked global ensemble of Hydrogen masers, and comparison to JPL's linear ion trap", Proc. 50th Annual Institute of Electronics Engineers (IEEE) International Frequency Control Symposium, 1159-1162, 1996.

[11] Zumberge, J.F., M.B. Heflin, D.C. Jefferson, M.M. Watkins, and F.H. Webb, "Precise point positioning for the efficient and robust analysis of GPS data from large networks", J. Geophys.Res., 102(B3), 5005-5017, 1997.

[12] Zumberge, J.F., M.M. Watkins, and F.H. Webb, "Characteristics and applications of precise GPS clock solutions every 30 seconds", Navigation, 44(4), 449-456, 1998a.

[13] Zumberge, J.F., F.H. Webb, and M.M. Watkins, "Efficient estimation of precise high-rate GPS clocks", in 1998 IGS Analysis Center Workshop Proceedings, European Space Operations Centre, Darmstadt, Germany, 55, 1998b.

T.A. Springer: Common Interests of the IGS and the IVS, IVS 2000 General Meeting Proceedings, p.296-305
http://ivscc.gsfc.nasa.gov/publications/gm2000/springer

Common Interests of the IGS and the IVS

T.A. Springer

Astronomical Institute, University of Berne, Switzerland
e-mail: springer@aiub.unibe.ch

1. Introduction

With the advent of the International Laser Ranging Service (ILRS) and the International VLBI Service (IVS) all three major space geodetic techniques, GPS, SLR, and VLBI, have a dedicated service. The availability of these three services, IGS, ILRS, and IVS, will simplify the cooperation and exchange of information amongst the three services.

The routine availability of reference frame products, station coordinates and Earth rotation parameters with their full covariance matrix, from all three techniques will enable an accurate combination of the reference frames from the different techniques. This is very important because it has become clear over the last few years that there are biases between the techniques at the several centimeter level, e.g., a 5 cm bias has been observed between the SLR range observations from the GPS satellites and the computed ranges based on IGS orbits and ITRF SLR station positions [11]. Each of the three techniques has its own unique capability and none of the three techniques can provide all the answers we are looking for. Already each technique profits from the other, e.g., GPS and SLR rely on the VLBI based UT1, SLR may use the GPS and VLBI based X- and Y-polar motion, and GPS heavily relies on SLR based models like, e.g., the Earth's gravity field. When combining the three techniques we should be able to get the best out of each technique. Last but not least the availability of products from different techniques may help understanding and resolving technique dependent problems.

1.1. The International GPS Service

Over the last decade GPS started playing a major role in regional and global studies of the Earth. In view of a continued growth and diversification of GPS applications, the scientific community has made an effort to promote international standards for GPS data acquisition and analysis, and to deploy and operate a common, comprehensive global tracking network. As part of this effort, the International GPS Service (IGS) was established by the International Association of Geodesy (IAG) in 1993 and began official operation in January 1994. Usually, the International Association of Geodesy (IAG) General Meeting in August 1989 in Edinburgh, UK, is considered as the starting point for the IGS. The IGS planning committee was created shortly thereafter and the IGS call for participation was sent out in February 1991. At the XXth IUGG General Assembly in Vienna in August 1991 the IGS planning committee was reorganized and renamed IGS campaign oversight committee. This oversight committee organized the 1992 IGS Test Campaign scheduled from June 21 to September 23.

The 1992 operations were so successful, that data collection, processing, and product dissemination continued without interruption after September 23, 1992, first on a "best effort" basis, then, starting November 1, 1992, as the "IGS Pilot Service". During this pilot phase in 1993, the

IGS Terms of Reference were written and the current IGS structure was established. The official start of the IGS took place in January 1994. In December 1997 the name of the IGS was slightly changed. The original name was International GPS Service for Geodynamics. Due to the enormous expansion of the IGS the term "for Geodynamics" was no longer considered to accurately reflect all IGS activities, which by that time also included atmospheric studies. For more information concerning this early phase of the IGS see, e.g., [5, 3].

The IGS is based on the voluntary contributions of a large number of organizations. The current structure of the IGS consists of [4]: global network of tracking stations, operational centers, regional data centers, global data centers, analysis centers (AC), associate analysis centers (AAC), analysis center coordinator (ACC), central bureau (CB), governing board (GB), and working groups.

According to the Terms of Reference the accuracy of the IGS products should be sufficient to support current scientific objectives including: scientific satellite orbit determinations, monitoring Earth rotation, realization and easy global accessibility to the International Terrestrial Reference Frame (ITRF), monitoring deformations of the solid Earth, and variations in the liquid Earth, climatological research, eventually weather prediction, and ionosphere monitoring.

The primary objective of the IGS is to provide the reference system for a wide variety of scientific and practical applications involving GPS. To fulfill its role the IGS produces a number of "fundamental" products, which are: GPS data from a global network of about 200 stations, GPS satellite orbits, GPS satellite clocks, Earth rotation parameters, station coordinates and velocities, station specific tropospheric zenith path delays (ZPD), global ionosphere maps, and GPS receiver clocks. For more information about the IGS and all its components see, e.g., the IGS Annual Reports [12, 4, 6].

At the start of the IGS Test Campaign in 1992 the focus was mainly on the GPS satellite orbits. The goal was to provide orbits of an accuracy which would allow the "normal" geodetic GPS user to avoid orbit determination. The effect of an orbit error dR on an estimated baseline component is given by the following "rule of thumb", see [2]:

$$dx \approx dR \cdot \frac{L}{R} \tag{1}$$

where L and dx are baseline length and baseline component error and R, dR are satellite distance and orbit error. From eqn. (1) we see that for a baseline with length $L = 400$ km, $dR = 2$ m (typical error for the GPS broadcast orbits), and $R = 20000$ km the baseline component error will be about 40 mm. Using IGS orbits, assuming an orbit error (dR) of about 100 mm, the baseline component error due to the orbit error will be at the 2 mm level. Figure 1 illustrates the effect of the orbit quality on baseline estimates quite nicely. A European baseline of approximately 400 km was processed once using broadcast orbits and once using precise IGS orbits; both solutions were performed over a period of 100 days. The coordinates of one station were kept fixed, whereas the coordinates of the second station were solved for. Figure 1 shows the variation of the daily position estimates of the second, free station, from both solutions. The RMS of the variations using broadcast orbits is 13, 24, and 23 mm in the north, east, and up directions, respectively. This corresponds quite well with the estimated orbit effect of 40 mm. In the case of the IGS orbits the RMS of the variations is 2, 3, and 6 mm in the north, east, and up directions, respectively.

Figure 2 shows the weighted orbit RMS (WRMS) of the individual Analysis Center solutions with respect to the combined IGS final orbit products. Figure 2 reflects the quality improvement of the IGS products as a function of time since 1994. The quality of the IGS orbit estimates has

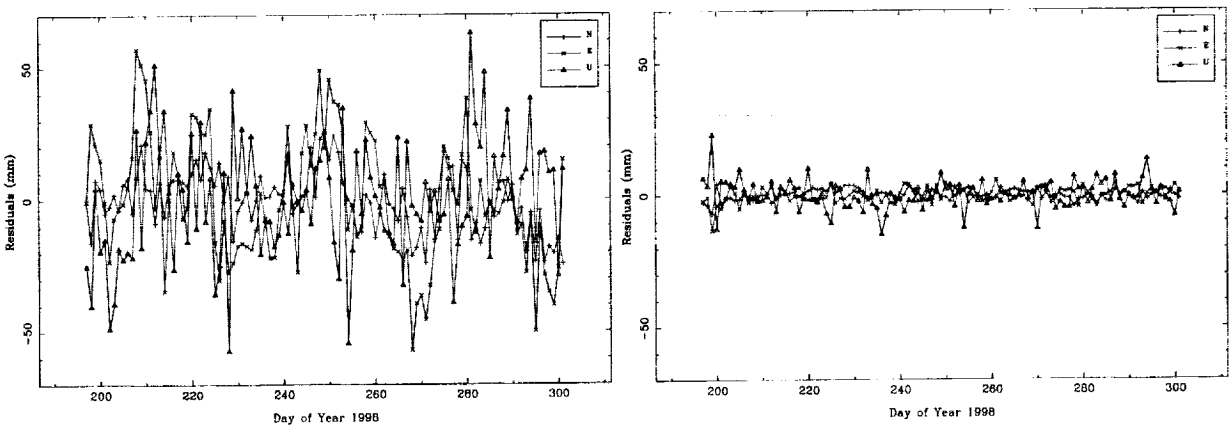

(a) Using broadcast orbits

(b) Using IGS orbits

Figure 1. Residuals of daily position estimates on a 400 km baseline using orbits of different quality.

improved from the 200 mm to the 30 mm level in a time period of 5 to 6 years. The routine combinations of the products of the different IGS Analysis Centers have played a major role in the improvements of the IGS product quality. We are convinced that without the feedback coming from the IGS combinations the quality improvements would have been significantly smaller. Of course, Figure 2 only shows the internal consistency of the IGS products and not their accuracy. However, similar levels of accuracy are indicated by the IGS 7-day arc orbit analysis and by the comparisons with satellite laser ranging observations of the GPS satellites PRN 5 and 6. Notice also the quality of the IGS rapid orbit (IGR) in Figure 2. This orbit product is available with a delay of currently only 17 hours after the end of observation and its quality is comparable to that of the best individual Analysis Center final products.

2. Common Interests of the IGS and the IVS

In GPS and VLBI analysis there are a relatively large number of common parameters; station coordinates, Earth rotation parameters (X, Y, and LOD), tropospheric zenith delays and gradients, and the station clock offsets in those cases where the GPS and VLBI receivers are connected to the same external oscillator. The station coordinates, and their time evolution (velocity), and the Earth rotation parameters are of interest to all geodetic techniques and these will become (or already are) available in the SINEX (Software INdependent EXchange format) product files from the Analysis Centers of the different techniques. The tropospheric zenith delays and gradients, and the station clock offsets are common to GPS and VLBI.

The availability of the SINEX products from the different techniques will allow the routine comparison (or combination) of the reference frames of the individual techniques. The progress made within the IGS has shown how effective and useful the comparisons of different results are. The IGS has also defined exchange formats for tropospheric zenith delay and station clock estimates. It would be very valuable if the IVS would adopt the IGS formats, with enhancements where necessary, for these estimates because it would make comparisons of the results very easy.

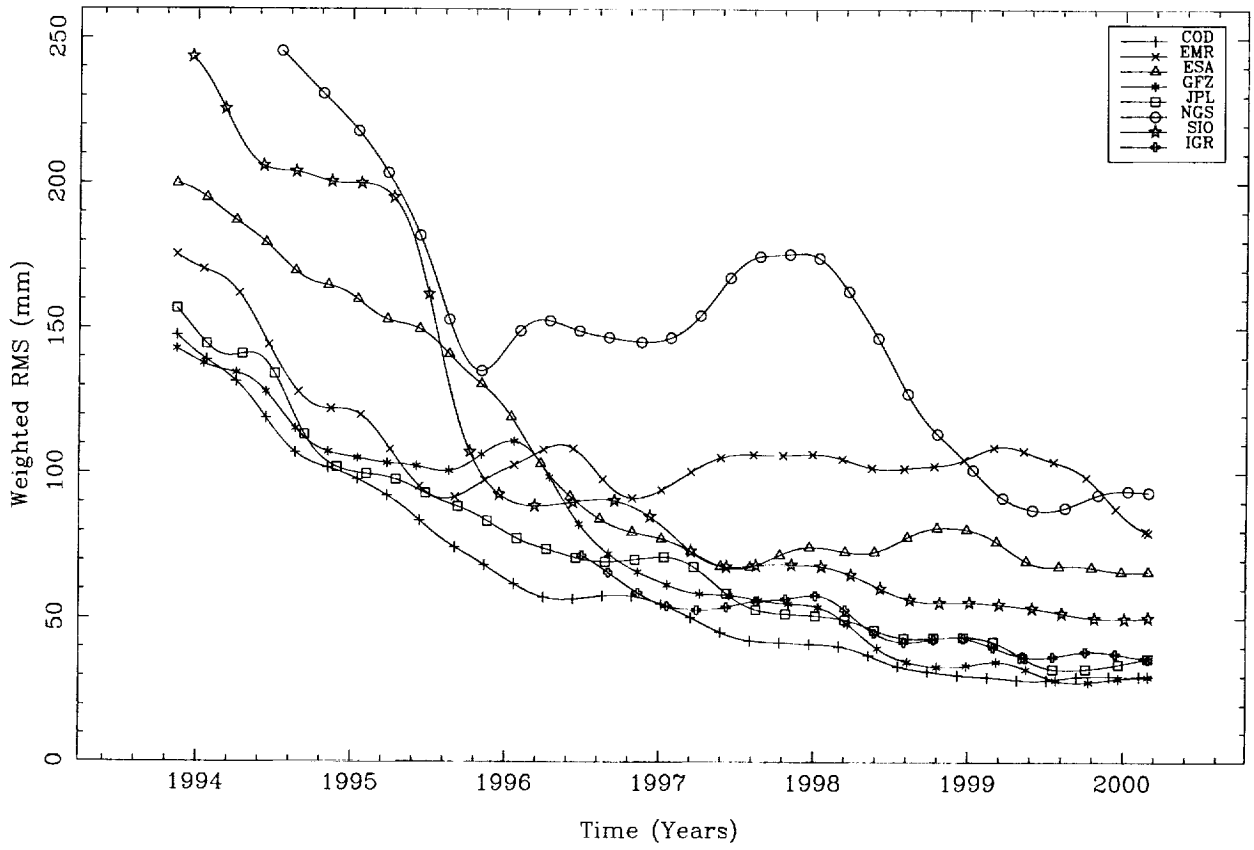

Figure 2. Weighted orbit RMS (cm) of the Analysis Center and IGS Rapid (IGR) orbit solutions with respect to the IGS final orbits. The weekly WRMS values from the IGS orbit combination summaries were smoothed, for plotting purposes, using a sliding 10 week window.

We are convinced that both techniques will greatly benefit from comparisons of all these products.

Furthermore, in the GPS (IGS) results there are currently two interesting problems which cannot be resolved by using GPS alone. For both problems the IGS needs the support of some other technique. The first problem, or at least interesting result, is that the time series of the coordinate estimates show similar signals for stations in the same geographical area. The question which has to be solved here is whether these signals represent real geophysical phenomena or whether they are some artificial signal caused by modeling problems in the GPS data analysis. One way to try to resolve this problem is by comparing the time series from different IGS Analysis Centers, which is routinely done within the IGS. However, it will be much more informative to compare time series from different Analysis Centers using different techniques. Here clearly the IVS may help the IGS.

The second problem is the question of where the GPS satellite transmitter phase center is located. Recently it has become clear that there may be an error on the meter level in the location of the transmitter phase center. Because of correlations between the estimated parameters, especially with tropospheric zenith delays, the transmitter phase center location cannot be solved for using GPS data. For this purpose the IGS has requested the IVS to evaluate whether VLBI observations of the GPS satellites could help to solve this problem. Tom Herring proposed this at the IGS 1999 Analysis Center workshop held at the Scripps Institute for Oceanography, in La Jolla, California. Both problems will be discussed in more detail below.

2.1. Geographically Correlated Station Position Variations

It has become clear that the GPS time series of station coordinate estimates from the different IGS Analysis Centers show similar signals for stations in the same geographical area. The main question is whether these signals represent real geophysical phenomena or whether they are an artifact of the GPS data analysis. Figure 3 shows an example of these geographically correlated station position variations for two different areas, Eastern and Western Europe, over a time period of three years. These figures are based on the results of the CODE (Center for Orbit Determination in Europe) Analysis Center of the IGS [10].

Figure 3 shows that the height variations of the stations are as large as 20 mm with an approximately annual period. The coherence between the stations within a certain geographical area is very high. The difference between geographical areas, e.g., East and West Europe, are quite large. In Western Europe the height variation seems to have a maximum around the start of the year whereas in Eastern Europe a minimum is observed around this time. The size of these effects is such that they could easily be caused by geophysical processes like, e.g., atmospheric loading (which is in general not accounted for by the IGS analysis centers). However, there are several reasons why GPS results could show annual signals. First of all the solar radiation pressure, which is the dominant error source in the GPS orbit model, has an annual period. Secondly the 4 minute change per day of the station–satellite geometry, because the orbital revolution period of the GPS satellites is approximately half a sidereal day, also leads to an annual period in the station–satellite geometry. It is very likely that this annual period will show up in the results because of multipath effects which strongly depend on the station–satellite geometry.

The best way to resolve this problem is to compare the GPS based time series with time series from one or more of the other geodetic techniques. Of course also the (inter)comparison of GPS results from the different IGS Analysis Centers may give some idea. However, in most cases the

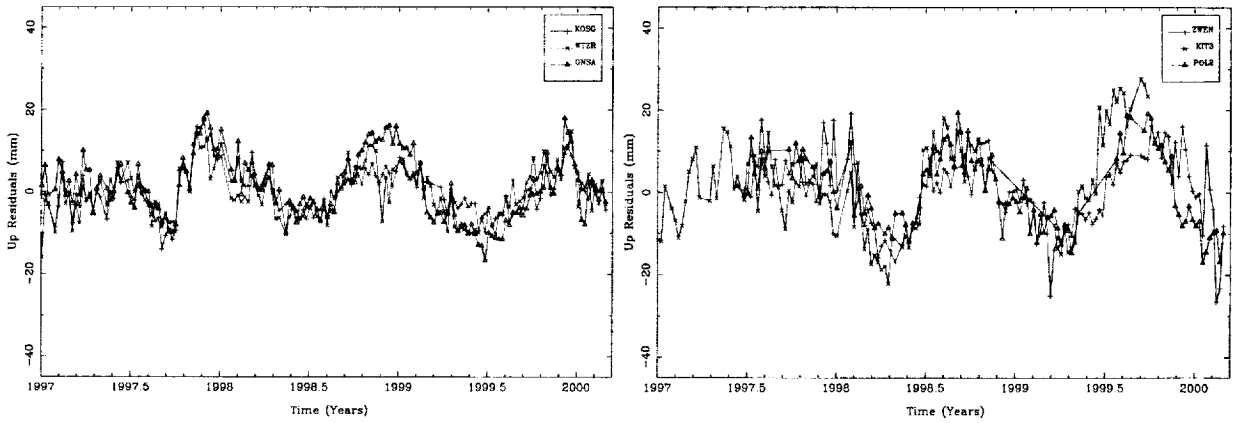

(a) Western Europe

(b) Eastern Europe

Figure 3. Residuals of daily height estimates from global GPS solutions for stations in the same geographical area.

GPS time series agree quite well which each other. The only exceptions are observed in some of the "remote" areas where only a few IGS stations are present. Clearly the comparisons of station coordinate time series from the IGS and the IVS will be most useful to resolve this issue.

2.2. GPS Satellite Transmitter Antenna Phase Center Offset

One of the major remaining problems in GPS data processing is the location of the satellite and receiver antenna phase centers. The recently observed bias (1 meter!) in the phase center location of the first block IIR satellite (PRN 13) has made it clear that the position of the satellite phase center offset is not well known [1]. Also, the elevation-dependent phase center variations of the receiver antennas are a major error source. A complicating factor is that the phase center offset estimates are highly correlated with the estimated tropospheric zenith delays and the terrestrial scale. To study the effects of the antenna phase center offsets we generated a series of test solutions using different processing strategies. The solutions should give a better understanding of the correlations between the antenna phase center offsets, the elevation dependent phase center variations, the tropospheric zenith delays, and the terrestrial scale. The following four processing options were modified in the test solutions:

- Constrained or free terrestrial scale. The "constrained" solutions are generated by constraining the coordinates of 37 reference stations to 1 mm. The free solution is generated by using minimal constraints (3 rotational constraints).
- The satellite transmitter phase center offset (Z-offset) is either fixed, artificially changed, or estimated. We call this a Z-offset because the direction of the satellite phase center offset corresponds with the Z-axis of the satellite-fixed reference frame. The Z-axis is the axis pointing from the center of mass of the satellite to the geocenter.
- Either relative receiver antenna phase center variations, relative to the Dorne Margolin antennas [8], or absolute variations using anechoic phase chamber values [7] are used.

	Differences w.r.t. Reference Solution			
Solution Description	Scale (ppb)	Tropos. (mm ZPD)	Z-off (m)	RMS (mm)
Scale Fixed	0.1	0	-	1.46
Scale Free, 15° cut-off	-0.3	1	-	1.40
Scale Free, 20° cut-off	-1.0	4	-	1.36
Scale Free, Z-off. +1 meter	-8.3	5	(+1.0)	1.46
Scale Fixed, Z-off Est.	1.5	-1	-0.2	1.44
Scale Free, Z-off Est.	13.2	-7	-1.6	1.44
Scale Free, Z-off Est. 15° cut-off	17.0	-12	-2.0	1.39
Scale Free, Z-off Est. 20° cut-off	22.8	-18	-2.5	1.34
Scale Fixed, Abs. P.C. Var.	8.5	-10	-	1.57
Scale Free, Abs. P.C. Var.	14.3	-18	-	1.53
Scale Fixed, Abs. P.C. Var., Z-off. Est.	-1.4	-9	2.1	1.49
Scale Free, Abs. P.C. Var., Z-off. Est.	-29.7	9	5.5	1.46

Table 1. Influence of small processing changes on the terrestrial scale, tropospheric zenith delay, and satellite antenna offset.

- Different elevation cut-off angles (10°, 15°, or 20°) are used.

Combinations of these processing options were tested and the results are summarized in Table 1. The reference solution was a minimally constrained (3 rotational constraints) solution, which means in particular that the terrestrial scale was free. The other processing options of the reference solution were identical with those of our official IGS solution, i.e., 10° cut-off angle with elevation-dependent weighting, relative phase center variations introduced, and no Z-offset estimated. The normalized RMS of the one-way L_1 phase observations of this reference solution was 1.46 mm. The first column of Table 1 identifies the processing option which was changed w.r.t. the reference solution. The next three columns show the mean difference between the test solution and the reference solution, in terrestrial scale, tropospheric zenith path delay, and estimated satellite antenna offsets. The last column gives the normalized RMS of the one-way L_1 phase observations.

We first wanted to know whether there were significant differences between the solutions with a fixed or free scale. No significant differences were found. Secondly, we tested the influence of the elevation cut-off angle by changing it from 10° to 15° and 20°. Here a change of 1.0 ppb in the terrestrial scale was observed going from a 10° to a 20° cut-off angle. This change corresponds to a 6 mm height change of the station heights. The formal errors of the height estimates, however, were 3–5 mm and 3–6 mm for the 10° and 20° solutions, respectively. Thus a 1.0 ppb scale change is practically within the 1σ formal error, and therefore not significant. It is interesting to note that the noise of the normalized observation residuals (RMS) seems to decrease with increasing elevation despite the fact that we use elevation-dependent weighting for the observations.

Next we artificially changed the satellite phase center offsets of all satellites by one meter. In Table 1 we see that this change has a large impact on both the terrestrial scale and the tropospheric zenith delays. The scale changed by 8 ppb (50 mm in station height) and the zenith delays were changed by 5 mm (15 mm in station height). A comparison of the station coordinate estimates

showed that they agreed at the few mm level after a 7 parameter transformation. Apart from the scale change of 8 ppb the coordinate transformation showed a small translation in the Z-direction of 5 mm. A comparison of the orbit estimates, without any parameter transformation, showed that they agreed on the mm level, which is remarkable considering the relatively large changes in the other parameters. These results underline the strong correlation between the satellite antenna phase center offset, the terrestrial scale, and the tropospheric zenith delays.

We then made the attempt to estimate the phase center offset of the satellites by estimating one offset for each individual satellite. It should be mentioned that the observability of this offset is rather poor due to the fact that the "observation angle" between the satellite–receiver and satellite–geocenter vectors is at maximum 14^o. This means that the major part of the Z-offset shows up as a range bias which may be absorbed by ambiguities and/or clock offsets and is strongly reduced in double difference observations. In this context the test where we changed the Z-offset by one meter is quite convincing. Only 70 mm (7%) of the 1 meter change showed up in the results.

The remaining effect of the Z-offset will have an elevation-dependent signature because the "observation angle" increases with decreasing satellite elevation. This elevation-dependent signature explains the correlation between the Z-offset and the estimated tropospheric delays. In addition, it is well known that the tropospheric delays correlate with the station heights and therefore with the terrestrial scale. The results of the four tests which were performed with Z-offset estimation are quite remarkable. If the scale of the terrestrial network is constrained the results look quite reasonable. However, as soon as the scale is left free to adjust the results differ quite significantly from the reference solutions with changes of 22 ppb in scale, 18 mm in zenith delay, and more than 2 m in satellite antenna phase center offset. Notice that the formal errors of the station heights (3–6 mm) and the tropospheric zenith delays (1–2 mm) barely change. The formal errors of the Z-offset estimates are a few centimeters only but increasing strongly with growing cut-off angle (from 40 to 70 mm going from 10^o to 20^o). Besides the scale change the coordinate transformation again showed small translations in the Z-direction of up to 15 mm. Also the orbits were now different but only by 20 mm in RMS without showing significant orientation differences. Quite disturbing is the pronounced elevation-dependency of the results.

In the last four tests we introduced the absolute receiver phase center offset and variations from anechoic chamber measurements. Earlier investigations had shown that the introduction of these absolute phase center measurements resulted in a 15 ppb terrestrial scale change of the GPS results [9]. In our earlier tests we noticed that the satellite antenna offsets also cause large scale effects in the terrestrial network. We therefore hoped to find a solution for the satellite antenna offset which would enable us to use the absolute phase center measurements without any residual effects on the terrestrial scale and the estimated tropospheric zenith delays.

The first two solutions, where we introduced the absolute phase center variations, confirm the fact that these give a 15 ppb terrestrial scale change and also large changes in the tropospheric delays. It is remarkable that, in the solution where the scale is constrained, the change of the scale is as large as 8 ppb! Notice also, that the RMS of these solutions is increased.

In the latter two solutions we solved for the satellite phase center offset in addition to introducing the chamber measurements. The solution with the constrained terrestrial scale looks quite acceptable although the Z-offset change of 2 meters is large. However, the minimal constrained solution shows a dramatic scale change of almost 30 ppb (180 mm station height). Also, the estimated Z-offset is very large (5 m). This solution is not acceptable which means that we are still not in a position to use the absolute phase center variations.

We conclude that it is not feasible to accurately solve for the satellite antenna offsets in an absolute sense due to the correlation with the terrestrial scale, the tropospheric delays, the receiver antenna phase center offsets, and elevation-dependent variations. However, we are able to solve for these offsets in a relative way, e.g., by adopting a specific value for a single satellite. The offsets of the other satellites may then be determined relative to this adopted value. Significant Z-offset differences were observed between the individual satellites. Two other IGS ACs, GFZ and JPL, which also estimated the satellite antenna offsets, observed very similar differences for individual satellites [1]. We furthermore conclude that biases observed in the terrestrial scale and tropospheric delays, based on GPS microwave measurements, are very likely the result of inaccurately known phase center positions (and their elevation dependency) of both the satellite and the receiver antennas. We hope that the IVS will be capable of tracking the GPS satellites and that this will allow us to determine the phase center offset and the elevation dependency of the GPS transmitter antenna. It is clear that this problem can not be resolved using GPS alone.

3. Outlook

The availability of service type of organizations for the three major space geodetic techniques will greatly improve the exchange of information and consequently the cooperation between the different techniques. At the same time this should help the scientists to get a better insight in the strengths *and* weaknesses of the individual techniques.

The combination of the reference frame products from the different techniques on the SINEX level should enable us to get the best out of all three techniques and truly unify the reference frames of the different techniques. It is quite clear that at present systematic differences at the few centimeter level exist between the techniques. The scientific community may therefore look forward to some very interesting results coming from the inter-technique comparisons based on the reference frame products which will be, or already are, routinely provided in the software independent exchange (SINEX) format.

Each of the three techniques has its own specialism and none of the techniques can provide all the answers. It is therefore clear the all three techniques are needed, also because they all depend on each other. In the previous section we have given two examples where GPS needs the help of one or more other techniques. From this perspective the establishment of the combined IVS, IGS, and ILRS working group during the IVS 2000 General Meeting which was held in Kötzting, Germany, is an excellent development. In this working group analysis experts from the three different techniques will work together and try to resolve problems and inconsistencies between the techniques. The first item on the list of this working group is the determination of the location of the GPS transmitter phase center offset. Secondly, the working group will study the observed SLR–microwave bias.

References

[1] Yoaz E. Bar-Sever. Estimation of the GPS Transmit Antenna Phase Center Offset. *presented at the AGU Spring Meeting, EOS Transactions*, 79(45):183, November 1998.

[2] I. Baueršíma. NAVSTAR/Global Positioning System (GPS), II. Mitteilungen der Satelliten-Beobachtungsstation Zimmerwald, No. 10, Astronomical Institute, University of Berne, 1983.

[3] G. Beutler, I. I. Mueller, and R. E. Neilan. The International GPS Service for Geodynamics (IGS):

Development and Start of Official Service on January 1, 1994. *Bulletin Géodésique*, 68(1):39–70, 1994.

[4] IGS. *IGS 1997 Annual Report.* IGS Central Bureau, IGS Central Bureau, JPL, Pasadena, California, USA, 1997.

[5] I. I. Mueller and G. Beutler. The International GPS Service for Geodynamics - Development and Current Structure. In *Proceedings 6th International Geodetic Symposium on Satellite Positioning, Vol. 2*, pages 823–835, Ohio State University, Columbus, Ohio, USA, 1992.

[6] Ivan Mueller, Ruth Neilan, and Ken Gowey. *IGS 1997 Technical Reports.* IGS Central Bureau, Jet Propulsion Laboratory, Pasadena, California U.S.A., 1997.

[7] C. Rocken, C. Meertens, B. Stephens, J. Braun, T. VanHove, S. Perry, O. Ruud, M. McCallum, and J. Richardson. Receiver and antenna test report. Technical report, UNAVCO Academic Research Infrastructure (ARI), 1996.

[8] M. Rothacher, W. Gurtner, S. Schaer, R. Weber, and H. O. Hase. Azimuth- and Elevation-Dependent Phase Center Corrections for Geodetic GPS Antennas Estimated from GPS Calibration Campaigns. In W. Torge, editor, *IAG Symposium No. 115*, pages 335–339. Springer-Verlag, 1996.

[9] M. Rothacher, S. Schaer, L. Mervart, and G. Beutler. Determination of Antenna Phase Center Variations Using GPS Data. In G. Gendt and G. Dick, editors, *IGS Workshop Proceedings on Special Topics and New Directions*, pages 77–92, Potsdam, Germany, May 15–18 1995. GeoForschungsZentrum.

[10] M. Rothacher, T.A. Springer, S. Schaer, G. Beutler, D. Ineichen, U. Wild, A. Wiget, C. Boucher, S. Botton, and H. Seeger. Annual Report 1997 – CODE Analysis Center of the IGS. In Ivan Mueller, Ruth Neilan, and Ken Gowey, editors, *IGS 1997 Technical Reports*, pages 77–91, Jet Propulsion Laboratory, Pasadena, California U.S.A., October 1998. IGS Central Bureau.

[11] T.A. Springer. *Modeling and Validating Orbits and Clocks Using the Global Positioning System.* PhD thesis, Astronomical Institute, University of Berne, Berne, Switzerland, November 1999.

[12] J. F. Zumberge, D. E. Fulton, and R. E. Neilan. *1996 Annual Report of the International GPS Service for Geodynamics.* IGS Central Bureau, Jet Propulsion Laboratory, Pasadena, California, U.S.A., November 1997. Workshop proceedings.

Poster Session

Analysis Reports

Maria Sokolskaya et al.: EOP Determination with OCCAM and ERA Packages, IVS 2000 General Meeting Proceedings, p.309–313
http://ivscc.gsfc.nasa.gov/publications/gm2000/sokolskaya2

EOP Determination with OCCAM and ERA Packages

Maria Sokolskaya, Elena Skurikhina

Institute of Applied Astronomy RAS
Contact author: Maria Sokolskaya, e-mail: smy@quasar.ipa.nw.ru

Abstract

The EOP series were obtained with OCCAM v. 3.5 and ERA v. 7 packages from VLBI NEOS-A and CORE-A measurements for the period 1997–1999. The EOP estimations provided by OCCAM were compared with those provided by ERA. The correlations of OCCAM and ERA results with the EOP(IERS)C04 were studied. It was found that the results obtained with OCCAM agree satisfactorily with the results obtained with ERA. The differences between the EOP estimated from NEOS-A and CORE-A observations were also calculated with OCCAM and ERA. These differences were verified to be similar and of significant correlation.

1. Introduction

Recently two packages for VLBI data processing are available for the IAA EOP Service. The first of them is OCCAM, which is used in the IAA for the regular estimation of the EOP since 1997. The version 3.5 [1] is now in use. This version is an improvement on OCCAM v. 3.4 [2]. OCCAM v. 3.5 permits both EOP and station positions estimation.

The package ERA v. 7 [3] was advanced for VLBI data processing in 1998 [4]. The package makes available not only the EOP and station positions estimation but also determination of radio source coordinates and subdiurnal tidal terms in UT1.

The estimation of EOP with ERA and OCCAM from NEOS-A and CORE-A observations seems important because it helps to compare and analyze packages and might show evidence for systematical errors. In this paper the single factor statistical analysis of EOP is made. Our next step is to perform the results of multi-factor analysis of the EOP, obtained with different packages from different programs. The paper with graphical representation of result is available on the web page http://www.ipa.nw.ru/PAGE/DEPFUND/GEO/ENG/lab_e.htm.

2. Observations and Reductions

There are 155 NEOS-A and 62 CORE-A VLBI sessions accumulated for the period 1997–1999 which have been processed with OCCAM and ERA. For more detailed information on observations see Table 1.

Both ERA and OCCAM packages process the data with models compliant with IERS Conventions (1996). The station coordinates are taken from the ITRF97. Coordinates of radio sources are taken from either RSC(IAA)99R02 or for newly observed sources from NGS files.

The ERA package requires a special representation of VLBI data in the table form. To estimate EOP with ERA the observations from NGS files were databased in ERA tables. It should be noted that the ERA tables containing the required VLBI processing information are more compact than the corresponding NGS files. The coefficient of compression varies from 4.5 to 5.0 for the data

Table 1. The observations processed.

Year	Network	Period	Number of sessions	Number of observations	Number of stations	Number of radio sources
1997	NEOS-A	weekly	52	53698	7	227
1998	NEOS-A	weekly	52	58191	11	234
1999	NEOS-A	weekly	51	61217	11	252
1997	CORE-A	biweekly	23	22590	5	46
1998	CORE-A	biweekly	25	35377	6	67
1999	CORE-A	biweekly	14	18807	8	63

under consideration. In spite of this advantage the process of databasing takes time while OCCAM deals directly with NGS files.

In the ERA processing the five Earth Orientation Parameters, their diurnal linear trends and coefficients of Legendre polynomials, that approximate station clocks and troposphere zenith path delays were estimated in the least square solutions. In the OCCAM package Kalman filtering is used for estimation of stochastic parameters such as tropospheric path delay and station clocks by random walk model.

3. Comparison of the EOP Obtained with ERA and OCCAM Packages

The differences between the EOP estimations obtained with OCCAM and ERA packages were studied from NEOS-A observations for the period 1994–1999, from CORE-A observations for the period 1994–1999. They were found mostly within 1 milliarcsec for the pole coordinates X_p and Y_p and the nutation parameter $d\epsilon$, within 1.5 milliarcsec for $d\psi$ and 0.025 milliarcsec for $UT1$ (see Table 2). The EOP data for the period 1997–1996 were taken from EOP(IAA)99R01 and EOP(IAA)99R02. The graphical comparison of the differences can be found on the web page http://www.ipa.nw.ru/PAGE/DEPFUND/GEO/ENG/lab_e.htm.

The parameters of linear trend and values of *rms* after/before fitting are given in Table 3, columns 2–3 for each EOP. *Rms* value can be used as a criterion of the coincidence for the data. It is clear from Table 3 that in the sense of *rms* the agreement between ERA and OCCAM in Y_p, $d\psi$ and $d\epsilon$ is better for NEOS-A, in X_p and $UT1$ is a little better for CORE-A. There occur linear trends in X_p and $UT1$ EOP(ERA)−EOP(OCCAM) from NEOS-A differences. The linear trend in $UT1$ differences EOP(ERA)−EOP(OCCAM) from CORE-A can also be detected. No significant trends are found for the other differences. The correlation analysis of the differences EOP(ERA)−EOP(OCCAM) obtained from NEOS-A and those obtained from CORE-A shows low level of relations. The corresponding coefficients of correlation are presented in Table 5, column 1. They are evidence for the fact that there are no systematics in OCCAM and ERA.

4. Comparison of the Obtained EOP with the EOP(IERS)C04

The analysis of systematics in the differences EOP(ERA)−EOP(IERS)C04 and EOP(OCCAM)-EOP(IERS)C04 was carried out for NEOS-A and CORE-A. The parameters of linear trends in the EOP differences are shown in Table 4. The calculated parameters mostly coincide (within 3σ)

Table 2. The statistical characteristics of differences between the EOP (ERA-OCCAM) .

NEOS-A	$X_p(mas)$	$Y_p(mas)$	$UT1(0.1\ ms)$	$d\psi(mas)$	$d\epsilon(mas)$
min	-1.19	-1.06	-0.38	-2.14	-1.28
max	1.34	0.77	0.27	2.20	0.75
mean	-0.12	0.11	-0.07	-0.06	0.10
CORE-A	$X_p(mas)$	$Y_p(mas)$	$UT1(0.1\ ms)$	$d\psi(mas)$	$d\epsilon(mas)$
min	-0.73	-0.91	-0.23	-2.50	-0.90
max	1.20	0.80	0.18	1.72	1.29
mean	-0.05	0.07	0.01	-0.25	0.07

for ERA and OCCAM both for NEOS-A and CORE-A. The trend in X_p is revealed only for the ERA processing of NEOS-A. It can explain the trend in X_p differences in Table 3. The trend might occur because the data were taken from EOP(IAA)99R01 and EOP(IAA)99R02 obtained with ITRF96. The linear trend in Y_p is surely detected for NEOS-A with ERA and OCCAM and less surely for CORE-A. The parameters of the trend are similar that evidence for the fact that this trend does really exist. The trend can be explained by the complex effects of the input C04. The residual of trends in $UT1$ detected with ERA and OCCAM for NEOS-A is positive and explains the increase of differences in $UT1$ with time. No trend in $UT1$ was found for CORE-A. The significant value of bias is detected for $d\epsilon$ for NEOS-A.

The coefficients of correlation between differences EOP(ERA)−EOP(IERS)C04 and differences EOP(OCCAM)−EOP(IERS)C04 obtained for NEOS-A are given in Table 5, column 3. The coefficients of correlation between differences EOP(ERA)−EOP(IERS)C04 and differences EOP(OCCAM)−EOP(IERS)C04 obtained for CORE-A are given in Table 5, column 4.

The similar coefficients of correlation in Table 5, column 3-4 and *rms* from Tables 3-4 analysis make it clear that the OCCAM and ERA packages agree between each other within deviations from C04, and agree satisfactorily with C04.

5. Correlation between Observational Programs

The level of agreement of EOP estimations obtained from different networks NEOS-A and CORE-A was also studied with the OCCAM and ERA packages. The EOP obtained with ERA and OCCAM from simultaneous NEOS-A and CORE-A sessions were compared (62 sessions for the period 1997–1999). Differences between the EOP obtained from NEOS-A and CORE-A with ERA and OCCAM are shown on the web page
http://www.ipa.nw.ru/PAGE/DEPFUND/GEO/ENG/lab_e.htm. From the figure it can be concluded that these differences are similar and of significant correlation. This is evidence for systematic differences between observational programs. The correlation coefficients between the differences NEOS-A−CORE-A obtained with ERA and NEOS-A−CORE-A obtained with OCCAM are given in Table 5, column 2. The parameters of linear trends in EOP are presented in Table 3. The *rms* value characterizes the root mean square of the series, *crms*—the root mean square of the differences after linear fitting. It is easy to conclude from Table 3 that there are few significant parameters of the linear trends.

Table 3. Parameters of linear trends in the differences between the obtained EOP.

	ERA−OCCAM		NEOS-A−CORE-A	
	NEOS-A	CORE-A	ERA	OCCAM
$T_0(year-1900)$	94.01	97.08	97.08	97.08
X_p, mas,bias	-0.41 ± 0.03	-0.01 ±0.07	-0.03 ±0.11	-0.15 ±0.09
$\dot{X}_p, mas/year$	0.10 ± 0.01	-0.03 ±0.05	-0.05 ±0.07	-0.04 ±0.06
$crms/rms$	0.30/ 0.36	0.29 / 0.29	0.45 / 0.46	0.37 / 0.43
Y_p, mas,bias	0.13 ± 0.03	0.02 ±0.08	0.04 ±0.11	-0.04 ±0.07
$\dot{Y}_p, mas/year$	-0.01 ± 0.01	0.04 ±0.05	-0.08 ±0.07	-0.03 ±0.05
$crms/rms$	0.28/ 0.30	0.33 / 0.34	0.44 / 0.45	0.28 / 0.29
$UT1, 0.1\ ms$,bias	-0.16 ± 0.01	-0.05 ±0.02	-0.02 ±0.03	0.03 ±0.03
$\dot{UT}1, 0.1\ ms/year$	0.03 ± 0.00	0.05 ±0.01	0.05 ±0.02	0.05 ±0.02
$crms/rms$	0.08/ 0.12	0.07 / 0.08	0.12 / 0.13	0.14 / 0.18
$d\psi, mas$,bias	-0.04 ± 0.03	-0.08 ±0.07	0.05 ±0.10	0.02 ±0.05
$\dot{d\psi}, mas/year$	0.00 ± 0.01	-0.01 ±0.05	0.01 ±0.06	0.01 ±0.03
$crms/rms$	0.26/ 0.26	0.30 / 0.31	0.39 / 0.39	0.20 / 0.20
$d\epsilon, mas$,bias	0.10 ± 0.03	0.22 ±0.08	-0.10 ±0.10	0.06 ±0.07
$\dot{d\epsilon}, mas/year$	0.00 ± 0.01	-0.12 ±0.06	0.13 ±0.07	-0.03 ±0.04
$crms/rms$	0.27/ 0.28	0.34 / 0.35	0.41 / 0.42	0.27 / 0.27

Table 4. Parameters of linear trends in the differences between the obtained EOP and EOP(IERS)C04.

	NEOS-A		CORE-A	
	ERA	OCCAM	ERA	OCCAM
$T_0(year-1900)$	96.99	96.66	98.46	98.46
X_p, mas,bias	-0.23 ± 0.02	-0.10 ± 0.02	0.03 ± 0.05	0.09 ± 0.03
$\dot{X}_p, mas/year$	0.10 ± 0.01	0.00 ± 0.01	-0.00± 0.06	0.06 ± 0.04
$crms$	0.23	0.34	0.22	0.34
Y_p, mas,bias	0.07 ± 0.02	-0.04 ± 0.01	0.24 ± 0.04	0.16 ± 0.03
$\dot{Y}_p, mas/year$	0.05 ± 0.01	0.06 ± 0.01	0.12 ± 0.05	0.04 ± 0.04
$crms$	0.19	0.28	0.23	0.30
$UT1, 0.1\ ms$,bias	-0.02 ± 0.01	0.05 ± 0.01	0.03 ± 0.01	0.05 ± 0.02
$\dot{UT}1, 0.1\ ms/year$	-0.02 ± 0.01	-0.04 ± 0.00	-0.00 ± 0.02	0.05 ± 0.02
$crms$	0.11	0.11	0.12	0.10
$d\psi, mas$,bias	-0.09 ± 0.03	-0.03 ± 0.01	-0.37 ± 0.09	-0.15 ± 0.06
$\dot{d\psi}, mas/year$	0.01 ± 0.02	-0.01 ± 0.01	0.05 ± 0.12	0.02 ± 0.08
$crms$	0.34	0.62	0.45	0.66
$d\epsilon, mas$,bias	0.14 ± 0.01	0.04 ± 0.01	0.04 ± 0.04	-0.00 ± 0.03
$\dot{d\epsilon}, mas/year$	-0.00 ± 0.01	0.00 ± 0.01	-0.10 ± 0.06	0.03 ± 0.04
$crms$	0.15	0.23	0.24	0.30

Table 5. Correlation coefficients between the EOP differences.

	1	2	3	4
$X_p(mas)$	0.26	0.65	0.46	0.56
$Y_p(mas)$	-0.15	0.30	0.43	0.41
$UT1(0.1\ ms)$	0.34	0.77	0.75	0.76
$d\psi(mas)$	0.01	0.22	0.28	0.30
$d\epsilon(mas)$	-0.01	0.07	0.12	0.30

6. Conclusions

- The similar values of trends in EOP obtained with different packages from different programs might show evidence for systematic differences between $C04$ and VLBI results.
- Differences between EOP obtained with ERA and OCCAM both from NEOS-A and CORE-A are of low correlation and have *rms* similar to that of EOP(ERA)−EOP(IERS)C04 differences.
- The comparison of the obtained EOP with C04 shows that the OCCAM results are in a little better agreement with C04 for X_p, Y_p, $d\psi$, $d\epsilon$, than the ERA results. For $UT1$ the agreement with C04 is approximately the same for both packages.
- The accuracy of the EOP obtained from NEOS-A network for the period 1997–1999 is a little better than from CORE-A network.
- Differences between the EOP obtained from NEOS-A and CORE-A both with ERA and OCCAM are similar and of significant correlation. This shows us that these differences are caused rather by systematics between the programs than between packages. It is important to extend this study for other packages.

Acknowledgments

Authors are grateful to George Krasinsky for his participation in installation and exploration of ERA package.

References

[1] Skurikhina, E. A.: Determination of EOP from VLBI in IAA. IAU Colloquium 178. Polar motion: historical and scientific problems. Italy, Cagliary, 1999.

[2] Titov, O. A, Zarraoa: OCCAM 3.4 User's Guide. Comm of the IAA N 69, 1997.

[3] Krasinsky, G. A.,Vasyliev, M.: ERA: Knowledge base for ephemeris and dynamical astronomy. In: Proc. IAA Coll. 165, Poznan, Poland, Kluwer Acad. Publ., 239–244, 1997.

[4] Krasinsky, G. A.: Ocean tidal effects on universal time as obtained from VLBI observations of 1984–1998. In *Trudy IPA RAN, v. 4, Astrometry, geodynamics and celestial mechanics.* – SPb.:IPA RAN, 12–21 (in Russian), 1999.

Maria Sokolskaya et al.: A Catalogue of Radio Source Coordinates Obtained from NEOS and CORE VLBI Programs, IVS 2000 General Meeting Proceedings, p.314–318
http://ivscc.gsfc.nasa.gov/publications/gm2000/sokolskaya1

A Catalogue of Radio Source Coordinates Obtained from NEOS and CORE VLBI Programs

Maria Sokolskaya, Zinovy Malkin

Institute of Applied Astronomy RAS
Contact author: Zinovy Malkin, e-mail: malkin@quasar.ipa.nw.ru

Abstract

A new catalogue of radio source coordinates is constructed as a combination of catalogues derived from NEOS and CORE VLBI programs for the period 1997–1999 using ERA package. One of the main goals of this study was an attempt to investigate systematic differences between source coordinates derived from geodetic VLBI observations made by various sets of stations and estimate a possible proper or apparent motion of radio sources. At the first stage nine catalogues were obtained from observations of NEOS-A, CORE-A and CORE-B programs for 1997, 1998 and 1999. At the next stage six catalogues were derived: three catalogues for years 1997, 1998, 1999 using all observations for these years and three catalogues for each program NEOS-A, CORE-A, and CORE-B for the whole period 1997–1999. Finally, after analysis of differences between catalogues and time variations of source coordinates a combined catalogue was made.

1. Introduction

The improvement of the ICRF is one of the most urgent tasks of modern astrometry and this problem can be solved only by the VLBI method. Modern VLBI observations can provide accuracy of CRF determination at the level 0.1–0.3 mas [1]. To achieve such accuracy one should account for many factors contributing to the CRS error budget.

This paper presents preliminary results of investigation of the influence of radio source structure on CRF. There are at least two possible errors caused by complicated structure.

The first one is the dependence of radio source coordinates of VLBI network configuration. To investigate this effect we compare catalogues of source coordinates derived from observations collected in various VLBI programs NEOS-A, CORE-A, and CORE-B.

The second factor is the apparent (or proper) motion of radio sources. It is evident that for extragalactic radio sources only apparent motion caused by displacement of source emission barycenter can be detected with modern technology. This effect can amount to a few tenths of a mas/y [2]. It can be investigated from coordinate time series, e.g. from a series of catalogues derived from a relatively short period of observations. We used a series of catalogues obtained for one year observation period.

The strategy of this study was the following. At the first stage nine catalogues were obtained from observations of NEOS-A, CORE-A and CORE-B observations for 1997, 1998 and 1999. These catalogues were computed using ERA v. 7 program package from global solutions for observations collected from each program during every year. Hereafter they will be referred as "primary" catalogues.

At the second stage six catalogues were derived from the "primary" ones: three catalogues for years 1997, 1998, 1999 averaged over observational programs and three catalogues for each

Table 1. Statistics of observations.

Year	Network	Period	Number of sessions	Number of observations	Number of stations	Number of radio sources
1997	NEOS-A	weekly	52	53698	7	227
1998	NEOS-A	weekly	52	58191	11	234
1999	NEOS-A	weekly	51	61217	11	252
1997	CORE-A	biweekly	23	22590	5	46
1998	CORE-A	biweekly	25	35377	6	67
1999	CORE-A	biweekly	14	18807	8	63
1997	CORE-B1	bimonthly	5		8	
	CORE-B2	bimonthly	5	21503	9	45
	CORE-B3	bimonthly	5		10	
1998	CORE-B1	bimonthly	6		11	
	CORE-B2	bimonthly	6	39225	9	56
	CORE-B3	bimonthly	6		9	
1999	CORE-B4	bimonthly	5		6	
	CORE-B5	bimonthly	4	21853	7	59
	CORE-B6	bimonthly	5		10	

program NEOS-A, CORE-A, and CORE-B averaged over the period 1997–1999. Finally, after analysis of differences between catalogues and time variations of source coordinates a combined catalogue was made. The paper with the combined catalogue is presented on the web page http://www.ipa.nw.ru/PAGE/DEPFUND/GEO/ENG/lab_e.htm.

2. Observations and Primary Processing

The are 155 NEOS-A, 62 CORE-A, and 47 CORE-B sessions for the period 1997–1999 that were processed. The information on observations is given in Table 1.

At this step equations of conditions accumulated for every year/program were processed in global adjustment to derive corrections to a priori values of radio source coordinates which were taken from RSC(IAA)99R02.

After solving corresponding normal systems nine catalogues have been derived for NEOS-A, CORE-A, and CORE-B for 1997, 1998, and 1999. These "primary" catalogues were used for further study.

The station positions and subdiurnal tidal terms in UT1 were also estimated at this stage, but have not been analyzed in this paper.

3. Comparison of Catalogues Obtained from Different Observational Programs

The differences in right ascension and declination were studied for NEOS-A and CORE-A, NEOS-A and CORE-B, CORE-A and CORE-B observational programs. To calculate these differences three catalogues for NEOS-A, CORE-A, and CORE-B averaged over 1997–1999 were used. The differences of angular positions obtained from different observational programs are shown in

Table 2. Differences between catalogues obtained from different observational programs.

Differences	NEOS-A – CORE-A	NEOS-A – CORE-B	CORE-A – CORE-B
All	51	50	58
> 1.5 mas	2	2	6
< 0.5 mas	43	39	40
< 0.25 mas	33	27	29
< 0.10 mas	11	5	9
$\Delta\alpha, \mu$as	–39±19	–71±17	–30±30
$\Delta\delta, \mu$as	–10±19	–20±19	–23±31
$\Delta\alpha_\alpha, \mu$as	64±30	65±24	75±36
$\Delta\delta_\alpha, \mu$as	23±27	52±27	45±45

Fig. 1. The sources with differences in right ascension or declination greater than 1.5 mas are not presented. For NEOS-A–CORE-A differences such sources are 0106+013, and 1451-375; for NEOS-A–CORE-B, 0106+013, 1313-333; for CORE-A–CORE-B, 0106+013, 0919-260, 0920-397, 1313-333, 2134-00 and 2255-282. 1255-316 has a few observations and a large error and also is not presented. The differences of right ascension and declination are mostly within 0.25 mas. The statistics of these differences are given in Table 2.

We tried also to estimate bias ($\Delta\alpha$ and $\Delta\delta$) and periodic term in differences between catalogues ($\Delta\alpha_\alpha$ and $\Delta\delta_\alpha$).

4. Analysis of Apparent Motion of the Radio Sources

A simple way to analyze the time variability of radio sources is to estimate rates of change of their coordinates with time. For this purpose the differences between catalogues derived from annual series of observations were analyzed. We used both "primary" catalogues based on observations collected with each observational program NEOS-A, CORE-A, and CORE-B, and three catalogues for years 1997, 1998, and 1999 averaged over observational programs.

Two approaches were tried. The first one is based on the analysis of differences 1997–1998, 1998–1999, and 1997–1999 between "primary" catalogues. The second method is least squares estimation of linear trend in coordinates from averaged catalogues.

Formally, one may consider as meaningful a value of computed apparent motion that is greater than say two or three standard deviations. But it is well known that formal estimates of standard deviation do not reflect actual error of observations. So, we plan to use supplemental criteria and longer series of observations to find radio sources having detectable proper or apparent motion.

At this stage we found only several candidates that might have detectable apparent motion. As can be expected they mostly belong to "candidates" or "others" sources according to ICRF classification.

5. Combined Catalogue

A combined catalogue was constructed as a weighted average from nine "primary" catalogues. It is presented on the web page http://www.ipa.nw.ru/PAGE/DEPFUND/GEO/ENG/lab_e.htm.

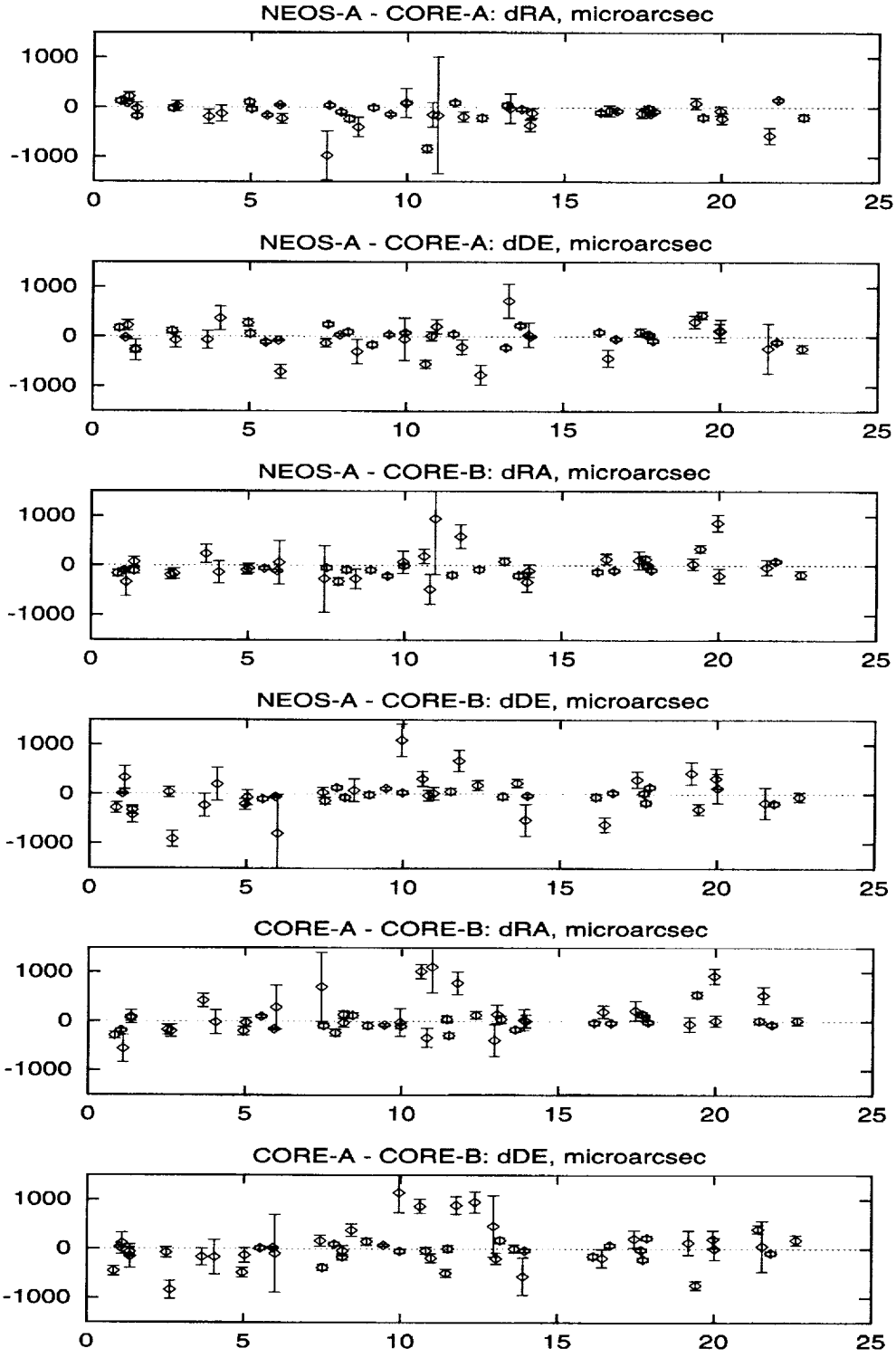

Figure 1. Differences in radio source coordinates obtained from different observational programs as function of RA.

As usual, we can suspect that formal errors in coordinates are underestimated. So, we consider a new procedure for estimation of standard deviation of coordinates which could reflect actual accuracy of observations.

6. Conclusions

This study is based on analysis of "primary" year/program catalogues. It is found that this is an appropriate way to investigate both systematic differences between source directions derived from different observational programs (i.e. on different configuration of network) and detect time variations of coordinates of radio sources. Besides, comparison of annual catalogues allows us to obtain more realistic estimates of errors in source coordinates in the combined catalogue.

Of course, the amount and especially the period of observations are not sufficient to get a definite solution of the problem under investigation. So, we plan to extend this study for all available VLBI observations.

It is clear also that splitting observational data in VLBI programs is only a first approach in studying the dependence of source coordinates on network configuration. Evidently, the next step should be to derive separate catalogues using observations collected from definite network configurations stable during long periods.

Acknowledgments

Authors wish to thank George Krasinsky for his participation in installation and exploration of ERA package.

References

[1] Gontier A.-M., Feissel M., Ma C.: The contribution of VLBI to the realization of a celestial reference system. IERS Technical Note 23, Observatoire de Paris, I-6–I-14, 1997.

[2] Fey P., Charlot P.: VLBA Observations of radio reference frame sources. II. Astrometric suitability based on observed structure. Astrophys. J. Suppl., 111, 95–142, 1997.

[3] Krasinsky G. A., Vasilyev M. V.: ERA: Knowledge base for ephemeris and dynamical astronomy. In: Proc. IAA Coll. 165, Poznan, Poland, Kluwer Acad. Publ., 239–244, 1997.

Wolfgang Schwegmann et al.: Status of IADA: an Intelligent Assistant for Data Analysis in VLBI, IVS 2000 General Meeting Proceedings, p.319–323
http://ivscc.gsfc.nasa.gov/publications/gm2000/schwegmann

Status of IADA: an Intelligent Assistant for Data Analysis in VLBI

Wolfgang Schwegmann, Harald Schuh

Deutsches Geodätisches Forschungsinstitut (DGFI)
Contact author: Wolfgang Schwegmann, e-mail: schwegmann@dgfi.badw.de

Abstract

A faster and semiautomatic data analysis is important if the VLBI procedure shall be accelerated. Most of the tasks during the VLBI data analysis are very complex and require typical knowledge-based techniques. Thus, a Knowledge-Based System (KBS) called IADA (Intelligent Assistant for Data Analysis in VLBI) is being built which can be adapted to different geodetic VLBI software packages. The concept of IADA is described and it is shown how the knowledge about the VLBI data analysis process can be modeled and applied to the data analysis by the problem solving component of the KBS, to automate the data analysis. An interface has to be developed to transfer data and information between the existing software, e.g. the Mark III data analysis software package SOLVE, and IADA. The concept of the interface and the data flow between the KBS and SOLVE is described.

1. Introduction

The VLBI data analysis is a very complex process and needs a lot of manual interactions. It is very time consuming and a partial automation would be very useful to accelerate the VLBI procedure in particular with regard to the increasing number of geodetic observing sessions to be expected in the future. Most tasks of the geodetic VLBI data analysis require a comprehensive knowledge of the whole procedure of data analysis. Thus, a *Knowledge-Based System (KBS)* for support and guidance of the analyst is developed at DGFI to automate the geodetic VLBI data analysis. In this KBS the knowledge about the data analysis is stored and processed according to specific rules and instructions. The concept of an *Intelligent Assistant for Data Analysis in VLBI (IADA)* will be described in section 3.

The KBS can be adapted to different geodetic VLBI software packages by developing an interface between the existing data analysis software and IADA. The interface is used to transfer data and information between both the existing software and the KBS. Whenever the latter is activated the interface collects all necessary data from the database. This information is evaluated by the KBS and possible errors are corrected. The results are transferred back to the existing software and the regular analysis is continued. At present the interface is being built for one of the most widely used geodetic VLBI data analysis software packages, called SOLVE [1]. The concept of the interface and the data flow between IADA and SOLVE will be described in section 4.

2. Advantages of a Knowledge-Based System

Knowledge-Based Systems are software systems in which the knowledge about a problem domain is isolated and stored in a so-called Knowledge Base (KB) and is processed and evaluated by a domain-independent problem-solving component. Modifications of the KB as well as its exten-

sions do not influence the problem-solving component. Only the KB has to be modified to adapt the KBS to new situations or tasks.

A KBS can be used to administer, store and evaluate specific knowledge needed for VLBI data analysis, to provide targeted information for the user and to solve the complex tasks within the data analysis automatically. It is less susceptible to errors, allows to conserve the analyst's knowledge and to check his/her decisions. Moreover, it can be used to guide and to support the analyst during the data analysis, to evaluate situations, to solve new problems and to analyse and check the data and the results. The KBS can be used as a teaching system for less experienced analysts and to exonerate the analyst in his/her routine work.

3. Concept of the KBS

The most important and even critical task when developing a KBS is to build the KB, i.e. to collect, structure and organize the knowledge about the VLBI data analysis (*knowlege acquisition*) and to store it in the KB (*knowledge representation*). The efficiency of a KBS depends on the quality of the knowledge within the KB, which should be modular, flexible and extensible. Several knowledge representation techniques are applied to store the knowledge in the KB:

- *Frames* to represent objects. They consist of several slots to describe the attributes of the object.
  Figure 1 shows an editor to administer frame-based knowledge about VLBI stations in the Knowledge Base of IADA.
- *Behaviors* to change the attributes of an object.
- *Prolog* to analyse a situation, e. g. to check the clock parameterization.
- *Rules* to model knowledge which depends on conditions. Rules consist of a condition part and an action part which is carried out if the condition part is true.

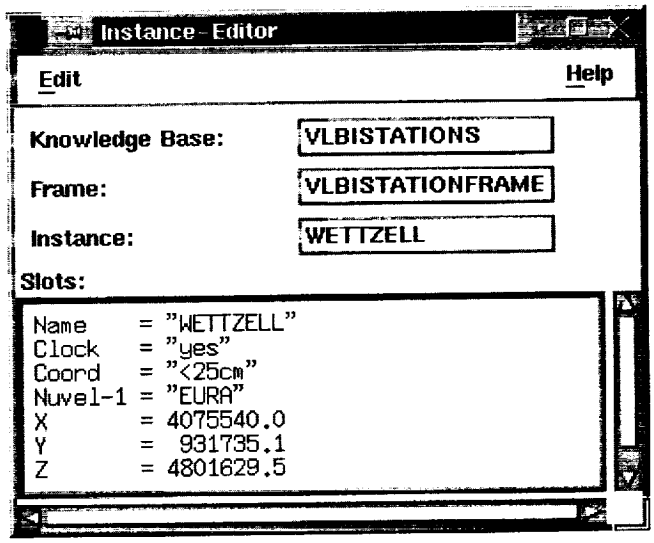

Figure 1. An editor to administer frame-based knowledge.

The representation of the knowledge about the VLBI data analysis using these formalisms is described in more detail in [2].

The structure of the Knowledge Base of IADA is shown in figure 2. The KB contains several components to be modular and easy to maintain as well as to fulfill different tasks like supervising the data analysis, evaluating current situations and deriving a qualitative description of a situation, detecting problems, treating specific situations, solving problems or simulating new situations. The components of the KB are:

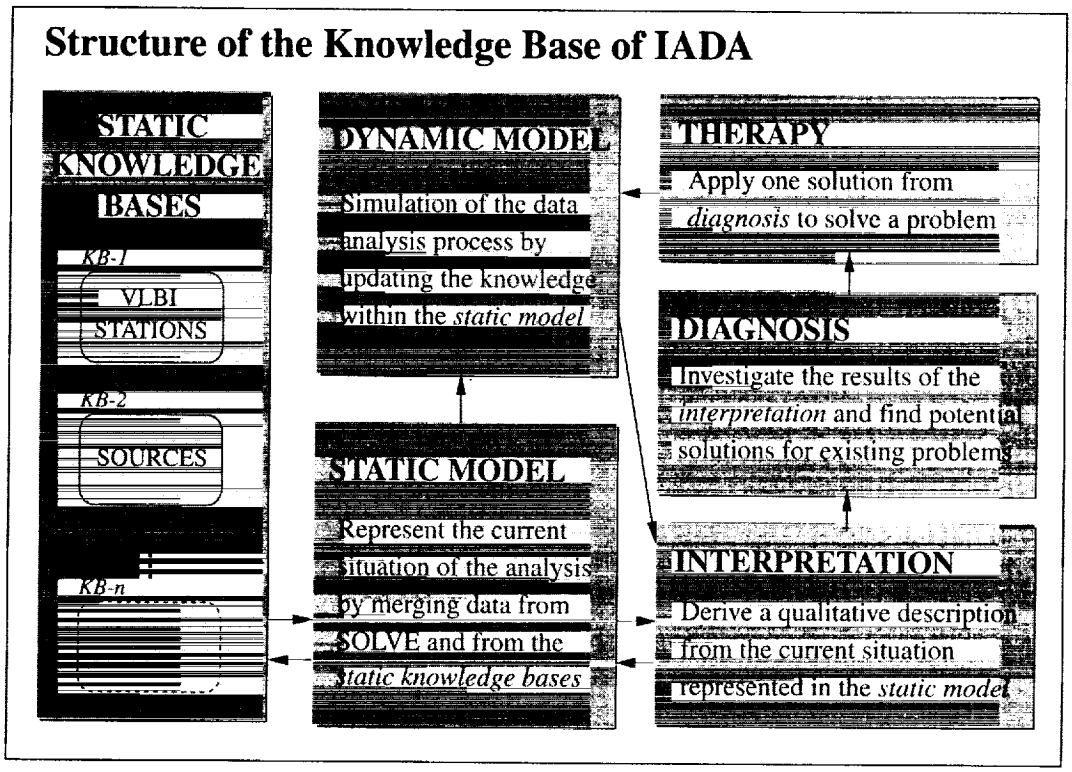

Figure 2. Structure of the Knowledge Base of IADA.

Static Knowledge Bases The static KBs contain general knowledge about the VLBI data analysis which does not depend on the current experiment. Normally the static knowledge bases don't have to be modified during the data analysis.

Static Model The current situation of the analysis is represented in the static model of the KB. This situation is generated by merging static data and information from the static knowledge bases and dynamic information about the status of the analysis which has to be obtained from the VLBI analysis software via the interface. The dynamic knowledge changes during the data analysis depending on the current situation.

Dynamic Model The dynamic model can be used to simulate the analysis process by continuously updating the parameters of the static model. Thus, the system is able to predict the effects of possible changes of the static model and to verify possible solutions of detected problems by using one or several of the components described below.

Interpretation This component evaluates the current situation represented in the static model. It investigates the parameters of the static model and derives a qualitative description of the situation by using rules.

Diagnosis This component evaluates the results of the interpretation, detects possible problems and finds potential solutions for existing problems.

Therapy The results of the interpretation and diagnosis are applied by this component to solve an existing problem.

Due to the modularity of the KB and the mutual independence of its components the analyst is able to use the KBS in different ways. One possible application could be to interpret the current situation, to find possible solutions of a problem, to apply one of these solutions and to use the dynamic model to simulate the effects of this solution. The results may be investigated by the interpretation component and compared with the original situation. On the other hand the analyst is able to simulate the effects following his/her own solutions.

4. Data Flow between SOLVE and IADA

The system interface is being developed to extract data and information from SOLVE and to transfer them to IADA. These data are processed by the KBS to control and/or automate the data analysis. Figure 3 shows the data flow between SOLVE and the KBS when the latter is used to control the VLBI data analysis as a background process. The KBS starts to check the current parameterization in SOLVE any time the analyst is going to start the least-squares solution. Thus, the interface reads the information entered by SOLVE into so-called *scratch files*. The information is transferred to the KBS which builds up the static model according to the current analysis situation and starts the interpretation and diagnosis of that situation. If problems were detected it tries to find potential solutions and applies one of them by updating the parameters of the static model. Then the user is asked whether the solution found by the KBS is correct or not. The KBS tries to find another solution unless the analyst does accept the solution. If the problem is solved the parameters of the static model are extracted by the interface and stored in the scratch files which are used by SOLVE. Finally, the analysis is going to be continued in SOLVE.

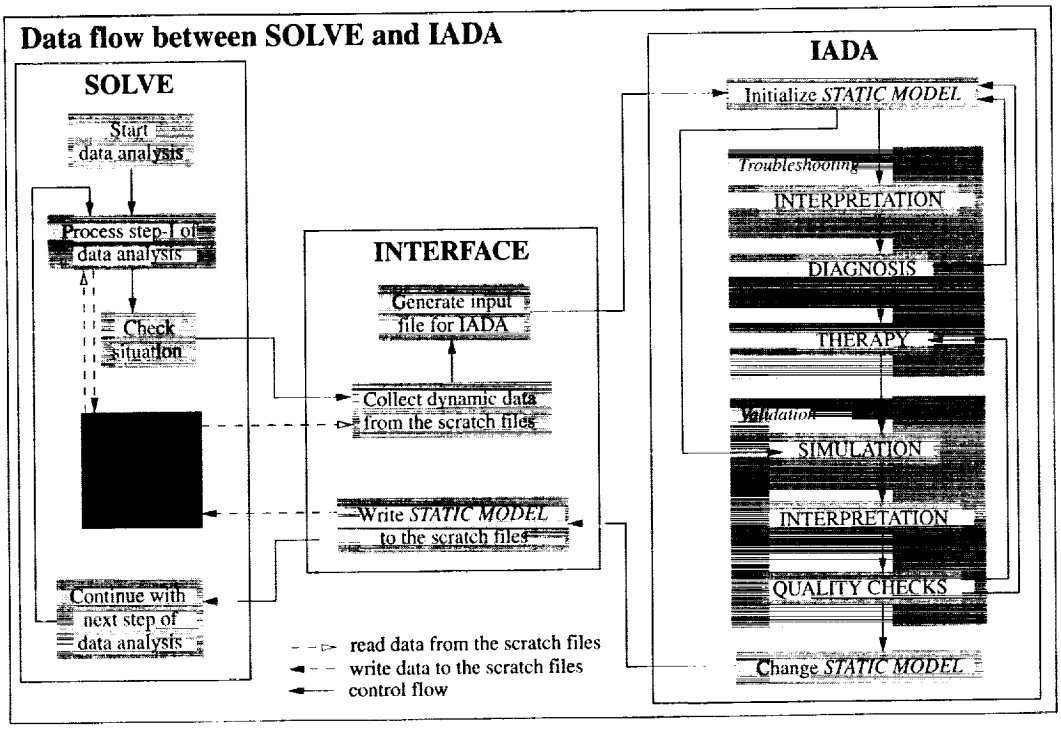

Figure 3. Data flow between SOLVE and IADA.

Figure 4 gives an example of a message which is generated if a problem occured. The analyst has to accept the solution found by the KBS, i.e. he has to confirm the message; if he does not, the KBS tries to find another solution. As soon as the analyst accepts the solution the regular VLBI data analysis will be continued in SOLVE.

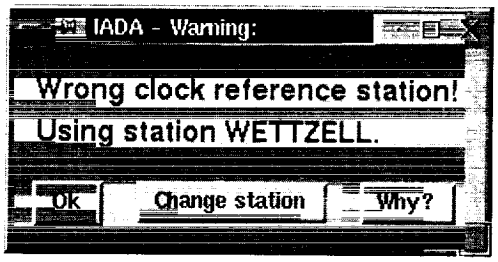

Figure 4. An example of a warning message generated by IADA.

5. Conclusions

The application of knowledge-based techniques for the automation of the VLBI data analysis brings many benefits because they allow an explicit modelling of the multifaceted knowledge needed for these tasks. Thus, the knowledge of several analysts can be conserved and applied by the KBS to automate considerable parts of the data analysis. The importance of the Knowledge Base of a KBS has been pointed out and the modular structure of the KB of IADA has been described. This modularity allows the use of the KBS for several tasks like interpretation, diagnosis and simulation. The interface between the VLBI data analysis software package SOLVE and IADA allows the exchange of data and information between these two systems to control and/or to automate by the KBS the regular analysis done in SOLVE.

6. Acknowledgements

The Knowledge-Based System IADA is developed at DGFI within the research project "Applications of Methods of Artificial Intelligence for the VLBI Data Analysis". This project is supported by the Deutsche Forschungsgemeinschaft (DFG), project Schu 1103/2-1.

References

[1] Ryan, J. W., Ma, C. and Vandenberg, N. R., "The Mark III VLBI Data Analysis System", NASA Goddard Space Flight Center, publication X-945-80-25, 1980.

[2] Schwegmann, W. and Schuh, H., "On the Automation of the Mark III VLBI Data Analysis System", in Proceedings of the 13^{th} Working Meeting on European VLBI for Geodesy and Astrometry, held at Viechtach, February 12-13, 1999, edited by W. Schlüter and H. Hase, Bundesamt für Kartographie und Geodäsie, Wettzell, 1999.

Ulrich Meyer et al.: GINS: A New Multi-Technique Software for VLBI Analysis, IVS 2000 General Meeting Proceedings, p.324–328
http://ivscc.gsfc.nasa.gov/publications/gm2000/meyer

GINS: A New Multi-Technique Software for VLBI Analysis

Ulrich Meyer [1], *Patrick Charlot* [2], *Richard Biancale* [1]

[1]) *Centre National d'Etudes Spatiales, Groupe de Recherches de Géodésie Spatiale/Toulouse*

[2]) *Observatoire de Bordeaux*

Contact author: Ulrich Meyer, e-mail: meyer@step.iapg.verm.tu-muenchen.de

Abstract

The GINS software, developed initially for analysis of satellite geodetic technique data, has recently been extended with a VLBI module for analysis of both Earth-based and space VLBI observations. This report presents the current status of its development and discusses future plans. These include analysis of space VLBI data from the VSOP/HALCA satellite as well as multi-technique (VLBI/SLR/DORIS/GPS) combinations of geodetic data at the observation level.

1. Introduction

The "Groupe de Recherches de Géodésie Spatiale" (GRGS) has developed for many years the GINS/DYNAMO software package for precise satellite orbit computation and geopotential model estimation (e.g. the GRIM models) as well as for reference system determination (e.g. station coordinates and velocities). This package can process angular (optical), range (SLR, PRARE, altimetric), doppler (TRANET, PRARE, DORIS) and GPS data. The corresponding measurement functions were progressively added to the software during the past 20 years following the emergence of each of these techniques in space geodesy.

The VLBI measurement function was not included until recently because an orbit computation is not needed for this technique. However, the launch in 1997 of the Japanese space VLBI satellite HALCA (Highly Advanced Laboratory for Communication in Astronomy) in the framework of the VLBI Space Observatory Program (VSOP) gave a chance, for the first time, to test the concept of space VLBI geodesy. The HALCA satellite consists of an 8 m antenna and observes extragalactic radio sources jointly with Earth-based VLBI stations at frequencies of 1.6 and 5 GHz to provide images of these sources with an unprecedented angular resolution (Hirabayashi 1998). It also measures space VLBI delay and delay rate which can be used for HALCA orbit recovery and geodetic applications, although only on a test basis as such data are of limited accuracy (Fejes 1999).

Adding the VLBI measurement function to GINS fulfils the multi-disciplinarity approach of this software package and beyond space VLBI data analysis also offers new possibilities for combining geodetic data at the observation level, e.g. for Earth orientation determination. The following sections describe the VLBI model implemented in GINS, including the space VLBI capability, and discuss comparisons and tests carried out to ensure its accuracy. Preliminary results of analysis of a single space VLBI experiment from HALCA are also presented.

2. The VLBI Model in GINS

The general structure of the GINS software is shown in Fig. 1. Since the original purpose of GINS is satellite orbit integration and reconstruction, all types of measurements between the Earth and a satellite are easily implemented. In the case of a purely Earth-based technique like VLBI, the orbit integration is omitted and the satellite is replaced by a second ground station, unless if dealing with HALCA data.

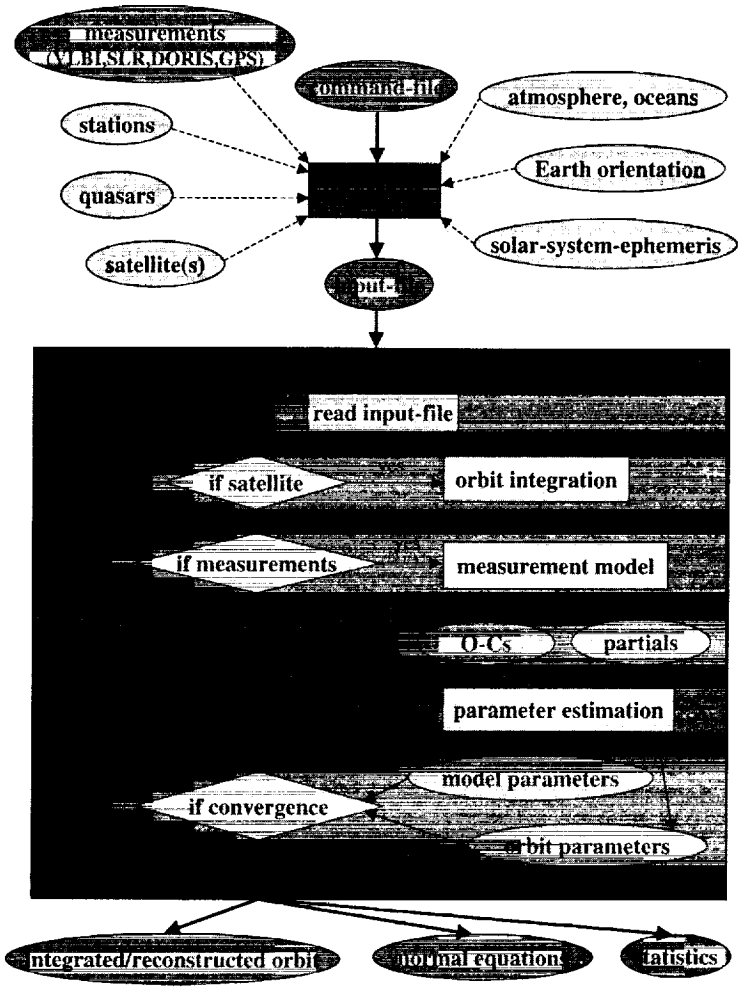

Figure 1. General structure of the orbit integration and reconstruction software package GINS.

The VLBI model implemented in GINS is basically the same as that used in MODEST and described in Sovers et al. (1998); only some of the minor effects (for example, some specific

antenna types) have been omitted for the sake of simplicity. In the initial step, the actual station positions are determined and rotated from the terrestrial frame to a celestial geocentric frame. Station motions like tectonic, tidal, and loading effects, were already part of GINS and have been kept unchanged. The same holds for the rotation part including UT1, polar motion, nutation and precession. These rotated station coordinates are then transformed from the geocentric frame to a barycentric frame by applying a Lorentz transformation which incorporates relativistic effects. In the barycentric frame, the geometric delay is calculated, corrected for a gravitational delay and scaled to a proper delay before it is transformed back to the geocentric frame by the inverse Lorentz transformation. Back in the geocentric frame the delay is corrected for an antenna axis offset delay which depends on the antenna type and the refracted elevation angle of the observed source. Finally atmospheric delays are applied. The ionospheric delays are usually retrieved from the measurement file (in the case of dual-frequency VLBI experiments) while the tropospheric delays are calculated based on surface pressure and temperature (also available from the measurement file) and then are mapped to the elevation angle of the observed source.

Thereon, the difference between observed and calculated delay is formed which goes into a least-squares parameter estimation. The following VLBI parameters may be estimated in the current version of GINS: clock offsets and drifts, wet zenith delays, source coordinates, station coordinates, and Earth orientation parameters (polar motion and UT1). It is possible to use only the original uncertainty of each observation for weighting, but station-dependent or technique-dependent (in the case of a multi-technique analysis) weighting can also be applied.

Specific options were introduced for space VLBI analysis because (i) the satellite and the orbit integration must not be omitted, (ii) the ionospheric and tropospheric corrections must be switched off for the satellite which is sufficiently high to not be influenced by the atmosphere, and (iii) meteorological data and ionospheric delays are usually not available for the ground stations. For the calculation of the tropospheric correction, an option is provided to use standard surface temperature and pressure, while for the ionospheric correction a model has been implemented which calculates the ionospheric delay as a function of the total electron content (TEC), the elevation angle of the radio source and the observed frequency. A crude TEC model in the form of standard daily-varying TEC values is also provided for cases where no TEC measurements are available.

3. Tests of Accuracy

The newly implemented VLBI model and capability of GINS has been evaluated by carefully comparing results obtained with GINS to those obtained with the MODEST software developed by Sovers et al. (1998) and available at Bordeaux Observatory. Most parts of the model showed a very good agreement but some relatively minor differences were also discovered in the course of this comparison.

While the model for tectonic station motion is in exact agreement with that of MODEST, the models for tidal station motions and loading effects apparently differ from the ones implemented in MODEST and cause small deviations.

The Lorentz transformation between the geocentric frame and the barycentric frame gives results that are in accordance with MODEST at the mm level. Small differences are due to the fact that GINS stores and interpolates the solar system ephemeris data while MODEST calls it directly whenever it is needed. The computation of the gravitational delay is in agreement at the sub-mm level and the scaling factor is the same (19.7 ppm as is commonly used in satellite

geodesy).

While the calculation of the axis offset delay in GINS follows the scheme used in MODEST, differences at the mm level were found due to the fact that for calculating the refracted elevation angle GINS uses actual meteorological data stored in the measurement file while MODEST normally uses mean values. The same holds for the calculation of the tropospheric delay.

4. Analysis of Space VLBI Data

The space VLBI capability of GINS has been used to process the delay data acquired in the framework of the space geodesy demonstration experiment (GEDEX) on the HALCA satellite. Further details about this experiment can be found in Fejes (1999). The data file analyzed contains 83 observations on baselines from HALCA to three ground stations (HARTRAO in South-Africa, USUDA64 in Japan, and AT in Australia) covering two periods of about two hours each on December 4, 1997. The observed frequency is 1.6 GHz and the formal errors for the delays on the space baselines are about 2–3 ns. A reconstructed HALCA orbit at the time of the experiment with a claimed accuracy of 10 m is available from the Jet Propulsion Laboratory and is used in our analysis to evaluate the actual accuracy of the space VLBI delays.

While the HALCA perigee height of 544 km is high enough so that no tropospheric and ionospheric corrections have to be considered for HALCA, such corrections are not canceled out for the ground stations and must be modeled. Of these, the ionospheric delay is the largest one because of the relatively low observing frequency of 1.6 GHz. Unfortunately, the TEC describing the ionosphere model cannot be estimated from the data because only a single frequency was observed. The default daily-varying TEC values were thus used in our analysis to calculate the ionospheric delays although these are known to poorly represent the actual behaviour of the ionosphere. The tropospheric corrections were calculated using standard surface temperature and pressure.

The results of our analysis show that the space VLBI delay residuals are at the level of a few meters after estimating a single clock offset and drift and a single wet zenith delay per station (see Fig. 2). These results, although preliminary, are promising and suggest that the HALCA orbit is somewhat better than the claimed accuracy.

5. Future Prospects

The VLBI model implemented in GINS is currently known to be accurate at the few mm level based on comparisons with the MODEST software. Further tests are planned to determine the origin of the small deviations found, especially for the tidal and loading effects. This should ensure a sub-mm accuracy in the near future.

The space VLBI capability of GINS will also be further developed by adding VLBI partials for orbit estimation and a geometric model for the HALCA satellite. The analysis presented here will then be repeated, including also a more sophisticated ionospheric model like that produced routinely by the GPS satellites.

The new VLBI capability of GINS will be useful in the future to carry out multi-technique analyses combining VLBI, SLR, GPS and DORIS measurements at the observation level for Earth orientation estimation and reference frame unification.

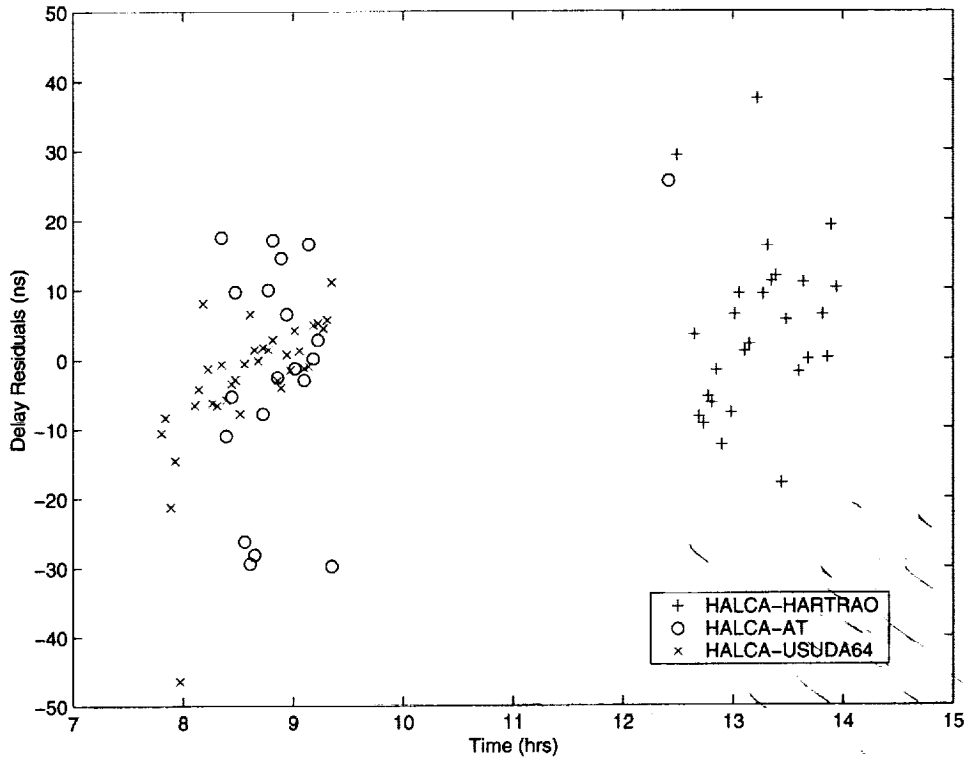

Figure 2. Space VLBI delay residuals (in nanoseconds) for the data of Dec 4, 1997 on three baselines to the HALCA satellite. These were obtained after estimating a single clock offset and drift and a single wet zenith delay per station.

Acknowledgements

We are indebted to Sándor Frey for providing the HALCA space VLBI observations from the GEDEX database in Penc, Hungary and for advice in processing these data. The implementation of the VLBI measurement function in GINS would not have been possible without the substantial support of Sylvain Loyer and Jean-Michel Lemoine while the comparisons with the MODEST software were carried out with the assistance of Ojars Sovers and Chris Jacobs.

References

Fejes, I.: 1999, The Status and Perspective of the Space VLBI Geodesy Demonstration Experiment (GEDEX), *Adv. Space Res.*, 23, 781.

Hirabayashi, H.: 1998, The VSOP Mission – A New Era for VLBI, *IAU Colloquium 164: Radio Emission from Galactic and Extragalactic Compact Sources*, Eds. J. A. Zensus, G. B. Taylor, & J. M. Wrobel, *ASP Conference Series*, Vol. 144, 11.

Sovers, O. J., Fanselow, J. L., & Jacobs, C. S.: 1998, Astrometry and Geodesy with Radio Interferometry: Experiments, Models, Results, *Reviews of Modern Physics*, 70 (4).

Ryuichi Ichikawa et al.: An Experimental Campaign for Evaluation of Wet Delay Variations Using Water Vapor Radiometers in the Kanto District, Central Japan, IVS 2000 General Meeting Proceedings, p.329–333
http://ivscc.gsfc.nasa.gov/publications/gm2000/ichikawa

An Experimental Campaign for Evaluation of Wet Delay Variations Using Water Vapor Radiometers in the Kanto District, Central Japan

Ryuichi Ichikawa [1], *Y. Koyama* [1], *T. Kondo* [1], *H. Okubo* [1], *H. Hanado* [2], *K. Aonashi* [3], *Y. Shoji* [3], *Y. Hatanaka* [4], *J. Yamamoto* [5], *T. Takamura* [5], *K. Matsushige* [6]

[1] *Kashima Space Research Center, Communications Research Laboratory*
[2] *Communications Research Laboratory*
[3] *Meteorological Research Institute, Japan Meteorological Agency*
[4] *Geographical Survey Institute*
[5] *Center for Environmental Remote Sensing (CEReS), Chiba University*
[6] *National Institute for Environmental Studies*

Contact author: Ryuichi Ichikawa, e-mail: richi@crl.go.jp

Abstract

Anisotropic mapping functions are considered a powerful tool for removing the effects of atmospheric variability from GPS and VLBI analyses. However, the assumption of simple linear form of atmosphere is not always appropriate in the context of intense mesoscale phenomena. Thus, in June 1998 we initiated a field experiment for characterizing water vapor variations using water vapor radiometers (WVRs) in the Kanto district of central Japan. In spite of the relatively short distance between Tsukuba and Kashima (about 54 km) the atmospheric gradients solutions from WVR are significantly different. This result suggests that the mesoscale weather pattern caused these large differences.

1. Introduction

Radio signal delay associated with the neutral atmosphere is one of the major error sources for space-based geodetic techniques such as the Global Positioning System (GPS) and Very Long Baseline Interferometry (VLBI). Recently, several anisotropic mapping functions have been developed for the purpose of better modeling these propagation delays, thereby improving the repeatability of horizontal site coordinates (MacMillan, 1995; Chen and Herring, 1997). The anisotropic mapping function is considered a powerful tool for removing or calibrating the effects of horizontal variability of atmosphere from GPS and VLBI analyses. Atmospheric gradients are assumed to have a simple linear form in the anisotropic mapping function. However, it is suggested that this assumption is not always appropriate in the context of intense mesoscale phenomena such as the passing of cold fronts, heavy rainfall events, and severe storms. Thus, in June 1998 we initiated a field experiment for detecting and characterizing water vapor variations using water vapor radiometers (WVRs) in the Kanto district of central Japan. In this short report we present a preliminary analysis of our findings.

2. Observation

Three WVRs were installed on the east-west line from Kashima to Tsukuba as shown in Figure 1. Dual-frequency geodetic GPS receivers were installed nearby these WVR sites, allowing

intercomparison of the atmospheric delay parameters derived using each technique. The delay estimates derived from WVR observations are calibrated in standard fashion by comparing WVR results with those obtained by numerical integration of operational radiosonde profiles observed by the Japan Meteorological Agency (JMA) at Tsukuba (Tateno). Figure 2 shows that calibrated WVR delays are very consistent with the delay derived from radiosonde profiles during the period 28 April - 10 June 1998. GPS-derived delays are also consistent with the other measurements as shown in the same figure.

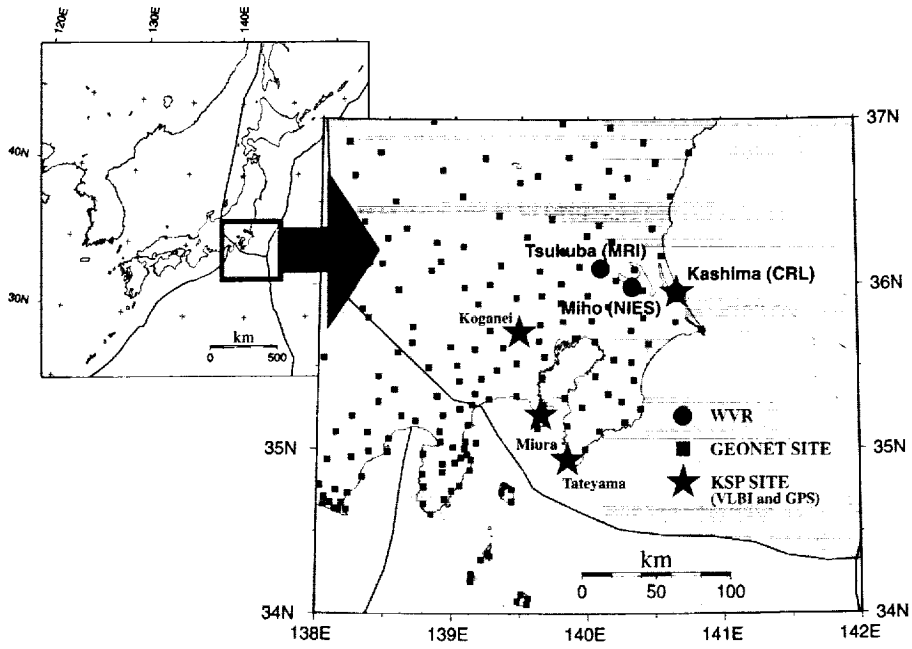

Figure 1. Map showing the WVR and GPS stations operated during the field experiment.

3. Results

Time series of atmospheric gradients estimated by WVR slant delays at Tsukuba and Kashima are compared to each other as shown in Figure 3.

In this figure we show the estimates of the EW (upper) and NS (lower) gradient delay during July 1998. Here, the gradient vector was estimated as a piecewise linear function with three-hour intervals. Both series of the EW and NS gradient components are smoothed with a 24-hour window. In spite of the relatively short distance between Tsukuba and Kashima (about 54 km) the atmospheric gradients solutions are significantly different. The magnitude of the NS gradient component at Kashima is approximately several times larger than that at Tsukuba during 3–4, 9–10, and 30–31 July 1998. We investigated the zenith wet delay (ZWD) field retrieved by the permanent GPS array of the Geographical Survey Institute (GEONET), by constructing maps in which ZWD is represented as a continuous spatial function (by interpolating between the GPS stations). In the vicinity of Kashima, for the period 3–4 July 1998, the ZWD field had a strong NS gradient of up to 1 cm/10 km (see Figure 4).

But the gradient in Tsukuba during this time period was very much smaller. This result

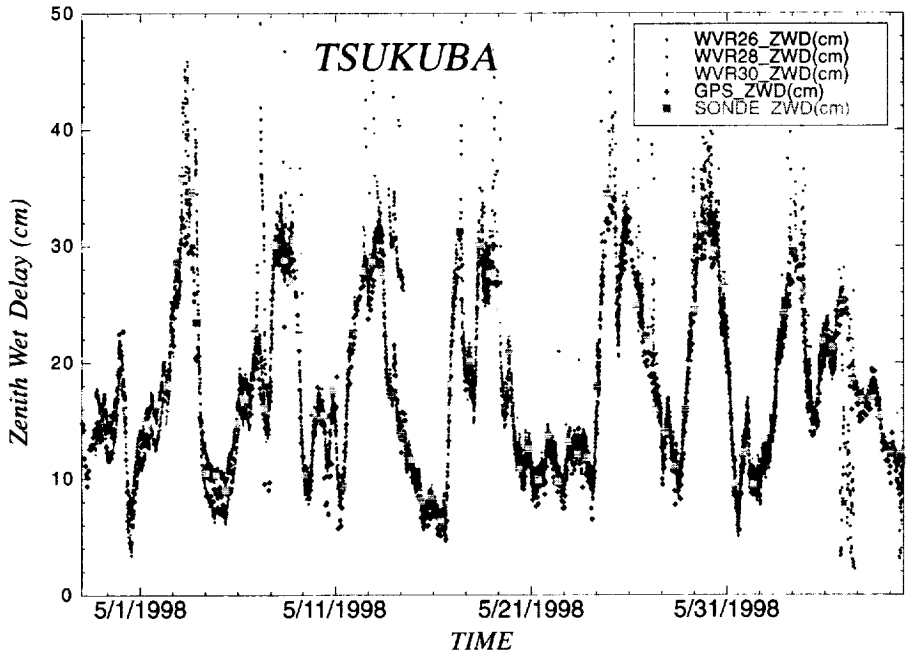

Figure 2. Zenith wet delay at Tsukuba as measured by WVR, GPS, and radiosondes from 28 April to 10 June 1998. The WVR wet delay is calibrated by comparing with the delay based on the radiosonde data.

suggests that the mesoscale weather pattern caused large differences to develop in the NS gradient (between Kashima and Tsukuba). We are now analyzing the output of high resolution numerical weather prediction models in order to investigate these results more deeply.

References

[1] Chen, G. and T. A. Herring, "Effects of atmospheric azimuthal asymmetry on the analysis of space geodetic data", J. Geophys. Res., 102, 20489-20502, 1997.

[2] MacMillan, D.S., "Atmospheric gradients from very long baseline interferometry observations", Geophys. Res. Lett., 22, 1041-1044, 1995.

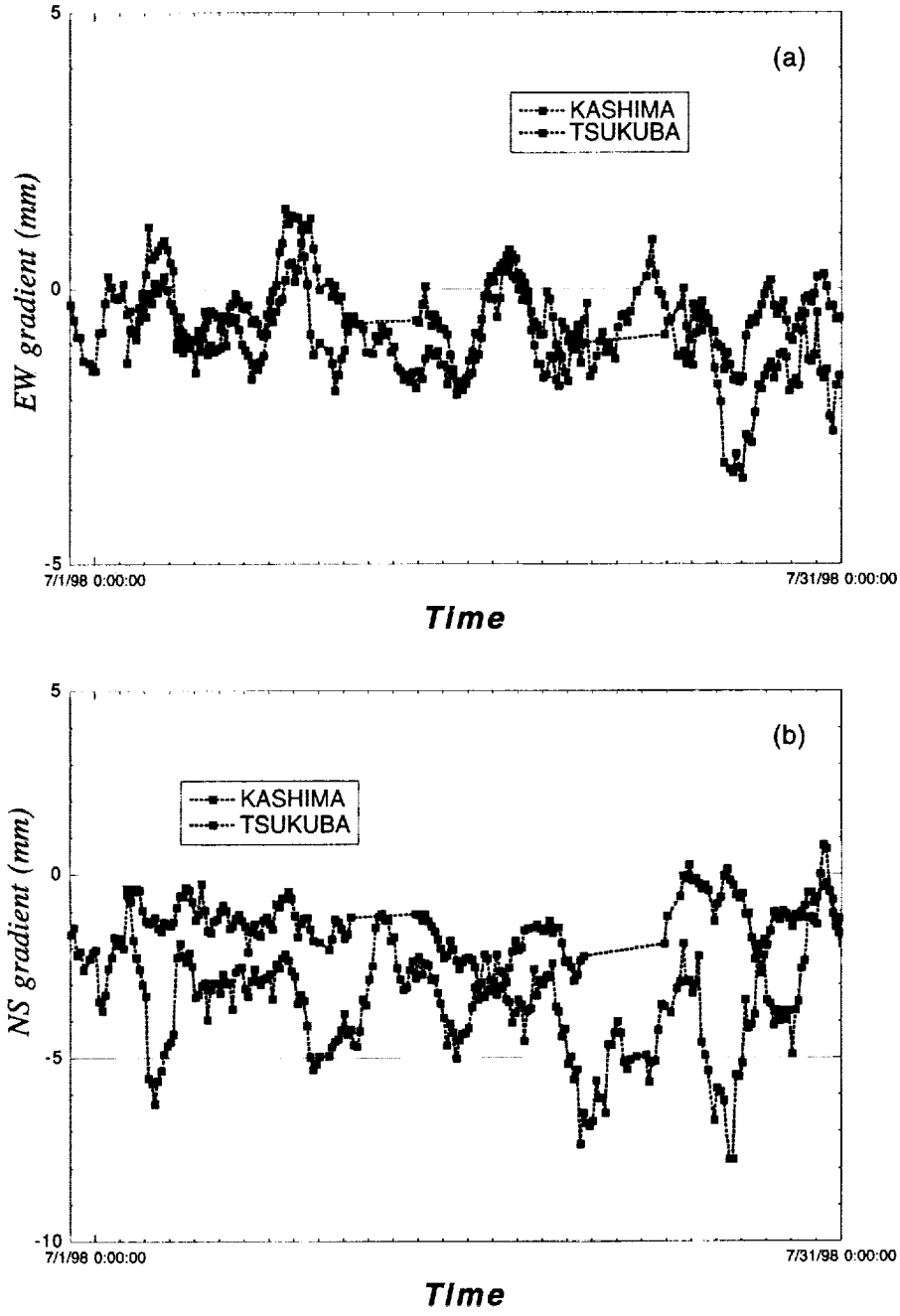

Figure 3. Estimates of the gradients at Tsukuba and Kashima obtained by WVR slant path delays in (a) the east-west direction and (b) the north-south direction. The gradient components estimated with three-hour intervals are smoothed with a 24-hour window.

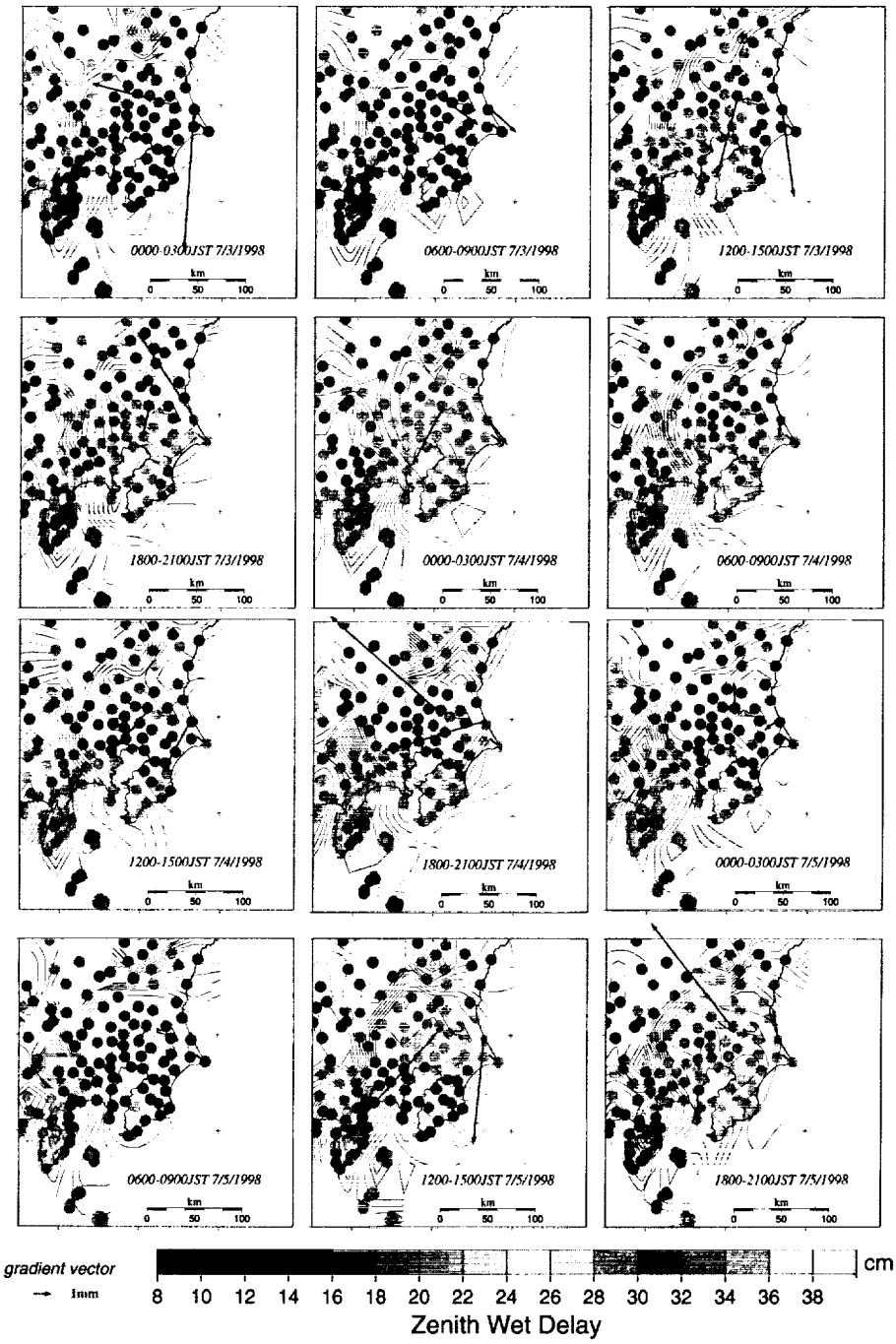

Figure 4. Zenith wet delay images retrieved from the Geographical Survey Institute (GSI) GPS array during 0000 JST July 3–2100 JST July 5, 1998. Contour Interval is 1 cm. Gradient vectors estimated from slant path delays using WVRs are also indicated in this figure.

Junichi Nakajima et al.: Optical Linked VLBI in Japan, IVS 2000 General Meeting Proceedings, p.334–337
http://ivscc.gsfc.nasa.gov/publications/gm2000/nakajima

Optical Linked VLBI in Japan

Junichi Nakajima [1], *Yasuhiro Koyama* [1], *Tetsuro Kondo* [1], *Mamoru Sekido* [1], *Yukio Takahashi* [1], *Eiji Kawai* [1], *Hiroshi Okubo* [1], *Hitoshi Kiuchi* [1], *Noriyuki Kawaguchi* [2], *Moritaka Kimura* [2], *Kenta Fujisawa* [2]

[1)] *Kashima Space Research Center, Communications Research Laboratory*

[2)] *National Astronomical Observatory*

[3)] *Institute of Space and Astronautical Science*

Contact author: Junichi Nakajima, e-mail: nakaji@crl.go.jp

1. Introduction

Optical linked VLBI is the key technology to change historical VLBI style in this decade. It will not only achieve high sensitivity by the fast data transfer beyond magnetic tapes, but other features are also attractive for the VLBI operation. The optical linked data transfer without the media transport and its real-time correlation capability enables the quick look of observations. This means our global VLBI network will serve as a connected interferometer. Dynamic scheduling and real-time fringe checks eliminate independent fringe tests before observation and after standby. These features of optical linked VLBI minimize observation failure usually known long after observation and maximize telescope resources. Currently operated optical VLBI network KSP (Key Stone Project), GALAXY (Giga-bit Astronomical Large Array Xross-connect) and other experimental based optical VLBI in Japan are briefly summarized in this report.

2. Currently Operated Optical Linked VLBI in Japan

2.1. Key Stone Network

One of the long operated optical linked VLBI for geodetic data production is the KSP-VLBI around the Tokyo metropolitan area. The 256 Mbps VLBI data is transmitted via ATM (Asynchronous Transfer Mode). The retrieved data from four telescopes are adjusted for their data epoch at buffers in front of the Koganei correlator. The highly reliable KSP VLBI is operated every other day and additional R&D observations are scheduled between the geodetic regular schedule [Kiuchi *et al.* 1999].

2.2. GALAXY

In 1998 the geodetic KSP network and astronomical VSOP/OLIVE network were mutually connected. The GALAXY (Giga-bit Large Array Xross-connect) appears under three different institutes. The network consists of Usuda 64 m (ISAS), Nobeyama 45 m (NRO), Kashima 34 m (CRL) and four 11m in Kashima, Koganei, Miura, and Tateyama [Kiuchi *et al.* 1999]. Correlation capability is four station maximum at the Koganei correlator and there is additional limitation in telescope combinations. Possible observation frequencies are listed in Table 1. The GALAXY network performed dynamical change of schedule when they found the HR1099 flare up stars

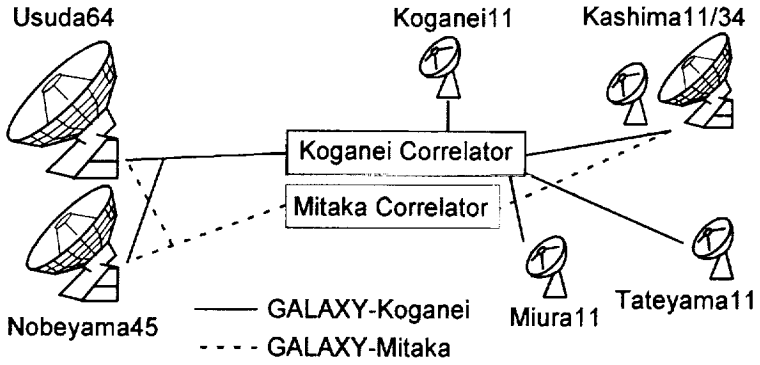

Figure 1. Optical Connection of KSP and GALAXY domestic optical VLBI.

variability during the observations. Mitaka VSOP-FX correlator is planned to share the processing.

Table 1. Two currently operated optical VLBI networks in Japan.

	KSP real time VLBI	GALAXY real time VLBI
Telescopes	4 x 11 m (KSP)	Usuda 64 m, Nobeyama 45 m, Kashima 34 m, 4 x 11 m (KSP)
Receiver Frequency	2/8 GHz	1.6/2/5/8/22 GHz
Correlator (Terminal)	Koganei (K4)	Koganei (K4), Mitaka (VSOP-FX)
Baseline Maximum Length	134 km	208 km
Scheduling	Automatic, static schedule	Operator control, dynamic schedule

3. Optical Linked VLBI with Experimental Results

3.1. Giga-bit ftp-VLBI

CRL has been developing the Giga-bit VLBI system which has a capability to perform 1024 Mbps VLBI observations. In this system, we realized ftp based data transfer which enables us to perform a fringe check during observation sessions. Using large memory 1024 Mbit (=128 MByte) the unit freezes the stream data at the assigned epoch. Besides the continuous tape recording, a connected PC starts ftp transfer from one station to the other. After the ftp, immediately software correlation starts and shows the result. The software correlator has an advantage in its flexibility to extended lag windows. Although the delay resolution is less than 1 ns at 1024 Mbps/1-bit/ch system, we are able to know the precise clock offset before tape correlation. Except for small telescope combinations, one second of the Giga-bit observations is enough to detect fringes from strong sources. The amount of ftp data is reduced when large telescopes are used. Figure 2 shows the ftp-VLBI 3C279 fringe between Nobeyama 45 m and Kashima 34 m from 12.8 MByte (0.1 sec) data. The processed lag window is expanded to about 50000 in this case. Starting from ftp, it takes about 10 to 15 minutes to see the fringes when the observation is normal.

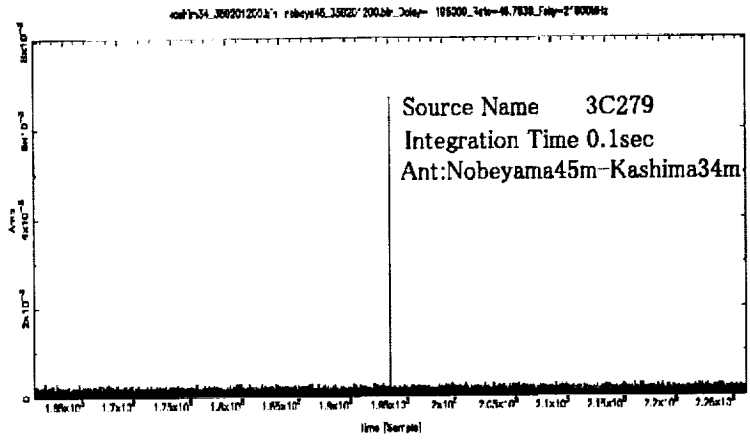

Figure 2. Gigabit ftp-VLBI fringe between Kashima 34m and Nobeyama 45m.

3.2. Giga-bit SDI-based Optical System

There are several approaches to establish over Giga-bit VLBI data transmission. One method is the high speed ATM and IP enhancement. The standardized transfer protocol promises commercial based extension in future. On the other hand, the interface employed in high speed consumer instruments are focused for local usage. In this case, the technology is concentrated into key devices and much cheaper than the ATM under its strict definition. SDI (Serial Data Interface) used in HDTV (High Definition TV) instrument connection supports optical data transmission up to 1.5 Gbps and 20 km distance without an optical repeater. We have developed the interface 1024 Mbps VLBI data and attribution data transfer shown in Figure 3 [Nakajima *et al.* 1999]. Large digital delay is occurring at parallel to serial data transfer. To compensate for this delay the concept of VSI (VLBI standard Interface, [Whitney, in this volume]) plays an important role. In the idea, 1 PPS tick label the data at DAS (Data Acquisition System). This will eliminate all digital delays introduced at later digital/analog component and only the clock offset between the telescopes remains in processing. There is no need to use a cable counter when the DAS is located near the receiver and the digital optical transmission is installed. We confirmed fringes and 1024 Mbps transmission performance by experimentally installing the unit in the correlation system as in Figure 4. Short distance interferometry experiments between Kashima 34m and Kashima 26m are planned.

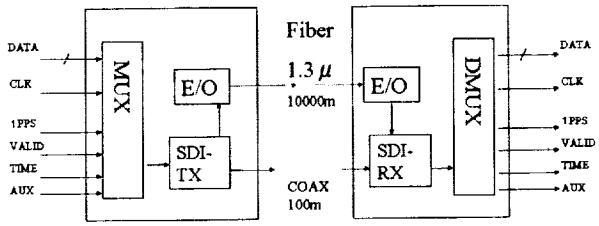

Figure 3. SDI Gigabit optical transmission system.

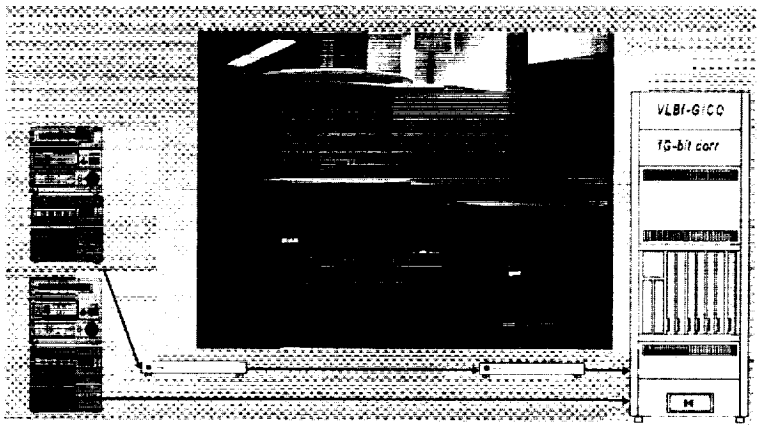

Figure 4. Giga-bit optical transmitter SPO1152TX/RX test in VLBI correlation

3.3. Other Optical-based VLBI Experiments in Progress

The other optical based VLBI projects are as follows. A 155 Mbps STM-1 ATM transmitter is completed to provide real-time VLBI. The unit will support VLBI via an international optical link or a satellite link [Kiuchi, personal communication]. Recently, the National Astronomical Observatory carried out a 2048 Mbps VLBI data transmission test which will fully utilize 2.5 Mbps ATM performance. They succeeded in send-back more than hundreds km [Kawaguchi, personal communication]. The GALAXY network is expected to enhance the performance up to 1024 Mbps in future. NTT (Nippon Telegram and Telecom) is developing a high speed "IP over ATM" interface which will adapt the KSP system for future expansion. CRL is also developing an IP-based VLBI system less than 1 Mbps. The variable rate IP-VLBI is realized by PC computer based technology. Experimenting with a simple frequency standard, the system will provide the possibility of preliminary VLBI experiment at many dishes never used for VLBI. This will give experience and opportunity to join the VLBI network to new groups. In the future, when we can afford to use broadband optical links between remote places this will bring us standard bandwidth VLBI observations. All real-time VLBI progress brought about direct results never obtained by tape based VLBI. But it should be noted that the fringe finding method and observation procedure is more difficult than tape based VLBI. Since most of the current VLBI systems were designed under a tape based concept, the future system should be improved to adapt automatic optical linked VLBI operations.

References

[1] H. Kiuchi, T. Kondo, M. Sekido, Y. Koyama, M. Imae, T. Hoshino, and H Uose, "Real-time Data transfer and Correlation System", J. Commun. Res. Lab., Vol. 46, p. 1, 1999

[2] H. Kiuchi, Y. Takahashi, A. Kaneko, H. Uose, S. Iwamura, T. Hoashino, N. Kawaguchi, H. Kobayashi, L. Fujisawa, J. Amagai, J. Nakajima, T. Kondo, S. Iguchi T. Miyaji, K.Sorai, K. Sebata, T.Yoshino, and N. Kurihara, IECE Trans. Commun., VOL. E83-B. NO.2, FEB.,2000

[3] J. Nakajima, "Optical and Coaxial Serial Data Transmitter/Receiver for Giga-it VLBI and VSI", IVS TDC Center News.,Commun. Res. Lab., Ser. 15, p26, 1999

Olexandr A. Molotaj: Celestial Reference Frame RSC(GAOUA)99 C 03, IVS 2000 General Meeting Proceedings, p.338-341
http://ivscc.gsfc.nasa.gov/publications/gm2000/molotaj

Celestial Reference Frame RSC(GAOUA)99 C 03

Olexandr A. Molotaj

Astronomical Observatory of National Taras Shevchenko University of Kyiv
e-mail: mol@aoku.freenet.kiev.ua

Abstract

The last version of Kyiv compiled series of celestial reference frames RSC(GAO UA)99 C 03 comprises positions of 736 radio sources (RSs). It was formed by Kyiv arc length method on base of 6 various institutions' initial solutions prepared in 1999, namely RSC(USNO) 99 R 01, RSC(GIUB)99 R 01, RSC(SHA)99 R 01, RSC(FFI)99 R 01, RSC(IAA)99 R 01, and RSC(GSFC)99 R 00. Averaged formal uncertainties of 212 defining RSs of the frame are equal to 0.06 and 0.07 mas in right ascension and declination, respectively. Axes of the frame are aligned to those of the ICRF with accuracy of 0.021 mas. This paper discusses accuracy of the ICRF, of all used initial frames, and of Kyiv compiled frames obtained during 1997–1999 span.

1. Introduction

Since 1997 the investigations are restored at Kyiv to construct annual celestial compiled VLBI frames. Their objective concludes in testing the arc length approach *(Yatskiv and Kur'yanova, 1990)*, which is fully independent from that of the IERS CB and can be used, too, for maintenance of the ICRF. Besides, the annual compiled frame is useful for VLBI institutions as well as for VLBI analysis groups due to its operative possibilities to compare their results. During these three years five reference frames are obtained by using Kyiv approach to VLBI initial celestial frames of various institutions, submitted to the IERS CB (see last publication *Molotaj et al., 1998*). This work has objective on base of mutual comparisons of used initial and obtained compiled frames to evaluate their accuracy and to show a formal accuracy progress of current VLBI analysis.

2. Kyiv Arc Length Approach

From known different approaches to compile initial VLBI RS positions into a joint celestial reference frame only three fully independent ones are used currently:

- very straightforward approach adopted by the IAU Working Group on Reference Frames to combine RS positions at the observational level *(Ma et al, 1997)*;
- the IERS CB approach based on development of traditional ideas of fundamental astrometry (see *IERS Annual Reports*);
- Kyiv approach based on analysis of lengths of arcs (below simply *arcs*) between RSs with the following steps: (a) selection of basic frames as part from all collected individual (observational) ones; (b) calculation of the arcs between all common defining radio sources in each basic frame; (c) intercomparison of the arcs in all basic catalogues; (d) determination of mean values of the arcs and residuals "arc minus mean arc"; (e) construction of individual frames defined by positions of two selected RSs and based on the arcs; (f) construction of

Table 1. **List of VLBI frames used for construction GAOUA compiled series.** N is number of RSs in frame; N_d is number of defining RSs which are common for basic frames; σ_α and σ_δ are internal uncertainties in *mas* for right ascension and declination respectively; W is weight of basic frame used for the rigid frame constructing; $\Delta\bar{\alpha}_*$ and $\bar{\Delta\delta}$ are mean differences in terms of "Frame – ICRF" calculated for 212 defining RSs; $|\Delta\alpha_*|$ and $|\Delta\delta|$ are r.m.s. of those differences

Frame	N	N_d	σ_α	σ_δ	W	$\Delta\bar{\alpha}_*$	$\bar{\Delta\delta}$	$\lvert\Delta\alpha_*\rvert$	$\lvert\Delta\delta\rvert$
a) 1997									
RSC(USNO) 95 R 04	556	27	0.07	0.08	0.57				
RSC(NOAA) 95 R 01	249	27	0.18	0.25	0.07				
RSC(JPL) 95 R 01	287	27	0.14	0.21	0.03				
RSC(GSFC) 95 R 01	550	27	0.12	0.09	0.33				
RSC(GIUB) 95 R 01	89	5	0.17	0.24	-				
RSC(SHA) 95 R 01	45	3	0.06	0.08	-				
RSC(GAOUA)97 C 01	598	212	0.15	0.18	-	.00	.20	.27	.31
b) 1998									
RSC(GSFC)97 R 01	600	82	0.14	0.18	0.49				
RSC(USNO)97 R 08	615	82	0.15	0.18	0.36				
RSC(JPL)97 R 01	287	82	0.20	0.28	0.15				
RSC(GAOUA)97 R 01	129	17	0.21	0.38	-				
RSC(GIUB)97 R 01	266	26	0.78	0.59	-				
RSC(GAOUA)98 C 01	631	212	0.11	0.13	-	.00	.00	.24	.26
c) 1999-1									
RSC(USNO) 98 R 01	640	187	0.14	0.16	0.69				
RSC(GIUB) 98 R 01	580	187	0.18	0.21	0.22				
RSC(JPL) 98 R 01	522	187	0.46	0.52	0.09				
RSC(GAOUA)98 R 01	198	54	0.24	0.41	-				
RSC(GAOUA)99 C 01	655	212	0.11	0.12	-	-.01	-.05	.32	.30
d) 1999-2									
RSC(USNO) 98 R 01	640	187	0.14	0.16	0.39				
RSC(GIUB) 98 R 01	580	187	0.18	0.21	0.15				
RSC(JPL) 98 R 01	522	187	0.46	0.52	0.06				
RSC(GSFC) 99 R **	644	187	0.11	0.14	0.41				
RSC(GAOUA)98 R 01	198	54	0.24	0.41	-				
RSC(GAOUA)99 C 02	673	212	0.08	0.09	-	.00	-.04	.26	.28
d) 1999-3									
RSC(USNO) 99 R 01	652	205	0.12	0.14	0.46				
RSC(GIUB) 99 R 01	602	205	0.15	0.17	0.20				
RSC(SHA) 99 R 01	720	205	0.15	0.18	0.09				
RSC(GSFC) 99 R **	644	205	0.11	0.14	0.25				
RSC(IAA)99 R 01	506	82	0.46	0.56	-				
RSC(FFI)99 R 01	431	58	0.16	0.12	-				
RSC(GAOUA)99 C 03	726	212	0.06	0.07	-	.00	.00	.23	.27

$\Delta\alpha_* = \Delta\alpha \cdot \cos\delta$; ** - this frame is received directly from the GSFC

Table 2. **Rotational angles** $A1, A2$, and $A3$ of VLBI initial frames' axes to align theirs to those of the RSC(GAOUA)99 C 03 solution. The angles are calculated for common RSs of Table 1. σ is r.m.s. error of angles; all values in *mas*

Frame	$A1$	$A2$	$A3$	σ
RSC(USNO) 99 R 01	0.013	0.039	0.012	0.006
RSC(GIUB) 99 R 01	0.724	−0.502	0.053	0.009
RSC(SHA) 99 R 01	0.015	−0.006	−0.019	0.012
RSC(GSFC) 99 R **	0.014	0.021	−0.002	0.008
RSC(IAA)99 R 01	0.054	0.123	−0.259	0.060
RSC(FFI)99 R 01	0.113	−0.102	−0.345	0.074

a combined rigid frame using the data of previous steps; (g) alignment of combined rigid frame to the ICRF and construction of compiled reference frame under the conditions: no net rotation and minimum displacements among common RSs; (h) expansion of the reference frame obtained to the rest of RSs, involved in the process of constructing the compiled frame.

3. Celestial Reference Frames of Kyiv Series during 1997–1999

Table 1 lists main characteristics of all compiled catalogues of the GAOUA series as well as the used initial frames conveyed to us by the IERS CB during 1997–1999 span. The frames are ordered as follows: basic frames, other ones, compiled frame obtained. A calculation procedure follows the steps as mentioned above. Some distinctions were determined by number of common defining RSs. The more this number, the more is number of celestial zones, selected to coincide the rigid frame with the ICRF. Also in different solutions the different pairs of basic RSs were selected to construct the rigid frames. This circumstance is not strong because, in principle, any RSs' pair can be taken as basic one.

4. Conclusions

Uncertainties in right ascension are systematically better than those in declination for solutions of all institutions.

In southern declinations both positional differences and their uncertainties grow in comparison with northern ones.

Formal accuracy of GAOUA series improves more than twice while real accuracy of initial frames improves only 20%. Probably, these peculiarities are connected with an accumulation of observations.

The USNO and GSFC solutions are approximately equal in accuracy and during this span they have maximal weights. The weights of other institutions are more than two times smaller.

The GIUB solution differs a valuable rigid rotation around the ICRF (see values of rotational angles of all solutions in Table 2).

Table 3. **List of large positional differences** for defining RS in terms of "RSC(GAOUA)99 C 03 – RSC(WGRF)99 R 01". σ_α and σ_δ are the GAOUA uncertainties; all values in *mas*

RS Designation	$\Delta\alpha$	σ_α	RS Designation	$\Delta\delta$	σ_δ
0629-418	-0.61	0.21	0629-418	-0.79	0.25
2312-319	-0.63	0.18	2312-319	-1.14	0.22
0138-097	+1.63	0.09	0131-522	0.70	0.11
1143-245	-0.79	0.08	0440-003	-1.25	0.10
1448+762	+0.84	0.32	0458+138	-0.97	0.24
			0812+367	+0.72	0.06
			1038+064	-0.62	0.03
			1616+063	-0.66	0.11
			1718-649	+1.08	0.36
			2059+034	-0.76	0.08

Axes of all Kyiv solutions are aligned to those of the ICRF with accuracy 0.02 mas by all 212 common defining radio sources.

Comparisons between GAOUA solutions and the ICRF give zero mean differences in right ascension. Behaviour of declination differences is more complex. While the RSC(GAOUA)97 C 01 big difference is explained by the effect of tropospheric gradient, not taken into account in some initial frames at 1995, one can see that the difference grows in the two first solutions of 1999. This effect can be introduced by the different subsamples of the ICRF sources used in the arc method. Thus in Table 3 the RSs are listed with the differences more than 0.6 mas in any coordinate between the RSC(GAOUA)99 C 03 and RSC(WGRF)99 R 01.

Acknowledgements

Author is grateful to the Central Bureau of the IERS as well as Dr. Chopo Ma for providing him the initial VLBI reference frames used in this work.

References

1998 IERS Annual Report. 1999, Central Bureau of IERS - Observatoire de Paris,Paris

Ma C., Arias E.F., Eubanks T.M., Fey A.L., Gontier A.-M., Jacobs C.S., Sovers O.J., Archinal B.A., Charlot P., 1997, The International Celestial Reference Frame realized by VLBI. *IERS Technical Note 23.* Central Bureau of IERS - Observatoire de Paris, Paris, p.II-3

Molotaj O.A., Tel'nyuk-Adamchuk V.V., Yatskiv Ya.S., 1998, Celestial Reference Frame RSC (GAOUA)98 C 01. *Kinematika i fizika nebesnykh tel*, **14**, 6, 512

Yatskiv Ya.S., Kur'yanova A.N., 1990, A new approach to the construction of a compiled catalogue of positions of extragalactic radio sources. *Inertial Coordinate System on the Sky*, Proc. 141th IAU Symp. held in Leningrad, Kluwer, p.295

Z. Paragi et al.: Indications for Frequency Dependent Radio Core Position in 1823+568, IVS 2000 General Meeting Proceedings, p.342–345
http://ivscc.gsfc.nasa.gov/publications/gm2000/paragi

Indications for Frequency Dependent Radio Core Position in 1823+568

Z. Paragi, I. Fejes, S. Frey

FÖMI Satellite Geodetic Observatory
Contact author: Z. Paragi, e-mail: paragi@sgo.fomi.hu

Abstract

The International Celestial Reference Frame (ICRF) defining source 1823+568 was observed as a calibrator in our multi-frequency very long baseline interferometry (VLBI) experiment. Images taken at 5, 8.4, 15 and 22 GHz reveal that there is a shift in position of the source between these frequencies. The shift of the "radio core" in this object is qualitatively in agreement with predictions of conical jet models developed for radio-loud active galactic nuclei (AGN). This effect can be quite common in quasars, and "ultra-precise" astrometric projects may require a correction for it in the future.

1. Introduction

The central engine of radio-loud active galactic nuclei (AGN) is assumed to be located within a compact radio component, called the radio core. A sub-group of radio-loud AGN are core dominated quasars, where the core (i.e. location of the central engine) is routinely associated with the most compact, flat spectrum component, which is usually also the brightest one. Flat spectrum means that the observed flux density is a weak function of frequency. Core dominated quasars are subject to astrophysical studies in order to understand e.g. particle acceleration mechanisms in astrophysical jets, and are also targeted by geodetic VLBI projects.

Quasars are at huge distances from us and therefore their proper motion is practically below detection limits (but cf. Ma et al. 1998). Their radio structure is compact and simple, so they are good candidates for defining the International Celestial Reference Frame (ICRF). In this paper we present multi-frequency very long baseline interferometry (VLBI) images of one of the ICRF defining sources, 1823+568, and interpret its structure in the context of compact jets.

2. Compact Jets in Radio-loud AGN and in Microquasars

Spectral properties of VLBI cores in quasars were interpreted by the conical jet model of Blandford and Königl (1979). In this model the compact cores are in fact unresolved jets that have different radiative properties at different frequencies, but their integrated spectrum remains nearly flat. One of the consequences of this model is that the jet reaches its peak brightness at different distances from the central engine at different frequencies.

The reason for the shift of the peak brightness in the jet is local absorption of the emitted synchrotron radiation. This so-called synchrotron self-absorption is more significant closer to the central engine, and much more effective at low frequencies. Due to this effect, the low frequency VLBI core component is observed at a greater distance to the central engine, with respect to the higher frequency ones. However, as i) the central engine itself cannot be seen, ii) the positional information is lost in astrophysical VLBI experiments, and iii) the effect was assumed to

be very small, images taken at different frequencies are usually aligned by the observed radio core components.

The dependence of core position shift on physical conditions within compact jets was studied in detail by Lobanov (1998). Calculations indicated that a shift of a few tenths of a milli-arcsecond (mas) may be quite common in quasars between 5 and 22 GHz. In fact, frequency dependent position shifts of VLBI cores were observed in some quasars (see Lobanov 1998, and references therein). There are two ways of determining the core position shift: i) directly by phase-referencing to another source, or ii) indirectly, by aligning optically thin jet components. In the latter case we select a jet component observed at two (or more) frequencies. These components are in general optically thin to synchrotron radiation, i.e. absorption effects do not affect their observed position. We align the images taken at different frequencies with the help of these components, and estimate the core position shift.

The latter method was used in aligning images of the microquasar SS433 obtained at 1.6, 5 and 15 GHz (Paragi et al. 1999). In this case the shift of the core-jets was 4 mas between 1.6 and 5 GHz. The use of optically thin jet components in aligning images (instead of the brightest core-jet components, which would be located at the phase centre after the first self-calibration step at all frequencies) was checked independently by fitting the well established kinematic model to the observed radio structure. The kinematic centre (i.e. the central engine of SS433) was located in a radio quiet gap in between the approaching and receding core-jets, and the position shift of these features with frequency was confirmed.

3. The ICRF Defining Source 1823+568

The source 1823+568 is a BL Lac type object at a redshift of z=0.664 showing apparent superluminal motion (Gabuzda & Cawthorne 1996, and references therein). It has a core-jet VLBI structure with structure index of 1 in both S and X bands (Fey & Charlot 1997). The structure index may have values from 1 to 4 (with increasing structural effects), and is defined by the error delay introduced by the source structure. The error delay is below 3 picoseconds for the most compact sources. Based on its observational history, stable position and small structure index, 1823+568 was selected to be a defining source of the ICRF (Ma et al. 1998).

We observed 1823+568 with the NRAO Very Long Baseline Array (VLBA) as a calibrator source on 26 March 1998. The experiment was carried out at 5, 8.4, 15 and 22 GHz, the target source was again SS433. Initial data calibration was done in the NRAO AIPS package (Cotton 1995; Diamond 1995). We used DIFMAP (Shepherd et al. 1994) for imaging. We imaged the calibrator as well at all frequencies from the few minutes of data (5–7 minutes per frequency, each observed at three different hour angles). We were able to reconstruct the well known mas scale structure of the source at all frequencies.

We also performed model-fitting in DIFMAP. The bright jet component located at 6.56 mas distance from the VLBI core at 5 GHz, is found to have an increasing separation with frequency: 7.19, 7.35 and 8.00 mas at 8.4, 15 and 22 GHz, respectively (with an estimated accuracy of 0.1 mas). We attribute this apparent position shift to the shift of the radio core with respect to the optically thin jet component, as the theory of compact jets predicts.

Note that the measured position is very uncertain at 22 GHz, and is not in agreement with the lower frequency separation values, as the expected core position shift is proportional roughly with $(\nu_2 - \nu_1)/\nu_1\nu_2$ (Lobanov 1998). Still, there is a clear tendency of increasing component separation

with frequency. The VLBI images at 5, 8.4, 15 and 22 GHz are shown in Fig. 1. We applied the same restoring beam in all cases (2×1 mas at $PA = 0°$), and aligned the optically thin jet components in order to illustrate the VLBI core position shift.

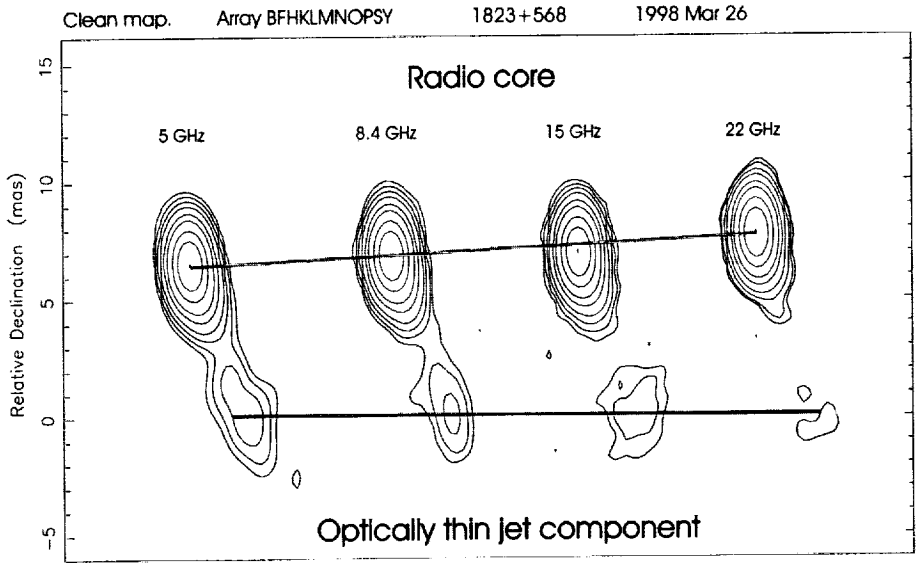

Figure 1. VLBA images of the ICRF defining source 1823+568 at 5, 8.4, 15 and 22 GHz, respectively. The restoring beam size is 2×1 mas at $PA = 0°$ in all cases. We shifted all images according to the model-fitting results, in order to align them by the optically thin jet component (assumed to be at the same physical location in the sky at all frequencies)

4. The Effect of VLBI Core Position Shift on Astrometric Analysis

The VLBI position of quasars determined by astrometry is the position of the phase centre, which is presumably located in the VLBI core (for core dominated quasars with simple structure). If source structural effects are taken into account, the measured position is that of an arbitrarily selected reference point. One way – though not necessarily the best – is to select a reference point that minimizes the calculated source structure delays. In this case the reference point is also found to be at or near the peak brightness distribution, i.e. in the radio core (Fey & Charlot 1997).

If there is a VLBI core position shift in a quasar, then the reference points selected in the S and X band images do not correspond to the same physical location in the sky. The maximum difference of the group delays measured in the S and X bands due to this effect is given by:

$$\Delta_{\rm gd}^{\rm max} = 1.6 \times 10^{-8}\,{\rm s}\,\left[\frac{B}{1000\,{\rm km}}\right]\left[\frac{\Delta r}{1\,{\rm mas}}\right]\,, \qquad (1)$$

where B is the projected length of the baseline. This difference in the group delays depends purely on the source-baseline geometry, and so will be baseline dependent.

In the process of ionospheric correction one forms a linear combination of the group delays measured in the S and X bands, in order to correct for the ionospheric delay contribution. The maximum group delay error introduced by the shift between the S and X band reference points on

a given baseline is:

$$\tau_{\rm err}^{\rm max} = 0.08\ \Delta_{\rm gd}^{\rm max}\ . \qquad (2)$$

For an 8000 km baseline and 0.1 mas shift in the reference point the maximum error delay is only 1 ps, which is very small compared to the present level of accuracy. However, VLBI core position shifts as large as 1 mas (if such large shifts exist) must be accounted for in future ultra-precise astrometric analysis (cf. Charlot 1990).

Note that the separation of the VLBI core from the central engine at a given frequency depends on physical conditions within compact jets. If these change, both the position of the core at a given frequency *and* the observed position shift between two frequencies may change. As physical conditions determine the emitted radiation from the source, it follows that these position changes must be coupled by changes in the observed flux density. These effects must be studied in detail in the future.

Also note that the conical jet model cannot be applied to all sources, for example it does not apply to compact symmetric objects (CSO), and to sources that are dominated by a bright jet component that was ejected recently. Future observations are needed to establish what fraction of core-jet sources show a measurable shift of radio core position with frequency.

Acknowledgements

The authors would like to thank Patrick Charlot and Leonid Petrov for useful comments on the manuscript. This research was supported by the Hungarian Space Office (MŰI), the Netherlands Organization for Scientific Research (NWO) and the Hungarian Scientific Research Fund (OTKA). The National Radio Astronomy Observatory is operated by Associated Universities, Inc. under a Cooperative Agreement with the National Science Foundation.

References

Blandford R.D., Königl A., 1979, Astrophys. J. 232, 34

Charlot P., 1990, Astron. J. 99, 1309

Cotton W.D. 1995, in: Zensus J.A., Diamond P.J., Napier P.J. (eds.) Very Long Baseline Interferometry and the VLBA, ASP Conference Series 82, 189

Diamond P.J., 1995, in: Zensus J.A., Diamond P.J., Napier P.J. (eds.) Very Long Baseline Interferometry and the VLBA, ASP Conference Series 82, 227

Fey A.L., Charlot P., 1997, Astrophys. J. Suppl. 111, 95

Gabuzda D.C., Cawthorne T.V., 1996, Mon. Not. R. Astron. Soc. 283, 759

Lobanov A.P., 1998, Astron. Astrophys. 330, 79

Ma C., Arias E.F., Eubanks T.M. et al., 1998, Astron. J. 116, 516

Paragi Z., Vermeulen R.C., Fejes I., Schilizzi R.T., Spencer R.E., Stirling A.M., 1999, Astron. Astrophys. 348, 910

Shepherd M.C., Pearson T.J., Taylor G.B., 1994, Bull. Am. Astron. Soc. 26, 987

Yusuke Kono et al.: The Differential VLBI Observation of Lunar Prospector, IVS 2000 General Meeting Proceedings, p.346–349
http://ivscc.gsfc.nasa.gov/publications/gm2000/kono

The Differential VLBI Observation of Lunar Prospector

Yusuke Kono [1], *Hideo Hanada* [2], *Kenzaburo Iwadate* [3], *Hiroshi Araki* [3], *Nobuyuki Kawano* [2], *Yasuhiro Koyama* [4], *Yoshihiro Fukuzaki* [5]

[1] *Graduate University for Advanced Study, Department of Astronomical Science*
[2] *National Astronomical Observatory, Division of Earth Rotation*
[3] *National Astronomical Observatory, Mizusawa Astrodynamics Observatory*
[4] *Communications Research Laboratory, Kashima Space Research Center*
[5] *Geographical Survey Institute*

Contact author: Yusuke Kono, e-mail: kono@miz.nao.ac.jp

Abstract

We performed a differential VLBI observation of Lunar Prospector (LP) and a QSO as a test observation for SELENE. Purpose of such observations for SELENE is estimation of the orbit and lunar gravity field. We developed a software for correlation of signals from LP. This software correlates carrier signal and calculates change of fringe phases. On the other hand, signals from a QSO were correlated by a conventional VLBI correlator. In correlation of LP, we could see the phase variation caused by the orbital motion around the Moon. The phase error was within about 0.6 degrees. This phase error suggests that we can determine position of LP within accuracy of 20 cm, if we could solve 2π ambiguity of phases. Because LP transmitted only one frequency signal, we could not solve the ambiguity. This 2π ambiguity can be solved by multi-frequency differential VLBI observations in SELENE project.

1. Introduction

Differential VLBI can measure the angular distance between two radio sources which are close to each other with higher sensitivity by canceling the effects of excess path delay in the ionosphere and the troposphere. The lunar gravimetry mission in the Japanese lunar exploration project SELENE (SELenological and ENgineering Explorer) puts a radio source on the lunar orbiter and that on the Moon for differential VLBI observations. These radio sources emit four carrier waves in order to resolve phase ambiguity [1], [2]. As a preliminary experiment of SELENE, we performed differential VLBI observations of LP which transmitted one carrier wave.

In this paper, we describe the observations and the receiving system profile and discuss the method of correlation and the phase error.

2. Observation Profile

We performed differential VLBI observation of LP on Sep. 21, 1998 by using three VLBI stations. These were Kashima, Mizusawa and Tsukuba (Figure 1).

2.1. Radio Sources

LP was launched on Jan. 6, 1998, and the mission ended on July 31, 1999 [3]. LP transmitted a S-band signal. It seemed that the signal was a carrier wave during our observations. In order

to correlate the signals, the frequency stability of the oscillator on LP must satisfy the following condition. The maximum synchronization error between two signals is a half of sampling period. Therefore, phase variation during (e.g. $\pm 2.5\mu$sec when sampling period is 5μsec) must not exceed the expected phase measurements error (e.g. 10 deg).This condition is as follows,

$$2\pi \frac{\Delta f}{f} f \times 2.5 \times 10^{-6} < 2\pi \frac{10}{360} \quad (1)$$

$$\frac{\Delta f}{f} < 5.1 \times 10^{-6} \quad (2)$$

where, $\frac{\Delta f}{f}$ is frequency stability of the oscillator and f is nominal transmitting frequency. Figure 2 shows that the oscillator satisfies this condition.

LP and the QSO 3C273B were observed alternately with switching interval 4 minutes. Figure 3 shows positions LP and 3C273B in the observations.

2.2. Receiving System

Diameters of antennas used in the observation are 34 m of Kashima, 10 m of Mizusawa and 4 m of GSI respectively. The largest baseline length is about 350km. Figure 4 shows the receiving system. Because LP transmitted a signal with very narrow bandwidth, we could record the data from LP at very low sampling rate of 200 ksps with a special recorder. One the other hand, we recorded the signal from the QSO with a conventional VLBI recorder.

3. Correlation Software

Because sampling rate is so low sampled data can be correlated using a work station. This data processing is almost the same as general one for VLBI (Figure 5).

For prediction of position of LP, GEODYN-II calculated position of LP. DE200, IERS Technical note 23 and ITRF 1996 were adopted for lunar ephemeris, the Earth rotation, positions of ground stations respectively. Initial orbit was given from the Web site (http://fdd.gsfc.nasa.gov/lp/)

4. Data Processing and Result

As a result of the processing mentioned above, cross spectrums are obtained every 0.7 sec. parameter period (PP). Figure 6 shows an example of a cross spectrum. After integrating of this cross spectrum over only 150 Hz bandwidth around a carrier frequency, residual fringe phases are obtained every PP. In order to see a short period variation of phases, we fitted the phases obtained for 40 sec observations to 4th-order polynomial functions. Figure 7 shows residual from the function. The standard deviation is about 0.6 degrees which corresponds to a position error of 20 cm at the Moon.

I correlated the sampled data for one hour. The observed phases for the first 40 sec switching interval are approximated by a 4th-order polynomial, then the estimated phases at the second PP are calculated through extrapolation of the polynomial. The observed phase at the second PP is shifted by 2πn (n is integer) which gives the smallest difference observed phase from estimated one. This process is continued from the first PP to the last PP. Finally the observed phases could be connected over the whole observation though all of the phase has a constant ambiguity (Figure 8).

On the other hand, the QSO's signals are correlated by conventional VLBI correlator NAOCO (New Advanced One unit COrrelator) of NAO. Figure 9 shows the variation of residual fringe phases from prediction.

5. Conclusion

We performed a differential VLBI observation of Lunar Prospector at S-Band. Using our new correlation software, we tracked the residual fringe phases with accuracy of 0.6 degrees which corresponds to the position error of 20cm at the Moon.

References

[1] Hideo Hanada et al.: "Observation system of radio sources on the Moon by VLBI in SELENE project", Proceedings of the International Workshop on GEMSTONE, jun. 25-28, pp126-130,1999.

[2] Hideo Hanada, Masatsugu Ooe, Noriyuki Kawaguti, Nobuyuki Kawano, Seisuke Kuji, Tetsuo Sasao, Seiitsu Tsuruta, Mitsumi Fujisita and Masaki Morimoto: "Study of the Lunar Core by VLBI Observations of Artificial Radio Sources on the Moon",J. Geomag. Geoelectr., 45, 1405-1414, 1993.

[3] Alan B. Binder: "Lunar Prospector:Overview",Science, 281,1475-1476, 1998.

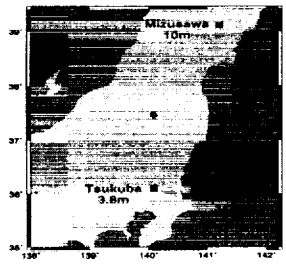

Figure 1. Configuration of VLBI Stations

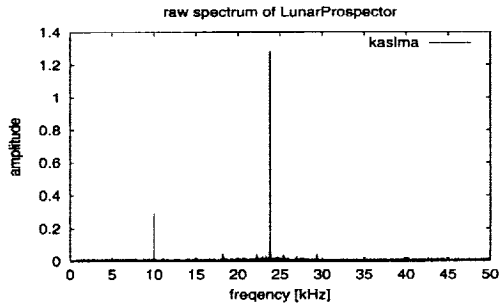

Figure 2. Spectrum of a signal from LP

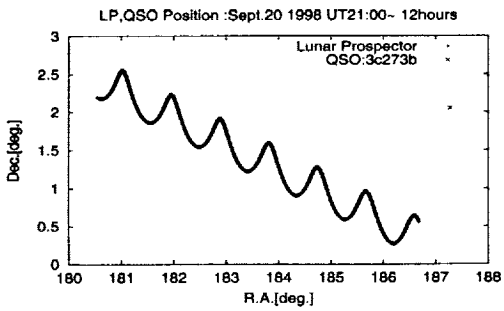

Figure 3. Positions of LP and 3C273B

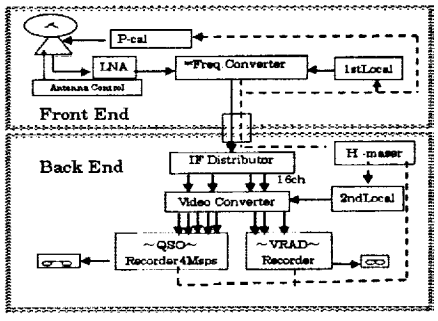

Figure 4. Receiving system

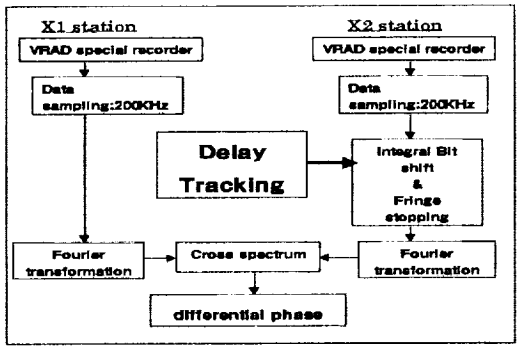

Figure 5. Data processing

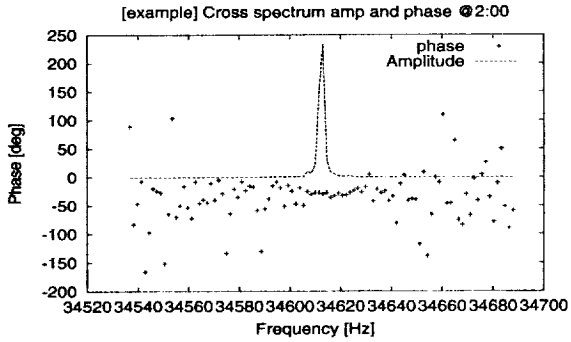

Figure 6. Example of amplitudes and phases of cross spectrum

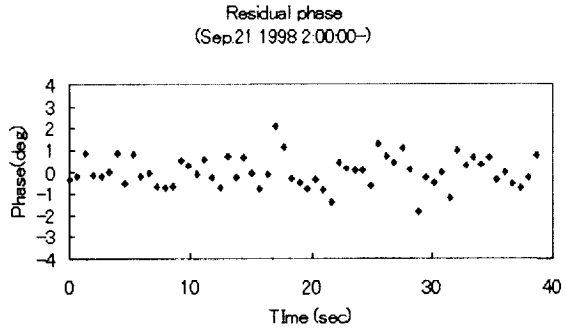

Figure 7. Residual fringe phases in one switching period for LP

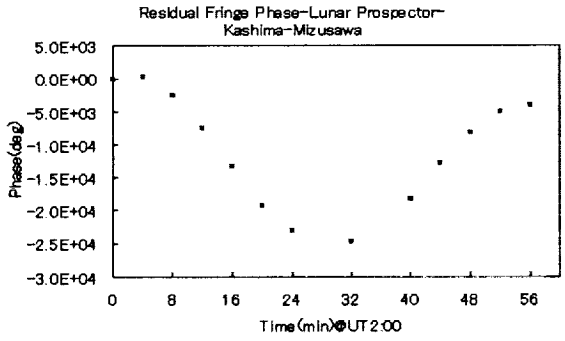

Figure 8. Residual fringe phase for LP

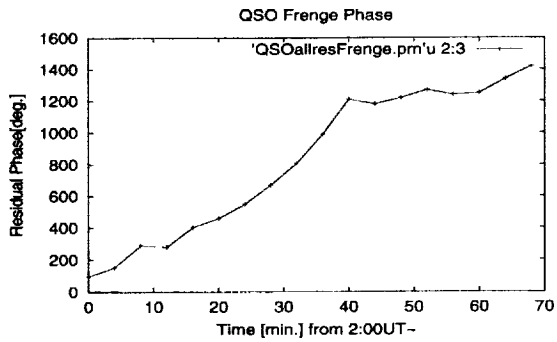

Figure 9. Residual fringe phase for QSO

Elena Skurikhina: EOP and Station Positions Determined with OCCAM Package, IVS 2000 General Meeting Proceedings, p.350–354
http://ivscc.gsfc.nasa.gov/publications/gm2000/skur

EOP and Station Positions Determined with OCCAM Package

Elena Skurikhina

Institute of Applied Astronomy RAS
e-mail: sea@quasar.ipa.nw.ru

Abstract

The preliminary results of EOP [Pole coordinates, UT1 and corrections to nutation angles ($\Delta\psi$ and $\Delta\epsilon$)] and station positions determination from NEOS-A, CORE-A, CORE-B and IRIS-A observation programs using package OCCAM version 3.5 in IAA RAS are reported in this paper. The EOP series for period 1984–1999 were obtained from these four programs. Comparison of the series with EOP(IERS)C04 shows both bias and rate in X_P pole coordinate arise from one in IRIS-A series. Station positions were estimated for every observational session. Station positions at epoch 1997.0 and velocities for 23 stations were derived from station positions time series by LSM estimations.

1. Introduction

The OCCAM package [1] is used for IAA EOP Service since 1997. Now version 3.5 [2] is in use for the Service. Observation data from IRIS-A, NEOS-A, CORE-A and CORE-B programs were processed and EOP [pole coordinates (X_P and Y_P), Universal Time (UT1), corrections to nutation angles ($\Delta\psi$ and $\Delta\epsilon$)] and station positions were obtained for every session.

2. EOP from IRIS-A, CORE-A, CORE-B and NEOS-A

EOP were calculated from all these programs beginning from 1984.0 until 2000.0 and as a result a 15-year EOP series consisting of 1071 points was produced. The processing of data was carried out using the catalog of stations positions ITRF97 and radio source positions catalog RSC(IAA)99R02. The station WETTZELL was used as clock reference for processing NEOS-A observations, the station WESTFORD or WETTZELL for IRIS-A, and mostly Gilmore Creek for CORE-A and CORE-B.

The produced common time series and separate series for each observational program were compared with EOP(IERS)C04 series. The results are presented in Figure 1 and Table 1. Table 1 shows values of bias and rate for differences between EOP series (common and obtained for each observational program) and EOP(IERS)C04 series. This comparison shows any trend in X_P in common series. It is due to trend in X_P in IRIS-A mostly and also in CORE-A and CORE-B series. For Y_P, UT1 and nutation trend is insignificant.

RMS of differences between the IAA EOP series and EOP(IERS)C04 corrected for trend as given in Table 1 are presented in Table 2.

From Figure 1 and Table 1 one can see that the significant trend existing for X_P IRIS-A series makes RMS of common series considerably worse; see Table 2.

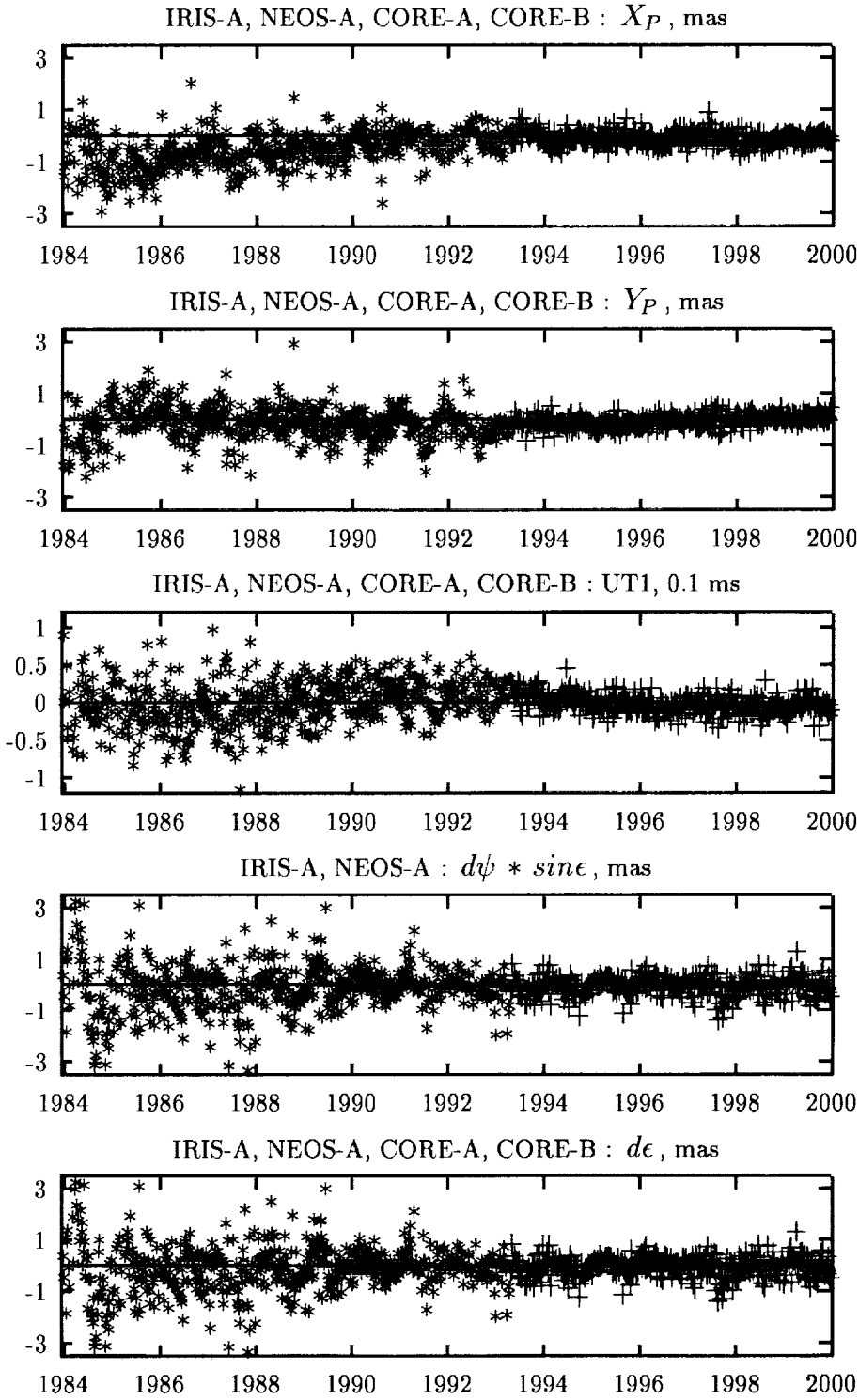

Figure 1. Differences between EOP estimations of OCCAM (* - for IRIS-A, +- for NEOS-A, CORE-A and CORE-B) and EOP(IERS)C04.

Table 1. Parameters of linear trends in the differences between the EOP obtained from different observational programs and EOP(IERS)C04.

	Common series	IRIS-A	NEOS-A	CORE-A	CORE-B
X_p,mas,	-0.32±0.02	-0.48±0.03	-0.08±0.01	0.09±0.03	-0.17±0.04
$\dot{X}_p$, mas/y	0.06±0.01	0.12±0.01	-0.01±0.01	0.06±0.04	-0.03±0.05
Y_p, mas	-0.05±0.02	-0.09±0.03	-0.05±0.01	0.17±0.03	0.03±0.05
$\dot{Y}_p$, mas/y	0.00±0.00	-0.03±0.01	0.04±0.01	0.04±0.04	0.14±0.05
$UT1$, 0.1 ms,	0.00±0.01	0.02±0.01	-0.01±0.01	0.05±0.02	0.01±0.03
$\dot{UT}1, 0.1\ ms/y$	0.00±0.00	0.03±0.01	-0.02±0.01	0.05±0.02	-0.03±0.03
$\Delta\psi$, mas	-0.02±0.02	0.00±0.03	-0.04±0.01	-0.15±0.06	-0.00±0.10
$\dot{\Delta}\psi$, mas/y	-0.01±0.00	0.00±0.01	0.00±0.01	0.02±0.08	0.06±0.12
$\Delta\epsilon$, mas, bias	0.02±0.01	0.01±0.01	0.04±0.01	-0.00 ±0.03	0.03±0.03
$\dot{\Delta}\epsilon$, mas/y	-0.00±0.00	-0.01±0.01	-0.00±0.01	0.03±0.04	-0.06±0.04

Table 2. RMS of differences between EOP series (common and separate) and EOP(IERS)C04 series.

	Common series 1984–1993 1071 sess.	IRIS-A 1984–1993 612 sess.	NEOS-A 1993–1999 350 sess.	CORE-A 1997–1999 62 sess.	CORE-B 1997-1999 47 sess.
X_p(mas)	0.55	0.65	0.24	0.22	0.24
Y_p(mas)	0.57	0.71	0.20	0.23	0.27
$UT1$(0.1 ms)	0.25	0.29	0.12	0.12	0.17
$\Delta\psi$(mas)	0.63	0.75	0.35	0.45	0.59
$\Delta\epsilon$(mas)	0.27	0.31	0.17	0.24	0.19

3. Station Position Estimations

Station positions (X, Y, Z Cartesian coordinates) were estimated for 23 stations. Station positions were obtained simultaneously with corrections to nutation angles and no additional constraints were used. The calculations were carried out for each observational session. Produced station position time series were analysed by LSM to estimate station positions at epoch 1997.0 and station velocities. Some stations (first 13 in Table 3) took part in few observational programs, and therefore their positions and velocities were obtained from all available data. Analysis of station coordinate time series shows a significant periodic component with period about one year for some stations. In any case its amplitude consists more than 1 cm. For instance, amplitude of year's term for X-coordinate of station Fortaleza is about 1.5 cm, X-coordinate of Kokee is 1.1 cm, Y-coordinate of Richmond is 1.2 cm, Z-coordinate of Hartrao is 1.2 cm, Y-coordinate of Hobart26 is 1.1 cm, Z-coordinate of Mojave12 is 1.1 cm.

The results of station position estimation corrected for year's term are presented in Table 3.

References

[1] Titov O., Zarraoa N.: (1997) OCCAM 3.4 User's Guide. Comm of the IAA N 69.

[2] Skurikhina E.: Determination of EOP from VLBI in IAA. Presented at IAU Coll. 178 "Polar Motion: Historical and Scientific Problems", Cagliari, September 27-30, 1999.

Table 3. Station positions (m) and velocities (m/y).

Station	X V_X	Y V_Y	Z V_Z	SX SV_X	SY SV_Y	SZ SV_Z	Nsess
ALGOPARK	918034.740	-4346132.276	4561971.169	0.0007	0.0010	0.0021	106
	-0.0157	-0.0070	0.0069	0.0004	0.0005	0.0009	
FORTLEZA	4985370.058	-3955020.338	-428472.319	0.0011	0.0008	0.0009	250
	-0.0023	-0.0025	0.0124	0.0006	0.0004	0.0005	
GILCREEK	-2281547.302	-1453645.074	5756993.138	0.0005	0.0004	0.0008	314
	-0.0220	-0.0056	-0.0059	0.0002	0.0001	0.0003	
KOKEE	-5543837.633	-2054567.857	2387851.922	0.0010	0.0006	0.0010	295
	-0.0068	0.0604	0.0304	0.0005	0.0003	0.0005	
MATERA	4641938.782	1393003.022	4133325.550	0.0010	0.0007	0.0017	91
	-0.0189	0.0174	0.0182	0.0004	0.0003	0.0006	
MEDICINA	4461369.994	919596.820	4449559.216	0.0020	0.0019	0.0027	26
	-0.0173	0.0184	0.0130	0.0007	0.0007	0.0008	
NOTO	4934563.134	1321201.259	3806484.490	0.0044	0.0015	0.0078	15
	-0.0162	0.0174	0.0153	0.0014	0.0004	0.0022	
NRAO20	883772.748	-4924385.591	3944042.470	0.0008	0.0011	0.0015	178
	-0.0135	-0.0035	0.0038	0.0006	0.0007	0.0010	
NRAO85 3	882325.558	-4925137.990	3943397.633	0.0026	0.0026	0.0033	157
	-0.0150	0.0015	-0.0078	0.0010	0.0010	0.0013	
NYALES20	1202462.752	252734.402	6237765.995	0.0076	0.0005	0.0017	87
	-0.0148	0.0073	0.0090	0.0006	0.0004	0.0012	
ONSALA60	3370606.037	711917.490	5349830.743	0.0016	0.0008	0.0030	106
	-0.0137	0.0142	0.0101	0.0003	0.0001	0.0005	
WESTFORD	1492206.591	-4458130.535	4296015.555	0.0005	0.0008	0.0012	600
	-0.0149	-0.0037	0.0049	0.0001	0.0001	0.0002	
WETTZELL	4075539.895	931735.269	4801629.355	0.0001	0.0001	0.0001	941
	-0.0158	0.0170	0.0072	0.0000	0.0000	0.0000	
MOJAVE12	-2356171.047	-4646755.819	3668470.547	0.0057	0.0063	0.0080	193
	-0.0137	0.0065	-0.0082	0.0009	0.0010	0.0013	
HARTRAO	5085442.772	2668263.474	-2768697.014	0.0061	0.0036	0.0047	41
	-0.0092	0.0157	0.0153	0.0043	0.0024	0.0031	
HOBART26	-3950236.756	2522347.559	-4311562.587	0.0068	0.0053	0.0100	32
	-0.0350	-0.0011	0.0703	0.0065	0.0049	0.0090	
HRAS 085	-1324210.998	-5332023.165	3232118.353	0.0052	0.0065	0.0071	364
	-0.0119	-0.0033	-0.0068	0.0006	0.0007	0.0008	
KASHIMA	-3997892.299	3276581.230	3724118.264	0.0064	0.0046	0.0067	18
	-0.0077	0.0098	-0.0069	0.0058	0.0042	0.0061	
RICHMOND	961258.049	-5674090.067	2740533.782	0.0028	0.0065	0.0044	430
	-0.0089	-0.0022	-0.0009	0.0004	0.0009	0.0006	
SESHAN25	-2831686.961	4675733.727	3275327.757	0.0283	0.0032	0.0165	5
	-0.0068	-0.0381	-0.0586	0.0169	0.0018	0.0090	
URUMQI	228310.665	4631922.755	4367063.988	0.0281	0.0252	0.0385	9
	-0.0013	0.0232	-0.0076	0.0179	0.0160	0.0225	
DSS15	-2353538.841	-4641649.480	3676669.980	0.0068	0.0142	0.0140	6
	-0.0223	-0.0010	0.0001	0.0049	0.0102	0.0100	
DSS65	4849336.672	-360488.773	4114748.882	0.0235	0.0130	0.0168	5
	0.0144	0.0091	-0.0253	0.0153	0.0093	0.0090	

Valery I. Altunin et al.: VLBI in the Deep Space Network: Challenges and Prospects, IVS 2000 General Meeting Proceedings, p.355–360
http://ivscc.gsfc.nasa.gov/publications/gm2000/altunin

VLBI in the Deep Space Network: Challenges and Prospects

Valery I. Altunin [1], *George M. Resch* [1], *David H. Rogstad* [1], *Pamela R. Wolken* [2]

[1)] *Jet Propulsion Laboratory*

[2)] *Honeywell Corporation*

Contact author: Valery I. Altunin, e-mail: Valery.I.Altunin@jpl.nasa.gov

Abstract

The purpose of this paper is to highlight the current status and prospects for VLBI in the NASA DSN. Although the prime purpose of the DSN is to support spacecraft operations and space research in deep space, this unique facility is also used on a noninterference basis with flight projects to support ground-based science experiments. The DSN VLBI capabilities are an integral part of a number of space- and ground-based projects. They include support of experiments at major radio astronomy VLBI networks (e.g., VLBA, EVN, APT), space VLBI co-observing, as well as VLBI geodesy and astrometry programs. The paper will describe for the potential DSN VLBI users 1) DSN VLBI objectives, 2) the current organizational structure and 3) current and projected capabilities.

1. Introduction

The NASA Deep Space Network (DSN) is a unique set of facilities distributed worldwide with the prime goal of supporting spacecraft operations and research in deep space. To conduct tracking of spacecraft in deep space, the DSN uses state-of-the art technology and instrumentation which is sometimes similar and often identical to radio astronomy instrumentation. From the time of the DSN's creation in the early 1960s, the radio astronomy community recognized great value in this facility for radio astronomy. Since then, the unique features of the DSN have been regularly used to do ground-based radio astronomy of which Very Long Baseline Interferometry (VLBI) is a very large part.

The DSN supports scientific experiments on a noninterference basis with the flight operations of space projects. This scientific support is carried out in three scientific disciplines: Radio Astronomy (radiometry, spectroscopy, polarization, VLBI), Radio Science (utilizing signals of interplanetary spacecraft to obtain information on the solar system's interplanetary environment, planetary atmospheres and fundamental physics), and Radar Astronomy (utilizing 0.5 megawatt transmitters).

2. DSN VLBI Objectives

The prime function of the VLBI capabilities at the DSN is to provide direct or indirect support to flight projects. This support can include: 1) VLBI navigation (including the maintenance of the navigation reference sources catalog), 2) Platform Parameters (station locations, calibration of Earth rotation and pole motion), 3) ground-based observing in support of space astronomy missions (e.g., Space VLBI, Gravity Probe-B). The infrastructure developed for these prime VLBI capabilities is also utilized to develop and support other DSN capabilities as, for example, antenna arraying and space VLBI telemetry acquisition and tracking (SVLBI spacecraft phase/clock synchronization and precision navigation).

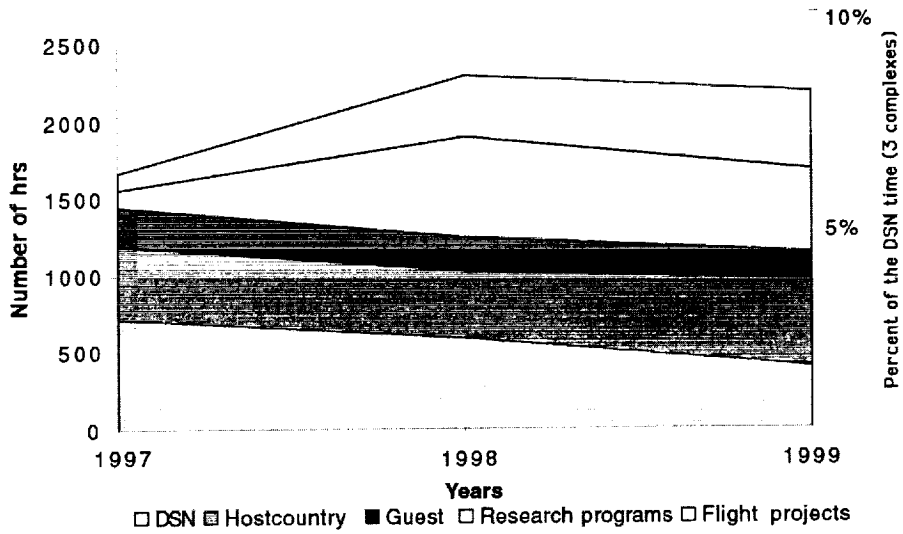

Figure 1. DSN time utilization for VLBI programs

Additionally, the DSN provides support for VLBI radio astronomy, geodesy and astrometry programs by 1) participating in operations of the major radio astronomy VLBI networks (e.g., Very Long Baseline Array, European VLBI Network, Asian Pacific Telescope), 2) providing an opportunity for "host country" radio astronomers to conduct their research at the Madrid (Spain) and Canberra (Australia) DSN complexes, and 3) carrying out various JPL/NASA research programs using DSN antennas.

The objectives of the DSN's participation in such research activities are 1) to realize and exploit the scientific and technical potentials of the DSN for enhancement of VLBI radio astronomy, geodesy, and astrometry sciences, and 2) to develop new DSN capabilities for support of scientific observations with ever-evolving VLBI techniques. Support of these activities requires developing and maintaining capabilities that are in addition to those required for deep space communication.

3. DSN VLBI Programs and Customers

DSN antennas have been used for VLBI since the inception of VLBI in the late 1960s. Radio astronomers were using them for pioneering VLBI experiments taking advantage of their superb sensitivity and longest baselines. A number of outstanding results in the fields of astrophysics, astrometry, and geodesy were obtained in VLBI experiments with DSN antennas.

A number of VLBI programs are currently conducted at the DSN:

1. Two VLBI radio astronomy programs are currently conducted at the DSN in support of flight missions: 1) VSOP (space VLBI co-observing at 70 m telescopes) and 2) Gravity Probe-B (monitoring of the proper motion of reference radio stars).

2. Two long-term ground-based VLBI programs: one geodesy (CORE) and one astrometry (VLBI detection of the extrasolar planets) are currently supported by the NASA Space Science Office.

3. Although the prime goal of NASA's Deep Space Network is to support space flight missions, in recognition of the value of large DSN radio telescopes for radio astronomy, NASA is allocating up to 3% of the DSN antennas time for ground-based radio astronomy research (guest observing programs). VLBI radio astronomers have been for a long time the major users of the DSN's radio astronomy guest observing time. The DSN antennas in Goldstone, CA, and Madrid, Spain, are participating in observational sessions of the EVN, VLBA, and Global VLBI.

4. The intergovernmental agreements between the US and Spain, and the US and Australia provide to radio astronomers in Spain and Australia so-called "host country" time at the DSN telescopes. This time accounts for about 1-2% of the DSN radio telescopes' time. The VLBI radio astronomy experiments, including astrometry and geodesy experiments (e.g. European Geodetic VLBI program, astrometric catalog of Southern hemisphere radio sources to extend the ICRF), consume a major portion of "host country" time in Spain and Australia.

5. Additionally, the DSN/JPL maintains DSN internal VLBI programs to monitor the earth rotation parameters (Clock Sync) and astrometric catalog of the reference sources for spacecraft navigation, Catalog Maintenance and Enhancement (CAT M&E). The results of these measurements are provided to the IERS Central Bureau on a regular basis.

Figure 1 shows the DSN time utilization for VLBI experiments and programs.

4. DSN VLBI Hardware and Operations Status

The DSN facilities include three major installations around the world: Goldstone, California, Madrid (Robledo), Spain, and Canberra (Tidbinbilla), Australia. The extremely large baselines between the DSN antennas/complexes and its strategic locations permit very high angular resolutions (close to the maximally possible at the surface of the earth) to be realized in VLBI observations between the DSN antennas and with other radio telescopes and interferometric networks. Additionally, high sensitivity (large collecting area, state of the art LNAs) and the ability to do VLBI phase referencing (fast antenna re-pointing, antenna clusters) have made the DSN facilities very valuable astronomical resources to conduct state-of-the-art VLBI experiments. Table 1 provides the current status of the DSN equipment which is utilized for VLBI observations.

All receivers have ambient loads and noise generators to provide automated measurements of the system temperature. Additionally, a Dicke-type beam switch is available which provides the capability for K-band radiometric measurement with reduced sensitivity to atmospheric fluctuations. The MKIV recording terminals (with dual recorder transports at each station) include the control computer running the PC Field System (PCFS) which can be controlled locally as well as remotely and automatically. The system configuration also includes the power meters to monitor the IF input levels.

The Deep Space Network has evolved to support the operations of deep space missions. The security required to support these operations with high reliability creates significant differences in the operating environment for the DSN radio telescopes compared to regular radio telescopes. While the PCFS computer provides a high level of compatibility with other VLBI installations, it cannot function as a prime DSN station computer. Instead, two additional computers, the Equipment Activity Controller (EAC) and the Radio Astronomy Controller (RAC), are used to interface the PCFS computer with other DSN subsystems. In effect, the EAC and RAC make the rest of the DSN appear like a radio astronomy observatory to the PCFS while providing a high

Table 1. Current Status of DSN Equipment Used for VLBI

DSN Complex, Location	Antenna	Dia - meter (m)	Frequency Bands (GHz)	SEFD (Jy)	Polarization, Channels configuration	Frequency standard, Clock	VLBI recorders
Goldstone, CA, USA	DSS13	34	31.9-32.1, 40-50,	300, 900	LCP, RCP, S&X simult.	Hydrogen maser, GPS	MKIV
Goldstone, CA, USA	DSS14	70	1.6-1.73, 2.2-2.3, 7.9-8.7, 18-26	40, 15, 20, 55	LCP& RCP simult., S&X simult.	Hydrogen maser, GPS	MKIV
Goldstone, CA, USA	DSS15	34	2.2-2.3, 8.4-8.5,	165, 130	LCP, RCP, S&X simult.	Hydrogen maser, GPS	MKIV
Canberra, Australia	DSS43	70	1.6-1.73, 2.2-2.3, 7.9-8.7, 12-18, 18-26	40, 15, 20, 50, 55	LCP& RCP simult., S&X simult.	Hydrogen maser, GPS	MKIV, S2
Canberra, Australia	DSS45	34	2.2-2.3, 8.4-8.5,	165, 130	LCP, RCP, S&X simult.	Hydrogen maser, GPS	MKIV, S2
Madrid, Spain	DSS63	70	1.6-1.73, 2.2-2.3, 7.9-8.7, 18-26	40, 15, 20, 55	LCP& RCP simult., S&X simult.	Hydrogen maser, GPS	MKIV
Madrid, Spain	DSS65	34	2.2-2.3, 8.4-8.5,	165, 130	LCP, RCP, S&X simult.	Hydrogen maser, GPS	MKIV

degree of security to the DSN. Additionally, the DSN VLBI Schedule Processor (DVSP) provides a bridge between a user which submits its VLBI schedule file through the Internet and the secure networks internal to the DSN. The schedule (VEX format) is preprocessed at the DVSP to check its validity (including correctness of the scheduled DSN time, format, etc.).

The DSN VLBI capability includes also the XF type VLBI correlator (Block II) which is capable of processing the MKIV VLBI data. The correlator has four MKIV playbacks. It is used mainly to process the DSN/JPL internal VLBI programs data.

5. DSN VLBI Organization

The Plans and Commitments Office of JPL's Tracking and Mission Operations Directorate (TMOD) is the prime organization within the DSN which establishes and maintains the interface with the DSN VLBI external customers. Among its responsibilities are: 1) establishing appropriate technical and organizational interfaces with the projects and VLBI organizations, 2) managing the space VLBI co-observing operations and VLBI operations for radio astronomy and geodesy, 3) organizing a review of the proposals for guest observations at the DSN, 4) providing the requests for the allocation of the necessary DSN time, 5) providing the guest radio astronomers with the

necessary expertise to successfully execute observations with the DSN radio telescopes.

The development and implementation of VLBI capabilities at the DSN is the responsibility of the DSN Engineering Office while operation and maintenance are under the purview of the DSN Operations Office, both within the TMOD. These offices respond to the requirements provided by the Plans and Commitments Office, allocate the budget for necessary developments, and manage implementation and maintenance of the VLBI equipment including the correlator.

The day-to-day VLBI operations are the responsibilities of the JPL/NASA contractor personnel. The Customer Service Representative (CSR) and Network Operations Engineer (NOPE) are the prime contact for users to monitor the status of the project and resolve inconsistencies in the schedule. The station radio astronomy engineer and "friend" of the DSN telescopes (in Madrid and Canberra) usually help with the setup of the experiment configuration, calibration and conduct the observations. (For contact information see http://deepspace.jpl.nasa.gov/dsnscience/)

6. Opportunities and Challenges

The space VLBI requirements have been the major driver for the upgrades and improvements of the VLBI DSN system in the last decade. They have initiated at the DSN the upgrade of the VLBI recorders to MKIV and the upgrade of the K-band receivers at the 70 m sub-network. A new VLBI user interface and operational system based on a PCFS and three other controllers (DVSP, EAC, RAC) provides simpler access to users to the VLBI DSN system and more reliable operations. Additionally, the 11 m antenna sub-network has been built through the extensive use of VLBI technology to collect high data rate spacecraft telemetry (up to 144 Mbit/s) and provide clock synchronization and high accuracy navigation in order to support the space VLBI missions operations.

It is likely that the space VLBI missions will be the most demanding customers for the DSN VLBI in the future. Particularly, future SVBI missions will need 1) ground telescope co-observing support (only one antenna in space; at least one other antenna required to have the interferometric fringes), 2) ground telescopes with large apertures (antenna in space rather small), 3) high-precision apertures able to operate at millimeter wavelengths, and 4) telescopes located around the world and especially located close to the spacecraft tracking stations to enable real-time correlation. These future SVLBI VLBI needs for co-observing are naturally fulfilled by the DSN capabilities.

The future space and ground-based VLBI technology driven by science tends to evolve to 1) higher frequencies (space VLBI 22, 43, 86 GHz, millimeter wavelength VLBI), 2) wideband (up to 1–8 Gbit/s) recording and processing, 3) precision calibration, and 4) highly reliable VLBI operations. These and other capabilities need to be implemented at the DSN to enable support for future space VLBI missions as well as to participate in the work of the major radio astronomy and geodesy VLBI networks.

The DSN already began the implementation of the S2 VLBI recording at the DSN complexes. In addition to the S2 recorder in CDSCC which is maintained by CSIRO, the DSN will install in the next two years S2 recorders at all three complexes and interface them with the operational DSN equipment. Also, the DSN is developing a software correlator which will eventually be installed at each complex and used for real-time fringe verification. Currently, the prototype of this correlator is used for the ground-based testing of the SVLBI project Radioastron space radio telescope. To provide support for the internal DSN VLBI projects, the DSN is implementing a new VLBI correlator successor to Block II. The correlator will be capable of processing the MKIV data and

will have four playbacks.

The DSN is currently undergoing significant organizational changes which may influence the interfaces with the DSN VLBI science users. Two major paradigms are the themes of these changes: the service provider and full cost accounting. VLBI became one of the services (along with other science services: Radio astronomy, Planetary radar, Radio science) which the DSN provides customers. These may, for example, introduce certain difficulties in rapidly implementing the new capabilities. "Full cost accounting" will eventually assign a cost of the DSN operations to every project supported by the DSN. The algorithm and procedures are still evolving. The impact of the implementation of full cost accounting on the DSN science services is not clear yet.

David Gordon: Geodesy/Astrometry with the VLBA, IVS 2000 General Meeting Proceedings, p.361–361
http://ivscc.gsfc.nasa.gov/publications/gm2000/gordon

Geodesy/Astrometry with the VLBA

David Gordon

Raytheon ITSS/NASA Goddard Space Flight Center
e-mail: dgg@leo.gsfc.nasa.gov

1. Introduction

The RDV experiments are a joint effort between VLBI scientists at NASA Goddard Space Flight Center, the U.S. Naval Observatory, and the National Radio Astronomy Observatory (an NSF facility operated by Associated Universities, Inc.). Six RDV geodesy/astrometry experiments are conducted yearly, using the 10 VLBA antennas and up to 10 Mark 4 antennas. Correlation is done on the VLBA correlator, a station-based, geocenter referenced correlator, similar to the new Mark 4 correlators. VLBA correlator output is in the form of cross-spectra phase and amplitude visibility data, which must be further processed using the NRAO AIPS software package to obtain geodetic observables. Most of the geodetic processing has been done at GSFC, using steps developed by NRAO and GSFC staff. These steps are given in a geodesy processing guide, available on-line in AIPS by typing "EXPLAIN ASTROMET". The first 17 RDV experiments, spanning 2.6 years, have been processed and, except for one problem (known as the southern source problem), the results are fairly good. The baseline repeatabilities are generally as good as, or better than, an equivalent span of Mark3/4 data, and many of the experiments can be phase connected between most of the VLBA antennas.

2. The Southern Source Problem

Many of the RDV experiments exhibit a problem with excess noise on southern sources. Though not well defined, this problem shows up most prominently in SOLVE solutions in a statistics parameter called "NRD(15psec)". NRD15 is an RMS residual delay, normalized with noise equal to the delay sigma combined with 15 psec in an RSS manner. Expected values are around unity. NRD15's greater than about 2 usually indicate a problem, such as poor antenna performance, source structure, etc. On plots of NRD15 vs. declination, many of the RDV's show a flareup of NRD15 values at southern declinations. A recent analysis indicates that this problem has a seasonal dependence, being most pronounced in the spring, summer, and early fall, and least pronounced in the winter, implicating the atmosphere in some manner. In late 1999, 6 stations from RDV11 were correlated on the Mark3A Washington Correlator and the results compared with the same 6 stations processed with the VLBA correlator and AIPS. The initial conclusion of this comparison is that the southern source problem shows up in the VLBA/AIPS version, but not in the Mark3A/Fourfit version. Thus, the problem appears to be a result of some error in the VLBA/AIPS processing, rather than in the data itself. Investigation of this problem is ongoing. We are currently concentrating on looking separately at the correlator model and the fringe residual portions of the observables and looking for whatever dependencies exist.

H. B. Iz et al.: VLBI Baseline Rates from Baseline Measurements of Collocated Antennas using Composite Models, IVS 2000 General Meeting Proceedings, p.362–367
http://ivscc.gsfc.nasa.gov/publications/gm2000/iz

VLBI Baseline Rates from Baseline Measurements of Collocated Antennas using Composite Models

H. B. Iz, Brent A. Archinal

United States Naval Observatory
Contact author: H. B. Iz, e-mail: baki@tos.usno.navy.mil

Abstract

At a given site, occasionally a new VLBI antenna has replaced an older one for operational use. Large-scale VLBI solutions account for these situations by assuming the motion of the old and new antenna is the same. We alternatively used composite models in which the common baseline rates are represented directly and estimated from collocated baseline measurements. Because the baseline lengths are invariant under rotations and translations, the baseline models are less prone to the common systematic effects and consequently simpler than those of large-scale solutions. We investigated the compatibility of the baseline measurements from different nearby antennas and compared the composite model solutions with the single baseline solutions for baseline measurements from the a) ALGOPARK to NRAO85-3 and NRAO20, b) GILCREEK to NRAO85-3 and NRAO20, and c) HARTRAO to KAUAI and KOKEE antennas. We have found data that contribute significantly to the estimated rates and calculate solutions that are more robust. We also evaluate the gain in efficiency in estimating baseline rates because of the increased number of observations in the composite models.

1. Baseline Measurements

The majority of VLBI baseline measurements are generated on a global basis through the observing programs of NASA's Goddard Space Flight Center, in close cooperation with the U.S. Naval Observatory's Earth Orientation Department, and other national and international participants. The baseline data used in this study is from the NASA Goddard Space Flight Center's VLBI terrestrial reference frame solution number 1102g, 1998 August. At a given site, occasionally a new VLBI antenna has replaced an older one for operational use. Large-scale VLBI solutions account for these situations by assuming the motion of the old and new antenna is the same. In this study, we alternatively use composite models in which the common baseline rates are represented directly and estimated from collocated baseline measurements. Because the baseline lengths are invariant under rotations and translations, the baseline models are less prone to the common systematic effects and consequently simpler than those of large-scale solutions. We investigate the compatibility of the baseline measurements from different nearby antennas and compared the composite model solutions with the single baseline solutions for baseline measurements from the a) ALGOPARK to NRAO85-3 and NRAO20, b) GILCREEK to NRAO85-3 and NRAO20, and c) HARTRAO to KAUAI and KOKEE antennas. Although most of the time the measurements are the products of weekly session (network) solutions, the three baselines with collocated antennas have varying numbers of measurements. Figure 1 shows the baseline measurements from ALGOPARK to NRAO85-3 and NRAO20 for a total of 117. The NRAO85-3 antenna was replaced by a new one within one km that became operational in October 1995 (54 measurements). The GILCREEK to NRAO85-3 and NRAO20 baselines consist of 561 measurements; 116 of them are from the GILCREEK to the new NRAO20 antenna (figure 2). The baseline measurements are

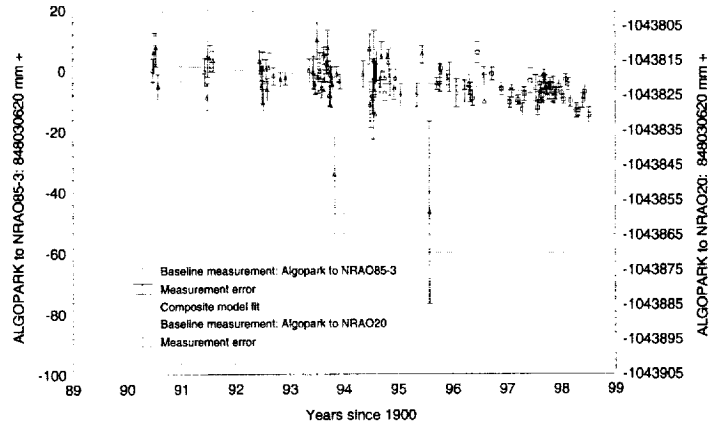

Figure 1. Baseline measurements: ALGOPARK to NRAO85-3 and NRAO20. The left Y-axis is for the ALGOPARK – NRAO85-3 baseline measurements. The offset between the two Y-axes is the difference in the intercept parameters.

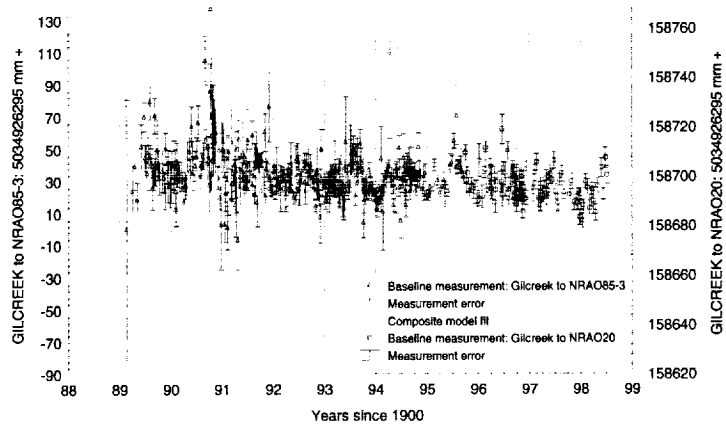

Figure 2. Baseline measurements: GILCREEK to NRAO85-3 and NRAO20. The left Y-axis is for the GILCREE – NRAO85-3 baseline measurements. The offset between the two Y-axes is the difference in the intercept parameters.

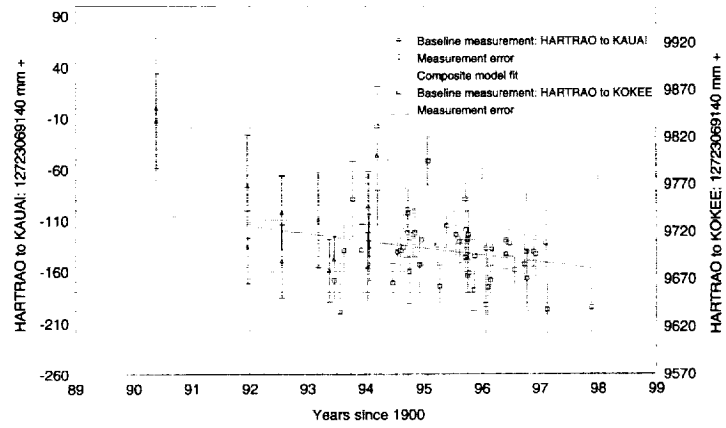

Figure 3. Baseline measurements: HARTRAO to KAUAI and KOKEE. The left Y-axis is for the HARTRAO – KAUAI baseline measurements. The offset between the two Y-axes is the difference in the intercept parameters.

more complete than the previous case but some of the early results are noisier. There are only 61 measurements from the HARTRAO to KOKEE and KAUAI baselines (figure 3). Only 13 data points belong to the HARTRAO to KAUAI baseline.

2. Single Baseline Model

The typical approach for estimating baseline rates is as follows,

$$y_{1_i} = a + bt_i + u_{1_i} \qquad i = 1, ..., m \tag{1}$$

In the above expression, y_{1_i} denotes the m baseline observations, a and b are the intercept and the slope parameters, t_i is the epoch of the observation expressed in Julian years that are shifted by an appropriate number of years in order to work with fewer digits for well conditioned solutions. The subscript 1 indicates that the single baseline model represents the data. The above expression in matrix notation reads as,

$$\boldsymbol{y}_1 = \boldsymbol{A}_1\boldsymbol{x}_1 + \boldsymbol{u}_1 \tag{2}$$

The $m \times 1$ vector of disturbances, $\boldsymbol{u}_1$, has the following assumed statistical properties,

$$E(\boldsymbol{u}_1) = \boldsymbol{0}, E(\boldsymbol{u}_1\boldsymbol{u}_1) = diag(\sigma^2_{u_{1_i}}) = \sigma_1^2 \cdot \boldsymbol{W}_1 \tag{3}$$

where σ_1^2 is the *a priori* variance of unit weight which is assumed to be unity. This value is subsequently replaced by the estimated *a posteriori* variance of unit weight.

A weighted least square solution to equation (2) is well-known and is given by,

$$\hat{\boldsymbol{x}}_1 = (\boldsymbol{A}_1\boldsymbol{W}_1^{-1}\boldsymbol{A}_1)^{-1}\boldsymbol{A}_1\boldsymbol{W}_1^{-1}\boldsymbol{y}_1 \tag{4}$$

where $\hat{\boldsymbol{x}}_1$ is the 2×1 vector of the least-square estimate of the unknown parameter vector $\boldsymbol{x}_1$ which consists of the intercept and the slope.

The following expression gives the *a posteriori* variance of unit weight $\hat{\sigma}_1^2$ of the observations,

$$\hat{\sigma}_1^2 = \frac{(\boldsymbol{y}_1 - \boldsymbol{A}_1\hat{\boldsymbol{x}}_1)\boldsymbol{W}_1^{-1}(\boldsymbol{y}_1 - \boldsymbol{A}_1\hat{\boldsymbol{x}}_1)}{m - 2} \tag{5}$$

3. Composite Model

The following composite model includes two intercepts to accommodate the collocated antennas [1]

$$y_{2_j} = \alpha a_1 + \beta a_2 + bt_j + u_{2_j} \qquad j = 1, ..., n \tag{6}$$

$\alpha = 1$, $\beta = 0$ when the measurements refer to the initial baseline, and $\alpha = 0$, $\beta = 1$ when the measurements refer to the baseline with collocated antenna. The subscript in y is to denote that the data is represented by the composite model. We express the observation of the new model in matrix notation as

$$\boldsymbol{y}_2 = \boldsymbol{A}_2\boldsymbol{x}_2 + \boldsymbol{u}_2 \tag{7}$$

[1] Or alternatively, one intercept and a parameter to represent the offset between collocated antennas.

The $n \times 1$ vector of disturbances, $\boldsymbol{u}_2$, has the following assumed statistical properties,

$$E(\boldsymbol{u}_2) = \boldsymbol{0}, E(\boldsymbol{u}_2\boldsymbol{u}_2) = diag(\sigma^2_{u_{2_j}}) = \sigma_2^2 \cdot \boldsymbol{W}_2 \tag{8}$$

where the unknown parameter vector $\boldsymbol{x}_2$ includes two intercept parameters and a slope parameter due to the plate motion common to all observations. A weighted least square solution to this new model is given by,

$$\hat{\boldsymbol{x}}_2 = (\boldsymbol{A}_2\boldsymbol{W}_2^{-1}\boldsymbol{A}_2)^{-1}\boldsymbol{A}_2\boldsymbol{W}_2^{-1}\boldsymbol{y}_2 \tag{9}$$

$$\Sigma_{\hat{\boldsymbol{x}}_2} = \hat{\sigma}_2^2(\boldsymbol{A}_2\boldsymbol{W}_2^{-1}\boldsymbol{A}_2)^{-1}$$

The *a posteriori* variance of unit weight of this solution is

$$\hat{\sigma}_2^2 = \frac{(\boldsymbol{y}_2 - \boldsymbol{A}_2\hat{\boldsymbol{x}}_2)\boldsymbol{W}_2^{-1}(\boldsymbol{y}_2 - \boldsymbol{A}_2\hat{\boldsymbol{x}}_2)}{n-3} \tag{10}$$

4. Are the Data from Two Different Baselines Compatible?

The *a posteriori* variances of unit weight of the simple and composite models are statistically *dependent.* However, the estimated variance of the *added* observations given by

$$\hat{\sigma}_{21}^2 = \frac{f_2\hat{\sigma}_2^2 - f_1\hat{\sigma}_1^2}{f_2 - f_1} \tag{11}$$

with $f_1 = m-2$ and $f_2 = n-m-1$, is *independent* from the *a posteriori* variance of unit weight of the simple model. Hence, for normally distributed observations, the following variance ratios are F-distributed with $m-1$ degrees of freedom in the numerator and $n-m-1$ degrees of freedom in the denominator,

$$F = \frac{\hat{\sigma}_1^2}{\hat{\sigma}_{21}^2} \tag{12}$$

This expression enables us to test the equality of the variances using a two-tailed hypothesis testing procedure at a given *p-level* [2]. When the computed variance ratio exceeds its corresponding theoretical value the null hypothesis is rejected at the given *p-level.*

The application of this testing procedure shows that all the baseline measurements from different antennas (pairwise) are compatible at 0.0001 *p-level.* Hence, we can use all the measurements directly in the composite models.

5. Solutions – Influential Data Analyses

The estimated baseline rates from the simple as well as composite models are given in Table 1. Despite the statistical agreement between the measurements from different antennas, there are large differences between single baseline estimates but the differences are not statistically significant when their errors are considered. One apparent reason for the deviations is the varying number of observations in each solution. Another is a result of more precise baseline measurements in the latter epochs. The composite model solution rates are therefore more in agreement with those single model solution rates that make use of less noisy data. In all cases, the baseline rates

[2]Defined as the statistical significance of a result is an estimated measure of the degree to which it is *true.*

Table 1. Numerical results

Baseline	Estimated Rate (mm/yr)	Nuvel 1A NNR Rate (mm/yr)	$\hat{\sigma}^2$	No. of data
ALGOPARK-NRAO20	-2.3±0.6	0.0	1.55	70
ALGOPARK-NRAO85 3	-0.5±0.4		1.19	48
ALGOPARK-NRAO20+ ALGOPARK-NRAO85	-1.3±0.3		1.36	118
Modified composite solution [3]	-0.1 ±0.4		1.32	117
GILCREEK-NRAO20	-2.7±0.7	0.0	1.96	116
GILCREEK-NRAO85 3	-1.3±0.3		1.53	446
GILCREEK-NRAO20+ GILCREEK-NRAO85	-1.6±0.3		1.63	562
Modified composite solution	None [4]		None	
HARTRAO-KAUAI	-24.2±10.3	-3.0	1.03	13
HARTRAO-KOKEE	-5.2±4.6		1.25	49
HARTRAO-KAUAI+ HARTRAO-KOKEE	-7.4±4.1		1.25	49

from the composite model solutions are not markedly better than those of individual solutions. However, note that composite models include much more data. Figure 4 shows that two of the baseline solutions from single as well as composite models are considerably influenced by a single data point (this is known as *influential data*). The plots show the change in the baseline rate estimate when each data point is sequentially removed from the solution. An influential data point in the ALGOPARK to NRAO85 and NRAO20 composite model solution accounts for 30 percent of the estimated baseline rate (Figure 4a) and there is an almost 50 percent change for another influential point in the HARTRAO to KAUAI and KOKEE composite model solution rate (Figure 4c). Observe that the maximum contributions are located either at the beginning or at the end of single baseline measurements where, by design, they are more effective. The corresponding measurement errors of the influential data are not necessarily the largest errors.

6. Conclusion

The above results show that all the baseline measurements from different antennas are compatible (pairwise) at 0.001 *p-level*. Simple and composite model rates are not markedly different from each other. They are also overall compatible with the NUVEL-1A solution (except HARTRAO-KAUAI baseline solution). Precise baseline measurements dominate the composite model rates as expected. The variances of the composite model rates are not significantly better than those of the simple models. Nevertheless, the resulting series are preferable for further exploratory analyses since they include more data. Composite models are also intuitively more appealing. There are

[3]Modified composite solution is the composite model solution where the influential data point is excluded.

[4]There are no data points in this solution that have a strong influence on the baseline rate.

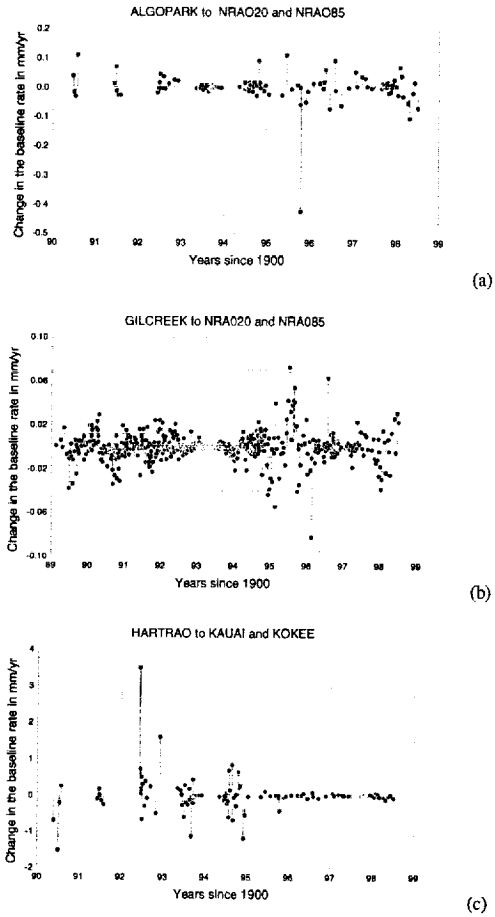

Figure 4. The contribution of each data point to the composite baseline solution rate. Note that the maximum contributions are located either at the beginning or at the end of single baseline measurements. The corresponding measurement errors are not necessarily the largest ones.

data points that influence the estimated baseline rates significantly (up to 50 percent) if they are removed from the solutions. This is especially true for those baselines with fewer observations. Modified composite solutions, where the influential data point is removed, are statistically more reliable since the estimated rates are homogeneously dependent on all data points. For all baselines with few observations and *influential* data points, new observations are strongly encouraged.

7. References

DeMets et al., Effect of recent revisions to the geomagnetic reversal time scale on estimates of current plate motions, Geophys. Res. Lett. Vol. 21 No. 20, p. 2191-2194, 1994. Ma, C., and J. W. Ryan, NASA Space Geodesy Program GSFC DATA Analysis 1998, VLBI Geodetic Results 1979-1998, August, 1998.

Jinling Li et al.: Polar Motion from VLBI Measurements, IVS 2000 General Meeting Proceedings, p.368–372
http://ivscc.gsfc.nasa.gov/publications/gm2000/li_jl

Polar Motion from VLBI Measurements

Jinling Li, Guangli Wang

Joint Radio Astronomy Research Laboratory, Shanghai Astronomical Observatory, National Astronomical Observatory, Chinese Academy of Sciences

Contact author: Jinling Li, e-mail: jll@center.shao.ac.cn

Abstract

From the reduction of 2893 globally distributed astrometric and geodetic VLBI sessions from August 1979 to December 1998, coordinates of 722 radio sources at J2000.0, coordinates and velocities of 128 stations at J1997.0 and about 20 years Earth Orientation Parameters were estimated. From the analysis of polar motion series the following are demonstrated: (1) During the VLBI data span the Markowitz wobble does not appear. (2) The amplitudes of both annual and Chandler wobble show temporal variations, with the former being more obvious than the latter. (3) Wavelet analysis shows that all the signals in the polar motion series are characterized by temporal variation in amplitudes. If we take any signal as strictly periodic, it is impossible to remove it completely from the polar motion series by least-squares fit because the hypothesis of a constant amplitude conflicts with VLBI measurements. (4) By applying a low-pass filter the secular polar motion was found to be 2.74±0.01 mas/yr towards 83.9±0.3 °W longitude, which is smaller in rate and more westward in direction compared with those determined from optical observations.

1. Introduction

Very Long Baseline Interferometry is so far the sole space geodetic technique to simultaneously provide the celestial reference frame (CRF), the terrestrial reference frame (TRF) and the linking Earth Orientation Parameters (EOP), which permits the unification of CRF, TRF and EOP. Due to the outstanding characteristics of high stability and precision, VLBI has been the principal technique to determine EOP since the 1980s. Astrometric and geodetic VLBI has accumulated nearly 20 years of observations. With the CALC8.2/SOLVE software system we performed a reduction of these observations. The resultant polar motion series were analyzed for the determination of the spectrum structure and the secular polar motion.

2. Data Reduction

Data reduction is performed by applying software system CALC8.2/SOLVE. IERS 1996 Conventions (McCarthy, 1996) are adopted. The terrestrial reference frame is connected to ITRF96 (Boucher et al., 1998) at 1997.0 by applying no-net-horizontal-translation and no-net-rotation constraints to the position adjustments of 12 stations with uniform station weighting for both constraints. The evolution of the TRF is connected to NNR-NUVEL1A (DeMets et al., 1994) by applying no-net-horizontal-translation and no-net-rotation constraints to the velocity adjustments of five stations with uniform station weighting for both constraints. The celestial reference frame is connected to RSC (WGRF) 95 R 01 (Ma and Feissel, 1997) (ICRF95) by applying no-net-rotation constraints to the position adjustments of the 212 ICRF95 defining sources with weighting proportional to the precision of the source positions. The New Mapping Function (Neill, 1996) is used

for the correction of troposphere delay with cut-off angle at 7 degrees. Clock behavior and wet troposphere effect are modeled as piecewise linear functions. Station positions and velocities and source positions are estimated as global parameters, Earth Orientation Parameters x, y, UT1, $\delta\psi$ and $\delta\epsilon$ are estimated as arc ones. Axis offset and asymmetric atmosphere effects are considered as well.

From the data reduction, the weighted-root-mean-squares of post-fit residuals is about 25ps. The coordinates of 722 radio sources at J2000.0, the coordinates and velocities of 128 stations at J1997.0 and about 20 years of Earth Orientation Parameters resulted. Comparisons show that the differences in orientation between our solution and ICRF95 are about 0.02 mas. The relative deformation parameters are at the same level of precision and are not significant. The relative rotation angles and their rates of change between our solution and ITRF96 are respectively at the precision level of 0.3 mas and 0.1 mas/yr. The systematic differences and relative drifts between our solution and EOP (IERS) C 04 are respectively at the precision level of 0.4 mas and 0.05 mas/yr.

3. Analysis of the Polar Motion Series

The polar motion series from the VLBI data reduction was smoothed and interpolated into a normal series with a sample interval of 30 days. This series is the basis of the following analysis.

After the normal series was de-trended spectrum analysis and wavelet analysis were applied. The results are shown in Figures 1 and 2, from which it is clear that the spectrum at high frequencies is very complicated. However, the annual and Chandler wobble are easily identifiable. In the spectrum there also exist long periodic terms.

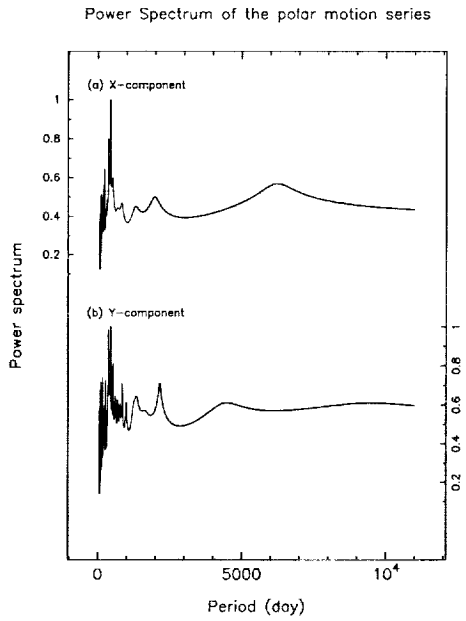

Figure 1. Spectrum analysis of the polar motion series

It is believed that in the polar motion series there exists the Markowitz wobble with period around 25 years and amplitude about 20 mas. There are debates about its existence. For instance, it may be solely associated with errors of star catalogues or the motion of stations. With Hipparcos

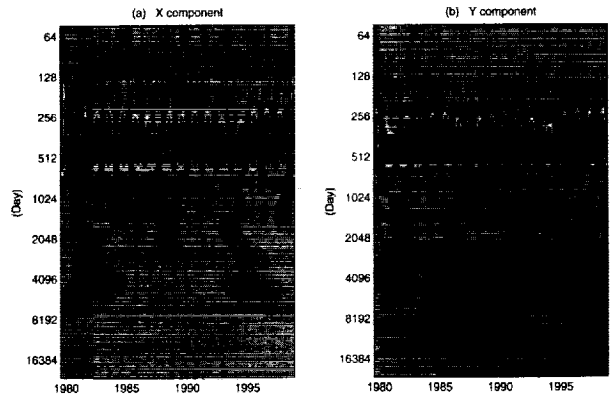

Figure 2. Wavelet analysis of the polar motion series.

catalogue Vondrak (1997) re-reduced the historical optical observations taking into consideration station motions based on plate motion model. The resultant polar motion series is more than 90 years in data span. However, since the observation data span of the Hipparcos catalogue is only 37 months, the average precision in proper motion of stars is about 1 mas/yr. When deducing star positions at the beginning of the 20^{th} century from the mean observation epoch (1991.25) of Hipparcos catalogue, the errors in star position will be magnified. In addition, space geodetic determinations show that the motions of stations are usually different from the predictions of plate motion models at the centimeter level (for instance, the difference for Shanghai VLBI station is about 9 mm/yr). Therefore, the re-reduction of the polar motion series based on Hipparcos catalogue does not fundamentally clear up the suspicions about the existence of Markowitz wobble. As shown in Figure 1 and 2, Markowitz wobble does not appear in the spectrum of the polar motion series from VLBI measurements, which of course still requires further support from future space measurements since the data span utilized here is only about 20 years.

In Figure 3 the characteristics of signals with periods near 400 days are demonstrated by applying wavelet analysis to the polar motion series as shown in a through d corresponding to x-component and e through h for y-component. From top downwards, the signals are respectively (a/e) the full information near the period of 400 days, (b/f) residuals after the removal of annual wobble by least-squares (LS) fit, (c/g) residuals after the removal of the LS solution to Chandler wobble and (d/h) residuals after the removal of LS solutions to both annual and Chandler wobble. In a and e, the beating phenomenon of the annual and Chandler wobble is very clear, which takes place mainly at the annual frequency. In b and f the Chandler wobble is manifested, with relatively slight variation in amplitude. In c and g, it is mainly the annual wobble. Compared with Chandler wobble in b and f, the variation in amplitude of the annual wobble is more obvious. In d and h, since the LS solutions to annual and Chandler wobble are removed, only the variations in amplitudes are shown. It can be seen that the absolute variation in amplitude at the annual frequency is comparable to that at the Chandler frequency. Within the VLBI data span, the amplitudes of annual and Chandler wobble in x- and y-component are respectively 80 mas and 72 mas, 178 mas and 175 mas. Hence, the relative variation in amplitude of the annual wobble is more significant than of Chandler wobble. The annual wobble is usually taken as stable. After its LS solution is removed the residuals are taken as Chandler wobble and so its characteristic parameters are studied. This conflicts with the demonstration in Figure 3.

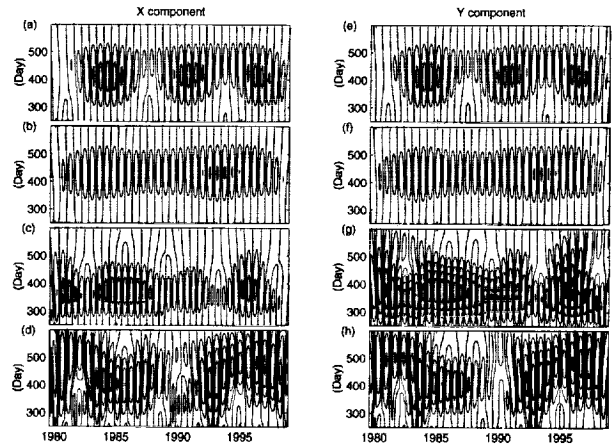

Figure 3. Wavelet analysis of phenomena nearby 400 day period.

Table 1. Estimations of the secular polar motion

Observations	Data span	Rate (mas/yr)	Direction (Degree W)	Reference
International Latitude Service	1899-1979	3.52±0.09	80.1±1.6	Dickman, 1981
Optical	1900-1992	3.51±0.01	79.2±0.2	Gross & Vondrak, 1999
Space geodetic	1976-1994	3.39±0.53	85.4±4.0	McCarthy & Luzum, 1996
Optical and space geodetic	1899-1994	3.33±0.08	75.0±1.1	McCarthy & Luzum, 1996
Latitude	1900-1978	1.6	70	Zhao et al., 1986
Latitude	1900-1978	3.51	79	Zhao & Dong, 1988
Optical	1899-1992	3.31±0.05	76.1±0.8	Schuh et al., 2000
VLBI	1979-1999	2.74±0.01	83.9±0.3	This analysis

LS fit is widely used in the analysis of polar motion series. When we remove a signal at a specified frequency by LS fit, the a priori hypothesis is that the signal is constant in amplitude. However, it is demonstrated by wavelet analysis in Figure 2 that all the signals have some temporal variations in amplitudes. It is easy to understand that under such circumstances, after the removal of the LS solution to a signal at a specified frequency, there still exists signal with almost the same frequency in the spectrum of the residuals. When we solve the LS solutions to two or more signals within narrow frequency span, it is hard to overcome the singularity of normal equation, which leads to unstable solutions. This is a commonly encountered problem in the analysis of signals characterized by temporal variation in amplitude. In view of this, we applied a filter to determine the secular polar motion. By referring to Figure 1 and 2 the cutoff period was set at 8000 days and a low pass filter was applied to the polar motion series. The secular polar motion was found to be 2.74±0.01 mas/yr towards 83.9±0.3°W longitude. From a comparison of results in Table 1 it can be seen that the secular polar motion determined here is smaller in rate and more westwards in direction than those from optical observations.

In conclusion, from the analysis of the VLBI observed polar motion series the following are demonstrated: (1) During the VLBI data span the Markowitz wobble does not appear. (2) The

relative temporal variation in amplitude of the annual wobble is more obvious than that of the Chandler wobble. (3) All the signals in the polar motion series are characterized by temporary variation in amplitudes. (4) A low-pass filter was used to estimate the secular polar motion, which is 2.74±0.01 mas/yr towards 83.9±0.3°W longitude.

Acknowledgements This work is partly supported by the Chinese National Major Basic Research Project *No. 970231003*, Major Project of National Natural Scientific Foundation Committee *No. 19833030*, Major Project of the Chinese Academy of Sciences *No. KJ951-1-304* and National Major Basic Research Project *No. 95-13-03-02*.

References

[1] Boucher C, Altamimi Z, Sillard P. Results and analysis of the ITRF96. *IERS Technical Note 24*, Observatorie de Paris, 1998. 1–22

[2] DeMets C, Gordon R G, Argus D F, et al. Effect of recent revisions to the geomagnetic reversal time scale on estimates of current plate motions. *Geophys Res Let*, 1994, 21: 2191–2194

[3] Dickman S R. Investigation of controversial polar motion features using homogeneous international latitude service data. *J Geophys Res*, 1981, 86: 4904–4912

[4] Gross R, Vondrak J. Astrometric and space-geodetic observations of polar wander. *Geophys Res Let*, 1999, 26: 2085–2088

[5] Ma C, Feissel M. Definition and realization of the international celestial reference system by VLBI astrometry of extragalactic objects. *IERS Technical Notes 23*. Observatorie de Paris, 1997. II-1–II-44

[6] McCarthy D. IERS Conventions (1996). *IERS Technical Notes 21*. Observatorie de Paris, 1996. 4–94

[7] McCarthy D D, Luzum B J. Path of the mean rotational pole from 1899 to 1994. *Geophys J Int*, 1996, 125: 623–629

[8] Neill A E. Global mapping functions for the atmospheric delay of radio wavelengths. *J Geophys Res*, 1996, 101: 3227–3246

[9] Schuh H, Nagel S and Seitz T. Linear drift and periodic variations observd in long time series of polar motion. *(private communication)*, 2000

[10] Vondrak J, Ron C, Pesek I. Earth rotation in the Hipparcos reference frame. *Celes Mech Dyn Astron*, 1997, 66: 115–122

[11] Zhao M, Dong D. A new research for the secular polar motion in this century. *The Earth's Rotation and Reference Frames for Geodesy and Geodynamics*, ed by A K Babcock and G A Wilkins, pp.385–392. d Reidel, Dordrecht, Holland. 1988

[12] Zhao M, Dong D D, Chen Y F. Re-research of the secular polar motion. *Acta Astronomica Sinica*, 1986. 27: 352–359

http://ivscc.gsfc.nasa.gov/publications/gm2000/berube

Canadian Transportable VLBI Antenna (CTVA)

Mario Bérubé, Jacques Lafrance

Geodetic Survey Division, Natural Resources Canada
Contact author: Mario Bérubé, e-mail: mario@geod.nrcan.gc.ca

Abstract

The Canadian Transportable VLBI Antenna (CTVA) is an integral part of the activities in the Canadian VLBI Technical Development Center and has been involved in a number of S2 frequency-switched VLBI system tests. In this paper we present the CTVA specifications and discuss site preparation and antenna assembly.

1. Objectives

Provide fiducial reference for the Canadian Active Control System (CACS) and the Canadian Base Net (CBN), part of the Canadian Spatial Reference System.

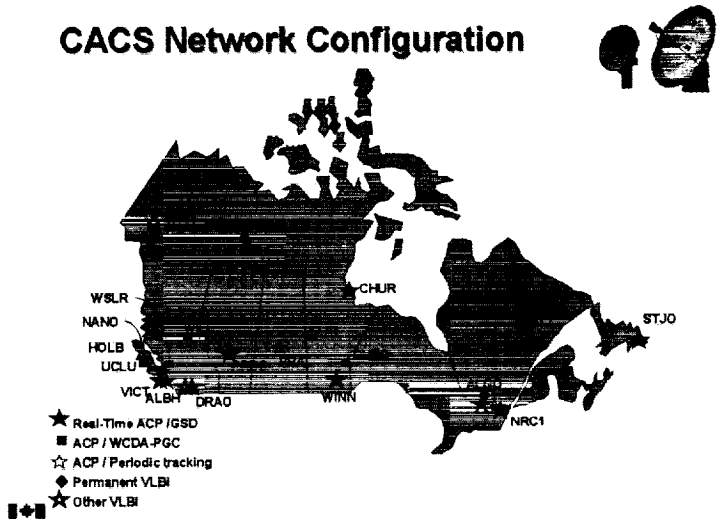

Along with the Algonquin 46 m and Yellowknife 9 m antennas define a network of about 10 fiducial sites in Canada. The antenna will be co-located with CACS stations for a few months. These CACS stations should be revisited every 3-5 years.

2. Specifications

Reflector	3.6m diameter (2 panels)
Receiver (uncooled)	X band: Cassegrain (45cm sub-reflector) 8180 to 8980 Mhz
	S band: Prime focus 2210 to 2400 Mhz
Antenna SEFDs	X band: 70000
	S band: 100000
Antenna Slewing Rates	Azimuth: 150 degrees per minute
	Elevation: 60 degrees per minute
VLBI system	S2 Data Acquisition System (S2-DAS)
	S2 Record Terminal (S2-RT)
PCFS	Version : 9.4.6 (modified for S2-DAS)
Time standard	CH1-75 Transportable Hydrogen Maser
Transportability	Total weight is less than 1500kg
	Largest piece (half of reflector) 3.6mx1.8mx1m
	Heaviest part (positioner) 850kg

3. Site Preparation

The sites are selected so that the antenna is within few hundred metres of the GPS point and can be fixed to bedrock. A local network is established to determine relative positions between GPS and VLBI and provide a reference for measuring local stability.

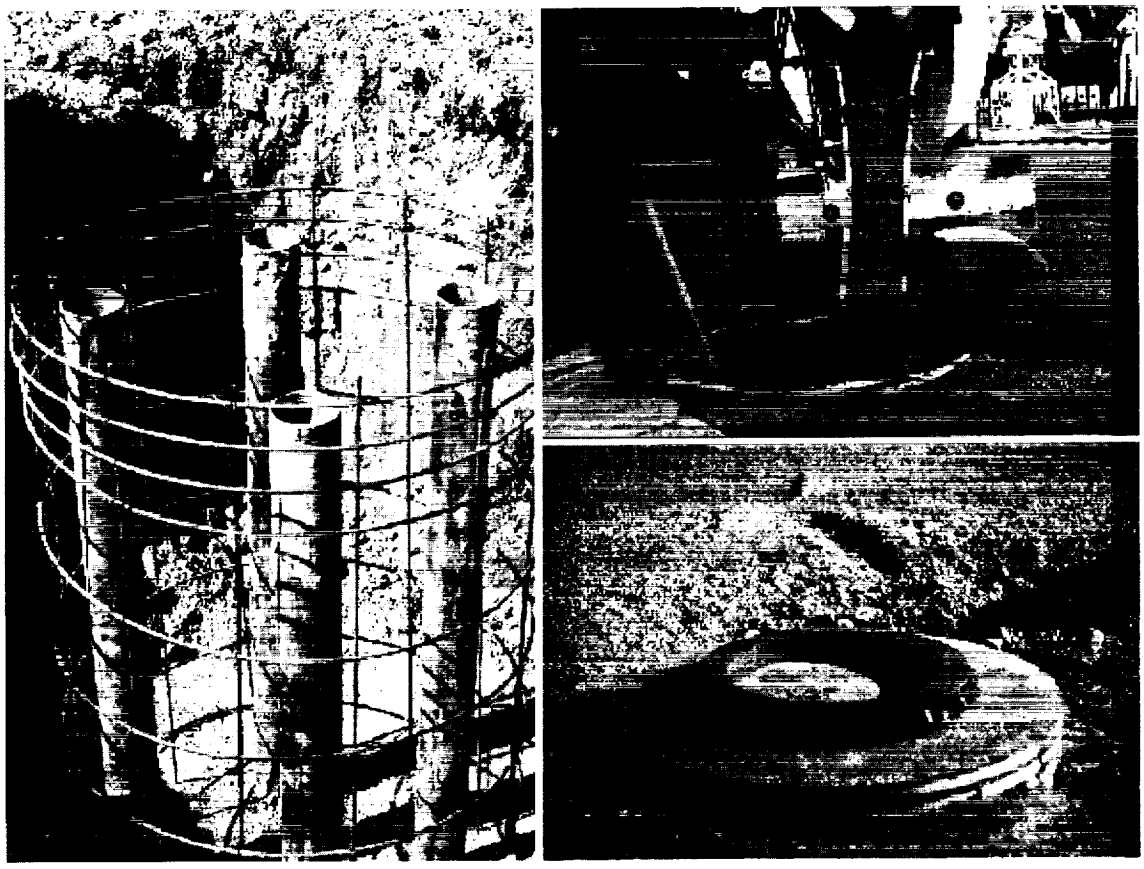

The concrete pad is anchored to bedrock using 15 cm diameter steel well casing and 1 cm reinforcing steel bar. A transition ring is used to fix the antenna to the pad. It takes about 2 weeks to prepare the site and survey the local stability network.

4. Re-assembly of the Antenna

The antenna is brought to the site in many parts. With three people, it takes less than a day to re-assemble.

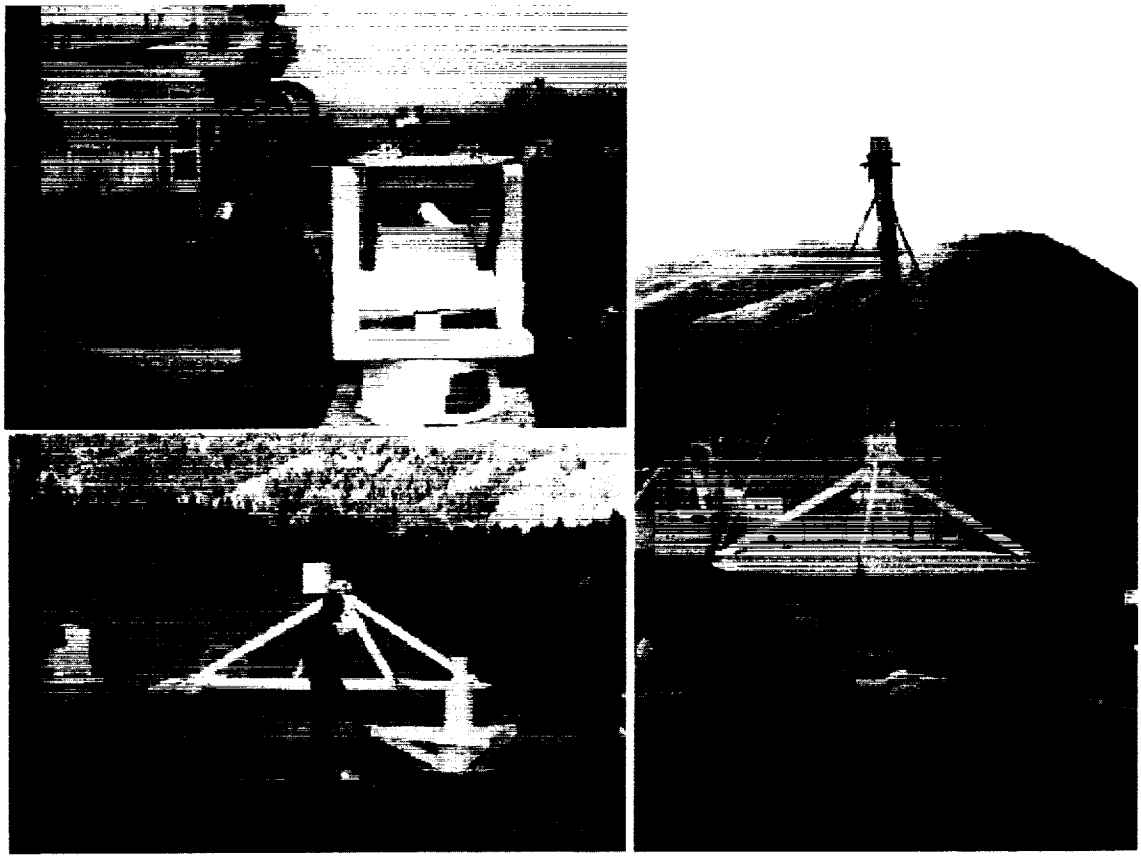

First, the two halves of the reflector, the quad legs, the sub-reflector and the S and X feeds are secured together on the ground. Second, the aluminum base is secured to the transition ring. Third, the positioner is secured to the base and levelled. Finally, the assembled dish is secured to the positioner.

5. Antenna Offset

The offset of the intersection of the elevation and azimuth axis with respect to the marker on the ground is determined by a precise survey method. This method uses two retro-reflectors installed on the CTVA. The marker is well defined in the local network. The same network is then used to position the two retro-reflectors defining a sphere and a circle centered at the antenna reference point. Surveys are done using high precision total station (distances 1 mm+1 ppm, angles 1"). The offset is determined with a precision of 2–3 mm.

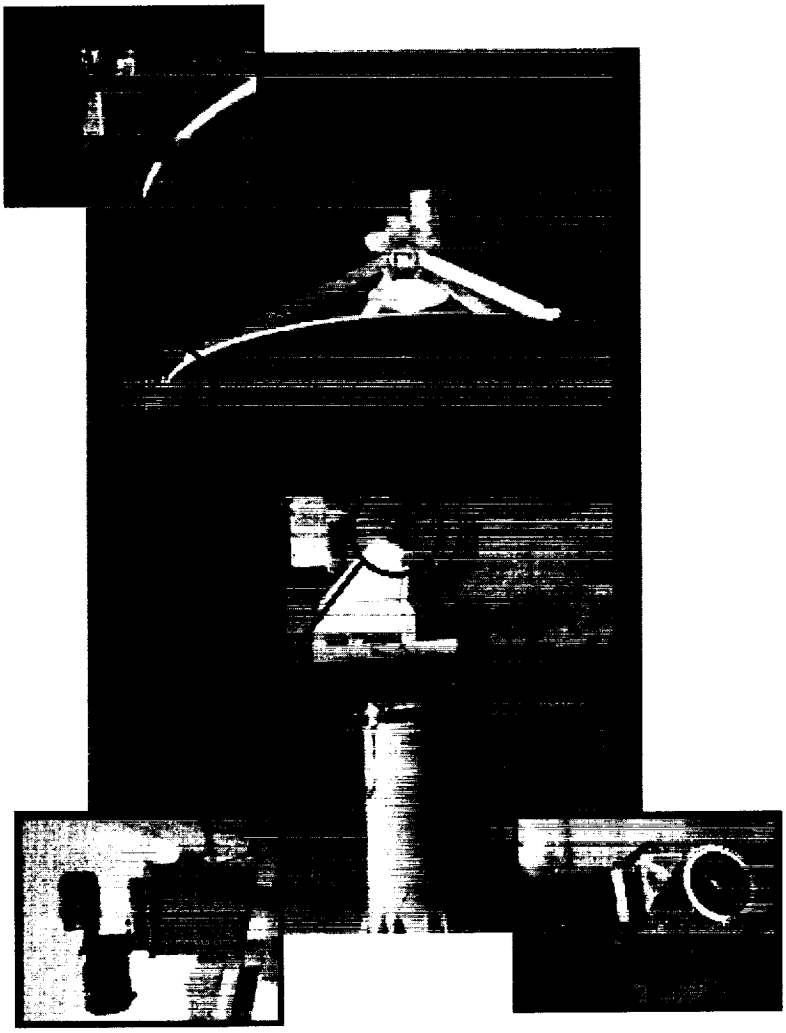

6. Status

The CTVA is at the Dominion Radio Astrophysical Observatory (DRAO) at Penticton for system validation. Initial geodetic experiments have been performed with Algonquin and Yellowknife. See [1] for details on the experiments, data analysis method and results. Trial operations will start in April. Next site for CTVA is St-John's (STJO). Another site has been prepared at Churchill (CHUR).

References

[1] Klatt, C., *et al.* "The S2 Geodetic VLBI program in Canada: System Validation Experiments and Results", This Volume.

William T. Petrachenko et al.: The S2 VLBI System: DAS, RT/PT and Correlator, IVS 2000 General Meeting Proceedings, p.378–382
http://ivscc.gsfc.nasa.gov/publications/gm2000/petrachenko1

The S2 VLBI System: DAS, RT/PT and Correlator

William T. Petrachenko [1], *Marc Bujold* [1], *Wayne H. Cannon* [5], *Brent R. Carlson* [3], *Peter E. Dewdney* [3], *Georg H. Feil* [2], *Paul Newby* [2], *Alexander Novikov* [2], *Josef Popelar* [1], *Richard D. Wietfeldt* [4]

[1] *Natural Resources Canada, Geodetic Survey Division*

[2] *Centre for Research in Earth and Space Technology, Space Geodynamics Laboratory*

[3] *National Research Council of Canada, Herzburg Institute of Astrophysics, Dominion Radio Astrophysical Observatory*

[4] *Jet Propulsion Laboratory, California Institute of Technology*

[5] *York University, Department of Physics and Astronomy*

Contact author: William T. Petrachenko, e-mail: Bill.Petrachenko@hia.nrc.ca

Abstract

The S2 VLBI system synthesizes wide IF bandwidths by rapidly switching the local oscillator (LO) frequency in a small (1-4) number of baseband converters (BBC's). Data are recorded on video cassettes using an array of 8 VHS transports. Characteristics of the S2 Data Acquisition System (DAS), the S2 Record and Playback Terminals (RT and PT) and the S2 Correlator are summarized. The bandwidth synthesis (BWS) frequency switching sequence used in a series of system validation experiments is presented.

1. Introduction

A major component of the Canadian Geodetic VLBI (CGLBI) Program involves the development of VLBI instrumentation for geodetic applications. The S2 VLBI system, including DAS, RT/PT and Correlator is a product of this effort.

The S2 is a general purpose VLBI system capable of a wide range of applications including geodesy/astrometry, astronomy (continuum, line and pulsar), and space VLBI. The successful application of the S2 DAS to geodetic applications is based on its use of LO's which can switch frequencies quickly. Each BBC LO is programmed to cycle through a set of frequencies sequentially, making it possible to synthesize wide IF bandwidths with a small number of BBC's. Since the sequences are flexible, this approach is very adaptable.

The S2 VLBI system is now essentially complete. Over the past several months, it has been undergoing a number of system validation tests. The tests have included five 24-hour geodetic observing runs (see Ref. [1]) and a few shorter tests which involve the continuous tracking of a single source.

The development of the S2 VLBI system has been funded by the Department of Natural Resources Canada (NRCan), the Centre for Research in Earth and Space Technology (CRESTech), the National Research Council (NRC) of Canada and the Canadian Space Agency (CSA).

2. S2 System Description

2.1. S2 Data Acquisition System (DAS)

At the heart of the S2 system's geodetic capability is the design of the BBC LO system (see Figure 1). In the S2 DAS, baseband conversion is a two-step process. Step 1 is an up-conversion using a 1350–2250 MHz frequency agile LO with settling time <1 ms and resolution 1 Hz. The effect of this mixing stage is to translate any frequency within the 100–1000 MHz IF input range up the centre of the 1225–1275 MHz bandpass filter. In step 2, the bandpass filter output is translated to baseband using a single sideband mixer (SSBM) and a fixed LO at 1250 MHz.

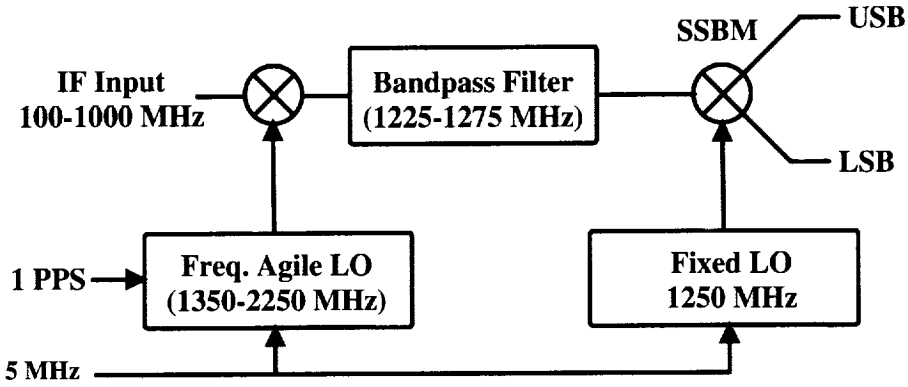

Figure 1. S2 BBC LO System.

The S2 BBC LO design provides two important advantages: 1) The two-step baseband conversion makes it possible to process the entire 100–1000 MHz IF input range independently in each BBC, i.e. no external IF processing steps, such as splitting of the IF input into sub-bands or the use of external mixing stages, are required to handle the 720 MHz X-band IF. 2) The rapid switching capability of the LO makes it possible to synthesize wide effective bandwidths by cycling through a sequence of LO frequencies, effectively removing the need for a large number of BBC's.

Characteristics of the S2 DAS are summarized below:

- Up to 4 IF inputs (100–1000 MHz) and 4 BBC's.
- Flexible switching of IF inputs to BBC's.
- Maximum output data rate, 512 Mbits/s.
- Phase coherent fast frequency switching LO: maximum switching rate, 50 Hz; settling time <1 ms; phase noise <2 degrees rms; frequency resolution, 1 Hz.
- VLBA compatible baseband channelization and sampling: bandwidths from .0625 to 16 MHz in factors of 2; 1 or 2-bit sampling with rate 32 Msamples/s.
- Data Quality Analysis: 2 PCAL tone extractors per BBC; one stream statistics accumulator per baseband channel.
- Control via terminal, serial multi-drop protocols, or Ethernet.
- Extensive debugging and self-test capabilities.

2.2. S2 Record and Playback Terminals (RT and PT)

The S2 RT and PT were the first components of the S2 VLBI system to be completed. They have been fully operational since the early 1990's and can be found at more than 20 radio telescopes world-wide, at three NASA Deep Space Network complexes where they are used for space VLBI and at two fully operational VLBI correlators. Architecturally, the RT and PT are made up of an array of 8 SVHS transports and a VME controller. The technology is mature, robust and the systems are convenient to use. SVHS cassettes are inexpensive and easy to handle.

Characteristics of the S2 RT/PT are summarized below:

- Data rates up to 128 Mbits/s.
- 6 hours continuous recording at 128 Mbits/s.
- BER in LP ≈1.e-5; BER in SLP ≈3.e-4
- Low media cost ($37 US per Tbit).
- S2 RT can be interfaced directly to the Canadian S2 DAS, the Australian S2 DAS and "other" DAS's in Russia and China.
- S2 RT can be interfaced to VLBA, Mk4, K4/VSOP or Australian LBA using S2-VIA module.
- S2 PT has a clean format-free non-data-replacement output interface.
- Control via terminal, serial multi-drop protocols or Ethernet interface.
- Supported by NASA VLBI Field System (PCFS).
- Extensive diagnostics, self-test and calibration software.
- Uses proven, reliable SVHS industrial transports.
- Transportable configuration includes 3 modules each weighing less than 37 kg.

2.3. Canadian S2 VLBI Correlator

The Canadian S2 VLBI Correlator (see Ref. [2]) was initially designed as Canada's contribution to the RadioAstron space VLBI project. It has many unique features for processing pulsar, spectral line and space VLBI data. With respect to geodetic applications, it handles the frequency switched BWS modes of operation. The correlator has been in full operational status for over 3 years in support of the VSOP and CGLBI programs.

Characteristics of the Canadian S2 VLBI Correlator are summarized below:

- XF station-based architecture.
- 6-station correlator.
- Handles 8 baseband channels per station/baseline.
- Channels can be 1 or 2-bit sampled at up to 32 Msamples/s.
- 8 sets of stream statistics and 8 9-bit tone extractors per station module.
- Two independent pulsar gates per station module.
- Handles the high fringe rates & accelerations characteristic of satellites (including perigee).

- Extensive diagnostic and self-test capability.
- Frequency switching capability.
- Up to 16,384 lags per baseline in spectral line or fringe search mode.
- Correlator "dump" interval as short as 1 ms.
- Standard output product for astronomy is "UVFITS".
- Utilities available to translate the geodetic multi-band "FRINGed" output into Calc & Solve dbase format.
- Special lag architecture and internal digital filters allow mixed bandwidth correlation as well as "zoom" mode for enhanced spectral line capability.

3. Frequency Sequence Design

3.1. S2 Frequency Sequence Capabilities

The S2 system was designed to provide a great deal of flexibility with respect to the implementation of frequency switched BWS. There are several factors that contribute to this flexibility.

1. IF Input Range. The IF input range is 100–1000 MHz. This allows IF channels up to 900 MHz bandwidth to be handled without band splitting.

2. Number of IF Inputs. Hardware for up to 4 IF inputs can be installed. This is more than adequate to handle the S-band and X-band inputs used in geodetic VLBI. The extra IF inputs could be used for additional bands, polarizations or to handle IF's wider than 900 MHz.

3. Number of BBC's. Up to 4 BBC's can be installed. This provides up to 4 simultaneous BWS frequencies and a potential output data rate of 512 Mbits/s.

4. Maximum Frequency Switching Rate. The maximum frequency switching rate is 50 Hz with LO switching transients settling in <1 ms.

5. Maximum Sequence Length. A sequence can have up to 16 unique states and (since states can occur more than once in a sequence) a total of 64 elements. For a 2 BBC system, the net effect is equivalent to 32 "virtual" BBC's. The sequence length limits are imposed in software and could be relaxed if necessary.

6. Sequence Length. The DAS software calculates which element of the frequency switching sequence to use at any particular time by assuming that the sequence starts at the beginning of the UT day. Removing the need to have a command to set the epoch at which the sequence starts makes the frequency switching command structure simpler and operationally more robust. A consequence of this assumption is, however, that the sequence length is constrained such that an integer number of cycles of the sequence must occur in a day.

7. LO Frequency Setting Resolution. The BBC LO frequency setting resolution is 1 Hz. This makes it possible to offset the LO frequency away from integer multiples of 1 MHz to avoid corruption of the PCAL tones.

3.2. Frequency Sequence for the S2 System Validation Tests

A BWS frequency switching sequence was selected to be used in the S2 system validation experiments. The design goal for the sequence was to match the performance of typical Mk3

sequences with respect to spanned bandwidth, rms bandwidth, ambiguity spacing and maximum sidelobe level. The sequence selected (see Table 1) uses a frequency switching period of 1 second per state and a total of 12 states.

State	X	S	BBC1(MHz)	BBC2(MHz)
1	•		8212.99	8932.99
2		•	2227.99	2352.99
3	•		8502.99	8642.99
4		•	2272.99	2307.99
5	•		8217.99	8972.99
6	•		8422.99	8722.99
7		•	2232.99	2347.99
8	•		8237.99	8907.99
9		•	2247.99	2332.99
10	•		8307.99	8837.99
11		•	2237.99	2342.99
12	•		8277.99	8867.99

Table 1. Frequency sequence used in the S2 system validation tests.

The performance of the sequence in Table 1 is summarized in Table 2. It very nearly matches the performance of the most commonly used Mk3 sequence except that it has the advantage that the X-band ambiguity spacing is 200 ns instead of 50 ns. The sequence performed very well in the system validation experiments. There was essentially no evidence of misidentification of fringes other than when signal levels were near or below the detection threshold.

Parameter	X-band	S-band
Spanned BW (MHz)	720	125
RMS BW (MHz)	280	49
Max sidelobe (%)	56	62
Ambiguity (ns)	200	200

Table 2. Performance of the frequency sequence used in the S2 system validation tests.

References

[1] Klatt, C., et al, "The S2 Geodetic VLBI Program in Canada: Operations, Experiments, and Results", This Volume.

[2] Carlson, B.R., et al, "The S2 VLBI Correlator: A Correlator for Space VLBI and Geodetic Signal Processing", in Publications of the Astronomical Society of the Pacific, 111:1025-1047, 1999 August.

Hayo Hase et al.: Transportable Integrated Geodetic Observatory (TIGO), IVS 2000 General Meeting Proceedings, p.383–387
http://ivscc.gsfc.nasa.gov/publications/gm2000/hase

Transportable Integrated Geodetic Observatory (TIGO)

Hayo Hase, Armin Böer, Stefan Riepl, Wolfgang Schlüter

BKG Wettzell

Contact author: Hayo Hase, e-mail: hase@wettzell.ifag.de

Abstract

TIGO is a transportable fundamental station for geodesy. TIGO consists of VLBI and SLR modules as well as of a so called basic service module which comprise a GPS array, atomic clock ensemble, superconducting gravity meter, seismometer, meteorological sensors including a water vapour radiometer and a server for the LAN. The energy module allows the operation of TIGO at remote sites with little infrastructure.

The primary purpose of TIGO is to contribute to the realization of global reference systems for geodesy (ITRF). Its transportability allows us to place TIGO at a site which improves homogeneity in the network of fundamental stations within the ITRF, if the necessary support of the hosting country can be made available to this project. After an Announcement of Opportunity for hosting TIGO and a reconnaissance of proposed sites as well as some analysis concerning the optimal use of TIGO, the Chilean city of Concepción got the highest priority for hosting TIGO beginning 2001.

1. Objectives of TIGO

The global reference frames ICRF (International Celestial Reference Frame) and ITRF (International Terrestrial Reference Frame) are the basis for all geodetic reference frames applied in continental and national areas. Today the geodetic space techniques are highly efficient and cost effective for scientific and practical applications. The geodetic space techniques such as VLBI (Very Long Baseline Interferometry), SLR (Satellite Laser Ranging), and microwave based observations of navigation systems like GPS (Global Positioning System) and DORIS (Doppler Orbitography and Radiolocation Integrated by Satellite) are realizing the global reference frame ITRF through an international network of geodetic stations—the International Space Geodetic Network (ISGN)—consisting of radio telescopes for VLBI, laser ranging systems for SLR/LLR, permanent GPS stations, DORIS ground beacons.

The global distribution of the geodetic stations is inhomogeneous. Concentrations of stations occur in North America, Europe and parts of Asia (Japan), whereas gaps in the network are obviously on the southern hemisphere.

For the minimization of systematic effects and errors the ideal distribution for the ISGN would be a homogeneous network. It is obvious that the realisation is an international task, regardless of political borders. International and bilateral cooperations are required, which finally result in the benefit for all by the existence of a highly precise global reference frame. The international coordination of the contributions is performed through the international services which are under the patronage of the International Association of Geodesy (IAG), namely the IVS (International VLBI Service)[1], ILRS (International Laser Ranging Service)[2], IGS (International GPS Service)[3].

[1] http://ivscc.gsfc.nasa.gov/
[2] http://ilrs.gsfc.nasa.gov/ilrs_home.html
[3] http://igscb.jpl.nasa.gov/

The combination of the products is guaranteed through the IERS (International Earth Rotation Service)[4].

The Bundesamt für Kartographie und Geodäsie (BKG) has developed the Transportable Integrated Geodetic Observatory (TIGO) as an additional fundamental station for the support of the realisation and for the maintenance of the ITRF and ICRF. TIGO is currently in a test phase and is operated in collocation with the Fundamentalstation Wettzell in Germany. It is planned to start the regular field operations in the year 2001. Due to the transportability the contribution to the ITRF can be optimised in dependence of the location and of the duration of operation at one site. In order to fill gaps in the ISGN the area for operation is preferably on the southern hemisphere. The minimum operation period at foreign sites is envisaged to be three years.

2. Transportable Integrated Geodetic Observatory (TIGO)

TIGO is a rigorous development of a fundamental station in order to provide observations for the

1. realisation of the geodetic global reference system,
2. maintenance of the global reference frame,
3. monitoring of the Earth orientation parameters,
4. monitoring of the crustal movements including tides.

All relevant geodetic space techniques are employed at TIGO:

- Very Long Baseline Interferometry (VLBI),
- Satellite Laser Ranging (SLR),
- Global Positioning System (GPS) and comparable navigation systems.

For the performance of observations with geodetic space techniques and for the correct interpretation of observational data additional local measurements are indispensable, like

- measurements concerning the local time and frequency keeping providing the UTC related time scale and reference frequencies,
- gravity measurements for monitoring Earth tides,
- seismic measurements for monitoring earthquakes,
- meteorological measurements for monitoring the troposphere,
- local survey measurements for monitoring the site stability and eccentricities between the various instrumental reference points.

TIGO has its own electric power generators in case there is no or unstable power supply at the remote site.

Transportability of the observatory is achieved by building the whole observatory into six 40-foot standard containers, which are certified for sea transportation. It is assumed that according to its specifications TIGO can be shipped to any remote location (outside arctic or antarctic environments) in the world. The un-/loading procedure of the containers from/to a truck at the selected

[4]http://hpiers.obspm.fr/

TIGO site is possible simply with muscle power (no crane will be needed!). After installation of TIGO some of the containers serve as the operation rooms. A more detailed description can be found in [3].

It is planned that TIGO will be operated jointly by BKG and partner institutions of the hosting country. With respect to the necessary training of staff and the risks of transportation the period of operation at the remote site should be at least three years.

3. TIGO in the Network of Fundamental Stations

Fundamental stations for geodesy realize fundamental reference points within the ITRF because of the possibility to tie global networks of different geodetic space techniques at one location by the local survey of the eccentricities between the various instrumental reference points.

In 1999 the ITRF contained only a few sites which deserve the title of a fundamental station. These are *Wettzell* (Germany), *Matera* (Italy), *KeyStone* (Japan), *Greenbelt*, (U.S.A.).

In addition there are some quasi-fundamental stations, where the distances between the different instruments are larger than 1 km. This makes the local survey more difficult, because its accuracy level should be one order of magnitude more accurate than those of the geodetic space techniques. However the results from these stations represent within a global reference frame the same region and are subject to almost the same geodynamic phenomena. The list of these stations consists of *Shanghai* (P.R.China), *Canberra-Tidbinbilla* (Australia), *Kokee Park-Maui* (Hawaii). An additional fundamental station at *Hartebeesthoek* (R.S.A.) will be created with the beginning of a permanent SLR operation with MOBLAS-6.

The TIGO project must be seen as a German contribution to the international effort to realize and to maintain the most accurate global reference system by densifying the existing networks. TIGO as a transportable fundamental station has the ability to be placed on those sites which contribute in an ideal way to the process of homogenisation of the inhomogeneous global network of fundamental stations.

A computation method in order to locate the most distant point from an existing point distribution on a sphere was developed by Hase [2]. Figure 1 shows the existing network of fundamental stations and the areas which they represent in terms of distance to other stations. From figure 1 it can be easily seen, that an additional fundamental station in South America would close the largest gap in the network.

Even if the choice for the best location can be quantified by the method described above, TIGO is dependent on the support by the hosting country in terms of operational staff, cost sharing and property provision. In July 1999 an *Announcement of Opportunity* for hosting TIGO was published by BKG [1]. By the due date September 30, 1999, several institutions from countries in South America and in near and far East Asia applied for participation in the TIGO project. During November and December 1999 the most promising 11 sites were inspected by BKG staff. A report [4] on the reconaissance and the received *Letters of Intent* were presented to the directing board of the German research group on satellite geodesy (FGS) who initiated the TIGO project in the early nineties.

Among the competitors a consortium with the Universidad de Concepción as main partner in Concepción, Chile, got the highest priority for hosting TIGO because of fulfilling the request from BKG for hosting and operating TIGO as well as the ideal geographical location within the global reference networks. A second priority was given to Cordoba, Argentina, and Bangalore, India.

Figure 1. Voronoi diagram with existing (quasi-)fundamental stations (marked with stars). The voronoi lines are the lines of largest distance between stations. The three numbered voronoi vertices are the three most remote points in the network of existing stations.

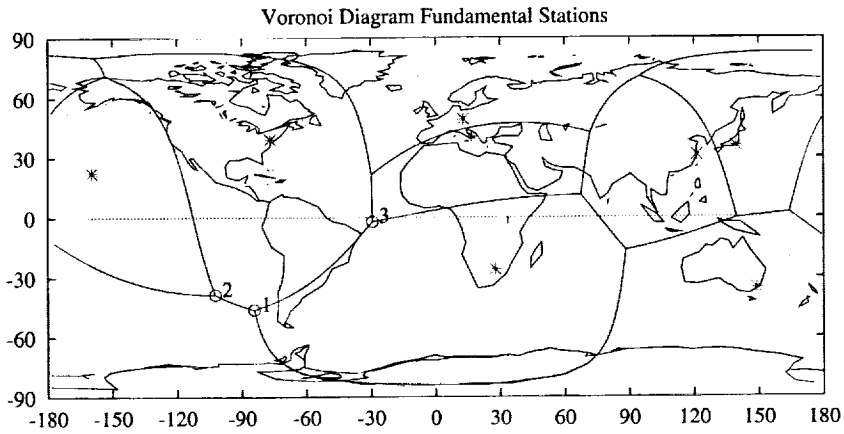

Figure 2 gives an impression of how the network changes in terms of approaching homogeneity in its point distribution by adding one new sites near the most remote locations (resp. close to the center of the largest gap).

Figure 2. Voronoi diagram with the network of existing (quasi-)fundamental stations plus the new site of Concepción possibly occupied with TIGO in the near future. (Compare with fig. 1.)

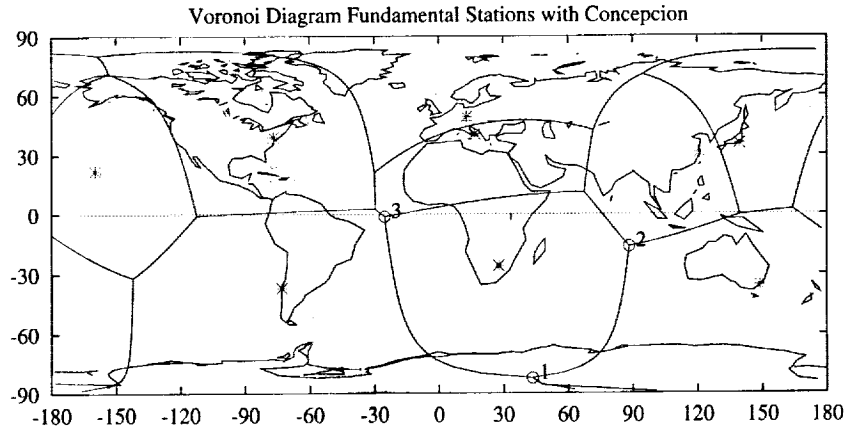

The gain of an additional fundamental station in the southern part of South America can be expressed in terms of the decrease of the maximum distance between the most remote point to any fundamental station (largest gap). Table 1 summarizes the gains of South American applicants.

Another way of looking at the improvement through an additional fundamental station in the network can be derived by the approximate volume of the Earth which follows from a Delaunay

Table 1. Improvement by an additional fundamental station in terms of reducing the largest distance to the fundamental points on a unit sphere Earth model.

New Site	Largest Distance	Gain
none	8648 km	0 (ref.)
Concepción, Chile	6087 km	29.6%
Cordoba, Argentina	6351 km	26.5%
Buenos Aires, Argentina	6486 km	25.0%
Fortaleza, Brazil	7758 km	10.3%

triangulation among the fundamental points on a unit sphere Earth model. Table 2 shows the increase in the approximate volume due to one additional site at different locations in the given network. The large relative increase of more than 57% can be achieved in South America with the realisation of an additional fundamental point by TIGO.

Table 2. Increase of volume of the unit sphere Earth model. Earth's approximate volume is derived from a Delaunay triangulation in the network of the fundamental stations. The listed sites had been proposed for hosting TIGO.

New Site	Volume	Increase
none	0.9727	0 (ref.)
Concepción, Chile	1.5294	57.2%
Cordoba, Argentina	1.5196	56.2%
Buenos Aires, Argentina	1.5129	55.5%
Fortaleza, Brazil	1.3085	34.5%
Bangalore, India	1.1537	18.6%
Serpong, Indonesia	1.1152	14.6%
Quezon City, Philippine	1.0278	5.7%

The next steps within the TIGO project comprises the negotiations with the Universidad de Concepción about the details of setting up TIGO and the operation beginning 2001 for a minimum period of three years.

References

[1] Announcement of Opportunity on Hosting TIGO, http://www.wettzell.ifag.de/tigo

[2] Hase, H.: New Method for the Selection of Additional Sites for the Homogenisation of an Inhomogeneous Cospherical Point Distribution, in: Int. Ass. of Geodesy Proceedings, Towards an Integrated Global Geodetic Observing System (IGGOS), Munich, October 5-9, 1998, edited by R. Rummel, H. Drewes, W. Bosch, H. Hornik

[3] Hase, H.: Theorie und Praxis globaler Bezugssysteme, Mitteilungen des Bundesamtes für Kartographie und Geodäsie, Band 13, Frankfurt am Main, 1999

[4] Schlüter, W., Hase, H.: Bericht zur Entscheidungsfindung über den ersten ausländischen TIGO-Standort, BKG-G-Az. 5165, 16. Januar 2000 (internal document)

Splinter Sessions

Reports

Ed Himwich: Planning the Chiefs Meeting for February 2001, IVS 2000 General Meeting Proceedings, p.391–392
http://ivscc.gsfc.nasa.gov/publications/gm2000/himwich3

Planning the Chiefs Meeting for February 2001

Ed Himwich

NVI, Inc./NASA Goddard Space Flight Center
e-mail: weh@vega.gsfc.nasa.gov

Abstract

This report summarizes the discussion at the splinter meeting to plan for the next Chiefs meeting.

1. Summary

There were 25 attendees, listed below. The chair opened the meeting by summarizing the comments received by e-mail before the meeting. Based on these comments, the chair made several proposals, some of which were modified based on the ensuing discussion. The resulting consensus is stated below:

1. The name is changed from "Chiefs Meeting" to "Operations Workshop" (OW). The feeling was that the old name confused some administrative managers who thought that the meeting was for administrators rather than a techincal meeting for the operators.

2. The format will be changed with the primary goal of having more hands-on sessions with smaller groups. To help accomplish this several things will be changed: (A) Analysis and science talks will be greatly curtailed, but not eliminated entirely. It was felt that the IVS General Meeting was a better forum for these topics. This will allow more time to be spent at the OW on training. However, it was felt that some overview was still worthwhile. (B) The OW will cover fewer topics. A poll will be taken of what topics people are most interested in. The available time will be used to cover the topics with the most interest at an appropriate level rather than trying to cover everything without enough depth. (C) The meeting will be focussed more strongly on the technical "Chiefs" at each station rather than accepting all operators. The Chief would then be responsible for sharing the training with the other operators at home. The goal is to reduce the number of attendees so that more topics can be covered. Some stations where the expertise is distributed over several individuals may need to send more than one individual. (D) The meeting will be longer, up to one week, so that more topics can be covered. To the extent possible the scheduling will be arranged to allow people who don't need to come for the whole meeting to come for a subset. (E) Last, but not least, meetings will be held every two years rather than every three. This will hopefully reduce the need to cover every topic at every meeting.

3. Participation in training sessions sponsored by other organizations, such as the EVN, would be encouraged. The first opportunity for this will be at the EVN recorder workshop the first week of May at Jodrell Bank.

2. Attendees

Walter Alef, Mario Berube, Francis Colomer, Pino Colucci, Ludwig Combrinck, Brian Corey, Clyde Cox, Helge Digre, Raymond Gonzalez, Hayo Hase, Ed Himwich (chair), Charles Ko-

dak, Kerry Kingham, Yasuhiro Koyama, Franco Mantovani, Arno Mueskens, Mike Poirier, Svein Rekkedal, Wolfgang Schlueter, David Shaffer, Dan Smythe, Richard Strand, Mike Titus, Vincenza Tornatore, Nancy Vandenberg

A. Nothnagel: Excerpts from the First IVS Analysis Workshop, IVS 2000 General Meeting Proceedings, p.393-396
http://ivscc.gsfc.nasa.gov/publications/gm2000/nothnagel2

Excerpts from the First IVS Analysis Workshop

A. Nothnagel

Geodetic Institute of the University of Bonn
e-mail: nothnagel@uni-bonn.de

Abstract

The first IVS Analysis Workshop was held in conjunction with the first IVS General Meeting at Kötzting. For the first time most of the representatives of the IVS Analysis Centers met in order to discuss a number of organisational and scientific topics which were considered essential for the current phase of the IVS data production and dissemination. Five working groups have been initiated which will discuss individual topics.

1. Introduction

On February 24, 2000 the first IVS Analysis Workshop was held in conjunction with the first IVS General Meeting at Kötzting in the Bavarian Forest, Germany. The fact that many colleagues attended the IVS General Meeting offered the opportunity to organize the Analysis Workshop at the same time. This saved a lot of travel time and money permitting more analysts to attend than would have been possible for a stand-alone meeting. Although the allocated time of one afternoon initially sounded too short for the many topics to be discussed the time frame of about 5 hours seemed to have been just right for start-up discussions. The meeting was attended by some 40 analysts from almost all IVS Analysis and Data Centers. We were very glad to also welcome to the workshop the IGS Analysis Coordinator, Tim Springer, the ILRS Analysis Coordinator, Ron Noomen, and the IERS-ITRF representative, Zuheir Altamimi, who all presented valuable contributions. It should be mentioned that the arrangements of the Local Organizing Committee, Wolfgang Schlüter and Hayo Hase, produced an appreciable environment which was a good basis for an efficient workshop.

The discussions of the scientific and organisational aspects of the IVS data production and product dissemination were preceeded by short introductory presentations in order to address the issues in question in a concise manner. The discussions were subdivided into three main groups: geophysical models, data reduction aspects, and general issues.

2. Geophysical Models

2.1. General

The discussions of the geophysical models were driven by the relationship between VLBI data analysis and the IERS Conventions 1996 (McCarthy, 1996). It was stated that some parts of the IERS Conventions are not as clear and consistent as would be necessary and it was pointed out that

1. often there are just computational recipes but the underlying background is neither explained nor referenced properly

2. sometimes there are several models available in the Conventions but there is no preference given which allows the use of one of the models as a standard
3. not enough software is provided to implement the recommended models.

However, it is understood that the IERS Conventions were never intended as a "Bible" for analysts but describe the basic characteristics of the IERS products in some general sense for the users and provide a reference solution framework against which the Analysis Centers are supposed to document their differences.

For this purpose, beyond others, the IAG/ETC Working Group 6 "Solid Earth Tides in Space Geodetic Techniques" had already published a report "Explanatory Supplement to the IERS Conventions (1996) Chapters 6 and 7" (SCHUH 1999). In this report several of the topics related to the IERS Conventions (1996) are discussed and described in more detail.

2.2. Earth Tides

The tidal models used in all routine VLBI analyses initially apply a single set of Love numbers for the complete range of frequencies as listed in the IERS Conventions. In a second step some corrections are necessary: the daily tides are corrected for Free Core Nutation (FCN) while long period tides are corrected for anelastic response of the mantle. Ideally, a correction for the permanent tide should be done as well using Love numbers for fluids. However, in order to take this into account the IERS Conventions suggest that this error is corrected by computing station coordinates on the "real" crust excluding the zero frequency part of the harmonic expansion.

This suggestion for a correction is ignored in all routine VLBI analyses. The IERS will be advised, pending a formal decision of the IVS, that a change in the current treatment of the permanent tide effects is deemed not to be necessary from an IVS point of view.

2.3. Ocean Loading

Hans-Georg Scherneck briefly introduced his new ocean loading model which is based on orthotides. The harmonic expansion of the tidal potential may be used for both ocean loading and solid Earth tides. Before it will be used routinely and even be suggested for inclusion in the IERS Conventions 200x it should be tested extensively by the IVS Analysis Centers. A standalone program, which needs to be modified slightly for use in analysis packages, is available from Scherneck via ftp://gere.oso.chalmers.se/pub/hgs/oload/Ttide-108.tar.Z

2.4. Atmospheric Loading

Time series for atmospheric loading displacements (vertical, east, north) are available for a large number of VLBI stations and VLBI experiments after 1989. After 1996 the files are continuous with 6 h sampling intervals, currently ending Jan. 31, 2000. Further explanations can be found at http://www.oso.chalmers.se/~hgs/apload.html

2.5. Nutation

Currently the best a priori for nutation in data analysis is the model in the IERS 1996 Conventions. If analysts want to compute residuals from the IAU 1980 nutation model they should use the following procedure: analyse the data with the model in the IERS 1996 Conventions, compute

total nutation angles, and subtract the IAU 1980 model angles for the respective epochs.

There will be a new nutation model following the work of an IAU Working Group on Nutation in the near future. As long as the complete series of VLBI sessions is computed with the same model always providing offsets to the same model no inconsistencies are to be expected.

3. Data Reduction Aspects

During the workshop a number of data submission and format issues were discussed. It was organized how the solutions for this year's annual submissions to the IERS are to be handled. For the combination of TRF solutions in SINEX format which will finally contribute to the realization of the ITRF2000 only minimally constrained solutions will be incorporated.

It was also emphasized that comparisons of VLBI analysis software packages as well as of analysis strategies should be carried out. There are a number of existing intercomparisons which are by-products of combinations of results. However, there are currently no direct comparisons for example on a session to session basis. A detailed analysis of the combination residuals are not carried out either. Older intercomparisons of software packages concentrated on the models themselves which seem to agree at the picosecond level.

Proposals were presented briefly which addressed naming conventions and data formats. A naming convention was proposed aiming at a unified procedure to issue names for sources and stations which are used in geodetic and astrometric VLBI sessions for the first time. Another proposal discussed a new generation of a Geo VLBI data format. The issue of an extension of the SINEX format for geodetic VLBI solutions was addressed briefly.

In view of the high quality results produced already it was suggested that the range of products should be extended by regularly producing baseline length results, high resolution EOP series, station clock information, and total atmospheric path delays and their contributions.

4. General Issues

One of the primary tasks of IVS is the regular production and dissemination of VLBI results and Earth orientation parameters in particular. The current status of submissions of both data and results is far behind proposed and expected dimensions. However, the operation of IVS is still in an initial stage and a number of obstacles still have to be smoothed out. It is expected that complete and timely submissions will be established soon which will be a prerequisite for routine combinations.

So far only the Analysis Coordinator's office is actively working towards the goal of regularly combining VLBI results. However, other Analysis Centers are encouraged to take up these tasks in parallel in order to establish quality control and redundancy.

5. IVS Analysis Working Groups

Five IVS Analysis Working Groups were set up at the end of the workshop which will establish and continue a detailed discussion of the respective topics. The groups are open to all VLBI analysts who wish to join them. First status reports of each of the Working Groups are due by June 30, 2000. The Working Groups are listed here with ad-hoc topics to be worked on:

- Geophysical Models

  discussion and coding of new models, interface for IERS Conventions, software implementation

- Data Analysis

  analysis methods, parameterization, constraints, weighting, correlations, editing, software implementation

- Comparisons and Combinations

  software packages, technique results, IVS solutions and products

- IVS Products

  types, formats, data flow

- ICRF

  maintenance, recommendations for additional sources to be observed

6. References

Schuh H. (ed.) (1999): *Explanatory Supplement to the IERS Conventions (1996) Chapters 6 and 7*, DGFI Report No. 71, Munich (http://dgfi2.dgfi.badw-muenchen.de/dgfi/DOC/report71.pdf)

McCarthy D.D. (ed.) (1996):*IERS Conventions (1996)*. IERS Technical Note 21, Observatoire de Paris

Brian E. Corey: RFI: Measurement Techniques, IVS 2000 General Meeting Proceedings, p.397–401
http://ivscc.gsfc.nasa.gov/publications/gm2000/corey2

RFI: Measurement Techniques

Brian E. Corey

MIT Haystack Observatory
e-mail: bcorey@haystack.mit.edu

Abstract

Some techniques for detecting radio frequency interference and for measuring its effect on the system temperature of a VLBI antenna are described.

1. Introduction

On 24 February 2000 a workshop on radio frequency interference (RFI) was held at the Fundamentalstation Wettzell during the IVS General Meeting. The topics discussed included (1) how RFI affects the VLBI observables (SNR, delay, etc.), (2) at what level RFI causes problems in geodetic VLBI, and (3) how to detect and measure RFI. The first two topics are treated in David Shaffer's companion paper, while the third topic is the subject of these notes.

Two general categories of measurement techniques may be distinguished by the type of equipment used:

- Measurements with a simple test set-up involving a small receiving antenna, an amplifier, and a spectrum analyzer.
- Measurements at a fully equipped VLBI station employing a VLBI antenna with receiver, a VLBI terminal, and a spectrum analyzer.

The first technique may of course be employed at a site with an existing VLBI antenna, but its most useful role is in surveying potential locations for future installation of a VLBI station. Specific examples of measurement procedures of both types are described in the next two sections.

As pointed out in Shaffer's paper, an increase as small as 10% in the power in a single baseband channel due to RFI can have a significant effect on the measured group delay. The methods described here are designed to be able to measure RFI-induced T_{sys} increases down to this level.

Most RFI sources are terrestrial and so are liable to be located near the horizon. RFI searches are therefore usually conducted by scanning the antenna around the horizon at, or slightly above, the minimum elevation angle normally observed.

2. RFI Measurements at a Site without a VLBI Antenna

Suppose we wish to characterize the RFI environment at a site where there will be a large VLBI antenna with antenna gain G_{vlbi} and system temperature T_{vlbi}. The goal is to detect RFI sources that would cause a 10% increase in the VLBI system temperature averaged over a bandwidth B_{vlbi} equal to the VLBI baseband bandwidth (typically 2 MHz or larger) anywhere in a given RF range, when the VLBI antenna is pointed more than a few beamwidths away from the source. (Ideally the search would be sensitive enough to detect sources so weak that they would increase T_{sys} by 10% only when the large antenna is pointed right at the source. Unless the RFI is much narrower

in bandwidth than B_{vlbi}, however, the procedure outlined here would require a search antenna as large as the VLBI antenna in order to detect such sources.)

The basic principle behind this method is the fact that, when a directional antenna is pointed more than a few beamwidths away from a source, the power received from the source is roughly the same as would be received by an omnidirectional antenna. There may be exceptions at some angles where the level is higher than this by (say) 10 dB, as when a prime-focus feed directly "sees" a source just beyond the edge of the primary reflector. But in general the power received away from the main beam will be within a factor of 2–3 of the omnidirectional level, or less.

2.1. Equipment and Configuration

- Test antenna with gain G_{ant} ($= 4\pi$ / beam solid angle in steradians, in the absence of losses in the antenna).
- RF amplifier with gain G_{amp}, with input attached directly to the antenna output.
- Spectrum analyzer that covers the desired RF range.
- Low-loss RF cable with loss L_{cab}, running from the amplifier output to the analyzer input.

See Figure 1. For convenience, define $G_{ac} = G_{amp}/L_{cab}$ [or, in dB units, $G_{ac}(\mathrm{dB}) = G_{amp}(\mathrm{dB}) - L_{cab}(\mathrm{dB})$]. G_{ac} is the net gain from the antenna output to the spectrum analyzer input.

2.2. Procedure

1. Set up the analyzer with frequency span covering the VLBI observing band, minimum input attenuation, narrow video BW (to minimize measurement noise – 10 kHz is often a good choice), and resolution BW B_{res} less than or equal to B_{vlbi}.
2. Scan the test antenna around the horizon slowly while observing the analyzer display.
3. Measure the total power P_{rfi} of each RFI signal observed. Doing this properly requires attention to the observed bandwidth B_{rfi} of the RFI signal. If $B_{rfi} = B_{res}$ (as will occur if the true signal BW is less than B_{res}), set P_{rfi} to the peak signal level. If $B_{rfi} > B_{res}$, set
   $P_{rfi}(\mathrm{dBm}) = P_{ave}(\mathrm{dBm}) + 10\log\left[B_{rfi}(\mathrm{Hz})/B_{res}(\mathrm{Hz})\right]$,
   where P_{ave} is the average power level over the RFI bandwidth. If $B_{rfi} > B_{vlbi}$, set
   $P_{rfi}(\mathrm{dBm}) = P_{ave}(\mathrm{dBm}) + 10\log\left[B_{vlbi}(\mathrm{Hz})/B_{res}(\mathrm{Hz})\right]$.
4. Calculate the effective power $P_{omni} = P_{rfi}/(G_{ant}G_{ac})$ that would be received by an omnidirectional antenna, and the corresponding noise temperature averaged over bandwidth B_{vlbi}.
   Calculate power in dBm:
   $P_{omni}(\mathrm{dBm}) = P_{rfi}(\mathrm{dBm}) - G_{ant}(\mathrm{dB}) - G_{ac}(\mathrm{dB})$
   Convert to milliwatts:
   $P_{omni}(\mathrm{mW}) = 10^{[P_{omni}(\mathrm{dBm})/10]}$
   Convert to noise temperature:
   $T_{omni}(\mathrm{K}) = P_{omni}(\mathrm{mW}) \,/\, [1.4 \times 10^{-20} \times B_{vlbi}(\mathrm{Hz})]$
   T_{omni} is the typical noise temperature increase due to RFI that will occur in a baseband channel when the VLBI antenna points away from the RFI source. If the VLBI antenna points directly at the source, the increase will be approximately $T_{omni}G_{vlbi}$, unless the source is in the near field (see Section 3), in which case the increase will be smaller than this.

5. Repeat steps 2-4 with other analyzer resolution bandwidths narrower than B_{vlbi}. The narrower B_{res} is, the greater the sensitivity to narrowband RFI, but at a cost of longer analyzer sweep times.

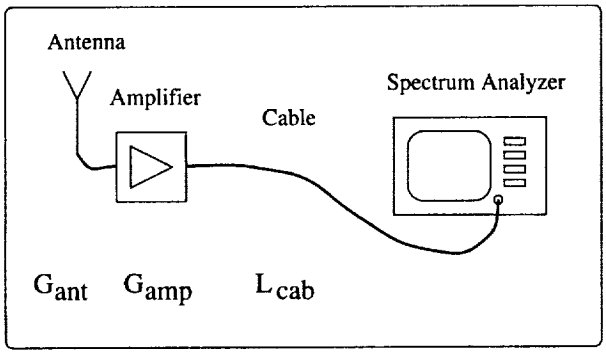

Figure 1. RFI measurement set-up without a VLBI system (courtesy of Armin Böer).

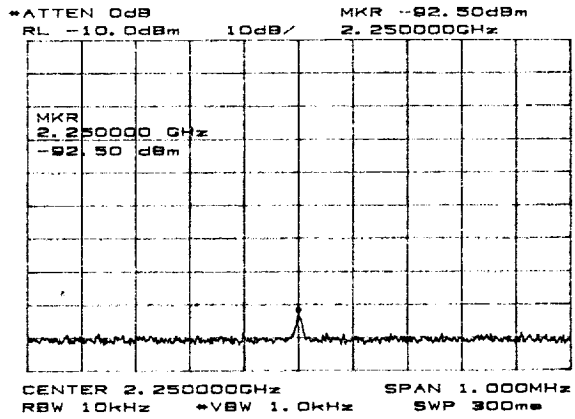

Figure 2. Sample analyzer display showing RFI (courtesy of Gerhard Kronschnabl).

2.3. Example

Figure 2 shows an RFI spike observed with the following equipment: an S-band horn with gain G_{ant} of 14 dB, an Avantek ABG240 amplifier with gain G_{amp} of 22 dB, an RF cable with loss L_{cab} of 6 dB, and an HP 8561A spectrum analyzer. The combined amplifier+cable gain G_{ac} is 22 − 6 = 16 dB. From the figure, the observed signal bandwidth is the same as the resolution bandwidth, and P_{rfi} is equal to −92.5 dBm. Step 4 above then gives:

$$\begin{aligned} P_{omni} &= -92.5 \text{ dBm} - 14 \text{ dB} - 16 \text{ dB} \\ &= -122.5 \text{ dBm} \\ P_{omni}(\text{mW}) &= 10^{-122.5/10} = 0.56 \times 10^{-12} \text{mW} \end{aligned}$$

For a baseband bandwidth B_{vlbi} of 2 MHz, the effective temperature would then be

$$\begin{aligned} T_{omni}(\text{K}) &= 0.56 \times 10^{-12} \text{ mW} / [1.4 \times 10^{-20} \times 2 \times 10^{6} \text{ Hz}] \\ &= 20 \text{ K} \end{aligned}$$

2.4. Requirements on the Equipment

Assume that the weakest RFI source that can be detected reliably is 3 dB above the noise floor P_{nf} on the analyzer, so the minimum detectable level is P_{nf}. Let T_{nf} be the equivalent noise temperature given by

$$T_{nf}(\text{K}) = P_{nf}(\text{mW}) / [1.4 \times 10^{-20} \times B_{res}(\text{Hz})]$$

T_{nf} for spectrum analyzers is typically 100,000 K or higher. Therefore, in order to be able to detect sources that could interfere with systems having noise temperatures below 50 K, it is essential to have an antenna and an amplifier with high gain and low noise ahead of the analyzer.

To be quantitative: Let T_{test} be the noise temperature of the test antenna and amplifier together, in the absence of RFI; T_{test} will include contributions from amplifier noise, atmospheric noise, and especially ground pickup. The noise floor on the spectrum analyzer is set by the sum of the antenna+amplifier noise at the analyzer input and the internal analyzer noise $T_{nf,sa}$:

$$T_{nf} = T_{test}G_{ac} + T_{nf,sa}$$

The requirement that the minimum detectable T_{omni} be less than 10% of T_{vlbi} is then equivalent to

$$(T_{test}G_{ac} + T_{nf,sa})/(G_{ant}G_{ac}) < T_{vlbi}/10$$

or

$$T_{test}/G_{ant} + T_{nf,sa}/(G_{ant}G_{ac}) < T_{vlbi}/10$$

In a well-designed system, the total system noise will be dominated by the noise from the antenna+amplifier, not by the internal spectrum analyzer noise. This requirement together with the last equation then yield

$$G_{ant} > 10\, T_{test}/T_{vlbi}$$

and

$$G_{ac} > T_{nf,sa}/T_{test}$$

For T_{test} = 300 K, T_{vlbi} = 30 K, and $T_{nf,sa} = 10^6$ K, these requirements become $G_{ant} > 100$ (= 20 dB) and $G_{ac} > 3000$ (= 35 dB).

3. RFI Measurements with a VLBI Antenna

Using a large antenna to look for RFI has the advantage of high sensitivity. A disadvantage is the narrow beamwidth, which necessitates scanning the antenna slowly if maximum sensitivity to RFI is desired. For example, a 20-meter antenna has a beamwidth of ~0.13° at X-band; a full sweep around the horizon at a single elevation angle with an integration time of 1 second per beamwidth would therefore take nearly an hour. [Note that, if a source is in the "near field" of the antenna, which extends out to distances of 2×(antenna diameter)^2/wavelength, or ~20 km for a 20-meter antenna at X-band, the effective antenna beamwidth is larger than the standard "far field" value measured on celestial sources. In other words, nearby sources appear larger.]

3.1. Measurements Using Baseband Detectors

A simple method for detecting RFI uses the baseband total power detectors built into most VLBI terminals. For example, MkIII/MkIV video converters and VLBA baseband converters all have total power integrators whose output can be read via the PC Field System command `tpi`. A procedure utilizing the `tpi` command is:

1. Set up the VLBI terminal as for an experiment, including frequencies and bandwidths.
2. Use the `tpi` command to log the baseband power levels in all channels every 1-2 seconds. For example, an appropriate command for a MkIII/MkIV system is
   `tpi=v1,v2,v3,v4,v5,v6,v7,v8,v9,v10,v11,v12,v13,v14@!,1s`
3. Scan the antenna around the horizon no faster than one beamwidth per `tpi` readout interval.

4. After the scan, examine the data for variations larger than 10% from sample to sample and between frequency channels. There may be some variability with time in the power levels due to weather (try to observe during good weather conditions!) and due to changing ground pickup (the horizon is unlikely to be perfectly flat!). Variability due to these two causes can usually be distinguished from RFI by the fact that clouds and ground generally increase T_{sys} by the same amount at all frequencies within a band (i.e., S or X), whereas RFI generally affects only a few channels at most.

3.2. Measurements Using a Spectrum Analyzer

A spectrum analyzer may be used instead of, or in addition to, the baseband power detectors to search for RFI. If the RFI is weak (raising T_{sys} by less than a factor of 2) and broadband (on the order of the bandwidth of a baseband channel or wider), the baseband detectors generally provide a more sensitive search method. But if the RFI is strong or narrowband, the spectrum analyzer approach works well and has the advantages of instant visual feedback and full IF coverage. (In the baseband detector approach, the measurements must be repeated for each observing frequency sequence.) To search for RFI with a spectrum analyzer:

1. Connect an IF signal from the receiver to the spectrum analyzer. Set the analyzer for a frequency span covering the full IF range, a narrow video BW, and a resolution BW B_{res} no larger than the baseband BW B_{vlbi}. Be sure the signal observed on the analyzer display is dominated by the receiver IF and not by internal analyzer noise.
2. Scan the antenna around the horizon at a rate no faster than one beamwidth per analyzer sweep time. If the sweep time is too long (and hence the scan rate is slower than desired), the video BW may be increased, but at the cost of increased noise.
3. For each RFI signal observed on the analyzer, note the signal bandwidth B_{rfi}. If $B_{rfi} = B_{res}$, set P_{rfi} to the peak signal level; if $B_{rfi} > B_{res}$, set P_{rfi} to the average power level of the RFI. Also note the power level P_{nf} of the noise floor away from the RFI.
4. Estimate the fractional increase $f = T_{rfi}/T_{sys}$ in T_{sys} due to the RFI signal according to

$$\begin{aligned} f(\text{dB}) &= P_{rfi}(\text{dBm}) - P_{nf}(\text{dBm}) + 10\log\left[B_{rfi}(\text{Hz})/B_{vlbi}(\text{Hz})\right] \\ f(\text{numeric}) &= 10^{f(\text{dB})/10} \end{aligned}$$

   The noise temperature due to the RFI is then $f \times T_{sys}$.
5. Repeat steps 2-4 as desired with narrower B_{res} settings in order to detect narrowband RFI at weaker levels.

Example: Suppose the plot in Figure 2 was obtained as described in this section. Then $P_{rfi} = -92.5$ dBm, $P_{nf} = -101$ dBm, and $B_{rfi} = 10$ kHz. By step 4 above, this signal would increase the system power in a 2 MHz bandwidth by the fractional amount

$$\begin{aligned} f(\text{dB}) &= -92.5\text{ dBm} - (-101\text{ dBm}) + 10\log\left[10^4\text{ Hz} \,/\, 2\times 10^6\text{ Hz}\right] \\ &= -14.5\text{ dB}\ , \end{aligned}$$

which equals 4%.

David B. Shaffer: RFI: Effects on Bandwidth Synthesis, IVS 2000 General Meeting Proceedings, p.402–406
http://ivscc.gsfc.nasa.gov/publications/gm2000/shaffer

RFI: Effects on Bandwidth Synthesis

David B. Shaffer

RadioMetrics/NVI, Inc./NASA Goddard Space Flight Center
e-mail: dbs@gemini.gsfc.nasa.gov

Abstract

I describe briefly how bandwidth synthesis works for VLBI, and then show how specific levels of RFI, expressed as a percentage increase above the nominal SEFD, affect the measured group delay.

1. Introduction

This note is a result of discussions held during an RFI workshop which took place at the Wettzell site on February 24, 2000 as part of the IVS meeting.

In the previous contribution, Brian Corey described radio frequency interference (RFI) measurements and how to determine the RFI power that may be incident on an antenna used for VLBI measurements.

The intent here is to describe quantitatively how RFI affects VLBI geodesy measurements and to quantify the level of RFI which is harmful.

2. Group Delay and Bandwidth Synthesis (BWS)

The most important quantity determined for a VLBI geodesy scan is the "group delay". This delay is the relative difference in the time of arrival of the random noise "signal" from a radio source at two antennas. As the Earth turns, the delay changes continuously, in a manner which depends on the relative location of the antennas and the position of the radio source. (Although many antennas participate in most VLBI experiments, in Mk III/Mk IV data analysis, the data from each pair of antennas is treated independently.)

Our ability to determine an accurate value for the group delay (at S- or X-band) depends on how much bandwidth is analyzed. Consider a wide bandwidth "signal" which is basically random noise. (This is what comes from the quasar radio sources.) The signal results from the addition of all the random electromagnetic fields within the overall bandwidth. This superposition of signals changes significantly on a time scale which depends on the maximum frequency difference (that is, the bandwidth). When we compare the two versions of this signal sampled (recorded) at different sites (this is what the correlator does!), we will find a non-zero correlation only if the two versions are closely aligned in time.

If B is the bandwidth that we process, the estimate of the group delay at which the signals are best aligned has an accuracy of about $1/B$. If the signal-to-noise ratio (SNR) is high, we can tell more accurately when the signals are aligned. In fact, the actual error (σ) in determining the best alignment delay is $\sigma = 1/(2\pi \cdot B_{rms} \cdot SNR)$. B_{rms} is the root-mean-square spanned bandwidth, which is about 40% of the total frequency span for the frequency sequences that we use.

How accurately must we measure the group delay?, *i.e.* what are the requirements on σ? We are trying to measure geodetic properties with a precision of better than a centimeter. Light

travels one centimeter in 33 trillionths of a second: $33 \cdot 10^{-12}$ seconds. One trillionth of a second is called a picosecond. Thus, we need to make group delay measurements with an accuracy of tens of picoseconds in order to achieve our desired geodetic goals. If we can achieve a modest SNR of 20, then we must analyze signals with bandwidths of hundreds of megahertz.

If we could record a complete bandwidth of several hundred MHz, our measurement of group delay would be relatively simple. We would just adjust the relative timing of the tapes until the correlator produced the maximum cross-correlation signal. However, the large bandwidth would require a very high data recording rate: twice the maximum bandwidth, or a sample rate approaching a gigabit per second. Although this rate should be achievable with the Mk IV, it is much higher than previous VLBI systems could record. Hence, a better way to sample a broad bandwidth was needed. Haystack's Alan Rogers showed in a 1970 paper that you don't need to record the entire bandwidth ("Very Long Baseline Interferometry with Large Effective Bandwidth for Phase Delay Measurements," *Radio Science*, **5**, 1239-1247). He demonstrated how to achieve nearly the same result by recording several narrow frequency channels spread out across the desired band. This technique, called "Bandwidth Synthesis" (BWS), is how we now record geodetic VLBI data, and is the reason for all the video converters in the data acquisition systems.

We must be careful how we combine the data from the BWS channels. In the case of a single very broad bandwidth, when the tapes are correlated at exactly the right delay, all parts of the processed bandwidth are in phase, with zero relative offset. If the estimated delay is not quite right, there will be a linear phase shift across the bandwidth. This shift arises because the real signal travel time between the two antennas does not match the delay picked by the correlator. In effect, the signal went a little farther (or a little less far) than the correlator estimated. At the higher frequencies in the band, the signal wavelength is shorter. Thus, at the higher frequencies, the extra distance that the signal went corresponds to more cycles (more phase) of the wavelength. If we can measure the shift of phase with frequency (the "phase slope") across the bandwidth, we can determine the difference between the delay used by the correlator (the "model delay") and the true delay. By adding the delay corresponding to the phase slope to the model delay, we get the actual delay. A set of such delays, determined for many scans, is then used to determine the overall geometry of the observations.

The BWS process takes advantage of this phase slope to measure the group delay correction to the correlator model: we process all the frequency channels, look at how the phase changes from channel to channel, and use this change to determine the delay.

This means we have to know how to align the various frequency channels. That is the purpose of the phase calibration system. The phase cal signals are injected in phase at the feed of the receiver. Any channel-to-channel variation of the phase cal phases when extracted from the individual frequency channels is due to differing path lengths through the VLBI equipment and differing video converter LO phases. The measured calibration phases are applied to the measured signal phases to take out the channel offsets. If the phase calibration fails, we can also observe a strong source to determine directly the phase offsets and apply the relative offsets to subsequent data: so-called "manual phase cal." This latter technique, however, does not let us keep track of time-dependent instrumental delay changes, so we really do prefer that the phase cal work!

Figure 1 shows a set of (fake!) BWS data, for our normal X-band observation mode, where eight frequency channels are used. The spacing of the channels is carefully chosen to maximize the effective spanned bandwidth and minimize confusing effects from combining the channels. At X-band, the channels that we use are often arranged in the sequence 0-1-4-10-21-29-34-36. These

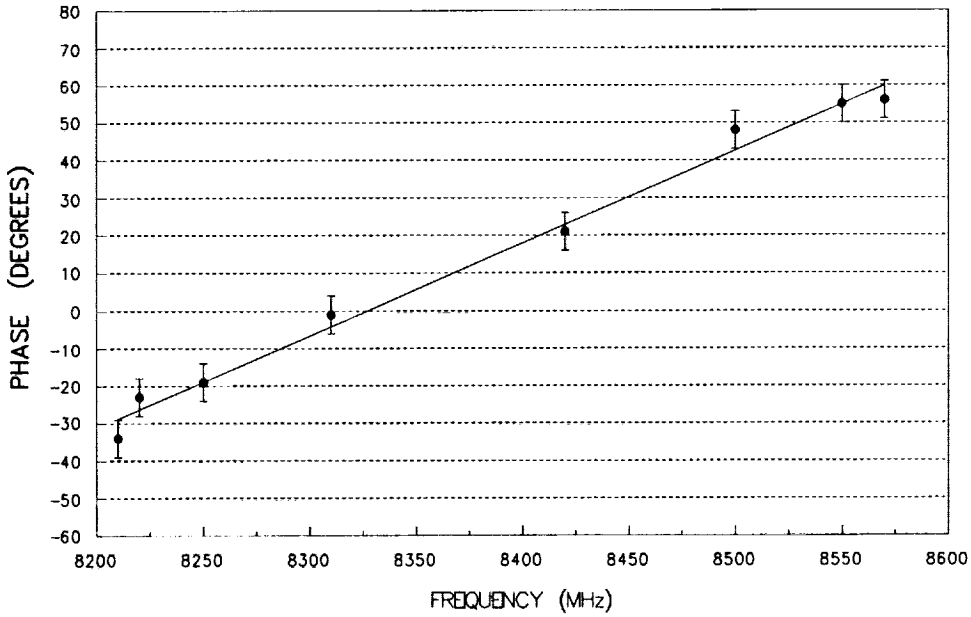

Figure 1. A (hypothetical) plot of phase versus frequency for an X-band experiment using the CDP standard narrowband sequence.

values denote the relative spacing between the channels. This sequence is usually multiplied by either 10 MHz or 20 MHz.

Because our equipment is not perfect and the phase calibration is not perfect, either, the amplitude of the correlated signal in the various channels is generally not the same, and there are residual phase offsets in each channel, too, as shown in Figure 1. Typical phase offsets are several degrees, resulting from such problems as phase offsets in the feeds, reflections in the phase cal system, and spurious phase cal signals. The amplitude and phase imperfections cause a group delay offset. As long as the phase offsets and the relative signal strength in each channel do not change, the group delay offset remains constant, and does not affect geodetic determinations. The offset is included in the clock offset term determined for each baseline.

3. RFI Effects

If the channel offsets change in a random sense during an experiment, there *will be* additional random group delay errors. If there are systematic changes, the delays will also be affected systematically. This is how RFI can cause serious problems.

Consider Figure 1. Determining the group delay is equivalent to fitting a line through the (frequency, phase) values for all the points. The slope of that line gives the group delay. Obviously, if the phase changes, a different slope (different delay) results. Generally, RFI does not cause phases to change. (However, some kinds of RFI—coherent signals at the phase cal frequencies—can cause the phase calibration phase to change, which will cause corresponding phase errors when the calibration is applied.) There is an error, however, on the measurement of the phase in each BWS channel. This error depends directly on the SNR in the channel. The size of this phase error *does* affect the fitting of the line through the phases: if the phase error in some channel is larger

(because the SNR is lower), that channel has a reduced effect on the fit. In the worst case, there may be so much RFI that a particular channel must be deleted from the fit. In this case, the effect of RFI is pretty obvious.

We can quantify the effect of RFI by noting how it affects the SNR in a frequency channel, and then how that affects the group delay determination. The channels for which RFI has the most effect are the end channels of the frequency sequences. These channels have the most leverage on the fit for the group delay. Since it is the overall SNR for the baseline (both antennas used together) that counts, we must relate the RFI level at one antenna to its effect on the interferometer.

The signal-to-noise ratio (SNR) of a VLBI observation depends on three parameters:

- the correlated flux density of the radio source: S_c
- the System Equivalent Flux Densities (SEFD) of the antennas
- the total number of bits correlated: N

Note that N depends on the scan length and the sample rate.

The exact expression for SNR is $SNR = S_c\sqrt{N}/\sqrt{SEFD_1 \cdot SEFD_2}$.

I now evaluate what happens to the group delay when a scan is affected by RFI at only one antenna. I assume that the correlated flux density, the SEFD at the second antenna, and the number of bits correlated do not change. Basically, the RFI increases the SEFD at the first antenna, which in turn reduces the overall SNR for the scan. The SEFD depends on the size of the antenna and the system noise power. (This power is usually expressed in terms of an equivalent noise temperature. Note that "temperature" and "power" are essentially equivalent, related by Boltzmann's equation: $P = kTB$.) When there is no RFI, the system noise temperature is determined by the internal noise power generated in the receiver amplifier, as well as the addition of some external radiation from the atmosphere and the ground. (Strictly speaking, the radio source itself also contributes to the system noise, but since most of the sources we observe add much less than one percent to the overall noise power, we usually neglect their noise contribution.) When there is RFI, the RFI power adds directly to the system noise power to increase the SEFD.

Thus, we can relate RFI to SEFD and then SNR by comparing the system power level with and without the RFI. If the RFI raises the power in a video convertor (as read by the Field System, using the `TPI` command, for example) by 10%, the effective SEFD in that channel will also increase by 10%, or a factor of 1.1, and the baseline SNR will be reduced by a factor of $1/\sqrt{1 \cdot 1.1} = 0.95$. If the RFI power is 100% of SEFD, it will double the power level, and the SEFD will also be a factor of 2 higher. Then the baseline SNR will be a factor of $1/\sqrt{1 \cdot 2} = 0.707$ lower.

Tables 1 and 2 show the effect RFI can have on group delay measurements when a single channel has a phase offset of 5 degrees, an offset which is not at all unusual. The RFI levels at one antenna are expressed as a fractional addition to the nominal system power level *in the affected channel only.* The "Relative Baseline SNR" shows the reduction in SNR, but only for the affected channel. I have applied the offset to the end channel of the frequency sequence to show the maximum effect. These tables show the group delay offset compared to the case of no phase error in the affected channel. The effect of RFI is to *reduce* the offset. This reduction, though, is not good—the original offset, without RFI, would just be absorbed into a clock offset. With RFI, what we consider in our analysis to be a clock offset is not constant!

The effect of RFI seems much worse at S-band. This is because the total frequency span is not as wide. In this case, a given phase offset has a larger effect on the slope of the phase line. Fortunately, the size of S-band delay errors is reduced by a factor of about 13 in our data analysis when the ionosphere correction is applied. (This correction combines the delays measured at S-

and X-band. We observe at two frequencies just so we can make this correction.)

Table 1. Effects of RFI at X-band

Single Antenna RFI Level	Relative Baseline SNR	Group Delay Offset
No RFI	1.000	16.9 picosec
10% RFI	0.953	15.9
20% RFI	0.913	15.0
30% RFI	0.977	14.2
40% RFI	0.845	13.4
50% RFI	0.816	12.8
100% RFI	0.707	10.3

Frequency Sequence is 0-1-4-10-21-29-34-36, multiplied by 10 MHz
RFI and a 5° phase offset occur in channel 8 only (frequency spacing 360 MHz)

Table 2. Effects of RFI at S-band

Single Antenna RFI Level	Relative Baseline SNR	Group Delay Offset
No RFI	1.000	96.9 picosec
10% RFI	0.953	92.1
20% RFI	0.913	87.9
30% RFI	0.977	83.9
40% RFI	0.845	80.3
50% RFI	0.816	77.1
100% RFI	0.707	64.0

Frequency Sequence is 0-1-4-10-15-17, multiplied by 5 MHz
RFI and a 5° phase offset occur in channel 6 only (frequency spacing 85 MHz)

At X-band, moderate RFI levels (those which increase the system noise power in one channel by less than 50%) can easily cause delay errors of several picoseconds, or more than 1 mm of geometric error. Larger RFI levels, of course, result in even larger errors, compared to the situation when there is no RFI. Notice that varying RFI (the usual case - RFI is seldom constant!) really causes a varying delay bias, rather than delay noise which could be either positive or negative. Thus, RFI will tend to "pull" the geodetic results, rather than just making the results noisier. For instance, if RFI is worse in a particular direction (a typical situation), the delays measured when the antenna is pointed in that direction will be affected systematically, leading to a biased position for the antenna. This biasing is probably the most serious reason why RFI is undesirable.

Based on simulations such as those used to generate the Tables, we have chosen an RFI level which causes a 10% increase in system noise power in a video converter bandwidth to be the level at which we begin to worry about degradation of VLBI observations. This is a quantifiable standard which we can present to other agencies as well as entities which are potential generators of RFI.

List of Participants

Registered Participants, IVS 2000 General Meeting Proceedings, p.409–413
http://ivscc.gsfc.nasa.gov/publications/gm2000/participants

Registered Participants

Name	Institution	Country	E-mail
Alef, Walter	Max Planck Institut for Radioastronomy	Germany	alef@mpifr-bonn.mpg.de
Altamimi, Zuheir	Institut Geographique National	France	altamimi@ensg.ign.fr
Altunin, Valery	Jet Propulsion Laboratory	USA	valery.altunin@jpl.nasa.gov
Andersen, Per Helge	FFI (Forsvarets forskningsinstitutt, Norw. Def. Res. Establ.)	Norway	per-helge.andersenffi.no
Appleby, Graham	NERC Space Geodesy Facility	UK	gapp@nerc.ac.uk
Archinal, Brent	U.S. Naval Observatory	USA	baa@casa.usno.navy.mil
Arias, Elisa Felicitas	BIPM	France	farias@bipm.fr
Bauernfeind, Erhard	Forschungseinrichtung Satellitengeodäsie, TU Munich	Germany	bauernfeind@wettzell.ifag.de
Becker, Matthias	Bundesamt fuer Kartographie und Geodaesie	Germany	becker@ifag.de
Behrend, Dirk	Institut d'Estudis Espacials de Catalunya (IEEC/CSIC)	Spain	behrend@ieec.fcr.es
Bergstrand, Sten	Onsala Space Observatory	Sweden	sten@oso.chalmers.se
Berube, Mario	Geodetic Survey Division, Natural Resources	Canada	mario@geod.nrcan.gc.ca
Bielmeier, Ewald	Technische Universitaet Muenchen	Germany	bielmeier@wettzell.ifag.de
Böhm, Johannes	TU Vienna	Austria	jboehm@luna.tuwien.ac.at
Boyer, William	NASA/ Goddard Space Flight Center	USA	wboyer@gemini.gsfc.nasa.gov
Brossmann, Michael	TU Dresden	Germany	brossman@kgise.geo.tu-dresden.de
Budrat, Heinz	Bundesministerium des Innern	Germany	Heinz.Budrat@bmi.bund400.de
Bürki, Beat	Geodesy and Geodynamics Lab, ETH Zurich	Switzerland	buerki@geod.baug.ethz.ch
Börger, Klaus	University of Bonn	Germany	boerger@uni-bonn.de
Campbell, James	Geodetic Institute of the University of Bonn	Germany	campbell@sn-geod-1.geod.uni-bonn.de
Cannon, Wayne	York University, Dept. Physics and Astronomy and Centre for Research in Earth and Space Technology	Canada	wayne@sgl.crestech.ca

Name	Institution	Country	E-mail
Capitaine, Nicole	Observatoire de Paris	France	capitain@danof.obspm.fr
Charlot, Patrick	Observatoire de Bordeaux	France	charlot@observ.u-bordeaux.fr
Clark, Tom	NASA/GSFC	USA	clark@tomcat.gsfc.nasa.gov
Colomer, Francisco	Observatorio Astronomico Nacional - Yebes	Spain	colomer@oan.es
Colucci, Giuseppe (Pino)	ASI/Telespazio	Italy	giuseppe.colucci@asi.it
Combrinck, Ludwig	HartRAO	South Africa	ludwig@ludwig.hartrao.ac.za
Corey, Brian	MIT Haystack Observatory	USA	bcorey@haystack.mit.edu
Cox, Clyde	Kokee Park Geophysical Observatory	USA	clyde.cox@alliedsignal.com
Dassing, Reiner	BKG-Wettzell	Germany	dassing@wettzell.ifag.de
Digre, Helge	Norwegian Mapping Authority	Norway	helge.digre@statkart.no
Drewes, Hermann	DGFI	Germany	drewes@dgfi.badw-muenchen.de
Dube, Maurice	Raytheon ITSS	USA	dube@cddis.gsfc.nasa.gov
Elgered, Gunnar	Onsala Space Observatory	Sweden	kge@oso.chalmers.se
Engelhardt, Gerald	BKG Leipzig	Germany	engelhardt@leipzig.ifag.de
Essaifi, Najat	Paris Observatory	France	Essaifi@hpopa.obspm.fr
Feissel, Martine	Paris Observatory/Institut Géographique National	France	feissel@ensg.ign.fr
Fernández, Laura I.	Observatorio Astronomico La Plata	Argentina	lauraf@fcaglp.unlp.edu.ar
Fey, Alan	U.S. Naval Observatory	USA	afey@usno.navy.mil
Gambis, Daniel	IERS/cb, Paris Observatory	France	Daniel.Gambis@obspm.fr
Gaume, Ralph	US Naval Observatory	USA	rgaume@usno.navy.mil
Gontier, Anne-Marie	Paris Observatory	France	Anne-Marie.Gontier@obspm.fr
Gonzalez, Raymond	NVI Inc. GSFC/NASA	USA	rgonzale@gemini.gsfc.nasa.gov
Gordon, David	Raytheon ITSS; NASA/GSFC	USA	dgg@leo.gsfc.nasa.gov
Grünreich, Dietmar	Bundesamt fuer Kartographie und Geodaesie	Germany	gruenreich@ifag.de
Haas, Rüdiger	Onsala Space Observatory	Sweden	haas@oso.chalmers.se
Harrison, Cynthia	Washington Correlator	USA	charrison@amsc-inc.com
Hase, Hayo	Bundesamt fuer Kartographie und Geodaesie - Wettzell	Germany	hase@wettzell.ifag.de
Herring, Thomas	MIT	USA	tah@mit.edu
Himwich, Ed	NVI/GSFC	USA	weh@vega.gsfc.nasa.gov

Name	Institution	Country	E-mail
Ihde, Johannes	Bundesamt für Kartographie und Geodäsie	Germany	ihde@leipzig.ifag.de
Johnson, Heidi	MIT Haystack Observatory	USA	hjohnson@haystack.mit.edu
Kawano, Nobuyuki	National Astronomical Observatory of Japan	Japan	kawano@miz.nao.ac.jp
Kermes, Roger	Lockheed Martin SO/Fairbanks NOAA/NESDIS CDA Station	USA	rkermes@mosquitonet.com
Kierulf, Halfdan Pascal	Statens kartverk. Norwegian mapping authority	Norway	halfdan.kierulf@statkart.no
Kihle, Roar	Norwegian Mapping Authority	Norway	roar.kihle@statkart.no
Kilger, Richard	FundamentalStation Wettzell	Germany	kilger@ifag.wettzell.de
Kingham, Kerry	U.S.N.O.	USA	kak@cygx3.usno.navy.mil
Klatt, Calvin	Geodetic Survey Division, Natural Resources Canada	Canada	klatt@geod.nrcan.gc.ca
Kluegel, Thomas	FESG, TU Munich	Germany	kluegel@wettzell.ifag.de
Kodak, Charles	AlliedSignal Technical Services Corporation	US	kodakc@thorin.atsc.allied.com
Kondo, Tetsuro	Communications Research Laboratory	Japan	kondo@crl.go.jp
Kono, Yusuke	GUAS of Japan	Japan	kono@miz.nao.ac.jp
Koyama, Yasuhiro	Kashima Space Research Center, CRL	Japan	koyama@crl.go.jp
Kronschnabl, Gerhard	Bundesamt fuer Kartographie und Geodaesie	Germany	kronschnabl@wettzell.ifag.de
Lanotte, Roberto	Telespazio	Italy	lanotte@asi.it
Lee, Shelton	Washington Correlator	USA	
Lewis, Deborah	Washington Correlator	USA	
Long, Jim	NASA/AlliedSignal	USA	longj@thorin.atsc.allied.com
Lucena, Macilio	INPE/CRAAE	Brazil	macilio@roen.inpe.br
Ma, Chopo	Goddard Space Flight Center	USA	cma@virgo.gsfc.nasa.gov
MacMillan, Dan	NVI, Inc./GSFC	USA	dsm@leo.gsfc.nasa.gov
Mantovani, Franco	Istituto di Radioastronomia	Italy	fmantovani@ira.bo.cnr.it
Matsuzaka, Shigeru	Geographical Survey Institute	Japan	shigeru@gsi-mc.go.jp
Meyer, Ulrich	IAPG, TU-München	Germany	meyer@step.iapg.verm.tu-muenchen.de
Müskens, Arno	University of Bonn / MPIfR Bonn / Mk3A-Mk4 correlator	Germany	mueskens@mpifr-bonn.mpg.de
Niell, Arthur	Haystack Observatory	USA	aniell@haystack.mit.edu
Nothnagel, Axel	Geodetic Institute of the University of Bonn	Germany	nothnagel@uni-bonn.de

Name	Institution	Country	E-mail
Paragi, Zsolt	FOMI Satellite Geodetic Observatory	Hungary	paragi@sgo.fomi.hu
Paunonen, Matti	Finnish Geodetic Institute	Finland	geodeet@csc.fi
Petrachenko, Bill	Geodetic Survey Div, NRCan	Canada	Bill.Petrachenko@hia.nrc.ca
Petrov, Leonid	Geodetic Institute of the University of Bonn	Germany	petrov@picasso.geod.uni-bonn.de
Poirier, Michael	MIT Haystack Observatory	USA	mpoirier@haystack.mit.edu
Ray, Jim	U.S. Naval Observatory	USA	jimr@maia.usno.navy.mil
Reinhart, Ewalt	BKG(retired)	Germany	reinhart@ifag.de
Resch, George	Jet Propulsion Laboratory	USA	George.Resch@jpl.nasa.gov
Riepl, Stefan	BKG	Germany	riepl@wettzell.ifag.de
Rizwan, Mamat	South Beijing Rd 40-5#	China	wwx@ms.xjb.ac.cn
Rothacher, Markus	Forschungseinrichtung Satellitengeodäsie, TU Munich	Germany	rothacher@bv.tum.de
Scherneck, Hans-Georg	Onsala Space Observatory	Sweden	hgs@oso.chalmers.se
Schlicht, Anja	TU Munich	Germany	schlicht@wettzell.ifag.de
Schlüter, Wolfgang	BKG-FS Wettzell	Germany	schlueter@wettzell.ifag.de
Schreiber, Ullrich	TU Munich	Germany	schreiber@wettzell.ifag.de
Schuh, Harald	Deutsches Geodaetisches Forschungsinstitut (DGFI)	Germany	schuh@dgfi.badw.de
Schupler, Bruce	AlliedSignal Technical Services Corporation	US	Bruce.Schupler@atsc.allied.com
Schwarz, Walter	Bundesamt fuer Kartographie und Geodaesie	Germany	Schwarz@wettzell.ifag.de
Schwegmann, Wolfgang	Deutsches Geodaetisches Forschungsinstitut (DGFI)	Germany	schwegmann@dgfi.badw.de
Seeger, Hermann	BKG (retired)	Germany	seeger@picasso.geod.uni-bonn.de
Shaffer, David	RadioMetrics/NVI/GSFC	USA	shaffer@nevada.edu
Smythe, Daniel	MIT Haystack Observatory	USA	Dsmythe@haystack.mit.edu
Sorgente, Mauro	University of Bonn	Germany	sorgente@mpifr-bonn.mpg.de
Sousa, Donald	MIT Haystack Observatory	USA	dsousa@haystack.mit.edu
Sovers, Ojars	RSA Systems, Inc.	USA	ojars@mail.rsasys.com
Springer, Tim	Astronomical Institute University of Berne	Switzerland	tim.springer@aiub.unibe.ch
Steinforth, Christoph	Geodetic Institute of the University of Bonn	Germany	steinfor@picasso.geod.uni-bonn.de
Strand, Richard	Gilmore Creek Geophysical Observatory	USA	oper@blizzard.gcgo.nasa.gov

Name	Institution	Country	E-mail
Tangen, Leif Morten	Norwegian Mapping Authority	Norway	leif.morten.tangen@statkart.no
Tesmer, Volker	Deutsches Geodaetisches Forschungsinstitut (DGFI)	Germany	tesmer@dgfi.badw.de
Thomas, Cynthia	NVI, Inc./GSFC	USA	cct@gemini.gsfc.nasa.gov
Thorandt, Volkmar	BKG Leipzig	Germany	vt@leipzig.ifag.de
Thornton, Bruce	Washington Correlator	USA	blt@casa.usno.navy.mil
Titus, Michael	MIT Haystack Observatory	USA	mtitus@haystack.mit.edu
To, Tran Din	Institute of Geology, National Center for Natural Sciences, Hanoi, c/o BKG	Vietnam	gps7@ifag.de
Tomasi, Paolo	Istituto di Radioastronomia	Italy	tomasi@ira.bo.cnr.it
Tornatore, Vincenza	Politecnico di Milano DIIAR	Italy	vin@ipmtf4.topo.polimi.it
Tuccari, Gino	Istituto di Radioastronomia CNR	Italy	tuccari@ira.noto.cnr.it
Van Langevelde, Huib	Joint Institute for VLBI in Europe	Netherlands	langevelde@jive.nl
Vandenberg, Nancy	NVI, Inc./GSFC	USA	nrv@gemini.gsfc.nasa.gov
Vespe, Francesco	Agenzia Spaziale Italiana	Italy	vespe@asi.it
Walker, R. Craig	NRAO	USA	cwalker@nrao.edu
Whitney, Alan	MIT Haystack Observatory	USA	awhitney@haystack.mit.edu
Wildes, William	GSFC NASA	USA	wtw@wildbill.gsfc.nasa.gov
Zeitlhoefler, Reinhard	Technische Universitaet Muenchen	Germany	zeitlhoefler@wettzell.ifag.de
Zernecke, Rudolf	FESG, TU Munich	Germany	zernecke@wettzell.ifag.de

Program

First IVS General Meeting Program, IVS 2000 General Meeting Proceedings, p.417–425
http://ivscc.gsfc.nasa.gov/publications/gm2000/program

First IVS General Meeting Program

Monday, February 21

Session 1. Highlights and Challenges of VLBI, Chair: Arthur Niell

09:00 Welcome

09:15 **IVS Chair's Address**
Wolfgang Schlüter—Bundesamt für Kartographie und Geodäsie (BKG)

09:30 **IVS Coordinating Center Report**
Nancy Vandenberg—NVI, Inc./Goddard Space Flight Center

09:45 **From Quasars to Benchmarks: VLBI Links Heaven to Earth** *(invited)*
James Campbell—Geodetic Institute, University of Bonn

10:15 **The Role of VLBI Among the Geodetic Space Techniques within CSTG** *(invited)*
Hermann Drewes—DGFI

10:45 BREAK/Poster Session 1

11:15 **Astronomical VLBI: Comparison and Contrast with Geodetic/Astrometric VLBI** *(invited)*
Craig Walker—NRAO

11:45 **The ICRF and Relationships Between Frames** *(invited)*
Chopo Ma—NASA Goddard Space Flight Center

12:00 **ITRF Status and Plans for ITRF2000** *(invited)*
Zuheir Altamimi—Institut Geographique National, France

12:15 LUNCH

14:00 **Geophysical Applications of Earth Rotation Measurements** *(invited)*
Tom Herring—MIT

14:30 **It's About Time!** *(invited)*
Tom Clark—NASA/GSFC

Session 2. Field Stations and Data Acquisition, Chair: Shigeru Matsuzaka

15:00 **IVS Network Coordinator Report**
Ed Himwich—NVI, Inc./GSFC

15:15 BREAK/Poster Session 1

15:45 **VLBI Electronics for Analysts: From the Feed to the Recorder** *(invited)*
Brian Corey—MIT Haystack Observatory

16:15 **VLBI Data Acquisition and Recorder Systems: A Summary and Comparison** *(invited)*
Bill Petrachenko—Geodetic Survey Division, NRCan

16:45 **An Introduction to the Field System** *(invited)*
Ed Himwich—NVI, Inc./GSFC

17:30 **Planning the Chiefs Meeting for February, 2001** *(splinter meeting)*
Ed Himwich—NVI, Inc./GSFC

Tuesday, February 22

Session 3. Technology and Data Acquisition, Chair: Wayne Cannon

09:00 **IVS Technology Coordinator Report**
Alan Whitney—MIT Haystack Observatory

09:20 **Geodetic VLBI Observations Using the Giga-Bit VLBI System**
Yasuhiro Koyama(1), Tetsuro Kondo(1), Junichi Nakajima(1), Mamoru Sekido(1) Ryuichi Ichikawa(1), Eiji Kawai(1), Hiroshi Okubo(1), Hiro Osaki(1), Hiroshi Takaba(2), Minoru Yoshida(2), and Ken-ichi Wakamatsu(2)—(1) Kashima Space Research Center, Communications Research Laboratory, (2) Gifu University

09:35 **Concept for an Affordable High-Data-Rate VLBI Recording and Playback System**
Alan Whitney—MIT Haystack Observatory

09:50 BREAK/Poster Session 2

Session 4. Local Surveys, Chair: Hayo Hase

10:30 **The Importance of Local Surveys for Tying Techniques Together** *(invited)*
John Bosworth (1) and Jim Long (2)—(1) NASA GSFC, (2) AlliedSignal Technical Services Corp.

11:00 **Local Surveys of VLBI Telescopes: Conceptual and Practical Issues** *(invited)*
Axel Nothnagel (1) and Ludwig Combrinck (2)—(1) Geodetic Institute, University of Bonn, (2) HartRAO

11:30 **A New GPS-VLBI Tie at the Onsala Telescope**
Sten Bergstrand, Rüdiger Haas, Jan M. Johansson—Onsala Space Observatory, Onsala, SWEDEN

11:45 **VLBI Determinations of Local Telescope Displacements**
R. Haas (1), A. Nothnagel (2), D. Behrend (3)—(1) OSO, Onsala/Sweden, (2) GIUB, Bonn/Germany, (3) IEEC, Barcelona/Spain

12:00 LUNCH

Session 5. Observing Programs, Chair: Paolo Tomasi

13:30 **The CORE Program**
Chopo Ma (1), Cynthia Thomas (2), Nancy Vandenberg (2)—(1) NASA GSFC, (2) NVI, Inc./GSFC

13:45 **The European VLBI Project**
James Campbell and Axel Nothnagel—Geodetic Institute, University of Bonn

14:00 **Current Activities in the EVN**
Huib van Langevelde—Joint Institute for VLBI in Europe

14:15 **Overview of Observations on the VLBA**
Craig Walker—NRAO

14:30 **Differential VLBI Observations Among a Lunar Orbiter, the Moon, and QSOs**
Nobuyuki Kawano(1), Hideo Hanada(1), Takahiro Iwata(2) and Yasuhiro Koyama(3)—(1)National Astronomical Observatory of Japan, (2)National Space Development Agency of Japan, (3)CRL

14:45 **A Southern Hemisphere Observing Program to Strengthen the ICRF: Benefits for Astrometry, Geodesy, and Astronomy**
A.L. Fey, K.J. Johnston (USNO); D.L. Jauncey, J.E. Reynolds, A.K. Tzioumis (ATNF); P. McCulloch, M.E. Costa, S.J. Ellingsen (UTas); G.D. Nicolson (HART RAO)

15:00 **A Proposed Astrometric Observing Program for Densifying the ICRF in the Northern Hemisphere**
P. Charlot (1), B. Viateau (1)(4), A. Baudry (1), C. Ma (2), A. Fey (3) , T. M. Eubanks (3), C. Jacobs (4), O. Sovers (4)—(1) Observatoire de Bordeaux, (2) NASA/GSFC, (3) USNO, (4) JPL

15:15 **The S2 Geodetic VLBI Program in Canada: Operations, Experiments, and Results**
Klatt(1), Berube(1), Bujold(1), Cannon(2), Feil(2), Novikov(2), Petrachenko(1), Popelar(1), Searle(2,1)—(1)Geodetic Survey Division, NRCan (2)SGL, CRESTech

15:30 **New Uses for the VLBI Network**
Tom Clark—NASA/GSFC

15:45 BREAK/Poster Session 2

Session 6. Correlators, Chair: Tetsuro Kondo

16:15 **How Do VLBI Correlators Work?** *(invited)*
Alan Whitney—MIT Haystack Observatory

16:45 **Early Experiences with the Mark IV Correlator**
Kerry Kingham and Jim Martin—U. S. Naval Observatory

17:00 **The Bonn Mark IV Correlator Project**
W. Alef (1), J.A. Zensus (1), A. Müskens (2), W. Schlüter (3)—(1) Max-Planck-Institut for Radioastronomie, Bonn, (2) Geodetic Institute, University of Bonn, (3) Bundesamt für Kartographie und Geodäsie

17:30 **Maintenance Support Issues** *(splinter meeting)*
Arthur Niell—MIT Haystack Observatory

19:00 Busses depart for IVS Dinner

19:30 IVS Dinner

Wednesday, February 23

Session 7. Analysis Part 1, Chair: Jim Ray

09:00 **IVS Analysis Coordinator Report**
Axel Nothnagel—Geodetic Institute, University of Bonn

09:15 **Geodetic Analysis Overview** *(invited)*
Harald Schuh—DGFI

09:45 **Instrumental Errors of Geodetic VLBI**
Leonid Petrov—Geodetic Institute of the University of Bonn

10:00 **Mark IV Data Analysis - Software Changes and Early Experiences**
Brent Archinal—U. S. Naval Observatory

10:15 **VLBI Data Analysis with a Full Variance-Covariance Matrix**
Harald Schuh and Volker Tesmer—DGFI, Munich, Germany

10:30 BREAK

11:00 **Optimal Estimation of Earth Orientation Parameters Using VLBI**
Leonid Petrov—Geodetic Institute of the University of Bonn

11:15 **Improvement of VLBI EOP Accuracy and Precision**
Dan MacMillan (1) and Chopo Ma (2)—(1) NVI, Inc./GSFC and (2) NASA Goddard Space Flight Center

11:30 **First Results of the 1999 Tsukuba-Wettzell UT1 Intensive Test Series**
Nothnagel A. (1), Hase H. (1), Kilger R. (1), Ogi S. (2), Takashima K .(2), Thorandt V. (1), Ullrich D. (1)—(1) Forschungsgruppe Satellitengeodaesie, Germany, (2) Geographical Survey Institute, Japan

11:45 **Ocean Loading Tides for, in and from VLBI**
Hans-Georg Scherneck, Rüdiger Haas, Alessandro Laudati—Onsala Space Observatory, Chalmers University of Technology

12:00 **Improved atmospheric mapping functions for VLBI and GPS**
Arthur Niell—MIT Haystack Observatory

12:15 LUNCH

Session 8. Analysis Part 2, Chair: Harald Schuh

14:00 **Atmospheric Parameters Derived from Simultaneous Observations with Space Geodetic and Remote Sensing Techniques at OSO**
R. Haas, L. P. Gradinarsky, G. Elgered, J. M. Johansson—Onsala Space Observatory (OSO)

14:15 **Calibration of Atmospherically Induced Delay Fluctuations**
G.M. Resch, C.S. Jacobs, S.J. Keihm, G.E. Lanyi, C.J. Naudet, A.L. Riley, H.W. Rosenberger, A.B. Tanner—Jet Propulsion Laboratory, California Institute of Technology

14:30 **Stability of the ICRF: A Time Series Approach**
Martine Feissel and Anne-Marie Gontier—Observatoire de Paris

14:45 **Improving the ICRF Using the Radio Reference Frame Image Database**
D.A. Boboltz, A.L. Fey, R.A. Gaume, K.J. Johnston—U. S. Naval Observatory

15:00 **Combination of VLBI, GPS, and SLR Data at the Observation Level - A Status Report**
P. H. Andersen—Forsvarets forskningsinstitutt, Kjeller, Norway, and Institute of Theoretical Astrophysics, University of Oslo, Norway

15:15 BREAK

15:45 **UTC and UT1: New Timing Products from the IGS** *(invited)*
Jim Ray—U. S. Naval Observatory

16:15 **Cooperation and Common Interests of the IGS and the IVS** *(invited)*
Tim Springer—University of Berne

16:45 **Closing Remarks and IVS Future Plans**
Wolfgang Schlüter—Bundesamt für Kartographie und Geodäsie (BKG)

17:00 ADJOURN

Poster Session 1. IVS Component Reports, Chair: Richard Kilger

Network Stations

Matera CGS VLBI Station Status P. Colucci, D. Del Rosso, E. Lunalbi, F. Vespe—ASI/Telespazio

The Geodetic Observatory O'Higgins: A Contribution to IVS in the Southern Hemisphere Andreas Reinhold(2), Hayo Hase(1),Wolfgang Schlüter(1), Reiner Wojdziak(2)—(1)Bundesamt für Kartographie und Geodäsie, Fundamentalstation Wettzell, (2) Aussenstelle Leipzig

The IVS Activities at Onsala Space Observatory R. Haas, G. Elgered, H.-G. Scherneck, J.M. Johansson, S. Bergstrand, L. P. Gradinarsky, B. Stoew, J, Boerjesson, H. Bouma—Onsala Space Observatory (OSO), Chalmers University of Technology (CUT), ONSALA (Sweden)

Noto VLBI Station: Technological Research Activity Gino Tuccari—Istituto di Radioastronomia CNR

VLBI Activities at GSI Shigeru Matsuzaka and Misao Ishihara—Geographical Survey Institute

TIGO: Its Contribution to ITRF/IERS Hayo Hase, Armin Boeer, Stefan Riepl, Wolfgang Schlüter—Bundesamt für Kartographie und Geodäsie (BKG)

20-m Radiotelescope at Fundamentalstation Wettzell Richard Kilger, et al.—Forschungsgruppe Satellitengeodaesie, Germany

The New 40-meter Radiotelescope of OAN at Yebes Francisco Colomer—OAN

Gilmore Creek Geophysical Observatory 2000 status Rich Strand—NASA/GCGO

Kokee Park Geophysical Observatory 2000 Clyde Cox—AlliedSignal Technical Services Corp.

Operation Centers

CORE Operations Center: 2000 and Beyond Cynthia Thomas and Nancy Vandenberg—NVI, Inc./Goddard Space Flight Center

Data Centers

The Paris Observatory Data Center (OPAR) Najat Essaifi—Paris Observatory

Status and Development of the IVS Data Center at BKG Leipzig Volkmar Thorandt, Dieter Ullrich, Rainer Wojdziak—Bundesamt für Kartographie und Geodäsie (BKG)

The IVS Data Center at the CDDIS: An Overview Carey Noll and Maurice Dube—NASA/GSFC

Analysis Centers

The Paris Observatory Analysis Centre OPAR Anne-Marie Gontier, Martine Feissel, Najat Essaifi, Didier Jean-Alexis—Paris Observatory

IAA Analysis Center Activity in 1999 Zinovy Malkin—IAA RAS

Contribution of the BKG analysis group to the IVS analysis activities Volkmar Thorandt, Dieter Ullrich, Gerald Engelhardt—Bundesamt für Kartographie und Geodäsie (BKG)

GSFC VLBI Analysis Center Activities Chopo Ma (1), David Gordon (2), Dan MacMillan (3), and Karen Baver (2)—(1) NASA/GSFC, (2) Raytheon ITSS and NASA/GSFC, (3) NVI, Inc. and NASA/GSFC

Technology Development Centers

Recent Activities at Communications Research Laboratory Tetsuro Kondo, et al.—CRL VLBI Group, Communications Research Laboratory

The Canadian Transportable VLBI Antenna Mario Berube—Geodetic Survey Division, NRCan

The S2 VLBI System: DAS, RT/PT and Correlator Petrachenko(1), Bujold(1), Cannon(2,4), Carlson(3), Dewdney(3), Feil(2), Newby(2), Novikov(2), Popelar(1), Wietfeldt(5)—(1)Geodetic Survey Division, NRCan (2)SGL, CRESTech, (3)DRAO, NRC, (4)York University, (5)JPL

Poster Session 2. IVS Analysis Reports, Chair: Rüdiger Haas

Determination of EOP with OCCAM and ERA Packages Elena Skurikhina and Maria Sokolskaya—Institute of Applied Astronomy, Russian Academy of Sciences

A Catalogue of Radio Source Coordinates Obtained from NEOS and CORE VLBI Programs Maria Sokolskaya, Zinovy Malkin—Institute of Applied Astronomy, Russian Academy of Sciences

Status of IADA: An Intelligent Assostant for Data Analysis in VLBI W. Schwegmann, H. Schuh—DGFI, Munich, Germany

GINS: A New Multi-Technique Software for VLBI Analysis U. Meyer (1), P. Charlot (2), R. Biancale (1)—(1) CNES/GRGS Toulouse, (2) Observatoire de Bordeaux

An Experimental Campaign for Evaluation of Wet Delay Variations Using WVRs in the Kanto District, Central Japan Ichikawa, et al.—Kashima Space Research Center, Communications Research

Optical Linked VLBI Observations Juichi Nakajima, et al.—CRL, Japan

Celestial Reference Frame RSC(GAOUA)99 C 03 O. A. Molotaj—Astronomical Observatory of Kyiv University

Multi-frequency VLBI Observations of the ICRF Source 1823+568 Z. Paragi et al.—FOMI Satellite Geodetic Observatory

Differential VLBI Observations of the Lunar Prospector Y. Kono[1], H. Hanada[2], K. Iwadate[2], H. Araki[2], N. Kawano[2], Y. Koyama[3] , Y. Fukuzaki[4]—[1] GUAS of Japan, [2] National Astronomical Observatory of Japan, [3] CRL, [4] Geographical Survey Institute

EOP Series and Station Positions from VLBI Observations for 1984-1999 Elena Skurikhina—Institute of Applied Astronomy, Russian Academy of Sciences

VLBI in the Deep Space Network: Challenges and Prospects V. Altunin(1), G. Resch (1), D. Rogstad(1), P. Wolken(2)—(1) JPL/NASA, (2) AlliedSignal

Geodesy/Astrometry from the VLBA David Gordon—Raytheon ITSS and NASA/GSFC

VLBI Baseline Rates from Simultaneous Solution of Baseline Measurements with Antenna Offsets H. B. Iz and B. A. Archinal—The U.S. Naval Observatory, Department of Earth Orientation, Washington D.C., USA

Polar Motion from VLBI Observations Jinling Li and Guangli Wang—Shanghai Observatory

Thursday, February 24

09:00 Excursion to Fundamentalstation Wettzell
- Introduction to activities at a fundamental station for geodesy (Schlüter)
- Visit to VLBI group at 20-m radio telescope (Kilger)
- Visit to Transportable Integrated Geodetic Observatory (TIGO) (Hase)
- Visit to the Wettzell Laser Ranging System (WLRS) (Riepl, Schreiber)
- Visit to the GPS control station (Roettcher, Hessels)
- Visit to the Time & Frequency Laboratory (Feil)
- Visit to the seismic and gravity meter station (Stoeger)

12:00 End of tour and departure for lunch

13:30 Analysis Centers Workshop (Haus des Gastes)
Axel Nothnagel

14:00 RFI Workshop (Wettzell)
Brian Corey and Hayo Hase

REPORT DOCUMENTATION PAGE

Form Approved
OMB No. 0704-0188

1. AGENCY USE ONLY *(Leave blank)*	2. REPORT DATE	3. REPORT TYPE AND DATES COVERED
	May 2000	Conference Publication

4. TITLE AND SUBTITLE
International VLBI Service for Geodesy and Astrometry
2000 General Meeting Proceedings

5. FUNDING NUMBERS
920.1

6. AUTHOR(S)
Nancy R. Vandenberg and Karen D. Baver, Editors

7. PERFORMING ORGANIZATION NAME(S) AND ADDRESS (ES)
Space Geodesy Networks & Sensor Calibration Office
Laboratory for Terrestrial Physics
Goddard Space Flight Center
Greenbelt, Maryland 20771

8. PEFORMING ORGANIZATION REPORT NUMBER
2000–02743–0

9. SPONSORING / MONITORING AGENCY NAME(S) AND ADDRESS (ES)
National Aeronautics and Space Administration
Washington, DC 20546-0001

10. SPONSORING / MONITORING AGENCY REPORT NUMBER
CP—2000–209893

11. SUPPLEMENTARY NOTES

12a. DISTRIBUTION / AVAILABILITY STATEMENT
Unclassified–Unlimited
Subject Category: 42
Report available from the NASA Center for AeroSpace Information,
7121 Standard Drive, Hanover, MD 21076-1320. (301) 621-0390.

12b. DISTRIBUTION CODE

13. ABSTRACT *(Maximum 200 words)*

This volume is the proceedings of the first General Meeting of the International VLBI Service for Geodesy and Astrometry (IVS), held in Kötzting, Germany, February 21–24, 2000. The content of this volume also appears on the IVS web site at: http://ivscc.gsfc.nasa.gov/publications/gm2000

The goal of the program committee for the General Meeting was to provide an interesting and informative program for a wide cross section of IVS members, including station operators, program managers, and analysts. The program included reports, tutorials, invited and contributed papers, and poster presentations. The tutorial papers should be particularly useful references because each one provides an overview and introduction to a topic relevant to VLBI.

14. SUBJECT TERMS
Geodesy, astrometry, VLBI, geophysics, Earth orientation, very long baseline interferometry, interferometry, radio astronomy, geodynamics, reference frames, terrestrial reference frame, celestial reference frame, length of day, Earth system science, Earth rotation.

15. NUMBER OF PAGES
425

16. PRICE CODE

17. SECURITY CLASSIFICATION OF REPORT	18. SECURITY CLASSIFICATION OF THIS PAGE	19. SECURITY CLASSIFICATION OF ABSTRACT	20. LIMITATION OF ABSTRACT
Unclassified	Unclassified	Unclassified	UL